THE REDOX AND CO-ORDINATION CHEMISTRY OF SOME DINUCLEAR DIPHOSPHAZANE-BRIDGED DERIVATIVES OF RUTHENIUM

by

STEPHEN FARRING WOOLLAM B.Sc.(Hons), (Natal)

A thesis submitted in partial fulfillment of the requirements for the degree of Doctor of Philosophy in the Faculty of Science, University of Natal, Pietermaritzburg

Department of Chemistry

University of Natal

Pietermaritzburg

November 1991

DECLARATION

I hereby certify that this research is the result of my own investigation which has not already been accepted in substance for any degree and is not being submitted in candidature for any other degree.

Signed: .....

S.F. WOOLLAM

I hereby certify that this statement is correct.

Signed: .....

PROFESSOR R J HAINES

(Supervisor)

Signed: .....

PROFESSOR J S FIELD

(Co-supervisor)

Department of Chemistry

University of Natal

Pietermaritzburg

November 1991

TO MY FAMILY

ACKNOWLEDGEMENTS

I wish to express my sincere gratitude to Professors R.J. Haines and J.S. Field for invaluable discussions and expert advice concerning this research project and for their continued interest and encouragement offered to me during the course of this investigation.

I also wish to extend my thanks to:-

Mr Martin Watson for efficient running of NMR spectra and in particular for the training received in the operation of NMR spectrometers;

Mr Hashim Desai for the synthesis of the diphosphazane ligands, for elemental analysis and technical assistance, and Mr Raj Somaru for elemental analysis;

Miss Niyum Ramesar and Mrs Karen Edwards for X-ray data collection and assistance with the computation of data;

The members of the technical staff in the Department of Chemistry and in the Faculty of Science Mechanical Instrument Workshop and Mr Paul Forder in the Glassblowing Workshop;

Mr Dave Crawley for assistance with the drawing of diagrams;

My colleagues in the laboratory for helpful discussions and support;

Mrs Shelagh Lellyett for most efficient typing;

The Foundation for Research Development and the University of Natal for financial assistance.

Finally, I would like to thank my parents and my brother for their patience and generous support throughout my academic career.

LIST OF ABBREVIATIONS AND SYMBOLS

A	anionic ligand
Bu	butyl
C	Celcius
cm	centimetre
Cp	cyclopentadienyl
Cp^*	pentamethylcyclopentadienyl
CV	cyclic voltammogram
Cy	cyclohexyl
Dc	calculated density
DEPT	Distortionless enhancement of polarization transfer
dmpm	bis(dimethylphosphino)methane
dppm	1,2-bis(diphenylphosphino)ethane
dppm	bis(diphenylphosphino)methane
Et	ethyl
ν	frequency
g	gram
$\{^1H\}$	proton noise decoupled
H_3PO_4	85% phosphoric acid
i	iso
IR	infrared
L	two electron donor ligand
M	transition metal
Me	methyl
mmol	millimole
n.m.	not measured
nmr	nuclear magnetic resonance
o,p	*ortho, para*
Ph	phenyl

Pr	propyl
py	pyridine
R	alkyl group
λ	radiation wavelength
TCNE	tetracyanoethylene
TCNQ	tetracyanoquinodimethane
TMS	trimethylsilane
THF	tetrahydrofuran
uv	ultraviolet
X	halogen, unless otherwise stated

SUMMARY

A review of the neutral binary carbonyls of iron, ruthenium and osmium is presented and the use of bridging ditertiary phosphine and phosphite ligands to stabilize dinuclear derivatives of these metals, and in particular of ruthenium, to fragmentation is discussed in some detail. The synthesis and reactivity of low oxidation state dinuclear diphosphorus-bridged transition metal complexes is summarized, while the chemistry of diruthenium complexes is surveyed in a little more detail, particularly that for systems having ruthenium in a low formal oxidation state.

With the object of producing suitable precursors for the synthesis of new diruthenium complexes, the reactions of $[Ru_2(\mu\text{-}CO)(CO)_4\{\mu\text{-}(RO)_2PN(Et)P(OR)_2\}_2]$ (R = Me or Pr^i) with the one-electron oxidants, silver(I) salts, in a variety of solvents, was investigated. The products obtained were found to be dicationic solvento species of the type $[Ru_2(CO)_5(solvent)\{\mu\text{-}(RO)_2PN(Et)P(OR)_2\}_2]^{2+}$ (solvent = alkyl or aryl nitrile, ketones, ethers, sulphides, etc). In order to establish the relative lability of the co-ordinated solvent in these complexes, they were reacted with a wide range of neutral and anionic donor ligands to afford complexes of the type $[Ru_2(CO)_5L\{\mu\text{-}(RO)_2PN(Et)P(OR)_2\}_2]^{2+}$, $[Ru_2(CO)_5A\{\mu\text{-}(RO)_2PN(Et)P(OR)_2\}_2]^{+}$, $[Ru_2(\mu\text{-}A)(CO)_4\{\mu\text{-}(RO)_2PN(Et)P(OR)_2\}_2]^{+}$, $[Ru_2(CO)_4A_2\{\mu\text{-}(RO)_2PN(Et)P(OR)_2\}_2]$ and $[Ru_2(\mu\text{-}A)A(CO)_3\{\mu\text{-}(RO)_2PN(Et)P(OR)_2\}_2]$ (L = neutral donor, A = anionic ligand).

It was established that organonitrile solvents are not readily displaced from the co-ordination sphere of the solvento species $[Ru_2(CO)_5(solvent)\{\mu\text{-}(RO)_2PN(Et)P(OR)_2\}_2]^{2+}$. Water readily displaces weakly co-ordinating oxygen-donor solvents such as acetone, THF and nitromethane,

to afford the aquo solvento species $[Ru_2(CO)_5(H_2O)\{\mu\text{-}(RO)_2PN(Et)P(OR)_2\}_2]^{2+}$, characterized X-ray crystallographically. Addition of a weak base to this species was found to result in the deprotonation of the co-ordinated water to give the hydroxycarbonyl species $[Ru_2(CO)_4\{\mu\text{-}OC(OH)\}\{\mu\text{-}(RO)_2PN(Et)P(OR)_2\}_2]^+$, resulting from the migration of the hydroxo group onto a carbon of an adjacent carbonyl ligand. This compound may be deprotonated further by a strong base to produce the carbon dioxide adduct $[Ru_2(CO)_4\{\mu\text{-}OC(O)\}\{\mu\text{-}(RO)_2PN(Et)P(OR)_2\}_2]$, the structure of which has been established X-ray crystallographically. It was thus apparent that the addition of ligands that may function as a base towards the solvento species, where the solvent is weakly co-ordinating, results in the deprotonation of the aquo solvento species by the base. This difficulty is circumvented through the addition of the acid form of the ligand to the solvento species, followed by deprotonation of the co-ordinated acid. Different products were found to be formed in the reactions involving carboxylic acids and carboxylate anions. While addition of the former gave $[Ru_2(CO)_5(OOCR')\{\mu\text{-}(RO)_2PN(Et)P(OR)_2\}_2]^+$, treatment with the latter led to $[Ru_2(CO)_4(\mu\text{-}OOCR')\{\mu\text{-}(RO)_2PN(Et)P(OR)_2\}_2]^+$, (R = H, Me or Ph). The structure of the acetato-bridged species $[Ru_2(CO)_4(\mu\text{-}OOCCH_3)\{\mu\text{-}(Pr^iO)_2PN(Et)P(OPr^i)_2\}_2]PF_6$ has been determined X-ray crystallographically. Carboxylate complexes of this type are useful precursors and were found to be displaced by a number of anionic ligands.

The redox behaviour of $[Ru_2(\mu\text{-}CO)(CO)_4\{\mu\text{-}(RO)_2PN(Et)P(OR)_2\}_2]$ towards the electron-acceptor ligand tetrachloro-*p*-benzoquinone and towards the diazonium salt $[PhN_2][PF_6]$ was also investigated. The former reaction afforded the chloro species $[Ru_2(CO)_5Cl\{\mu\text{-}(RO)_2PN(Et)P(OR)_2\}_2]^+$ while the latter gave a complex characterized X-ray crystallographically as the phenyldiazene species $[Ru_2(CO)_5\{N(H)=NPh\}\{\mu\text{-}(RO)_2PN(Et)P(OR)_2\}_2]$-

$(PF_6)_2$.

A further objective of this thesis was to investigate aspects of the co-ordination chemistry of the dinuclear diphosphazane-bridged derivatives $[Ru_2(\mu\text{-}CO)(CO)_4\{\mu\text{-}(RO)_2PN(Et)P(OR)_2\}_2]$. It was found that reaction of $[Ru_2(\mu\text{-}CO)(CO)_4\{\mu\text{-}(RO)_2PN(Et)P(OR)_2\}_2]$ with various alkynes afforded alkendiyl-bridged species of the type $[Ru_2(CO)_4(\mu\text{-}\sigma^2\text{-}R'C{=}CR'')\{\mu\text{-}(RO)_2PN(Et)P(OR)_2\}_2]$ and/or vinylidene-bridged species of the general formula $[Ru_2(CO)_4(\mu\text{-}\eta^1\text{-}C{=}CHR')\{\mu\text{-}(RO)_2PN(Et)P(OR)_2\}_2]$, the ratio of these isomers being dependent on the nature of the alkyne as well as the diphosphazane ligand. Mechanistic studies revealed that these isomers are formed via two different pathways and are not interconvertible. Protonation of the phenyl vinylidene-bridged species was found to afford the μ-vinyl derivative $[Ru_2(CO)_4\{\mu\text{-}\eta^1\text{-}\eta^2\text{-}C(H){=}CHPh\}\{\mu\text{-}(RO)_2PN(Et)P(OR)_2\}_2]BF_4$, the structure of the tetraisopropoxydiphosphazane species having been determined X-ray crystallographically.

As a consequence of studies aimed at understanding the mechanism of carbonyl substitution and oxidative addition reactions involving the dinuclear species $[Ru_2(\mu\text{-}CO)(CO)_4\{\mu\text{-}(RO)_2PN(Et)P(OR)_2\}_2]$ (R = Me or Pr^i) it was found that thermolysis of the isopropoxydiphosphazane-bridged derivative resulted in the formation of a co-ordinatively unsaturated species $[Ru_2(CO)_4\{\mu\text{-}(Pr^iO)_2PN(Et)P(OPr^i)_2\}_2]$, characterized by means of X-ray crystallography. This compound was found to be highly reactive towards both nucleophiles and electrophiles as well as radical sources. In particular, it reacts with dihydrogen to produce a dihydrido species $[Ru_2H_2(CO)_4\{\mu\text{-}(Pr^iO)_2PN(Et)P(OPr^i)_2\}_2]$, the structure of which has also been determined X-ray crystallographically.

As part of a programme exploring the redox chemistry of the unsaturated

species $[Ru_2(CO)_4\{\mu\text{-}(Pr^iO)_2PN(Et)P(OPr^i)_2\}_2]$, its electrochemistry was investigated by means of cyclic voltammetry. A two-electron oxidation in benzonitrile was found to result in the formation of a dicationic disolvento species *viz.* $[Ru_2(CO)_4(NCPh)_2\{\mu\text{-}(Pr^iO)_2PN(Et)P(OPr^i)_2\}_2]^{2+}$ which was confirmed by synthesis of the hexafluoroantimonate salt $[Ru_2(CO)_4(NCPh)_2\{\mu\text{-}(Pr^iO)_2PN(Et)P(OPr^i)_2\}_2](SbF_6)_2$ by addition of a twice molar amount of $AgSbF_6$ to $[Ru_2(CO)_4\{\mu\text{-}(Pr^iO)_2PN(Et)P(OPr^i)_2\}_2]$ in benzonitrile, and measurement of its CV. The structure of the dicationic dibenzonitrile solvento species was determined by means of X-ray crystallography.

CONTENTS

CHAPTER 1

DINUCLEAR DERIVATIVES OF RUTHENIUM

1.1 GENERAL INTRODUCTION

1.1.1 Introduction

The co-ordination chemistry of transition metals in low, zero or even negative formal oxidation states has been studied extensively and continues to receive increasing attention because of the utilization of transition metal complexes as homogeneous catalysts for a wide range of reactions of commercial importance. In spite of this there are few known dinuclear compounds of ruthenium in low formal oxidation states. The stability of complexes of transition metals in low oxidation states depends to a large extent on the presence of strong Π-acceptor ligands such as carbon monoxide which can accept electron density from the metal atom.[1] As described, a major motivation for the study of transition metal complexes of this type has been on the basis of their ability to catalyze important organic reactions. For instance, soluble metal carbonyl compounds, especially those of rhodium, ruthenium and cobalt, have been found to catalyze the transformation of synthesis gas (CO and H_2) into a wide variety of oxygenated products.[2] Further, the reductive oligomerisation of CO in the presence of H_2 to form linear hydrocarbons, alkenes and alcohols is a well established process. This process, known as the Fischer-Tropsch process,[3] has attracted considerable interest in the search for alternative sources of fuel and chemical feedstock.

$$CO + H_2 \xrightarrow[\Delta,\ \text{Pressure}]{\text{catalyst}} \text{linear } \alpha \text{ olefins, alcohols, alkanes, aldehydes carboxylic acids, esters and arenes.}$$

The disadvantages of this process are the high temperatures and pressures required, the lack of selectivity and the poor dispersion of molecular weights of the products formed. Additionally, a large quantity of the carbon content of coal must be discharged as CO_2 to form the H_2 necessary for the Fischer-Tropsch reaction (via the water-gas shift reaction). Iron and cobalt metal function as excellent Fischer-Tropsch catalysts, whereas ruthenium gives primarily high molecular weight linear hydrocarbons and rhodium low molecular weight materials. It has been found that ruthenium carbonyl can homogeneously catalyze the hydrogenation of CO at relatively low temperatures and pressure and that many properties of this catalyst were similar to that of the heterogeneous cobalt catalyst. The mononuclear species $[Ru(CO)_5]$ and $[H_2Ru(CO)_4]$ were detected in the catalytic solutions, suggesting these to be the catalytically active species. The primary products from this reaction are methanol and methyl formate.

Recent results in the search for new catalytic processes[4-8] have suggested an involvement of a dimetal centre during one or more steps of some catalytic reactions. Dinuclear systems offer the possibility of different types of oxidative-addition and reductive-elimination pathways, and of the stability of unusual oxidation states and of ligand coordination modes that are not possible for mononuclear compounds. One experimental approach to bimetallic activation involves the synthesis of compounds with metallic sites held in close proximity by bridging ligands which are assumed to be inert during the reaction which the complex undergoes.

1.1.2. Neutral Binary Carbonyls of the Group VIII Triad

The mononuclear iron pentacarbonyl species $[Fe(CO)_5]$ was first reported

in 1891[9] and was in fact the second known neutral binary carbonyl. Its structure, in the gaseous state, was established to be trigonal bipyramidal.[10] $[Ru(CO)_5]$ and $[Os(CO)_5]$ were reported some fifty years later,[11,12] as volatile colourless liquids. Both compounds are light-sensitive, particularly to ultraviolet light, and readily decarbonylate and condense to the trinuclear species $[Ru_3(CO)_{12}]$ and $[Os_3(CO)_{12}]$ respectively. The infrared spectra for $[Ru(CO)_5]$ and $[Os(CO)_5]$[13] are analogous to that found for $[Fe(CO)_5]$, suggesting all three penta-carbonyls have a trigonal bipyramidal structure.

The dinuclear iron carbonyl species $[Fe_2(CO)_9]$ was first described in 1905[14] and its single crystal X-ray structure, determined in 1939,[15] revealed the presence of three bridging carbonyl ligands, as shown in Figure 1.1. Its preparation was the first example of the photochemical generation of a polynuclear species from a mononuclear precursor.

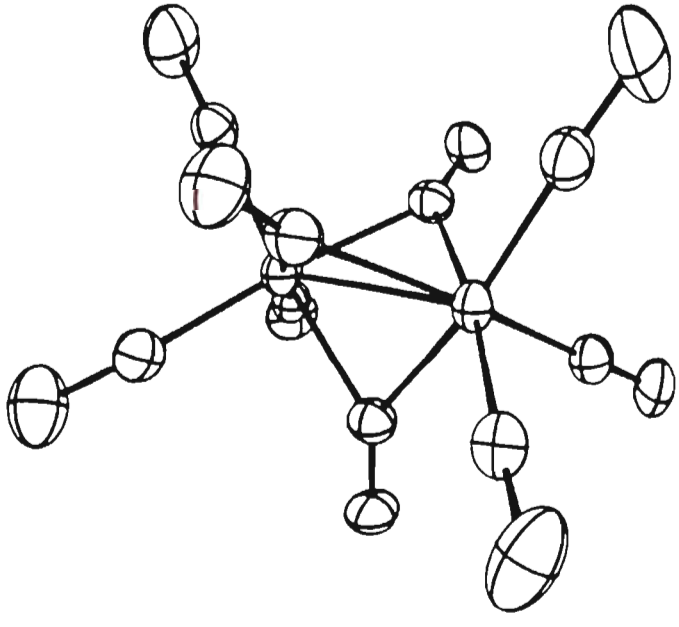

Figure 1.1: Structure of $[Fe_2(CO)_9]$

$[Fe_2(CO)_9]$ is insoluble in virtually all solvents but shows limited solubility in certain polar solvents. It is unstable in these solvents,

decomposing to $[Fe(CO)_4(solvent)]$[16] and $[Fe(CO)_5]$.[17]

$[Os_2(CO)_9]$ is prepared by the ultraviolet irradiation of $[Os(CO)_5]$ in n-heptane at -40°C .[18] It is light-sensitive and less thermally stable than its iron analogue, and in contrast to its iron analogue contains only one bridging carbonyl ligand, as shown in figure 1.2(a).

A dinuclear binary carbonyl complex of ruthenium *viz.* $[Ru_2(CO)_9]$ has been reported[19] but, in contrast with its iron and osmium analogues, is very unstable and has only been detected transiently in the photolysis of $[Ru(CO)_5]$ at temperatures of -40°C and less. Spectroscopic evidence indicated that the complex contains a single bridging carbonyl ligand, as well as terminal carbonyls, and has a structure analogous to that known for $[Os_2(CO)_9]$, (Figure 1.2(b)).

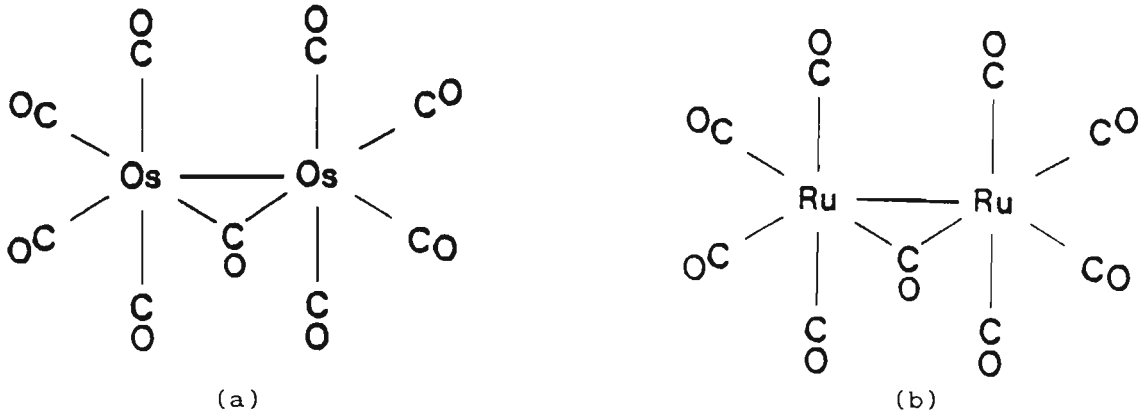

Figure 1.2: Structures of $[Os_2(CO)_9]$ (a) and $[Ru_2(CO)_9]$ (b)

In contrast to their dinuclear counterparts, the trinuclear dodeca-carbonyls of iron, ruthenium and osmium are all stable solids and their structures have been determined X-ray crystallographically. It was established that $[Fe_3(CO)_{12}]$[20] consists of an isosceles triangle of metal atoms with two carbonyl ligands bridging a single edge and ten terminal carbonyl ligands, as illustrated in Figure 1.3(a). In

contrast, the structures of $[Os_3(CO)_{12}]$[21] and $[Ru_3(CO)_{12}]$[22] were shown to contain twelve terminal carbonyl ligands; the structure of $[Ru_3(CO)_{12}]$ is shown in Figure 1.3(b). As a consequence of their stability, the trinuclear carbonyl complexes of iron, ruthenium and osmium have been extensively studied.

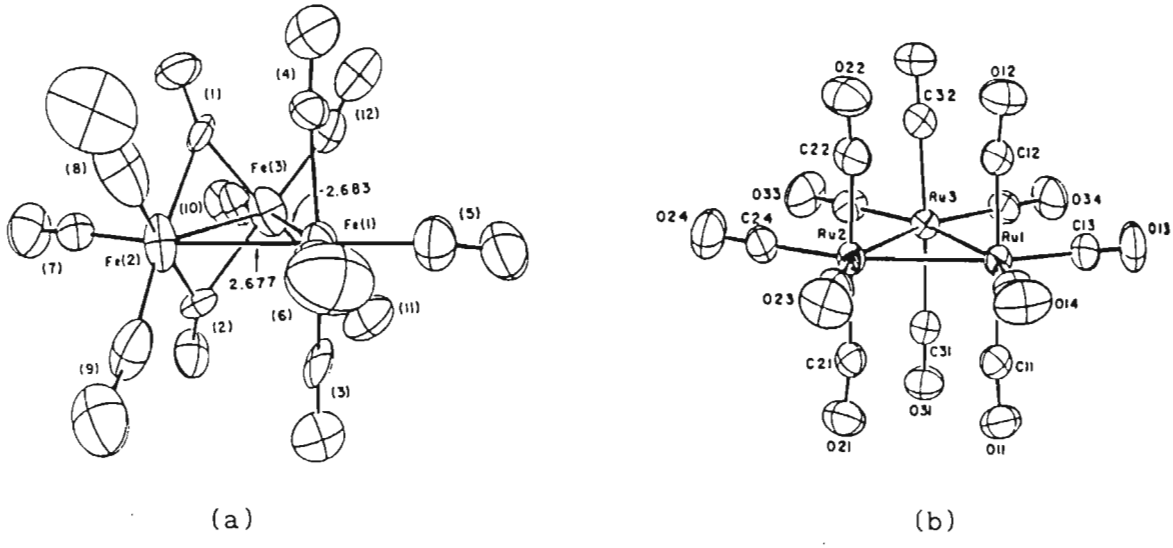

Figure 1.3: Structures of $[Fe_3(CO)_{12}]$ (a) and $[Ru_3(CO)_{12}]$ (b)

1.1.3 Stabilization of $[M_2(CO)_9]$ (M = Fe, Ru, Os) to fragmentation with bridging ditertiary phosphine and phosphite ligands

Iron, ruthenium and osmium have been found to form stable complexes with a wide range of neutral ligands such as CO, tertiary phosphines and phosphites, arsines, stibines, sulphides, nitric oxide, etc. Tertiary phosphines and phosphites bond strongly to transition metals through σ-bonding, as well as through Π-bonding by overlap of their low energy vacant d-orbitals with filled d-orbitals on the metal. They are therefore able to stabilize transition metal atoms in low formal oxidation states through the back donation of electron density from the metal onto the ligand. It stands to reason that tertiary phosphites $P(OR)_3$ are more effective in this context than are tertiary phosphines

PR_3.

The thesis that two metals kept in close proximity could react co-operatively with substrate molecules has led to the broad development of ligand systems which preferentially co-ordinate in the bridging rather than in the chelating co-ordination mode. Obviously, appropriate diphosphorus ligands would be good candidates for bridging two low oxidation state transition metals.

Diphosphorus ligands of the type R_2PYPR_2 (R = alkyl, aryl, alkoxy, aryloxy groups etc; Y = O, NR′ or CH_2; R′ = alkyl or aryl group) have been used extensively for this purpose. The tendency of these diphosphorus ligands, in which the two phosphorus atoms are linked through a single atom, to preferentially adopt the bridging co-ordination mode is because of their giving rise to closed more sterically stable five-membered rings in this situation as opposed to strained four-membered rings in the chelating mode. For the same geometric reason, 1,2-bisdiphenylphosphinoethane ($Ph_2P(CH_2)_2PPh_2$) is an excellent chelating ligand. Examples of compounds containing diphosphorus ligands adopting the bridging co-ordination mode include $[Rh_2Cl_2(CO)_2(\mu\text{-dppm})_2]$[24] and $[Fe_2(\mu\text{-CO})(CO)_4\{\mu\text{-}(EtO)_2POP(OEt)_2\}_2]$[25] whereas $[Ru_2(\mu\text{-OOCMe})(\mu\text{-CO})_2\text{-}(CO)_2(\mu\text{-dppe})_2]^+$ [26] contains chelating diphosphorus ligands.

In addition to holding two transition metals in close proximity thereby inhibiting fragmentation, the use of diphosphorus ligands of the type R_2PYPR_2 has many other advantages in co-ordination chemistry. For instance, the electronic and steric properties of the ligand can be systematically varied by changing the substituent R on the phosphorus atoms,[27] thus affecting the stereochemistry and electron density associated with the two transition metals. This is illustrated by the

reaction of $[Co_2(CO)_8]$ with $R_2PN(R')PR_2$ where $[Co_2(CO)_2\{\mu\text{-}F_2PN(R')\text{-}PF_2\}_3]$[28,29] for R = F, or $[Co_2(CO)_4\{\mu\text{-}(MeO)_2PN(Et)P(OMe)_2\}_2]$[30] for R = MeO, are formed.

By bridging the two metal atoms in a dinuclear complex, this type of ligand is able to promote reactions involving both metal centres, bridging by other groups and reactions which proceed by the formation and cleavage of metal-metal bonds.[31] These diphosphorus ligands preserve the binuclearity of the complexes during reactions while still allowing a certain amount of flexibility of the bimetallic framework, so as to accommodate a more favourable stereochemistry at each metal. For example, the complex $[Rh_2(CO)Cl_2\{\mu\text{-}(PhO)_2PN(Et)P(OPh)_2\}_2]$[32] is able to accommodate different geometries at each rhodium centre; at one it is four co-ordinate and square planar, while at the other it is five co-ordinate and approximately square pyramidal. In the complex $[Co_2(CO)_4\text{-}\{\mu\text{-}(MeO)_2PN(Et)P(OMe)_2\}_2]$[33] the cobalt atoms have identical sets of ligands co-ordinated to them, but the stereochemistry of the one cobalt is trigonal bipyramidal while the other is approximately square pyramidal.

1.1.4 Synthesis and reactivity of dinuclear transition metal complexes containing bridging diphosphorus ligands

The most extensively reported diphosphorus ligand with strong bridging properties is the ubiquitous bisdiphenylphosphinomethane (dppm).[34,35] Workers in our laboratories have however tended to focus their attention on tetra-alkoxydiphosphazane ligands of the type $(RO)_2PN(R')P(OR)_2$ (R = Me, Et, Pr^i, Ph; R' = Me, Et) which are less basic and more polarisable than their harder ditertiary phosphine counterparts. A result of this preference has been the isolation of products that are often more stable

and more soluble than the analogous ditertiary phosphine derivatives.

The vast majority of diphosphorus ligand-bridged complexes reported have involved the platinum group metals Rh, Ir, Pd and Pt with few having been reported for Ru and Os. The synthesis and reactivity of some of these and other dinuclear complexes bridged by diphosphorus ligands are outlined below.

The photochemical and thermal decarbonylation of mononuclear $R_2PN(R')PR_2$ metal carbonyl complexes of Cr, Mo and W has been found to provide routes to corresponding dinuclear complexes of these metals. For example, the mononuclear molybdenum complexes $[Mo(CO)_4\{\eta^2\text{-}R'N(PF_2)_2\}]$ (R' = CH_3 or C_6H_5) undergo facile pyrolysis to give the dinuclear derivatives $[Mo_2(\mu\text{-}CO)(CO)_4\{\mu\text{-}R'N(PF_2)_2\}_2]$.[36]

Complexes derived from manganese carbonyl and diphosphorus ligands have revealed a rich and interesting chemistry.[37,38] For instance, reaction of manganese carbonyl with dppm under thermal conditions results in the formation of the hexacarbonyldimanganese(o) derivative $[Mn_2(CO)_6(\mu\text{-}$

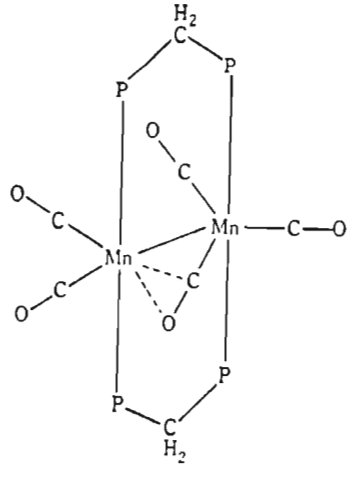

Figure 1.4: Structure of $[Mn_2(\mu\text{-}CO)(CO)_4(\mu\text{-}dppm)_2]$

dppm)$_2$].[39] This complex has been shown to readily lose carbon monoxide, under thermal conditions, to afford the red diamagnetic complex [$Mn_2(\mu$-CO)(CO)$_4(\mu$-dppm)$_2$]. The structure of this compound,[40] shown in Figure 1.4, revealed the presence of a bridging carbonyl ligand which functions as a four-electron donor. This complex is highly reactive and has proved to be an important precursor for the synthesis of diphosphorus dimanganese complexes, summarized in Scheme 1.1.[41]

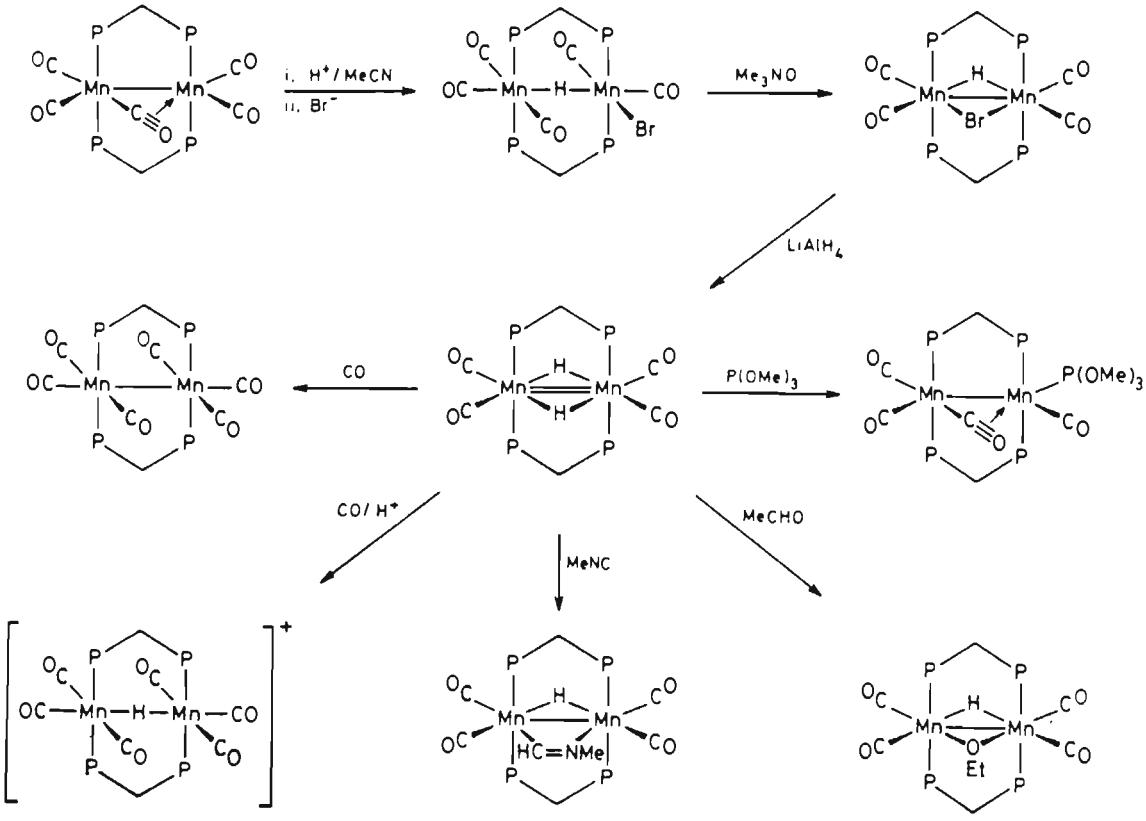

Scheme 1.1

The related rhenium carbonyls [$Re_2(CO)_6(\mu$-dppm)$_2$] and [$Re_2(CO)_6$-(μ-dmpm)$_2$] similarly exhibit high reactivity and, in particular, have been found to react readily with alkynes, alkenes, water, methanol and dihydrogen,[42,43] as outlined in Scheme 1.2.

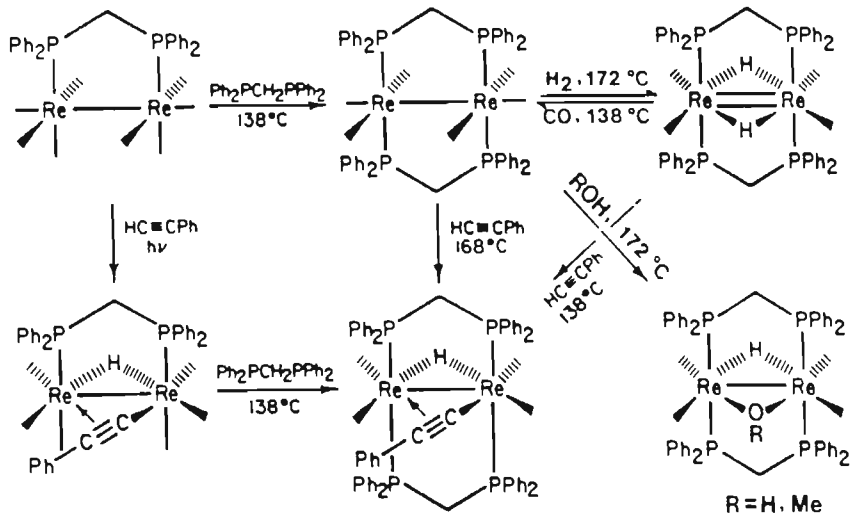

Scheme 1.2

The redox and co-ordination chemistry associated with diphosphorus ligand-bridged derivatives of rhodium has been extensively studied.[44-47] The dirhodium species $[Rh_2(\mu\text{-}CO)(CO)_2(\mu\text{-}dppm)_2]$ was first reported in 1980,[48] but it was only in 1985 that its X-ray crystal structure determination showed it to be a non A-frame complex,[49] the stereochemistry of which is shown in Figure 1.5. This complex reacts readily with a wide range of substrate molecules;[50,51] these reactions are described in more detail in Chapter 6.

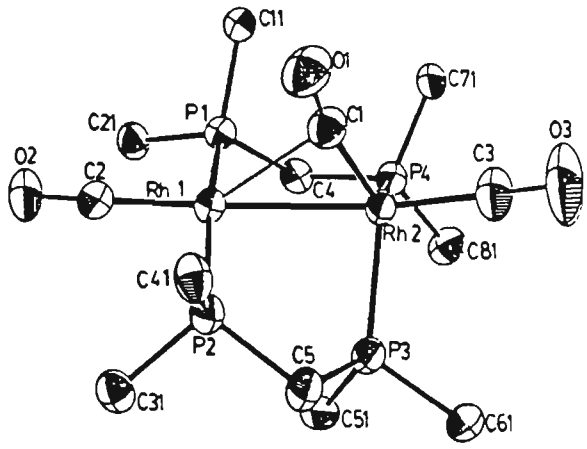

Figure 1.5: Structure of $[Rh_2(CO)_3(\mu\text{-}dppm)_2]$

The chemistry of dinuclear Rh(I) complexes of the type $[Rh_2Cl_2(CO)_2(\mu\text{-}R_2PYPR_2)_2]$ has also been extensively examined. The chloro and CO ligands in $[Rh_2Cl_2(CO)_2(\mu\text{-dppm})_2]$[24] are readily displaced by isocyanide ligands to give $[Rh_2(MeNC)_4(\mu\text{-dppm})_2]^{2+}$ which undergoes oxidative addition and adds unsaturated molecules such as CO and CS_2.[52-54]

Iridium A-frame complexes have shown similar reactivity[55,56] to their rhodium analogues. Of significance in this context are the reactions of $[Ir_2(\mu\text{-S})(CO)_2(\mu\text{-dppm})_2]$ and $[Ir_2(\mu\text{-Cl})(CO)_2(\mu\text{-dppm})_2]$ with CO, H_2,[57,58] acetylenes and $SnCl_2$[59] which are summarized in the scheme below.

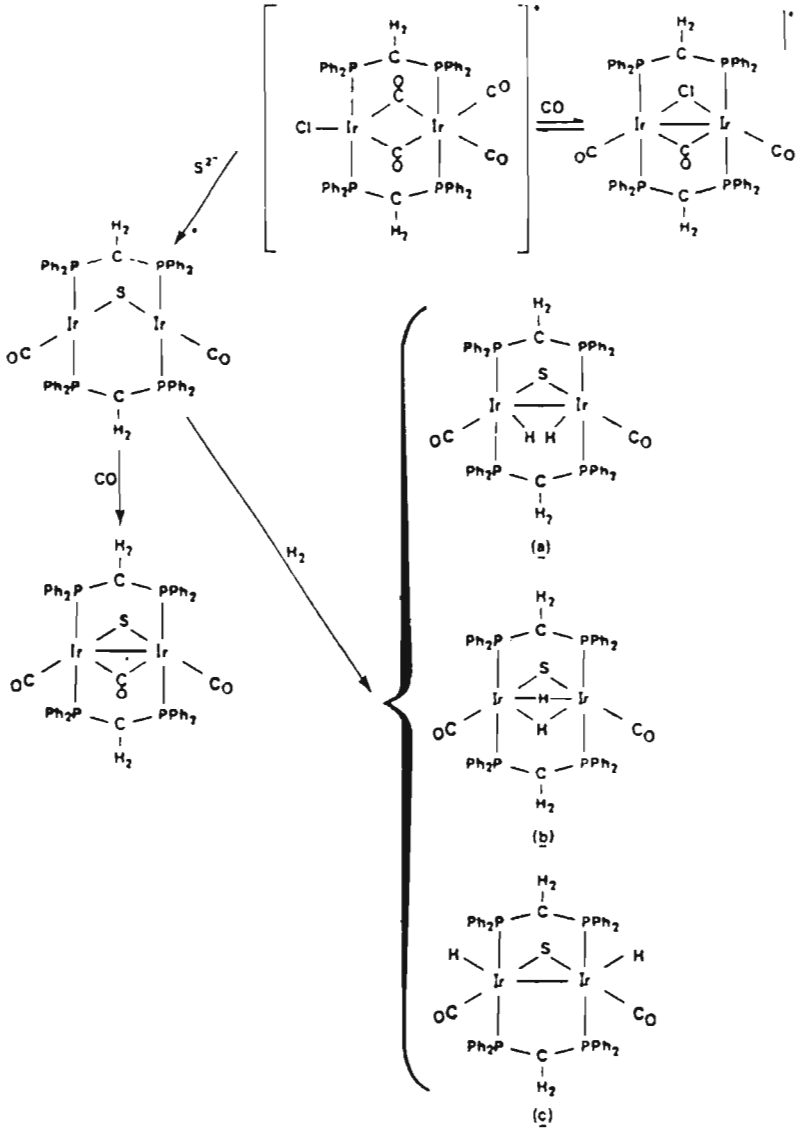

Scheme 1.3

Extensive studies of dinuclear diphosphorus ligand-bridged derivatives of platinum and palladium have also been undertaken. The dichloro derivatives $[M_2Cl_2(\mu\text{-dppm})_2]$ (M = Pd, Pt), in particular, are excellent precursors for a wide range of products containing small molecule compounds[60-62] such as acetylene, sulphur, sulphur dioxide, carbon disulphide, etc, as illustrated in Scheme 1.4.

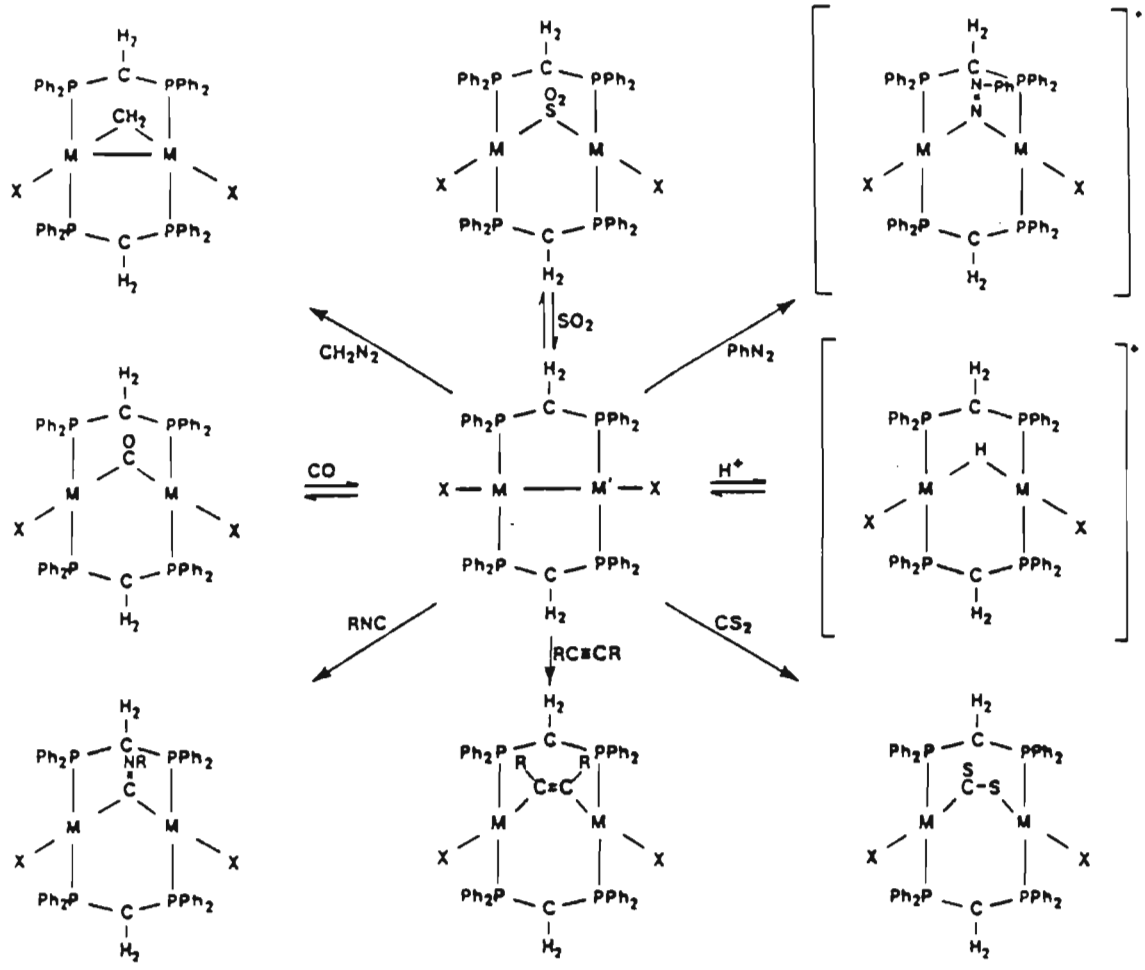

Scheme 1.4

Dinuclear metal complexes containing an "$M_2(\mu\text{-}R_2PYPR_2)_2$" skeleton have been shown to activate small molecule species which co-ordinate in the bridging position and as such are potential catalysts for reactions involving these species. Complexes which have demonstrated this potential include $[Rh_2(CO)_2(\mu\text{-dppm})_2]$ which catalyzes the hydrogenation of acetylene to ethylene[63] and $[Pd_2Cl_2(\mu\text{-dppm})_2]$, which catalyzes the

cyclotrimerisation of alkynes;[48] the catalytic properties of both complexes are associated with their ability to readily add alkynes across the two metal atoms. The dirhodium complex $[Rh_2(\mu\text{-}H)(CO)_3(\mu\text{-}dppm)_2]^+$, on the other hand, functions as a hydroformylation catalyst,[64] as well as catalyzing the water-gas shift reaction, but the exact mechanism of this reaction is not known.[65]

Surprisingly, the chemistry of dinuclear diphosphorus ligand-bridged derivatives of ruthenium, in which the ruthenium atoms are bridged by two diphosphorus ligands as in the above rhodium compound, has not been comprehensively examined, no doubt because of the lack of readily available precursors. In fact the only reported *bis* dppm-bridged ruthenium derivatives have been obtained by Lehmann and Wilkinson[66] through the reduction of $[Ru_3O(O_2CMe)_6(MeOH)_3]O_2CMe$ with zinc amalgam in the presence of dppm, affording $[Ru_2(O_2CMe)_4(\mu\text{-}dppm)_2]$ in two isomeric forms, and by Haines *et al.* who have reported the synthesis of the diruthenium(0) species $[Ru_2(\mu\text{-}CO)(CO)_4(\mu\text{-}dppm)_2]$. There are however a number of known dppm-related derivatives of ruthenium *viz.* $[Ru_2(\mu\text{-}CO)(CO)_4\{\mu\text{-}(RO)_2PN(Et)P(OR)_2\}_2]$,[67] reported by Haines *et al.*, and described in detail in Section 1.3 of this chapter, $[Ru_2Cl_6(\mu\text{-}dppm)_2]$,[68] recently reported by Cotton and co-workers, and $[Ru_2(\mu\text{-}CO)(CO)_4(\mu\text{-}dmpm)_2]$, very recently reported by Gladfelter.[69] There is, on the other hand, a larger contingent of diruthenium complexes containing a single bridging diphosphorus ligand as in $[Ru_2(\mu\text{-}CO)(CO)_6(\mu\text{-}dppm)]$[70-73] but which will not be discussed in detail in this thesis.

1.2 SURVEY OF DINUCLEAR DERIVATIVES OF RUTHENIUM

The chemisty of dinuclear derivatives of ruthenium in which the ruthenium atoms have relatively high formal oxidation states (*i.e.* ≥ +

2) has been extensively studied. In contrast, studies on ruthenium dimers in which the ruthenium atoms have low formal oxidation states have been limited, owing to the absence of suitable precursors and the low yields found for those that have been synthesized. The emphasis of this survey, however, will lie with those ruthenium dimers having low formal oxidation states since the chemistry established for such complexes will resemble more closely that of the work investigated for this thesis.

1.2.1 Higher oxidation state derivatives

a. Cyclopentadienyl Complexes. Since the discovery of $[Cp^*RuCl_2]_2$ ($Cp^* = C_5Me_5$) in 1984,[74] several groups have exploited the synthetic potential of this compound. This complex is highly reactive and is

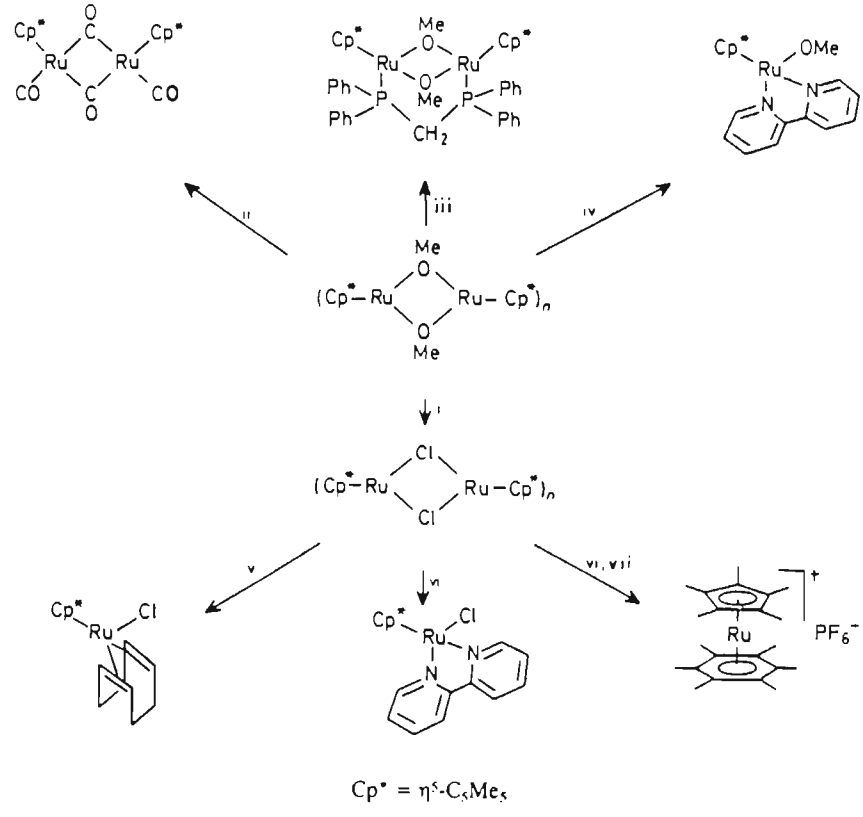

$Cp^* = \eta^5\text{-}C_5Me_5$

Reagents and conditions: i, Me_3SiCl; ii, CO, 60%; iii, dppm, 70%; iv, 2,2'-bipyridine; v, 1,5-cyclo-octadiene, 60%; vi, ıration of pentane, C_6Me_6 melt, 160 °C; vii, NH_4PF_6–H_2O, 50%.

Scheme 1.5

easily converted into a plethora of compounds under mild conditions. For example, Koelle and Kossakowski[75] have shown that $[Cp^*Ru(OMe)_2]_2$ can be readily prepared from $[Cp^*RuCl_2]_2$, and this in turn reacts with acceptor as well as strong donor ligands (2,2'-bipyridine) to give a number of complexes, shown in Scheme 1.5.

The related tetrahydride complex $[Cp^*Ru(\mu\text{-}H)_2]_2$[76] has been found to react with ethylene to give a novel dinuclear divinyl complex $[Cp^*Ru(CH_2{=}CH_2)(CH{=}CH_2)_2RuCp^*]$ via activation of a vinylic C-H bond.

b. Arene Complexes. Complexes of the type $[Ru(\eta\text{-}C_6H_6)X_2]_2$ (X = Cl, Br, I) have proved to be useful sythons in diruthenium chemistry. For instance, it has been shown that the reaction of these complexes with $AgPF_6$ affords triple halide-bridged complexes of the type $[Ru_2(\eta\text{-arene})_2(\mu\text{-}X)_3]PF_6$.[77] It was also found that the reaction of the chloro species $[Ru(\eta\text{-}C_6H_6)Cl_2]_2$[78] with NaOH or Na_2CO_3 followed by addition of $NaBPh_4$ gave, as major product, $[(\eta\text{-}C_6H_6)(OH)Ru(\mu\text{-}OH)Ru(H_2O)(\eta\text{-}C_6H_6)]BPh_4$ together with a small quantity of $[(\eta\text{-}C_6H_6)Ru(\mu\text{-}OH)_3Ru(\eta\text{-}C_6H_6)]BPh_4$.

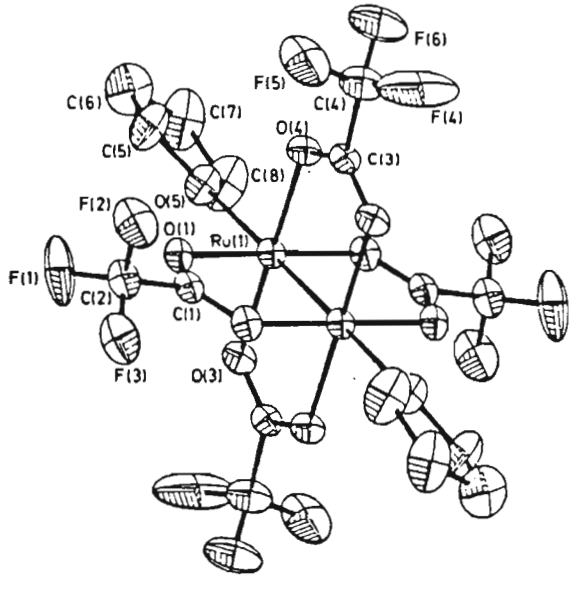

Figure 1.6: Structure of $[Ru_2(\mu\text{-}O_2CCF_3)_4(C_4H_8O)_2]$

c. Carboxylato Complexes. Since the discovery of $[Ru_2(\mu\text{-}O_2CR)_4]Cl$,[79] various studies have shown that these formally Ru(II)/Ru(III) species can be reduced in solution in a one electron reduction. In particular, reaction of $[Ru_2(O_2CMe)_4]Cl$ with Grignard reagents in THF has led to isolation of $[Ru_2(\mu\text{-}O_2CMe)_4.(C_4H_8O)_2]$,[80] the first carboxylate derivative with a Ru_2^{4+} core (Figure 1.6).

d. The Creutz-Taube Complex. The Creutz-Taube and related complexes have two (or more) ruthenium atoms bridged by bidentate ligands through which some degree of electron transfer can take place. These complexes have been studied extensively in recent years[81] because of the information they furnish in respect of electron exhange in binuclear systems. The title compound $[(NH_3)_5Ru(\mu\text{-pyrazine})Ru(NH_3)_5]^{5+}$ [82] is formally a mixed valence (Ru(II)/Ru(III) species with the unpaired electron being delocalized through the bridging ligand. Some ions with different bridging groups and ligands have also been shown to have trapped valencies.[83]

1.2.2. Lower oxidation state derivatives

a. Cyclopentadienyl Complexes. The first synthesis[84] of the now widely reported cyclopentadienyldicarbonylruthenium dimer $[(\eta\text{-}C_5H_5)_2Ru_2(CO)_4]$ (Figure 1.7) has been followed by an explosion of new diruthenium(I) chemistry.[85,86] The chemistry associated with this compound is governed by the blocking effect of the cyclopentadienyl rings to ligand entry and the thermodynamic stability of the metal carbonyl bond. Their reactivity is therefore often associated with more vigorous conditions (*i.e* high temperatures or UV irradiation), with the formation of product mixtures and generally with lower yields. Some of the reactivity patterns and chemistry established for these systems are

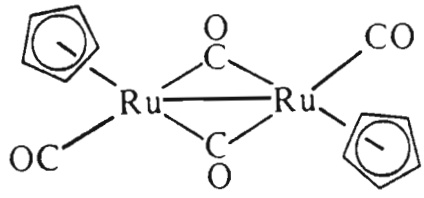

Figure 1.7

however similar to those found for the compounds which form the basis of the investigations reported in this thesis and as a consequence this chemistry will be reviewed in more detail. Some of the chemistry exhibited by this dimer, readily synthesized from $[Ru_3(CO)_{12}]$ and cyclopentadiene is summarized in Scheme 1.6 below.

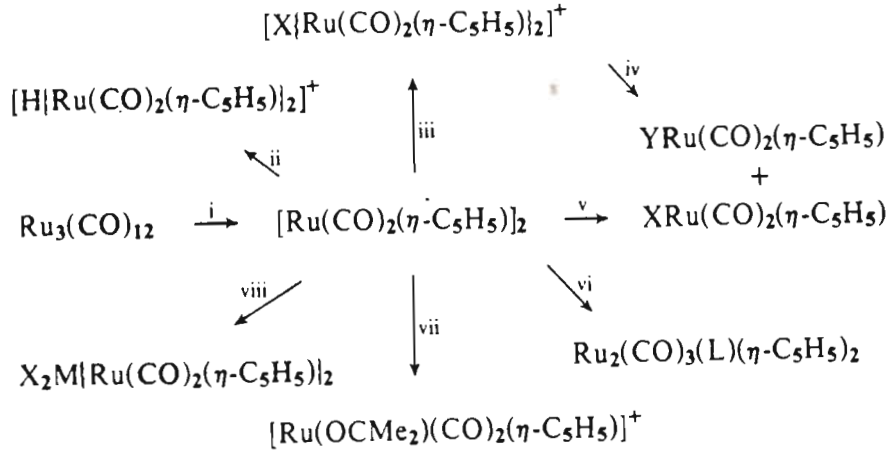

i, cyclopentadiene/air; ii, H^+; iii, X_2/toluene; iv, Y^- (halide or pseudohalide); v, $CHCl_3$/HCl (X = Cl); vi, L = PR_3, CNR; vii, Ag^+/acetone; viii, GeI_2 or $SnCl_2$

Scheme 1.6

Whereas the cyclopentadienylcarbonyl dimer of iron $[Fe_2(CO)_4(\eta\text{-}C_5H_5)_2]$ reacts with a range of alkynes under UV irradiation to produce dinuclear complexes containing the dimetallacyclopentenone unit (Figure 1.8), only diphenylacetylene has been found to produce an analogous complex with $[Ru_2(CO)_4(\eta\text{-}C_5H_5)_2]$.[87] Nevertheless, the product of the reaction, *viz.* $[Ru_2(\mu\text{-}CO)(CO)\{\mu\text{-}C(O)C_2Ph_2\}(\eta\text{-}C_5H_5)_2]$, undergoes alkyne exchange

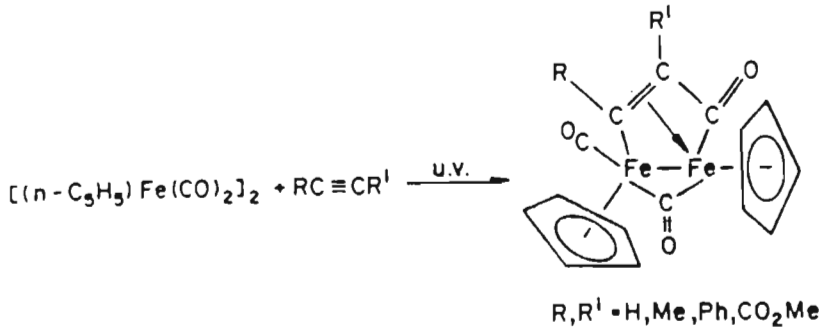

Figure 1.8

with HC_2H, MeC_2Me, MeC_2H, PhC_2H or PhC_2Me on heating in toluene to afford the appropriate dimetallacyclopentenone complexes $[Ru_2(\mu\text{-}CO)(CO)\text{-}\{\mu\text{-}C(O)C_2R_2\}(\eta\text{-}C_5H_5)_2]$.[88] In the case of $MeO_2CC_2CO_2Me$, the dimetallacyclobutene complex *cis*-$[Ru_2(\mu\text{-}CO)(CO)_2\{\mu\text{-}C_2(CO_2Me)\}(\eta\text{-}C_5H_5)_2]$ is the only product of the reaction, however (Figure 1.9).

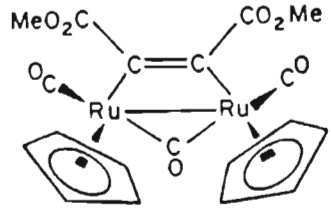

Figure 1.9: $[Ru_2(\mu\text{-}CO)(CO)_2\{\mu\text{-}C_2(CO_2Me)_2\}(\eta\text{-}C_5H_5)_2]$

Compounds of the type $[Ru_2(\mu\text{-}CO)(CO)\{\mu\text{-}C(O)C(R^1)C(R^2)\}(\eta\text{-}C_5H_5)_2]$ in which the $R^1 \neq R^2$ can exist in more than one isomeric form resulting from the linking of either end of the alkyne with CO. Steric factors apparently determine the relative stabilities of the two isomeric forms in the case of terminal acetylenes but electronic factors play a more dominant role for internal acetylenes.

Protonation of $[Ru_2(\mu\text{-}CO)(CO)\{\mu\text{-}C(O)C(R^1)C(R^2)\}(\eta\text{-}C_5H_5)_2]$ (R^1R^2 = H_2, Ph_2, H(Me), H(Ph)) with $HBF_4.OEt_2$ in acetone has been shown to lead to facile carbon-carbon bond cleavage and the generation of the μ-vinyl

complexes $[Ru_2(\mu\text{-}CO)(CO)_2\{\mu\text{-}C(R^1)\text{=}CH(R^2)\}(\eta\text{-}C_5H_5)_2]BF_4$. Significantly, treatment of this complex with $NaBH_4$ in acetone does not lead to the deprotonation of this cationic species but effects a rapid hydride addition at the β-carbon of the μ-vinyl group to produce the appropriate alkylidene complex $[Ru_2(\mu\text{-}CO)(CO)_2\{\mu\text{-}C(R^1)CH_2R^2\}(\eta\text{-}C_5H_5)_2]$, as shown in Scheme 1.7.

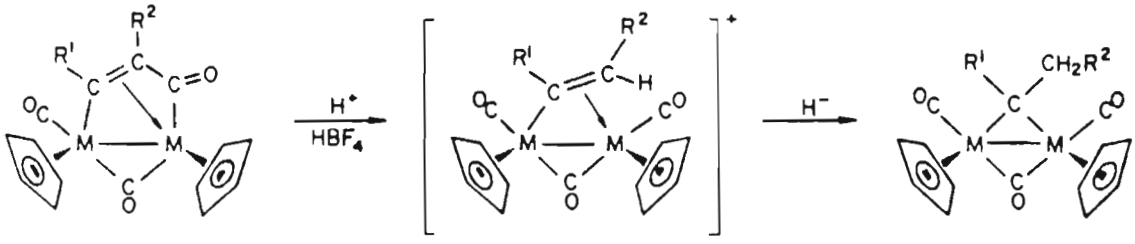

Scheme 1.7

The dimetallacyclopentenone complexes isomerise slowly in toluene at 105°C and in particular to the μ-vinylidene complexes $[Ru_2(\mu\text{-}CO)(CO)_2(\mu\text{-}CCHR)(\eta\text{-}C_5H_5)_2]$.[89,90]

The vinylidene complex $[Ru_2(\mu\text{-}CO)(CO)_2(\mu\text{-}CCH_2)(\eta\text{-}C_5H_5)_2]$ is converted quantitatively to the μ-ethylidyne species $[Ru_2(\mu\text{-}CO)(CO)_2(\mu\text{-}CMe)(\eta\text{-}C_5H_5)_2]^+$ on protonation with $HBF_4.OEt_2$.[90] This reaction is reversible and the latter can be converted to the μ-vinylidene complex on treatment with water, Et_3N or MeLi (Scheme 1.8). The μ-CMe complex can also be

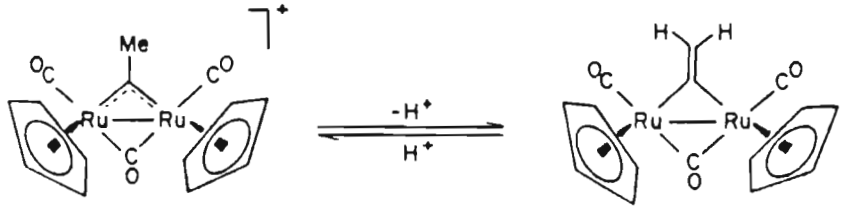

Scheme 1.8

synthesized in high yield by successive treatment of $[Ru(CO)_2(\eta\text{-}C_5H_5)]_2$ with MeLi and $HBF_4.OEt_2$. Carbyne-bridged compounds of the type $[Ru_2(\mu\text{-}CO)(CO)_2(\mu\text{-}CHR)(\eta\text{-}C_5H_5)_2]$ can be readily synthesized by reaction of $[Ru_2(\mu\text{-}CO)(CO)_2\{\mu\text{-}C(O)C_2Ph_2\}(\eta\text{-}C_5H_5)_2]$ with $Ph_3P{=}CHR$ in toluene under thermal conditions.[91] These compounds have been extensively studied and have been shown to have a rich chemistry associated with them.[92,93]

It is well documented that the pentamethylcyclopentadienyl ligand imparts very different steric and electronic effects on metal centres as compared to the cyclopentadienyl ligand. The pentamethylcyclopentadienyldicarbonyl dimer $[Ru_2(\mu\text{-}CO)_2(CO)_2(\eta\text{-}C_5Me_5)_2]$ may be synthesized by the direct treatment of $[Ru_3(CO)_{12}]$ with pentamethylcyclopentadiene.[94]

Treatment of $[Ru_2(CO)_4(\eta\text{-}C_5Me_5)_2]$ with $HBF_4.OEt_2$ in CH_2Cl_2 has been shown to afford the hydride-bridged dinuclear complex $[Ru_2(CO)_4H(\eta\text{-}C_5Me_5)_2]BF_4$ whereas UV irradiation of this species in the presence of CH_2X_2 (X = Cl, I_2) or PMe_3 has been shown to give rise to mononuclear products.[95] Knox and co-workers[96] have reported studies which show that the effect of the pentamethylcyclopentadienyl ligand on the organic chemistry of the diruthenium centre in $[Ru_2(CO)_4(\eta\text{-}C_5Me_5)_2]$ is quite significant. The result of these studies are summarized in Scheme 1.9.

Irradiation of a toluene solution of $[Ru_2(CO)_4(\eta\text{-}C_5Me_5)_2]$ with ultraviolet light while purging with ethylene has been shown to produce the ethylene complex $[Ru_2(\mu\text{-}CO)_2(C_2H_4)(CO)(\eta\text{-}C_5Me_5)_2]$ as well as the carbene derivative $[Ru_2(\mu\text{-}CO)(\mu\text{-}CHMe)(CO)_2(\eta\text{-}C_5Me_5)_2]$ and the unusual $[Ru_2(\mu\text{-}CO)\{\mu\text{-}C(Me)CHCH_2\}(CO)(\eta\text{-}C_5Me_5)_2]$. Sequential treatment of $[Ru_2(CO)_4(\eta\text{-}C_5Me_5)_2]$ with MeLi, HBF_4 and NEt_3 has been reported to give the μ-vinylidene complex $[Ru_2(\mu\text{-}CO)(CO)_2(\mu\text{-}CCH_2)(\eta\text{-}C_5Me_5)_2]$ which parallels the chemistry found for the corresponding cyclopentadienyl system.

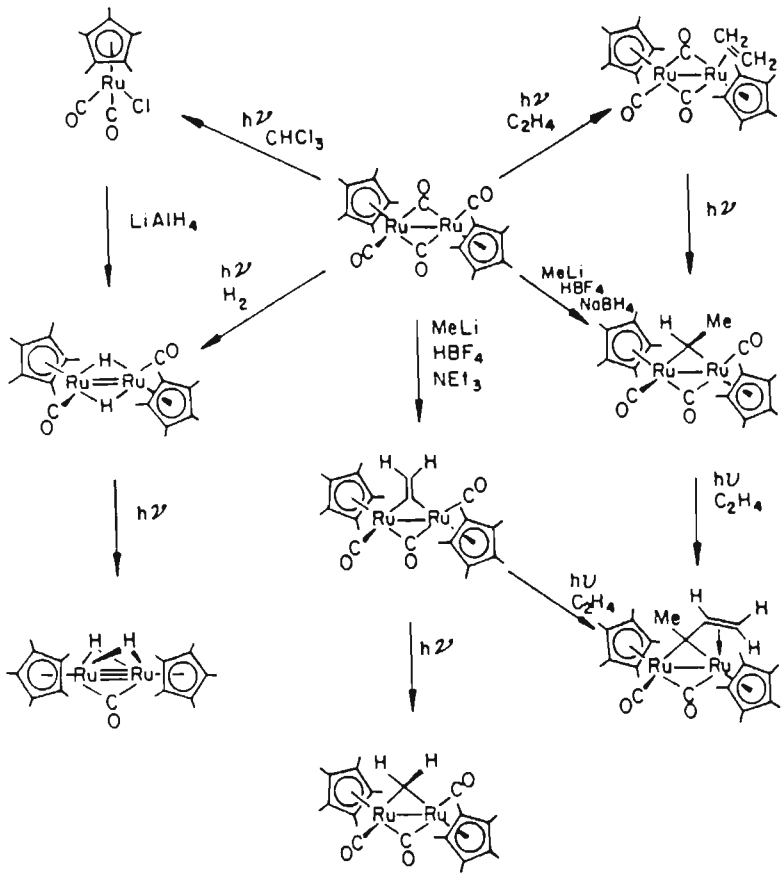

Scheme 1.9

Irradiation of this complex with ultraviolet light over several days produced the μ-methylene complex $[Ru_2(\mu\text{-}CO)(CO)_2(\mu\text{-}CH_2)(\eta\text{-}C_5Me_5)_2]$. Interestingly, addition of $AgBF_4$ to the vinylidene species results in the formation of the μ-ketene species $[Ru_2(\mu\text{-}CO)(CO)_2(\mu\text{-}\eta^2\text{-}C{\equiv}CH)(\eta\text{-}C_5Me_5)_2]$.[95] In contrast to the cyclopentadienyl analogue, treatment of $[Ru_2(CO)_4(\eta\text{-}C_5Me_5)_2]$ with dihydrogen under UV irradiation produces the multiply metal-metal bonded species $[Ru_2(\mu\text{-}H)_2(CO)_2(\eta\text{-}C_5Me_5)_2]$ and $[Ru_2(\mu\text{-}CO)(\mu\text{-}H)_2(\eta\text{-}C_5Me_5)_2]$.[96]

A high yield synthesis of the $\eta^5{:}\eta^5$ fulvalene dinuclear complex $[Ru_2(CO)_4(\eta^5{:}\eta^5\text{-}C_{10}H_8)]$ has recently been reported by Volhardt and Weideman[97] and its chemistry investigated. Irradiation of this complex in the absence of donor ligands leads to its isomerisation to the

unusual dinuclear oxidative product $[Ru_2(CO)_4(C_5H_4)_2]$ which converts back to the parent species under thermal conditions, as illustrated in the scheme below.

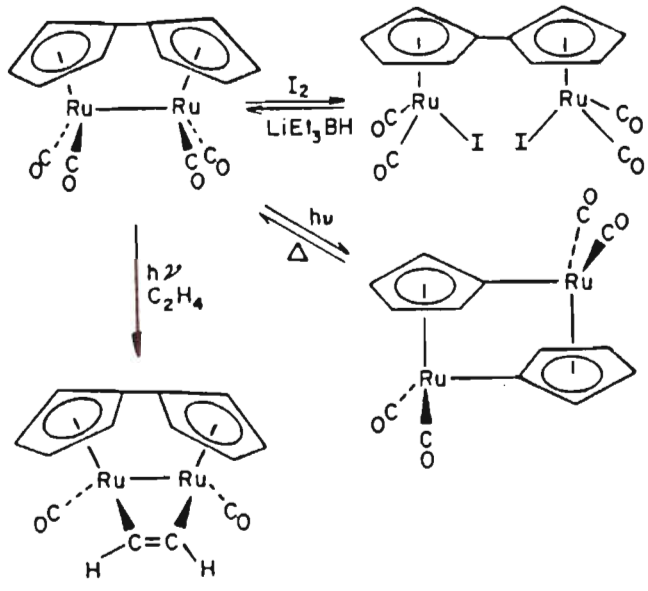

Scheme 1.10

Irradiation of the parent species $[Ru_2(CO)_4(\eta^5:\eta^5\text{-}C_{10}H_8)]$ with ultraviolet light in the presence of ethylene gives a diruthenacyclobutene complex in which the alkyne is bound in a "parallel" alkendiyl co-ordination mode. Similar complexes are afforded by the reaction of $[Ru_2(CO)_4(\eta^5:\eta^5\text{-}C_{10}H_8)]$ with diphenylacetylene and dimethylacetylenedicarboxylate. Iodine readily leaves the ruthenium-ruthenium bond in the parent species to give the diiodide complex $[Ru_2(CO)_4I_2(\eta^5:\eta^5\text{-}C_{10}H_8)]$ which, on treatment with $LiEt_3BH$ affords the parent species, indicating a very fast intramolecular dihydrogen elimination process.

b. Carboxylato-bridged complexes. Until recently the most common starting material for Ru(I) dimers was $[Ru_3(CO)_{12}]$. Ru(I) dimers obtained from this trimer are, however, obtained usually as by-products of its fragmentation under mild oxidizing conditions.[98] One of the most

commonly used precursors for Ru(I) complexes are the carboxylato-bridged species $[Ru(\mu\text{-}O_2CR)(CO)_2]_n$ and $[Ru(\mu\text{-}O_2CR)(CO)_2(NCMe)]_2$, synthesized for the first time by Lewis and Johnson.[99] This latter complex is now part of an extensive class of derivatives with the general formula $[M(\mu\text{-}O_2C\text{-}R)(CO)_2L]_2$ (M = Ru, Os; R = alkyl, fluoroalkyl or aromatic group; L = tertiary phosphine,[100] nitriles,[101] pyrazole,[102] CO,[103] carboxylic acid[104] or pyridine[105]). Recent interest in these complexes stems in part from the discovery that they are catalyst precursors for the hydroformylation of olefins,[106] and the addition of carboxylic acids to alkynes,[107,108] as well as the more recent demonstration that these Ru(I) carboxylate complexes exhibit catalytic activity for the homogeneous hydrogenation of carboxylic acids and dicarboxylic esters,[109] and the disproportionation of aldehydes. An intensive study by Singleton, Steyn *et al.*[26,110,111] has shown that these carboxylato species provide the basis for a consistent and reproducible route for the synthesis of Ru(I)-Ru(I) dimeric complexes. These species have been utilized as precursors for the synthesis of an unusual series of binuclear Ru(I) complexes, either through replacement of the carboxylate groups by other bridging anionic ligands, or by substitution of the labile groups *trans* to the Ru-Ru bond by bidentate diphosphine and dithioether ligands.

c. Organo -silicon, -tin and -germanium complexes. Very few examples exist of dinuclear Ru(I) complexes which have metal-metal bonds that are not supported by bridging ligands. An exception to this is demonstrated by the reaction of $[Ru_3(CO)_{12}]$ with organo-silicon and -germanium reagents under thermal or photochemical conditions,[112,113] affording complexes of the type $[Ru(CO)_4(ER_3)]_2$ (E = Si, R = Me, Et, Pr^i, Cl; ER_3 = $SiMeCl_2$). A new, low yield route has been devised[114] for the synthesis of the organo-tin analogue $[Ru(CO)_4(SnMe_3)]_2$ (Figure 1.10(a))

involving the treatment of $[Ru(CO)_4]^{2-}$ with trimethyltin chloride.

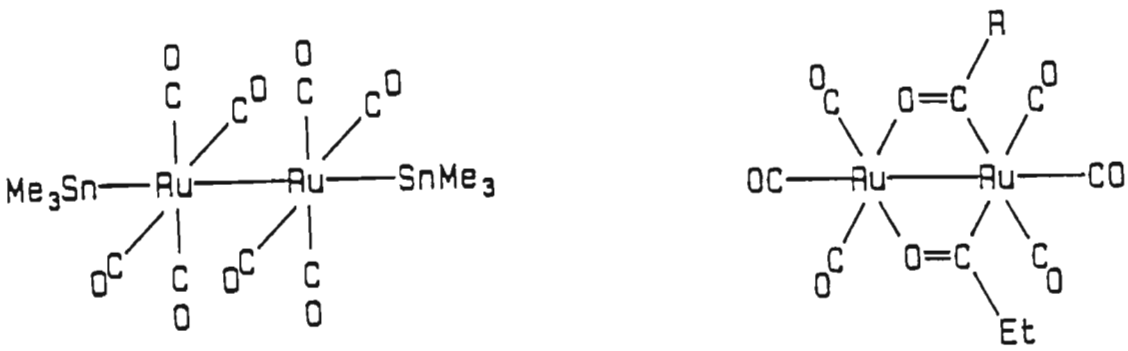

(a) (b)

Figure 1.10: $[Ru_2(CO)_8(SnMe_3)_2]$ (a) and $[Ru_2(CO)_6(\mu\text{-}OCEt)_2]$ (b)

d. Acyl complexes. Edge-bridged trinuclear hydrido clusters of ruthenium react with ethylene to form compounds containing bridging acyl groups. For example, $Na[Ru_3(\mu\text{-}CO)(\mu\text{-}H)(CO)_{10}]$ reacts with ethylene giving, on acidification $[Ru_3(\mu\text{-}H)(\mu\text{-}O{=}CEt)(CO)_{10}]$.[115] Further reaction with ethylene results in fragmentation giving $[Ru_3(CO)_{12}]$ and $[Ru_2(\mu\text{-}O{=}CEt)_2(CO)_6]$ (Figure 1.10(b)).

e. Pyrazolate complexes. A convenient high yield route to pyrazolato-bridged complexes of the type $[Ru(\mu\text{-}pz)(CO)_3]_2$ (pz = pyrazolyl or substituted pyrazolyl) involves the carbonylation of $RuCl_3.nH_2O$ in 2-methoxyethanol followed by zinc reduction in the presence of CO and the pyrazole ligand.[116] A more recent approach[117] has involved the displacement of acetate groups in $[Ru_2(CO)_4(O_2CCH_3)(NCMe)_2]$ by pyrazolate anions to afford complexes of the type $[Ru_2(CO)_4(\mu\text{-}pz)L_2]$.

f. Halo compounds. The synthesis of chloro-bridged Ru(I) dimers of the type $[Ru_2(\mu\text{-}Cl)_2(CO)_4\{P(Bu^t)_2R\}_2]$ can be effected by passage of CO through a solution of $RuCl_3.nH_2O$ in 2-methoxyethanol, followed by treatment of this solution with the phosphines $P(Bu^t)_2R$ (R = Bu^t, Ph or

p-tol).[118] A related iodo-bridged species $[Ru_2(\mu\text{-}I)_2(CO)_4(\mu\text{-dppm})]$ has been reported as one of the products of the reactions of $[Ru_3(CO)_8(\mu\text{-dppm})_2]$ with iodine in toluene under reflux, the other product of this fragmentation reaction being $[RuI_2(CO)(dppm)]$.[119]

g. Phosphido complexes. Reaction of $[Ru_3(CO)_{12}]$ with phosphine ligands is known to lead to cluster fragmentation and the formation of dinuclear products. Some of the earlier complexes of dinuclear derivatives synthesized by this procedure include complexes of the type $[Ru(\mu\text{-}ER_2)(CO)_3]_2$ (E = As, R = Ph; E = P, R = Ph, Me),[120,121] obtained by reaction of $[Ru_3(CO)_{12}]$ with secondary phosphines and arsines. Pyrolysis of the triphenylphosphine substituted derivative $[Ru_3(CO)_9(PPh_3)_3]$ gives the phenylphosphido-bridged product $[Ru_2(\mu\text{-}O{=}CPh)(\mu\text{-}PPh_2)(CO)_5(PPh_3)]$ in low yield as well as the known benzyne derivative $[Ru_3(CO)_7(PPh_2)_2(C_6H_4)]$.

h. Ditertiary phosphine and phosphite complexes. A new class of dinuclear ruthenium(0) complexes is emerging with the development of high yield synthetic routes to diphosphorus-ligand bridged complexes. The preparation and reactivity patterns for these derivatives are discussed in the following section of this chapter.

i. Dinuclear carbonylates of the type $[M_2(CO)_8]^{2-}$. The homonuclear dianions $[M_2(CO)_8]^{2-}$ (M = Ru, Os) are prepared by a procedure that involves the reductive disproportionation of CO_2 in its reaction with an alkali-metal salt of $[M(CO)_4]^{2-}$ to form $[M(CO)_5]$ which then reacts with additional $[M(CO)_4]^{2-}$ to give $[M_2(CO)_8]^{2-}$, the products being air and moisture sensitive.[122,123]

1.3 DINUCLEAR DIPHOSPHORUS LIGAND-BRIDGED DERIVATIVES OF RUTHENIUM(0)

As described previously, diphosphorus ligands of the type R_2PYPR_2 (R = alkyl, aryl, alkoxy, aryloxy groups, etc.; Y = O, NR′ or CH_2; R = alkyl or aryl group) bind strongly to many transition metals in low oxidation states.

1.3.1. Tetraalkoxydiphosphazane-Bridged Derivatives

Haines *et al.*[124] reported the first known substituted derivatives of the highly unstable $[Ru_2(CO)_9]$, and in particular showed that the reaction of $[Ru_3(CO)_{12}]$ with $(RO)_2PN(R')P(OR)_2$ (R = Me, Et, Pr^i, Ph etc.; R′ = Me, Et), in equimolar amounts under thermal or UV conditions affords the trinuclear substituted product $[Ru_3(CO)_{10}\{\mu\text{-}(RO)_2PN(R')P(OR)_2\}]$ which, on further irradiation in the presence of excess ligand, produces the dinuclear pentacarbonyl derivatives $[Ru_2(\mu\text{-}CO)(CO)_4\{\mu\text{-}(RO)_2PN(R')P(O\text{-}$

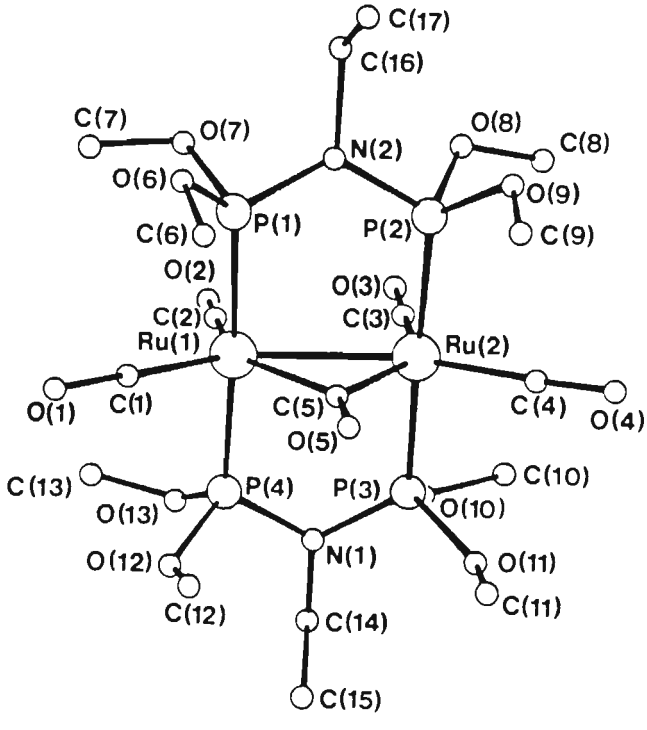

Figure 1.11: Structure of $[Ru_2(\mu\text{-}CO)(CO)_4\{\mu\text{-}(MeO)_2PN(Et)P(OMe)_2\}_2]$

$R)_2\}_2]$. On the basis of the structure established for the tetramethoxy-diphosphazane species $[Ru_2(\mu\text{-}CO)(CO)_4\{\mu\text{-}(MeO)_2PN(Et)P(OMe)_2\}_2]$, shown above, these compounds adopt structures analogous to those found for the di-iron diphosphorus ligand-bridged derivatives $[Fe_2(\mu\text{-}CO)(CO)_4\{\mu\text{-}(Et\text{-}O)_2POP(OEt)_2\}_2]$.[125,126]

These tetrasubstituted derivatives of $[Ru_2(CO)_9]$ are not entirely stable in solution decomposing, particularly in polar solvents, to $[Ru(CO)_3\{(R\text{-}O)_2PN(R')P(OR)_2\}]$. The analogous dppm derivative $[Ru_2(\mu\text{-}CO)(CO)_4\text{-}(\mu\text{-}dppm)_2]$[126] has also been prepared by the above photochemical procedure. Significantly, in contrast to that found for the reactions involving diphosphorus ligands, there was no evidence for the presence of $[Ru(CO)_4(\eta^1\text{-}dppm)]$ and/or $[Ru(CO)_3(dppm)]$ in solution, indicating that the mononuclear species, formed as a result of the fragmentation of $[Ru_3(CO)_{10}(\mu\text{-}dppm)]$, must rapidly associate to higher nuclearity species. The tetraphenyldiphosphazane ligand $Ph_2PN(Et)PPh_2$ was found to afford the trinuclear substitution product $[Ru_3(CO)_{10}\{\mu\text{-}Ph_2PN(Et)PPh_2\}]$ on reaction with an equimolar amount of $[Ru_3(CO)_{12}]$ under photochemical conditions. If a twice molar or greater amount of ligand is used however, photofragmentation occurs to give the mononuclear derivative $[Ru(CO)_3\{Ph_2PN(Et)PPh_2\}]$ as the sole product. It therefore became apparent that the reactivity and stability of these dinuclear derivatives was directly related to the steric and electronic properties of the bridging diphosphorus ligand.

The tetrasubstituted derivatives $[Ru_2(\mu\text{-}CO)(CO)_4\{\mu\text{-}(RO)_2PN(Et)P(OR)_2\}_2]$ are electron-rich because of the σ-donating property of the phosphorus atoms. As a result, these complexes have been found to be very reactive towards electrophiles and radical sources. Electrophilic attack may occur at the metal-metal bond or at the oxygen of the bridging carbonyl

ligand whereas nucleophilic attack may occur at a carbon of a terminally-bonded carbonyl ligand or at a carboxylic carbon of the diphosphorus ligand. Figure 1.12 summarizes the sites for potential attack on the diruthenium compound, using $[Ru_2(\mu\text{-}CO)(CO)_4\{\mu\text{-}(MeO_2PN(Et)\text{-}P(OMe)_2\}_2]$ as an example.

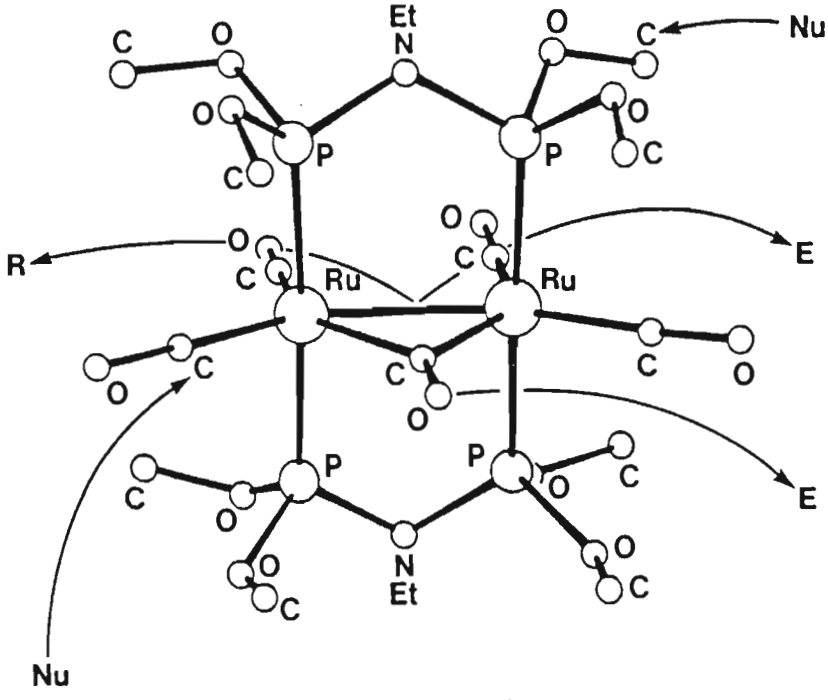

Figure 1.12

Electrophilic attack on $[Ru_2(\mu\text{-}CO)(CO)_4\{\mu\text{-}(RO)_2PN(Et)P(OR)_2\}_2]$ by the halogens chlorine, bromine and iodine has been shown to afford $[Ru_2X(CO)_5\{\mu\text{-}(RO)_2PN(Et)P(OR)_2\}_2]X$ (X = Cl, Br, I; R = Me, Pr^i, Ph) which decarbonylates in solution to give the halo-bridged complex $[Ru_2(\mu\text{-}X)(CO)_4\{\mu\text{-}(RO)_2PN(Et)P(OR)_2\}_2]X$, the rate of which is dependent upon the nature of the group R, and of the halogen employed. Further decarbonylation is achieved by heating or irradiation of solutions of $[Ru_2(\mu\text{-}X)(CO)_4\{\mu\text{-}(RO)_2PN(Et)P(OR)_2\}_2]X$ in THF with UV light, affording

tricarbonyl-dihalo complexes of the type $[Ru_2(\mu\text{-}X)X(CO)_3\{\mu\text{-}(RO)_2PN(Et)\text{-}P(OR)_2\}_2]$ with the structure of the complex for X = I and R = Pr^i having been established X-ray crystallographically.[127] These reactions are summarized in Scheme 1.11.

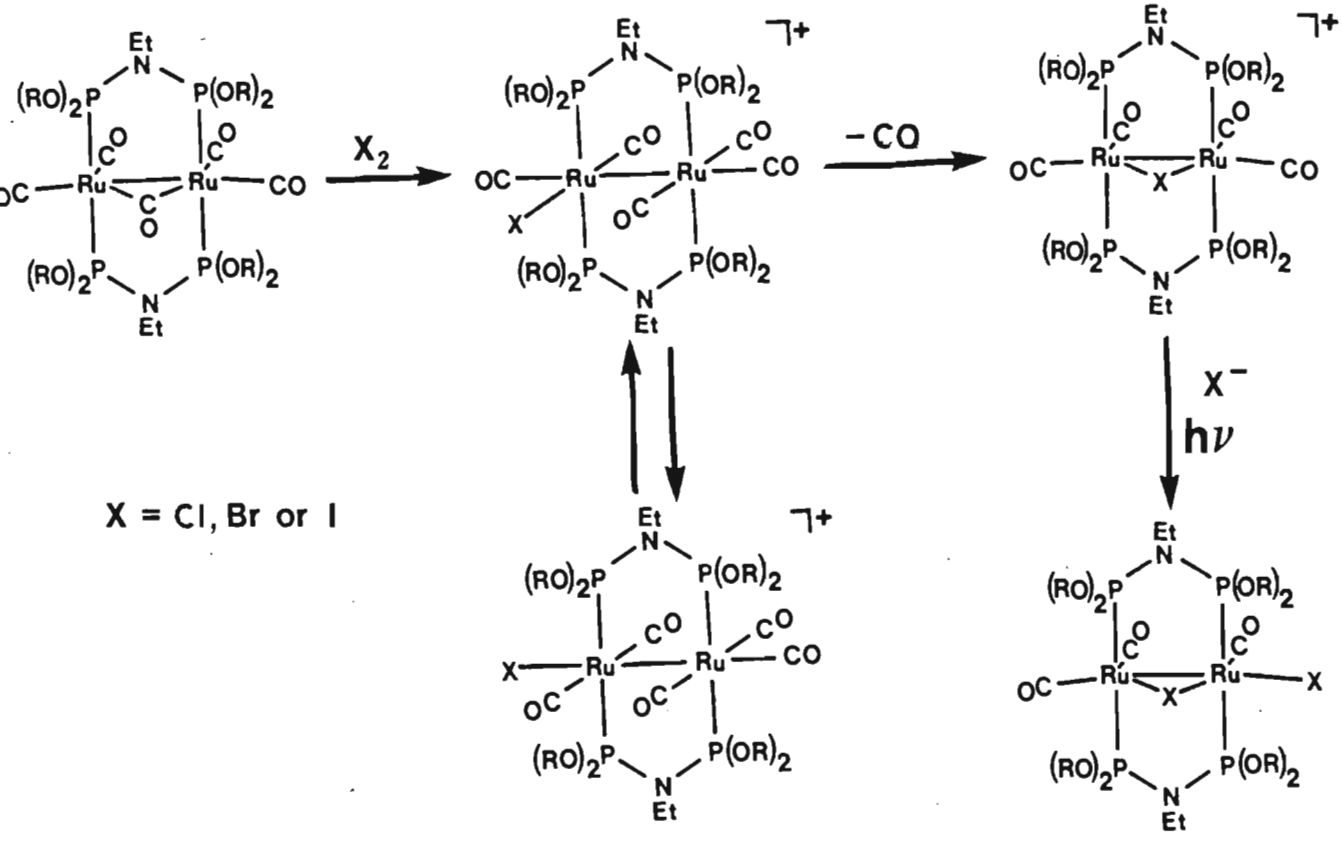

Scheme 1.11

Protonation of the ditertiary phosphine derivative $[Ru_2(\mu\text{-}CO)(CO)_4\{\mu\text{-}Ph_2PCH_2PPh_2)_2]$ was found to lead to a product in which the proton has effectively added across the two ruthenium atoms. On the other hand, the diphosphazane-bridged compounds $[Ru_2(\mu\text{-}CO)(CO)_4\{\mu\text{-}(RO)_2PN(Et)P\text{-}(OR)_2\}_2]$ (R = Me, Pr^i) gave, on protonation by HBF_4 or HPF_6, the complex $[Ru_2H(CO)_5\{\mu\text{-}(RO)_2PN(Et)P(OR)_2\}_2]X$ (X = BF_4 or PF_6),[128] which from infrared and nmr spectral data was judged to contain a terminally co-ordinated hydride ligand in both solution and solid state. Variable temperature $^{31}P\{^1H\}$ nmr spectroscopic studies indicated two isomers to be present in solution in dynamic equilibrium.

These protonated species are excellent precursors and have facilitated a wide range of metal hydride insertion reactions.[129] In particular, $[Ru_2H(CO)_5\{\mu\text{-}(RO)_2PN(Et)P(OR)_2\}_2]^+$ has been shown to be susceptible to attack by the unsaturated species PhC≡N, PhC≡CH and A=C=S (A = PhN or S) affording the three- four- and five-membered dimetalloheterocyclic compounds $[Ru_2\{\mu\text{-}\eta^1\text{-}N(CHPh)\}(CO)_4\{\mu\text{-}(RO)_2PN(Et)P(OR)_2\}_2]^+$, $[Ru_2\{\mu\text{-}\eta^2\text{-}OC(CHCHPh)\}(CO)_4\{\mu\text{-}(RO)_2PN(Et)P(OR)_2\}_2]^+$ and $[Ru_2\{\mu\text{-}\eta^2\text{-}AC(H)S\}(CO)_4\text{-}\{\mu\text{-}(RO)_2PN(Et)P(OR)_2\}_2]^+$ respectively, the structure of the former two being shown below.

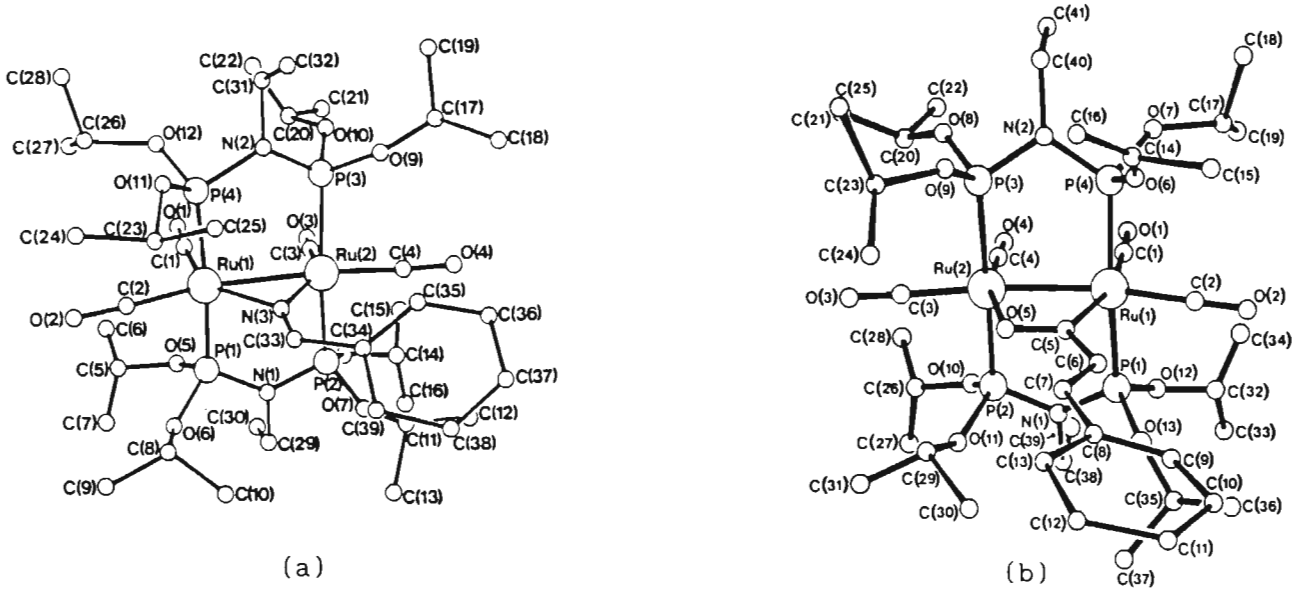

Figure 1.13: Structures of $[Ru_2\{\mu\text{-}\eta^1\text{-}N(CHPh)\}(CO)_4\{\mu\text{-}(RO)_2PN(Et)P\text{-}(OR)_2\}_2]^+$ (a) and $[Ru_2\{\mu\text{-}\eta^2\text{-}OC(CHCHPh)\}(CO)_4\{\mu\text{-}(RO)_2PN(Et)P(OR)_2\}_2]^+$ (b) (R = Pr^i)

The behaviour of $[Ru_2H(CO)_5\{\mu\text{-}(RO)_2PN(Et)P(OR)_2\}_2]^+$ towards acids having a potentially co-ordinating conjugate base has also been investigated.[130,131] In particular, it was found that reaction of $[Ru_2H(CO)_5\{\mu\text{-}(RO)_2PN(Et)P(OR)_2\}_2]^+$ with the acids HCl, HBr, HNO_3, H_2BO_2F, CF_3COOH, $PhSH/HPF_6$ and H_2CO_3/HPF_6 produces complexes of the type $[Ru_2A(CO)_5\{\mu\text{-}(RO)_2PN(Et)P(OR)_2\}_2]^+$ and/or $[Ru_2(\mu\text{-}A)(CO)_4\{\mu\text{-}(RO)_2PN(Et)P\text{-}(OR)_2\}_2]^+$ (A = Cl, Br, ON(O)O, OB(F)OH, $OC(CF_3)O$, SPh and OC(OH)). The formation of these complexes is proposed to occur via a diprotonated

species, *viz.* $[Ru_2H_2(CO)_5\{\mu\text{-}(RO)_2PN(Et)P(OR)_2\}_2]^{2+}$, as intermediate. The protonation step is presumed to be followed by the nucleophilic substitution of dihydrogen, presumably co-ordinated in the η^2- mode by HA or its conjugate base A^- while the final step in the reaction is the decarbonylation of $[Ru_2A(CO)_5\{\mu\text{-}(RO)_2PN(Et)P(OR)_2\}_2]^+$ to afford the bridged tetracarbonyl $[Ru_2(\mu\text{-}A)(CO)_4\{\mu\text{-}(RO)_2PN(Et)P(OR)_2\}_2]^+$. Thus reaction of $[Ru_2(\mu\text{-}CO)(CO)_4\{\mu\text{-}(RO)_2PN(Et)P(OR)_2\}_2]$ with excess trifluoroacetic acid produces the pentacarbonyl trifluoroacetate species $[Ru_2(CO)_5(OOCCF_3)\{\mu\text{-}(RO)_2PN(Et)P(OR)_2\}_2]^+$. This species is readily decarbonylated photochemically to afford the trifluoroacetate-bridged species $[Ru_2(CO)_4\{\mu\text{-}OC(CF_3)O\}\{\mu\text{-}(RO)_2PN(Et)P(OR)_2\}_2]^+$. Significantly, weaker carboxylic acids R'COOH (R' = H, Me, or Ph) were able to only partially protonate $[Ru_2(\mu\text{-}CO)(CO)_4\{\mu\text{-}(RO)_2PN(Et)P(OR)_2\}_2]$ without co-ordination of the carboxylate anion, according to the equilibrium

$$[Ru_2(\mu\text{-}CO)(CO)_4\{\mu\text{-}(RO)_2PN(Et)P(OR)_2\}_2] + R'COOH \rightleftharpoons [Ru_2H(CO)_5\{\mu\text{-}(RO)_2PN(Et)P(OR)_2\}_2]^+ + R'COO^-$$

Deprotonation of the species $[Ru_2H(CO)_5\{\mu\text{-}(RO)_2PN(Et)P(OR)_2\}_2]^+$ may also be achieved, but a strong base such as $NaBH_4$ is required.

The complexes $[Ru_2(\mu\text{-}CO)(CO)_4\{\mu\text{-}(RO)_2PN(Et)P(OR)_2\}_2]$ (R = Me, Pr^i) have also been shown to react readily with a range of metal-containing electrophiles[132] such as $[AuCl(PPh_3)]$, $[Cu(MeCN)_4]^+$ and $HgCl_2$ to give cationic products in which the metal substrate is either co-ordinated terminally as in $[Ru_2(HgCl)(CO)_5\{\mu\text{-}(RO)_2PN(Et)P(OR)_2\}_2]^+$ or in the bridging mode as in $[Ru_2\{\mu\text{-}M(L)\}(\mu\text{-}CO)(CO)_4\{\mu\text{-}(RO)_2PN(Et)P(OR)_2\}_2]^+$ (M = Au, L = PPh_3; M = Cu, L = MeCN). Reaction has also been found to occur with silver(I) salts, but the nature of the final product was found to be dependent on the nature of the ligand co-ordinated to the silver(I) ion. This will be discussed in more detail in the following chapter.

The carbonyls $[Ru_2(\mu\text{-}CO)(CO)_4\{\mu\text{-}(RO)_2PN(Et)P(OR)_2\}_2]$ (R = Me, Pr^i) have also been found to react with the nitrosonium ion NO^+. Not surprisingly, in view of this ion being isoelectronic with CO, a complex which is isostructural with $[Ru_2(\mu\text{-}CO)(CO)_4\{\mu\text{-}(RO)_2PN(Et)P(OR)_2\}_2]$ is produced.[133] The structure of the tetramethoxydiphosphazane derivative $[Ru_2(\mu\text{-}NO)(CO)_4\{\mu\text{-}(MeO)_2PN(Et)P(OMe)_2\}_2]^+$ is shown in Figure 1.14(b).

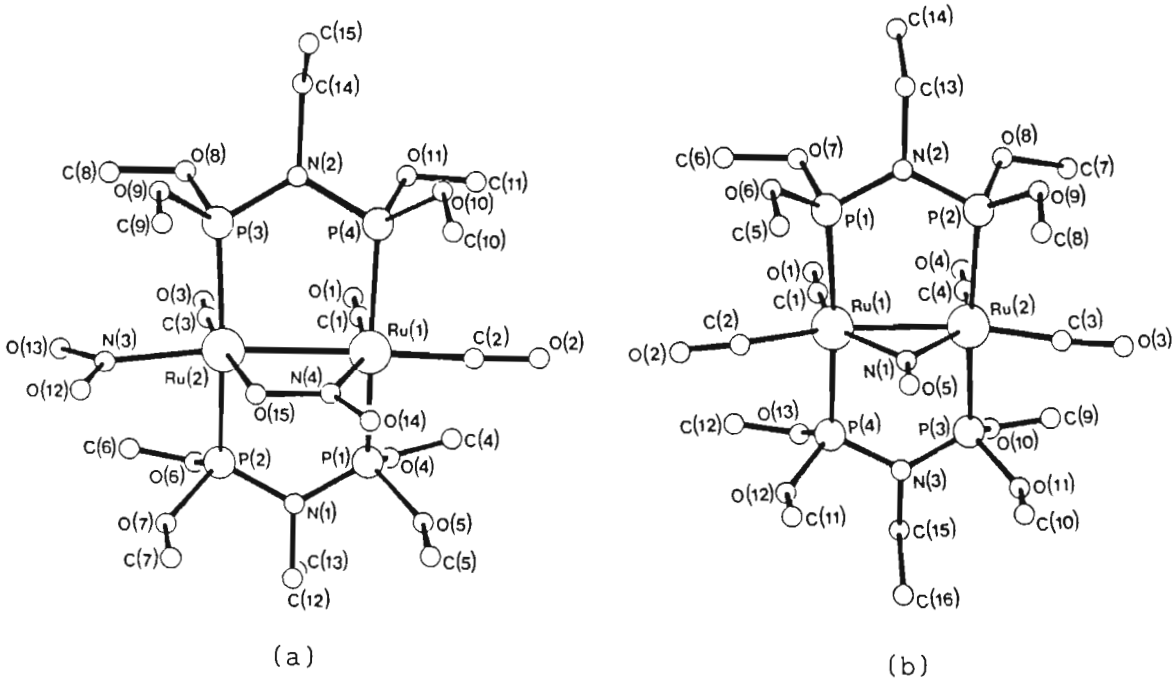

Figure 1.14: Structures of $[Ru_2(\mu\text{-}NO_2)(NO_2)(CO)_3\{\mu\text{-}(MeO)_2PN(Et)P(OMe)_2\}_2]$ (a) and $[Ru_2(\mu\text{-}NO)(CO)_4\{\mu\text{-}(MeO)_2PN(Et)P(OMe)_2\}_2]^+$ (b)

Reaction of a further molar equivalent of NO^+ results in the displacement of a carbonyl ligand by the nitrosonium ion to give the dicationic complexes $[Ru_2(\mu\text{-}CO)(CO)_2(NO)_2\{\mu\text{-}(RO)_2PN(Et)P(OR)_2\}_2]^{2+}$ in two isomeric forms. No reaction was observed on treatment of $[Ru_2(\mu\text{-}CO)(CO)_4\{\mu\text{-}(RO)_2PN(Et)P(OR)_2\}_2]$ with pure nitrogen oxide but, in the presence of trace amounts of air, the dinitro compound $[Ru_2(\mu\text{-}NO_2)(NO_2)(CO)_3\{\mu\text{-}(RO)_2PN(Et)P(OR)_2\}_2]$ was produced; the structure for R = Me, determined X-ray crystallographically, is shown in Figure 1.14(a).

The reaction of $[Ru_2(\mu\text{-}CO)(CO)_4\{\mu\text{-}(RO)_2PN(Et)P(OR)_2\}_2]$ with nitrogen dioxide or with the nitronium ion NO_2^+, was found to afford a penta-carbonyl nitro derivative $[Ru_2(CO)_5(NO_2)\{\mu\text{-}(RO)_2PN(Et)P(OR)_2\}_2]^+$. This complex may be decarbonylated to give the tetracarbonyl nitro-bridged species $[Ru_2(CO)_4\{\mu\text{-}ON(O)\}\{\mu\text{-}(RO)_2PN(Et)P(OR)_2\}_2]^+$.

The complexes $[Ru_2(\mu\text{-}CO)(CO)_4\{\mu\text{-}(RO)_2PN(Et)P(OR)_2\}_2]$ (R = Me, Pr^i) have also been shown to be susceptible to radical and diradical attack.[134] In particular, dissolution of the above complexes in CCl_4 was found to lead to the formation of the neutral dichloride $[Ru_2Cl_2(CO)_4\{\mu\text{-}(RO)_2PN(Et)P(OR)_2\}_2]$ (Figure 1.15(a)) via a radical pathway. These dichloro-derivatives isomerise in polar solvents to give $[Ru_2(\mu\text{-}Cl)(CO)_4\{\mu\text{-}(RO)_2PN(Et)P(OR)_2\}_2]Cl$. Reaction of $[Ru_2(\mu\text{-}CO)(CO)_4\{\mu\text{-}(RO)_2PN(Et)P(OR)_2\}_2]$ with Ph_2S_2 under photochemical conditions yielded a complex characterized as $[Ru_2(\mu\text{-}SPh)(CO)_4\{\mu\text{-}(RO)_2PN(Et)P(OR)_2\}_2]SPh$ (Figure 1.15(b)) which was presumed to have formed via $[Ru_2(CO)_4(SPh)_2\{\mu\text{-}(RO)_2PN(Et)P(OR)_2\}_2]$ based on the evidence found for analogous chloro-derivatives.

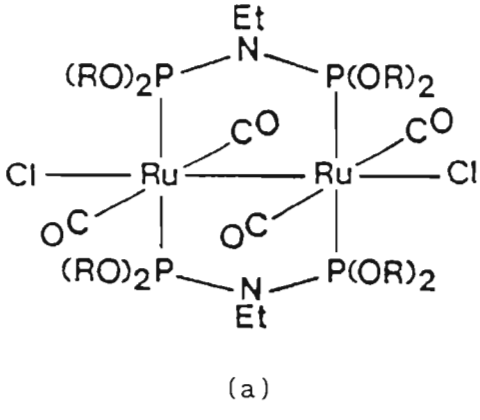

(a)

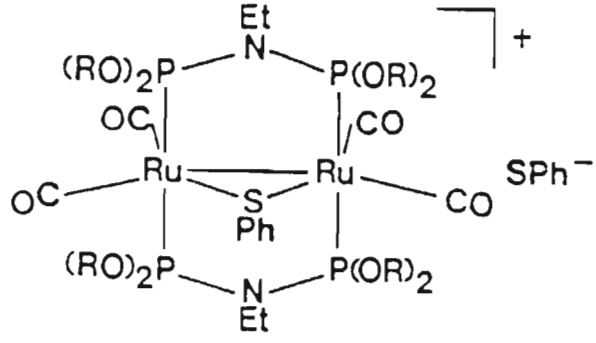

(b)

Figure 1.15: $[Ru_2Cl_2(CO)_4\{\mu\text{-}(RO)_2PN(Et)P(OR)_2\}_2]$ (a) and $[Ru_2(\mu\text{-}SPh)(CO)_4\{\mu\text{-}(RO)_2PN(Et)P(OR)_2\}_2]SPh$ (b)

Triplet state stannous chloride and sulphur dioxide are potentially

radical reagents. Reaction of $[Ru_2(\mu\text{-}CO)(CO)_4\{\mu\text{-}(RO)_2PN(Et)P(OR)_2\}_2]$ with $SnCl_2$ and SO_2 under photochemical conditions resulted in the addition of the substrate across the two ruthenium atoms with an accompanying loss of CO, to form $[Ru_2(\mu\text{-}SnCl_2)(CO)_4\{\mu\text{-}(RO)_2PN(Et)P(OR)_2\}_2]$ and $[Ru_2(\mu\text{-}SO_2)(CO)_4\{\mu\text{-}(RO)_2PN(Et)P(OR)_2\}_2]$ respectively.[135]

It was anticipated that reaction of $[Ru_2(\mu\text{-}CO)(CO)_4\{\mu\text{-}(RO)_2PN(Et)P(OR)_2\}_2]$ with the diradical tetrachloro-*o*-benzoquinone would lead to a product in which the quinone ligand chelates to one of the ruthenium atoms. Reaction takes place at room temperature but the $^{31}P\{^1H\}$ nmr spectrum of the product shows a very complex pattern of peaks. An X-ray crystal structure determination[135] on the tetramethoxydiphosphazane derivative revealed that a most unusual rearrangement had taken place resulting from the fission of a phosphorus-nitrogen bond of one of the diphosphazane ligands. Coupling of the $(RO)_2PN(Et)$ moiety with a co-ordinated carbon monoxide and of the $(RO)_2P$ moiety with the quinone

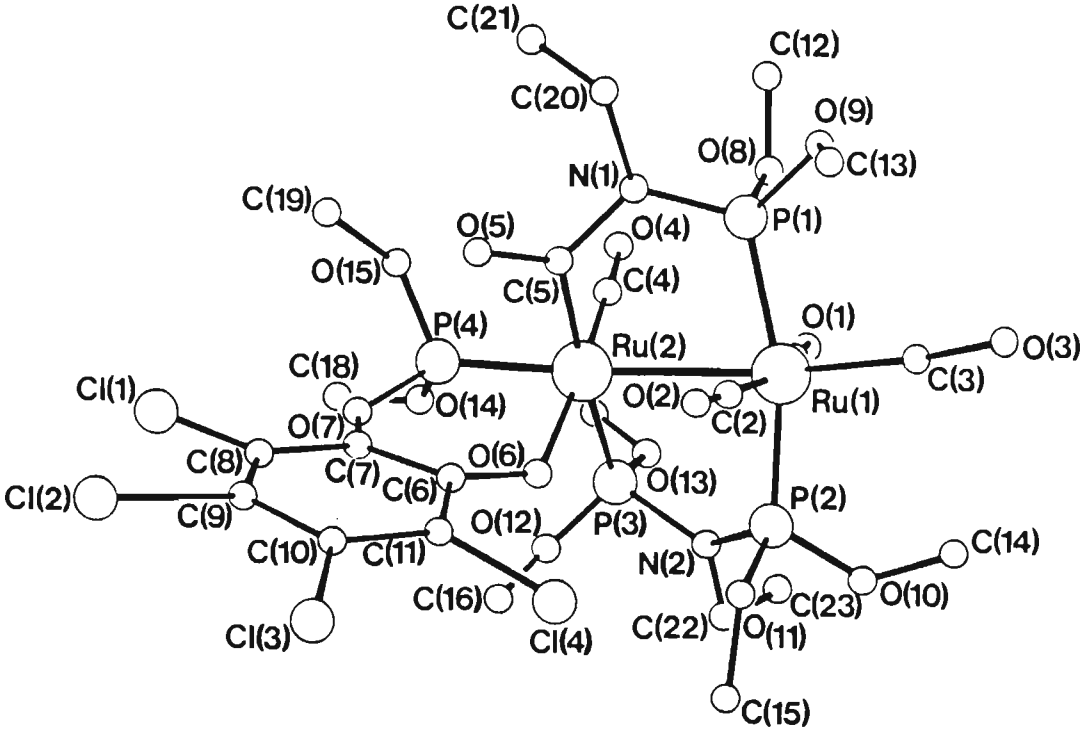

Figure 1.16: Structure of $[Ru_2\{\mu\text{-}(MeO)_2PN(Et)C(O)\}(CO)_4\{P(OMe)_2OC_6Cl_4O\}\{\mu\text{-}(MeO)_2PN(Et)P(OMe)_2\}]$

ligand, was found to have occurred producing, respectively, $(RO)_2PN(Et)C(O)$ and $(RO)_2POC_6Cl_4O$ moieties, as illustrated in the structure shown in Figure 1.16.

Complexes of the type $[Ru_2(\mu\text{-}CO)(CO)_4\{\mu\text{-}(RO)_2PN(Et)P(OR)_2\}_2]$ are relatively electron rich and as such, may function as donors to electron acceptor ligands. Thus, reaction of the above complexes with TCNQ and TCNE afford charge-transfer salts of the formula $[Ru_2(CO)_5(TCNX)\text{-}\{\mu\text{-}(RO)_2PN(Et)P(OR)_2\}_2]TCNX$ (X = Q or E; R = Me, Pr^i).[136] On the basis of the spectroscopic and cyclic voltammetric data, it has been established that these salts contain TCNX groups in both the inner (bonded through the nitrogen of a cyano group), and in the outer co-ordination sphere (as the $TCNX^{\bullet-}$ anion).

A preliminary investigation of the addition of small molecule compounds to $[Ru_2(\mu\text{-}CO)(CO)_4\{\mu\text{-}(RO)_2PN(Et)P(OR)_2\}_2]$ and their transformation on the metal centres has been undertaken.[137] It was found that reaction of $[Ru_2(\mu\text{-}CO)(CO)_4\{\mu\text{-}(RO)_2PN(Et)P(OR)_2\}_2]$ with phenyl acetylene PhC≡CH in a heated n-hexane solution, yielded a product characterized as the vinylidene-bridged species $[Ru_2(CO)_4(\mu\text{-}\eta^1\text{-}C{=}CHPh)\{\mu\text{-}(RO)_2PN(Et)P\text{-}(OR)_2\}_2]$.

1.3.2. Tetraalkyldiphosphorus Ligand-Bridged Derivatives

Recent reports in the literature have provided new synthetic routes to previously inaccessible diphosphorus ligand-bridged ruthenium(0) complexes. Takats and Kiel[138] have demonstrated that photolysis of $[Ru_3(CO)_{10}(dppm)]$ in the presence of CO affords $[Ru_2(CO)_7(dppm)]$ in good yield, although only small quantities of material may be prepared from each synthesis, owing to the poor solubility of $[Ru_3(CO)_{12}]$. The high

reactivity of this complex is demonstrated by its reaction with acetylene and diazomethane at low temperatures, affording the products $[Ru_2(CO)_5(\mu\text{-}C_2H_2CO)(dppm)]$ and $[Ru_2(CO)_6(\mu\text{-}CH_2)(dppm)]$ respectively (Scheme 1.12).

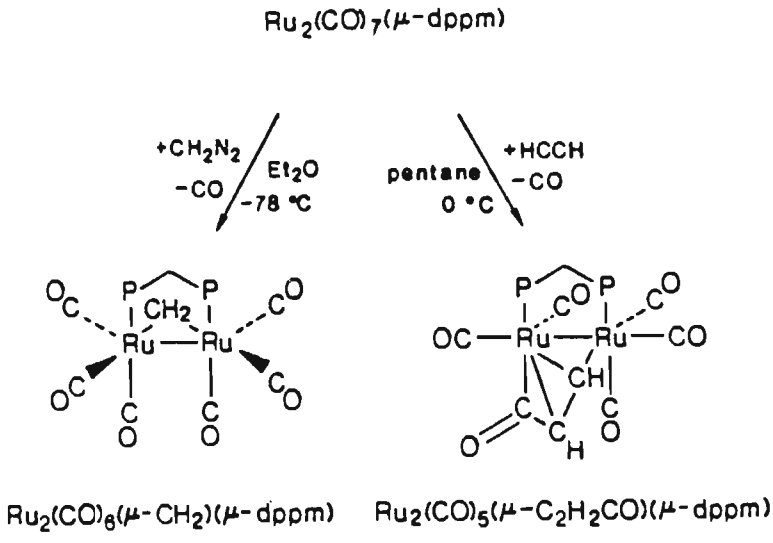

Scheme 1.12

Johnson and Gladfelter[69] have recently reported a high-yield synthesis for the dmpm-bridged diruthenium species $[Ru_2(\mu\text{-}CO)(CO)_4(\mu\text{-}dmpm)_2]$ by reaction of $[Ru_3(CO)_{12}]$ with dmpm under CO pressure at 120°C; the structure of this highly electron-rich air-sensitive product was determined X-ray crystallographically (Figure 1.17(a)). Protonation of this dmpm-bridged species is readily effected by $HBF_4.OEt_2$ in CH_2Cl_2 to afford a product analogous to that found for the protonation of $[Ru_2(\mu\text{-}CO)(CO)_4(\mu\text{-}dppm)_2]$.[128] The reaction of $[Ru_2(\mu\text{-}CO)(CO)_4(\mu\text{-}dmpm)_2]$ with the acetylenes PhC≡CPh and $MeO_2C\text{-}C{\equiv}C\text{-}CO_2Me$ has also been investigated and found to afford the alkendiyl-bridged products $[Ru_2(CO)_4(\mu\text{-}PhCCPh)(\mu\text{-}dmpm)_2]$ and $[Ru_2(CO)_4\{\mu\text{-}(MeO_2C)_2C_2\}(\mu\text{-}dmpm)_2]$ (Figure 1.17(b)) respectively.

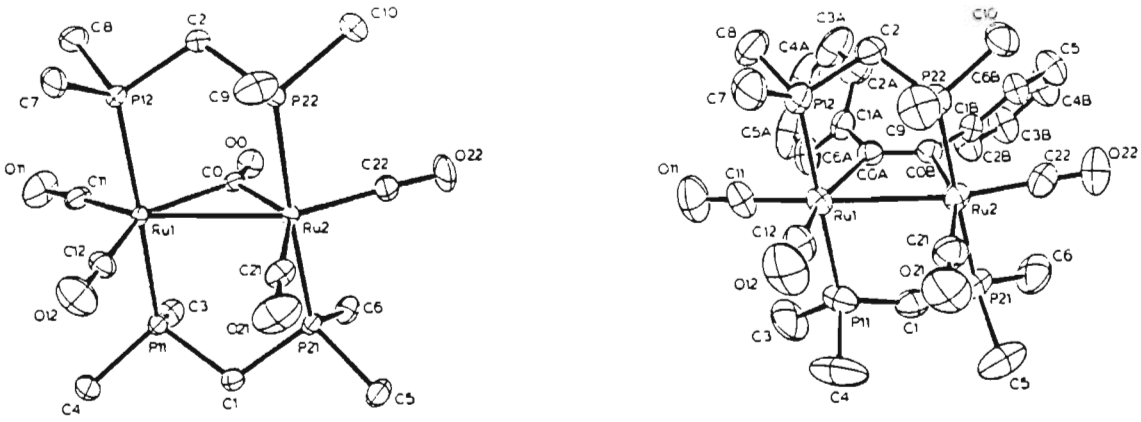

Figure 1.17: Structures of $[Ru_2(\mu\text{-}CO)(CO)_4(\mu\text{-}dmpm)_2]$ (a) and $[Ru_2\{\mu\text{-}C_2(CO_2Me)_2\}(CO)_4(\mu\text{-}dmpm)_2]$ (b)

The methylation of $[Ru_2(\mu\text{-}CO)(CO)_4(\mu\text{-}dmpm)_2]$ can be readily achieved using methyltriflate ($CF_3SO_3CH_3$), resulting in the formation of two products, namely $[Ru_2(CO)_5(CH_3)(\mu\text{-}dmpm)_2](CF_3SO_3)$ and $[Ru_2(CO)_4(\mu\text{-}CO\text{-}CH_3)(\mu\text{-}dmpm)_2](CF_3SO_3)$.[139]

CHAPTER 2

REACTION OF $[Ru_2(\mu\text{-}CO)(CO)_4\{\mu\text{-}(RO)_2PN(Et)P(OR)_2\}_2]$ WITH SILVER(I) SALTS IN NON-PROTIC SOLVENTS

2.1 INTRODUCTION

The known chemistry of dinuclear ruthenium(0) complexes of formula $[Ru_2(\mu\text{-}CO)(CO)_4(\mu\text{-}R_2PYPR_2)_2]$ (R = alkyl, aryl, alkoxy group, etc.; Y = O, CH_2, NR', etc.; R' = alkyl group) has been discussed in the previous chapter. A major part of the work described in this thesis involves the study of the redox chemistry of complexes of this type, with the aim of producing suitable precursors for the synthesis of new diruthenium species.

2.1.1 Synthesis of $[Ru_2(\mu\text{-}CO)(CO)_4\{\mu\text{-}(RO)_2PN(Et)P(OR)_2\}_2]$ (R = Me, Et, Pr^i)

The procedure originally developed for the synthesis of the tetraalkoxydiphosphazane derivatives $[Ru_2(\mu\text{-}CO)(CO)_4\{\mu\text{-}(RO)_2PN(Et)P(OR)_2\}_2]$[124] was modified slightly in order to achieve a more efficient preparation. The original synthesis involved, in the first instance, irradiation of $[Ru_3(CO)_{12}]$ and a three mole equivalent of the diphosphazane ligand in cyclohexane for one hour. The solvent was subsequently removed under reduced pressure and the residue redissolved in diethyl ether and allowed to stand at -10°C for 48 hours. This resulted in the separation of the dinuclear species from solution. Limitations of this procedure are the poor solubility of $[Ru_3(CO)_{12}]$ in cyclohexane, and the length of time taken to obtain the material in

crystalline form.

It was found that addition of benzophenone ketyl catalyst to $[Ru_3(CO)_{12}]$ in the presence of the diphosphazane ligand reduces the reaction time considerably and allows for greater quantities of material to be used for each synthesis. It was also found that the dinuclear species are only partially soluble in polar solvents such as methanol or ethanol. Methanol was therefore used to effect the rapid separation of these parent complexes from solution.

The method was modified further for the synthesis of a new mixed-ligand compound $[Ru_2(\mu\text{-}CO)(CO)_4\{\mu\text{-}(MeO)_2PN(Et)P(OMe)_2\}\{\mu\text{-}(Pr^iO)_2PN(Et)\text{-}P(OPr^i)_2\}]$ (**1**). In particular, the triruthenium species $[Ru_3(CO)_{10}\{\mu_2\text{-}(Pr^iO)_2PN(Et)P(OPr^i)_2\}]$ was irradiated in the presence of a twice molar amount of the tetramethoxydiphosphazane ligand $(MeO)_2PN(Et)P(OMe)_2$. The mixed-ligand species is formed, in *ca.* 50% yield, according to the equations:

$$[Ru_3(CO)_{12}] + (Pr^iO)_2PN(Et)P(OPr^i)_2 \xrightarrow{h\nu} [Ru_3(CO)_{10}\{\mu\text{-}(Pr^iO)_2PN(Et)P(OPr^i)_2\}] + 2CO$$

$$[Ru_3(CO)_{10}\{\mu\text{-}(Pr^iO)_2PN(Et)P(OPr^i)_2\}] + 2(MeO)_2PN(Et)P(OMe)_2 \xrightarrow{h\nu} [Ru_2(\mu\text{-}CO)(CO)_4\{\mu\text{-}(MeO)_2PN(Et)P(OMe)_2\}\{\mu\text{-}(Pr^iO)_2PN(Et)P(OPr^i)_2\}] + [Ru(CO)_3\{\eta^2\text{-}(MeO)_2PN(Et)P(OMe)_2\}] + 2CO$$

During the course of the investigation described in this thesis, specific trends became evident with regard to the band patterns as well as the frequencies of the carbonyl stretching vibrations in the infrared spectra of a range of compounds. These trends, as well as those evident for the chemical shifts in their respective $^{31}P\{^1H\}$ nmr spectra, warrant

particular comment. In general, the C-O stretching vibrations of tetramethoxydiphosphazane-bridged complexes were found to be approximately 10 cm^{-1} higher in frequency than their tetraisopropoxydiphosphazane-bridged analogues, as a consequence of the isopropoxydiphosphazane ligand being a slightly stronger donor than the methoxydiphosphazane ligand. Dicationic pentacarbonyl compounds of the type $[Ru_2(CO)_5(L)\{\mu\text{-}(RO)_2PN(Et)P(OR)_2\}_2]^{2+}$ (L = neutral ligand) were found to exhibit a band pattern in the C-O stretching region of their infrared spectra as shown in Figure 2.1(a); monocationic pentacarbonyl derivatives of the type $[Ru_2(CO)_5(A)\{\mu\text{-}(RO)_2PN(Et)P(OR)_2\}_2]^{+}$ (A = anionic ligand) exhibit the same band pattern in their infrared spectra, although the peaks are 10-15 cm^{-1} lower in frequency. Tetracarbonyl

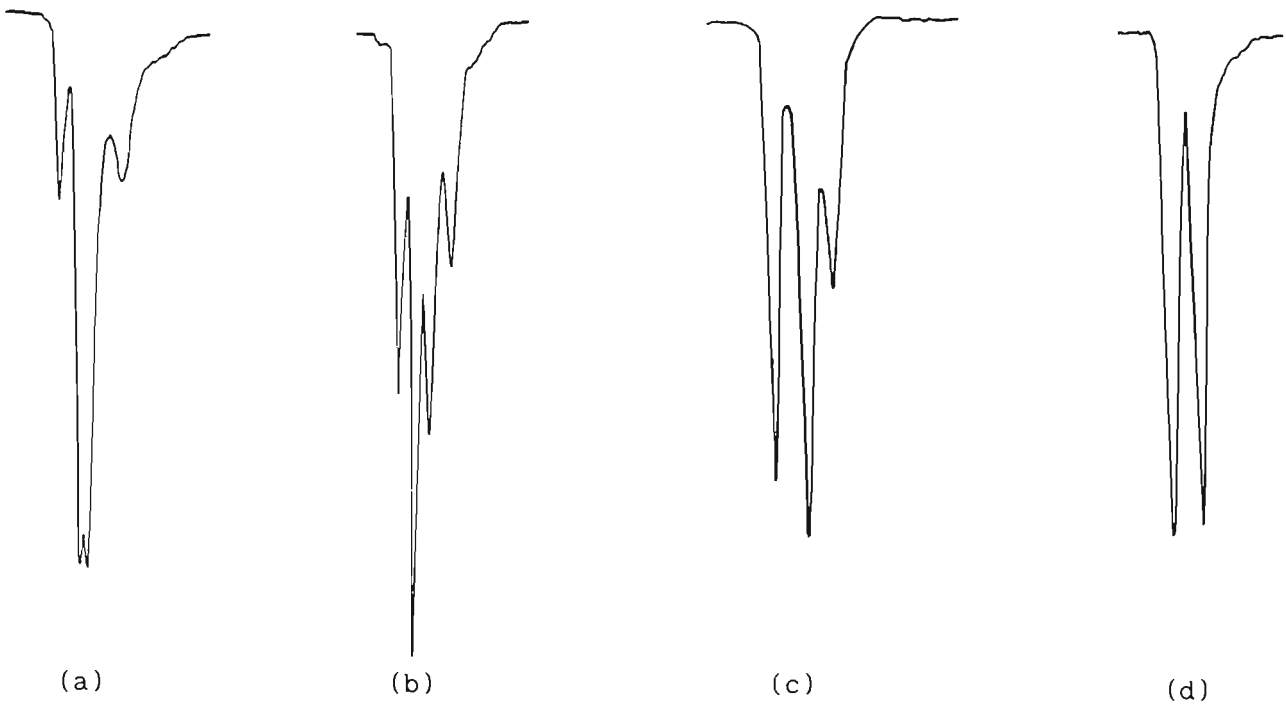

Figure 2.1: Infrared spectra for complexes of the type $[Ru_2(CO)_5(L)\{\mu\text{-}(RO)_2PN(Et)P(OR)_2\}_2]^{n+}$ (a), $[Ru_2(\mu\text{-}A)(CO)_4\{\mu\text{-}(RO)_2PN(Et)P(OR)_2\}_2]^{n+}$ (b), $[Ru_2(\mu\text{-}A)A(CO)_3\{\mu\text{-}(RO)_2PN(Et)P(OR)_2\}_2]$ (c) and $[Ru_2(L)_2(CO)_4\{\mu\text{-}(RO)_2PN\text{-}(Et)P(OR)_2\}_2]^{n+}$ (d)

complexes of the type $[Ru_2(\mu\text{-}A)(CO)_4\{\mu\text{-}(RO)_2PN(Et)P(OR)_2\}_2]^{n+}$ were found to exhibit a typical four-line band pattern in the C-O stretching region of their infrared spectra (Figure 2.1(b)), the frequencies of these bands being in the range 1880-2000 cm^{-1} for neutral compounds and 1950-2040 cm^{-1} for monocationic derivatives. Tricarbonyl complexes of general formula $[Ru_2(\mu\text{-}A)(A)(CO)_3\{\mu\text{-}(RO)_2PN(Et)P(OR)_2\}_2]$ exhibit a band pattern in the C-O stretching region of their infrared spectra as shown in figure 2.1(c). Neutral tetracarbonyl complexes of the type $[Ru_2(A)_2(CO)_4\{\mu\text{-}(RO)_2PN(Et)P(OR)_2\}_2]$ generally exhibit two bands in the C-O stretching region of their infrared spectra (Figure 2.1(d)); dicationic tetracarbonyl complexes of the type $[Ru_2(L)_2(CO)_4\{\mu\text{-}(RO)_2PN(Et)P(OR)_2\}_2]^{2+}$ exhibit the same band pattern although at higher frequencies (1985-2040 cm^{-1}).

The chemical shift of the peaks in the $^{31}P\{^1H\}$ nmr spectra were also found to be dependent on the nature of the diphosphazane ligand as well as the charge on the metal atoms. The chemical shifts of the resonances of tetraisopropoxydiphosphazane-bridged species were found to be 8-10 ppm upfield of their corresponding tetramethoxydiphosphazane-bridged analogues. In addition, neutral tetraisopropoxydiphosphazane-bridged complexes were found to have chemical shifts in the range 142-170 ppm, monocationic derivatives in the range 133-139 ppm whereas dicationic compounds exhibit resonances in the range 120-131 ppm. These trends have enabled accurate prediction of the arrangement of the carbonyl ligands as well as of the charge on the metal atoms based on the infrared and $^{31}P\{^1H\}$ nmr spectroscopic data.

2.1.2 Electrochemistry of $[Ru_2(\mu\text{-}CO)(CO)_4\{\mu\text{-}(RO)_2PN(Et)P(OR)_2\}_2]$

The redox chemistry of $[Ru_2(\mu\text{-}CO)(CO)_4\{\mu\text{-}(RO)_2PN(Et)P(OR)_2\}_2]$ (R = Me or

Pr^i) has been investigated electrochemically by means of cyclic voltammetry.[140,141] These studies were carried out both prior to and during the course of the investigation described in this chapter. Being electron-rich these diruthenium complexes were found to be readily oxidized but could not be reduced within the solvent limit of the solvents used, *viz.* acetone, dichloromethane and benzonitrile.

Figure 2.2 shows the CV of $[Ru_2(\mu\text{-}CO)(CO)_4\{\mu\text{-}(Pr^iO)_2PN(Et)P(OPr^i)_2\}_2]$

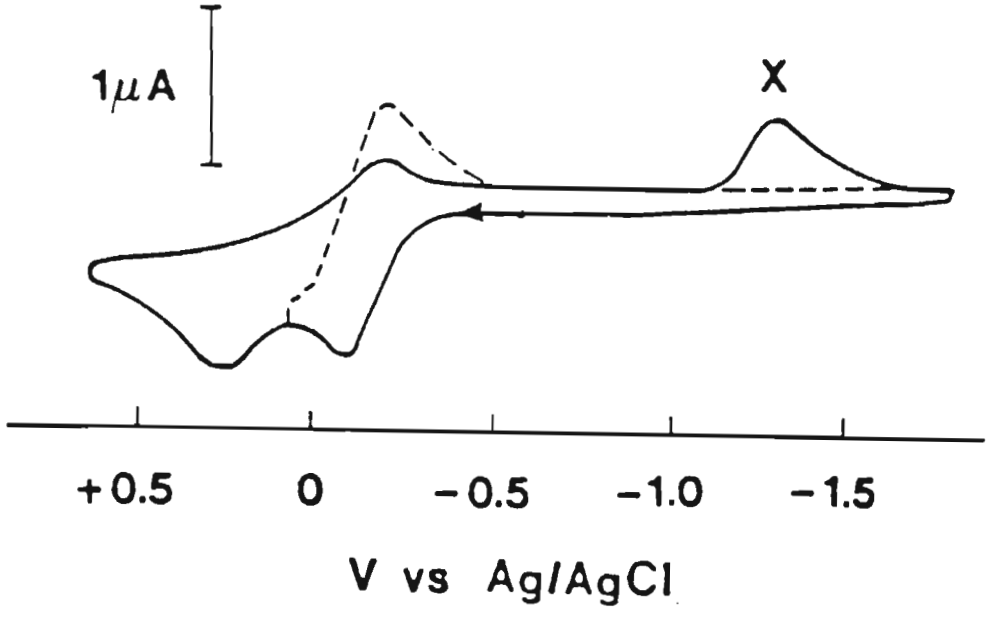

Figure 2.2: CV of 1.0m*M* $[Ru_2(\mu\text{-}CO)(CO)_4\{\mu\text{-}(Pr^iO)_2PN(Et)P(OPr^i)_2\}_2]$ in benzonitrile (0.1*M* TBAP) at Pt (298 K, 200 mV s^{-1})

measured in benzonitrile; similar CV's are obtained in acetone and dichloromethane. The initial anodic wave is reversible (i_{pc}/i_{pa} 1.0) and provided that the scan is not carried beyond this peak (E_{pa} -0.08 V) no additional cathodic wave is observed in the reverse scan. When the positive scan is extended, a second broad and irreversible oxidation wave is observed and, moreover, a new cathodic wave (X, Fig. 2.2) is

observed in the reverse scan. It has been possible to establish that the species formed following the removal of a second electron and which is subsequently reduced at X in the reverse scan (Fig. 2.2) is the dicationic solvento species $[Ru_2(CO)_5(solvent)\{\mu\text{-}(Pr^iO)_2PN(Et)P(OPr^i)_2\}_2]^{2+}$ (solvent = PhCN, acetone, CH_2Cl_2). This was achieved through the synthesis of $[Ru_2(CO)_5(PhCN)\{\mu\text{-}(Pr^iO)_2PN(Et)P(OPr^i)_2\}_2](SbF_6)_2$, described in section 2.2, and the measurement of its CV in benzonitrile. The primary reduction peak of this complex coincides with peak X in the CV of the parent neutral pentacarbonyl derivative and, furthermore, on reversal of the scan, two anodic waves are obtained which correspond to the oxidation of the parent complex $[Ru_2(\mu\text{-}CO)(CO)_4\{\mu\text{-}(Pr^iO)_2PN(Et)P(OPr^i)_2\}_2]$.

Figure 2.3 shows the CV of $[Ru_2(\mu\text{-}CO)(CO)_4\{\mu\text{-}(MeO)_2PN(Et)P(OMe)_2\}_2]$

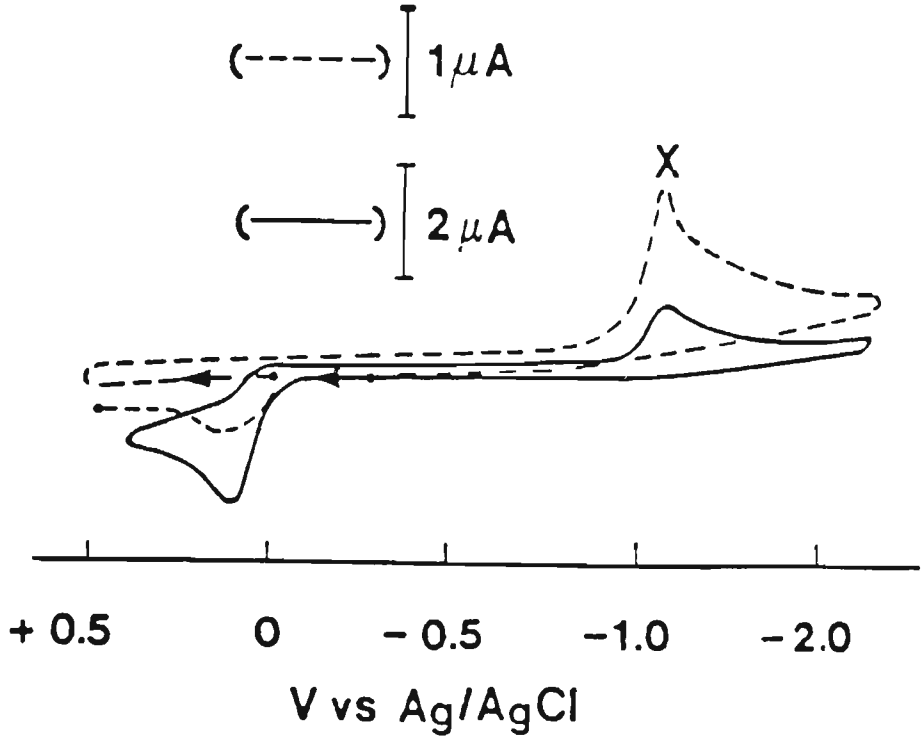

Figure 2.3: CV of 1.0m*M* $[Ru_2(\mu\text{-}CO)(CO)_4\{\mu\text{-}(MeO)_2PN(Et)P(OMe)_2\}_2]$ (———) and $[Ru_2(CO)_5(NCPh)\{\mu\text{-}(MeO)_2PN(Et)P(OMe)_2\}_2](SbF_6)_2$ (-----) **(5)** in benzonitrile (0.1*M* TBAP) at Pt (298 K, 200 mV s^{-1})

measured in benzonitrile. In contrast to that found for $[Ru_2(\mu\text{-}CO)(CO)_4\{\mu\text{-}(Pr^iO)_2PN(Et)P(OPr^i)_2\}_2]$, only one broad and irreversible wave is observed on scanning anodically, together with a broad cathodic wave (X, Figure 2.3) in the reverse scan. The peak current for the oxidation wave in the CV of $[Ru_2(\mu\text{-}CO)(CO)_4\{\mu\text{-}(MeO)_2PN(Et)P(OMe)_2\}_2]$ is twice that of the primary oxidation wave for $[Ru_2(\mu\text{-}CO)(CO)_4\{\mu\text{-}(Pr^iO)_2PN(Et)P(OPr^i)_2\}_2]$ under the same conditions. This indicates an ECE mechanism where $E_1^\circ > E_2^\circ$ (1 and 2 denoting the removal of the first and second electrons) giving rise to an overall two-electron transfer reaction. The implication is that the chemical step which follows the removal of the first electron allows the second electron to be removed more easily. The chemical step involves solvent co-ordination to a ruthenium atom in the radical cation, followed by the loss of a second electron to form the dicationic solvento species $[Ru_2(CO)_5(PhCN)\{\mu\text{-}(MeO)_2PN(Et)P(OMe)_2\}_2]^{2+}$. This was confirmed by synthesis of $[Ru_2(CO)_5(PhCN)\{\mu\text{-}(MeO)_2PN(Et)P(OMe)_2\}_2](SbF_6)_2$ and the measurement of its CV in benzonitrile. The reduction of this complex corresponds with peak X in the CV of the neutral parent compound and again an anodic wave is obtained on reversal of the scan, which corresponds to the oxidation of the parent complex $[Ru_2(\mu\text{-}CO)(CO)_4\{\mu\text{-}(MeO)_2PN(Et)P(OMe)_2\}_2]$. The CV of $[Ru_2(\mu\text{-}CO)(CO)_4\{\mu\text{-}(MeO)_2PN(Et)P(OMe)_2\}_2]$, recorded in acetone, exhibits the same pattern as the CV recorded in benzonitrile and an ECE mechanism therefore appears to operate in this solvent as well. On the other hand, the CV recorded in dichloromethane exhibits a reversible primary oxidation wave followed by an irreversible one with the appearance of a peak X in the reverse scan. Dichloromethane is a very weakly co-ordinating solvent which probably accounts for the stability of the radical cation $[Ru_2(CO)_5\{\mu\text{-}(MeO)_2PN(Et)P(OMe)_2\}_2]^{\cdot+}$ in dichloromethane, and accounting for an EEC mechanism.

Interestingly, the electrochemical oxidation of the more electron-rich bis(dimethylphosphino)methane derivative $[Ru_2(\mu\text{-}CO)(CO)_4(\mu\text{-}dmpm)_2]$ in benzonitrile also proceeds *via* an ECE mechanism, with the radical cation $[Ru_2(\mu\text{-}CO)(CO)_4(\mu\text{-}dmpm)_2]^{+\bullet}$ being rapidly attacked by the benzonitrile solvent in the chemical step, as found for the radical cation of $[Ru_2(\mu\text{-}CO)(CO)_4\{\mu\text{-}(MeO)_2PN(Et)P(OMe)_2\}_2]$.

Consistent with the potentials for the primary oxidations, $[Ru_2(\mu\text{-}CO)(CO)_4(\mu\text{-}dmpm)_2]$ is considerably more electron-rich than $[Ru_2(\mu\text{-}CO)(CO)_4\{\mu\text{-}(Pr^iO)_2PN(Et)P(OPr^i)_2\}_2]$ which in turn is more electron-rich than $[Ru_2(\mu\text{-}CO)(CO)_4\{\mu\text{-}(MeO)_2PN(Et)P(OMe)_2\}_2]$, whereas the mechanisms for the electrochemical oxidation of these complexes are ECE, EEC and ECE respectively. A common feature of $[Ru_2(\mu\text{-}CO)(CO)_4\{\mu\text{-}(MeO)_2PN(Et)P(OMe)_2\}_2]$ and $[Ru_2(\mu\text{-}CO)(CO)_4\{\mu\text{-}Me_2PCH_2PMe_2\}_2]$ is that the bridging bidentate ligands are relatively small in size in comparison to those in $[Ru_2(\mu\text{-}CO)(CO)_4\{\mu\text{-}(Pr^iO)_2PN(Et)_2P(OPr^i)_2\}_2]$. In order to test the hypothesis that the size of the bridging diphosphorus ligand plays a crucial role in determining the mechanism of the electrochemical oxidation of the compounds of the type $[Ru_2(\mu\text{-}CO)(CO)_4(\mu\text{-}R_2PYPR_2)_2]$, the mixed-ligand complex $[Ru_2(\mu\text{-}CO)(CO)_4\{\mu\text{-}(MeO)_2PN(Et)P(OMe)_2\}\{\mu\text{-}(Pr^iO)_2PN(Et)P(OPr^i)_2\}]$, which contains both the more bulky tetraisopropoxydiphosphazane and the less bulky tetramethoxydiphosphazane ligands was prepared by the author (see section 2.1.1) and its CV recorded in a range of solvents. Figure 2.4 shows the CV of this compound in benzonitrile.

Significantly, the primary oxidation wave has an i_{pc}/i_{pa} value of 0.8 and is therefore not fully reversible, the implication being that the radical cation $[Ru_2(CO)_5\{\mu\text{-}(MeO)_2PN(Et)P(OMe)_2\}\{\mu\text{-}(Pr^iO)_2PN(Et)P(OPr^i)_2\}]^{+\bullet}$ is not entirely stable to solvent attack on the time scale of

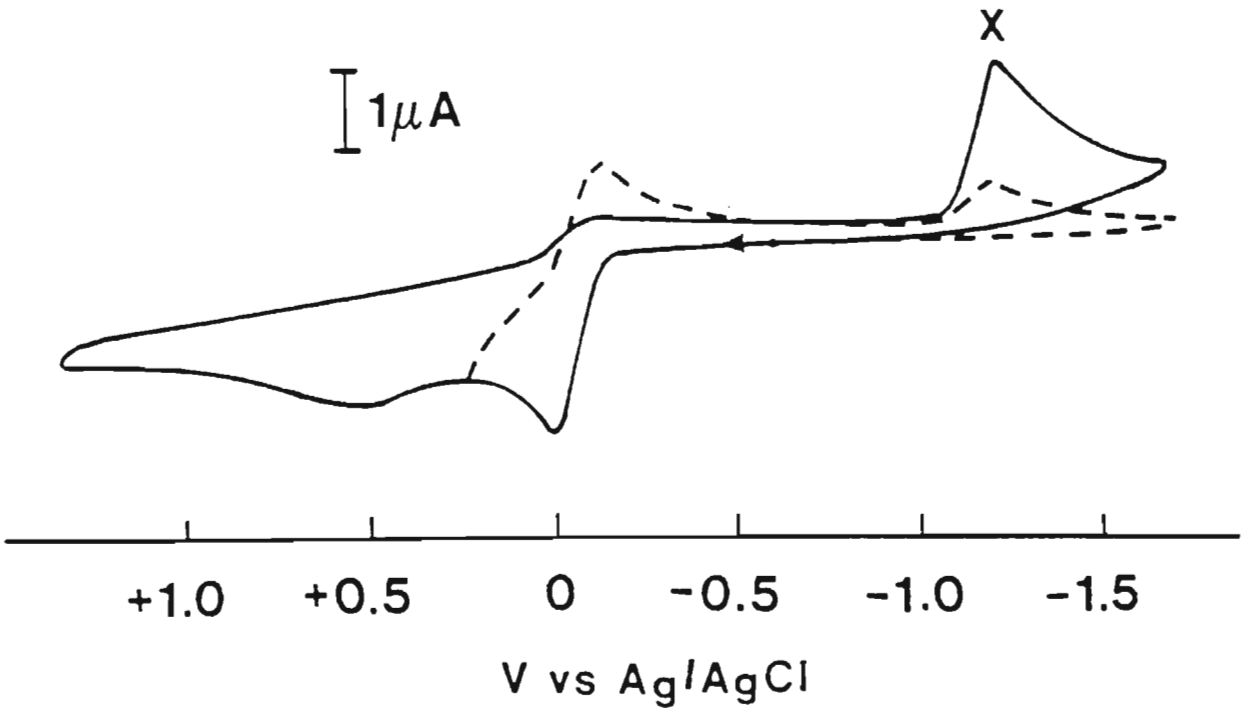

Figure 2.4: CV of 1.0m*M* $[Ru_2(\mu\text{-}CO)(CO)_4\{\mu\text{-}(MeO)_2PN(Et)P(OMe)_2\}\text{-}\{\mu\text{-}(Pr^iO)_2PN(Et)P(OPr^i)_2\}]$ (1) in benzonitrile (0.1M TBAP) at Pt (298 K, 200 mV s^{-1})

the experiment. Consistent with this interpretation it was observed that when the scan is carried just past the primary oxidation peak and reversed, the familiar peak X (Figure 2.4), due to the reduction of a dicationic solvento species is observed as a weak wave. It would thus appear that the radical cation is attacked by the benzonitrile ligand but relatively slowly. On scanning beyond the primary oxidation wave a second, broad and irreversible wave, as well as a significant enhancement in the height of peak X in the reverse scan is observed. Thus the CV of $[Ru_2(\mu\text{-}CO)(CO)_4\{\mu\text{-}(MeO)_2PN(Et)P(OMe)_2\}\{\mu\text{-}(Pr^iO)_2PN(Et)P(OPr^i)_2\}]$ displays features of both the EEC mechanism observed for $[Ru_2(\mu\text{-}CO)\text{-}(CO)_4\{\mu\text{-}(Pr^iO)_2PN(Et)P(OPr^i)_2\}_2]$ and the ECE mechanism observed for $[Ru_2(\mu\text{-}CO)(CO)_4\{\mu\text{-}(MeO)_2PN(Et)P(OMe)_2\}_2]$. The CV's of the mixed-ligand complex in acetone and dichloromethane follow this trend. These results are interpreted in terms of the stereochemistry of these complexes

playing a major role in determining the mechanism of their electrochemical oxidation. Ideally, the electrochemical behaviour of the mixed-ligand complex $[Ru_2(\mu\text{-}CO)(CO)_4(\mu\text{-}dmpm)\{\mu\text{-}(Pr^iO)_2PN(Et)P(OPr^i)_2\}]$ should have been undertaken to further substantiate these proposals, but the synthesis of this complex has not been achieved.

In summary, following the primary oxidation of $[Ru_2(\mu\text{-}CO)(CO)_4(\mu\text{-}R_2PYPR_2)_2]$ there are two possible pathways to the end-product of the oxidation process *viz.* a dicationic solvento species of general formula $[Ru_2(CO)_5(solvent)(\mu\text{-}R_2PYPR_2)_2]^{2+}$, with the pathway taken by a particular complex being determined by the extent to which the metal atom centre in the radical cation is open to attack by a solvent molecule. This is illustrated in the scheme below.

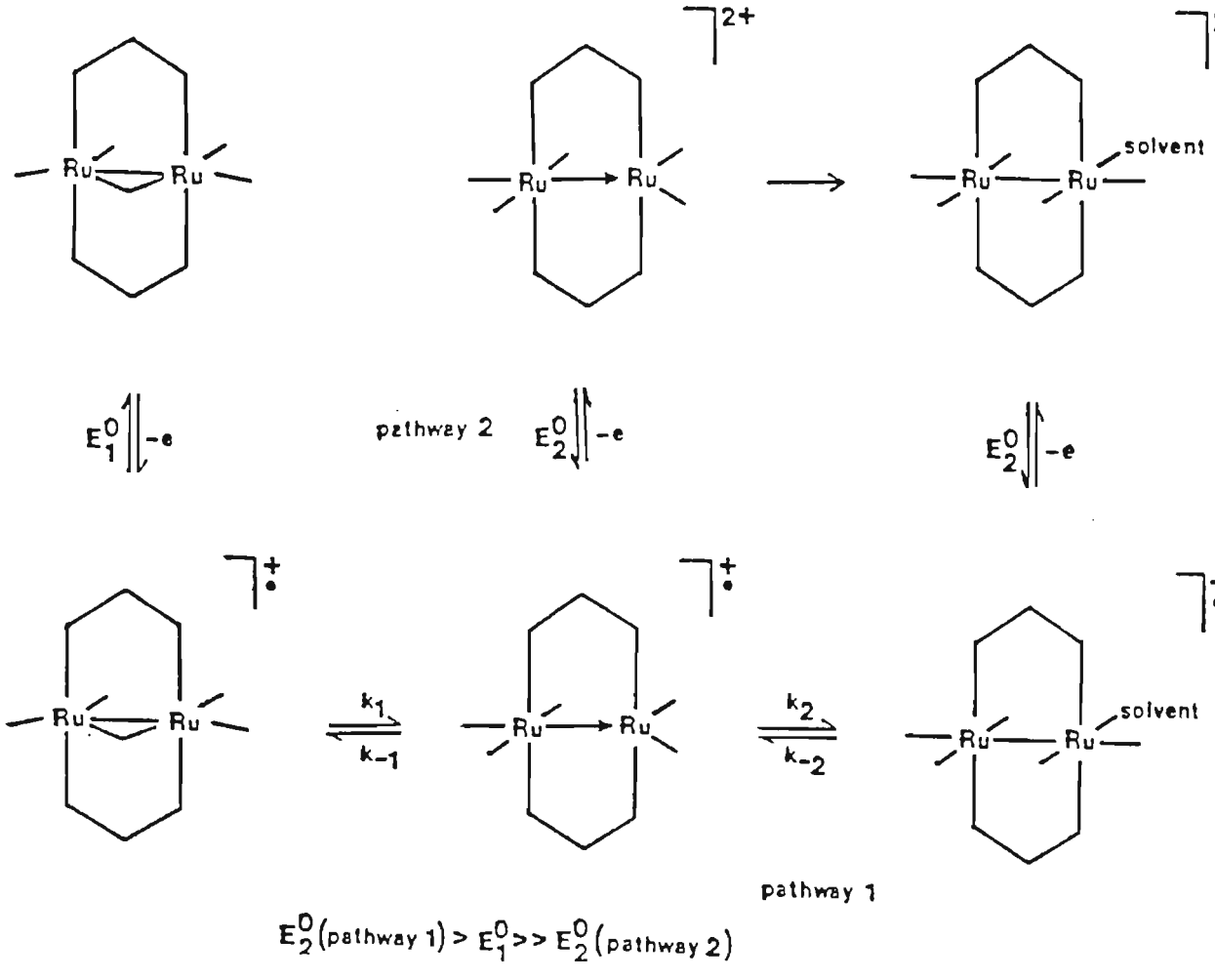

Scheme 2.1

2.1.3 The use of silver(I) salts as one-electron oxidants

Silver(I) salts are used extensively in inorganic and organometallic chemistry as one-electron oxidants,[142] while many examples are known of compounds which are formed by the addition of silver(I) complexes across a metal-metal bond in dinuclear and metal cluster derivatives.[143-146]

The use of silver(I) salts, in particular in the synthesis of solvento species, has been widely reported. For instance, Werner *et al.*[146] showed that reaction of the mononuclear complex $[ArRuX_2(L)]$ (X = Cl; Ar = C_6Me_6, C_6H_6 and *p*-cymene; L = CO and tertiary phosphines) with $AgPF_6$ in acetone yields $[ArRuCl(L)(acetone)]PF_6$. Many examples of the utilization of solvento species, which have been synthesized by this procedure, as precursors for the synthesis of a vast spectrum of products are known.[142,147,148] Manning *et al.*[149] have demonstrated that silver(I) salts may be used to cleave the metal-metal bond in di-iron cyclopentadienyl systems. The oxidative cleavage of $[Fe_2(\eta\text{-}C_5H_5)_2(CO)_{4-n}(CNMe)_n]$ (n = 0-2) by 2AgX was shown to be a two-electron process in most solvents but a one-electron process in acetonitrile, affording $[Fe_2(\eta\text{-}C_5H_5)_2(CO)(L)(CNMe)]^+$ (L = CO or CNMe) and $[Fe(\eta\text{-}C_5H_5)(CO)(L)]\cdot$. The co-ordinated solvent in the former compound is not labile, however, and could not be displaced by tertiary phosphines. The oxidative cleavage of the ruthenium analogue $[Ru_2(\eta\text{-}C_5H_5)_2(CO)_4]$ was found to afford the corresponding mononuclear ruthenium solvento species.[150]

Silver(I) salts have been used to effect transformations of complexes containing alkenes and related ligands. For example, treatment of the radical cation $[Ru_3(\mu\text{-}CO)_3(\mu_3\text{-}CMe)(\eta\text{-}C_5Me_5)_3]^{+\cdot}$ with Ag^+ gave the di-cationic species $[Ru_3(\mu\text{-}CO)_3(\mu_3\text{-}CMe)(\eta\text{-}C_5Me_5)_3]^{2+}$ which slowly deprotonated to form the corresponding μ_3-vinylidene complex

$[Ru_3(\mu\text{-}CO)_3(\mu_3\text{-}C{=}CH_2)(\eta\text{-}C_5Me_5)_3]^+$.[151] The ethene complex $[Ru_2(CO)(C_2H_4)(\mu\text{-}CO)_2(\eta\text{-}C_5H_5)_2]$ reacts with Ag^+ to afford the μ-vinyl cation $[Ru_2(CO)_2(\mu\text{-}CO)(\mu\text{-}CH{=}CH_2)(\eta\text{-}C_5H_5)_2]^+$.[152]

The diruthenium diphosphazane-bridged complexes $[Ru_2(\mu\text{-}CO)(CO)_4\{\mu\text{-}(RO)_2PN(Et)P(OR)_2\}_2]$ (R = Me or Pr^i) have been observed previously to react readily with silver(I) salts,[132] but the identity of the final product was found to be dependent on the nature of the ligand co-ordinated to the silver(I) ion. For example, treatment of $[Ru_2(\mu\text{-}CO)(CO)_4\{\mu\text{-}(MeO)_2PN(Et)P(OMe)_2\}_2]$ with an equimolar amount of $AgSbF_6$ in a weakly co-ordinating non-protic oxygen-donor solvent such as acetone was found to lead to the precipitation of elemental silver and the formation of a half molar amount of $[Ru_2(CO)_5(solvent)\{\mu\text{-}(MeO)_2PN(Et)P(OMe)_2\}_2]^{2+}$. On the other hand, reaction of $[Ru_2(\mu\text{-}CO)(CO)_4\{\mu\text{-}(MeO)_2PN(Et)P(OMe)_2\}_2]$ with an equimolar amount of $AgSbF_6$ in MeCN or with an equimolar amount of $[Ag(pyridine)_4]SbF_6$ in THF was found to give a product spectroscopically characterized as $[Ru_2(\mu\text{-}AgL)(\mu\text{-}CO)(CO)_4\{\mu\text{-}(MeO)_2PN(Et)P(OMe)_2\}_2]SbF_6$ (L = MeCN or pyridine). This complex was found to degrade to elemental silver and an intense purple, oxygen-sensitive species, presumed to be the one-electron oxidation product, $[Ru_2(\mu\text{-}CO)(CO)_4\{\mu\text{-}(MeO)_2PN(Et)P(OMe)_2\}_2]SbF_6$, on warming in the solid state under vacuum. The latter was found to spontaneously disproportionate to the dicationic solvento species $[Ru_2(CO)_5(solvent)\{\mu\text{-}(MeO)_2PN(Et)P(OMe)_2\}_2]^{2+}$ and the parent compound $[Ru_2(\mu\text{-}CO)(CO)_4\{\mu\text{-}(MeO)_2PN(Et)P(OMe)_2\}_2]$ on dissolution in weakly co-ordinating polar solvents such as acetone or benzonitrile. These results were interpreted in terms of the one-electron oxidation of $[Ru_2(\mu\text{-}CO)(CO)_4\{\mu\text{-}(RO)_2PN(Et)P(OR)_2\}_2]$ by silver(I) salts occurring *via* an inner sphere mechanism with the formation of the solvento species occurring *via* $[Ru_2(\mu\text{-}CO)(\mu\text{-}AgL)(CO)_4\{\mu\text{-}(RO)_2PN(Et)P(OR)_2\}_2]^+$ as intermediate. This is schematically

illustrated below.

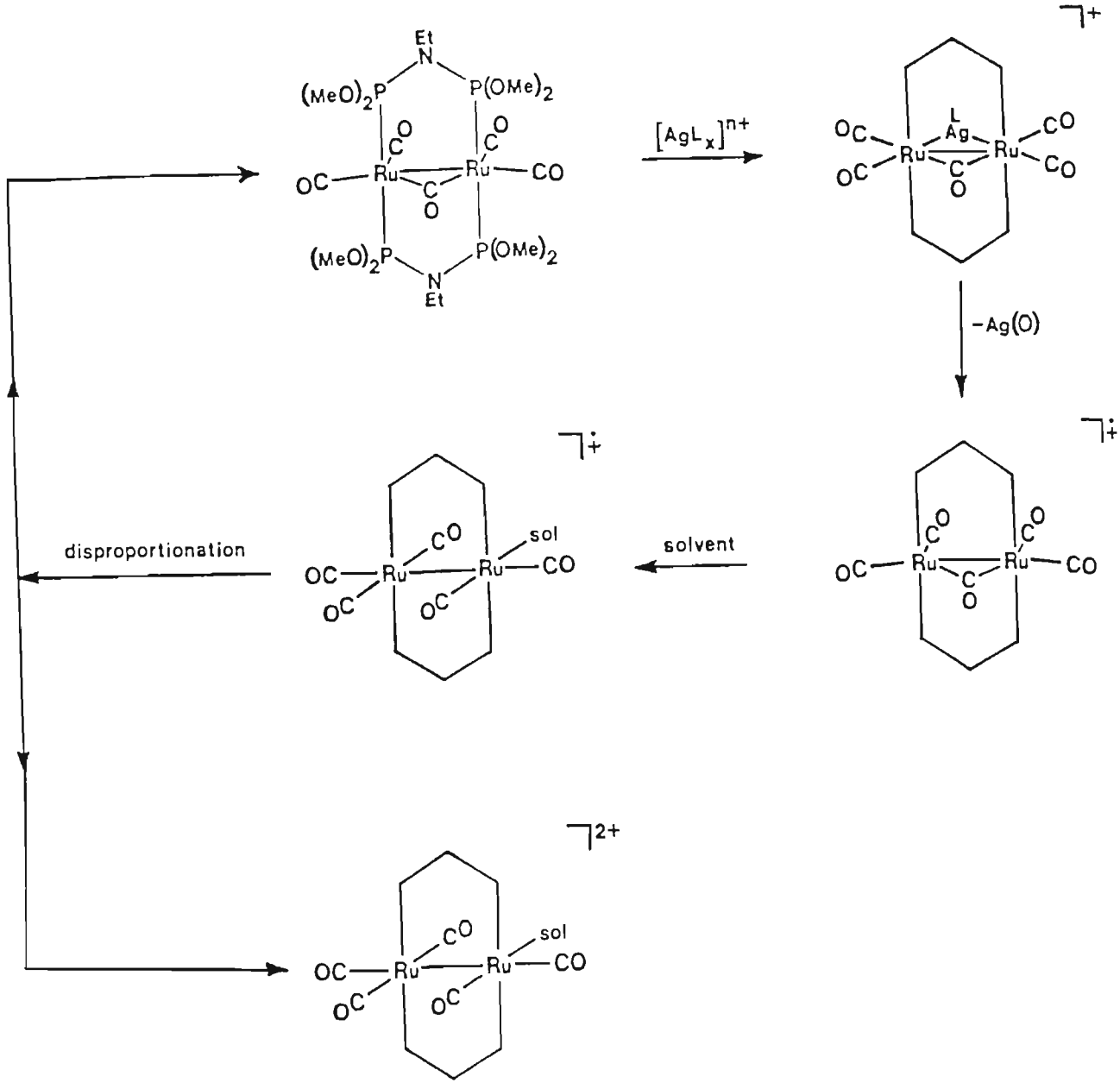

Scheme 2.2

This investigation was the first to provide evidence that the one-electron oxidation of polynuclear derivatives by silver(I) salts occurs *via* inner sphere intermediates and that the nature of the final product is dependent on the ligand co-ordinated to the silver.

Preliminary investigations in these laboratories have revealed that the solvent molecule in $[Ru_2(CO)_5(solvent)\{\mu\text{-}(RO)_2PN(Et)P(OR)_2\}_2]^{2+}$ may be partially replaced by neutral ligands such as carbon monoxide and isonitriles, or totally replaced by anionic ligands such as cyanides. The solvento species was therefore envisaged to be an excellent precursor for the synthesis of a wide range of dinuclear derivatives of ruthenium in low formal oxidation states. Many anomalous reactions of the solvento species were observed in the preliminary studies and thus an objective of the study reported in this thesis has been to gain a greater understanding of the redox chemistry of the parent complexes $[Ru_2(\mu\text{-}CO)(CO)_4\{\mu\text{-}(RO)_2PN(Et)P(OR)_2\}_2]$, as well as to study the co-ordination behaviour of a range of ligands towards the solvento species $[Ru_2(CO)_5(solvent)\{\mu\text{-}(RO)_2PN(Et)P(OR)_2\}_2]^{2+}$.

2.2 REACTION OF $[Ru_2(\mu\text{-}CO)(CO)_4\{\mu\text{-}(RO)_2PN(Et)P(OR)_2\}_2]$ (R = Me or Pr^i) WITH SILVER(I) SALTS IN ORGANONITRILE SOLVENTS

Addition of a twice molar amount of $AgSbF_6$ to $[Ru_2(\mu\text{-}CO)(CO)_4\{\mu\text{-}(RO)_2PN(Et)P(OR)_2\}_2]$ (R = Me or Pr^i) in either benzonitrile or acetonitrile, resulted in the immediate separation of metallic silver from the pale yellow solution. A white crystalline product could be isolated from this solution in almost quantitative yield and this was characterized as the dicationic solvento species $[Ru_2(CO)_5(solvent)\{\mu\text{-}(RO)_2PN(Et)P(OR)_2\}_2](SbF_6)_2$ (solvent = PhCN, MeCN; R = Me or Pr^i) by means of infrared and NMR spectroscopy as well as by means of microanalysis.

The infrared spectrum of the tetraisopropoxydiphosphazane-bridged derivative $[Ru_2(CO)_5(PhCN)\{\mu\text{-}(Pr^iO)_2PN(Et)P(OPr^i)_2\}_2](SbF_6)_2$ (**2**) exhibits a pattern of peaks in the C-O stretching region typical of monosubstituted pentacarbonyl species of the type $[Ru_2(CO)_5L\{\mu\text{-}(Pr^iO)_2P\text{-}$

$N(Et)P(OPr^i)_2\}_2]^{2+}$. In addition, a peak at 2245 cm^{-1} could be assigned as the C-N stretching mode of a co-ordinated benzonitrile. The frequency of this peak is considerably less than that for the corresponding mode for free benzonitrile (ν(C-N) *ca.* 2270 cm^{-1}). This is attributed to the reduction in the C-N bond order on co-ordination of benzonitrile to a dicationic centre. The ^1H nmr spectrum of this species is similar to that of the parent complex $[Ru_2(\mu\text{-}CO)(CO)_4\{\mu\text{-}(Pr^iO)_2PN(Et)P(OPr^i)_2\}_2]$ but contains, in addition, a multiplet in the aromatic region corresponding to the five protons of the co-ordinated benzonitrile. The $^{31}P\{^1H\}$ nmr spectrum of this compound, measured in acetone-d_6 at -77°C, exhibits an AA'BB' pattern of peaks, consistent with an asymmetric structure with non-equivalent ruthenium atoms *(vide infra)*. A sharp singlet is observed in the corresponding room temperature spectrum of this species indicating that the complex is involved in some fluxional process in solution. It is proposed that this process involves the intramolecular migration of the benzonitrile ligand from one ruthenium atom to the other as illustrated in Figure 2.5. A sharp singlet is also observed in the $^{31}P\{^1H\}$ nmr spectrum of this complex at room temperature in acetonitrile as well as in benzonitrile and dichloromethane, which contrasts with the AA'BB' pattern of

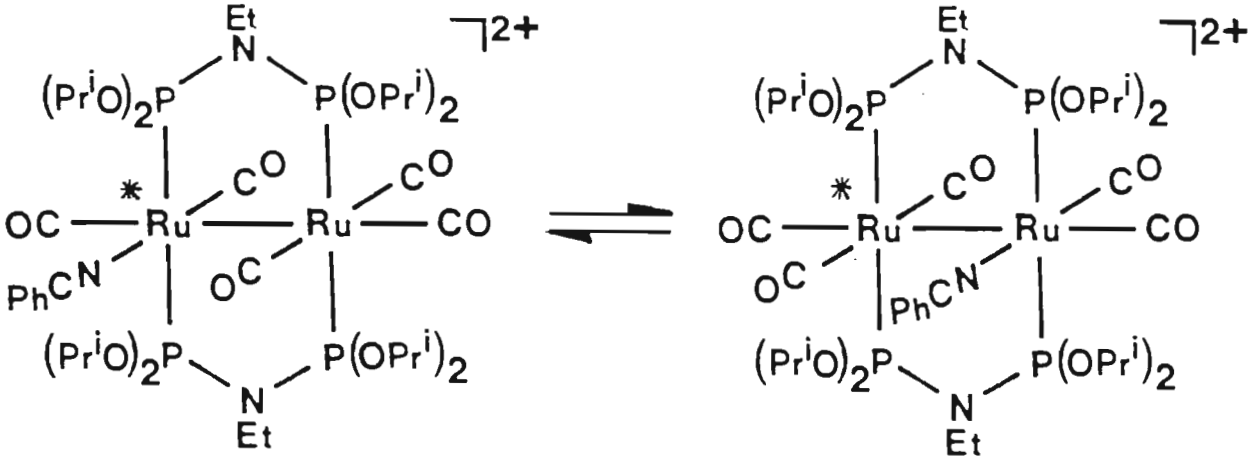

Figure 2.5

peaks observed for the acetonitrile solvento species $[Ru_2(CO)_5(NCMe)\{\mu\text{-}(Pr^iO)_2PN(Et)P(OPr^i)_2\}_2](SbF_6)_2$ in acetonitrile *(vide infra)*. Furthermore, addition of an excess of benzonitrile to the above acetonitrile solvento species in acetonitrile does not alter the $^{31}P\{^1H\}$ nmr spectrum of this compound. These observations are consistent with these complexes not exchanging their co-ordinated nitriles with free nitrile ligands, and with the fluxional process occurring *via* an intra- and not intermolecular mechanism. A single crystal X-ray structure determination was carried out for the tetraisopropoxydiphosphazane-bridged benzonitrile solvento species $[Ru_2(CO)_5(PhCN)\{\mu\text{-}(Pr^iO)_2PN(Et)P(OPr^i)_2\}_2](SbF_6)_2$. The stereochemistry of the dication is illustrated in Figure 2.6.

The two ruthenium atoms, each of which is approximately octahedral, are not only linked through two bridging tetraisopropoxydiphosphazane ligands *trans* disposed with respect to each other, but also by a formal ruthenium-ruthenium bond {Ru(1)-Ru(2) 2.890(3)Å}. Two of the carbonyl ligands are collinear with the Ru-Ru vector while the other three are orthogonal to it. The cation adopts an essentially staggered conformation, as reflected by P(1)-Ru(1)-Ru(2)-P(4) and P(2)-Ru(1)-Ru(2)-P(3) torsion angles of 28.4 and 31.0° respectively. The benzonitrile ligand is co-ordinated equatorially through its nitrogen atom with a ruthenium-nitrogen bond of 2.08(2)Å. The aromatic ring of the co-ordinated benzonitrile ligand lies approximately in the equatorial plane defined by the two ruthenium atoms and the two carbonyl groups bonded to the same ruthenium atom as the benzonitrile.

The infrared spectrum of $[Ru_2(CO)_5(MeCN)\{\mu\text{-}(Pr^iO)_2PN(Et)P(OPr^i)_2\}_2](SbF_6)_2$ **(3)** in the carbonyl stretching region exhibited an almost identical pattern to that found for the analogous benzonitrile solvento

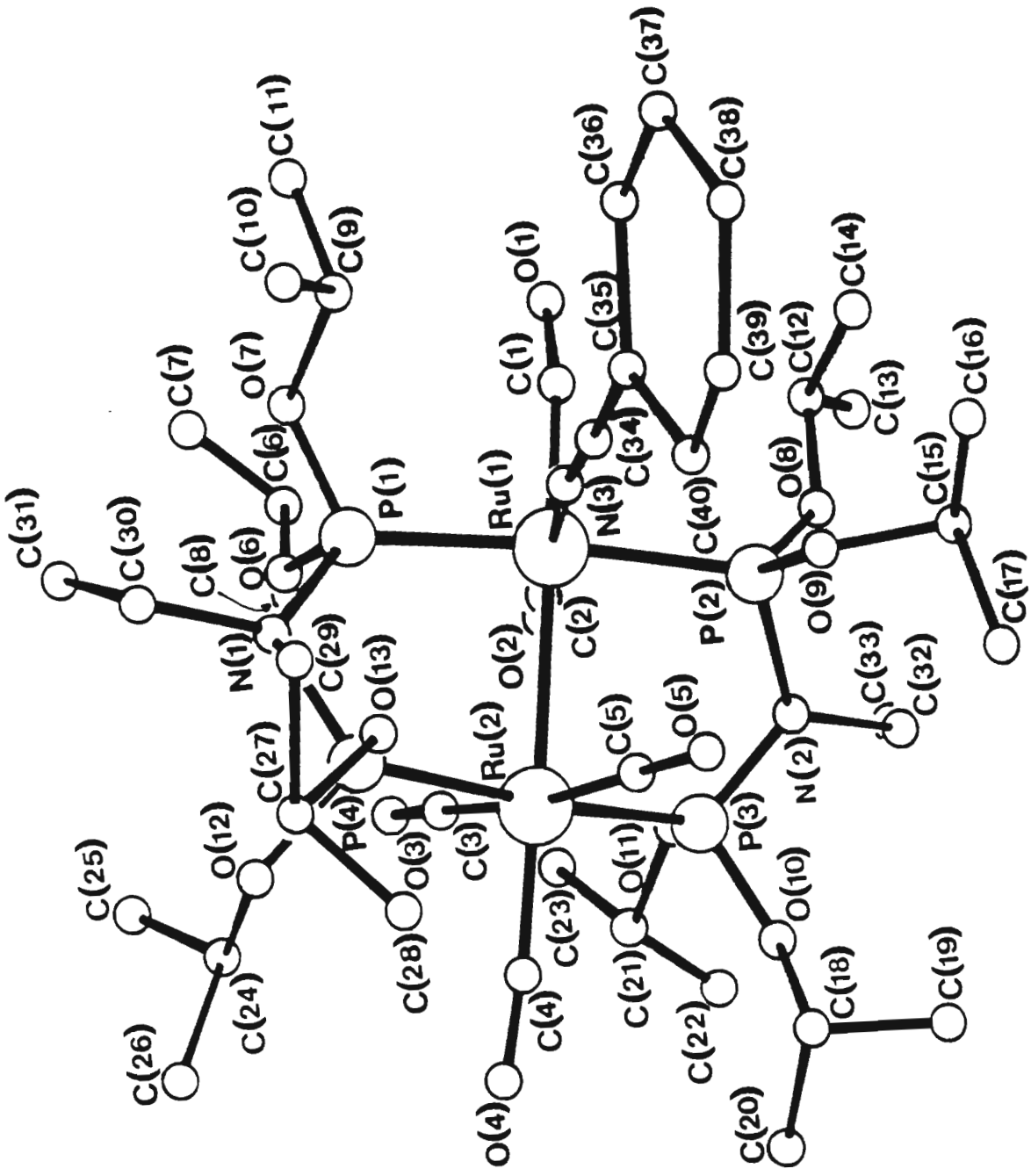

Figure 2.6: Structure of $[Ru_2(CO)_5(NCPh)\{\mu\text{-}(Pr^iO)_2PN(Et)P(OPr^i)_2\}_2]^{2+}$

species. The ^1H nmr spectrum is similar to that of the neutral parent complex, but contains, in addition, a singlet at 2.82 ppm assigned to the methyl protons of the co-ordinated acetonitrile. The room temperature $^{31}P\{^1H\}$ nmr spectrum of this complex in acetone-d_6 exhibits an AA'BB' pattern of peaks. This indicates that the complex is non-fluxional as opposed to the benzonitrile solvento species $[Ru_2(CO)_5(PhCN)\{\mu\text{-}(Pr^iO)_2PN(Et)P(OPr^i)_2\}_2](SbF_6)_2$, or if fluxional, the process is slow on the nmr time scale. This may be explained in terms of the acetonitrile, which is less bulky than benzonitrile, favouring co-ordination in an axial position instead of an equatorial one as established for the benzonitrile ligand. The migration of the aceto-nitrile from one ruthenium atom to the other will be more restricted in this situation.

The infrared spectrum of $[Ru_2(CO)_5(PhCN)\{\mu\text{-}(MeO)_2PN(Et)P(OMe)_2\}_2](SbF_6)_2$ (**4**) in the C-O stretching region gives the same pattern as that found for the analogous tetraisopropoxydiphosphazane derivative, although the peaks are approximately 10 cm^{-1} higher in frequency as a consequence of the isopropoxydiphosphazane ligand $(Pr^iO)_2PN(Et)P(OPr^i)_2$ being a slightly stronger donor than the tetramethoxydiphosphazane ligand $(MeO)_2PN(Et)P(OMe)_2$. In addition, a peak at 2237 cm^{-1} could be assigned as a C-N stretching vibration for the co-ordinated benzonitrile. The ^1H nmr spectrum of this species is similar to that of the parent complex $[Ru_2(\mu\text{-}CO)(CO)_4\{\mu\text{-}(MeO_2PN(Et)P(OMe)_2\}_2]$ but contains, in addition, a multiplet in the aromatic region corresponding to five protons of the co-ordinated benzonitrile. Variable temperature $^{31}P\{^1H\}$ nmr spectra of this complex were measured in acetone-d_6 and revealed the collapse of an AA'BB' pattern of peaks at -79°C and the formation of a sharp singlet at -55°C reflecting a fluxional process in solution as described for the analogous tetraisopropoxydiphosphazane derivative.

The infrared spectrum $[Ru_2(CO)_5(MeCN)\{\mu\text{-}(MeO)_2PN(Et)P(OMe)_2\}_2](SbF_6)_2$ (5) in the C-O stretching region is very similar to that of the analogous benzonitrile derivative. The ^1H nmr spectrum is similar to that of the parent complex but contains, in addition, a singlet at 2.75 ppm corresponding to the three protons of the co-ordinated acetonitrile. The room temperature $^{31}P\{^1H\}$ nmr spectrum of the complex in acetone-d_6 exhibits an AA'BB' pattern of peaks, centred at 137.03 ppm.

A large number of organonitrile complexes are known and the co-ordination chemistry of nitrile ligands has been reviewed.[153] The mode of co-ordination of these ligands is usually end-on through the nitrogen, although side-on bonding has been shown to occur.[154] The strength of the bond between nitriles, acetonitrile in particular, and transition metals is, in general, weak and as a consequence these ligands are readily displaced by other donor ligands under mild conditions. For example, Lewis *et al.*[155] have been able to isolate the unstable complexes $[Ru_3(CO)_{12-n}(NCMe)_n]$ (n = 1 or 2) from the low temperature reaction of $[Ru_3(CO)_{12}]$ with a 1:1 or 1:2 molar amount of trimethylamine-N-oxide, in dichloromethane in the presence of acetonitrile and to show that they react readily with phosphines and phosphites such as PPh_3 and $P(OMe)_3$ to give the compounds $[Ru_3(CO)_{12-n}L_n]$ (L = PPh_3 or $P(OMe)_3$; n = 1 or 2) in good yield. The cationic complexes $[(C_5H_5)Fe(CO)_2L]BF_4$ (L = RCN, R = Me, Et, Ph etc.) have been prepared by oxidative cleavage of $[(C_5H_5)Fe(CO)_2]_2$ in the presence of an excess of the nitrile L. The lability of the co-ordinated nitrile in these species has been demonstrated by its ready replacement by anionic nucleophiles (X^- = I^- and CN^-) or group Vb donor ligands ER_3 (E = P, R = C_6H_5, OCH_3, OC_6H_5; E = As, Sb, R = C_6H_5) affording the complexes $[(C_5H_5)Fe(CO)_2X]$ and $[(C_5H_5)Fe(CO)_2(ER_3)]^+$ in high yields.

Attempts to displace the co-ordinated nitrile in complexes of the type $[Ru_2(CO)_5(solvent)\{\mu\text{-}(RO)_2PN(Et)P(OR)_2\}_2](SbF_6)_2$ (solvent = acetonitrile or benzonitrile; R = Me or Pr^i) with neutral donor ligands such as pyridine and thioethers, or anionic ligands such as hydroxo and mercaptide ions were unsuccessful however. This indicated that the co-ordinated nitrile ligands in the above complexes are relatively strongly bound to the dicationic species and are not readily displaced. The synthesis of oxygen-donor solvento species was therefore attempted, and the ease of the displacement of these ligands by other donor ligands was investigated.

2.3 REACTION OF $[Ru_2(\mu\text{-}CO)(CO)_4\{\mu\text{-}(RO)_2PN(Et)P(OR)_2\}_2]$ WITH SILVER(I) SALTS IN KETONES, ETHERS AND NITROALKANES

2.3.1 Reaction of $[Ru_2(\mu\text{-}CO)(CO)_4\{\mu\text{-}(Pr^iO)_2PN(Et)P(OPr^i)_2\}_2]$ with $AgSbF_6$ in acetone

Addition of a twice molar amount of $AgSbF_6$ to a suspension of $[Ru_2(\mu\text{-}CO)(CO)_4\{\mu\text{-}(Pr^iO)_2PN(Et)P(OPr^i)_2\}_2]$ in acetone led to the separation of metallic silver from a pale yellow solution from which a white crystalline product was isolated in almost quantitative yield. The microanalysis of this compound was consistent with the formulation of the acetone solvento species $[Ru_2(CO)_5(Me_2CO)\{\mu\text{-}(Pr^iO)_2PN(Et)P(OPr^i)_2\}_2](SbF_6)_2$. The solid state infrared spectrum of the product in the carbonyl stretching region is similar to that found for the analogous benzonitrile solvento species apart from an additional peak at 1680 cm^{-1} assigned to the C-O stretching vibration of co-ordinated acetone; free acetone gives rise to a peak at approximately 1710 cm^{-1} while the frequencies of the C-O stretching vibrations for the co-ordinated acetone in the complexes $[Ru_2(\mu\text{-}O_2CR)_4(Me_2CO)_2]$ for R = Me, Et

and Ph occur at 1687, 1684 and 1690 cm^{-1} respectively.[156] These observations suggest that the product from the silver(I) salt reaction contains a co-ordinated acetone ligand. The $^{31}P\{^{1}H\}$ nmr spectrum of the product in acetone-d_6 exhibited two distinct sets of resonances however, a singlet at 129.42 ppm (X, Figure 2.7(a)) and an AA'BB' pattern centred at 127.45 ppm (Y, Figure 2.7(a)). It was found that on measuring this

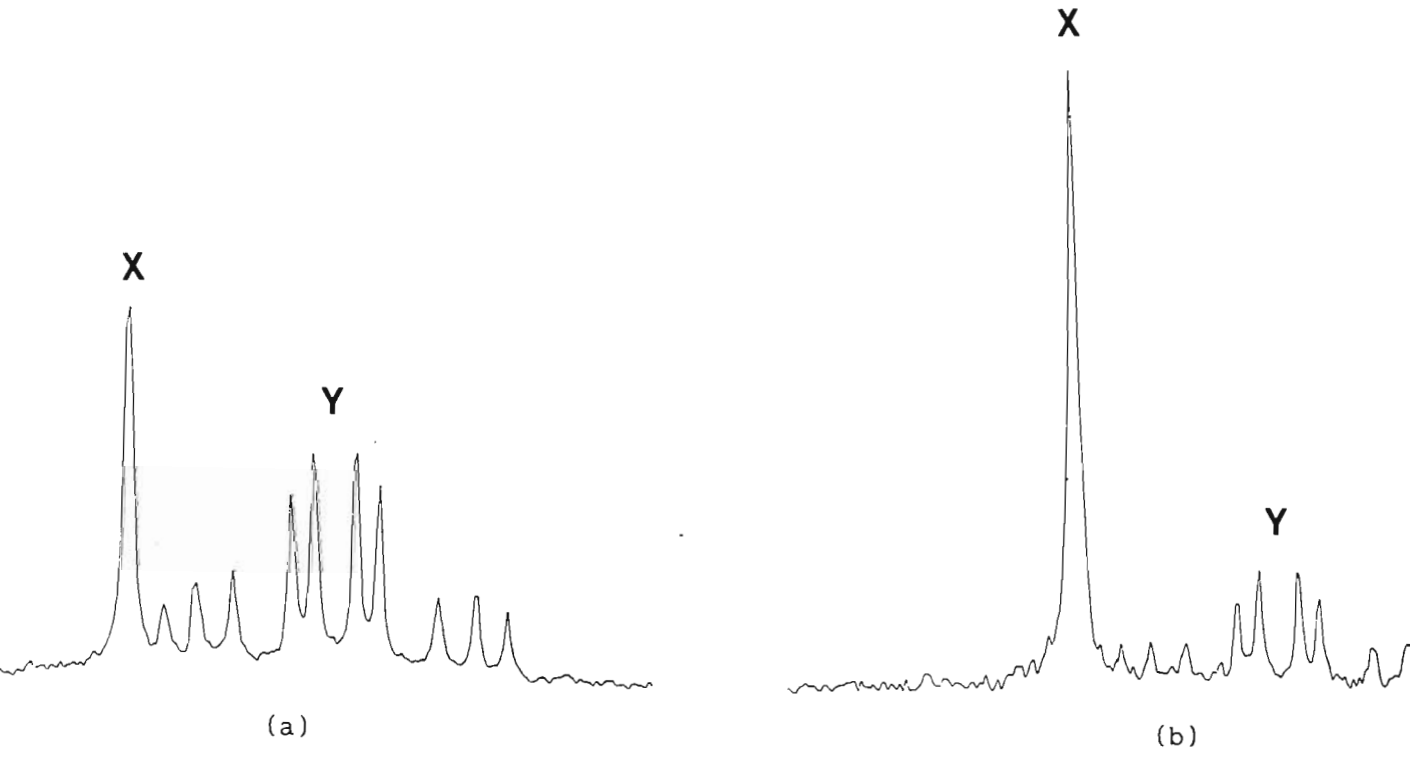

Figure 2.7: $^{31}P\{^{1}H\}$ nmr spectrum of $[Ru_2(CO)_5(H_2O)\{\mu\text{-}(Pr^iO)_2PN(Et)P\text{-}(OPr^i)_2\}_2]^{2+}$ and $[Ru_2(CO)_5(acetone)\{\mu\text{-}(Pr^iO)_2PN(Et)P(OPr^i)_2\}_2]^{2+}$ in acetone-d_6 (a) and in acetone-d_6/CD_2Cl_2 (b)

spectrum over a period of time the intensity of the singlet peak X increased while that of the AA'BB' pattern of resonances Y diminished. Low temperature $^{31}P\{^{1}H\}$ nmr studies revealed that the singlet peak X expands to an AA'BB' pattern of peaks centred at 136.90 ppm at -77°C. Two possible explanations could account for this behaviour. Firstly, the acetone solvento species may occur in two isomeric forms in solution with the acetone molecule co-ordinated in either an equatorial or in an

axial position. This would give rise to two different sets of resonances in the $^{31}P\{^{1}H\}$ nmr spectrum; the singlet at room temperature would be explained in terms of one of the isomers being involved in a fluxional process as described for the benzonitrile solvento species. Secondly, water present in trace amounts in the solution may preferentially displace the co-ordinated acetone, affording an aquo solvento species $[Ru_2(CO)_5(H_2O)\{\mu\text{-}(Pr^iO)_2PN(Et)P(OPr^i)_2\}_2](SbF_6)_2$.

In an attempt to explain the presence of two sets of resonances in the $^{31}P\{^{1}H\}$ nmr spectrum, dichloromethane, essentially a non co-ordinating solvent, was added to the above acetone-d_6 solution, thereby reducing the concentration of the acetone-d_6. The $^{31}P\{^{1}H\}$ nmr spectrum measured in this solvent mixture indicated a substantial enhancement of the singlet peak X with the accompanying reduction in the intensity of the AA'BB' pattern Y (Figure 2.7(b)). As the relative concentration of dichloromethane to acetone was increased, the corresponding relative intensity of peak X to resonance Y was also found to increase. Significantly, the $^{31}P\{^{1}H\}$ nmr spectrum of the product isolated from the above silver(I) salt reaction in acetone, measured in dichloromethane, exhibited a set of resonances at X only; the set of resonances centred at Y was absent. However, in contrast to that observed for the acetone-d_6 spectrum, where the peak at X is a singlet, this new set of resonances centred at X, has an AA'BB' pattern.

Isolation of the above product from dichloromethane affords a white crystalline material, the infrared spectrum in the carbonyl stretching region of which was essentially unchanged from that of the original product isolated from the reaction in acetone, but the peak at 1680 cm^{-1} corresponding to the carbonyl stretching mode of the co-ordinated acetone was absent. In addition, a broad peak at 3450 cm^{-1} was observed

in this spectrum.

The ^1H nmr spectrum of the dicationic acetone solvento species $[Ru_2(CO)_5(Me_2CO)\{\mu\text{-}(Pr^iO)_2PN(Et)P(OPr^i)_2\}_2](SbF_6)_2$ (**6**) measured in acetone-d_6 is essentially the same as that of the parent complex $[Ru_2(\mu\text{-}CO)(CO)_4\{\mu\text{-}(Pr^iO)_2PN(Et)P(OPr^i)_2\}_2]$ but contains in addition a complex set of resonances at 2.00 - 2.15 ppm assigned to both free and co-ordinated acetone, and a broad peak at 3.25 ppm which collapsed upon addition of D_2O. The ^1H nmr spectrum of the complex isolated from dichloromethane exhibited a broad peak at 3.62 ppm in CD_2Cl_2, the integral of which corresponded to two protons. It was possible to obtain single crystals on crystallisation of the acetone solvento species from an acetone/toluene mixture. A close examination of the crystals revealed that they occurred in two distinct geometric shapes. On mechanical separation it was found that one batch rapidly lost solvent and turned to a powder, whereas the other retained its crystallinity. A single crystal X-ray structure determination established these crystals to be the dicationic aquo solvento species $[Ru_2(CO)_5(H_2O)\{\mu\text{-}(Pr^iO)_2PN(Et)P(OPr^i)_2\}_2](SbF_6)_2$ (**7**). This species was found to be identical to the product isolated from the reaction of $[Ru_2(\mu\text{-}CO)(CO)_4\{\mu\text{-}(Pr^iO)_2PN(Et)P(OPr^i)_2\}_2]$ with $AgSBF_6$ in a THF/water mixture. The latter is discussed in further detail in Section 2.3.3 and in Chapter 3.

On the basis of the above results it is apparent that the acetone solvento species $[Ru_2(CO)_5(Me_2CO)\{\mu\text{-}(Pr^iO)_2PN(Et)P(OPr^i)_2\}_2](SbF_6)_2$ (**6**) and the aquo solvento species are present in equilibrium in acetone according to the equation:

$$[Ru_2(CO)_5(Me_2CO)\{\mu\text{-}(Pr^iO)_2PN(Et)P(OPr^i)_2\}_2]^{2+} + H_2O \rightleftharpoons [Ru_2(CO)_5(H_2O)\{\mu\text{-}(Pr^iO)_2PN(Et)P(OPr^i)_2\}_2]^{2+} + Me_2CO$$

It is also apparent that water preferentially displaces the co-ordinated acetone of the acetone solvento species, such that the acetone solvento species can only be isolated from acetone solutions containing only trace amounts of water or less. Even then it was always isolated together with small amounts of the aquo solvento species. Attempts to synthesize the acetone solvento species free of any aquo solvento species proved unsuccessful despite numerous attempts to obtain water-free acetone. The ratio of these two species could however be optimized by working under as anhydrous conditions as possible.

The $^{31}P\{^{1}H\}$ nmr spectrum of the aquo solvento species exhibits a sharp singlet in acetone-d_6 whereas in dichloromethane an AA'BB' pattern of peaks is observed. This can be explained in terms of the above equilibrium, between the acetone and aquo solvento species in acetone with the rapid exchange of the acetone and water molecules being accompanied by some fluxional process leading to the effective rapid exchange of the co-ordinated water from one ruthenium atom to the other in the dimer. This process is inhibited in dichloromethane. The rapid exchange of acetone and water is apparent from the observation that the acetone solvento species is immediately formed on dissolution of the aquo solvento species in acetone.

2.3.2 Reaction of $[Ru_2(\mu\text{-}CO)(CO)_4\{\mu\text{-}(MeO)_2PN(Et)P(OMe)_2\}_2]$ with $AgSbF_6$ in acetone

Addition of a twice molar amount of $AgSbF_6$ to an acetone solution of $[Ru_2(\mu\text{-}CO)(CO)_4\{\mu\text{-}(MeO)_2PN(Et)P(OMe)_2\}_2]$ led to the separation of metallic silver from a pale yellow solution from which a white crystalline product was isolated in almost quantitative yield, and characterized as the dicationic acetone solvento species $[Ru_2(CO)_5$-

(acetone){μ-$(MeO)_2PN(Et)P(OMe)_2$}$_2$]$(SbF_6)_2$ (8) by means of infrared and NMR spectroscopy and microanalysis.

The solid state infrared spectrum of [$Ru_2(CO)_5$(acetone){μ-$(MeO)_2PN(Et)P(OMe)_2$}$_2$]$(SbF_6)_2$ affords a similar pattern of terminal carbonyl stretching peaks as that found for the analogous tetraisopropoxydiphosphazane acetone solvento species although at slightly higher frequencies. A peak at 1652 cm^{-1} was assigned to the C-O stretch of the co-ordinated acetone. The $^{31}P\{^1H\}$ nmr spectrum of the compound in acetone-d_6 exhibits a single set of resonances of AA'BB' pattern. The ^1H nmr spectrum is essentially the same as that found for the parent complex but contains in addition a single resonance at 2.1 ppm, the integral of which corresponded to six protons. In contrast to its tetraisopropoxydiphosphazane analogue, the tetramethoxydiphosphazane solvento species is much more stable to attack by water. Only addition of a vast excess of water to an acetone solution of [$Ru_2(CO)_5$(acetone)-{μ-$(MeO)_2PN(Et)P(OMe)_2$}$_2$]$^{2+}$ resulted in the partial displacement of the co-ordinated acetone to afford the aquo solvento species. This suggests that the acetone bonds more strongly to the tetramethoxydiphosphazane dicationic species than for the corresponding tetraisopropoxydiphosphazane derivative. This is further endorsed by the lower C-O stretching frequency of the co-ordinated acetone found for the former derivative. This greater stability to attack by water would explain the presence of a single AA'BB' set of resonances in the $^{31}P\{^1H\}$ nmr spectrum of the compound, and the formation of one crystal morphology. Although well-formed crystals could be obtained, they were not suitable for single crystal X-ray diffraction studies.

2.3.3 Reaction of $[Ru_2(\mu\text{-}CO)(CO)_4\{\mu\text{-}(RO)_2PN(Et)P(OR)_2\}_2]$ (R = Me, Pr^i) with $AgSbF_6$ in THF

It was found that addition of a twice molar amount of $AgSbF_6$ to a solution of $[Ru_2(\mu\text{-}CO)(CO)_4\{\mu\text{-}(RO)_2PN(Et)P(OR)_2\}_2]$ (R = Me or Pr^i) in THF resulted in the separation of silver metal from a pale yellow solution. A white product was isolated from the solution and for both R = Me and R = Pr^i, was identified as the dicationic aquo solvento species $[Ru_2(CO)_5(H_2O)\{\mu\text{-}(RO)_2PN(Et)P(OR)_2\}_2](SbF_6)_2$, (R = Me (**9**); R = Pr^i (**7**)) as previously described. Despite using THF that had been rigorously dried according to literature procedures, the oxidation of the diruthenium species by silver(I) salts was always found to lead to the formation of the dicationic aquo solvento species, in which water, present in trace amounts in the THF solution, readily displaces the co-ordinated THF.

2.3.4 Reaction of $[Ru_2(\mu\text{-}CO)(CO)_4\{\mu\text{-}(Pr^iO)_2PN(Et)P(OPr^i)_2\}_2]$ with $AgSbF_6$ in diethyl ketone

Attempts were made to find an oxygen-donor solvent that would readily co-ordinate to the dicationic diruthenium species and that would be stable to displacement by water. Thus addition of a twice molar amount of $AgSbF_6$ to a solution of $[Ru_2(\mu\text{-}CO)(CO)_4\{\mu\text{-}(Pr^iO)_2PN(Et)P(OPr^i)_2\}_2]$ in diethyl ketone was found to lead to the separation of silver metal from a pale yellow solution from which a white crystalline product was isolated. Microanalytical results were consistent with the formulation for a diethyl ketone solvento species $[Ru_2(CO)_5(Et_2CO)\{\mu\text{-}(Pr^iO)_2PN(Et)P(OPr^i)_2\}_2](SbF_6)_2$ (**10**). The product showed a pattern of peaks in the carbonyl stretching region of the infrared spectrum typical of a dicationic pentacarbonyl species, in addition to a broad peak at 1650 cm^{-1}, assigned to the C-O stretching vibration of co-ordinated diethyl

ketone. When dissolved in dichloromethane however, the $^{31}P\{^{1}H\}$ nmr spectrum of the product exhibited two AA'BB' patterns of resonances, one centred at 125.68 ppm and the other centred at 125.00 ppm, the latter corresponding to the dicationic aquo solvento species previously described. This indicated that water displaces the co-ordinated ketone in $[Ru_2(CO)_5(Et_2CO)\{\mu\text{-}(Pr^iO)_2PN(Et)P(OPr^i)_2\}_2](SbF_6)_2$, although to a lesser extent than the displacement of acetone in the corresponding acetone solvento species, and that a vast excess of diethyl ketone is required to inhibit this displacement by water.

2.3.5 Reaction of $[Ru_2(\mu\text{-}CO)(CO)_4\{\mu\text{-}(Pr^iO)_2PN(Et)P(OPr^i)_2\}_2]$ with $AgSbF_6$ in nitromethane

Addition of a twice molar amount of $AgSbF_6$ to a solution of $[Ru_2(\mu\text{-}CO)(CO)_4\{\mu\text{-}(Pr^iO)_2PN(Et)P(OPr^i)_2\}_2]$ in nitromethane led to the separation of silver metal from a pale yellow solution from which a white crystalline material was isolated. Microanalysis results for the crystalline product were consistent with the expected values for a nitromethane solvento species $[Ru_2(CO)_5(CH_3NO_2)\{\mu\text{-}(Pr^iO)_2PN(Et)P(OPr^i)_2\}_2](SbF_6)_2$ (**11**). The infrared spectrum of this compound indicated it to be a new product with a band pattern in the carbonyl stretching region typical of that found for a dicationic solvento species. On dissolution in dichloromethane however, water displaced the co-ordinated solvent, presumably nitromethane, affording the dicationic aquo solvento species.

2.4 REACTION OF $[Ru_2(CO)_5(solvent)\{\mu\text{-}(RO)_2PN(Et)P(OR)_2\}_2]^{2+}$ (solvent = acetone or water; R = Me, Pr^i) WITH NEUTRAL DONOR LIGANDS

The solvent molecules in complexes of the type $[Ru_2(CO)_5(solvent)$-

$\{\mu\text{-}(RO)_2PN(Et)P(OR)_2\}_2]^{2+}$ (solvent = acetone or water; R = Me or Pr^i) are weakly co-ordinated and as such these complexes are excellent precursors for a wide range of products, as indeed has been found in some earlier preliminary investigations.

2.4.1 Reaction of $[Ru_2(CO)_5(solvent)\{\mu\text{-}(RO)_2PN(Et)P(OR)_2\}_2]^{2+}$ with organonitriles

It has been found that nitriles are capable of displacing oxygen-donor solvents, and in particular addition of an equimolar amount or excess of acetonitrile or benzonitrile to a solution of $[Ru_2(CO)_5(solvent)\text{-}\{\mu\text{-}(RO)_2PN(Et)P(OR)_2\}_2]^{2+}$ (solvent = acetone and H_2O; R = Me or Pr^i) results in the quantitative displacement of the co-ordinated acetone or water by the nitrile, affording the nitrile solvento species $[Ru_2(CO)_5\text{-}(R'CN)\{\mu\text{-}(RO)_2PN(Et)P(OR)_2\}_2]^{2+}$ (R = Me or Pr^i; R' = Me, Ph) previously described. The identity of the products were confirmed using infrared and $^{31}P\{^1H\}$ nmr spectroscopy.

2.4.2 Reaction of $[Ru_2(CO)_5(solvent)\{\mu\text{-}(RO)_2PN(Et)P(OR)_2\}_2]^{2+}$ with thioethers and sulphides

Not surprisingly, thioethers and sulphides were also found to displace the oxygen-donor solvent from $[Ru_2(CO)_5(solvent)\{\mu\text{-}(RO)_2PN(Et)P\text{-}(OR)_2\}_2]^{2+}$. Thus addition of an equimolar amount of tetrahydrothiophene (SC_4H_8) to a mixture of the acetone and aquo solvento species $[Ru_2(CO)_5\text{-}(solvent)\{\mu\text{-}(Pr^iO)_2PN(Et)P(OPr^i)_2\}_2](SbF_6)_2$ in acetone resulted in the immediate and quantitative displacement of the co-ordinated solvent by the tetrahydrothiophene. Microanalysis of the product was consistent with a complex of formula $[Ru_2(CO)_5(SC_4H_8)\{\mu\text{-}(Pr^iO)_2PN(Et)P(OPr^i)_2\}_2]\text{-}(SbF_6)_2$ (**12**). The band pattern of the C-O stretching peaks in the

infrared spectrum of the white crystals isolated were characteristic of a dicationic pentacarbonyl species. The $^{31}P\{^{1}H\}$ nmr spectrum of the product measured in CD_2Cl_2 showed an AA'BB' pattern of peaks, centred at 122.07 ppm. The ^{1}H nmr spectrum in CD_2Cl_2 is essentially the same as that of the parent complex but contains, in addition, multiplets at 2.07 - 2.22 ppm and 3.07 - 3.24 ppm corresponding to the eight protons of the co-ordinated tetrahydrothiophene. The structure of this compound was established X-ray crystallographically, and is illustrated in Figure 2.8. The structure is very similar to that of the analogous benzonitrile derivative $[Ru_2(CO)_5(PhCN)\{\mu\text{-}(Pr^iO)_2PN(Et)P(OPr^i)_2\}_2](SbF_6)_2$ with the tetrahydrothiophene co-ordinating equatorially, and with the cation adopting a staggered conformation {P(1)-Ru(1)-Ru(2)-P(4) and P(2)-Ru(1)- Ru(2)-P(3) torsion angles of 26.6 and 30.5° respectively}. A ruthenium-ruthenium distance of 2.926(2)Å is similar to that of the analogous benzonitrile solvento species and represents a formal metal-metal bond. A ruthenium-sulphur distance of 2.487(6)Å is slightly longer than those found for the pentaammineruthenium(III)-thioether complexes $[Ru(NH_3)_5L]^{3+}$ [157] {L = SC_4H_8, $S(CH_3)(C_2H_5)$ or $S(CH_3)_2$} {Ru-S distances: 2.367(1), 2,372(1) and 2.384(2)Å respectively}.

A slight excess of dimethyl sulphide (SMe_2) was added to a mixture of the tetraisopropoxydiphosphazane acetone and aquo solvento species $[Ru_2(CO)_5(solvent)\{\mu\text{-}(Pr^iO)_2PN(Et)P(OPr^i)_2\}_2]^{2+}$ (solvent = acetone or water) in acetone. A white crystalline material which was isolated from the reaction mixture had microanalytical results consistent with the formulation $[Ru_2(CO)_5(SMe_2)\{\mu\text{-}(Pr^iO)_2PN(Et)P(OPr^i)_2\}_2](SbF_6)_2$ (**13**). However, it was established by monitoring the reaction by means of $^{31}P\{^{1}H\}$ nmr spectroscopy that an excess of dimethyl sulphide was required for the rapid and quantitative displacement of the co-ordinated solvent. Under these conditions, a single set of peaks of AA'BB'

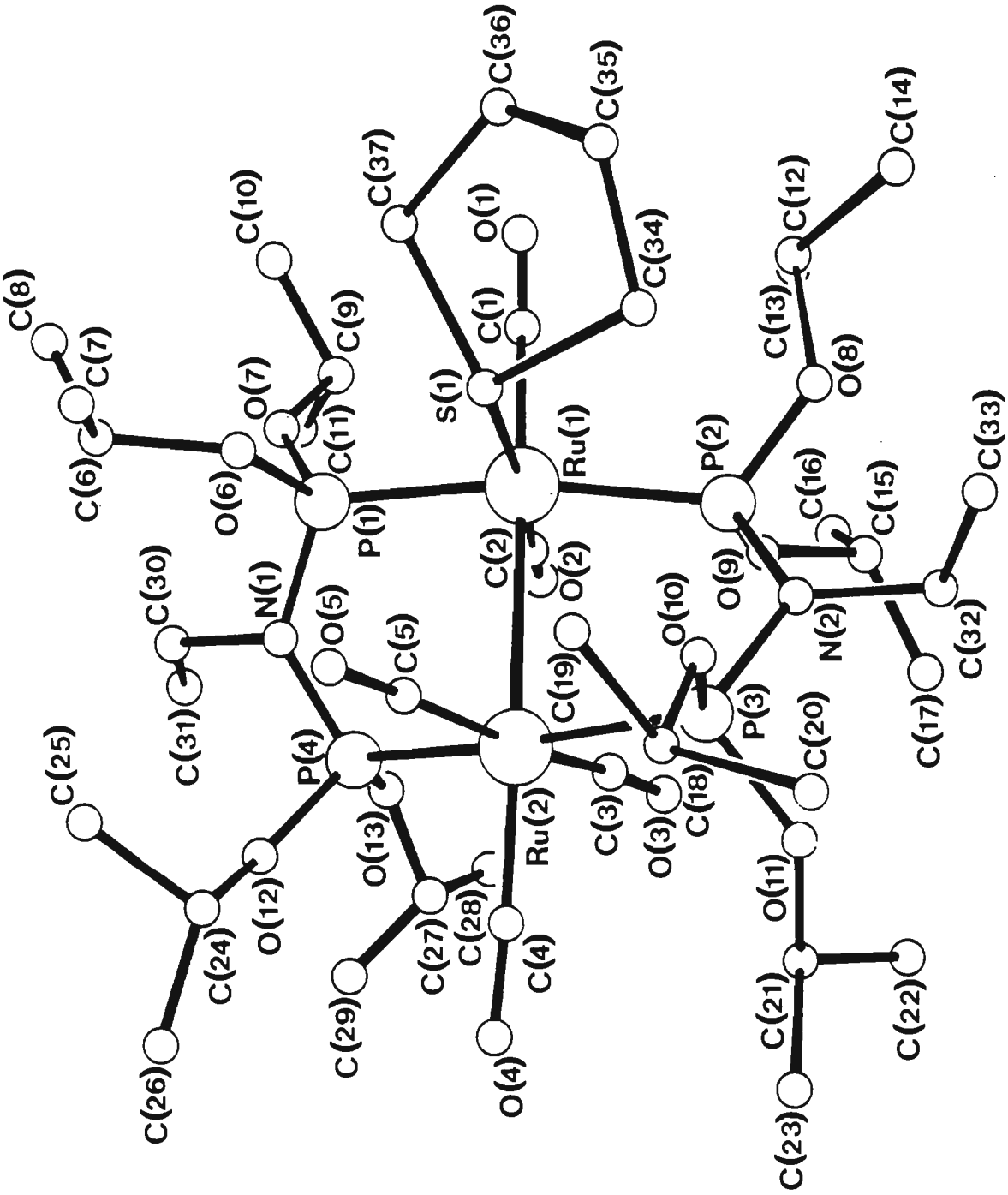

Figure 2.8: Structure of $[Ru_2(CO)_5(SC_4H_8)\{\mu\text{-}(Pr^iO)_2PN(Et)P(OPr^i)_2\}_2]^{2+}$

pattern centred at 121.17 ppm in CD_2Cl_2 was observed in the $^{31}P\{^1H\}$ nmr spectrum. On the other hand, the $^{31}P\{^1H\}$ nmr spectrum of $[Ru_2(CO)_5(SMe_2)\{\mu\text{-}(Pr^iO)_2PN(Et)P(OPr^i)_2\}_2]$ measured in CD_2Cl_2 contained in addition to the AA'BB' pattern of peaks centred at 121.17 ppm, an AA'BB' set of resonances centred at 125.00 ppm assigned to the phosphorus atoms of the aquo solvento species. The ^1H nmr spectrum of this material in CD_2Cl_2 was essentially the same as that found for the parent complex but had in addition two singlets at 2.56 and 2.62 ppm corresponding to both free and co-ordinated dimethylsulphide. It was thus apparent that the dimethyl sulphide in $[Ru_2(CO)_5(SMe_2)\{\mu\text{-}(Pr^iO)_2PN(Et)P(OPr^i)_2\}_2]^{2+}$ is partially displaced by water and/or acetone in solution and that, as described above, an excess of dimethyl sulphide is required for the isolation of $[Ru_2(CO)_5(SMe_2)\{\mu\text{-}(Pr^iO)_2PN(Et)P(OPr^i)_2\}_2](SbF_6)_2$ in a pure state.

The reaction of the solvento species $[Ru_2(CO)_5(solvent)\{\mu\text{-}(Pr^iO)_2PN(Et)\text{-}P(OPr^i)_2\}_2](SbF_6)_2$ (solvent = acetone and/or water) with hydrogen sulphide was also investigated. It was found that addition of $[Ru_2(CO)_5(solvent)\{\mu\text{-}(Pr^iO)_2PN(Et)P(OPr^i)_2\}_2](SbF_6)_2$ to a saturated solution of H_2S in acetone resulted in a colour change from clear to pale yellow. A $^{31}P\{^1H\}$ nmr spectrum of this solution measured within a short period of time, exhibited a singlet and a much weaker AA'BB' set of resonances; the resonances corresponding to the aquo and acetone solvento species were absent. An infrared spectrum of this solution in the C-O stretching region region revealed the presence of a mixture of penta- and tetracarbonyl species of the type $[Ru_2X(CO)_5\{\mu\text{-}(Pr^iO)_2PN(Et)\text{-}P(OPr^i)_2\}_2]^+$ and $[Ru_2(\mu\text{-}X)(CO)_4\{\mu\text{-}(Pr^iO)_2PN(Et)P(OPr^i)_2\}_2]^+$. The intensity of the singlet in the $^{31}P\{^1H\}$ nmr spectrum decreased while that of the AA'BB' pattern of peaks increased over a period of time, and to eventually become the sole resonance. The infrared spectrum of this

solution exhibited a typical four-line pattern in the C-O stretching region, with the frequencies of the bands indicating the compound present to be monocationic. Addition of potassium hydroxide to this solution resulted in the formation of a neutral compound which was isolated and identified as the sulphide-bridged species $[Ru_2(\mu\text{-}S)(CO)_4\{\mu\text{-}(Pr^iO)_2PN(Et)P(OPr^i)_2\}_2]$. This compound has been previously synthesized by addition of sodium sulphide to the dichloro species $[Ru_2Cl_2(CO)_4\{\mu\text{-}(Pr^iO)_2PN(Et)P(OPr^i)_2\}_2]$. The synthesis of the analogous tetramethoxydiphosphazane sulphide-bridged species $[Ru_2(\mu\text{-}S)(CO)_4\{\mu\text{-}(MeO)_2PN(Et)P(OMe)_2\}_2]$ has been achieved in the same way. Protonation of this species with $HBF_4.OEt_2$ was shown to afford $[Ru_2(\mu\text{-}SH)(CO)_4\{\mu\text{-}(MeO)_2PN(Et)P(OMe)_2\}_2]BF_4$. The above spectroscopic results are interpreted in terms of hydrogen sulphide displacing the solvent from $[Ru_2(CO)_5(solvent)\{\mu\text{-}(Pr^iO)_2PN(Et)P(OPr^i)_2\}_2]^{2+}$ to form a hydrogen sulphide species $[Ru_2(CO)_5(H_2S)\{\mu\text{-}(Pr^iO)_2PN(Et)P(OPr^i)_2\}_2]^{2+}$ which spontaneously deprotonates to form a pentacarbonyl HS^- species $[Ru_2(CO)_5(SH)\{\mu\text{-}(Pr^iO)_2PN(Et)P(OPr^i)_2\}_2]SbF_6$ (**14**). This compound slowly decarbonylates in solution affording the tetracarbonyl derivative $[Ru_2(\mu\text{-}SH)(CO)_4\{\mu\text{-}(Pr^iO)_2PN(Et)P(OPr^i)_2\}_2]SbF_6$ (**15**). This compound exhibits similar spectroscopic properties to those of the analogous tetramethoxydiphosphazane species $[Ru_2(\mu\text{-}SH)(CO)_4\{\mu\text{-}(MeO)_2PN(Et)P(OMe)_2\}_2]BF_4$, mentioned above, and may be deprotonated further by addition of an appropriate base, affording the sulphide-bridged complex $[Ru_2(\mu\text{-}S)(CO)_4\{\mu\text{-}(Pr^iO)_2PN(Et)P(OPr^i)_2\}_2]$ (**16**). This reaction pathway is illustrated in the scheme below.

The synthesis of $[Ru_2(\mu\text{-}S)(CO)_4\{\mu\text{-}(Pr^iO)_2PN(Et)P(OPr^i)_2\}_2]$ may also be achieved by addition of sulphur to the co-ordinatively unsaturated species $[Ru_2(CO)_4\{\mu\text{-}(Pr^iO)_2PN(Et)P(OPr^i)_2\}_2]$ (see Chapter 6).

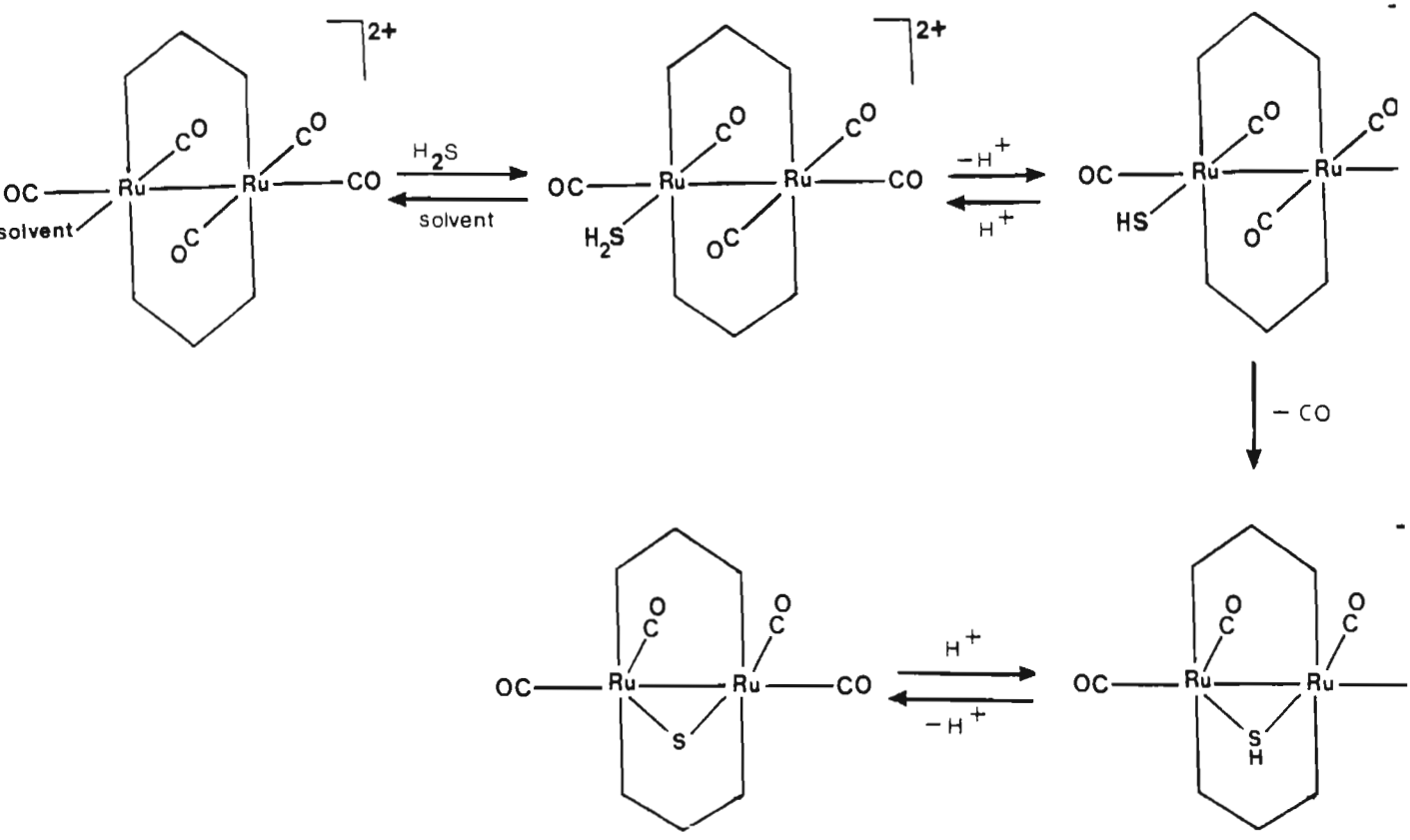

Scheme 2.3

Significantly, addition of an excess of tetrahydrothiophene or dimethyl sulphide to the tetramethoxydiphosphazane acetone solvento species $[Ru_2(CO)_5(acetone)\{\mu\text{-}(MeO)_2PN(Et)P(OMe)_2\}_2]^{2+}$ in acetone did not result in the displacement of the co-ordinated acetone by the thioether. This is, of course, in direct contrast to that found for the analogous tetra-isopropoxydiphosphazane solvento species and may be explained in terms of the acetone in $[Ru_2(CO)_5(acetone)\{\mu\text{-}(MeO)_2PN(Et)P(OMe)_2\}_2]^{2+}$ binding more strongly to the dinuclear centre than that of acetone in the analogous tetraisopropoxydiphosphazane species.

Surprisingly, addition of an excess of thiophene (SC_4H_4) to the solvento species $[Ru_2(CO)_5(solvent)\{\mu\text{-}(Pr^iO)_2PN(Et)P(OPr^i)_2\}_2]^{2+}$ (solvent = acetone and/or water) in acetone did not result in a ligand-substitution

reaction. This may, however, be explained in terms of the donor pair of electrons of the sulphur atom of thiophene being more associated with the π-orbitals of the carbon atoms such that this ligand is a poorer σ-donor ligand than the related tetrahydrothiophene. Less surprisingly, is that addition of an excess amount of carbon disulphide and phenyl-isothiocyanate also did not result in the displacement of the co-ordinated solvent in $[Ru_2(CO)_5(solvent)\{\mu\text{-}(Pr^iO)_2PN(Et)P(OPr^i)_2\}_2]^{2+}$.

2.4.3 Reaction of $[Ru_2(CO)_5(solvent)\{\mu\text{-}(RO)_2PN(Et)P(OR)_2\}_2]^{2+}$ (solvent = acetone or water; R = Me or Pr^i) with water and alcohols

The addition of an excess of the protic solvents H_2O, MeOH or EtOH to the solvento species $[Ru_2(CO)_5(solvent)\{\mu\text{-}(RO)_2PN(Et)P(OR)_2\}_2]^{2+}$ (solvent = acetone or water; R = Me or Pr^i) was found to result in the formation of the complexes $[Ru_2(CO)_5(H_2O)\{\mu\text{-}(RO)_2PN(Et)P(OR)_2\}_2]^{2+}$ or $[Ru_2(CO)_4\{\mu\text{-}\eta^2\text{-}OC(OR')\}\{\mu\text{-}(RO)_2PN(Et)P(OR)_2\}_2]^{+}$ (R' = Me or Et) respectively. The characterization of these complexes is discussed in detail in Chapter 3.

The reaction of the solvento species $[Ru_2(CO)_5(solvent)\{\mu\text{-}(RO)_2PN(Et)P\text{-}(OR)_2\}_2](SbF_6)_2$ (R = Me or Pr^i; solvent = acetone and/or water) with phenol was also investigated but in this case no reaction was observed even when a vast excess of phenol was employed.

2.4.4 Reaction of $[Ru_2(CO)_5(solvent)\{\mu\text{-}(RO)_2PN(Et)P(OR)_2\}_2]^{2+}$ (solvent = acetone or water; R = Me or Pr^i) with pyridine and related ligands

The reactions of the oxygen-donor solvento species $[Ru_2(CO)_5(solvent)\text{-}\{\mu\text{-}(RO)_2PN(Et)P(OR)_2\}_2](SbF_6)_2$ (R = Me or Pr^i; solvent = acetone and/or

water) with pyridine and related ligands was undertaken. It was found that addition of an equimolar amount or excess of pyridine to a solution of the dicationic aquo solvento species $[Ru_2(CO)_5(H_2O)\{\mu\text{-}(Pr^iO)_2PN(Et)P(OPr^i)_2\}_2]^{2+}$ in dichloromethane or THF resulted in the formation of a monocationic species $[Ru_2(CO)_4\{\mu\text{-}\eta^2\text{-}OC(OH)\}\{\mu\text{-}(Pr^iO)_2PN(Et)P(OPr^i)_2\}_2]^{+}$ *(vide infra)* as a consequence of the addition of pyridine effecting the deprotonation of the co-ordinated water, and the -OH group migrating onto a carbon of an adjacent carbonyl ligand. This is schematically illustrated below, and is discussed further in Chapter 3.

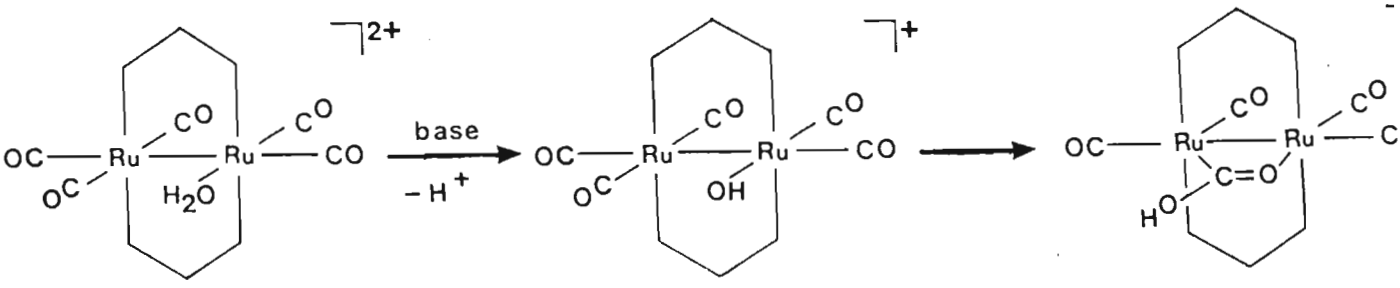

Scheme 2.4

The addition of an equimolar amount of pyridine to the dicationic solvento species $[Ru_2(CO)_5(solvent)\{\mu\text{-}(Pr^iO)_2PN(Et)P(OPr^i)_2\}_2]^{2+}$ (solvent = acetone and water) in acetone was monitored by means of $^{31}P\{^1H\}$ nmr and infrared spectroscopy, and it was found that in this solvent a mixture of two compounds is formed. In particular, the $^{31}P\{^1H\}$ nmr spectrum of the mixture exhibited an AA'BB' pattern of peaks corresponding to the monocationic species $[Ru_2(CO)_4\{\mu\text{-}\eta^2\text{-}OC(OH)\}\{\mu\text{-}(Pr^iO)_2PN(Et)P(OPr^i)_2\}_2]^{+}$ which formed as a result of the deprotonation of the dicationic aquo solvento species present in solution, by the pyridine. A second AA'BB' pattern of peaks of roughly equal intensity to the former was also observed in this spectrum. The two products could be separated by solvent extraction techniques and the second product was characterized as the dicationic pyridine solvento species $[Ru_2(CO)_5(NC_5H_5)\{\mu\text{-}(Pr^iO)_2P\text{-}$

$N(Et)P(OPr^i)_2\}_2](SbF_6)_2$ (**17**) which formed as a result of pyridine displacing the co-ordinated acetone from $[Ru_2(CO)_5(acetone)\{\mu\text{-}(Pr^iO)_2PN(Et)P(OPr^i)_2\}_2]^{2+}$. The infrared spectrum of the white crystalline material in the C-O stretching region is typical of that of a dicationic pentacarbonyl species. The $^{31}P\{^1H\}$ nmr spectrum of the product in acetone-d_6 exhibits an AA'BB' pattern of peaks centred at 126.86 ppm. This spectrum remained unchanged over a period of time indicating the stability of the complex to attack by acetone or water. The ^1H nmr spectrum in acetone-d_6 is essentially the same as that of the parent complex but contains an additional multiplet in the region 8.34 - 9.19 ppm corresponding to five protons of the co-ordinated pyridine.

Significantly, addition of an equimolar or excess amount of pyridine to an acetone solution of the tetramethoxydiphosphazane acetone solvento derivative $[Ru_2(CO)_5(solvent)\{\mu\text{-}(MeO)_2PN(Et)P(OMe)_2\}_2]^{2+}$ was observed to result in the sole formation of the monocationic product $[Ru_2(CO)_4\{\mu\text{-}\eta^2\text{-}OC(OH)\}\{\mu\text{-}(MeO)_2PN(Et)P(OMe)_2\}_2]^+$ with no dicationic pyridine solvento species being detected.

The reaction of the solvento species $[Ru_2(CO)_5(solvent)\{\mu\text{-}(Pr^iO)_2PN(Et)P(OPr^i)_2\}_2]^{2+}$ (solvent = acetone and water) with an equimolar amount of 4,4'-bipyridine in acetone was found to proceed in the same way as that for pyridine. The formation of the monocationic species $[Ru_2(CO)_4\{\mu\text{-}\eta^2\text{-}OC(OH)\}\{\mu\text{-}(Pr^iO)_2PN(Et)P(OPr^i)_2\}_2]^+$ and the dicationic species $[Ru_2(CO)_5(4,4'\text{-bipyridine})\{\mu\text{-}(Pr^iO)_2PN(Et)P(OPr^i)_2\}_2]^{2+}$ was confirmed using $^{31}P\{^1H\}$ nmr and infrared spectroscopy. It is sterically possible for the 4,4'-bipyridine ligand to bridge two dinuclear centres but the formation of a complex of this type was eliminated on the basis of the ^1H nmr spectral evidence which indicated the presence of one 4,4'-bipyridine ligand per dinuclear fragment.

2.4.5 Reaction of $[Ru_2(CO)_5(solvent)\{\mu\text{-}(RO)_2PN(Et)P(OR)_2\}_2]^{2+}$ (R = Me or Pr^i; solvent = acetone and/or water) with tertiary phosphines and phosphites.

Tertiary phosphines and phosphites have been shown to readily displace both oxygen- and nitrogen-donor co-ordinated solvents, but treatment of the solvento species $[Ru_2(CO)_5(solvent)\{\mu\text{-}(RO)_2PN(Et)P(OR)_2\}_2]^{2+}$ (R = Me or Pr^i; solvent = acetone and/or water) with an excess of trimethylphosphine or trimethylphosphite at room temperature, did not lead to any reaction, however.

2.5 REACTION OF $[Ru_2(CO)_5(solvent)\{\mu\text{-}(RO)_2PN(Et)P(OR)_2\}_2]^{2+}$ (solvent = acetone and H_2O; R = Me or Pr^i) WITH ANIONIC LIGANDS

The reaction of the tetramethoxydiphosphazane acetone solvento species $[Ru_2(CO)_5(acetone)\{\mu\text{-}(MeO)_2PN(Et)P(OMe)_2\}_2]^{2+}$ with halide, hydride and cyanide anions has previously been shown to afford products of the type $[Ru_2(CO)_5X\{\mu\text{-}(MeO)_2PN(Et)P(OMe)_2\}_2]^{+}$ (X = Cl, Br, I, H or CN) and $[Ru_2(\mu\text{-}X)(CO)_4\{\mu\text{-}(MeO)_2PN(Et)P(OMe)_2\}_2]^{+}$ (X = Cl, Br or I), in almost quantitative yield. It has also been demonstrated by co-workers that the reaction of the dicationic aquo or acetone solvento species with $TCNQ^{\bullet-}$ or $TCNE^{\bullet-}$ anions affords the hexafluoroantimonate salt of $[Ru_2(CO)_5(TCNX)\{\mu\text{-}(RO)_2PN(Et)P(OR)_2\}_2]^{+}$ (X = Q or E; R = Me or Pr^i) in which the $TCNQ^{\bullet-}$ or $TCNE^{\bullet-}$ ligand is co-ordinated to the dinuclear species by σ-donation of a lone pair of electrons on a nitrogen atom.

The reactions of the dicationic solvento species with anionic ligands has been further investigated. Preliminary investigations showed however, that reaction of the dicationic solvento species with anions that may function as a base results largely in the deprotonation of the

co-ordinated water in the aquo species $[Ru_2(CO)_5(H_2O)\{\mu\text{-}(RO)_2PN(Et)P(OR)_2\}_2]^{2+}$. This proved to be a major obstacle in pursuing the synthesis of novel pentacarbonyl and tetracarbonyl complexes of the type $[Ru_2(CO)_5X\{\mu\text{-}(RO)_2PN(Et)P(OR)_2\}_2]^{+}$ and $[Ru_2(\mu\text{-}X)(CO)_4\{\mu\text{-}(RO)_2PN(Et)P(OR)_2\}_2]^{+}$ (X = anionic ligand) using this approach.

2.5.1 Reaction of $[Ru_2(CO)_5(solvent)\{\mu\text{-}(Pr^iO)_2PN(Et)P(OPr^i)_2\}_2]^{2+}$ (solvent = acetone and water) with iodide ions

In demonstrating the use of the solvento species as a precursor for the synthesis of a wide range of products, the reactivity of $[Ru_2(CO)_5(solvent)\{\mu\text{-}(Pr^iO)_2PN(Et)P(OPr^i)_2\}_2]^{2+}$ (solvent = acetone and water) towards iodide ions, in particular, was investigated in detail.

Treatment of the solvento species $[Ru_2(CO)_5(solvent)\{\mu\text{-}(Pr^iO)_2PN(Et)P(OPr^i)_2\}_2]^{2+}$ (solvent = acetone and water) with an equimolar amount of tetrabutylammonium iodide in acetone was shown to result in a change in colour of the solution from clear to yellow. The $^{31}P\{^1H\}$ nmr spectrum of the solution revealed two AA'BB' patterns of peaks, which is interpreted in terms of both the axial and equatorial isomeric forms of the iodo species $[Ru_2(CO)_5I\{\mu\text{-}(Pr^iO)_2PN(Et)P(OPr^i)_2\}_2]^{+}$ (**18**) being present. This observation is consistent with that observed for the direct iodination of the parent complex $[Ru_2(\mu\text{-}CO)(CO)_4\{\mu\text{-}(Pr^iO)_2PN(Et)P(OPr^i)_2\}_2]$, previously described. Halo complexes of the type $[Ru_2X(CO)_5\{\mu\text{-}(RO)_2PN(Et)P(OR)_2\}_2]^{+}$ have been found to decarbonylate in solution with the rate of decarbonylation increasing along the series X = Cl < Br < I, with the tetraisopropoxydiphosphazane derivatives decarbonylating more readily than their tetramethoxydiphosphazane analogues, and with the decarbonylation being accelerated in polar, co-ordinating solvents such as dimethyl sulphoxide and acetone or under thermal or photochemical

conditions or by the use of the decarbonylating agent, trimethylamine-N-oxide dihydrate. Thus monitoring the decarbonylation process of $[Ru_2I(CO)_5\{\mu\text{-}(Pr^iO)_2PN(Et)P(OPr^i)_2\}_2]^+$ by means of $^{31}P\{^1H\}$ nmr spectroscopy, resulted in the detection within 24 hours of a singlet which corresponded with the tetracarbonyl iodo-bridged species $[Ru_2(\mu\text{-}I)(CO)_4\{\mu\text{-}(Pr^iO)_2PN(Et)P(OPr^i)_2\}_2]^+$ (**19**), in addition to the above two AA'BB' patterns of peaks. Addition of a slight excess of trimethylamine-N-oxide dihydrate accelerated this decarbonylation process such that all of the pentacarbonyl iodo species was converted to the tetracarbonyl iodo-bridged species $[Ru_2(\mu\text{-}I)(CO)_4\{\mu\text{-}(Pr^iO)_2PN(Et)P(OPr^i)_2\}_2]^+$ within 30 minutes. Addition of an equimolar amount of tetrabutylammonium iodide and trimethylamine-N-oxide dihydrate to the latter species resulted in the formation of a neutral product identified as the tricarbonyl diiodo derivative $[Ru_2I(\mu\text{-}I)(CO)_3\{\mu\text{-}(Pr^iO)_2PN(Et)P(OPr^i)_2\}_2]$ (**20**), by means of $^{31}P\{^1H\}$ nmr and infrared spectroscopy. This complex has been synthesized previously by irradiation of the parent complex $[Ru_2(\mu\text{-}CO)(CO)_4\{\mu\text{-}(Pr^iO)_2PN(Et)P(OPr^i)_2\}_2]$ in hexane in the presence of excess diiodomethane for five hours. The synthetic route to this complex *via* the solvento species is advantageous in that higher yields are obtained in a more rapid reaction, and under milder conditions.

Addition of an equimolar amount of tetrabutylammonium iodide to a solution of the pentacarbonyl iodo-species $[Ru_2I(CO)_5\{\mu\text{-}(Pr^iO)_2PN(Et)P(OPr^i)_2\}_2]^+$ in acetone, followed by the addition of an excess amount of $Me_3NO.2H_2O$, also resulted in the formation of a neutral product. This was extracted into toluene and characterized as the tetracarbonyl diiodo species $[Ru_2I_2(CO)_4\{\mu\text{-}(Pr^iO)_2PN(Et)P(OPr^i)_2\}_2]$ (**21**). A singlet was observed in the $^{31}P\{^1H\}$ nmr spectrum of this compound which is indicative of a symmetrical structure and the compound occurring as either the axial,axial isomer (Figure 2.9(a)) or the equatorial,equatorial

isomer (Figure 2.9(b)).

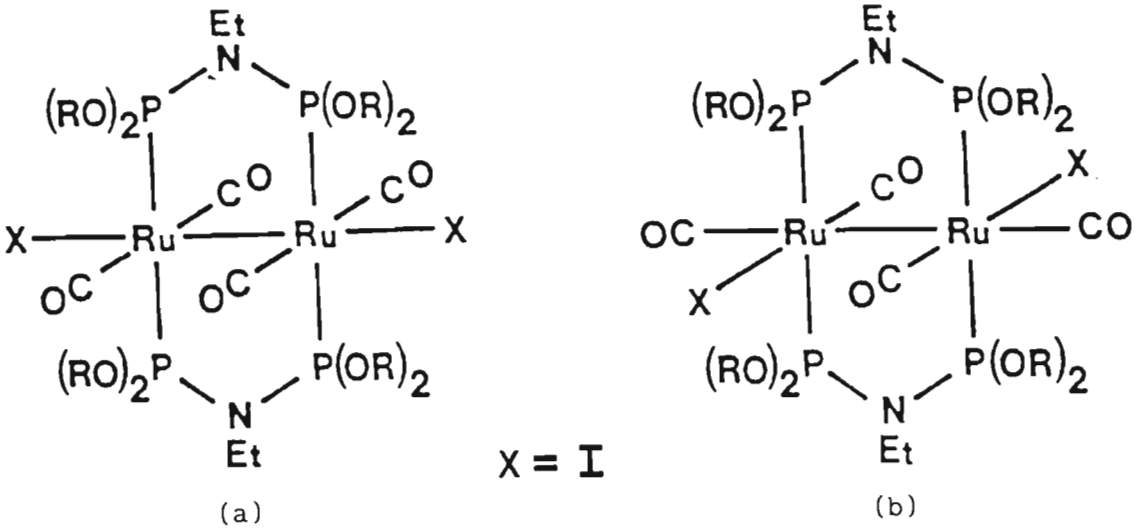

Figure 2.9: $[Ru_2I_2(CO)_4\{\mu\text{-}(RO)_2PN(Et)P(OR)_2\}_2]$; axial,axial isomer (a) and equatorial,equatorial isomer (b)

The band pattern in the C-O stretching region of the infrared spectrum of $[Ru_2I_2(CO)_4\{\mu\text{-}(Pr^iO)_2PN(Et)P(OPr^i)_2\}_2]$ is substantially different from that of $[Ru_2Cl_2(CO)_4\{\mu\text{-}(RO)_2PN(Et)P(OR)_2\}_2]$, which is interpreted in terms of these compounds occurring in different isomeric forms. A crystallographic investigation has shown that the dichloro compound occurs as the axial,axial isomer, and on this basis it is proposed that $[Ru_2I_2(CO)_4\{\mu\text{-}(Pr^iO)_2PN(Et)P(OPr^i)_2\}_2]$ is present as the equatorial, equatorial isomer. The ^1H nmr spectrum of the complex is essentially the same as that of the parent complex $[Ru_2(\mu\text{-}CO)(CO)_4\{\mu\text{-}(Pr^iO)_2PN(Et)P\text{-}(OPr^i)_2\}_2]$. Microanalysis for C, H, N, P and I were consistent with the proposed formulation. A field desorption mass spectrum exhibited a peak at 1124, which is the expected value for $[Ru_2(\mu\text{-}I)(CO)_4\{\mu\text{-}(Pr^iO)_2PN(Et)\text{-}P(OPr^i)_2\}_2]^+$. This ion is presumed to have formed as a result of a loss of an iodide ion from $[Ru_2I_2(CO)_4\{\mu\text{-}(Pr^iO)_2PN(Et)P(OPr^i)_2\}_2]$ in the ionization process. In contrast to the dichloro species, which degrades to $[Ru_2(\mu\text{-}Cl)(CO)_4\{\mu\text{-}(RO)_2PN(Et)P(OR)_2\}_2]^+$ (R = Me or Pr^i) in polar solvents, the diiodo species was found to be stable in both non-polar and polar solvents. Significantly, it could not be decarbonylated further

to afford the tricarbonyl diiodo species $[Ru_2I(\mu\text{-}I)(CO)_3\{\mu\text{-}(Pr^iO)_2PN(Et)P(OPr^i)_2\}_2]$ under thermal or photochemical conditions or with the use of excess $Me_3NO.2H_2O$. This diiodo species may also be synthesized by addition of a twice molar amount of iodine to the parent complex $[Ru_2(\mu\text{-}CO)(CO)_4\{\mu\text{-}(Pr^iO)_2PN(Et)P(OPr^i)_2\}_2]$, followed by the addition of an excess amount of $Me_3NO.2H_2O$, to afford the product in almost quantitative yield. Inherent crystal twinning prevented the structural confirmation of the tetracarbonyl diiodide derivative by means of X-ray crystallography.

The reactivity patterns of the tetramethoxydiphosphazane species $[Ru_2(\mu\text{-}CO)(CO)_4\{\mu\text{-}(MeO)_2PN(Et)P(OMe)_2\}_2]$ and the mixed-ligand derivative $[Ru_2(\mu\text{-}CO)(CO)_4\{\mu\text{-}(MeO)_2PN(Et)P(OMe)_2\}\{\mu\text{-}(Pr^iO)_2PN(Et)P(OPr^i)_2\}]$ with iodine and iodide ions were essentially the same as that for the tetraisopropoxydiphosphazane analogue described above. Some minor differences were observed however: the addition of $Me_3NO.2H_2O$ to the pentacarbonyl iodo-species $[Ru_2I(CO)_5\{\mu\text{-}(MeO)_2PN(Et)P(OMe)_2\}_2]^+$ in the presence of iodide ions afforded the diiodo species $[Ru_2I_2(CO)_4\{\mu\text{-}(MeO)_2PN(Et)P(OMe)_2\}_2]$ (**22**) as the major product, as found for the analogous tetraisopropoxydiphosphazane derivative reaction, as well as a small amount of the tricarbonyl species $[Ru_2I(\mu\text{-}I)(CO)_3\{\mu\text{-}(MeO)_2PN(Et)P(OMe)_2\}_2]$ (**23**). This is explained in terms of the two possible reaction pathways described previously. The addition of $Me_3NO.2H_2O$ to the mixed-ligand iodo-species $[Ru_2I(CO)_5\{\mu\text{-}(MeO)_2PN(Et)P(OMe)_2\}\{\mu\text{-}(Pr^iO)_2PN(Et)P(OPr^i)_2\}]^+$ in the presence of iodide ions afforded a mixture of both the axial,axial and the equatorial,equatorial isomers, $[Ru_2I_2(CO)_4\{\mu\text{-}(MeO)_2PN(Et)P(OMe)_2\}\{\mu\text{-}(Pr^iO)_2PN(Et)P(OPr^i)_2\}]$ (**24**), on the basis of the presence of two sets of AA'BB' peaks in its $^{31}P\{^1H\}$ nmr spectrum.

The pathways for the formation of $[Ru_2I_2(CO)_4\{\mu\text{-}(RO)_2PN(Et)P(OR)_2\}_2]$ and

$[Ru_2I(\mu\text{-}I)(CO)_3\{\mu\text{-}(RO)_2PN(Et)P(OR)_2\}_2]$ (R = Me, Et or Pr^i) from $[Ru_2(CO)_5(solvent)\{\mu\text{-}(RO)_2PN(Et)P(OR)_2\}_2]^{2+}$ are illustrated in Scheme 2.5. The scheme and the associated chemistry indicates that the nature of the product/s formed is dependent upon the order of addition of the halide ions and trimethylamine-N-oxide dihydrate as well as the rate of decarbonylation of the pentacarbonyl iodo species $[Ru_2X(CO)_5\{\mu\text{-}(RO)_2PN(Et)P(OR)_2\}_2]^+$ which, in turn, is dependent upon the factors described previously.

2.5.2 Reaction of $[Ru_2(CO)_5(solvent)\{\mu\text{-}(RO)_2PN(Et)P(OR)_2\}_2]^{2+}$ (solvent = acetone and water; R = Me or Pr^i) with hydroxide and alkoxide ions

The reactions of equimolar amounts of hydroxide or alkoxide ions $R'O^-$ (R' = H, Me or Et), with the solvento species $[Ru_2(CO)_5(solvent)\{\mu\text{-}(RO)_2PN(Et)P(OR)_2\}_2]^{2+}$ (solvent = acetone and water; R = Me or Pr^i) in acetone were monitored by means of $^{31}P\{^1H\}$ nmr and infrared spectroscopy. The reactions were found to lead to the formation of hydroxy- or alkoxycarbonyl complexes of the type $[Ru_2(CO)_4\{\mu\text{-}\eta^2\text{-}OC(OR')\}\{\mu\text{-}(RO)_2PN(Et)P(OR)_2\}_2]^+$ (R' = H, Me or Et) *(vide infra)*. This reactivity reflects the susceptibility of a carbonyl ligand of the solvento species $[Ru_2(CO)_5(solvent)\{\mu\text{-}(RO)_2PN(Et)P(OR)_2\}_2]^{2+}$ to nucleophilic attack, particularly by hard bases such as hydroxide or alkoxide ions.

2.5.3 Reaction of $[Ru_2(CO)_5(solvent)\{\mu\text{-}(RO)_2PN(Et)P(OR)_2\}_2]^{2+}$ (solvent = acetone and water; R = Me or Pr^i) with isothiocyanate and mercaptide ions

The reaction of equimolar amounts of the solvento species $[Ru_2(CO)_5(solvent)\{\mu\text{-}(Pr^iO)_2PN(Et)P(OPr^i)_2\}_2]^{2+}$ (solvent = acetone and water) with

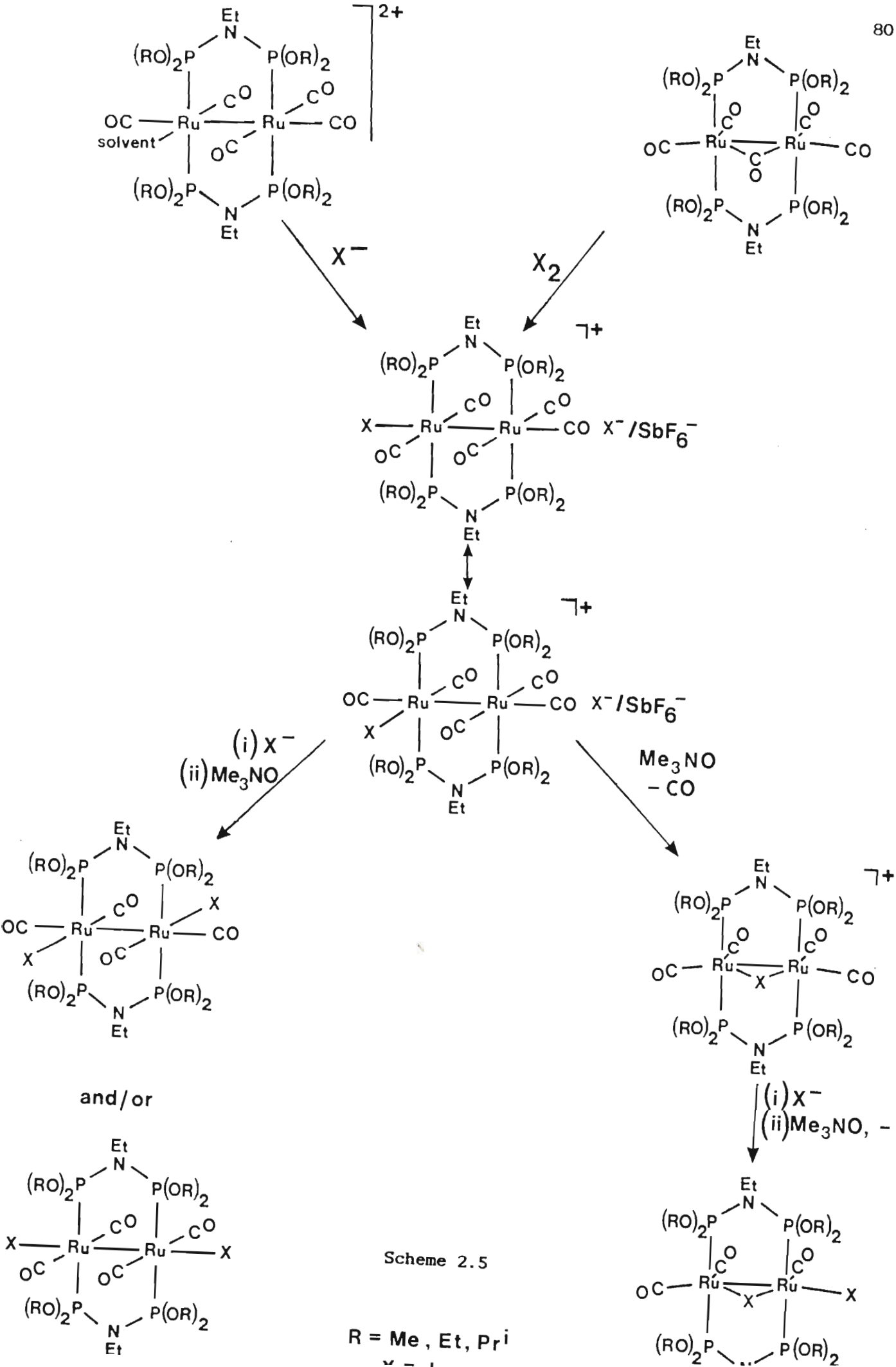

Scheme 2.5

R = Me , Et, Pr^i

sodium isothiocyanate (NaSCN) in acetone resulted in a change in the colour of the solution from clear to yellow. A $^{31}P\{^{1}H\}$ nmr spectrum of the solution revealed two sets of peaks of AA'BB' pattern, one corresponding to the hydroxycarbonyl species $[Ru_2(CO)_4\{\mu\text{-}\eta^2\text{-}OC(OH)\}\{\mu\text{-}(Pr^iO)_2PN(Et)P(OPr^i)_2\}_2]^+$ and the other to a monocationic species presumed to be $[Ru_2(CO)_5(NCS)\{\mu\text{-}(Pr^iO)_2PN(Et)P(OPr^i)_2\}_2]^+$ in which the thiocyanate ion had displaced the co-ordinated acetone from the solvento species. No attempts were made to isolate and fully characterize this product.

The treatment of the solvento species $[Ru_2(CO)_5(solvent)\{\mu\text{-}(Pr^iO)_2PN(Et)P(OPr^i)_2\}_2](SbF_6)_2$ (solvent = acetone and water) in acetone, with an equimolar amount of sodium phenyl mercaptide (NaSPh) was found to result in an immediate colour change of the solution from colourless to pale yellow. A $^{31}P\{^{1}H\}$ nmr spectrum of this solution again revealed two sets of peaks of AA'BB' pattern, one corresponding to the hydroxycarbonyl species $[Ru_2(CO)_4\{\mu\text{-}\eta^2\text{-}OC(OH)\}\{\mu\text{-}(Pr^iO)_2PN(Et)P(OPr^i)_2\}_2]^+$ and the other to a monocationic species later established to be the pentacarbonyl mercaptide species $[Ru_2(CO)_5(SPh)\{\mu\text{-}(Pr^iO)_2PN(Et)P(OPr^i)_2\}_2]^+$ (**26**) (see Section 2.6). Within a short period of time a singlet appeared in this spectrum which increased in intensity relative to that of the AA'BB' pattern of peaks associated with $[Ru_2(CO)_5(SPh)\{\mu\text{-}(Pr^iO)_2PN(Et)P(OPr^i)_2\}_2]^+$. As discussed above, this is as a result of the decarbonylation of this pentacarbonyl species to the tetracarbonyl mercaptide-bridged species $[Ru_2(CO)_4(\mu\text{-}SPh)\{\mu\text{-}(Pr^iO)_2PN(Et)P(OPr^i)_2\}_2]^+$ (**27**) (see Section 2.6).

2.5.4 Reaction of $[Ru_2(CO)_5(solvent)\{\mu\text{-}(RO)_2PN(Et)P(OR)_2\}_2]^{2+}$ (solvent = acetone and water) with acetate ions

The reaction of an equimolar amount of $AgOOCCH_3$ or $NaOOCCH_3$ with the solvento species $[Ru_2(CO)_5(solvent)\{\mu\text{-}(RO)_2PN(Et)P(OR)_2\}_2]^{2+}$ (solvent = acetone or water; R = Me or Pr^i) in acetone was found to afford the tetracarbonyl carboxylate-bridged species $[Ru_2(CO)_4(\mu\text{-}OOCCH_3)\{\mu\text{-}(RO)_2PN(Et)P(OR)_2\}_2]^+$ *(vide infra)* together with a small amount of $[Ru_2(CO)_4\{\mu\text{-}OC(OH)\}\{\mu\text{-}(RO)_2PN(Et)P(OR)_2\}_2]^+$ in the reaction involving $NaOOCCH_3$. There was no evidence for the formation of the pentacarbonyl pendant-acetato species $[Ru_2(CO)_5(OOCCH_3)\{\mu\text{-}(Pr^iO)_2PN(Et)P(OPr^i)_2\}_2]^+$. This contrasts with the reaction of the solvento species $[Ru_2(CO)_5(solvent)\{\mu\text{-}(Pr^iO)_2PN(Et)P(OPr^i)_2\}_2]^{2+}$ (solvent = acetone or water) with acetic acid which affords the pentacarbonyl acetato species $[Ru_2(CO)_5(OOCCH_3)\{\mu\text{-}(Pr^iO)_2PN(Et)P(OPr^i)_2\}_2]^+$ *(vide infra)*. As discussed above, the carbonyl groups of the solvento species $[Ru_2(CO)_5(solvent)\{\mu\text{-}(RO)_2PN(Et)P(OR)_2\}_2]^{2+}$ are susceptible to nucleophilic attack by hard nucleophiles. Thus a possible mechanism for the reaction of the solvento species with acetate ions involves the direct attack of an acetate on a co-ordinated carbon monoxide ligand. This step is followed by a decarbonylation process and the displacement of a co-ordinated solvent, as illustrated in pathway A in Scheme 2.6. An alternative mechanism involves the direct substitution of a carbonyl ligand of the solvento species, followed by a displacement of the solvent by the co-ordinated acetate ligand, as illustrated in pathway B in Scheme 2.6. A mechanism involving the direct displacement of the solvent by the acetate anion is eliminated on the basis that the pentacarbonyl pendant-acetato species $[Ru_2(CO)_5(OOCCH_3)\{\mu\text{-}(Pr^iO)_2PN(Et)P(OPr^i)_2\}_2]^+$ can only be decarbonylated under photochemical conditions, as discussed in section 2.6.2.

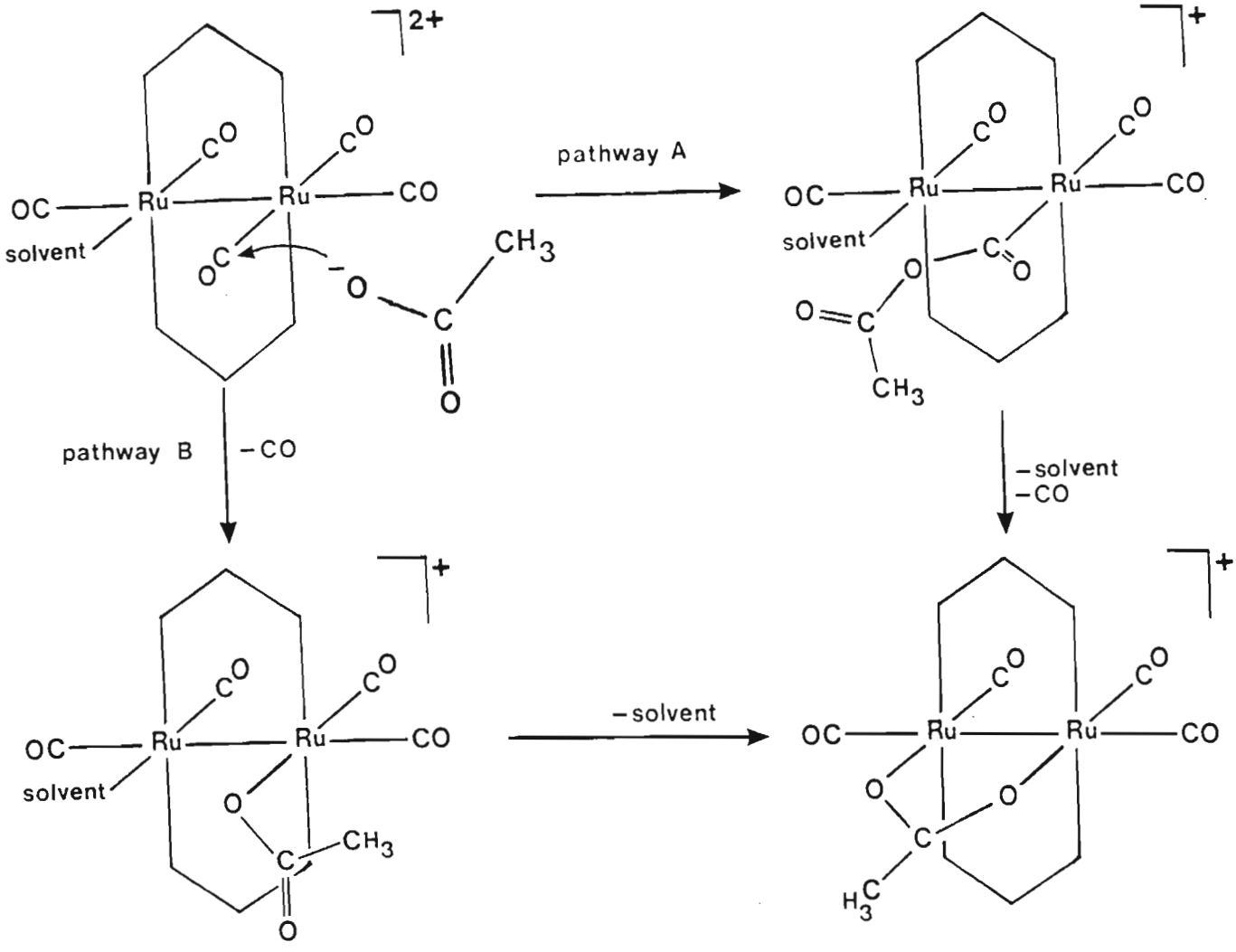

Scheme 2.6

In contrast to that observed above, the addition of an equimolar amount of $AgOOCCF_3$ to a mixture of the acetone and aquo solvento species $[Ru_2(CO)_5(solvent)\{\mu\text{-}(RO)_2PN(Et)P(OR)_2\}_2]^{2+}$ (solvent = acetone or water; R = Me or Pr^i) in acetone was found to lead to the formation of a penta-carbonyl carboxylate species *viz.* $[Ru_2(CO)_5(\mu\text{-}OOCCF_3)\{\mu\text{-}(RO)_2PN(Et)P\text{-}(OR)_2\}_2]^+$ (R = Me or Pr^i). This difference is explained in terms of the trifluoroacetate anion being more polarisable than its hard acetate counterpart and the site of nucleophilic attack by the former being at the metal itself thereby leading to the displacement of the co-ordinated solvent, as illustrated in Scheme 2.7 below.

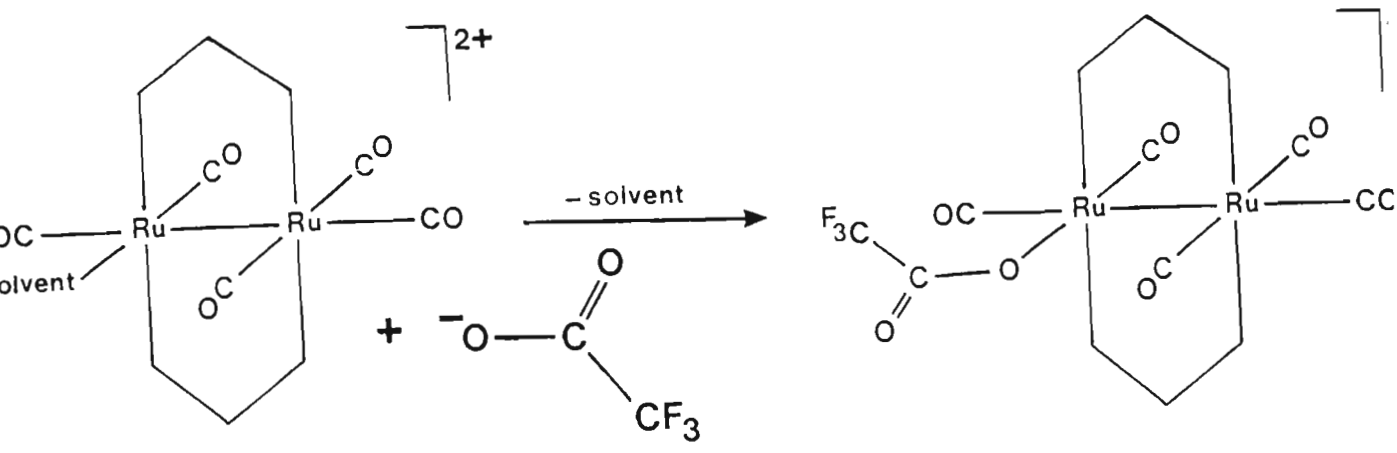

Scheme 2.7

The reaction of the dicationic solvento species with anionic ligands that may function as a base proved to be far more complex than originally envisaged, and it was concluded that an alternative synthetic route to penta- and tetracarbonyl complexes of the type $[Ru_2A(CO)_5\{\mu\text{-}(RO)_2PN(Et)P(OR)_2\}_2]^+$ and $[Ru_2(\mu\text{-}A)(CO)_4\{\mu\text{-}(RO)_2PN(Et)P(OR)_2\}_2]^+$ (A = anionic ligand) was required.

2.6 REACTION OF $[Ru_2(CO)_5(solvent)\{\mu\text{-}(RO)_2PN(Et)P(OR)_2\}_2]^{2+}$ (solvent = acetone and water; R = Me or Pr^i) WITH ACIDS CONTAINING A POTENTIALLY CO-ORDINATING CONJUGATE BASE

From the results discussed above, it became apparent that in order to replace the solvent molecule in $[Ru_2(CO)_5(solvent)\{\mu\text{-}(RO)_2PN(Et)P\text{-}(OR)_2\}_2]^{2+}$ softer, more polarisable Lewis bases were required. Initial investigations revealed that the addition of an excess amount of an acid having a potentially co-ordinating conjugate base to the dicationic solvento species resulted in the displacement of the co-ordinated solvent by the acid, followed by the ready deprotonation of the co-ordinated acid, affording penta- and possibly tetracarbonyl complexes of the type $[Ru_2X(CO)_5\{\mu\text{-}(RO)_2PN(Et)P(OR)_2\}_2]^+$ and $[Ru_2(\mu\text{-}X)(CO)_4\{\mu\text{-}(RO)_2PN(Et)P\text{-}$

$(OR)_2\}_2]^+$ (X = anionic ligand such as PhS^- or CH_3COO^- respectively), in almost quantitative yield. This approach circumvents the problems involved in the addition of a hard base to the solvento species.

2.6.1 Reaction of $[Ru_2(CO)_5(solvent)\{\mu\text{-}(RO)_2PN(Et)P(OR)_2\}_2]^{2+}$ (solvent = acetone and water) with phenyl mercaptan

The room temperature reaction of equimolar amounts of the solvento species $[Ru_2(CO)_5(solvent)\{\mu\text{-}(Pr^iO)_2PN(Et)P(OPr^i)_2\}_2](SbF_6)_2$ (solvent = acetone or water) and phenyl mercaptan in acetone resulted in an immediate change in colour of the solution from clear to pale yellow. The infrared spectrum of the solution exhibited a pattern of peaks in the C-O stretching region typical of a mixture of monocationic pentacarbonyl and tetracarbonyl derivatives, while the $^{31}P\{^1H\}$ nmr spectrum exhibited an AA'BB' pattern of peaks, and a singlet which increased in intensity over a period of time, and which eventually became the sole peak in the spectrum. The compound giving rise to this singlet was isolated and characterized as the mercaptide-bridged species $[Ru_2(\mu\text{-}SPh)(CO)_4\{\mu\text{-}(Pr^iO)_2PN(Et)P(OPr^i)_2\}_2]SbF_6$ (**27**). The infrared spectrum of this compound exhibited a four-line pattern in the C-O stretching region typical of a monocationic tetracarbonyl species while the $^{31}P\{^1H\}$ nmr spectrum measured in CD_2Cl_2 exhibited a sharp singlet at 129.93 ppm, as described above. The ^1H nmr spectrum was essentially the same as that of the parent complex but contained an additional multiplet at 7.14 - 7.43 ppm corresponding to the five protons of the bridging phenyl mercaptide ligand. On the basis of the above spectroscopic evidence, it is proposed that the formation of $[Ru_2(\mu\text{-}SPh)(CO)_4\text{-}\{\mu\text{-}(Pr^iO)_2PN(Et)P(OPr^i)_2\}_2]^+$ occurs via the intermediates shown in Scheme 2.8.

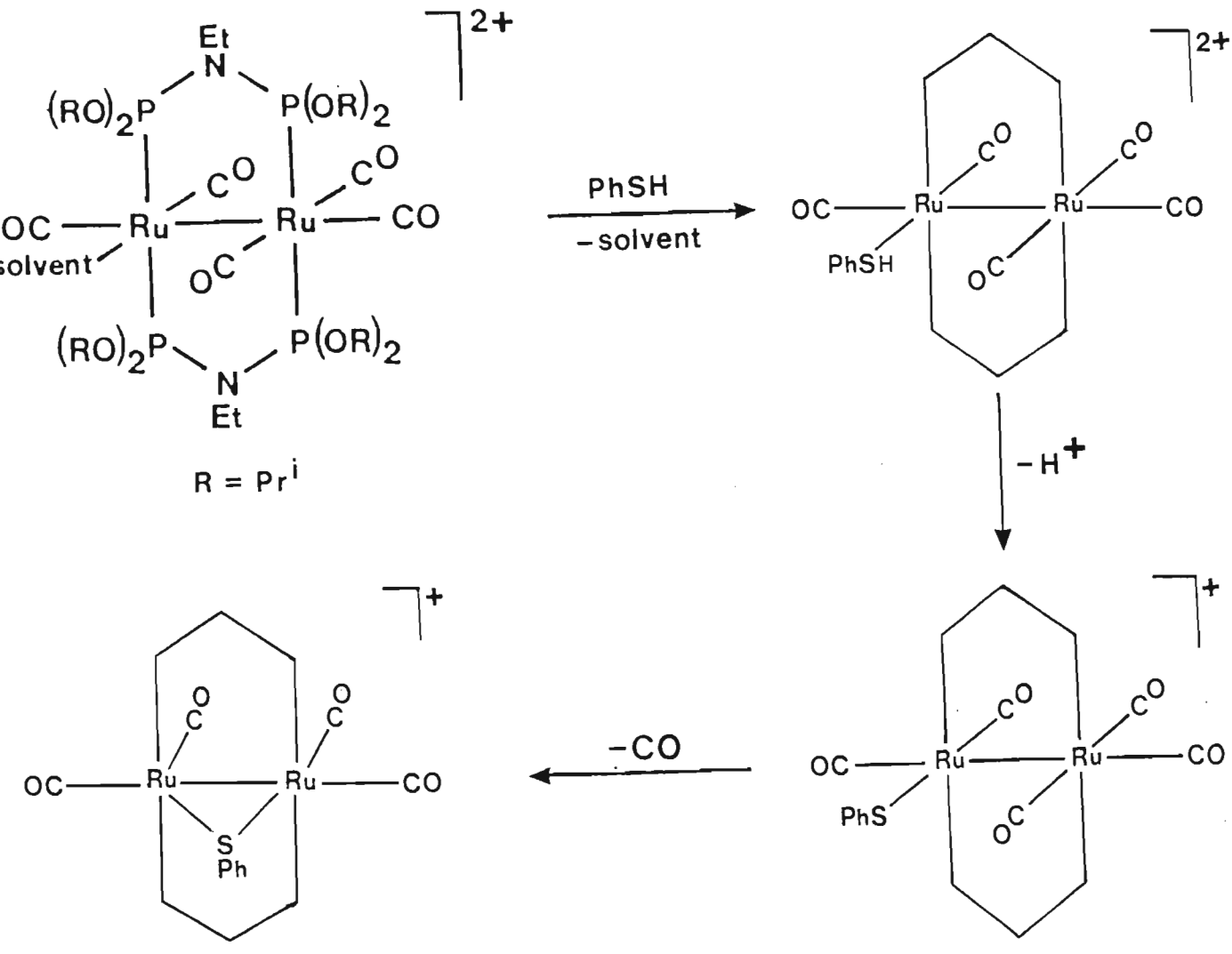

Scheme 2.8

The synthesis of the related tetramethoxydiphosphazane mercaptide-bridged species $[Ru_2(\mu\text{-SPh})(CO)_4\{\mu\text{-}(MeO)_2PN(Et)P(OMe)_2\}_2]PF_6$ has previously been achieved by addition of phenyl mercaptan to the hydrido species $[Ru_2(CO)_5H\{\mu\text{-}(MeO)_2PN(Et)P(OMe)_2\}_2]PF_6$, in the presence of HPF_6, in THF. Because of the inability to obtain single crystals of the hexafluoroanitmonate salt $[Ru_2(\mu\text{-SPh})(CO)_4\{\mu\text{-}(Pr^iO)_2PN(Et)P(OPr^i)_2\}_2]SbF_6$ (**27**) a single crystal structure determination was carried out on $[Ru_2(\mu\text{-SPh})(CO)_4\{\mu\text{-}(MeO)_2PN(Et)P(OMe)_2\}_2]PF_6$ which confirmed the presence of a bridging mercaptide-ligand, illustrated in in Figure 2.10. In contrast to $[Ru_2(CO)_5(PhCN)\{\mu\text{-}(Pr^iO)_2PN(Et)P(OPr^i)_2\}_2]^{2+}$ and $[Ru_2(CO)_5(SC_4H_8)\{\mu\text{-}$

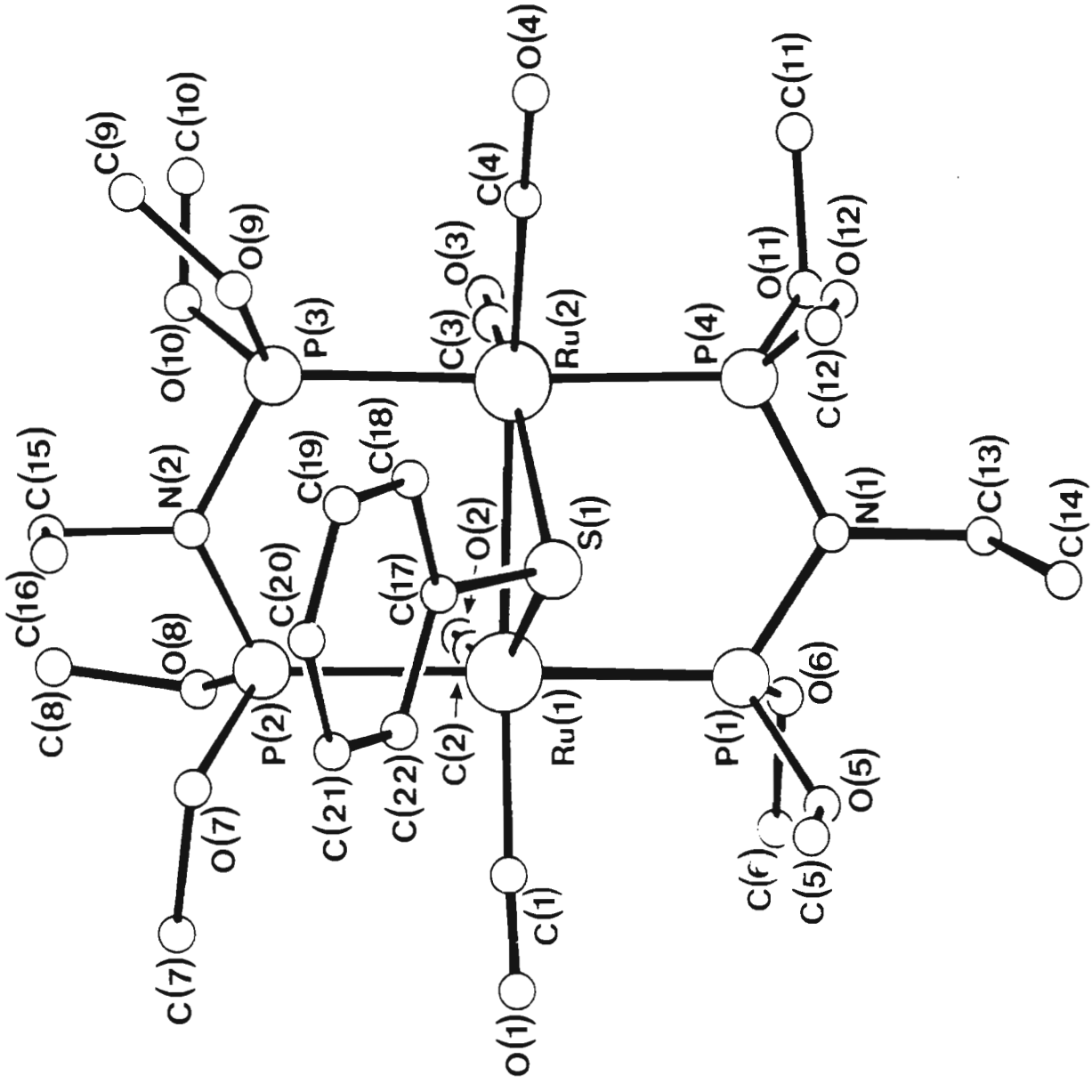

Figure 2.10: Structure of $[Ru_2(\mu\text{-SPh})(CO)_4\{\mu\text{-}(MeO)_2PN(Et)P(OMe)_2\}_2]^+$

$(Pr^iO)_2PN(Et)P(OPr^i)_2\}_2]^{2+}$, this cation adopts an eclipsed conformation as reflected by P(1)-Ru(1)-Ru(2)-P(4) and P(2)-Ru(1)-Ru(2)-P(3) torsion angles of 2.10 and 1.69° respectively, with the two ruthenium atoms bridged by the phenylmercapto ligand and separated by a distance of 2.796(1)Å.

2.6.2 Reaction of $[Ru_2(CO)_5(solvent)\{\mu-(RO)_2PN(Et)P(OR)_2\}_2]^{2+}$ (solvent = acetone and water) with carboxylic acids

In an attempt to understand the contrasting behaviour of $[Ru_2(CO)_5(solvent)\{\mu-(RO)_2PN(Et)P(OR)_2\}_2]^{2+}$ (solvent = acetone or water) towards harder and softer nucleophiles, the solvento species was reacted with a range of carboxylic acids; the reaction of this species with harder carboxylate anions is discussed in Section 2.5.4 and in Chapter 3.

An excess of acetic acid (CH_3COOH) was thus added to the solvento species $[Ru_2(CO)_5(solvent)\{\mu-(Pr^iO)_2PN(Et)P(OPr^i)_2\}_2](SbF_6)_2$ (solvent = acetone or water) in acetone. An infrared spectrum of the resultant solution afforded a band pattern in the C-O stretching region typical of a pentacarbonyl species with the frequencies of the constituent peaks being more typical of a dicationic than of a monocationic species. Furthermore, the $^{31}P\{^1H\}$ nmr spectrum revealed a singlet peak, of chemical shift typical of a dicationic pentacarbonyl species. This spectral evidence is interpreted in terms of the formation of an acetic acid species $[Ru_2(CO)_5(HOOCCH_3)\{\mu-(Pr^iO)_2PN(Et)P(OPr^i)_2\}_2]^{2+}$ resulting from the displacement of the co-ordinated solvent of the solvento species, by the acetic acid. Attempts to isolate this acetic acid adduct $[Ru_2(CO)_5(HOOCCH_3)\{\mu-(Pr^iO)_2PN(Et)P(OPr^i)_2\}_2](SbF_6)_2$ were unsuccessful because water was found to partially displace the co-ordinated acetic acid in the absence of excess acetic acid. An excess

of pyridine was added to the solution from which a white crystalline product was isolated and was characterized as the monocationic pentacarbonyl acetate species, $[Ru_2(CO)_5(OOCCH_3)\{\mu\text{-}(Pr^iO)_2PN(Et)P(OPr^i)_2\}_2]\text{-}SbF_6$ (**28**). The infrared spectrum of the compound exhibits a pattern of peaks in the C-O stretching region, typical of a monocationic pentacarbonyl derivative, as well as an additional broad peak at 1610 cm^{-1}, assigned to the acetate carbonyl stretching vibration. The $^{31}P\{^1H\}$ nmr spectrum exhibits an AA'BB' pattern of peaks centred at 128.02 ppm while the ^1H nmr spectrum is essentially the same as that of the parent complex with an additional peak at 1.93 ppm in $CDCl_3$ corresponding to the three protons of the acetate ligand.

An excess of formic acid (HCOOH) was also added to a mixture of the acetone and aquo solvento species $[Ru_2(CO)_5(solvent)\{\mu\text{-}(Pr^iO)_2PN(Et)P\text{-}(OPr^i)_2\}_2]^{2+}$ (solvent = acetone or water) in acetone and the mixture stirred for one hour. The $^{31}P\{^1H\}$ nmr spectrum of the solution exhibited a singlet, assigned to the dicationic formic acid adduct $[Ru_2(CO)_5(HOOCH)\{\mu\text{-}(Pr^iO)_2PN(Et)P(OPr^i)_2\}_2]^{2+}$. An excess of pyridine was added to this compound in acetone and a product characterized as the monocationic formate species $[Ru_2(CO)_5(OOCH)\{\mu\text{-}(Pr^iO)_2PN(Et)P(OPr^i)_2\}_2]\text{-}SbF_6$ (**29**) was isolated from the resultant solution. The infrared spectrum in the terminal C-O stretching region of this compound is similar to that of the analogous acetate derivative, and contains a broad peak at 1620 cm^{-1} assigned to the carbonyl stretching vibration of the co-ordinated formate. The $^{31}P\{^1H\}$ nmr spectrum in acetone-d_6 exhibits an AA'BB' pattern of peaks centred at 128.35 ppm, consistent with an asymmetric structure. Evidence for the presence of a formate group was confirmed by the presence of a triplet centred at 7.98 ppm in the $\{^1H\}$ nmr spectrum of this species in $CDCl_3$ corresponding to the proton of the co-ordinated formate, the triplet arising from long-range

coupling to the two phosphorus atoms. In addition, a downfield peak at 167.82 ppm was observed in the ^{13}C $\{^1H\}$ nmr spectrum of this species and this was shown to result from a primary carbon by a DEPT experiment, consistent with the presence of a formate ligand.

Interestingly, a rhodium A-frame hydride complex $[Rh_2(\mu\text{-}H)(CO)_2(\mu\text{-}dppm)_2]^+$ has been shown to undergo reaction with carbon dioxide to yield the bridging formate derivative $[Rh_2(CO)_2(\mu\text{-}OOCH)(\mu\text{-}dppm)_2]^+$. Reaction of this complex with CO occurs with concomitant expulsion of CO_2 and is thought to transpire *via* a change in formate co-ordination from bridging to terminal, followed by decarboxylation through a β-elimination step. This is illustrated schematically below. The ter-

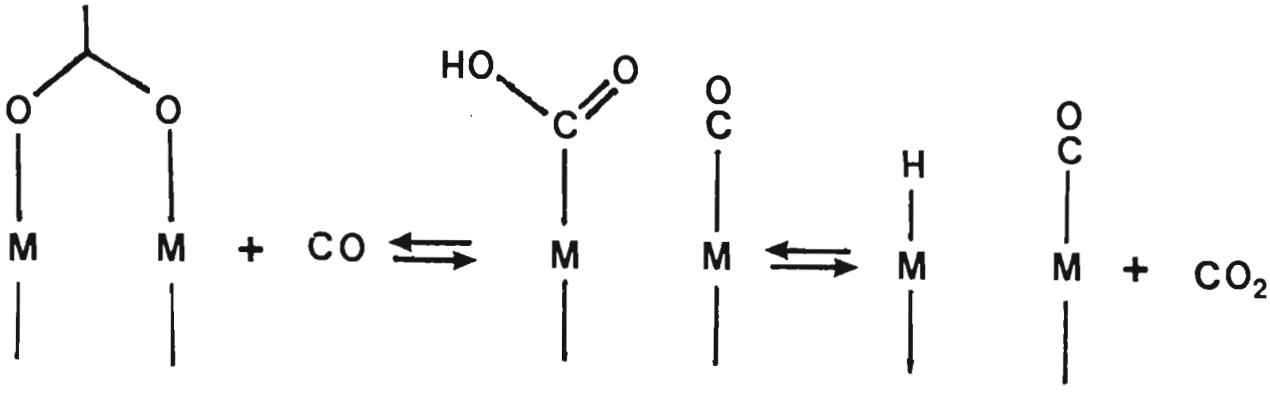

Scheme 2.9

minally co-ordinated formate in $[Ru_2(CO)_5(OOCH)\{\mu\text{-}(Pr^iO)_2PN(Et)P(OPr^i)_2\}_2]^+$ has however been shown to be stable to decarboxylation.

Treatment of an acetone solution of the solvento species $[Ru_2(CO)_5(solvent)\{\mu\text{-}(Pr^iO)_2PN(Et)P(OPr^i)_2\}_2](SbF_6)_2$ (solvent = acetone and water), with an excess of trifluoroacetic acid (CF_3COOH) resulted in the formation of a white product identified as the monocationic trifluoroacetate species $[Ru_2(CO)_5(OOCCF_3)\{\mu\text{-}(Pr^iO)_2PN(Et)P(OPr^i)_2\}_2]SbF_6$ (**30**).

The infrared spectrum of the compound in the terminal C-O stretching region is essentially the same as that of the analogous acetate derivative, but with a broad peak at 1690 cm^{-1} corresponding to the carbonyl stretching mode of the co-ordinated trifluoroacetate. The $^{31}P\{^1H\}$ nmr spectrum exhibited an AA'BB' pattern of peaks in acetone-d_6, centred at 130.82 ppm, while the ^1H nmr spectrum is similar to that of the parent complex $[Ru_2(\mu\text{-}CO)(CO)_4\{\mu\text{-}(Pr^iO)_2PN(Et)P(OPr^i)_2\}_2]$. The presence of a trifluoroacetate ligand was confirmed by the observation of a singlet at -70.3 ppm in the $^{19}F\ \{^1H\}$ nmr spectrum.

An acetone solution of the solvento species $[Ru_2(CO)_5(solvent)\text{-}\{\mu\text{-}(Pr^iO)_2PN(Et)P(OPr^i)_2\}_2](SbF_6)_2$ (solvent = acetone and water) was allowed to react with a vast excess of benzoic acid (PhCOOH) in acetone for 48 hours. A white product was isolated from the solution and characterized as the monocationic benzoate complex $[Ru_2(CO)_5(OOCPh)\text{-}\{\mu\text{-}(Pr^iO)_2PN(Et)P(OPr^i)_2\}_2]SbF_6$ (**31**). The infrared spectrum of this compound in the C-O stretching region is similar to that of the analogous acetate derivative. The $^{31}P\{^1H\}$ nmr spectrum exhibits an AA'BB' pattern of peaks, centred at 128.63 ppm in $CDCl_3$. The presence of a benzoate ligand was confirmed by the observation of a multiplet at 7.29 - 8.08 ppm, corresponding to five protons, in the ^1H nmr spectrum.

The pendant-carboxylate complexes of the type $[Ru_2(CO)_5(OOCR)\{\mu\text{-}(Pr^iO)_2\text{-}PN(Et)P(OPr^i)_2\}_2]SbF_6$ (R = H, CH_3, CF_3 or Ph) are stable in solution but were found to undergo decarbonylation in the presence of ultraviolet light to afford the tetracarbonyl carboxylate-bridged species $[Ru_2(CO)_4\text{-}\{\mu\text{-}OC(R)O\}\{\mu\text{-}(Pr^iO)_2PN(Et)P(OPr^i)_2\}_2]SbF_6$, the identity of which were established by means of $^{31}P\{^1H\}$ nmr and infrared spectroscopy. The carboxylate-bridged complexes $[Ru_2(CO)_4\{\mu\text{-}OC(R)O\}\{\mu\text{-}(Pr^iO)_2PN(Et)P\text{-}(OPr^i)_2\}_2]^+$ (R = Me or Ph) are, however, best synthesized by treatment

of the parent complex $[Ru_2(\mu\text{-}CO)(CO)_4\{\mu\text{-}(Pr^iO)_2PN(Et)P(OPr^i)_2\}_2]$ with silver acetate (R = Me) or silver benzoate (R = Ph). These syntheses and the characterization of carboxylate-bridged products are discussed in detail in Chapter 3.

The reactivity patterns described for the addition of carboxylic acids to the solvento species $[Ru_2(CO)_5(solvent)\{\mu\text{-}(Pr^iO)_2PN(Et)P(OPr^i)_2\}_2]^{2+}$ are summarized in Scheme 2.10.

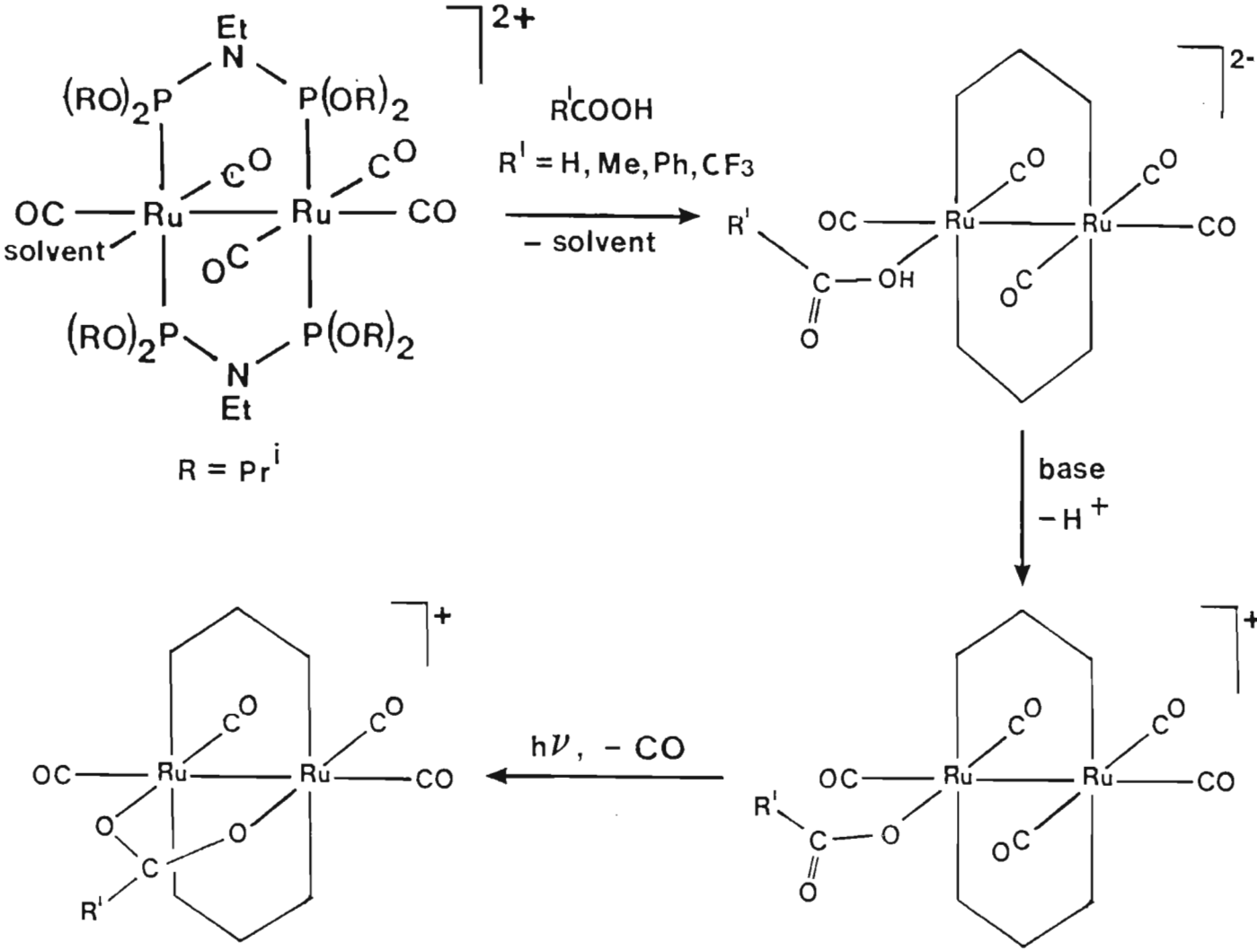

Scheme 2.10

2.7 EXPERIMENTAL

2.7.1 *Synthesis of* $[Ru_2(\mu\text{-}CO)(CO)_4\{\mu\text{-}(MeO)_2PN(Et)P(OMe)_2\}\{\mu\text{-}(Pr^iO)_2PN(Et)P(OPr^i)_2\}]$ (1)

An ether solution (130 ml) of $[Ru_3(CO)_{10}\{\mu\text{-}(Pr^iO)_2PN(Et)P(OPr^i)_2\}]$ (0.780 g, 0.844 mmol) and $(MeO)_2PN(Et)P(OMe)_2$ (0.387 g, 1.688 mmol) was irradiated with UV light for 30 minutes. After removal of the solvent under reduced pressure, the orange oily residue was dissolved in warm methanol (25 ml, 40°C) and kept at -25°C for 15 hours. Yellow crystals of the title compound, which separated from the solution, were separated, washed with cold methanol (5 ml, 0°C) and dried. Yield: 0.470 g, 0.515 mmol, 60%. *M* (**1**) = 912.77 g/mol.

2.7.2 *Synthesis of* $[Ru_2(CO)_5(NCPh)\{\mu\text{-}(RO)_2PN(Et)P(OR)_2\}_2](SbF_6)_2$ (*R = Me* (**4**), Pr^i (**2**))

A twice molar amount of a solution of $AgSbF_6$ (0.100 g, 0.291 mmol) in benzonitrile (3 ml) was added to a solution of $[Ru_2(\mu\text{-}CO)(CO)_4\{\mu\text{-}(RO)_2PN(Et)P(OR)_2\}_2]$ (R = Me: 0.116 g, 0.146 mmol; R = Pr^i: 0.150 g, 0.146 mmol) in benzonitrile (5 ml) and the mixture stirred for one hour, during which time a precipitate of silver metal separated. The pale yellow solution was filtered through a glass fibre fritte and the volume of the filtrate was concentrated under reduced pressure to *ca.* 3 ml. Toluene (5 ml) was added and the solution was kept at -10° to effect the separation of the title compound in crystalline form. Yield; 80-90%. *M*(**2**) = 1611.63 g/mol; *M*(**4**) = 1374.76 g/mol.

2.7.3 *Synthesis of* $[Ru_2(CO)_5(NCMe)\{\mu\text{-}(RO)_2PN(Et)P(OR)_2\}_2](SbF_6)_2$ *(R = Me (5), Pr^i (3))*

A twice molar amount of a solution of $AgSbF_6$ (0.100 g, 0.291 mmol) in acetonitrile (3 ml) was added to a solution of $[Ru_2(\mu\text{-}CO)(CO)_4\{\mu\text{-}(RO)_2P\text{-}N(Et)P(OR)_2\}_2]$ (R = Me: 0.116 g, 0.146 mmol; R = Pr^i: 0.150 g, 0.146 mmol) in acetonitrile (5 ml) and the mixture stirred for two hours, during which time a precipitate of silver metal separated. The pale yellow solution was filtered through a glass fibre fritte and the filtrate was concentrated under reduced pressure to *ca.* 3 ml. Toluene (5 ml) was added and the solution was kept at -10° to effect the separation of the title compound in crystalline form. Yield; 80-90%. *M*(**5**) = 1084.89 g/mol; *M*(**3**) = 1537.56 g/mol.

2.7.4 *Synthesis of* $[Ru_2(CO)_5(Me_2CO)\{\mu\text{-}(RO)_2PN(Et)P(OR)_2\}_2](SbF_6)_2$ *(R = Me (8), Pr^i (6))*

A twice molar amount of a solution of $AgSbF_6$ (1.201 g, 0.582 mmol) in acetone (5 ml) was added to a solution of $[Ru_2(\mu\text{-}CO)(CO)_4\{\mu\text{-}(RO)_2PN(Et)\text{-}P(OR)_2\}]$ (R = Me: 0.232g, 0.291 mmol; R = Pr^i: 0.300 g, 0.291 mmol) in acetone (5 ml) and the mixture stirred for one hour, during which time a precipitate of silver metal separated. The pale yellow solution was filtered through a glass fibre fritte and the volume of the filtrate was concentrated under reduced pressure to *ca.* 2 ml. Crystallization of the title compound as colourless crystals was achieved by addition of ether (3 ml, for R = Me) or of toluene (5 ml, for R = Pr^i) to the solution which was then set aside at -10°. Yield: 80-90%. *M*(**8**) = 1329.70 g/mol; *M*(**6**) = 1554.60 g/mol.

2.7.5 *Synthesis of* $[Ru_2(CO)_5(H_2O)\{\mu\text{-}(RO)_2PN(Et)P(OR)_2\}_2](SbF_6)_2$ *(R = Me (9), Pr^i (7))*

A twice molar amount of a solution of $AgSbF_6$ (0.201 g, 0.582 mmol) was added to a solution of $[Ru_2(\mu\text{-}CO)(CO)_4\{\mu\text{-}(RO)_2PN(Et)P(OR)_2\}]$ (R = Me: 0.232 g, 0.291 mmol; R = Pr^i: 0.300 g, 0.291 mmol) in THF (10 ml), containing 1% water, and the mixture stirred for one hour, during which time a precipitate of silver metal separated. The solution was filtered through a glass fibre fritte and the filtrate was evaporated to dryness. A white product was extracted into dichloromethane (2 x 10 ml) to which diethyl ether was added to effect the crystallization of the title compound. Yield: 80-90%. *M*(**9**) = 1289.70 g/mol, *M*(**7**) = 1514.53 g/mol.

2.7.6 *Synthesis of* $[Ru_2(CO)_5(L)\{\mu\text{-}(Pr^iO)_2PN(Et)P(OPr^i)_2\}_2]SbF_6$ *(L = Et_2CO (**10**), $MeNO_2$ (**11**))*

A twice molar amount of a solution of $AgSbF_6$ (0.100 g, 0.291 mmol) was added to a solution of $[Ru_2(\mu\text{-}CO)(CO)_4\{\mu\text{-}(Pr^iO)_2PN(Et)P(OPr^i)_2\}]$ (0.150 g, 0.146 mmol) in diethyl ketone or nitromethane (5 ml) and the mixture stirred for 90 minutes, during which time a precipitate of silver metal separated. The solution was filtered through a glass fibre fritte and the volume of the filtrate was reduced under vacuum to *ca.* 1 ml. Diethyl ether (5 ml) was added and the solution was kept at -10° to effect the crystallization of the title compounds. Yield: 40-50%. *M*(**10**) = 1582.66 g/mol; *M*(**11**) = 1557.55 g/mol.

2.7.7 *Synthesis of* $[Ru_2(CO)_5(L)\{\mu\text{-}(Pr^iO)_2PN(Et)P(OPr^i)_2\}_2](SbF_6)_2$ *(L = SC_4H_8 (**12**), SMe_2 (**13**))*

A slight excess of tetrahydrothiophene (0.009 g, 0.100 mmol) or dimethyl

sulphide (0.007 g, 0.113 mmol) was added to a mixture of the acetone and aquo solvento species $[Ru_2(CO)_5(solvent)\{\mu\text{-}(Pr^iO)_2PN(Et)P(OPr^i)_2\}]\text{-}(SbF_6)_2$ (solvent = acetone and water) (0.150 g, 0.090 mmol) in acetone (5 ml). White crystals of the title compound were obtained by addition of diethyl ether (10 ml) to this solution. Yield: 90-95%. *M*(**12**) = 1584.69 g/mol, *M*(**13**) = 1558.65 g/mol.

2.7.8 *Synthesis of* $[Ru_2(CO)_5(SH)\{\mu\text{-}(Pr^iO)_2PN(Et)P(OPr^i)_2\}_2]SbF_6$ (**14**), $[Ru_2(\mu\text{-}SH)(CO)_4\{\mu\text{-}(Pr^iO)_2PN(Et)P(OPr^i)_2\}_2]SbF_6$ (**15**) *and* $[Ru_2(\mu\text{-}S)(CO)_4\{\mu\text{-}(Pr^iO)_2PN(Et)P(OPr^i)_2\}_2]$ (**16**)

$[Ru_2(CO)_5(solvent)\{\mu\text{-}(Pr^iO)_2PN(Et)P(OPr^i)_2\}_2](SbF_6)_2$ (0.200 g, 0.195 mmol) was added to a saturated solution of hydrogen sulphide in acetone (10 ml) resulting in an immediate change in colour of the solution to pale yellow. A species was identified in solution as being the mono-cationic mercaptide species $[Ru_2(CO)_5(SH)\{\mu\text{-}(Pr^iO)_2PN(Et)P(OPr^i)_2\}_2]SbF_6$ (**14**) by means of infrared and $^{31}P\{^1H\}$ nmr spectroscopy. The solution was stirred for 15 hours after which time a species was spectroscopically identified in solution as being the mercaptide-bridged species $[Ru_2(\mu\text{-}SH)(CO)_4\{\mu\text{-}(Pr^iO)_2PN(Et)P(OPr^i)_2\}_2]SbF_6$ (**15**). The solvent was then removed under reduced pressure, the residue washed with diethyl ether and then extracted into chloroform. An excess of an aqueous potassium hydroxide solution was added to this solution and the two-layered mixture stirred for 5 minutes, during which time the chloroform solution became orange in colour. The chloroform solution was separated from the aqueous layer and the solvent then removed under vacuum. A neutral orange compound was extracted into toluene and was identified as the sulphide-bridged species $[Ru_2(\mu\text{-}S)(CO)_4\{\mu\text{-}(Pr^iO)_2PN(Et)P(OPr^i)_2\}_2]$. Yield: 80%. *M*(**14**) = 1293.8 g/mol, *M*(**15**) = 1265.8 g/mol, *M*(**16**) = 1033.0 g/mol.

2.7.9 *Synthesis of* $[Ru_2(CO)_5(NC_5H_5)\{\mu\text{-}(Pr^iO)_2PN(Et)P(OPr^i)_2\}_2](SbF_6)_2$ (**17**)

An equimolar amount of pyridine (0.015 g, 0.195 mmol) was added to a mixture of the acetone and aquo solvento species $[Ru_2(CO)_5(solvent)\text{-}\{\mu\text{-}(Pr^iO)_2PN(Et)P(OPr^i)_2\}](SbF_6)_2$ (solvent = acetone and water) (0.200 g, 0.195 mmol) in acetone (5 ml). The solvent was removed under vacuum and the residue washed with chloroform (3 x 5 ml). The remaining white residue was extracted into dichloromethane (3 ml), the extract filtered through a glass fibre fritte and diethyl ether (5 ml) was added to the filtrate. The solution was cooled to -10° to effect the separation of the title compound in crystalline form. Yield: 35%. *M*(**17**) = 1575.61 g/mol.

2.7.10 *Synthesis of* $[Ru_2I_2(CO)_4\{\mu\text{-}(RO)_2PN(Et)P(OR)_2\}\{\mu\text{-}(R'O)_2PN(Et)\text{-}P(OR')_2\}]$ (*R = R' = Me* (**22**), *Et* (**25**), Pr^i (**21**); *R = Me*, *R'* = Pr^i (**24**))

i) A twice molar amount of tetrabutylammonium iodide (0.050 g, 0.136 mmol) was added to a mixture of acetone and the aquo solvento species $[Ru_2(CO)_5(solvent)\{\mu\text{-}(RO)_2PN(Et)P(OR)_2\}_2](SbF_6)_2$ (R = Me : 0.090 g, 0.068 mmol; R = Pr^i : 0.104 g, 0.068 mmol) in acetone (5 ml) and the mixture stirred for 30 minutes, during which time the solution became yellow in colour. An excess of $Me_3NO.2H_2O$ (0.030 g, 0.270 mmol) was added and the solution was stirred for a further 30 minutes. The solvent was removed under reduced pressure and an orange product was extracted into toluene (2 x 5 ml) and the extract then filtered through a glass fibre fritte. The volume of the extract was reduced *in vacuo* to 2 ml and ethanol was added (5 ml). The solution was set aside at -10° for 15 hours during which time orange crystals of the title compounds

separated from the mother liquor. Yield: 75%.

ii) A twice molar amount of iodine (0.150 g, 0.591 mmol) was added to a solution of $[Ru_2(\mu\text{-}CO)(CO)_4\{\mu\text{-}(RO)_2PN(Et)P(OR)_2\}\{\mu\text{-}(R'O)_2PN(Et)P(OR')_2\}]$ (R = R' = Me : 0.236 g, 0.296 mmol; R = R' = Et : 0.270 g, 0.296 mmol; R = R' = Pr^i : 0.303 g, 0.296 mmol; R = Me, R' = Pr^i : 0.270 g, 0.296 mmol) in acetone (15 ml) and the mixture stirred for 30 minutes, during which time the solution became dark orange in colour. An excess of $Me_3NO.2H_2O$ (0.060 g, 0.540 mmol) was added and the solution was stirred for a further 30 minutes by which time the solution had become light orange in colour. The solvent was removed under reduced pressure and the title compounds were extracted into toluene (2 x 5 ml) and crystallized in the same way as above. Yield: 80-90%. *M* (**22**) = 1026.32 g/mol, *M* (**25**) = 1138.56 g/mol, *M* (**24**) = 1250.80 g/mol, *M* (**21**) = 1138.56 g/mol.

2.7.11 *Synthesis of* $[Ru_2I(\mu\text{-}I)(CO)_3\{\mu\text{-}(RO)_2PN(Et)P(OR)_2\}_2]$ *(R = Me (**23**), Pr^i (**20**)*

An equimolar amount of tetrabutylammonium iodide (0.050 g, 0.136 mmol) was added to a mixture of the acetone and aquo solvento species $[Ru_2(CO)_5(solvent)\{\mu\text{-}(RO)_2PN(Et)P(OR)_2\}_2](SbF_6)_2$ (R = Me : 0.090 g, 0.068 mmol); R = Pr^i : 0.104 g, 0.068 mmol) in acetone (5 ml) and the mixture stirred for 30 minutes, during which time the solution became yellow in colour. An excess $Me_3NO.2H_2O$ (0.060 g, 0.540 mmol) was added and the solution was stirred for 30 minutes. An excess of tetrabutylammonium iodide (0.075 g, 0.204 mmol) and further $Me_3NO.2H_2O$ (0.030 g, 0.270 mmol) was added and the mixture stirred for a further 30 minutes. The solvent was removed under reduced pressure and an orange product was extracted into toluene (2 x 5 ml) and the extract then filtered through a glass fibre fritte. The volume of the extract was

reduced *in vacuo* to 2 ml and ethanol was added (5 ml). The solution was set aside at -10° for 15 hours during which time orange crystals of the title compounds separated from the mother liquor. Yield: 70%. *M*(**23**) = 998.31 g/mol; *M*(**20**) = 1222.79 g/mol.

2.7.12 *Synthesis of* $[Ru_2(CO)_5(SPh)\{\mu\text{-}(Pr^i)_2PN(Et)P(OPr^i)_2\}_2]SbF_6$ *(R =* Pr^i *(**26**)) and* $[Ru_2(CO)_4(\mu\text{-}SPh)\{\mu\text{-}(Pr^iO)_2PN(Et)P(OPr^i)_2\}_2]SbF_6$ *(R =* Pr^i *(**27**))*

An equimolar amount of phenyl mercaptan (0.011 g, 0.096 mmol) was added to a mixture of the acetone and aquo solvento species $[Ru_2(CO)_5(solvent)\{\mu\text{-}(Pr^iO)_2PN(Et)P(OPr^i)_2\}_2](SbF_6)_2$ (0.150 g, 0.096 mmol) in acetone, resulting in an immediate change in colour of the solution to yellow. A species was identified in solution as being the monocationic mercaptide complex $[Ru_2(CO)_5(SPh)\{\mu\text{-}(Pr^iO)_2PN(Et)P(OPr^i)_2\}_2]^+$ by means of infrared and $^{31}P\{^1H\}$ nmr spectroscopy. The solution was stirred for 48 hours and the solvent then removed under reduced pressure. The residue was washed with diethyl ether and dried under vacuum. The title compound was crystallized from acetone/diethyl ether. Yield: 70-80%. *M* (**27**) = 1341.86 g/mol.

2.7.13 *Synthesis of* $[Ru_2(CO)_5(OOCR')\{\mu\text{-}(Pr^iO)_2PN(Et)P(OPr^i)_2\}_2]SbF_6$ *(R' = H (**29**),* CH_3 *(**28**),* CF_3 *(**30**), Ph (**31**))*

An excess of R'COOH (R' = H : 0.050 g, 1.087 mmol; R' = CH_3 : 0.050 g, 0.833 mmol; R' = CF_3 : 0,050 g, 0.439 mmol; R' = Ph : 0.075 g, 0.615 mmol) was added to a mixture of the acetone and aquo solvento species $[Ru_2(CO)_5(solvent)\{\mu\text{-}(Pr^iO)_2PN(Et)P(OPr^i)_2\}_2](SbF_6)_2$ (0.150 g, 0.096 mmol) in acetone (5 ml) and the mixture stirred for 1 hour (for R' = H, CH_3, CF_3) or 48 hours (for R' = Ph). The solvent was removed under

reduced pressure and the residue washed with warm water (3 x 5 ml, 50°), followed by diethyl ether (3 x 5 ml). The residue was dried and recrystallized from $CHCl_3$/hexane to afford the title compounds. Yield: 70-80%. *M*(**29**) = 1305.78 g/mol; *M*(**28**) = 1319.81 g/mol; *M*(**30**) = 1373.78 g/mol; *M*(**31**) = 1381.88 g/mol.

2.7.14 *Crystal Structure Determination of* $[Ru_2(CO)_5(NCPh)\{\mu\text{-}(Pr^iO)_2PN(Et)P(OPr^i)_2\}_2](SbF_6)_2$ (**2**), $[Ru_2(CO)_5(SC_4H_8)\{\mu\text{-}(Pr^iO)_2PN(Et)P(OPr^i)_2\}_2](SbF_6)_2\cdot CH_2Cl_2$ (**12**) *and* $[Ru_2(\mu\text{-}SPh)(CO)_4\{\mu\text{-}(MeO)_2PN(Et)P(OMe)_2\}_2]PF_6$ (**27**)

The intensity data collection is described in Appendix A.3(a) and the general approach to the structure solution in Appendix A.3(b). For (**2**), the crystallographic data are given in Table 2.5, the fractional co-ordinates and isotropic thermal parameters in Table 2.6, the anisotropic thermal parameters in Table 2.7, the interatomic distances in Table 2.8 and the interatomic angles in Table 2.9. The difference fourier of this structural solution showed considerable disorder associated with one of the hexafluoroantimonate anions, and which was therefore defined as a rigid group and refined as such. For (**12**), the crystallographic data are given in Table 2.5, the fractional co-ordinates and isotropic thermal parameters in Table 2.10, the anisotropic thermal parameters in Table 2.11, the interatomic distances in Table 2.12 and the interatomic angles in Table 2.13. For (**27**) the crystallographic data are given in Table 2.5, the fractional co-ordinates and isotropic thermal parameters in Table 2.14, the anisotropic thermal parameters in Table 2.15, the interatomic distances in Table 2.16 and the interatomic angles in Table 2.17. The observed and calculated structure factors for (**2**), (**12**) and (**27**) may be found on microfiche in an envelope fixed to the inside cover.

TABLE 2.1

MICROANALYTICAL DATA

	COMPLEX	ANALYSIS : Found (Calculated) % %C	%H	%N
1	$[Ru_2(\mu\text{-}CO)(CO)_4\{\mu\text{-}(MeO)_2PN(Et)P(OMe)_2\}\{\mu\text{-}(Pr^iO)_2PN(Et)P(OPr^i)_2\}]$	32.65(32.88)	5.63(5.53)	3.12(3.07)
2	$[Ru_2(CO)_5(NCPh)\{\mu\text{-}(Pr^iO)_2PN(Et)P(OPr^i)_2\}_2](SbF_6)_2$	32.07(30.55)	4.53(4.45)	2.65(2.61)
3	$[Ru_2(CO)_5(NCMe)\{\mu\text{-}(Pr^iO)_2PN(Et)P(OPr^i)_2\}_2](SbF_6)_2$	27.76(27.34)	4.66(4.53)	2.93(2.73)
4	$[Ru_2(CO)_5(NCPh)\{\mu\text{-}(MeO)_2PN(Et)P(OMe)_2\}_2](SbF_6)_2$	21.87(20.97)	2.88(2.87)	3.22(3.02)
5	$[Ru_2(CO)_5(NCMe)\{\mu\text{-}(MeO)_2PN(Et)P(OMe)_2\}_2](SbF_6)_2$	17.77(17.38)	2.76(2.84)	3.25(3.20)
6	$[Ru_2(CO)_5(OCMe_2)\{\mu\text{-}(Pr^iO)_2PN(Et)P(OPr^i)_2\}_2](SbF_6)_2$	27.75(27.79)	4.35(4.59)	1.99(1.81)
7	$[Ru_2(CO)_5(H_2O)\{\mu\text{-}(Pr^iO)_2PN(Et)P(OPr^i)_2\}_2](SbF_6)_2$	26.44(26.17)	4.44(4.53)	1.84(1.84)
8	$[Ru_2(CO)_5(OCMe_2)\{\mu\text{-}(MeO)_2PN(Et)P(OMe)_2\}_2](SbF_6)_2$	18.18(18.16)	3.01(3.04)	2.18(2.11)
9	$[Ru_2(CO)_5(H_2O)\{\mu\text{-}(MeO)_2PN(Et)P(OMe)_2\}_2](SbF_6)_2$	15.51(15.82)	2.82(2.82)	2.17(2.17)
10	$[Ru_2(CO)_5(OCEt_2)\{\mu\text{-}(Pr^iO)_2PN(Et)P(OPr^i)_2\}_2](SbF_6)_2$	27.86(28.84)	4.88(4.85)	1.88(1.77)
11	$[Ru_2(CO)_5(MeNO_2)\{\mu\text{-}(Pr^iO)_2PN(Et)P(OPr^i)_2\}_2](SbF_6)_2$	27.30(26.22)	4.32(4.47)	2.82(2.70)
12	$[Ru_2(CO)_5(SC_4H_8)\{\mu\text{-}(Pr^iO)_2PN(Et)P(OPr^i)_2\}_2](SbF_6)_2$	27.74(28.04)	4.71(4.71)	1.81(1.77)
13	$[Ru_2(CO)_5(SMe_2)\{\mu\text{-}(Pr^iO)_2PN(Et)P(OPr^i)_2\}_2](SbF_6)_2$	27.87(27.97)	4.47(4.67)	1.99(1.80)
17	$[Ru_2(CO)_5(NC_5H_5)\{\mu\text{-}(Pr^iO)_2PN(Et)P(OPr^i)_2\}_2](SbF_6)_2$	28.74(28.97)	4.35(4.55)	2.94(2.67)

TABLE 2.1 (continued)

	COMPLEX	ANALYSIS : Found (Calculated) % %C	%H	%N
21	$[Ru_2I_2(CO)_4\{\mu\text{-}(Pr^iO)_2PN(Et)P(OPr^i)_2\}_2]^a$	31.01(30.72)	5.40(5.33)	2.24(2.21)
22	$[Ru_2I_2(CO)_4\{\mu\text{-}(MeO)_2PN(Et)P(OMe)_2\}_2]^b$	19.22(18.72)	3.34(3.35)	3.30(2.73)
24	$[Ru_2I_2(CO)_4\{\mu\text{-}(MeO)_2PN(Et)P(OMe)_2\}\{\mu\text{-}(Pr^iO)_2PN(Et)P(OPr^i)_2\}]$	25.65(25.32)	4.47(4.44)	2.63(2.46)
25	$[Ru_2I_2(CO)_4\{\mu\text{-}(EtO)_2PN(Et)P(OEt)_2\}_2]$	26.06(25.32)	5.15(4.44)	2.02(2.46)
27	$[Ru_2(\mu\text{-}SPh)(CO)_4\{\mu\text{-}(Pr^iO)_2PN(Et)P(OPr^i)_2\}_2]SbF_6$	33.88(34.01)	5.89(5.34)	2.21(2.09)
28	$[Ru_2(CO)_5(OOCCH_3)\{\mu\text{-}(Pr^iO)_2PN(Et)P(OPr^i)_2\}_2]SbF_6$	30.87(31.85)	4.88(5.28)	2.40(2.12)
29	$[Ru_2(CO)_5(OOCH)\{\mu\text{-}(Pr^iO)_2PN(Et)P(OPr^i)_2\}_2]SbF_6$	31.41(31.27)	5.12(5.18)	2.49(2.14)
30	$[Ru_2(CO)_5(OOCCF_3)\{\mu\text{-}(Pr^iO)_2PN(Et)P(OPr^i)_2\}_2]SbF_6$	30.98(30.60)	4.79(4.85)	2.08(2.04)
31	$[Ru_2(CO)_5(OOCPh)\{\mu\text{-}(Pr^iO)_2PN(Et)P(OPr^i)_2\}_2]SbF_6$	36.55(34.76)	5.21(5.19)	2.13(2.03)
32	$[Ru_2(CO)_4(\mu\text{-}OOCCF_3)\{\mu\text{-}(Pr^iO)_2PN(Et)P(OPr^i)_2\}_2]SbF_6$	30.25(30.34)	4.86(4.95)	1.87(2.08)

[a] % P 10.23(9.90), % I 21.02(20.29)

[b] % P 12.67(12.07), % I 26.41(24.73)

TABLE 2.2

INFRARED SPECTROSCOPIC DATA

COMPLEX	ν(C≡O), cm^{-1}					OTHER	MEDIUM	COLOUR
1	1993(s)	1948(s)	1916(s)	1898(s)		1710(ms), ν(C=O)	Cyclohexane	Yellow
	1990(s)	1939(s)	1909(s)	1892(s)		1710(ms), ν(C=O)	Nujol	
2	2093(w)	2051(s)	2030(s)	2001(m)			CH_2Cl_2	White
	2100(w)	2043(s)	2031(s)	1993(m)		2145(w), ν(C≡N)	Nujol	
3	2094(w)	2053(s)	2031(s)	2003(m)			CH_2Cl_2	White
	2094(w)	2057(s)	2027(s)	2004(m)			Nujol	
4	2103(w)	2059(s)	2041(s)	2012(m)		2240(w), ν(C≡N)	CH_2Cl_2	White
	2106(w)	2054(s)	2039(s)	2012(m)		2237(w), ν(C≡N)	Nujol	
5	2104(w)	2060(s)	2041(s)	2011(m)			CH_3CN	White
	2105(w)	2060(sh)	2040(s)	2013(m)			Nujol	
6	2099(w)	2054(sh)	2033(s)	1980(m)		1680(m), ν(C=O)	Nujol	White
7	2097(w)	2045(sh)	2034(s)	1987(m)		3450(m,br), ν(O-H)	Nujol	White
8	2098(w)	2050(s)	2035(vs)	1998(ms)		1652(m), ν(C=O)	Nujol	White
9	2105(w)	2061(s)	2050(s)	2031(s)	2005(s)	3550(m,br), ν(O-H)	Nujol	White

TABLE 2.2 (continued)

COMPLEX	$\nu(C\equiv O)$, cm^{-1}				OTHER	MEDIUM	COLOUR
10	2091(w)	2043(s)	2023(s)	1985(m)	1650(m), $\nu(C=O)$	Nujol	White
	2084(w)	2031(s)	2020(s)	1970(m)		Et_2CO	
11	2092(w)	2051(s)	2028(vs)	2005(m)		CH_2Cl_2	White
	2094(w)	2051(s)	2030(vs)	2006(m)		Nujol	
12	2097(m)	2044(s)	2031(s)	1994(ms)		CH_2Cl_2	White
	2097(m)	2050(s)	2031(s)	1997(ms)		Nujol	
13	2096(w)	2046(s)	2032(s)	1994(m)		CH_2Cl_2	White
	2102(w)	2050(s)	2036(vs)	1989(m)		Nujol	
17	2086(w)	2043(s)	2023(s)	1994(m)		CH_2Cl_2	White
	2087(w)	2047(s)	2026(s)	1991(m)		Nujol	
21	2021(w)	1975(vs)	1938(m)			Hexane	Orange
	2019(m)	1966(s)	1931(m)			Nujol	
22	2015(m)	1985(s)	1950(m)			CH_2Cl_2	Orange
24	2022(w)	2007(m)	1979(vs)	1943(m)		Hexane	Orange
	2020(w)	2004(m)	1977(vs)	1941(m)		Nujol	

TABLE 2.2 (continued)

COMPLEX	ν(C≡O), cm^{-1}				OTHER	MEDIUM	COLOUR
25	1986(s)	1944(vs)				$CHCl_3$	Orange
	1981(s)	1938(s)	1925(sh)			Nujol	
26	2086(w)	2028(s)	2014(sh)	1970(m)		CH_2Cl_2	Yellow
27	2032(m)	2001(s)	1973(m)	1951(w)		CH_2Cl_2	Yellow
	2033(ms)	2004(s)	1975(m)	1956(m)		Nujol	
28	2084(w)	2031(s)	2020(s)	1968(m)	1600(m), ν(C=O)	$CHCl_3$	White
	2084(w)	2028(s)	2015(s)	1963(m)	1610(m), ν(C=O)	Nujol	
29	2087(w)	2032(s)	2023(s)	1972(m)	1610(m), ν(C=O)	$CHCl_3$	White
	2086(w)	2031(s)	2019(s)	1965(m)	1620(m), ν(C=O)	Nujol	
30	2087(w)	2038(s)	2021(s)	1974(m)	1685(m), ν(C=O)	CH_2Cl_2	White
	2088(w)	2036(s)	2025(s)	1974(m)	1690(m), ν(C=O)	Nujol	
31	2086(w)	2032(s)	2018(s)	1966(m)	1600(m), ν(C=O)	$CHCl_3$	White
	2085(w)	2031(s)	2015(s)	1960(m)	1608(m), ν(C=O)	Nujol	
32	2035(s)	2008(vs)	1980(s)	1956(m)	1645(m), ν(C=O)	$CHCl_3$	Pale Yellow
	2042(s)	2014(vs)	1991(s)	1963(m)	1635(m), ν(C=O)	Nujol	

TABLE 2.3

^{1}H AND $^{31}P\{^{1}H\}$ NMR SPECTROSCOPIC DATA

COMPLEX	δ ^{1}H (ppm)	δ $^{31}P\{^{1}H\}$ (ppm)
1	1.17t (3H); 1.38t (3H); 1.31-1.40m (24H); 3.10-3.25m (2H); 3.30-3.41m (2H); 3.59-3.65m (12H); 4.85-5.05m (4H)	156.46 (AA'BB')[a]
2	1.32-1.65m (54H); 3.54-3.78m (4H); 4.92-5.27m (8H); 7.21-8.11, (5H)	128.51(s), 133.75 (AA'BB') (-77°C)[b]
3	1.39-1.57m (54H); 2.83t (3H); 3.50-3.60m (4H); 4.91-4.99m (8H)	130.00 (AA'BB')[b]
4	1.35t (6H); 3.70-3.81m (4H); 4.00-4.22m (24H); 7.72-8.01m (5H)	140.47(s), 141.48 (AA'BB') (-96°C)[b]
5	1.37t (6H); 2.75s (3H); 3.60-3.81m (4H); 3.93-4.14m (24H)	137.03 (AA'BB')[b]
6	1.20-1.63m (54H); 2.00-2.15m (6H); 3.23-3.31m (4H); 5.04-5.11m (8H)	127.50 (AA'BB')[b]
7	1.28-1.54m (54H); 3.42-3.53m (6H); 3.62s,br (2H); 5.04-5.21m (8H)	125.00 (AA'BB')[c]
8	1.29t (6H); 2.10s (6H); 3.40-3.64m (4H); 3.74-4.02m (24H)	139.42 (AA'BB')[b]
9	Insufficiently soluble in CD_2Cl_2	
12	1.2[illegible]-1.54m (54H); 2.07-2.22m (4H); 3.06-3.28m (4H); 3.37-3.46m (4H); 4.70-4.90m (8H)	120.22 (AA'BB')[c]

TABLE 2.3 (Continued)

COMPLEX	δ ^{1}H (ppm)	δ $^{31}P\{^{1}H\}$ (ppm)
13	1.31-1.57m (54H); 2.62s (6H); 3.40-3.55m (4H); 4.60-5.00m (8H)	121.17 (AA'BB')[c]
17	1.25-1.50m (54H); 3.27-3.41m (4H); 4.60-5.02m (8H); 8.34-9.19m (5H)	126.86 (AA'BB')[b]
21	1.25-1.58m (54H); 3.25-3.42m (4H); 5.30-5.50m (8H)	134.33(s)[a]
22	1.20t (6H); 2.80-3.90m (28H)	144.81(s)[a]
24	0.97-1.62m (30H); 3.30-4.10m (16H); 5.28-5.46m (4H)	139.28 (AA'BB')[a,e]
		138.80 (AA'BB')[a,f]
27	0.90t (6H); 1.23-1.47m (48H); 3.01-3.10m (4H); 4.54-4.83m (8H) 7.14-7.43m (5H)	129.93(s)[d]
28	1.18-1.49m (54H); 1.93s (3H); 3.25-3.42m (4H); 4.60-4.95m (8H)	128.02 (AA'BB')[d]
29	1.24-1.50m (54H); 3.26-3.45m (4H); 4.55-4.92m (8H); 7.98t (1H); (^{4}J(PH) 1.85 Hz)	128.35 (AA'BB')[d]
30	1.29-1.56m (54H); 3.42-3.61m (4H); 4.75-5.10m (8H)	130.82 (AA'BB')[b,g]
31	0.83-1.54m (54H); 3.26-3.44m (4H); 4.60-5.14m (8H); 7.28-8.08m (5H)	128.62 (AA'BB')[d]
32	1.23-1.51m (54H); 3.40-3.55m (4H); 4.57-4.75m (8H)	132.95 (AA'BB')[d]

s = singlet, AA'BB' = midpoint of AA'BB' pattern, m = multiplet, t = triplet
[a]Recorded in C_6D_6, [b]Recorded in acetone-d_6, [c]Recorded in CD_2Cl_2, [d]Recorded in $CDCl_3$, [e]Major isomer, [f]Minor isomer, [g]$\delta^{19}F\{^{1}H\}$ = 70.3 ppm(s)

TABLE 2.4

$^{13}C\{^{1}H\}$ NMR SPECTROSCOPIC DATA

COMPLEX	δ $^{13}C\{^{1}H\}$ (ppm)
21[a]	17.19s ($-NCH_2\mathit{C}H_3$); 23.75-24.82m ($-OCH(\mathit{C}H_3)_2$); 40.00s ($-N\mathit{C}H_2CH_3$); 71.52-74.08m ($-O\mathit{C}H(CH_3)_2$); 206.68q ($-\mathit{C}{\equiv}O$)
29[b]	16.67s ($-NCH_2\mathit{C}H_3$); 23.46-24.27m ($-OCH(\mathit{C}H_3)_2$); 41.93s ($-N\mathit{C}H_2CH_3$); 73.19-74.01m ($-O\mathit{C}H(CH_3)_2$); 167.85s ($-OO\mathit{C}H$)

s = singlet, m = multiplet, q = quintet, [a]Recorded in C_6D_6, [b]Recorded in $CDCl_3$

TABLE 2.5

CRYSTAL DATA FOR $[Ru_2(CO)_5(NCPh)\{\mu\text{-}(Pr^iO)_2PN(Et)P(OPr^i)_2\}_2](SbF_6)_2$ (2)

and $[Ru_2(CO)_5(SC_4H_8)\{\mu\text{-}(Pr^iO)_2PN(Et)P(OPr^i)_2\}_2](SbF_6)_2$ (12)

	2	12
Formula	$C_{40}H_{71}N_3F_{12}O_{13}P_4Ru_2Sb_2$	$C_{37}H_{74}N_2F_{12}O_{13}P_4SRu_2Sb_2.CH_2$
Molecular mass	1599.5	1669.7
Crystal dimensions, mm	0.50 x 0.23 x 0.16	0.46 x 0.31 x 0.19
Crystal system	orthorhombic	orthorhombic
Space group	$P2_12_12$	$Pna2_1$
a(Å)	22.710(5)	27.167(2)
b(Å)	23.695(5)	14.629(2)
c(Å)	12.256(3)	16.704(2)
α(°)	90	90
β(°)	90	90
γ(°)	90	90
V(Å^3)	6594.9	6638.9
Z	4	4
D_C (g cm^{-3})	1.61	1.67
F(000)	3176	3248
λ(Mo-K_α) (Å)	0.71069	0.71069
μ(Mo-K_α) (cm^{-1})	13.1	16.33
Reflections measured	5104	3821
Unique reflections	4617	3304
Observed reflections [$I > 3\sigma(I)$]	3877	2788
Crystal stability	Decay = 10%	Decay = 12%
Absorption corrections	Not applied	Not applied
No. of parameters	319	349
R	0.101	0.058
R_w	0.101	0.066

TABLE 2.5 (continued)

CRYSTAL DATA FOR $[Ru_2(\mu\text{-SPh})(CO)_4\{\mu\text{-}(MeO)_2PN(Et)P(OMe)_2\}_2]PF_6$ (27)

	27
Formula	$C_{22}H_{39}N_2F_6O_{12}P_5SRu_2$
Molecular mass	1028.7
Crystal dimensions, mm	0.50 x 0.23 x 0.19
Crystal system	triclinic
Space group	$P\bar{1}$
a(Å)	9.424(8)
b(Å)	12.899(1)
c(Å)	16.628(2)
$\alpha(^\circ)$	93.386(9)
$\beta(^\circ)$	102.118(8)
$\gamma(^\circ)$	99.135(9)
V(Å^3)	1942.3
Z	2
D_c (g cm^{-3})	1.76
F(000)	1028
λ(Mo-K_α) (Å)	0.71069
μ(Mo-K_α) (cm^{-1})	13.95
Reflections measured	5603
Unique reflections	5133
Observed reflections [$I > 3\sigma(I)$]	4692
Crystal stability	No decay
Absorption corrections	Applied
No. of parameters	341
R	0.053
R_w	0.076

TABLE 2.6: Fractional co-ordinates ($\times 10^4$) and equivalent isotropic temperature factors ($Å^2$, $\times 10^3$) for $[Ru_2(CO)_5(NCPh)\{\mu\text{-}(Pr^iO)_2PN(Et)P(OPr^i)_2\}_2](SbF_6)_2$ (2)

	x/a	y/b	z/c	U_{eq}
Ru(1)	1565(1)	1802(1)	8821(2)	39(1)
Ru(2)	1523(1)	1571(1)	6507(2)	41(1)
P(1)	652(3)	2098(4)	6471(7)	48(2)
P(2)	2395(4)	1058(4)	6712(7)	52(2)
P(3)	1093(3)	2663(3)	8432(7)	44(2)
P(4)	2071(3)	947(3)	9001(7)	44(2)
O(1)	458(10)	2381(10)	5365(18)	63(6)*
O(2)	65(8)	1764(8)	6768(14)	48(5)*
O(3)	2977(10)	1442(9)	6553(19)	65(6)*
O(4)	2503(10)	566(10)	5841(19)	70(7)*
O(5)	1577(9)	3115(8)	8167(15)	55(5)*
O(6)	660(10)	2928(10)	9228(19)	70(7)*
O(7)	2512(10)	885(9)	10016(19)	62(6)*
O(8)	1680(10)	395(9)	9148(18)	66(6)*
O(9)	1458(11)	1858(11)	11305(22)	85(7)*
O(10)	380(10)	1270(10)	9059(19)	67(6)*
O(11)	858(10)	485(10)	7066(19)	68(6)*
O(12)	1572(14)	1283(13)	4083(26)	112(10)*
O(13)	2246(11)	2646(10)	6250(21)	76(7)*
N(1)	2512(11)	733(10)	7938(20)	53(7)*
N(2)	615(10)	2635(10)	7324(20)	46(6)*
N(3)	2381(11)	2196(10)	8691(21)	50(6)*
C(1)	808(16)	2573(16)	4427(31)	69(10)*
C(2)	515(17)	2275(17)	3477(35)	85(12)*
C(3)	787(23)	3209(22)	4295(43)	119(17)*
C(4)	-242(16)	1361(16)	6026(31)	75(11)*
C(5)	-706(21)	1702(21)	5393(40)	110(16)*
C(6)	-483(20)	908(20)	6745(39)	105(15)*
C(7)	3538(30)	1273(27)	5785(54)	156(23)*
C(8)	3429(29)	1676(26)	4917(52)	156(22)*
C(9)	4006(35)	1669(33)	6378(72)	216(33)*
C(10)	2059(20)	155(19)	5372(38)	95(14)*
C(11)	2077(22)	-351(21)	5970(43)	117(17)*
C(12)	2269(33)	27(33)	4420(59)	192(29)*

TABLE 2.6 (continued)

C(13)	1482(21)	3747(19)	8166(36)	99(13)*
C(14)	2030(25)	3919(23)	8785(49)	139(20)*
C(15)	1565(27)	3895(24)	6935(46)	142(20)*
C(16)	641(18)	2972(18)	10407(32)	80(11)*
C(17)	12(24)	3079(21)	10747(38)	117(16)*
C(18)	1072(26)	3374(24)	10821(48)	141(21)*
C(19)	2839(16)	1347(16)	10631(30)	70(10)*
C(20)	3453(21)	1386(17)	10160(34)	92(12)*
C(21)	2847(20)	1123(20)	11837(38)	106(15)*
C(22)	1345(18)	263(17)	10158(34)	87(13)*
C(23)	1750(16)	-107(16)	10783(29)	73(11)*
C(24)	840(17)	-65(17)	9650(31)	80(11)*
C(25)	1503(17)	1406(14)	4989(29)	67(9)*
C(26)	846(12)	1469(12)	8920(25)	47(7)*
C(27)	1984(15)	2235(14)	6352(30)	64(9)*
C(28)	1540(18)	1916(16)	10395(30)	73(10)*
C(29)	1093(12)	895(12)	6855(23)	42(7)*
C(30)	3057(17)	361(17)	8041(33)	85(12)*
C(31)	2905(22)	-190(22)	8598(44)	126(17)*
C(32)	173(14)	3108(14)	7233(26)	61(9)*
C(33)	-428(15)	2929(16)	7638(32)	75(11)*
C(34)	2776(14)	2482(14)	8680(28)	60(9)*
C(35)	3295(13)	2825(12)	8716(26)	55(8)*
C(36)	3476(17)	3089(16)	7742(31)	79(10)*
C(37)	4058(20)	3404(21)	7841(40)	106(15)*
C(38)	4264(18)	3543(18)	8767(39)	92(13)*
C(39)	4077(19)	3310(18)	9704(35)	88(13)*
C(40)	3536(19)	2985(18)	9780(33)	85(12)*
Sb(1)	2597(1)	3004(1)	2702(3)	89(1)*
F(1)	2448(17)	2679(16)	1335(37)	197(15)*
F(2)	3012(15)	3591(15)	2085(30)	172(13)*
F(3)	3220(14)	2548(15)	2568(32)	169(13)*
F(4)	2002(17)	3479(17)	2562(36)	202(16)*
F(5)	2176(13)	2438(13)	3338(26)	145(11)*
F(6)	2813(19)	3255(18)	3906(37)	216(17)*
Sb(2)	10000	0	3498(5)	115(2)*
F(7)	9376(1)	461(1)	3445(5)	306(16)*

TABLE 2.6 (continued)

F(8)	10323(1)	369(1)	2375(5)	306(16)*
F(9)	10356(1)	472(1)	4428(5)	306(16)*
Sb(3)	5000	0	1332(8)	189(3)*
F(10)	4826(1)	725(1)	1078(8)	408(24)*
F(11)	5529(1)	16(1)	248(8)	408(24)*
F(12)	5559(1)	213(1)	2277(8)	408(24)*

* isotropic temperature factor.

$$U_{eq} = \frac{1}{3} \Sigma_i \Sigma_j U_{ij} a_i^* a_j^* (a_i \cdot a_j)$$

TABLE 2.7: Anistropic temperature factors ($Å^2$, $x10^3$) for

$[Ru_2(CO)_5(NCPh)\{\mu\text{-}(Pr^iO)_2PN(Et)P(OPr^i)_2\}_2](SbF_6)_2$ (2)

	U(11)	U(22)	U(33)	U(23)	U(13)	U(12)
Ru(1)	37(1)	45(1)	34(1)	2(1)	-1(1)	-2(1)
Ru(2)	36(1)	49(1)	39(1)	1(1)	4(1)	2(1)
P(1)	47(4)	59(5)	37(4)	-1(4)	1(4)	6(4)
P(2)	42(4)	64(5)	51(5)	7(4)	8(4)	13(4)
P(3)	48(4)	39(4)	44(4)	-1(4)	4(4)	4(4)
P(4)	39(4)	44(5)	50(5)	13(4)	1(4)	7(4)

TABLE 2.8: Interatomic distances (Å) for

$[Ru_2(CO)_5(NCPh)\{\mu\text{-}(Pr^iO)_2PN(Et)P(OPr^i)_2\}_2](SbF_6)_2$ (2)

Ru(1)-Ru(2)	2.889(3)	Ru(1)-P(3)	2.353(8)
Ru(1)-P(4)	2.341(8)	Ru(1)-N(3)	2.08(2)
Ru(1)-C(26)	1.82(3)	Ru(1)-C(28)	1.95(4)
Ru(2)-P(1)	2.339(8)	Ru(2)-P(2)	2.337(8)
Ru(2)-C(25)	1.90(4)	Ru(2)-C(27)	1.90(3)
Ru(2)-C(29)	1.92(3)	P(1)-O(1)	1.58(2)
P(1)-O(2)	1.59(2)	P(1)-N(2)	1.65(3)
P(2)-O(3)	1.62(2)	P(2)-O(4)	1.60(2)
P(2)-N(1)	1.71(3)	P(3)-O(5)	1.57(2)
P(3)-O(6)	1.52(3)	P(3)-N(2)	1.74(3)
P(4)-O(7)	1.60(3)	P(4)-O(8)	1.59(2)
P(4)-N(1)	1.72(3)	O(1)-C(1)	1.47(4)
O(2)-C(4)	1.49(4)	O(3)-C(7)	1.63(6)
O(4)-C(10)	1.51(5)	O(5)-C(13)	1.51(5)
O(6)-C(16)	1.45(4)	O(7)-C(19)	1.52(4)
O(8)-C(22)	1.49(4)	O(9)-C(28)	1.14(4)
O(10)-C(26)	1.17(3)	O(11)-C(29)	1.14(3)
O(12)-C(25)	1.16(4)	O(13)-C(27)	1.15(4)
N(1)-C(30)	1.52(4)	N(2)-C(32)	1.51(4)
N(3)-C(34)	1.12(4)	C(1)-C(2)	1.52(5)
C(1)-C(3)	1.51(6)	C(4)-C(5)	1.54(6)
C(4)-C(6)	1.49(5)	C(7)-C(8)	1.45(8)
C(7)-C(9)	1.59(9)	C(10)-C(11)	1.41(6)
C(10)-C(12)	1.30(7)	C(13)-C(14)	1.51(7)
C(13)-C(15)	1.56(6)	C(16)-C(17)	1.51(6)
C(16)-C(18)	1.46(6)	C(19)-C(20)	1.51(6)
C(19)-C(21)	1.57(6)	C(22)-C(23)	1.48(5)
C(22)-C(24)	1.52(5)	C(30)-C(31)	1.51(6)
C(32)-C(33)	1.51(4)	C(34)-C(35)	1.43(4)
C(35)-C(36)	1.41(5)	C(35)-C(40)	1.46(5)
C(36)-C(37)	1.52(6)	C(37)-C(38)	1.27(6)
C(38)-C(39)	1.34(5)	C(39)-C(40)	1.45(5)
Sb(1)-F(1)	1.87(4)	Sb(1)-F(2)	1.84(4)
Sb(1)-F(3)	1.79(3)	Sb(1)-F(4)	1.77(4)
Sb(1)-F(5)	1.82(3)	Sb(1)-F(6)	1.66(5)

TABLE 2.8 (continued)

Sb(2)-F(7)	1.789(0)	Sb(2)-F(8)	1.789(0)
Sb(2)-F(9)	1.790(0)	Sb(3)-F(10)	1.791(0)
Sb(3)-F(11)	1.790(0)	Sb(3)-F(12)	1.790(0)

TABLE 2.9: Interatomic angles (°) for

$[Ru_2(CO)_5(NCPh)\{\mu\text{-}(Pr^iO)_2PN(Et)P(OPr^i)_2\}_2](SbF_6)_2$ (2)

Ru(2)-Ru(1)-P(3)	87.2(2)	Ru(2)-Ru(1)-P(4)	86.8(2)
P(3)-Ru(1)-P(4)	173.5(3)	Ru(2)-Ru(1)-N(3)	92.3(7)
P(3)-Ru(1)-N(3)	90.1(7)	P(4)-Ru(1)-N(3)	87.6(7)
Ru(2)-Ru(1)-C(26)	87.3(10)	P(3)-Ru(1)-C(26)	88.9(9)
P(4)-Ru(1)-C(26)	93.4(9)	N(3)-Ru(1)-C(26)	178.9(11)
Ru(2)-Ru(1)-C(28)	175.4(11)	P(3)-Ru(1)-C(28)	93.9(11)
P(4)-Ru(1)-C(28)	92.3(11)	N(3)-Ru(1)-C(28)	92.2(13)
C(26)-Ru(1)-C(28)	88(2)	Ru(1)-Ru(2)-P(1)	86.9(2)
Ru(1)-Ru(2)-P(2)	88.0(2)	P(1)-Ru(2)-P(2)	174.9(3)
Ru(1)-Ru(2)-C(25)	179.0(11)	P(1)-Ru(2)-C(25)	94.0(11)
P(2)-Ru(2)-C(25)	91.1(11)	Ru(1)-Ru(2)-C(27)	85.6(11)
P(1)-Ru(2)-C(27)	91.2(10)	P(2)-Ru(2)-C(27)	88.6(10)
C(25)-Ru(2)-C(27)	95(2)	Ru(1)-Ru(2)-C(29)	87.5(8)
P(1)-Ru(2)-C(29)	91.1(8)	P(2)-Ru(2)-C(29)	88.5(8)
C(25)-Ru(2)-C(29)	91.9(14)	C(27)-Ru(2)-C(29)	172.6(14)
Ru(2)-P(1)-O(1)	118.8(9)	Ru(2)-P(1)-O(2)	116.0(8)
O(1)-P(1)-O(2)	100.0(11)	Ru(2)-P(1)-N(2)	116.3(9)
O(1)-P(1)-N(2)	101.7(12)	O(2)-P(1)-N(2)	101.3(11)
Ru(2)-P(2)-O(3)	112.7(9)	Ru(2)-P(2)-O(4)	115.9(9)
O(3)-P(2)-O(4)	101.8(12)	Ru(2)-P(2)-N(1)	117.4(9)
O(3)-P(2)-N(1)	103.4(13)	O(4)-P(2)-N(1)	103.6(12)
Ru(1)-P(3)-O(5)	108.4(8)	Ru(1)-P(3)-O(6)	121.5(10)
O(5)-P(3)-O(6)	107.6(12)	Ru(1)-P(3)-N(2)	114.1(9)
O(5)-P(3)-N(2)	107.6(11)	O(6)-P(3)-N(2)	96.5(12)
Ru(1)-P(4)-O(7)	117.3(9)	Ru(1)-P(4)-O(8)	116.6(9)
O(7)-P(4)-O(8)	100.8(12)	Ru(1)-P(4)-N(1)	117.9(9)
O(7)-P(4)-N(1)	101.4(12)	O(8)-P(4)-N(1)	99.8(12)
P(1)-O(1)-C(1)	131(2)	P(1)-O(2)-C(4)	125(2)
P(2)-O(3)-C(7)	125(3)	P(2)-O(4)-C(10)	128(2)
P(3)-O(5)-C(13)	125(2)	P(3)-O(6)-C(16)	134(3)
P(4)-O(7)-C(19)	129(2)	P(4)-O(8)-C(22)	124(2)
P(2)-N(1)-P(4)	116(2)	P(2)-N(1)-C(30)	117(2)
P(4)-N(1)-C(30)	126(2)	P(1)-N(2)-P(3)	119.5(14)
P(1)-N(2)-C(32)	124(2)	P(3)-N(2)-C(32)	116(2)
Ru(1)-N(3)-C(34)	169(3)	O(1)-C(1)-C(2)	103(3)

TABLE 2.9 (continued)

O(1)-C(1)-C(3)	112(3)	C(2)-C(1)-C(3)	112(4)
O(2)-C(4)-C(5)	107(3)	O(2)-C(4)-C(6)	106(3)
C(5)-C(4)-C(6)	115(4)	O(3)-C(7)-C(8)	97(5)
O(3)-C(7)-C(9)	97(5)	C(8)-C(7)-C(9)	93(5)
O(4)-C(10)-C(11)	109(4)	O(4)-C(10)-C(12)	104(5)
C(11)-C(10)-C(12)	105(5)	O(5)-C(13)-C(14)	99(4)
O(5)-C(13)-C(15)	102(4)	C(14)-C(13)-C(15)	109(5)
O(6)-C(16)-C(17)	108(3)	O(6)-C(16)-C(18)	112(4)
C(17)-C(16)-C(18)	115(4)	O(7)-C(19)-C(20)	108(3)
O(7)-C(19)-C(21)	103(3)	C(20)-C(19)-C(21)	112(4)
O(8)-C(22)-C(23)	104(3)	O(8)-C(22)-C(24)	99(3)
C(23)-C(22)-C(24)	112(3)	Ru(2)-C(25)-O(12)	170(4)
Ru(1)-C(26)-O(10)	175(3)	Ru(2)-C(27)-O(13)	178(3)
Ru(1)-C(28)-O(9)	163(4)	Ru(2)-C(29)-O(11)	178(3)
N(1)-C(30)-C(31)	111(3)	N(2)-C(32)-C(33)	112(3)
N(3)-C(34)-C(35)	177(4)	C(34)-C(35)-C(36)	118(3)
C(34)-C(35)-C(40)	119(3)	C(36)-C(35)-C(40)	122(3)
C(35)-C(36)-C(37)	114(4)	C(36)-C(37)-C(38)	121(4)
C(37)-C(38)-C(39)	123(4)	C(38)-C(39)-C(40)	123(4)
C(35)-C(40)-C(39)	113(4)	F(1)-Sb(1)-F(2)	92(2)
F(1)-Sb(1)-F(3)	79(2)	F(2)-Sb(1)-F(3)	91(2)
F(1)-Sb(1)-F(4)	92(2)	F(2)-Sb(1)-F(4)	83(2)
F(3)-Sb(1)-F(4)	169(2)	F(1)-Sb(1)-F(5)	89(2)
F(2)-Sb(1)-F(5)	178(2)	F(3)-Sb(1)-F(5)	90.6(14)
F(4)-Sb(1)-F(5)	96(2)	F(1)-Sb(1)-F(6)	173(2)
F(2)-Sb(1)-F(6)	87(2)	F(3)-Sb(1)-F(6)	94(2)
F(4)-Sb(1)-F(6)	95(2)	F(5)-Sb(1)-F(6)	92(2)
F(7)-Sb(2)-F(8)	89.9(0)	F(7)-Sb(2)-F(9)	89.9(0)
F(8)-Sb(2)-F(9)	90.0(0)	F(8)-Sb(2)-F(8)	79.3(0)
F(9)-Sb(2)-F(9)	100.9(0)	F(10)-Sb(3)-F(11)	90.0(0)
F(10)-Sb(3)-F(12)	89.9(0)	F(11)-Sb(3)-F(12)	89.9(0)
F(11)-Sb(3)-F(11)	84.3(0)	F(12)-Sb(3)-F(12)	99.4(0)

TABLE 2.10: Fractional co-ordinates ($x10^4$) and equivalent isotropic temperature factors ($Å^2$, $x10^3$) for $[Ru_2(CO)_5(SC_4H_8)\{\mu\text{-}(Pr^iO)_2PN(Et)P(OPr^i)_2\}_2](SbF_6)_2\cdot CH_2Cl_2$ (12)

	x/a	y/b	z/c	U
Ru(1)	759(1)	7345(1)	1405	45(1)*
Ru(2)	1289(1)	8535(1)	2517(1)	44(1)*
P(1)	1376(2)	7707(3)	468(3)	49(1)*
P(2)	166(3)	7230(3)	2436(4)	62(2)*
P(3)	936(3)	7675(3)	3568(3)	59(2)*
P(4)	1588(2)	9330(3)	1410(3)	52(1)*
S(1)	1230(2)	5979(3)	1839(4)	64(2)*
O(1)	229(7)	6090(11)	251(10)	94(5)
O(2)	249(6)	9034(9)	807(9)	70(4)
O(3)	390(7)	9768(10)	2600(9)	80(4)
O(4)	1856(7)	9877(10)	3574(10)	85(5)
O(5)	2169(7)	7224(10)	2353(8)	74(4)
O(6)	1793(6)	6982(10)	505(9)	74(4)
O(7)	1233(8)	7755(11)	-440(10)	84(5)
O(8)	-179(6)	6347(10)	2532(9)	78(4)
O(9)	-214(7)	8049(10)	2306(9)	84(5)
O(10)	1217(6)	6740(9)	3818(9)	74(4)
O(11)	881(6)	8164(9)	4398(8)	69(4)
O(12)	2117(5)	9809(8)	1504(8)	60(3)
O(13)	1272(5)	10175(8)	1144(7)	55(3)
N(1)	1615(6)	8754(9)	562(8)	50(4)
N(2)	386(8)	7254(10)	3358(9)	59(4)
C(1)	427(9)	6609(13)	698(12)	67(6)
C(2)	439(9)	8387(14)	1072(12)	66(6)
C(3)	721(8)	9283(12)	2568(12)	57(5)
C(4)	1647(9)	9328(13)	3208(11)	56(5)
C(5)	1814(10)	7705(13)	2398(12)	60(5)
C(6)	2255(12)	6873(19)	34(18)	103(9)
C(7)	2526(14)	6119(25)	537(23)	136(11)
C(8)	2205(14)	6685(22)	-771(23)	127(11)
C(9)	769(11)	7715(16)	-823(17)	85(7)
C(10)	817(18)	6982(30)	-1417(31)	170(16)
C(11)	713(15)	8624(24)	-1285(23)	135(12)
C(12)	-369(10)	5746(15)	1889(15)	82(7)

TABLE 2.10 (continued)

C(13)	-730(15)	6235(24)	1457(25)	137(11)
C(14)	-589(14)	4959(22)	2322(20)	124(11)
C(15)	-703(12)	8200(18)	2600(17)	93(8)
C(16)	-996(17)	8584(26)	1908(26)	148(13)
C(17)	-682(14)	8808(24)	3383(22)	126(11)
C(18)	1691(12)	6697(20)	4258(20)	105(9)
C(19)	1992(12)	5890(19)	3974(17)	106(9)
C(20)	1503(22)	6660(37)	5125(38)	203(21)
C(21)	881(12)	9084(18)	4595(18)	99(8)
C(22)	378(15)	9335(23)	4955(24)	133(11)
C(23)	1331(15)	9178(24)	5238(23)	133(12)
C(24)	2533(10)	9430(15)	1917(14)	78(6)
C(25)	2840(12)	8878(19)	1362(18)	101(8)
C(26)	2802(14)	10312(24)	2219(20)	128(11)
C(27)	1217(10)	11075(16)	1594(14)	79(6)
C(28)	699(14)	11458(19)	1420(22)	113(9)
C(29)	1619(12)	11685(19)	1505(19)	100(8)
C(30)	1897(10)	9169(16)	-130(15)	82(7)
C(31)	1755(12)	10002(20)	-479(17)	107(9)
C(32)	32(12)	6957(19)	4051(18)	101(8)
C(33)	167(13)	5925(21)	4314(21)	119(10)
C(34)	874(9)	5199(13)	2521(14)	66(5)
C(35)	901(13)	4268(21)	2088(20)	114(10)
C(36)	936(14)	4371(23)	1255(22)	127(11)
C(37)	1273(9)	5161(13)	1022(12)	64(5)
Sb(1)	3178(1)	8260(1)	4163(1)	86(1)*
Sb(2)	983(1)	2438(2)	4094(2)	117(1)*
F(1)	471(9)	2277(14)	4819(14)	151(7)
F(2)	914(13)	3641(24)	4103(26)	241(14)
F(3)	970(13)	1239(24)	3860(21)	224(13)
F(4)	1407(18)	2635(26)	3322(30)	258(17)
F(5)	557(15)	2520(18)	3282(24)	221(13)
F(6)	1399(20)	2408(29)	4928(36)	292(21)
F(7)	2458(9)	3476(15)	8790(13)	157(8)
F(8)	1207(11)	3014(19)	9559(17)	183(10)
F(9)	2012(10)	3496(17)	10191(17)	181(9)
F(10)	1595(12)	3298(20)	8152(20)	202(11)

TABLE 2.10 (continued)

F(11)	1921(12)	2098(22)	9289(23)	217(12)
F(12)	1765(12)	4531(22)	9094(22)	221(12)
C(38)	2458(25)	3296(40)	2236(36)	206(23)
Cl(1)	3081(9)	2937(16)	2164(16)	278(9)
Cl(2)	2504(12)	4469(22)	2407(21)	366(14)

* $U_{eq} = \frac{1}{3} \Sigma_i \Sigma_j U_{ij} a_i^* a_j^* (a_i \cdot a_j)$

TABLE 2.11: Anistropic temperature factors ($Å^2$, $x10^3$) for $[Ru_2(CO)_5(SC_4H_8)\{\mu\text{-}(Pr^iO)_2PN(Et)P(OPr^i)_2\}_2](SbF_6)_2 \cdot CH_2Cl_2$ (12)

	U(11)	U(22)	U(33)	U(23)	U(13)	U(12)
P(1)	41(5)	48(2)	59(3)	-2(2)	6(3)	6(2)
P(2)	59(6)	49(2)	78(3)	8(3)	11(3)	-1(2)
P(3)	73(6)	51(3)	54(3)	10(2)	10(3)	1(3)
P(4)	59(5)	42(2)	55(3)	9(2)	-2(3)	-7(2)

TABLE 2.12: Interatomic distances (Å) for $[Ru_2(CO)_5(SC_4H_8)\{\mu\text{-}(Pr^iO)_2PN(Et)P(OPr^i)_2\}_2](SbF_6)_2\cdot CH_2Cl_2$ (12)

Ru(1)-Ru(2)	2.925(2)	Ru(1)-P(1)	2.355(6)
Ru(1)-P(2)	2.365(7)	Ru(1)-S(1)	2.482(5)
Ru(1)-C(1)	1.84(2)	Ru(1)-C(2)	1.84(2)
Ru(2)-P(3)	2.362(6)	Ru(2)-P(4)	2.332(5)
Ru(2)-C(3)	1.89(2)	Ru(2)-C(4)	1.90(2)
Ru(2)-C(5)	1.88(2)	P(1)-O(6)	1.55(2)
P(1)-O(7)	1.57(2)	P(1)-N(1)	1.672(15)
P(2)-O(8)	1.60(2)	P(2)-O(9)	1.60(2)
P(2)-N(2)	1.65(2)	P(3)-O(10)	1.621(15)
P(3)-O(11)	1.567(14)	P(3)-N(2)	1.65(2)
P(4)-O(12)	1.606(15)	P(4)-O(13)	1.569(13)
P(4)-N(1)	1.649(15)	S(1)-C(34)	1.88(2)
S(1)-C(37)	1.82(2)	O(1)-C(1)	1.19(3)
O(2)-C(2)	1.16(3)	O(3)-C(3)	1.15(3)
O(4)-C(4)	1.16(3)	O(5)-C(5)	1.20(3)
O(6)-C(6)	1.49(4)	O(7)-C(9)	1.41(4)
O(8)-C(12)	1.48(3)	O(9)-C(15)	1.43(4)
O(10)-C(18)	1.48(4)	O(11)-C(21)	1.38(3)
O(12)-C(24)	1.44(3)	O(13)-C(27)	1.52(3)
N(1)-C(30)	1.51(3)	N(2)-C(32)	1.57(4)
C(6)-C(7)	1.57(5)	C(6)-C(8)	1.38(5)
C(9)-C(10)	1.47(5)	C(9)-C(11)	1.54(4)
C(12)-C(13)	1.41(5)	C(12)-C(14)	1.49(4)
C(15)-C(16)	1.51(5)	C(15)-C(17)	1.58(5)
C(18)-C(19)	1.51(4)	C(18)-C(20)	1.54(7)
C(21)-C(22)	1.54(5)	C(21)-C(23)	1.63(5)
C(24)-C(25)	1.49(4)	C(24)-C(26)	1.57(4)
C(27)-C(28)	1.54(5)	C(27)-C(29)	1.42(4)
C(30)-C(31)	1.40(4)	C(32)-C(33)	1.62(4)
C(34)-C(35)	1.54(4)	C(35)-C(36)	1.40(5)
C(36)-C(37)	1.53(4)	Sb(2)-F(1)	1.86(3)
Sb(2)-F(2)	1.77(4)	Sb(2)-F(3)	1.80(4)
Sb(2)-F(4)	1.75(5)	Sb(2)-F(5)	1.79(4)
Sb(2)-F(6)	1.79(6)	C(38)-Cl(1)	1.78(7)
C(38)-Cl(2)	1.74(7)		

TABLE 2.13: Interatomic angles (°) for $[Ru_2(CO)_5(SC_4H_8)\{\mu\text{-}(Pr^iO)_2PN(Et)P(OPr^i)_2\}_2](SbF_6)_2\cdot CH_2Cl_2$ (12)

Ru(2)-Ru(1)-P(1)	86.4(1)	Ru(2)-Ru(1)-P(2)	85.1(1)
P(1)-Ru(1)-P(2)	170.3(2)	Ru(2)-Ru(1)-S(1)	92.3(1)
P(1)-Ru(1)-S(1)	90.4(2)	P(2)-Ru(1)-S(1)	94.7(2)
Ru(2)-Ru(1)-C(1)	179.3(6)	P(1)-Ru(1)-C(1)	93.1(7)
P(2)-Ru(1)-C(1)	95.3(7)	S(1)-Ru(1)-C(1)	88.2(7)
Ru(2)-Ru(1)-C(2)	86.1(7)	P(1)-Ru(1)-C(2)	87.1(7)
P(2)-Ru(1)-C(2)	87.6(7)	S(1)-Ru(1)-C(2)	177.1(8)
C(1)-Ru(1)-C(2)	93.4(9)	Ru(1)-Ru(2)-P(3)	87.4(1)
Ru(1)-Ru(2)-P(4)	88.0(1)	P(3)-Ru(2)-P(4)	175.2(2)
Ru(1)-Ru(2)-C(3)	88.3(6)	P(3)-Ru(2)-C(3)	86.8(6)
P(4)-Ru(2)-C(3)	91.8(6)	Ru(1)-Ru(2)-C(4)	177.8(6)
P(3)-Ru(2)-C(4)	94.7(6)	P(4)-Ru(2)-C(4)	89.9(6)
C(3)-Ru(2)-C(4)	92.2(9)	Ru(1)-Ru(2)-C(5)	85.5(7)
P(3)-Ru(2)-C(5)	92.4(6)	P(4)-Ru(2)-C(5)	88.5(6)
C(3)-Ru(2)-C(5)	173.9(9)	C(4)-Ru(2)-C(5)	94.0(9)
Ru(1)-P(1)-O(6)	109.8(6)	Ru(1)-P(1)-O(7)	118.4(8)
O(6)-P(1)-O(7)	104.6(9)	Ru(1)-P(1)-N(1)	114.8(6)
O(6)-P(1)-N(1)	109.8(9)	O(7)-P(1)-N(1)	98.5(8)
Ru(1)-P(2)-O(8)	121.9(6)	Ru(1)-P(2)-O(9)	106.7(6)
O(8)-P(2)-O(9)	103.9(9)	Ru(1)-P(2)-N(2)	115.5(8)
O(8)-P(2)-N(2)	97.8(9)	O(9)-P(2)-N(2)	110.1(9)
Ru(2)-P(3)-O(10)	116.7(6)	Ru(2)-P(3)-O(11)	117.0(6)
O(10)-P(3)-O(11)	101.6(8)	Ru(2)-P(3)-N(2)	114.0(6)
O(10)-P(3)-N(2)	99.5(8)	O(11)-P(3)-N(2)	105.7(9)
Ru(2)-P(4)-O(12)	116.8(5)	Ru(2)-P(4)-O(13)	115.3(5)
O(12)-P(4)-O(13)	100.0(7)	Ru(2)-P(4)-N(1)	116.2(5)
O(12)-P(4)-N(1)	105.5(8)	O(13)-P(4)-N(1)	100.6(7)
Ru(1)-S(1)-C(34)	113.6(7)	Ru(1)-S(1)-C(37)	110.1(7)
C(34)-S(1)-C(37)	95.1(9)	P(1)-O(6)-C(6)	132(2)
P(1)-O(7)-C(9)	131(2)	P(2)-O(8)-C(12)	127.6(14)
P(2)-O(9)-C(15)	132(2)	P(3)-O(10)-C(18)	125(2)
P(3)-O(11)-C(21)	131(2)	P(4)-O(12)-C(24)	125.7(12)
P(4)-O(13)-C(27)	126.5(13)	P(1)-N(1)-P(4)	122.1(9)
P(1)-N(1)-C(30)	119.5(12)	P(4)-N(1)-C(30)	118.3(13)
P(2)-N(2)-P(3)	122.2(11)	P(2)-N(2)-C(32)	117(2)

TABLE 2.13 (continued)

P(3)-N(2)-C(32)	120(2)	Ru(1)-C(1)-O(1)	176(2)
Ru(1)-C(2)-O(2)	175(2)	Ru(2)-C(3)-O(3)	177(2)
Ru(2)-C(4)-O(4)	173(2)	Ru(2)-C(5)-O(5)	175(2)
O(6)-C(6)-C(7)	101(2)	O(6)-C(6)-C(8)	117(3)
C(7)-C(6)-C(8)	115(3)	O(7)-C(9)-C(10)	105(3)
O(7)-C(9)-C(11)	106(2)	C(10)-C(9)-C(11)	107(3)
O(8)-C(12)-C(13)	108(2)	O(8)-C(12)-C(14)	104(2)
C(13)-C(12)-C(14)	111(3)	O(9)-C(15)-C(16)	107(3)
O(9)-C(15)-C(17)	110(2)	C(16)-C(15)-C(17)	116(3)
O(10)-C(18)-C(19)	110(2)	O(10)-C(18)-C(20)	100(3)
C(19)-C(18)-C(20)	117(3)	O(11)-C(21)-C(22)	109(2)
O(11)-C(21)-C(23)	104(2)	C(22)-C(21)-C(23)	113(3)
O(12)-C(24)-C(25)	111(2)	O(12)-C(24)-C(26)	102(2)
C(25)-C(24)-C(26)	113(3)	O(13)-C(27)-C(28)	108(2)
O(13)-C(27)-C(29)	115(2)	C(28)-C(27)-C(29)	117(2)
N(1)-C(30)-C(31)	122(2)	N(2)-C(32)-C(33)	109(2)
S(1)-C(34)-C(35)	103(2)	C(34)-C(35)-C(36)	112(3)
C(35)-C(36)-C(37)	112(3)	S(1)-C(37)-C(36)	106(2)
F(1)-Sb(2)-F(2)	92.4(14)	F(1)-Sb(2)-F(3)	90.2(13
F(2)-Sb(2)-F(3)	166(2)	F(1)-Sb(2)-F(4)	173(2)
F(2)-Sb(2)-F(4)	85(2)	F(3)-Sb(2)-F(4)	91(2)
F(1)-Sb(2)-F(5)	91(2)	F(2)-Sb(2)-F(5)	83(2)
F(3)-Sb(2)-F(5)	83.5(14)	F(4)-Sb(2)-F(5)	82(2)
F(1)-Sb(2)-F(6)	88(2)	F(2)-Sb(2)-F(6)	95(2)
F(3)-Sb(2)-F(6)	99(2)	F(4)-Sb(2)-F(6)	99(2)
F(5)-Sb(2)-F(6)	177(2)	Cl(1)-C(38)-Cl(2)	103(4)

TABLE 2.14: Fractional co-ordinates ($x10^4$) and equivalent isotropic temperature factors ($Å^2$, $x10^3$) for $[Ru_2(CO)_4(\mu\text{-}SPh)\{\mu\text{-}(MeO)_2PN(Et)P(OMe)_2\}_2]PF_6$ (27)

	x/a	y/b	z/c	U_{eq}
Ru(1)	804(1)	3428(1)	3297(1)	29(1)
Ru(2)	52(1)	1331(1)	2610(1)	32(1)
P(1)	2328(2)	2938(1)	4441(1)	31(1)
P(2)	-788(2)	3941(2)	2176(1)	41(1)
P(3)	-1536(2)	1800(2)	1474(1)	48(1)
P(4)	1627(2)	780(1)	3709(1)	34(1)
S(1)	2143(1)	2567(1)	2479(1)	32(1)
O(1)	2317(7)	5690(4)	3864(4)	86(2)
O(2)	-1622(6)	3288(5)	4249(4)	76(2)
O(3)	-2411(5)	809(5)	3516(4)	79(2)
O(4)	-124(7)	-781(4)	1660(4)	90(2)
O(5)	3918(4)	3661(3)	4757(3)	42(1)
O(6)	1749(5)	2993(3)	5270(3)	46(1)
O(7)	-258(6)	4937(4)	1725(3)	59(1)
O(8)	-2161(5)	4218(4)	2513(3)	59(1)
O(9)	-1309(7)	1269(4)	627(3)	74(1)
O(10)	-3247(7)	1455(7)	1409(6)	118(2)
O(11)	840(5)	52(3)	4283(3)	54(1)
O(12)	2724(5)	40(3)	3498(3)	51(1)
N(1)	2697(5)	1721(4)	4410(3)	37(1)
N(2)	-1418(6)	3076(4)	1324(3)	47(1)
C(1)	1751(7)	4869(5)	3630(4)	48(2)*
C(2)	-712(8)	3347(5)	3897(4)	51(2)*
C(3)	-1508(8)	990(5)	3158(4)	52(2)*
C(4)	-11(7)	15(6)	2002(4)	50(2)*
C(5)	4883(7)	3891(5)	4195(4)	53(2)*
C(6)	1753(10)	3925(8)	5750(6)	79(2)*
C(7)	-51(10)	6010(8)	2061(6)	84(2)*
C(8)	-3542(11)	4365(8)	2026(7)	87(3)*
C(9)	-2198(18)	856(13)	-142(11)	146(5)*
C(10)	-4004(19)	560(16)	1407(12)	168(6)*
C(11)	151(10)	-1027(7)	4017(6)	81(2)*
C(12)	3651(9)	263(7)	2919(5)	72(2)*
C(13)	3722(7)	1386(5)	5156(4)	51(2)*

TABLE 2.14 (continued)

C(14)	5302(9)	1544(7)	5075(5)	71(2)*
C(15)	-2107(8)	3441(5)	518(4)	56(2)*
C(16)	-991(9)	3552(7)	-62(6)	76(2)*
C(17)	2315(6)	3001(4)	1498(3)	38(1)*
C(18)	2175(8)	2248(6)	837(5)	59(2)*
C(19)	2576(10)	2550(7)	104(6)	79(2)*
C(20)	3133(9)	3635(7)	64(5)	71(2)*
C(21)	3208(8)	4325(6)	684(5)	59(2)*
C(22)	2805(7)	4046(5)	1426(4)	42(1)*
P(5)	5343(3)	7569(2)	2092(2)	94(1)
F(1)	3916(14)	7810(17)	2009(13)	321(9)
F(2)	5979(14)	8434(9)	2799(7)	206(4)
F(3)	6763(12)	7359(13)	2011(9)	257(6)
F(4)	4755(20)	6703(13)	1432(11)	309(7)
F(5)	5451(32)	6841(15)	2722(12)	365(11)
F(6)	5445(25)	8295(16)	1451(10)	310(9)

* isotropic temperature factor.

$$U_{eq} = \frac{1}{3} \Sigma_i \Sigma_j U_{ij} a_i^* a_j^* (a_i \cdot a_j)$$

TABLE 2.15: Anistropic temperature factors ($Å^2$, $x10^3$) for

$[Ru_2(CO)_4(\mu\text{-SPh})\{\mu\text{-}(MeO)_2PN(Et)P(OMe)_2\}_2]PF_6$ (27)

	U(11)	U(22)	U(33)	U(23)	U(13)	U(12)
Ru(1)	28(1)	30(1)	30(1)	2(1)	6(1)	9(1)
Ru(2)	30(1)	31(1)	33(1)	0(1)	6(1)	2(1)
P(1)	31(1)	31(1)	29(1)	3(1)	4(1)	5(1)
P(2)	42(1)	46(1)	37(1)	9(1)	5(1)	19(1)
P(3)	39(1)	52(1)	44(1)	4(1)	-6(1)	4(1)
P(4)	40(1)	30(1)	34(1)	6(1)	10(1)	9(1)
S(1)	29(1)	34(1)	33(1)	4(1)	8(1)	7(1)
O(1)	106(5)	31(3)	95(4)	-10(3)	-22(4)	4(3)
O(2)	60(3)	113(5)	82(4)	27(3)	50(3)	38(3)
O(3)	47(3)	111(5)	84(4)	6(4)	38(3)	2(3)
O(4)	113(5)	62(3)	79(4)	-38(3)	0(4)	18(3)
O(5)	32(2)	46(2)	42(2)	0(2)	0(2)	-1(2)
O(6)	57(3)	44(2)	40(2)	3(2)	16(2)	7(2)
O(7)	78(3)	55(3)	59(3)	24(2)	28(3)	26(3)
O(8)	41(2)	86(4)	55(3)	10(3)	7(2)	33(3)
O(9)	108(4)	66(3)	32(3)	-15(2)	-3(3)	-6(3)
O(10)	51(4)	126(6)	152(7)	30(5)	-11(4)	-21(4)
O(11)	67(3)	33(2)	63(3)	13(2)	24(2)	-6(2)
O(12)	63(3)	43(2)	54(3)	6(2)	19(2)	22(2)
N(1)	43(3)	32(2)	38(3)	9(2)	12(2)	9(2)
N(2)	42(3)	57(3)	36(3)	6(3)	-5(2)	14(3)
P(5)	106(2)	84(2)	86(2)	-29(1)	1(2)	35(2)
F(1)	158(10)	407(26)	388(23)	-148(19)	16(12)	146(13)
F(2)	272(13)	177(9)	136(8)	-74(7)	-22(8)	62(9)
F(3)	159(9)	401(22)	237(14)	-34(15)	44(9)	148(12)
F(4)	334(18)	235(15)	278(19)	-160(14)	-51(15)	38(13)
F(5)	701(42)	225(16)	237(18)	129(15)	148(25)	182(22)
F(6)	441(27)	301(22)	213(16)	128(16)	64(17)	117(20)

TABLE 2.16: Interatomic distances (Å) for

$[Ru_2(CO)_4(\mu\text{-}SPh)\{\mu\text{-}(MeO)_2PN(Et)P(OMe)_2\}_2]PF_6$ (27)

Ru(1)-Ru(2)	2.796(1)	Ru(1)-P(1)	2.316(2)
Ru(1)-P(2)	2.335(2)	Ru(1)-S(1)	2.380(2)
Ru(1)-C(1)	1.923(6)	Ru(1)-C(2)	1.899(8)
Ru(2)-P(3)	2.326(2)	Ru(2)-P(4)	2.323(2)
Ru(2)-S(1)	2.387(1)	Ru(2)-C(3)	1.895(8)
Ru(2)-C(4)	1.909(7)	P(1)-O(5)	1.600(4)
P(1)-O(6)	1.589(5)	P(1)-N(1)	1.661(5)
P(2)-O(7)	1.590(6)	P(2)-O(8)	1.596(6)
P(2)-N(2)	1.690(5)	P(3)-O(9)	1.599(6)
P(3)-O(10)	1.582(7)	P(3)-N(2)	1.669(6)
P(4)-O(11)	1.589(5)	P(4)-O(12)	1.590(5)
P(4)-N(1)	1.673(4)	S(1)-C(17)	1.788(6)
O(1)-C(1)	1.114(8)	O(2)-C(2)	1.131(10)
O(3)-C(3)	1.140(10)	O(4)-C(4)	1.122(9)
O(5)-C(5)	1.447(9)	O(6)-C(6)	1.402(11)
O(7)-C(7)	1.430(11)	O(8)-C(8)	1.428(11)
O(9)-C(9)	1.40(2)	O(10)-C(10)	1.25(2)
O(11)-C(11)	1.440(10)	O(12)-C(12)	1.441(11)
N(1)-C(13)	1.533(8)	N(2)-C(15)	1.499(9)
C(13)-C(14)	1.506(11)	C(15)-C(16)	1.566(13)
C(17)-C(18)	1.393(10)	C(17)-C(22)	1.374(8)
C(18)-C(19)	1.408(13)	C(19)-C(20)	1.425(12)
C(20)-C(21)	1.305(12)	C(21)-C(22)	1.414(11)
P(5)-F(1)	1.41(2)	P(5)-F(2)	1.524(10)
P(5)-F(3)	1.438(14)	P(5)-F(4)	1.47(2)
P(5)-F(5)	1.45(2)	P(5)-F(6)	1.47(2)

TABLE 2.17: Interatomic angles (°) for

$[Ru_2(CO)_4(\mu\text{-SPh})\{\mu\text{-}(MeO)_2PN(Et)P(OMe)_2\}_2]PF_6$ (27)

Ru(2)-Ru(1)-P(1)	90.4(0)	Ru(2)-Ru(1)-P(2)	90.5(0)
P(1)-Ru(1)-P(2)	177.9(1)	Ru(2)-Ru(1)-S(1)	54.2(0)
P(1)-Ru(1)-S(1)	87.0(1)	P(2)-Ru(1)-S(1)	95.1(1)
Ru(2)-Ru(1)-C(1)	164.8(2)	P(1)-Ru(1)-C(1)	88.5(2)
P(2)-Ru(1)-C(1)	91.1(2)	S(1)-Ru(1)-C(1)	110.6(2)
Ru(2)-Ru(1)-C(2)	95.5(2)	P(1)-Ru(1)-C(2)	88.6(2)
P(2)-Ru(1)-C(2)	89.4(2)	S(1)-Ru(1)-C(2)	149.3(2)
C(1)-Ru(1)-C(2)	99.6(3)	Ru(1)-Ru(2)-P(3)	90.9(1)
Ru(1)-Ru(2)-P(4)	91.9(0)	P(3)-Ru(2)-P(4)	177.1(1)
Ru(1)-Ru(2)-S(1)	54.0(0)	P(3)-Ru(2)-S(1)	95.0(1)
P(4)-Ru(2)-S(1)	86.2(1)	Ru(1)-Ru(2)-C(3)	94.4(2)
P(3)-Ru(2)-C(3)	91.7(2)	P(4)-Ru(2)-C(3)	88.7(2)
S(1)-Ru(2)-C(3)	147.7(2)	Ru(1)-Ru(2)-C(4)	164.0(2)
P(3)-Ru(2)-C(4)	89.0(2)	P(4)-Ru(2)-C(4)	88.2(2)
S(1)-Ru(2)-C(4)	110.1(2)	C(3)-Ru(2)-C(4)	101.5(3)
Ru(1)-P(1)-O(5)	116.6(2)	Ru(1)-P(1)-O(6)	115.2(2)
O(5)-P(1)-O(6)	99.4(2)	Ru(1)-P(1)-N(1)	118.6(2)
O(5)-P(1)-N(1)	103.5(2)	O(6)-P(1)-N(1)	100.7(3)
Ru(1)-P(2)-O(7)	120.5(2)	Ru(1)-P(2)-O(8)	106.2(2)
O(7)-P(2)-O(8)	105.1(3)	Ru(1)-P(2)-N(2)	117.9(2)
O(7)-P(2)-N(2)	97.4(3)	O(8)-P(2)-N(2)	108.8(3)
Ru(2)-P(3)-O(9)	111.4(2)	Ru(2)-P(3)-O(10)	117.1(4)
O(9)-P(3)-O(10)	102.8(4)	Ru(2)-P(3)-N(2)	118.3(2)
O(9)-P(3)-N(2)	103.6(3)	O(10)-P(3)-N(2)	101.7(4)
Ru(2)-P(4)-O(11)	115.3(2)	Ru(2)-P(4)-O(12)	117.6(2)
O(11)-P(4)-O(12)	99.0(3)	Ru(2)-P(4)-N(1)	116.9(2)
O(11)-P(4)-N(1)	100.9(3)	O(12)-P(4)-N(1)	104.3(2)
Ru(1)-S(1)-Ru(2)	71.8(0)	Ru(1)-S(1)-C(17)	120.1(2)
Ru(2)-S(1)-C(17)	121.0(2)	P(1)-O(5)-C(5)	120.6(4)
P(1)-O(6)-C(6)	124.9(5)	P(2)-O(7)-C(7)	124.8(6)
P(2)-O(8)-C(8)	126.5(6)	P(3)-O(9)-C(9)	136.8(9)
P(3)-O(10)-C(10)	130.7(11)	P(4)-O(11)-C(11)	122.2(5)
P(4)-O(12)-C(12)	123.9(5)	P(1)-N(1)-P(4)	120.1(3)
P(1)-N(1)-C(13)	119.3(4)	P(4)-N(1)-C(13)	118.4(4)
P(2)-N(2)-P(3)	116.3(3)	P(2)-N(2)-C(15)	120.3(5)

TABLE 2.17 (continued)

P(3)-N(2)-C(15)	122.2(4)	Ru(1)-C(1)-O(1)	176.4(7)
Ru(1)-C(2)-O(2)	179.2(6)	Ru(2)-C(3)-O(3)	177.1(6)
Ru(2)-C(4)-O(4)	175.8(7)	N(1)-C(13)-C(14)	112.3(6)
N(2)-C(15)-C(16)	110.3(6)	S(1)-C(17)-C(18)	118.8(5)
S(1)-C(17)-C(22)	120.4(4)	C(18)-C(17)-C(22)	120.0(6)
C(17)-C(18)-C(19)	120.2(7)	C(18)-C(19)-C(20)	118.3(8)
C(19)-C(20)-C(21)	120.0(9)	C(20)-C(21)-C(22)	123.0(7)
C(17)-C(22)-C(21)	118.6(6)	F(1)-P(5)-F(2)	92.0(10)
F(1)-P(5)-F(3)	169.0(11)	F(2)-P(5)-F(3)	94.0(8)
F(1)-P(5)-F(4)	89.4(11)	F(2)-P(5)-F(4)	177.6(9)
F(3)-P(5)-F(4)	84.9(10)	F(1)-P(5)-F(5)	104(2)
F(2)-P(5)-F(5)	86.0(8)	F(3)-P(5)-F(5)	85.3(14)
F(4)-P(5)-F(5)	91.8(10)	F(1)-P(5)-F(6)	83.5(13)
F(2)-P(5)-F(6)	93.6(8)	F(3)-P(5)-F(6)	86.9(12)
F(4)-P(5)-F(6)	88.5(10)	F(5)-P(5)-F(6)	172(2)

CHAPTER 3

REACTION OF $[Ru_2(\mu\text{-}CO)(CO)_4\{\mu\text{-}(RO)_2PN(Et)P(OR)_2\}_2]$ WITH SILVER(I) SALTS IN PROTIC SOLVENTS, AND WITH SILVER(I) CARBOXYLATES

3.1 INTRODUCTION

The synthesis of the solvento species $[Ru_2(CO)_5(solvent)\{\mu\text{-}(RO)_2PN(Et)P(OR)_2\}_2]^{2+}$ by reaction of the neutral dimer $[Ru_2(\mu\text{-}CO)(CO)_4\{\mu\text{-}(RO)_2PN(Et)P(OR)_2\}_2]$ with silver(I) salts in non-protic solvents as well as the synthesis and reactivity of the aquo solvento species $[Ru_2(CO)_5(H_2O)\{\mu\text{-}(RO)_2PN(Et)P(OR)_2\}_2]^{2+}$ has been discussed, briefly in the case of the aquo solvento species, in Chapter 2. The investigations of the reactions of the parent dimer with silver(I) salts has been extended to include the solvents methanol and ethanol in order to gain a better understanding of the properties of the solvento species $[Ru_2(CO)_5(solvent)\{\mu\text{-}(RO)_2PN(Et)P(OR)_2\}_2]^{2+}$, where the solvent is protic.

The initial aim of the investigation was to develop a synthetic route to

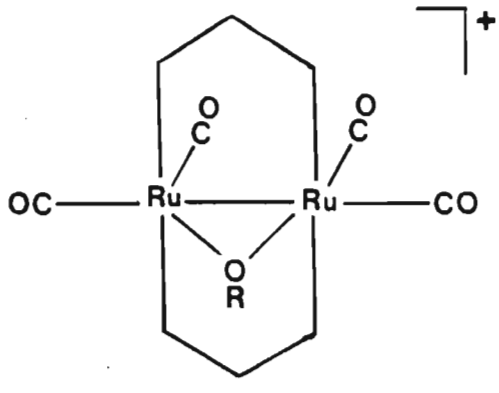

R = H, Me etc

Figure 3.1

bridged hydroxy and alkoxy complexes of the type $[Ru_2(CO)_4(\mu\text{-}OR')\{\mu\text{-}(RO)_2PN(Et)P(OR)_2\}_2]^+$ (R' = H, Me, Et etc; R = Me, Pr^i) (Figure 3.1). The addition of alkoxide ions to the solvento species $[Ru_2(CO)_5(solvent)\{\mu\text{-}(RO)_2PN(Et)P(OR)_2\}_2]^{2+}$ (solvent = acetone) with concommitant loss of carbon monoxide, was envisaged to be a possible route to complexes of this type.

However, it has become apparent from this investigation that a carbonyl group of the solvento species is a potential site for nucleophilic attack and that addition of hydroxide or alkoxide ions results in the formation of hydroxy- or alkoxycarbonyl complexes of stoichiometry $[Ru_2(CO)_4\{\mu\text{-}OC(OR')\}\{\mu\text{-}(RO)_2PN(Et)P(OR)_2\}_2]^+$ (R' = H, Me or Et) (Scheme 3.1).

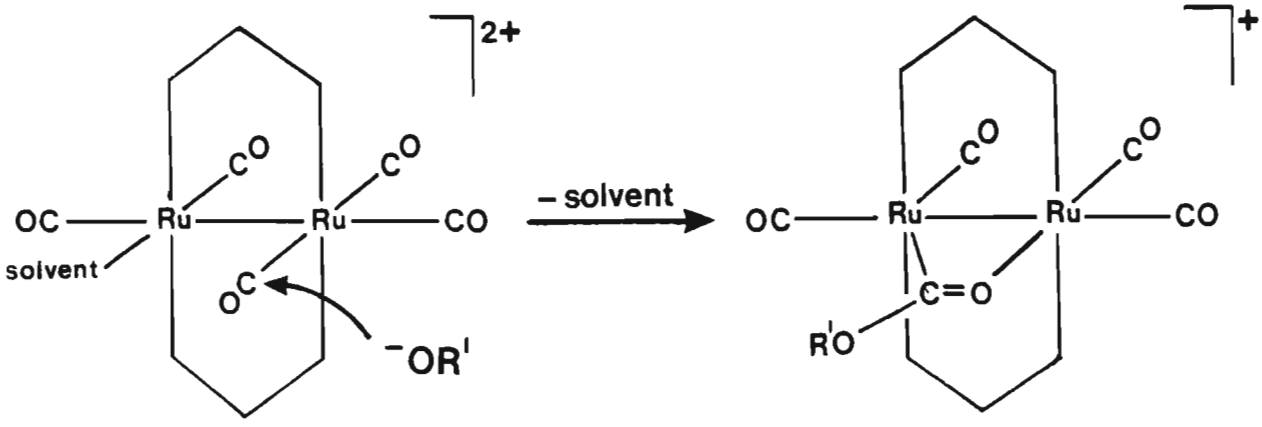

Scheme 3.1

A commonly accepted explanation for the relative scarcity of low-valent metal-alkoxide derivatives is that such linkages are characteristically weak due to a mismatch of these hard, basic ligands, with soft group (VIII) transition metal centres.[158] The difficulty in isolating metal alkoxide complexes and the ease with which they decompose (presumably by β-hydride elimination) to metal hydrides support this hypothesis. Despite this, a number of hydroxide- and alkoxide-bridged binuclear

complexes of group VIII metals have appeared in the literature. For example, dirhodium complexes of the type $[Rh_2(\mu\text{-}OR)(CO)_2(\mu\text{-}dppm)_2]^+$ (R = H, Me, Et) have been prepared by addition of RONa to $[RhCl(CO)(dppm)]_2$,[159] while a related iridium hydroxide complex $[Ir_2(\mu\text{-}OH)(CO)_2(\mu\text{-}dppm)_2]^+$ has been obtained from the reaction of $[IrCl(CO)(dppm)]_2$ with excess NaOH.[5]

Homogeneously catalyzed reactions involving carbon monoxide have been the subject of intensive experimental investigation in recent years. The renewed attention has been based, in part, upon the desirability of using synthesis gas (CO/H_2 mixture) as a feedstock for the production of organic chemicals and fuels. Reactions of particular interest have included the reduction of CO by dihydrogen[160] and the water-gas shift (WGS).[161,162] A key step in the mechanisms proposed for a number of these catalyzed reactions is that involving nucleophilic attack at a co-ordinated carbon monoxide, as shown in the equation below:

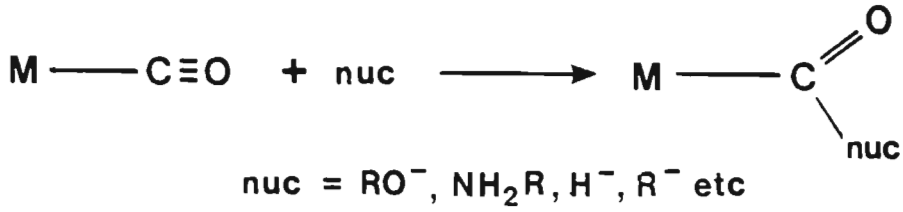

Equation 3.1

For example, the homogeneous catalysis of the water-gas shift by metal carbonyls in solution has been proposed to proceed via a cycle such as that shown in Scheme 3.2. The transformation of CO in this scheme involves the reaction of a co-ordinated carbonyl group with hydroxide ions to give a hydroxycarbonyl complex, $[M(CO)_x(CO_2H)]^-$. Subsequent decarboxylation of the latter leads to the formation of the metal-

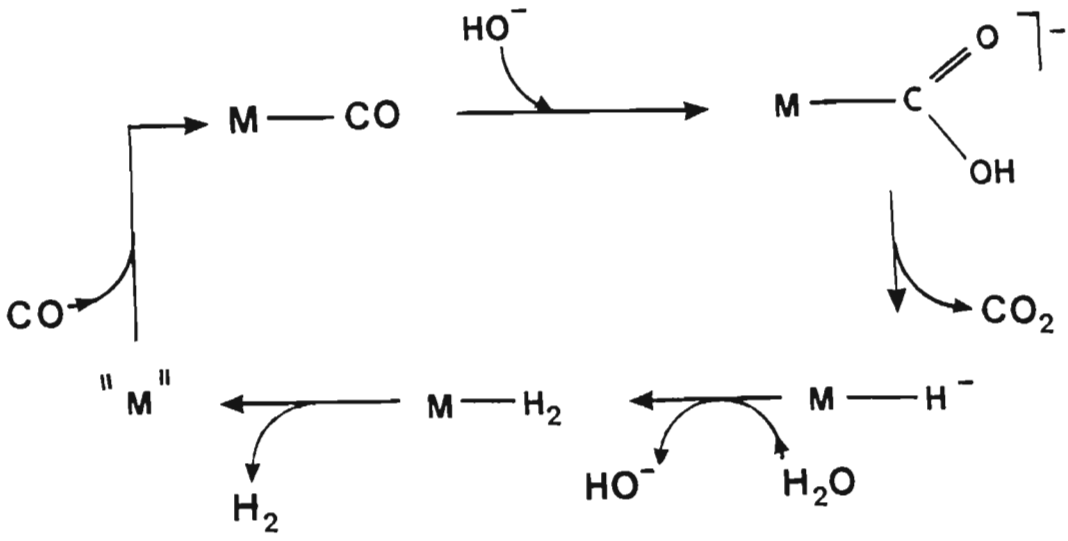

Scheme 3.2

hydride anion $[M(CO)_xH]^-$. The conversion of CO via reactions of this type and involving H_2O or a base, is important not only for the water-gas shift adjustment of the CO/H_2 ratios in synthesis gas feedstocks, but also in using CO/H_2O mixtures for the catalytic reduction and hydroformylation/hydromethylation of various organic substrates.[163-165] The reactions of the nucleophiles MeO^- and OH^- with the mononuclear pentacarbonyl complexes $[M(CO)_5]$ (M = Fe, Ru, Os) have been described by Ford and co-workers.[166] For the methoxide ion, the product in each case was shown to be the methoxycarbonyl adduct $[M(CO)_4(CO_2CH_3)]^-$. Reaction with NaOH, on the other hand, gives the hydroxycarbonyl adduct $[M(CO)_4(CO_2H)]^-$. This reaction was shown to be somewhat slower and to be followed by decarboxylation to afford the metal hydride complex $[HM(CO)_4]^-$. This was shown to occur via a base-independent β-elimination pathway, *i.e.* a concerted process involving the transfer of hydrogen to the metal and cleavage of the metal-carbon bond. The reactions of the triangular clusters $[M_3(CO)_{12}]$ (M = Fe, Ru or Os, with methoxide and hydroxide ions have also been studied.[167] Addition of methoxide ions to both the ruthenium and osmium species results in the

formation of the stable methoxycarbonyl adducts $[M_3(CO)_{11}(CO_2CH_3)]Na$, whereas for the triiron analogue, this adduct undergoes fragmentation to give mononuclear $[Fe(CO)_4(CO_2CH_3)]^-$. Significantly, monosubstitution of the ruthenium cluster with $(CH_3O)_3P$ markedly reduces its susceptibility to attack by the anionic nucleophile. The reaction of the triruthenium species $[Ru_3(CO)_{12}]$ with hydroxide ions results in the formation of the analogous hydroxycarbonyl species $[Ru_3CO)_{11}(CO_2H)]^-$ which readily degrades to the hydride species $[HRu_3(CO)_{11}]^-$. This species has received considerable attention as a homogeneous catalyst for the water-gas shift reaction[167,168] and for the hydrogenation,hydroformylation and hydrosilation of alkenes.[169]

Carboxylate complexes have until recently constituted a large proportion of the studies involving binuclear ruthenium(I) derivatives, largely as a result of the readily available and versatile precursors $[Ru(CO)_2(OOCR)]_n$ and $[Ru_2(CO)_4(\mu\text{-}OOCR)_2(MeCN)_2]$.[99] These polymeric and dinuclear carboxylato complexes have been shown to be useful starting materials for the synthesis of new binuclear ruthenium(I) complexes on the basis that the bridging carboxyate ligands may be readily displaced by a wide range of potentially bridging ligands. For example, the synthesis of the dppm-bridged acetato species $[Ru_2(CO)_4(\mu\text{-}OOCCH_3)(\mu\text{-}dppm)_2]PF_6$ has very recently been reported[26] and was shown to be achieved by reaction of $[Ru(\mu\text{-}OOCCH_3)(CO)_2]_n$ with two molar equivalents of dppm in refluxing ethanol, followed by the addition of NH_4PF_6.[117] The binuclear ruthenium complexes of general formula $[Ru_2(CO)_4(\mu\text{-}XY)_2(PPh_3)_2]$ (XY^- = $NC_5H_4O^-$, $S_2NC_3H_4^-$) have been synthesized by reaction of $[Ru_2(CO)_4(\mu\text{-}OOCCH_3)_2$-$(PPh_3)_2]$ with sodium 2-oxypyridinate and sodium 2-mercaptothiazolate respectively. The related pyrazolato-bridged complex $[Ru_2(CO)_4(\mu\text{-}XY)_2$-$(PPh_3)_2]$ (XY^- = $N_2C_3H_3^-$), on the other hand, was synthesized by reaction of $[Ru_2(CO)_4(\mu\text{-}OOCCH_3)_2(MeCN)_2]$ with sodium pyrazolate, followed by

addition of PPh_3.

It has been demonstrated previously in these laboratories that reaction of the dinuclear tetramethoxydiphophazane-bridged complex $[Ru_2(\mu\text{-}CO)(CO)_4\{\mu\text{-}(MeO)_2PN(Et)P(OMe)_2\}_2]$ with silver acetate readily leads to the formation of an acetato-bridged tetracarbonyl species, $[Ru_2(CO)_4(\mu\text{-}OOCCH_3)\{\mu\text{-}(MeO)_2PN(Et)P(OMe)_2\}_2]^+$. This result would appear to be inconsistent with the observed stability of the pentacarbonyl unidentate acetato-species $[Ru_2(CO)_5(OOCCH_3)\{\mu\text{-}(Pr^iO)_2PN(Et)P(OPr^i)_2\}_2]^+$ to decarbonylation, as described in the previous chapter. A study of the reactions of the dinuclear diphosphazane-bridged derivatives with a range of silver(I) carboxylates was thus undertaken in an attempt to clarify this anomaly. The establishment with which the acetate ligands in the complex $[Ru_2(CO)_4(\mu\text{-}OOCCH_3)_2(PPh_3)_2]$, described above, were shown to be displaced also prompted the investigation of the substitution of the acetate ligand in the complexes $[Ru_2(CO)_4(\mu\text{-}OOCR')\{\mu\text{-}(RO)_2PN(Et)P(OR)_2\}_2]^+$ (R = Me or Pr^i; R' = Me or Ph) by 2-oxypyridinate and pyrazolate anions, as well as by other anionic ligands such as hydroxide (OH^-), alkoxide (OR^-) and thiolate (SR^-) ions.

3.2 REACTIONS OF $[Ru_2(\mu\text{-}CO)(CO)_4\{\mu\text{-}(RO)_2PN(Et)P(OR)_2\}_2]$ (R = Me or Pr^i) WITH $AgSbF_6$ IN THF/WATER AND IN ACETONE/WATER

Addition of a twice molar amount of $AgSbF_6$ to a solution of the tetramethoxy- or tetraisopropoxydiphosphazane-bridged derivative $[Ru_2(\mu\text{-}CO)(CO)_4\{\mu\text{-}(RO)_2PN(Et)P(OR)_2\}_2]$ (R = Me or Pr^i) in THF or acetone, containing 1% water, was found to result in the immediate separation of silver metal from the pale yellow solution and the formation of a readily isolable product, characterized as the dicationic aquo solvento species $[Ru_2(CO)_5(H_2O)\{\mu\text{-}(RO)_2PN(Et)P(OR)_2\}_2](SbF_6)_2$.

The infrared spectrum of the tetraisopropoxydiphosphazane-bridged derivative $[Ru_2(CO)_5(H_2O)\{\mu\text{-}(Pr^iO)_2PN(Et)P(OPr^i)_2\}_2](SbF_6)_2$ (**7**) exhibits a pattern of peaks in the C-O stretching region similar to that of dicationic solvento species described previously, and a broad peak at 3450 cm^{-1} which can be assigned to the O-H stretching vibration of the co-ordinated water. The frequency of the latter is similar to those found for $[Ru_2(\mu\text{-}OOCMe)_4(H_2O)_2]$ (ν(OH) 3490, 3370 and 3250 cm^{-1}).[156] The ^1H nmr spectrum of this compound is also consistent with the presence of a co-ordinated water molecule; a broad peak at 3.15 ppm, the integral of which corresponds to two protons, was observed to collapse upon addition of D_2O. The $^{31}P\{^1H\}$ nmr spectrum of this compound, measured in CD_2Cl_2, exhibits an AA'BB' pattern of peaks at 125.00 ppm, consistent with an asymmetric structure.

The infra-red spectrum of the tetramethoxydiphosphazane-bridged analogue $[Ru_2(CO)_5(H_2O)\{\mu\text{-}(MeO)_2PN(Et)P(OMe)_2\}_2](SbF_6)_2$ (**9**) exhibits a band pattern similar to that of the tetraisopropoxydiphosphazane derivative in the C-O stretching region and a broad peak at 3520 cm^{-1} which can be assigned to the O-H stretching vibration of the co-ordinated water. The product was insufficiently soluble in non co-ordinating solvents such as dichloromethane to obtain $^{31}P\{^1H\}$ and ^1H nmr spectra.

A single crystal X-ray structure determination was carried out for the tetraisopropoxy derivative $[Ru_2(CO)_5(H_2O)\{\mu\text{-}(Pr^iO)_2PN(Et)P(OPr^i)_2\}_2](SbF_6)_2$ using a crystal isolated from the reaction of $AgSbF_6$ with the parent complex in an acetone/water mixture. The stereochemistry of the dicationic species is illustrated in Figure 3.2. The two ruthenium atoms, each of which is approximately octahedral, are separated by a distance of 2.871(1)Å, consistent with a formal Ru-Ru bond. The cation adopts an essentially staggered conformation, while the water molecule

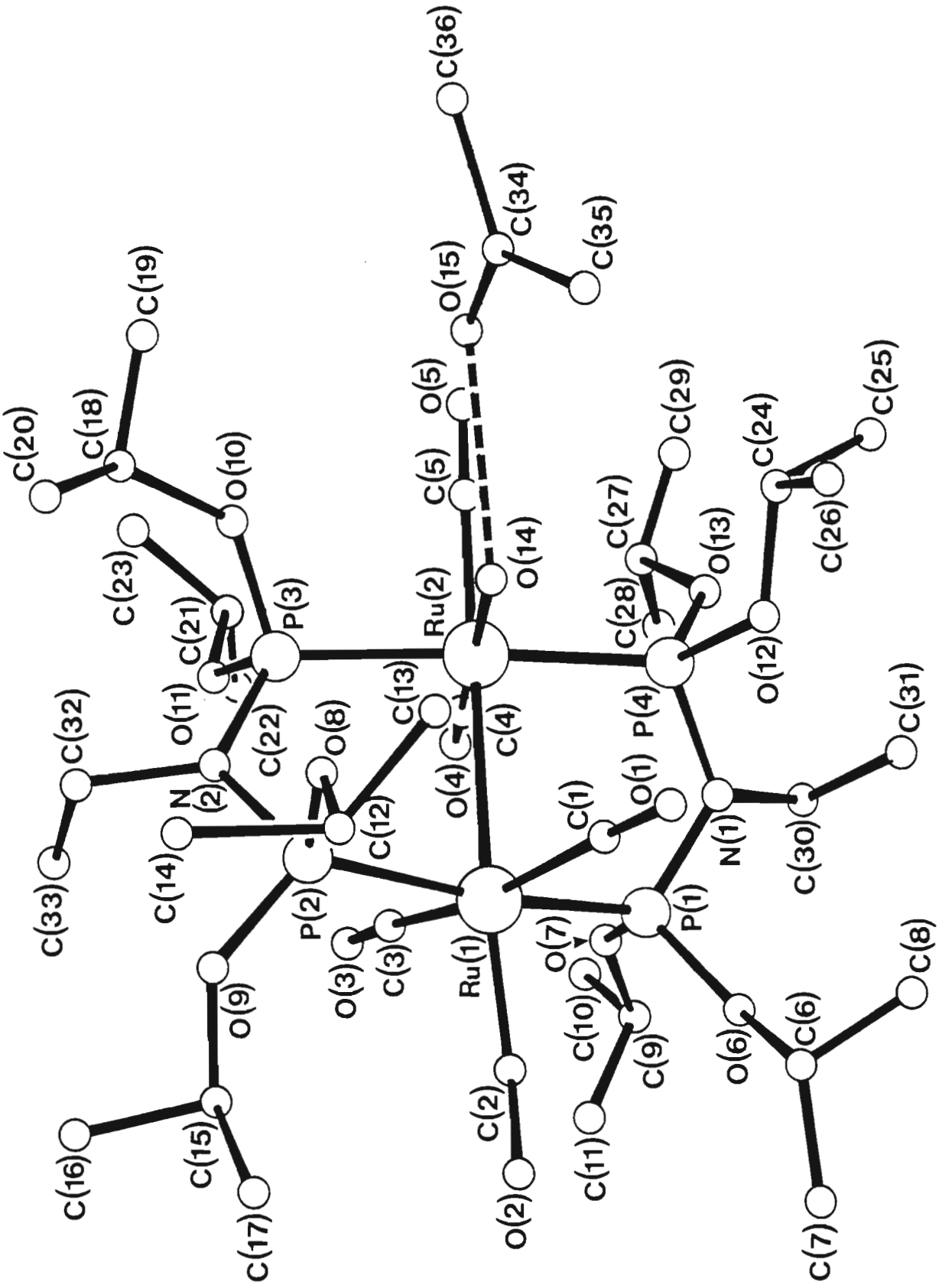

Figure 3.2:

Structure of $[Ru_2(CO)_5(H_2O)\{\mu\text{-}(Pr^iO)_2PN(Et)P(OPr^i)_2\}_2].OC(CH_3)_2^{2+}$

is co-ordinated equatorially with a ruthenium-oxygen separation of 2.212(8)Å. An interesting feature of the structure is the presence of an acetone molecule hydrogen-bonded to the co-ordinated water (O(water)...O(acetone) 2.656Å). Although the position of the hydrogens of the co-ordinated water could not be located in the refinement of the crystal data, it could be assumed that the oxygen-hydrogen bonds are directed towards the oxygen atom of the acetone molecule.

It was anticipated that the hydrogens of the co-ordinated water in the complexes $[Ru_2(CO)_5(H_2O)\{\mu\text{-}(RO)_2PN(Et)P(OR)_2\}_2]^{2+}$ (R = Me or Pr^i) would be very acidic and that these complexes could be readily deprotonated by weak bases. Consistent with this, addition of an equimolar amount of pyridine or triethylamine to these complexes was found to lead to the formation of a monocationic species, $[Ru_2(CO)_4\{\mu\text{-}OC(OH)\}\{\mu\text{-}(RO)_2PN(Et)P(OR)_2\}_2]^+$, resulting from the deprotonation of the aquo solvento species, and the subsequent migration of the hydroxo ligand onto the carbon of an adjacent carbonyl ligand. The monocationic pentacarbonyl hydroxo derivative $[Ru_2(CO)_5(OH)\{\mu\text{-}(RO)_2PN(Et)P(OR)_2\}_2]^+$ is proposed to be an intermediate in the formation of the hydroxycarbonyl species but it was not detected using $^{31}P\{^1H\}$ nmr and infrared spectroscopy. Two isomeric forms are possible for the hydroxycarbonyl species, *viz.* $[Ru_2(CO)_4\{\mu\text{-}OC(OH)\}\{\mu\text{-}(RO)_2PN(Et)P(OR)_2\}_2]^+$ (Figure 3.3 (a)) and

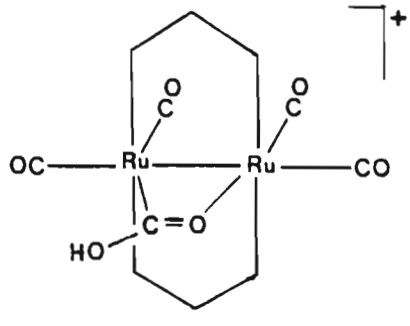

(a)

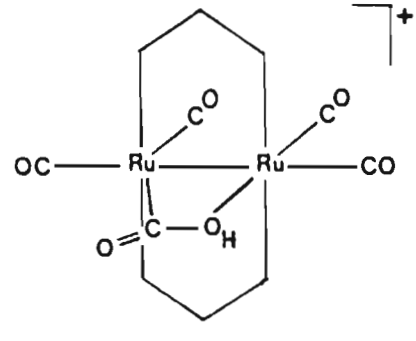

(b)

Figure 3.3

$[Ru_2(CO)_4\{\mu\text{-}HOC(O)\}\{\mu\text{-}(RO)_2PN(Et)P(OR)_2\}_2]^+$ (Figure 3.3 (b)). However, on the basis of the structures established X-ray crystallographically for the analogous methoxy- and ethoxycarbonyl species, discussed in Section 3.3, it is concluded that the hydroxycarbonyl derivative occurs as isomer (a).

The infrared spectrum of $[Ru_2(CO)_4\{\mu\text{-}OC(OH)\}\{\mu\text{-}(Pr^iO)_2PN(Et)P(OPr^i)_2\}_2]\text{-}SbF_6$ (**33**) contains four bands in the C-O stretching region at 2033(s), 2000(vs), 1973(s) and 1952(m) cm^{-1}, the pattern of which is typical for monocationic complexes of the type $[Ru_2(\mu\text{-}X)(CO)_4\{\mu\text{-}(Pr^iO)_2PN(Et)P\text{-}(OPr^i)_2\}_2]^+$ (X = bridging anionic ligand), and a broad weak band at 1700 cm^{-1} which can be assigned to the C-O stretching vibration of the bridging hydroxycarbonyl ligand. The $^{31}P\{^1H\}$ nmr spectrum, measured in $CDCl_3$, exhibits an AA'BB' pattern of peaks at 139.88 ppm, while the ^1H nmr spectrum contains resonances associated with the protons of the diphosphazane ligands, as well as a broad peak at 1.75 ppm which can be assigned to the proton of the hydroxycarbonyl moiety.

The deprotonation of $[Ru_2(CO)_5(H_2O)\{\mu\text{-}(Pr^iO)_2PN(Et)P(OPr^i)_2\}_2]^{2+}$ is reversible and, significantly, treatment of $[Ru_2(CO)_4\{\mu\text{-}OC(OH)\}\text{-}\{\mu\text{-}(Pr^iO)_2PN(Et)P(OPr^i)_2\}_2]^+$ with $HBF_4.OEt_2$ in dichloromethane, was found to produce the dicationic aquo solvento species in quantitative yield.

The hydroxycarbonyl species $[Ru_2(CO)_4\{\mu\text{-}OC(OH)\}\{\mu\text{-}(Pr^iO)_2PN(Et)P\text{-}(OPr^i)_2\}_2]^+$ can be deprotonated further provided stronger bases such as potassium hydroxide or an excess of triethylamine are employed. Thus addition of an aqueous solution of potassium hydroxide to a solution of $[Ru_2(CO)_4\{\mu\text{-}OC(OH)\}\{\mu\text{-}(Pr^iO)_2PN(Et)P(OPr^i)_2\}_2]^+$ in dichloromethane and vigorous stirring of the two layer mixture led to the formation of a

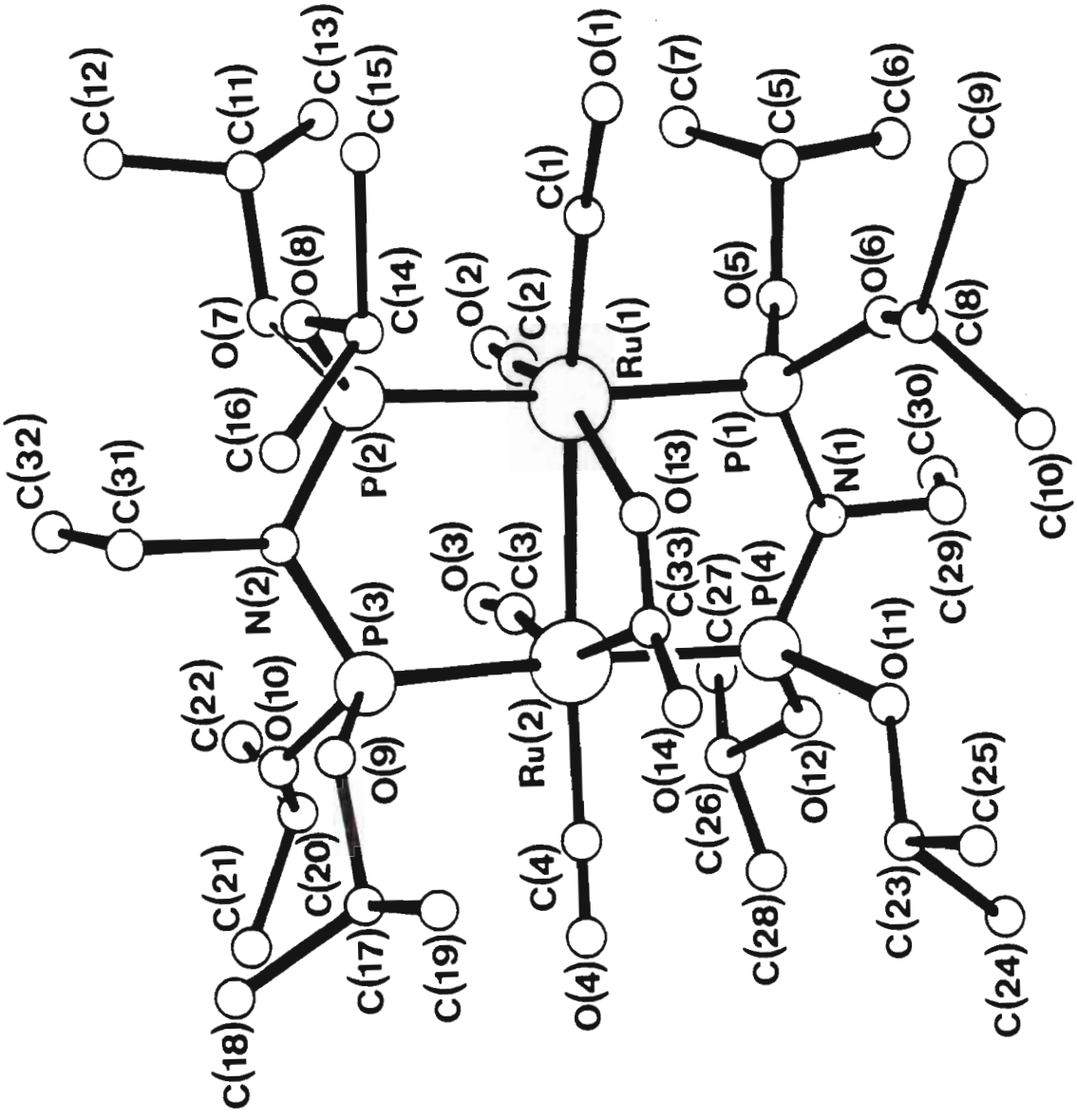

Figure 3.4: Structure of $[Ru_2(CO)_4\{\mu\text{-}OC(O)\}\{\mu\text{-}(Pr^iO)_2PN(Et)P(OPr^i)_2\}_2]$

neutral product characterized as the carbon dioxide adduct $[Ru_2(CO)_4\{\mu\text{-}OC(O)\}\{\mu\text{-}(Pr^iO)_2PN(Et)P(OPr^i)_2\}_2]$ (35).

The infrared spectrum of this complex contains a typical four-line band pattern in the C-O stretching region as well as broad peaks at 1710 and 1505 cm^{-1} which can be assigned to the C-O stretching vibrations of the co-ordinated CO_2 ligand. The $^{31}P\{^1H\}$ nmr spectrum, measured in $CDCl_3$, exhibits an AA'BB' pattern of peaks at 140.24 ppm, while the ^1H nmr spectrum is similar to that of the parent complex.

A single crystal structure determination was carried out to confirm the identity of this compound and to establish the mode of co-ordination of the carbon dioxide. The stereochemistry of the complex is illustrated in Figure 3.4. The carbon dioxide adopts a novel bridging co-ordination mode bonding to the two ruthenium atoms through the carbon and one of the oxygen atoms; the bond distances associated with the co-ordinated CO_2 are summarized in Figure 3.5. The C(33)-O(13) distance {1.25(2)Å} is longer than the C(33)-O(14) distance {1.13(2)Å} with the former representing a C-O single bond. These distances are comparable to those

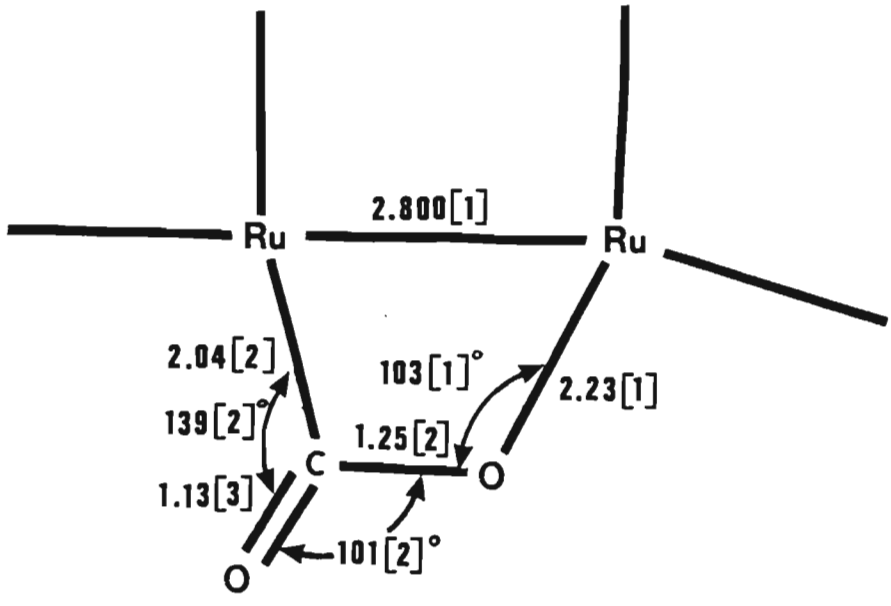

Figure 3.5

found in the related carbon dioxide derivative $[\{(Cy)_3P\}_2Ni(\eta^2\text{-}CO_2)]$,[170] which was found to have C-O distances of 1.22(2) and 1.17(2)Å (Figure 3.6).

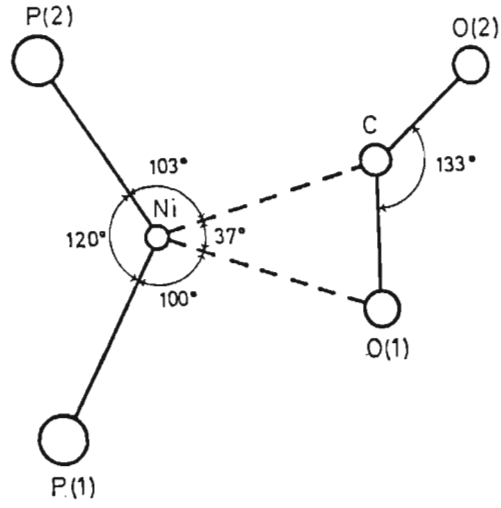

Figure 3.6: Mode of bonding of CO_2 in $[(Cy_3P)_2Ni(\eta^2\text{-}CO_2)]$. C-O(1) 1.22(2), C-O(2) 1.17(2)Å

A ruthenium-ruthenium distance of 2.800(1)Å in $[Ru_2(CO)_4\{\mu\text{-}OC(O)\}\{\mu\text{-}(Pr^iO)_2PN(Et)P(OPr^i)_2\}_2]$ represents a formal metal-metal bond, and which lies approximately within the plane formed by the atoms of the CO_2 ligand.

The number of structurally characterized carbon dioxide complexes is limited and are mostly mononuclear. In these complexes carbon dioxide has been shown to adopt one of three co-ordination modes as shown in Figure 3.7. The mode of co-ordination of carbon dioxide in $[Ru_2(CO)_4\{\mu\text{-}$

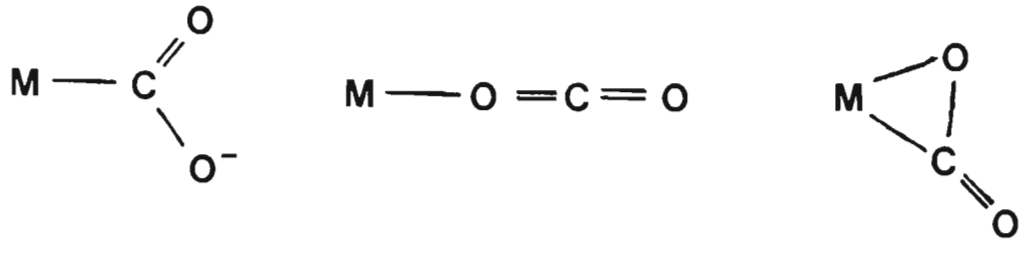

Figure 3.7

$OC(O)\}\{\mu\text{-}(Pr^iO)_2PN(Et)P(OPr^i)_2\}_2]$, in which it bridges across two metal atoms separated by a relatively short distance, is novel and, in fact, no other compounds of this type have been reported.

Interest in the co-ordination of carbon dioxide has been stimulated by a search for inexpensive chemical feedstocks, and has been extensively reviewed. [171,172]

Carbon dioxide is a weak electrophilic ligand which only co-ordinates to very basic centres. It is also a very labile ligand that is easily displaced, although it can undergo a range of chemical transformations, such as deoxygenation, dimerisation, or disproportionation when bound to a metal. For these reasons, X-ray diffraction studies are, in general, essential to establish the authenticity of a carbon dioxide complex.[173]

It is recognised that some metallocarboxylic acid derivatives such as $[CpRe(CO)(NO)\{OC(OH)\}]$[174] readily lose CO_2 upon deprotonation, via a presumed CO_2 complex (Scheme 3.3). However, decarboxylation is not a

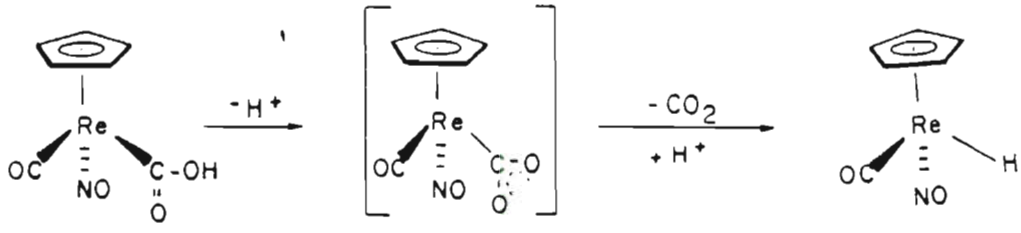

Scheme 3.3

reliable criterion for the involvement of an intermediate carbon dioxide complex. This is demonstrated by the decomposition of transition metal formates M-OCHO to hydrides with the loss of CO_2. This process has in some instances been shown to be an intramolecular reaction and which

need not involve a vacant co-ordination site.[175] Since metallo-carboxylic acids can be derived from attack of hydroxide ions or water on electron-deficient carbonyl groups,[176,177] labile carbon dioxide complexes would seem to be mandatory intermediates in the "water-gas shift reaction".

A series of cobalt-salen derivatives, developed by Floriani,[178] have been shown to react reversibly with carbon dioxide. It has been proposed that the complex $[Co(Pr^{n}\text{-salen})K(CO_2)(thf)]$ {salen = N,N'-ethylene-bis(salicylideneaminato)dianion} adopts a structure in solution where one of the oxygen atoms of the CO_2, co-ordinated to the cobalt through its carbon atom, is weakly bound to the potassium ion. A related carbon dioxide derivative, $[OsRh_2(\mu\text{-}H)_2(\mu_3\text{-}CO_2)(C_8H_{12})_2(PMe_2Ph)_3]$, in which a carbon dioxide molecule bridges three metal atoms through its carbon and both of its oxygen atoms, has more recently been reported.[179]

Significantly, the CO_2 adduct $[Ru_2(CO)_4\{\mu\text{-}OC(O)\}\{\mu\text{-}(Pr^{i}O)_2PN(Et)P(OPr^{i})_2\}_2]$ was found to be susceptible to protic attack with stepwise protonation of this compound by $HBF_4.OEt_2$, in dichloromethane, leading to the formation of $[Ru_2(CO)_4\{\mu\text{-}OC(OH)\}\{\mu\text{-}(Pr^{i}O)_2PN(Et)P(OPr^{i})_2\}_2]^{+}$ and $[Ru_2(CO)_5(H_2O)\{\mu\text{-}(Pr^{i}O)_2PN(Et)P(OPr^{i})_2\}_2]^{2+}$ respectively.

It was also found that the warming of crystals or of a solution of $[Ru_2(CO)_4\{\mu\text{-}OC(O)\}\{\mu\text{-}(Pr^{i}O)_2PN(Et)P(OPr^{i})_2\}_2]$ in hexane above -10°C leads to the formation of an extremely air-sensitive intense purple-red species, assumed to have formed as a result of the decarboxylation of this compound. The nature of this product was unknown at this stage however, and was only later established to be the formally co-ordinatively unsaturated species $[Ru_2(CO)_4\{\mu\text{-}(Pr^{i}O)_2PN(Et)P(OPr^{i})_2\}_2]$

(see Chapter 6). The latter was established to react quantitatively with carbon monoxide, producing the parent pentacarbonyl species $[Ru_2(\mu\text{-}CO)(CO)_4\{\mu\text{-}(Pr^iO)_2PN(Et)P(OPr^i)_2\}_2]$ thereby completing the cycle shown in Scheme 3.4.

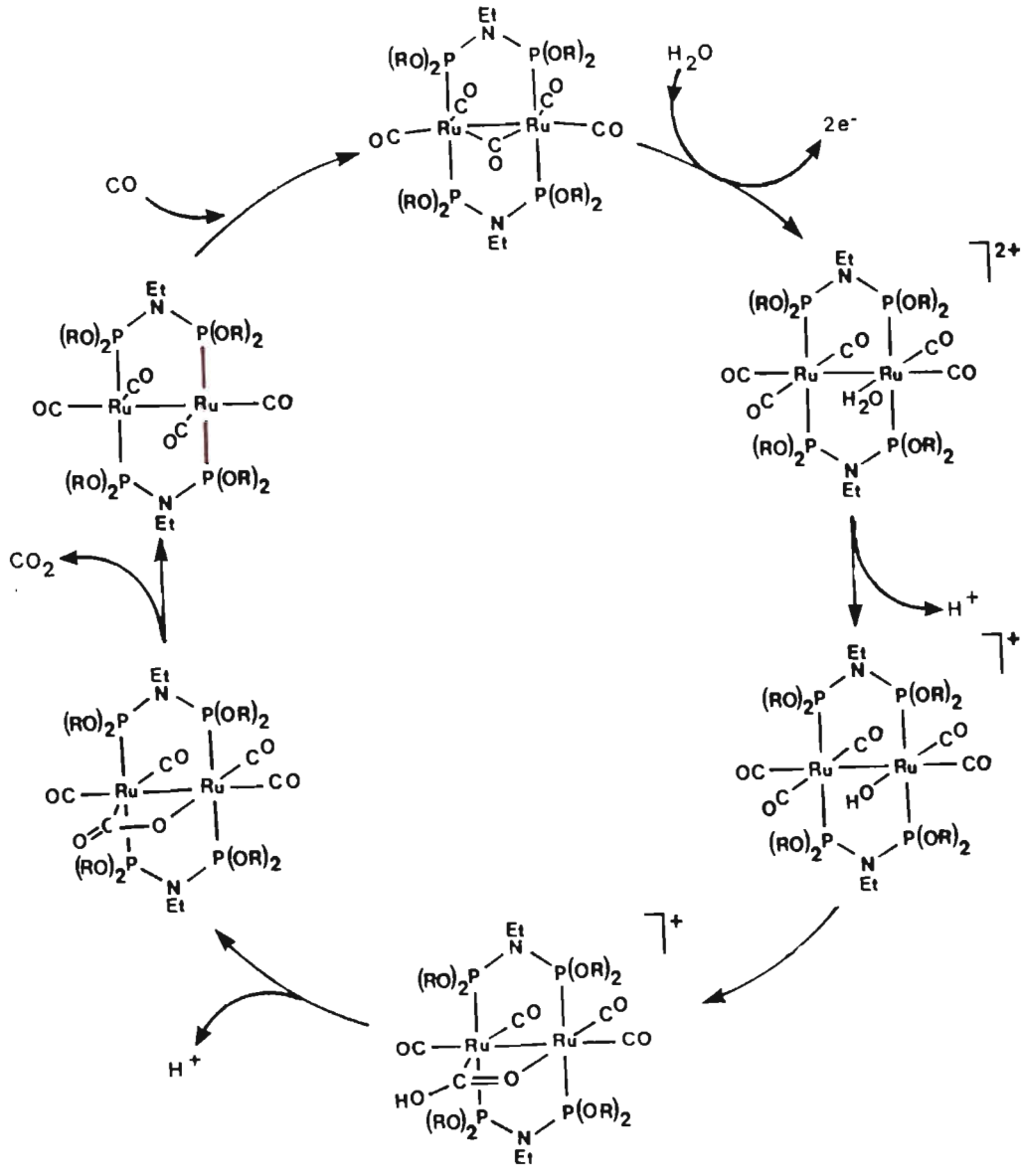

Scheme 3.4

The electronic influence of other ligands in the metal's co-ordination sphere plays a major role in the co-ordination chemistry of carbon dioxide. Since the metal-CO_2 bond is stabilized mainly by back-donative interactions it would be expected that good donor ligands (such as phos-

phines) would enhance the binding ability of carbon dioxide to the metal centre. This has been verified both experimentally[170] and theoretically,[180] as well as having been demonstrated to be of importance in carbon dioxide insertion processes.[181] For this reason, it would be of value to investigate the formation of analogous carbon dioxide complexes of more electron-rich species, containing bridging ditertiary phosphine ligands, such as $R_2PCH_2PR_2$ (R = Me, Ph or cyclohexyl).

3.3 REACTIONS OF $[Ru_2(\mu\text{-}CO)(CO)_4\{\mu\text{-}(RO)_2PN(Et)P(OR)_2\}_2]$ (R = Me or Pr^i) WITH $AgSbF_6$ IN METHANOL AND ETHANOL

Treatment of a suspension of the tetramethoxy- or tetraisopropoxydiphosphazane derivatives $[Ru_2(\mu\text{-}CO)(CO)_4\{\mu\text{-}(RO)_2PN(Et)P(OR)_2\}_2]$ (R = Me or Pr^i) in methanol or ethanol with a twice molar amount of $AgSbF_6$ was found to lead to the immediate separation of metallic silver from the pale yellow solution and the formation of a pale yellow product characterized as the monocationic alkoxycarbonyl species $[Ru_2(CO)_4\{\mu\text{-}OC(OR')\}\{\mu\text{-}(RO)_2PN(Et)P(OR)_2\}_2]SbF_6$ (R = Me, Pr^i; R' = Me, Et).

The infrared spectrum of the methoxycarbonyl tetraisopropoxydiphosphazane-bridged species $[Ru_2(CO)_4\{\mu\text{-}OC(OMe)\}\{\mu\text{-}(Pr^iO)_2PN(Et)P(OPr^i)_2\}_2]SbF_6$ (36) exhibits a four-line pattern of peaks in the C-O stretching region typical of complexes of the type $[Ru_2(\mu\text{-}X)(CO)_4\{\mu\text{-}(RO)_2PN(Et)P(OR)_2\}_2]^+$ (X = anionic ligand) as well as a broad band at 1630 cm^{-1} readily assigned to the carbonyl stretching vibration of the methoxycarbonyl fragment. The $^{31}P\{^1H\}$ nmr spectrum, measured in CD_3OD, exhibits an AA'BB' pattern of peaks, centred at 139.72 ppm, while the ^1H nmr spectrum exhibits a singlet at 3.78 ppm, the integral of which corresponds to three protons, assigned to the methyl protons of the methoxycarbonyl ligand.

The infrared spectrum of the methoxycarbonyl tetramethoxydiphosphazane-bridged species $[Ru_2(CO)_4\{\mu\text{-}OC(OMe)\}\{\mu\text{-}(MeO)_2PN(Et)P(OMe)_2\}_2]SbF_6$ (37) in the C-O stretching region is similar to that of the analogous tetra-isopropoxydiphosphazane derivative but in contrast to that observed for the latter, the $^{31}P\{^1H\}$ nmr spectrum, measured in acetone-d_6, exhibits a singlet at 149.51 ppm in the room temperature spectrum, although an AA'BB' pattern of peaks, centred at 150.54 ppm, is observed when the spectrum is recorded at -40°C. These results are interpreted in terms of the complex being involved in some fluxional process in solution. The first example of fluxional behaviour involving the migration of ligands of the type OC(R) (R = Me, Et, Ph, NH_2R etc) and in particular of the acyl ligand OC(Et), was demonstrated by Kaesz[182] in their studies of the triosmium species $[Os_3\{\mu_2\text{-}OC(R)\}_2(CO)_{10}]$ (R = Me, Et, Ph), in which a rapid interconversion between the vicinal and geminal isomers of these complexes was shown to occur. The ^1H nmr spectrum of $[Ru_2(CO)_4\{\mu\text{-}OC(OMe)\}\{\mu\text{-}(MeO)_2PN(Et)P(OMe)_2\}_2]SbF_6$ is similar to that of the parent complex but contains, in addition, a singlet at 3.76 ppm, assigned to the methyl protons of the methoxycarbonyl group.

The infrared spectrum of the ethoxycarbonyl derivative $[Ru_2(CO)_4\{\mu\text{-}OC(OEt)\}\{\mu\text{-}(Pr^iO)_2PN(Et)P(OPr^i)_2\}_2]SbF_6$ (38) in the C-O stretching region is similar to that of the analogous methoxycarbonyl species. The $^{31}P\{^1H\}$ nmr spectrum of this compound, on the other hand, exhibits a singlet at 135.51 (measured in $CDCl_3$). This is in contrast to that observed for the analogous methoxycarbonyl species in which an AA'BB' pattern of peaks is observed in its $^{31}P\{^1H\}$ nmr spectrum, but may be explained in terms of a fluxional process occurring in solution as described for the tetramethoxydiphosphazane methoxycarbonyl species $[Ru_2(CO)_4\{\mu\text{-}OC(OMe)\}\{\mu\text{-}(MeO)_2PN(Et)P(OMe)_2\}_2]SbF_6$. The ^1H nmr spectrum contains, in addition to the resonances of the protons of the diphosphazane ligands,

a quartet at 4.10 ppm as well as a set of resonances overlapping the multiplet in the region 1.14 - 1.65 ppm, the integrals of which correspond to two and three protons respectively. These additonal resonances are attributed to the presence of an ethoxy group.

The infrared spectrum of $[Ru_2(CO)_4\{\mu\text{-}OC(OEt)\}\{\mu\text{-}(MeO)_2PN(Et)P(OMe)_2\}_2]SbF_6$ (39) in the C-O stretching region is similar to that of the analogous methoxycarbonyl speices. As for $[Ru_2(CO)_4\{\mu\text{-}OC(OMe)\}\{\mu\text{-}(MeO)_2PN(Et)P(OMe)_2\}_2]SbF_6$ and $[Ru_2(CO)_4\{\mu\text{-}OC(OEt)\}\{\mu\text{-}(Pr^iO)_2PN(Et)P(OPr^i)_2\}_2]SbF_6$ the $^{31}P\{^1H\}$ nmr spectrum of this compound, measured in acetone-d_6, exhibits a singlet at room temperature but an AA'BB' pattern of peaks at -40°C, indicating that the complex is also involved in a fluxional process in solution. The presence of an ethoxy group is confirmed by the appearance of a quartet (2 protons) and a triplet (3 protons), at 4.25 and 1.22 ppm respectively, in its ^1H nmr spectrum.

An X-ray crystal structure determination was carried out for the methoxycarbonyl·tetramethoxydiphosphazane-bridged species $[Ru_2(CO)_4\{\mu\text{-}OC(OMe)\}\{\mu\text{-}(MeO)_2PN(Et)P(OMe)_2\}_2]SbF_6$ which confirmed the presence of an unusual μ_2-methoxycarbonyl ligand. Despite a structural solution being obtained, inherent crystal twinning prevented refinement of the intensity data. A single crystal structure determination was therefore carried out for the ethoxycarbonyl derivative, $[Ru_2(CO)_4\{\mu\text{-}OC(OEt)\}\{\mu\text{-}(MeO)_2PN(Et)P(OMe)_2\}_2]SbF_6$, the stereochemistry of which is shown in Figure 3.8. The structure shows the two ruthenium atoms to be linked not only by two bridging diphosphazane ligands, but also by an ethoxycarbonyl group, giving rise to a four-membered Ru_2OC ring. The separation of 2.777(1)Å between the two ruthenium atoms represents a formal metal-metal bond. The molecule adopts a slightly staggered conformation, as reflected by P(1)-Ru(1)-Ru(2)-P(4) and P(2)-Ru(1)-

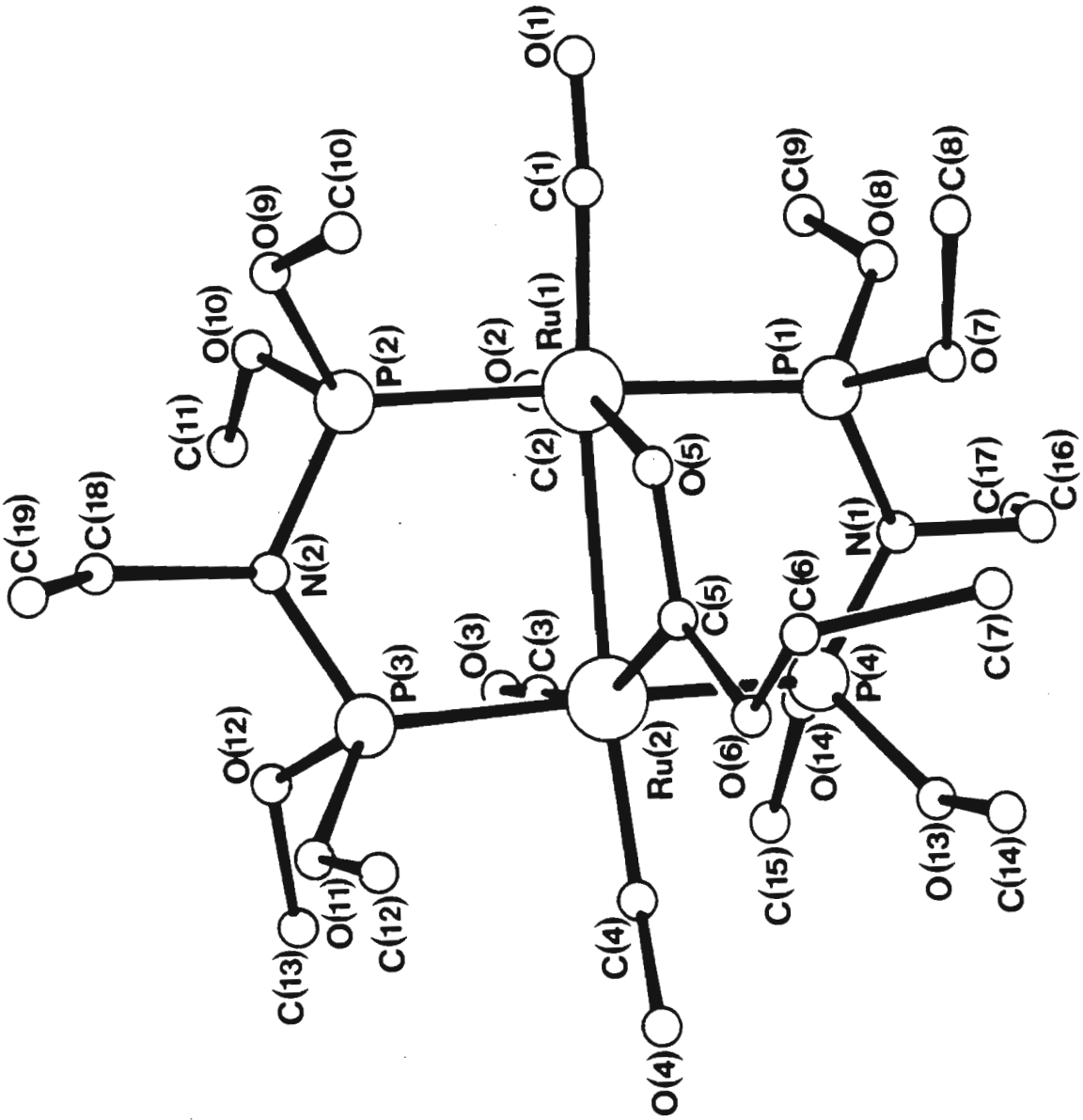

Figure 3.8:

Structure of $[Ru_2(CO)_4\{\mu\text{-}OC(OEt)\}\{\mu\text{-}(MeO)_2PN(Et)P(OMe)_2\}_2]^+$

Ru(2)-P(3) torsion angles of 14.84 and 6.35°. The relatively large difference in these torsion angles is as a consequence of there being both a twist about the metal-metal bond and a buckle of one of the diphosphazane ligands due to the presence of an asymmetric bridging ethoxycarbonyl ligand. As expected the C(5)-O(5) distance (1.27(1)Å) is slightly shorter than the C(5)-O(6) distance (1.31(1)Å), the former representing a C-O double bond.

Many examples exist in which two transition metals are bridged by an acyl group OC(R) (R = alkyl group), giving rise to a four-membered M_2OC ring. One such example is the doubly-bridged acyl derivative $[Ru_2\{\mu\text{-}OC(Et)\}_2(CO)_6]$, reported by Kaesz and Kampe.[115] The ethoxycarbonyl complex $[Ru_2(CO)_4\{\mu\text{-}OC(OEt)\}\{\mu\text{-}(MeO)_2PN(Et)P(OMe)_2\}_2]SbF_6$ is, however, only the second structurally characterized complex containing a bridging OC(OR) ligand (R = alkyl group). The first example of this type of compound, described by Lewis *et al.*,[183] was the hexaosmium cluster $[Os_6H_3(CO)_{19}\{\mu_2\text{-}OC(OMe)\}(\mu_3\text{-}PH)]$. This compound is obtained by reaction of $[Os_6H_2(CO)_{20}(MeCN)(\mu_3\text{-}PH)]$ with methoxide ion to afford $[Os_6H_2(CO)_{19}\{\mu_2\text{-}OC(OMe)\}(\mu_3\text{-}PH)]^-$ which is then protonated to yield the above neutral derivative.

$$[Os_6H_2(CO)_{20}(MeCN)(\mu_3\text{-}PH)] \xrightarrow[-MeCN]{MeO^{\ominus}} [Os_6H_2(CO)_{19}\{\mu_2\text{-}OC(OMe)\}(\mu_3\text{-}PH)]^- \xrightarrow{CF_3COOH} [Os_6H_3(CO)_{19}\{\mu_2\text{-}OC(OMe)\}(\mu_3\text{-}PH)]$$

The alkoxycarbonyl derivatives $[Ru_2(CO)_4\{\mu\text{-}OC(OR')\}\{\mu\text{-}(RO)_2PN(Et)P(OR)_2\}_2]^+$ (R = Me or Pr^i; R′ = Me or Et) are susceptible to protic attack and on treatment with $HBF_4.OEt_2$ in acetone were found to afford a mixture of the acetone and aquo solvento species $[Ru_2(CO)_5(solvent)\{\mu\text{-}(RO)_2PN(Et)P(OR)_2\}_2]^{2+}$ (solvent = acetone or water; R = Me or Pr^i). Addition of excess methanol or ethanol to this mixture was shown to lead to the formation of the corresponding alkoxycarbonyl species. It is

therefore concluded that the reaction of the parent complexes $[Ru_2(\mu\text{-}CO)(CO)_4\{\mu\text{-}(RO)_2PN(Et)P(OR)_2\}_2]$ (R = Me or Pr^i) with silver(I) salts in methanol or ethanol, produces alcohol solvento species $[Ru_2(CO)_5(HOR')\{\mu\text{-}(RO)_2PN(Et)P(OR)_2\}_2]^{2+}$ (R = Me or Pr^i; R' = Me or Et) as intermediates. A proton of the co-ordinated alcohol is readily abstracted by the free alcohol, it being sufficiently basic to effect this deprotonation, which is followed by the migration of the alkoxide ligand onto the carbon of an adjacent carbonyl ligand, affording the alkoxycarbonyl derivatives. None of the postulated intermediates could be detected using $^{31}P\{^1H\}$ nmr spectroscopy however. The reactions of $[Ru_2(\mu\text{-}CO)(CO)_4\{\mu\text{-}(RO)_2PN(Et)P(OR)_2\}_2]$ with silver(I) salts in protic solvents is summarized in Scheme 3.5.

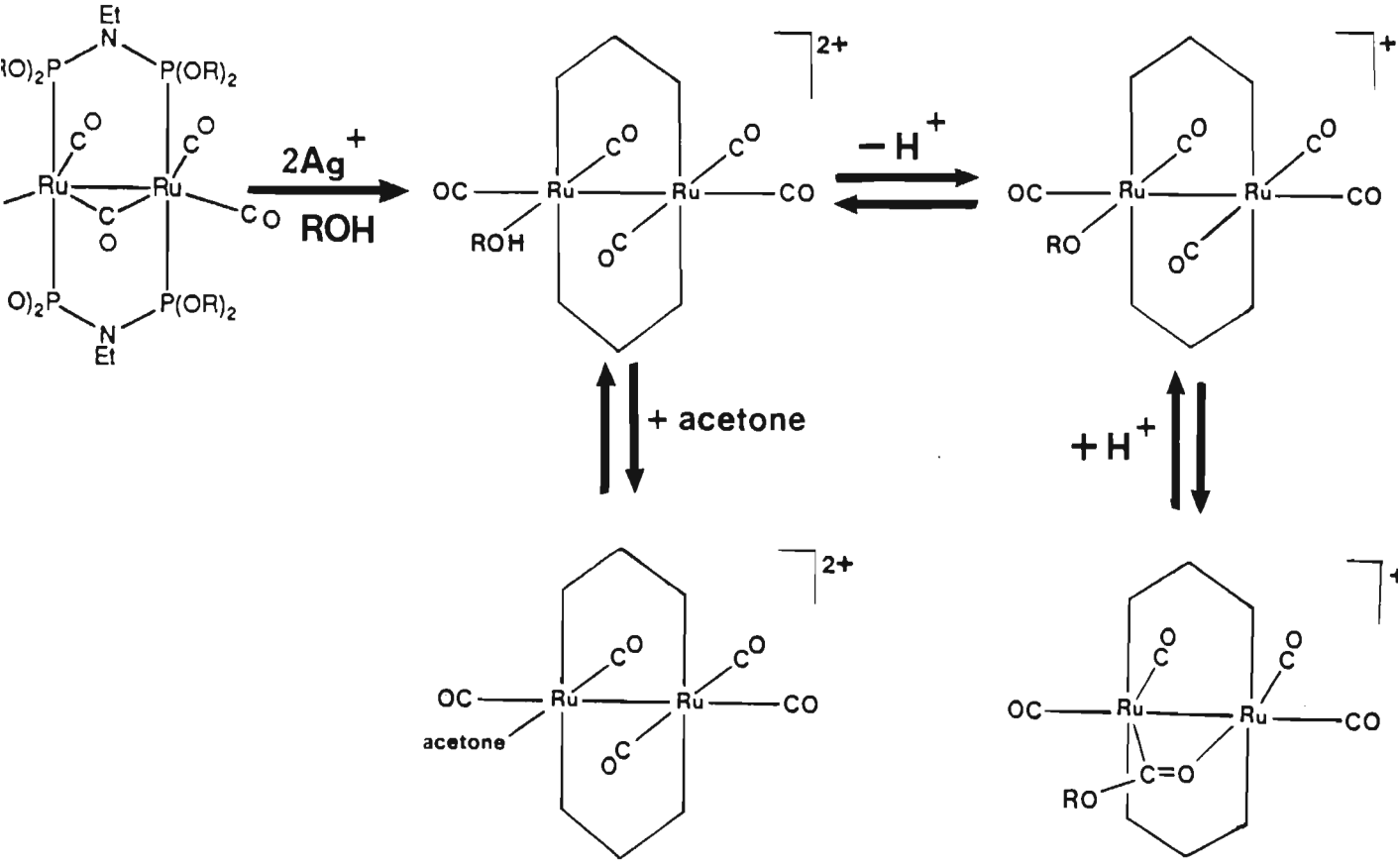

Scheme 3.5

3.4 REACTIONS OF $[Ru_2(\mu\text{-}CO)(CO)_4\{\mu\text{-}(RO)_2PN(Et)P(OR)_2\}_2]$ WITH AgOOCR′ (R′ = Me, Ph, CF_3)

The addition of a twice molar amount of AgOOCR′ (R′ = Me, Ph or CF_3) to $[Ru_2(\mu\text{-}CO)(CO)_4\{\mu\text{-}(RO)_2PN(Et)P(OR)_2\}_2]$ (R = Me or Pr^i) was found to lead to the separation of metallic silver and the formation of a pale yellow solution from which carboxylato-bridged tetracarbonyl species $[Ru_2(CO)_4(\mu\text{-}OOCR')\{\mu\text{-}(RO)_2PN(Et)P(OR)_2\}_2]^+$ could be isolated, as the hexafluorophosphate salts, for R′ = Me or Ph and from which the mono-ligated carboxylato pentacarbonyl species $[Ru_2(CO)_5(\mu\text{-}OOCR')\{\mu\text{-}(RO)_2PN(Et)P(OR)_2\}_2]^+$ could be isolated, again as the hexafluorophosphate salt, for R = CF_3. These compounds were characterized by means of elemental analysis and infrared and nmr spectroscopy.

The infrared spectrum of $[Ru_2(CO)_4(\mu\text{-}OOCCH_3)\{\mu\text{-}(Pr^iO)_2PN(Et)P(OPr^i)_2\}_2]PF_6$ (**40**) exhibits a four-line pattern of peaks in the terminal C-O stretching region. In addition, a band observed at 1555 cm^{-1} could be assigned to the C-O stretching vibration of the bridging acetate ligand; the frequency of this peak is comparable to those for related acetato-bridged species such as $[Ru_2(CO)_4(\mu\text{-}OOCCH_3)_2(PPh_3)_2]$ which affords a strong band at 1571 cm^{-1} in its infrared spectrum. The $^{31}P\{^1H\}$ nmr spectrum of this compound, measured in $CDCl_3$, exhibits a singlet at 135.56 ppm, consistent with the compound having a symmetrical structure. The ^1H nmr spectrum contains a singlet at 1.81 ppm, the integral of which corresponds to three protons, thereby confirming the presence of an acetate ligand.

The infrared spectrum of the benzoate-bridged species $[Ru_2(CO)_4(\mu\text{-}OOCPh)\{\mu\text{-}(Pr^iO)_2PN(Et)P(OPr^i)_2\}_2]PF_6$ (**41**) in the C-O stretching region is similar to that of the analogous acetato-bridged species, described

above. A peak at 1534 cm^{-1} in this spectrum was assigned to the carbonyl stretching mode of the bridging benzoate ligand. The $^{31}P\{^1H\}$ nmr spectrum, measured in $CDCl_3$, exhibits a singlet at 134.16 ppm, while the ^1H nmr spectrum of the complex contains a multiplet between 7.24 and 7.56 ppm, the integral of which corresponds to five protons, readily assigned to the protons of the benzoate group.

The infrared spectrum of the tetramethoxydiphosphazane derivative $[Ru_2(CO)_4(\mu\text{-}OOCPh)\{\mu\text{-}(MeO)_2PN(Et)P(OMe)_2\}_2]PF_6$ (**42**) in the C-O stretching region is similar to that of the analogous acetato-bridged species, while a peak at 1530 cm^{-1} could be assigned to the carbonyl stretching mode of the bridging benzoate ligand. The $^{31}P\{^1H\}$ nmr spectrum, measured in $CDCl_3$, exhibits a singlet at 145.44 ppm, while the ^1H nmr spectrum contains a multiplet in the region 7.25 - 7.60 ppm, corresponding to the five protons of the co-ordinated benzoate ligand.

A single crystal structure determination was carried out for $[Ru_2(CO)_4(\mu\text{-}OOCCH_3)\{\mu\text{-}(Pr^iO)_2PN(Et)P(OPr^i)_2\}_2]PF_6$ and confirmed the presence of a bridging acetate ligand; the stereochemistry of the cation is shown in Figure 3.9. The two ruthenium atoms have approximate octahedral geometries, with the angles about the ruthenium atoms ranging from 81.3(2) to 96.8(4)°, and are bridged by two tetraisopropoxydiphosphazane ligands in a *trans* arrangement as well as by an acetato group, as described above. The Ru-Ru separation is 2.806(1)Å, which is consistent with a formal metal-metal bond. The ion adopts a slightly staggered conformation, as reflected by torsion angles of 17.27 and 13.83°. The Ru-C distances for the axial {1.942(8)Å} and equatorial {1.844(9)Å} carbonyl ligands are significantly different, with similar differences in these distances having been observed for $[Ru_2(CO)_6(\mu\text{-}OOCCH_3)_2]$.[101]

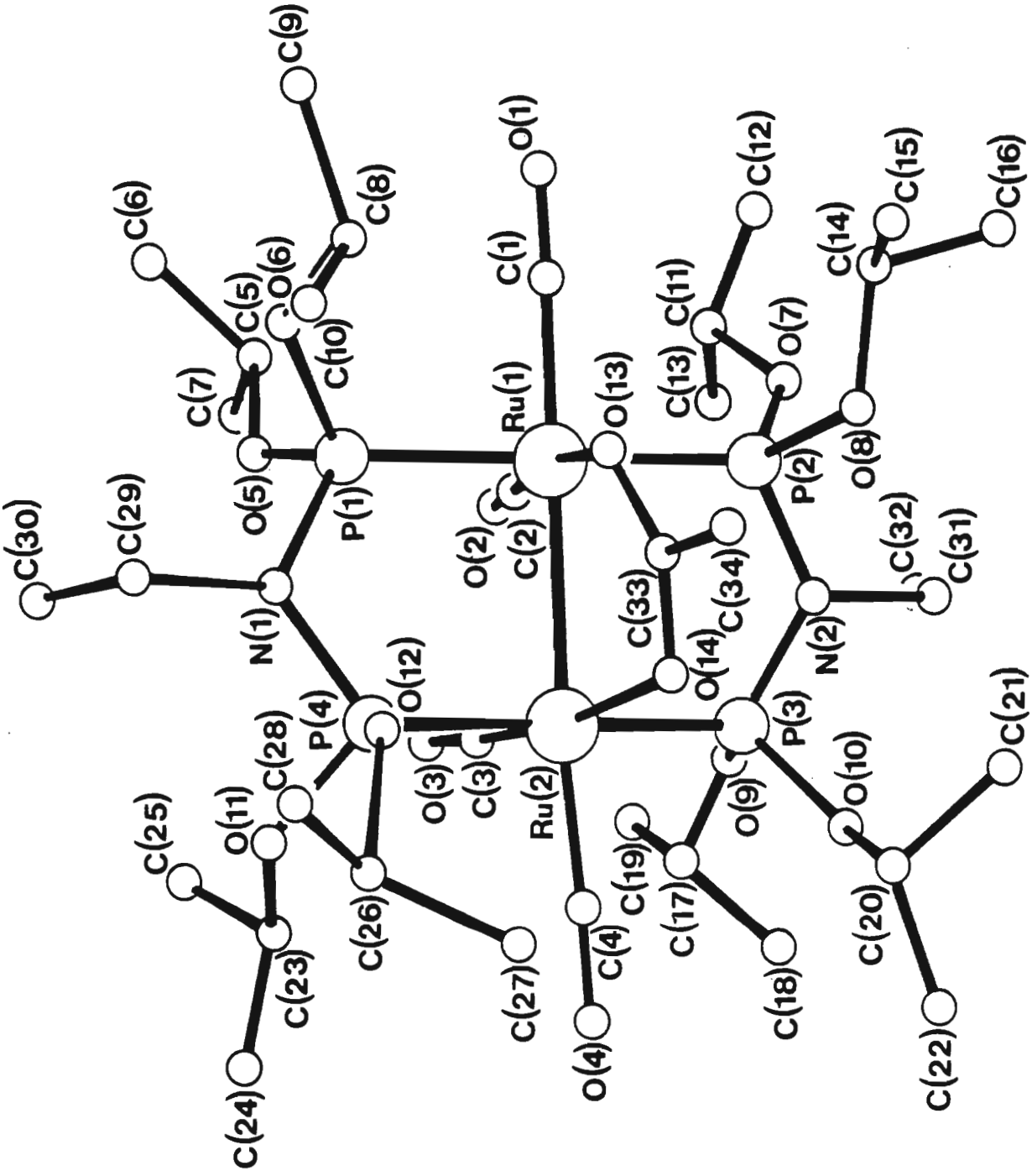

Figure 3.9:

Structure of $[Ru_2(CO)_4(\mu\text{-}OOCCH_3)\{\mu\text{-}(Pr^iO)_2PN(Et)P(OPr^i)_2\}_2]^+$

Significantly, the acetato-bridged species $[Ru_2(CO)_4(\mu\text{-}OOCCH_3)\{\mu\text{-}(Pr^iO)_2PN(Et)P(OPr^i)_2\}_2]^+$ and the methoxycarbonyl species $[Ru_2(CO)_4\{\mu\text{-}OC(OCH_3)\}\{\mu\text{-}(Pr^iO)_2PN(Et)P(OPr^i)_2\}_2]^+$ are structural isomers with, as described above, the structures of both having been determined X-ray crystallographically. Attempts to interconvert these two either thermally or under photochemical conditions were unsuccessful, indicating the stability of the two modes of co-ordination. This result is not surprising in view of the reported stability of the group VIB metal derivatives $[M(CO)_5(COOH)]^-$ and $[M(CO)_5\{OC(O)H\}]^-$ (M = Cr, Mo, W) to intramolecular interconversion.[184]

The reaction of $[Ru_2(\mu\text{-}CO)(CO)_4\{\mu\text{-}(Pr^iO)_2PN(Et)P(OPr^i)_2\}_2]$ with silver acetate was monitored by means of $^{31}P\{^1H\}$ nmr spectroscopy, but a set of resonances corresponding to the pentacarbonyl acetato species $[Ru_2(CO)_5(OOCCH_3)\{\mu\text{-}(Pr^iO)_2PN(Et)P(OPr^i)_2\}_2]^+$ described in Chapter 2, was not observed. This suggests that formation of the tetracarbonyl acetato-bridged species occurs via a pathway that does not involve this species.

It has been established previously (see Chapter 2) that treatment of the iodide-bridged tetracarbonyl diruthenium species $[Ru_2(\mu\text{-}I)(CO)_4\{\mu\text{-}(Pr^iO)_2PN(Et)P(OPr^i)_2\}_2]^+$ with iodide ions in the presence of $Me_3NO.2H_2O$, leads to the formation of the triiodide species $[Ru_2(\mu\text{-}I)(I)(CO)_3\{\mu\text{-}(Pr^iO)_2PN(Et)P(OPr^i)_2\}_2]$. Attempts to synthesize the analogous diacetate tricarbonyl species by reaction of $[Ru_2(CO)_4(\mu\text{-}OOCCH_3)\{\mu\text{-}(Pr^iO)_2PN(Et)P(OPr^i)_2\}_2]^+$ with acetate ions were, however, unsuccessful.

The identity of the trifluoroacetate pentacarbonyl species $[Ru_2(CO)_5(OOCCF_3)\{\mu\text{-}(Pr^iO)_2PN(Et)P(OPr^i)_2\}_2]^+$ (**43**) formed from the reaction of $[Ru_2(\mu\text{-}CO)(CO)_4\{\mu\text{-}(Pr^iO)_2PN(Et)P(OPr^i)_2\}_2]$ with $AgOOCCF_3$, was confirmed

by means of comparitive $^{31}P\{^{1}H\}$ nmr and infrared spectra (Chapter 2).

The formation of the carboxylato species $[Ru_2(CO)_5(OOCCF_3)\{\mu\text{-}(RO)_2PN(Et)P(OR)_2\}_2]^+$ and $[Ru_2(CO)_4(\mu\text{-}OOCR')\{\mu\text{-}(RO)_2PN(Et)P(OR)_2\}_2]^+$ (R = Me or Pr^i; R' = Me or Ph) from the reaction of $[Ru_2(\mu\text{-}CO)(CO)_4\{\mu\text{-}(RO)_2PN(Et)P(OR)_2\}_2]$ with silver(I) carboxylates is assumed to involve a dicationic solvento species $[Ru_2(CO)_5(solvent)\{\mu\text{-}(RO)_2PN(Et)P(OR)_2\}_2]^{2+}$ as intermediate. As discussed in Chapter 2, this has been confirmed by addition of acetate or benzoate ions to the dicationic solvento species which resulted in the formation of the tetracarbonyl species $[Ru_2(CO)_4(\mu\text{-}OOCR')\{\mu\text{-}(RO)_2PN(Et)P(OR)_2\}_2]^+$ (R = Me or Pr^i; R' = Me or Ph), and by the addition of trifluoroacetate ions to the dicationic solvento species which led to the formation of the pentacarbonyl species $[Ru_2(CO)_5(OOCCF_3)\{\mu\text{-}(RO)_2PN(Et)P(OR)_2\}_2]^+$ (R = Me or Pr^i). This difference in co-ordination behaviour is explained in terms of the carboxylate ions, in the former reaction, displacing a carbonyl ligand from the solvento species with concomittant loss of the co-ordinated solvent, to afford the tetracarbonyl acetato-bridged species and of the trifluoroacetate ion, which is a weaker base than the acetate or benzoate ions, simply displacing the co-ordinated solvent to afford the pentacarbonyl monodentate trifluoroacetato species.

A number of diruthenium carboxylato complexes have thus far been described, in which the carboxylato ligands have been shown to bond in either a pendant or a bridging mode. It has been established that the frequencies of the C-O stretching vibration for these two modes of co-ordination are appreciably different. In particular, a shift of approximately 60 cm^{-1} to lower frequencies is observed on decarbonylation of the pendant-carboxylato species $[Ru_2(CO)_5(OOCR')\{\mu\text{-}(Pr^iO)_2PN(Et)P(OPr^i)_2\}_2]^+$ to the carboxylato-bridged derivatives $[Ru_2(CO)_4$-

$(\mu\text{-OOCR}')\{\mu\text{-}(Pr^iO)_2PN(Et)P(OPr^i)_2\}_2]^+$; Table 3.1 provides the frequencies of the C-O stretching vibrations of the carboxylate ligand in complexes of this type.

Complex	ν(c=O), cm^{-1}			
	R′			
	H	CH_3	Ph	CF_3
$[Ru_2(CO)_5(OOCR')\{\mu\text{-}(Pr^iO)_2PN(Et)P(OPr^i)_2\}_2]^+$	1620	1610	1608	1690
$[Ru_2(CO)_4(\mu\text{-}OOCR')\{\mu\text{-}(Pr^iO)_2PN(Et)P(OPr^i)_2\}_2]^+$	nm	1550	1534	1635

Table 3.1

3.5 REACTIONS OF $[Ru_2(CO)_4(\mu\text{-}OOCMe)\{\mu\text{-}(RO)_2PN(Et)P(OR)_2\}_2]PF_6$ WITH ANIONIC LIGANDS

With the object of synthesizing compounds of the type $[Ru_2(\mu\text{-}X)(CO)_4\{\mu\text{-}(RO)_2PN(Et)P(OR)_2\}_2]^+$ (X = anionic ligand) the acetato-bridged species $[Ru_2(CO)_4(\mu\text{-}OOCMe)\{\mu\text{-}(RO)_2PN(Et)P(OR)_2\}_2]^+$ (R = Me or Pr^i) was reacted with a range of anions. In particular, $[Ru_2(CO)_4(\mu\text{-}OOCMe)\{\mu\text{-}(MeO)_2PN(Et)P(OMe)_2\}_2]PF_6$ was reacted with sodium 2-oxypyridinate and found to afford a product characterized as $[Ru_2(CO)_4(\mu\text{-}NC_5H_4O)\{\mu\text{-}(MeO)_2PN(Et)P(OMe)_2\}_2]PF_6$ **(44)**. The infrared spectrum of this complex in the C-O stretching region is very similar to that of the acetato-bridged derivative. The $^{31}P\{^1H\}$ nmr spectrum, measured in $CDCl_3$, exhibits an AA′BB′ pattern of peaks at 143.76 ppm, while the ^1H nmr spectrum contains a multiplet in the region 6.23 - 7.74 ppm, corresponding to the four protons of the oxypyridinate ligand, as well as resonances corresponding to the protons of the diphosphazane ligands. In contrast to that observed for the tetramethoxydiphosphazane species, reaction of sodium 2-oxypyridinate with the tetraisopropoxydiphosphazane derivative

$[Ru_2(CO)_4(\mu\text{-}OOCCH_3)\{\mu\text{-}(Pr^iO)_2PN(Et)P(OPr^i)_2\}_2]PF_6$ did not lead to the displacement of the acetate ligand.

An X-ray structure determination was carried out on a single crystal of $[Ru_2(CO)_4(\mu\text{-}NC_5H_4O)\{\mu\text{-}(MeO)_2PN(Et)P(OMe)_2\}_2]PF_6$ to confirm the presence of a bridging oxypyridinate ligand; the stereochemistry of the cation is illustrated in Figure 3.10. The ruthenium atoms are bridged by an oxypyridinate ligand, as well as by the two diphosphazane ligands with the oxypyridinate ligand having a bite distance of *ca.* 2.30Å. Since this distance is appreciably less than the ruthenium-ruthenium distance of 2.797(1)Å, and because of the steric interactions between the diphosphazane and oxypyridinate ligands, the two octahedral geometries about the ruthenium atoms are twisted about the ruthenium-ruthenium bond. This is reflected by P(1)-Ru(1)-Ru(2)-P(4) and P(2)-Ru(1)-Ru(2)-P(3) torsion angles of 25.16 and 20.33° respectively; these are appreciably larger than those established for the related acetato-bridged species $[Ru_2(CO)_4(\mu\text{-}OOCCH_3)\{\mu\text{-}(Pr^iO)_2PN(Et)P(OPr^i)_2\}_2]PF_6$, described above. The distances involving all the carbonyl groups are normal, as are the Ru-O {2.094(8)Å} and Ru-N {2.148(8)Å} distances of the oxypyridinate group, comparing well with analogous distances in related species.[117]

A neutral product was found to be formed in the reaction of the acetato-bridged species $[Ru_2(CO)_4(\mu\text{-}OOCCH_3)\{\mu\text{-}(Pr^iO)_2PN(Et)P(OPr^i)_2\}_2]PF_6$ with sodium pyrazolate. This was characterized as the dipyrazolato tricarbonyl species $[Ru_2(CO)_3(\mu\text{-}N_2C_3H_3)(N_2C_3H_3)\{\mu\text{-}(Pr^iO)_2PN(Et)P(OPr^i)_2\}_2]$ (**45**) (Figure 3.11.). The infrared spectrum of this compound in the C-O stretching region closely resembles that of the dichloro tricarbonyl species $[Ru_2(\mu\text{-}Cl)(Cl)(CO)_3\{\mu\text{-}(Pr^iO)_2PN(Et)P(OPr^i)_2\}_2]$, described in Chapter 4. A broad peak at 1555 cm^{-1} was assigned to the N-N stretching vibration of the co-ordinated pyrazolate ligands. The $^{31}P\{^1H\}$ nmr

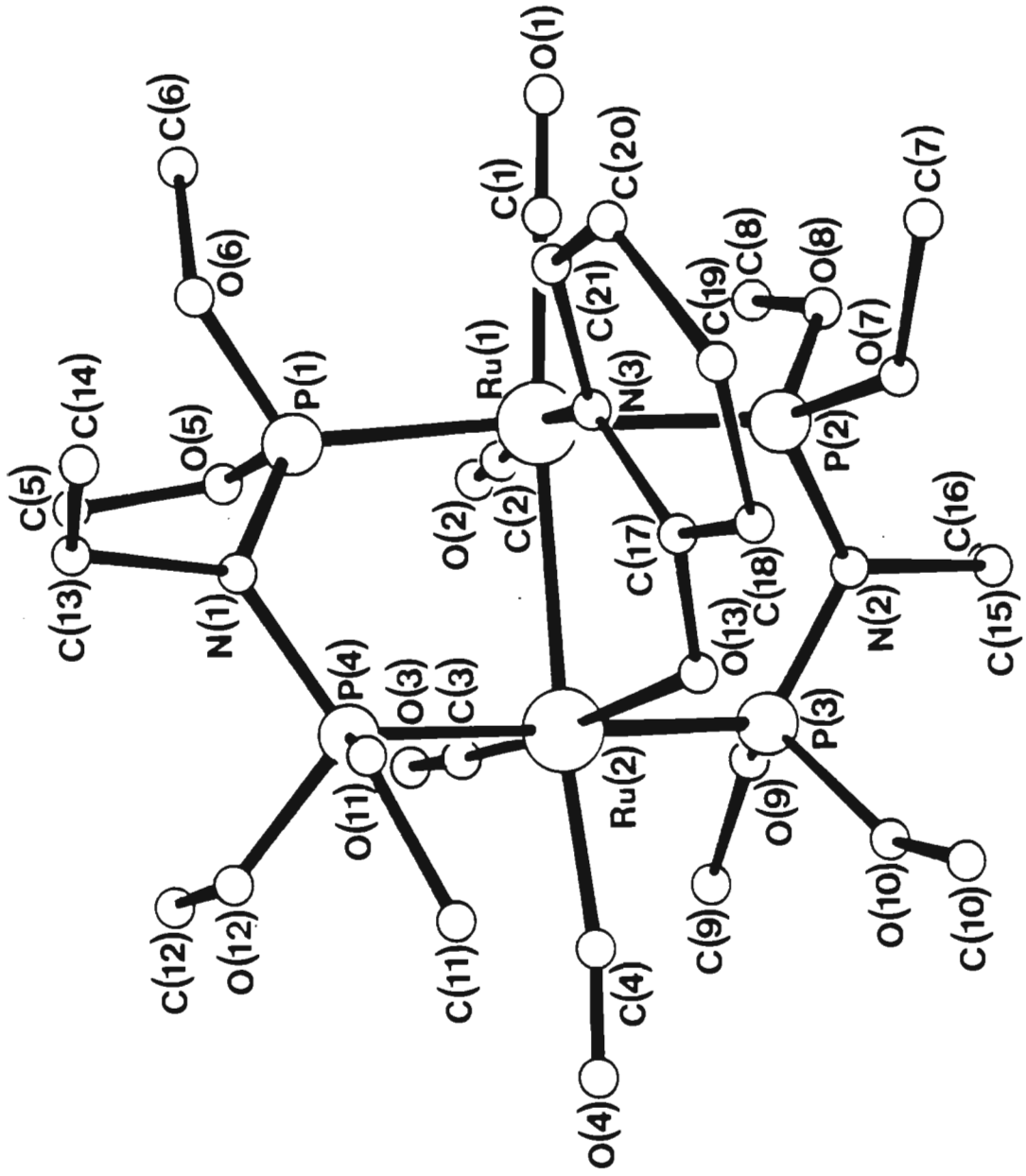

Figure 3.10: Structure of $[Ru_2(CO)_4(\mu\text{-}NC_5H_4O)\{\mu\text{-}(MeO)_2PN(Et)P(OMe)_2\}_2]^+$

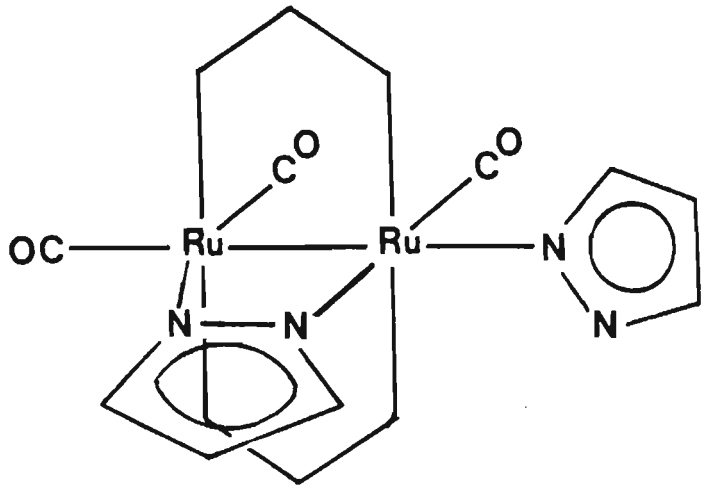

Figure 3.11

spectrum, measured in acetone-d_6, exhibits an AA'BB' pattern of peaks at 146.95 ppm, consistent with an asymmetric structure. The ^1H nmr spectrum contains multiplets in the regions 6.03 - 6.26 and 7.45 - 7.59 ppm, corresponding to six protons of the two pyrazolate ligands. There was no evidence for the formation of a tetracarbonyl pyrazolate-bridged species $[Ru_2(CO)_4(\mu\text{-}N_2C_3H_3)\{\mu\text{-}(Pr^iO)_2PN(Et)P(OPr^i)_2\}_2]^+$.

The reactions of $[Ru_2(CO)_4(\mu\text{-}OOCCH_3)\{\mu\text{-}(Pr^iO)_2PN(Et)P(OPr^i)_2\}_2]PF_6$ with sodium mercaptide, sodium methoxide and potassium hydroxide were also investigated but no reaction was observed, as determined by monitoring with $^{31}P\{^1H\}$ nmr spectroscopy.

3.6 EXPERIMENTAL

3.6.1 *Synthesis of* $[Ru_2(CO)_4\{\mu\text{-}OC(OH)\}\{\mu\text{-}(RO)_2PN(Et)P(OR)_2\}_2]SbF_6$ *(R = Me (34), Pr^i (33))*

An excess of pyridine (0.032 g, 0.400 mmol) in THF (1 ml) was added

dropwise to a stirred solution of $[Ru_2(CO)_5(H_2O)\{\mu\text{-}(RO)_2PN(Et)P(OR)_2\}_2]$-$(SbF_6)_2$ (R = Me : 0.150 g, 0.116 mmol; R = Pr^i: 0.150 g, 0.099 mmol) in THF (5 ml). The solvent was removed under reduced pressure and the residue was washed with water (3 x 5 ml) and dried. The title compound was crystallized from acetone/ether. Yield: 80-90%. *M* (**34**) = 1053.29 g/mol; *M* (**33**) = 1277.77 g/mol.

3.6.2 *Synthesis of* $[Ru_2(CO)_4\{\mu\text{-}OC(O)\}\{\mu\text{-}(Pr^iO)_2PN(Et)P(OPr^i)_2\}_2]$ (**35**)

An excess of an aqueous solution (3 ml) of potasium hydroxide (0.030 g, 0.536 mmol) was added to a solution of $[Ru_2(CO)_5(H_2O)\{\mu\text{-}(Pr^iO)_2P$-$N(Et)P(OPr^i)_2\}_2](SbF_6)_2$ (0.200 g, 0.132 mmol) in dichloromethane (3 ml) and the two-layered mixture was vigorously stirred for a further 30 minutes. The dichloromethane layer was separated from the aqueous solution, and the solvent was removed under reduced pressure. The title compound was extracted into hexane (5 x 3 ml) and isolated in crystalline form by cooling the combined hexane extracts to -20°C . Yield: 30%. *M* (**35**) = 1041.01 g/mol.

3.6.3 *Synthesis of* $[Ru_2(CO)_4\{\mu\text{-}OC(OMe)\}\{\mu\text{-}(RO)_2PN(Et)P(OR)_2\}_2]SbF_6$ (*R = Me* (**37**), Pr^i (**36**))

A solution of a twice molar amount of $AgSbF_6$ (0.100 g, 0.291 mmol) in methanol (1 ml) was added dropwise to a stirred suspension of $[Ru_2(\mu\text{-}CO)(CO)_4\{\mu\text{-}(RO)_2PN(Et)P(OR)_2\}_2]$ (R = Me: 0.116 g, 0.146 mmol; R = Pr^i: 0.150 g, 0.146 mmol) in methanol (5 ml) and the mixture stirred for a further two hours, during which time a precipitate of silver metal separated. The pale yellow solution was filtered through a glass fibre fritte and the volume of the filtrate reduced under vacuum to 3 ml. Toluene (3 ml) was added and the solution was kept at -10° to effect the

separation of the title compound in crystalline form. Yield; 80-90%. *M*(**37**) = 1067.32 g/mol; *M*(**36**) = 1291.80 g/mol.

3.6.4 *Synthesis of* $[Ru_2(CO)_4\{\mu\text{-}OC(OEt)\}\{\mu\text{-}(RO)_2PN(Et)P(OR)_2\}_2]SbF_6$ (*R = Me* (**39**), Pr^i (**38**))

A solution of a twice molar amount of $AgSbF_6$ (0.100 g, 0.291 mmol) in ethanol (2 ml) was added dropwise to a stirred suspension of $[Ru_2(\mu\text{-}CO)(CO)_4\{\mu\text{-}(RO)_2PN(Et)P(OR)_2\}_2]$ (R = Me: 0.116 g, 0.146 mmol; R = Pr^i: 0.150 g, 0.146 mmol) in ethanol (8 ml) and the mixture stirred for a further two hours, during which time a precipitate of silver metal separated. The pale yellow solution was filtered through a glass fibre fritte and the volume of the filtrate reduced under vacuum to 5 ml. Toluene (3 ml) was added and the solution was kept at -10° to effect the separation of the title compound in crystalline form. Yield; 70-80%. *M*(**39**) = 1081.35 g/mol; *M*(**38**) = 1376.12 g/mol.

3.6.5 *Synthesis of* $[Ru_2(CO)_4(\mu\text{-}OOCCH_3)\{\mu\text{-}(Pr^iO)_2PN(Et)P(OPr^i)_2\}_2]PF_6$ (**40**)

A twice molar amount of solid $AgOOCCH_3$ (0.065 mg, 0.390 mmol) was added to a solution of $[Ru_2(\mu\text{-}CO)(CO)_4\{\mu\text{-}(Pr^iO)_2PN(Et)P(OPr^i)_2\}_2]$ (0.200 mg, 0.195 mmol) in acetone (10 ml) and the mixture stirred for 15 hours, during which time a precipitate of silver metal separated. The pale yellow solution was filtered through a glass fibre fritte and excess NH_4PF_6 (*ca.* 0.5 g) was added to the filtrate. The solvent was removed under reduced pressure and the resultant yellow solid was washed with water (5 x 5 ml) and dried. The title compound was crystallized from $CHCl_3$/ether. Yield; 65-75%. *M*(**40**) = 1201.02 g/mol.

3.6.6 *Synthesis of* $[Ru_2(CO)_4(\mu\text{-}OOCPh)\{\mu\text{-}(RO)_2PN(Et)P(OR)_2\}_2]PF_6$ *(R = Me (**42**), Pr^i (**41**))*

A twice molar amount of solid AgOOCPh (0.100 mg, 0.437 mmol) was added to a solution of $[Ru_2(\mu\text{-}CO)(CO)_4\{\mu\text{-}(RO)_2PN(Et)P(OR)_2\}_2]$ (R = Me: 0.175 g, 0.219 mmol; R = Pr^i: 0.224 g, 0.219 mmol) in acetone (10 ml) and the mixture stirred for 15 hours, during which time a precipitate of silver metal separated. The pale yellow solution was filtered through a glass fibre fritte and excess NH_4PF_6 (*ca.* 0.5 g) was added to the filtrate. The solvent was removed under reduced pressure and the resultant yellow residue was washed with water (5 x 5 ml) and dried. The yellow solid was crystallized from $CHCl_3$/ether to afford yellow crystals of the title compound. Yield; 70-80%. *M*(**42**) = 1038.61 g/mol; *M*(**41**) = 1263.09 g/mol.

3.6.7 *Synthesis of* $[Ru_2(CO)_5(\mu\text{-}OOCCF_3)\{\mu\text{-}(Pr^iO)_2PN(Et)P(OPr^i)_2\}_2]PF_6$ *(**43**)*

A twice molar amount of solid $AgOOCCF_3$ (0.100 g, 0.452 mmol) was added to a solution of $[Ru_2(\mu\text{-}CO)(CO)_4\{\mu\text{-}(Pr^iO)_2PN(Et)P(OPr^i)_2\}_2]$ (0.232 g, 0.226 mmol) in acetone (10 ml) and the mixture stirred for 15 hours. The pale yellow solution was filtered through a glass fibre fritte and an excess amount of NH_4PF_6 (*ca.* 0.5 g) was added to the filtrate. The solvent was removed under reduced pressure and the resultant residue washed with water (5 x 5 ml) and dried. The yellow solid was crystallized from $CHCl_3$/ether, affording title compound as yellow crystals. Yield; 75%. *M*(**43**) = 1283.00 g/mol.

3.6.8 *Synthesis of* $[Ru_2(CO)_4(\mu\text{-}NC_5H_4O)\{\mu\text{-}(MeO)_2PN(Et)P(OMe)_2\}_2]PF_6$ (**44**)

A slight excess of sodium 2-oxypyridinate (0.020 g, 0.171 mmol) was added to a solution of $[Ru_2(CO)_4(\mu\text{-}OOCCH_3)\{\mu\text{-}(MeO)_2PN(Et)P(OMe)_2\}_2]PF_6$ (0.150 g, 0.153 mmol) in THF (15 ml) and the solution refluxed for 5 hours. The volume of the pale yellow solution was reduced under reduced pressure and diethyl ether was added to effect the separation of the title compound in crystalline form. Yield: 30%. *M* (**44**) = 1011.58 g/mol.

3.6.9 *Synthesis of* $[Ru_2(CO)_3(\mu\text{-}N_2C_3H_3)((N_2C_3H_3)\{\mu\text{-}(Pr^iO)_2PN(Et)P(OPr^i)_2\}_2]$ (**45**)

An excess of solid sodium pyrazolate (0.050 g, 0.555 mmol) was added to a solution of $[Ru_2(CO)_4(\mu\text{-}OOCCH_3)\{\mu\text{-}(Pr^iO)_2PN(Et)P(OPr^i)_2\}_2]PF_6$ (0.200 g, 0.167 mmol) in THF resulting in an immediate colour change to intense yellow. The mixture was stirred for 1 hour after which the solvent was removed under reduced pressure. The resultant solid was extracted with hexane (3 x 3 ml) and the combined extracts were set aside at -20°C to effect the separation of the title compound in crystalline form. Yield: 25%. *M* (**45**) = 1103.11 g/mol.

3.6.10 *Crystal Structure Determinations of* $[Ru_2(CO)_5(H_2O)\{\mu\text{-}(Pr^iO)_2PN(Et)P(OPr^i)_2\}_2](SbF_6)_2\cdot OC(CH_3)_2$ (**7**), $[Ru_2(CO)_4\{\mu\text{-}OC(OEt)\}\{\mu\text{-}(MeO)_2PN(Et)P(OMe)_2\}_2]SbF_6$ (**39**), $[Ru_2(CO)_4\{\mu\text{-}OC(O)\}\{\mu\text{-}(Pr^iO)_2PN(Et)P(OPr^i)_2\}_2]$ (**35**), $[Ru_2(CO)_4(\mu\text{-}OOCCH_3)\{\mu\text{-}(Pr^iO)_2PN(Et)P(OPr^i)_2\}_2]PF_6$ (**40**) *and* $[Ru_2(CO)_4(\mu\text{-}NC_5H_4O)\{\mu\text{-}(MeO)_2PN(Et)P(OMe)_2\}_2]PF_6$ (**44**)

The method for the intensity data collections is described in Appendix A.3(a) while the general approach to the structure solutions is given in Appendix A.3(b). The crystallographic data for (7), (39), (35), (**40**) and (**44**) are summarized in Table 3.5. The fractional co-ordinates and isotropic thermal parameters for (7), (39), (35), (**40**) and (**44**) are given in Tables 3.6, 3.10, 3.14, 3.18 and 3.22 respectively, the anisotropic thermal parameters in Tables 3.7, 3,11, 3,15, 3,19 and 3,23 respectively, the interatomic distances in Tables 3.8, 3.12, 3.16, 3.20 and 3.24 respectively, and the interatomic angles in Tables 3.9, 3.13, 3.17, 3.21 and 3.25. The observed and calculated structure factors for (**7**), (39), (35), (**40**) and (**44**) may be found on microfiche in an envelope fixed to the inside cover of the thesis.

TABLE 3.2

MICROANALYTICAL DATA

	COMPLEX	ANALYSIS : Found (Calculated) % %C	%H	%N
33	$[Ru_2(CO)_4\{\mu\text{-}OC(OH)\}\{\mu\text{-}(Pr^iO)_2PN(Et)P(OPr^i)_2\}_2]SbF_6$	31.29(31.02)	5.33(5.30)	2.44(2.19)
35	$[Ru_2(CO)_4\{\mu\text{-}OC(O)\}\{\mu\text{-}(Pr^iO)_2PN(Et)P(OPr^i)_2\}_2]$	37.70(38.07)	6.25(6.40)	3.32(2.69)
36	$[Ru_2(CO)_4\{\mu\text{-}OC(OMe)\}\{\mu\text{-}(Pr^iO)_2PN(Et)P(OPr^i)_2\}_2]SbF_6$	31.83(31.61)	5.40(5.39)	2.20(2.17)
37	$[Ru_2(CO)_4\{\mu\text{-}OC(OMe)\}\{\mu\text{-}(MeO)_2PN(Et)P(OMe)_2\}_2]SbF_6$	20.07(20.25)	3.41(3.50)	2.75(2.62)
38	$[Ru_2(CO)_4\{\mu\text{-}OC(OEt)\}\{\mu\text{-}(Pr^iO)_2PN(Et)P(OPr^i)_2\}_2]SbF_6$	31.27(30.55)	5.29(5.21)	2.29(2.03)
39	$[Ru_2(CO)_4\{\mu\text{-}OC(OEt)\}\{\mu\text{-}(MeO)_2PN(Et)P(OMe)_2\}_2]SbF_6$	21.29(21.10)	3.68(3.64)	2.74(2.59)
40	$[Ru_2(CO)_4(\mu\text{-}OOCCH_3)\{\mu\text{-}(Pr^iO)_2PN(Et)P(OPr^i)_2\}_2]PF_6$	34.09(34.00)	5.82(5.80)	2.38(2.33)
41	$[Ru_2(CO)_4(\mu\text{-}OOCPh)\{\mu\text{-}(Pr^iO)_2PN(Et)P(OPr^i)_2\}_2]PF_6$	37.58(37.08)	5.45(5.68)	2.20(2.22)
42	$[Ru_2(CO)_4(\mu\text{-}OOCPh)\{\mu\text{-}(MeO)_2PN(Et)P(OMe)_2\}_2]PF_6$	26.57(26.60)	3.89(3.79)	2.51(2.70)
44	$[Ru_2(CO)_4(\mu\text{-}NC_5H_4O)\{\mu\text{-}(MeO)_2PN(Et)P(OMe)_2\}_2]PF_6$	25.29(24.93)	3.95(3.79)	4.28(4.15)
45	$[Ru_2(CO)_3(\mu\text{-}N_2C_3H_3)(N_2C_3H_3)\{\mu\text{-}(Pr^iO)_2PN(Et)P(OPr^i)_2\}_2]$	40.72(40.35)	6.85(6.43)	7.30(7.43)

TABLE 3.3

INFRARED SPECTROSCOPIC DATA

COMPLEX	ν(C≡O), cm^{-1}				OTHER	MEDIUM	COLOUR
33	2033(s)	2000(vs)	1973(s)	1952(m)	1700(w), ν(C=O)	CH_2Cl_2	White
	2034(s)	1998(vs)	1963(s)	1950(s)	1700(w), ν(C=O)	Nujol	
35	2010(s)	1972(vs)	1940(s)	1923(s)		Hexane	Yellow
	2007(s)	1974(s)	1939(s)	1921(s)	1710(s), 1505(m), $\nu(CO_2)$	Nujol	
36	2033(s)	2000(vs)	1972(s)	1951(m)		CH_2Cl_2	Pale yellow
	2036(s)	2004(vs)	1992(s)	1956(m)	1630(w), ν(C=O)	Nujol	
37	2042(s)	2014(vs)	1987(s)	1966(m)	1608(w), ν(C=O)	CH_2Cl_2	Pale yellow
	2041(s)	2004(vs)	1993(s)	1955(m)	1713(w), ν(C=O)	Nujol	
38	2033(s)	2000(vs)	1973(s)	1950(m)	1600(w), ν(C=O)	CH_2Cl_2	Pale yellow
	2034(s)	2001(vs)	1974(s)	1953(s)	1710(w), ν(C=O)	Nujol	
39	2041(m)	2012(vs)	1985(s)	1965(sh)	1605(w), ν(C=O)	CH_2Cl_2	Pale yellow
	2046(s)	2005(vs)	1987(s)	1955(s)		Nujol	
40	2030(s)	2001(vs)	1972(s)	1947(m)	1550(m), ν(C=O)	$CHCl_3$	Pale yellow
41	2031(s)	2001(vs)	1972(s)	1949(m)		$CHCl_3$	Pale yellow
	2025(s)	1995(vs)	1966(m)	1944(m)	1534(m), ν(OOCPh)	Nujol	
42	2035(s)	2008(vs)	1982(s)	1952(m)	1540(m), ν(OOCPh)	$CHCl_3$	Pale yellow
	2039(s)	2011(vs)	1980(s)	1958(s)	1535(m), ν(OOCPh)	Nujol	

TABLE 3.3 (continued)

COMPLEX	ν(C≡O), cm^{-1}				OTHER	MEDIUM	COLOUR
44	2039(m)	2016(vs)	1981(s)	1963(s)		CH_2Cl_2	Yellow
45	1994(sh)	1985(s)	1934(vs)	1908(sh)	1566(m), ν(N=N)	Hexane	Yellow
	1971(sh)	1963(s)	1923(vs)	1916(sh)	1555(m), ν(N=N)	Nujol	

vs = very strong, s = strong, m = medium, w = weak, sh = shoulder.

TABLE 3.4

^{1}H AND $^{31}P\{^{1}H\}$ NMR SPECTROSCOPIC DATA

COMPLEX	δ ^{1}H (ppm)	δ $^{31}P\{^{1}H\}$ (ppm)
33	1.18-1.52m (54H); 1.80s (1H); 3.04-3.57m (4H); 4.38-4.82m (8H)	135.49 (AA'BB')[a]
35	1.17-1.41m (54H); 3.05-3.62m (4H); 4.35-5.05m (8H)	140.24 (AA'BB')[a,d]
36	1.30-1.65m (54H); 3.40-3.55m (4H); 3.78s (3H); 4.44-4.85m (8H)	139.72 (AA'BB')[b]
37	1.30t (6H); 3.35-3.50m (4H); 3.73-3.95m (27H)	149.51(s)[c], 150.54 (AA'BB')[c,d]
38	1.14-1.65m (57H); 3.21-3.57m (4H); 4.10q (2H); 4.40-4.89m (8H)	135.51(s)[a]
39	1.22t (6H); 1.30t (3H); 3.35-3.60m (4H); 3.77-4.05m (24H); 4.25q (2H)	149.62(s)[c], 150.64 (AA'BB')[c,d]
40	1.22-1.59m (54H); 1.81s (3H); 3.40-3.55m (4H); 4.53-4.73m (8H);	135.56(s)[a]
41	0.96-1.60m (54H); 3.25-3.45m (4H); 4.48-4.76m (8H); 7.24-7.56m (5H)	134.16(s)[a]
42	1.22t (6H); 3.25-3.82m (28H); 7.25-7.61m (5H)	145.44(s)[a]
44	1.09-1.32m (6H); 3.09-3.93m (28H); 6.23-7.74m (4H)	143.76 (AA'BB')[a]
45	0.91-1.45m (54H); 3.30-3.50m (4H); 4.10-5.30m (8H); 6.05-7.60m (6H)	146.95 (AA'BB')[c]

m = multiplet, s = singlet, t = triplet, q = quartet

[a]Recorded in $CDCl_3$, [b]Recorded in CD_3OD, [c]Recorded in acetone-d_6, [d]Measured at -40°C

TABLE 3.5

CRYSTAL DATA FOR

$[Ru_2(CO)_5(H_2O)\{\mu\text{-}(Pr^iO)_2PN(Et)P(OPr^i)_2\}_2](SbF_6)_2.OC(CH_3)_2$ (7), AND
$[Ru_2(CO)_4\{\mu\text{-}OC(OEt)\}\{\mu\text{-}(MeO)_2PN(Et)P(OMe)_2\}_2]SbF_6$ (39)

	7	39
Formula	$C_{33}H_{68}F_{12}N_2O_{14}P_4Ru_2Sb_2$	$C_{19}H_{39}F_6N_2O_{14}P_4Ru_2Sb$
Molecular mass	1572.6	1081.4
Crystal dimensions, mm	0.46 x 0.15 x 0.15	0.38 x 0.12 x 0.12
Crystal system	monoclinic	monoclinic
Space group	$P2_1/n$	$P2_1/c$
a(Å)	12.181(2)	11.492(8)
b(Å)	23.389(2)	15.698(5)
c(Å)	22.901(2)	21.542(8)
α(°)	90	90
β(°)	99.55(1)	103.09(4)
γ(°)	90	90
V(Å^3)	6434.3	3785.3
Z	4	4
D_c (g cm^{-3})	1.62	1.90
F(000)	3000	2128
λ(Mo-K_α) (Å)	0.71069	0.71069
μ(Mo-K_α) (cm^{-1})	15.70	18.27
Reflections measured	9457	5653
Unique reflections	7742	4658
Observed reflections [$I > 3\sigma(I)$]	5987	3770
Crystal stability	Decay = 20%	Decay = 11%
Absorption corrections	Applied	Applied
No. of parameters	336	338
R	0.083	0.070
R_w	0.094	0.076

Table 3.5 (continued)

CRYSTAL DATA FOR

$[Ru_2(CO)_4\{\mu\text{-}OC(O)\}\{\mu\text{-}(Pr^iO)_2PN(Et)P(OPr^i)_2\}_2](SbF_6)_2$ (**35**) AND
$[Ru_2(CO)_4(\mu\text{-}OOCCH_3)\{\mu\text{-}(Pr^iO)_2PN(Et)P(OPr^i)_2\}_2]PF_6$ (**40**)

	35	**40**
Formula	$C_{33}H_{66}N_2O_{14}P_4Ru_2$	$C_{34}H_{69}F_6N_2O_{14}P_5Ru_2$
Molecular mass	1041.0	1201.0
Crystal dimensions, mm	0.77 x 0.46 x 0.27	0.23 x 0.19 x 0.08
Crystal system	orthorhombic	triclinic
Space group	*Pbca*	*P*1
a(Å)	16.858(5)	10.517(2)
b(Å)	17.994(2)	11.995(2)
c(Å)	31.602(5)	13.055(1)
α(°)	90	108.153(10)
β(°)	90	112.648(10)
γ(°)	90	100.756(10)
V(Å^3)	9586.1	1353.1
Z	8	1
D_c (g cm^{-3})	1.44	1.47
F(000)	4304	616
λ(Mo-K_α) (Å)	0.71069	0.71069
μ(Mo-K_α) (cm^{-1})	8.07	7.78
Reflections measured	7307	3952
Unique reflections	5786	3928
Observed reflections [$I > 3\sigma(I)$]	4602	3886
Crystal stability	Decay = 14%	No decay
Absorption corrections	Applied	Applied
No. of parameters	356	396
R	0.072	0.040
R_w	0.090	0.046

Table 3.5 (continued)

CRYSTAL DATA FOR

$[Ru_2(CO)_4(\mu\text{-}NC_5H_4O)\{\mu\text{-}(MeO)_2PN(Et)P(OMe)_2\}_2]PF_6$ (**44**)

	44
Formula	$C_{21}H_{38}F_6N_2O_{13}P_5Ru_2$
Molecular mass	1011.6
Crystal dimensions, mm	0.46 x 0.27 x 0.23
Crystal system	orthorhombic
Space group	$Pna2_1$
a(Å)	30.917(7)
b(Å)	10.574(1)
c(Å)	11.508(1)
α(°)	90
β(°)	90
γ(°)	90
V(Å^3)	3762.1
Z	4
D_c (g cm^{-3})	1.88
F(000)	2024
λ(Mo-K_α) (Å)	0.71069
μ(Mo-K_α) (cm^{-1})	11.45
Reflections measured	2993
Unique reflections	2660
Observed reflections [$I > 3\sigma(I)$]	2581
Crystal stability	No decay
Absorption corrections	Applied
No. of parameters	451
R	0.036
R_w	0.038

TABLE 3.6: Fractional co-ordinates ($x10^4$) and equivalent isotropic temperature factors ($Å^2$, $x10^3$) for $[Ru_2(CO)_5(H_2O)\{\mu\text{-}(Pr^iO)_2PN(Et)P(OPr^i)_2\}_2](SbF_6)_2 \cdot OC(CH_3)_2$ (7)

	x/a	y/b	z/c	U_{eq}
Ru(1)	3015(1)	8318(1)	1682(1)	46(1)
Ru(2)	5337(1)	8111(1)	1681(1)	43(1)
P(1)	3539(3)	8955(2)	2463(2)	56(1)
P(2)	2733(2)	7645(1)	916(1)	47(1)
P(3)	4899(3)	7184(1)	1322(1)	48(1)
P(4)	5699(3)	9031(1)	2084(2)	53(1)
O(1)	3336(8)	9294(4)	842(4)	73(3)*
O(2)	580(10)	8608(5)	1730(5)	98(3)*
O(3)	3049(8)	7311(4)	2546(4)	78(3)*
O(4)	5517(8)	7702(4)	2934(4)	73(3)*
O(5)	7796(9)	7928(5)	1606(5)	90(3)*
O(6)	2717(8)	9458(4)	2537(4)	76(3)*
O(7)	3629(8)	8644(4)	3079(4)	73(3)*
O(8)	2991(7)	7882(4)	299(4)	66(2)*
O(9)	1576(7)	7353(4)	727(4)	65(2)*
O(10)	5618(11)	7091(6)	802(6)	64(3)*
O(11)	5074(9)	6662(5)	1767(5)	85(3)*
O(12)	5751(7)	9547(4)	1650(4)	61(2)*
O(13)	6853(8)	9118(4)	2519(4)	67(2)*
O(14)	5130(7)	8421(3)	756(3)	56(2)*
N(1)	4775(9)	9281(4)	2492(5)	58(3)*
N(2)	3567(8)	7063(4)	1037(4)	54(3)*
C(1)	3242(10)	8931(5)	1151(5)	55(3)*
C(2)	1484(12)	8497(6)	1701(6)	64(3)*
C(3)	3041(10)	7683(5)	2231(6)	55(3)*
C(4)	5400(11)	7857(6)	2447(6)	60(3)*
C(5)	6869(11)	7981(6)	1635(6)	62(3)*
C(6)	1974(18)	9829(9)	2047(9)	110(6)*
C(7)	969(21)	9942(10)	2296(10)	122(7)*
C(8)	2714(24)	10299(13)	1928(13)	154(9)*
C(9)	3176(19)	8732(10)	3581(10)	117(7)*
C(10)	3866(27)	8396(14)	4071(14)	169(11)*
C(11)	2001(24)	8588(13)	3534(13)	155(10)*
C(12)	2213(17)	8138(9)	-160(9)	102(6)*

TABLE 3.6 (continued)

C(13)	2871(21)	8566(10)	-483(11)	129(7)*
C(14)	1745(25)	7695(14)	-562(14)	166(10)*
C(15)	578(17)	7352(9)	1001(9)	104(6)*
C(16)	191(26)	6669(13)	1010(14)	161(10)*
C(17)	-234(21)	7734(11)	645(12)	136(8)*
C(18)	5708(21)	6680(10)	381(11)	127(7)*
C(19)	6954(20)	6674(10)	382(10)	121(7)*
C(20)	4910(24)	6733(14)	-187(13)	152(10)*
C(21)	6143(17)	6515(9)	2171(9)	101(6)*
C(22)	5818(20)	6357(11)	2725(11)	131(8)*
C(23)	6634(34)	6114(18)	1849(17)	220(16)*
C(24)	6573(12)	9600(7)	1274(7)	72(4)*
C(25)	7516(17)	10024(8)	1575(9)	101(6)*
C(26)	6060(17)	9898(8)	712(9)	101(6)*
C(27)	7571(13)	8676(7)	2874(7)	74(4)*
C(28)	7375(18)	8716(10)	3498(10)	114(6)*
C(29)	8750(19)	8845(10)	2853(10)	119(7)*
C(30)	5173(16)	9672(9)	3033(9)	99(5)*
C(31)	5570(21)	10212(12)	2843(11)	136(8)*
C(32)	3207(16)	6457(8)	853(8)	93(5)*
C(33)	2786(22)	6170(12)	1431(12)	144(9)*
Sb(1)	5344(1)	2001(1)	2074(1)	104(1)
F(1)	6666(14)	2396(7)	2059(8)	176(6)*
F(2)	4104(14)	1560(7)	2099(7)	170(6)*
F(3)	6062(17)	1739(8)	2815(9)	197(7)*
F(4)	4897(17)	2248(9)	1383(9)	210(8)*
F(5)	5925(13)	1367(7)	1758(7)	157(5)*
F(6)	4742(12)	2596(7)	2455(7)	152(5)*
Sb(2A)	0	0	0	130(1)
F(7)	662(19)	9392(10)	486(10)	228(8)*
F(8)	-13(19)	10499(11)	604(11)	251(10)*
F(9)	1486(20)	10250(10)	-47(10)	239(9)*
Sb(2B)	5000	0	5000	129(1)
F(10)	9280(19)	4426(10)	317(10)	239(9)*
F(11)	9082(20)	5538(11)	224(11)	251(10)*
F(12)	10953(15)	5045(7)	689(8)	178(6)*
O(15)	3169(12)	1685(6)	-173(7)	112(4)*

TABLE 3.6 (continued)

C(34)	3009(16)	1455(9)	282(9)	98(5)*
C(35)	3736(19)	992(10)	591(10)	116(6)*
C(36)	2126(24)	1639(11)	598(12)	146(9)*

* isotropic temperature factor.

$$U_{eq} = \frac{1}{3} \Sigma_i \Sigma_j U_{ij} a_i^* a_j^* (a_i \cdot a_j)$$

TABLE 3.7: Anistropic temperature factors ($Å^2$, $x10^3$) for

$[Ru_2(CO)_5(H_2O)\{\mu\text{-}(Pr^iO)_2PN(Et)P(OPr^i)_2\}_2](SbF_6)_2 \cdot OC(CH_3)_2$ (7)

	U(11)	U(22)	U(33)	U(23)	U(13)	U(12)
Ru(1)	41(1)	49(1)	48(1)	-2(1)	10(1)	-1(1)
Ru(2)	39(1)	45(1)	46(1)	-1(1)	7(1)	-3(1)
P(1)	55(2)	61(2)	55(2)	-12(2)	19(2)	-2(2)
P(2)	39(2)	54(2)	48(2)	-3(1)	2(1)	-4(1)
P(3)	44(2)	44(2)	56(2)	-6(1)	6(1)	0(1)
P(4)	48(2)	51(2)	60(2)	-8(2)	10(2)	-9(1)
Sb(1)	113(1)	95(1)	106(1)	-19(1)	24(1)	-12(1)
Sb(2A)	76(1)	182(2)	133(2)	-5(2)	16(1)	-2(1)
Sb(2B)	152(2)	98(1)	120(2)	-12(1)	-20(2)	6(1)

TABLE 3.8: Interatomic distances (Å) for

$[Ru_2(CO)_5(H_2O)\{\mu\text{-}(Pr^iO)_2PN(Et)P(OPr^i)_2\}_2](SbF_6)_2 \cdot OC(CH_3)_2$ (7)

Ru(1)-Ru(2)	2.871(1)	Ru(1)-P(1)	2.332(3)
Ru(1)-P(2)	2.343(3)	Ru(1)-C(1)	1.929(13)
Ru(1)-C(2)	1.918(14)	Ru(1)-C(3)	1.942(13)
Ru(2)-P(3)	2.349(3)	Ru(2)-P(4)	2.353(3)
Ru(2)-O(14)	2.212(8)	Ru(2)-C(4)	1.843(14)
Ru(2)-C(5)	1.911(14)	P(1)-O(6)	1.572(11)
P(1)-O(7)	1.575(10)	P(1)-N(1)	1.679(11)
P(2)-O(8)	1.596(10)	P(2)-O(9)	1.561(9)
P(2)-N(2)	1.693(10)	P(3)-O(10)	1.606(15)
P(3)-O(11)	1.581(11)	P(3)-N(2)	1.670(10)
P(4)-O(12)	1.572(9)	P(4)-O(13)	1.596(9)
P(4)-N(1)	1.683(12)	O(1)-C(1)	1.12(2)
O(2)-C(2)	1.14(2)	O(3)-C(3)	1.13(2)
O(4)-C(4)	1.16(2)	O(5)-C(5)	1.15(2)
O(6)-C(6)	1.58(2)	O(7)-C(9)	1.37(3)
O(8)-C(12)	1.42(2)	O(9)-C(15)	1.46(2)
O(10)-C(18)	1.38(3)	O(11)-C(21)	1.51(2)
O(12)-C(24)	1.43(2)	O(13)-C(27)	1.50(2)
N(1)-C(30)	1.55(2)	N(2)-C(32)	1.52(2)
C(6)-C(7)	1.46(4)	C(6)-C(8)	1.47(4)
C(9)-C(10)	1.51(4)	C(9)-C(11)	1.46(4)
C(12)-C(13)	1.54(3)	C(12)-C(14)	1.44(4)
C(15)-C(16)	1.67(4)	C(15)-C(17)	1.48(3)
C(18)-C(19)	1.52(4)	C(18)-C(20)	1.49(4)
C(21)-C(22)	1.44(3)	C(21)-C(23)	1.39(5)
C(24)-C(25)	1.59(2)	C(24)-C(26)	1.50(2)
C(27)-C(28)	1.49(3)	C(27)-C(29)	1.50(3)
C(30)-C(31)	1.45(3)	C(32)-C(33)	1.64(4)
Sb(1)-F(1)	1.86(2)	Sb(1)-F(2)	1.84(2)
Sb(1)-F(3)	1.88(2)	Sb(1)-F(4)	1.69(2)
Sb(1)-F(5)	1.84(2)	Sb(1)-F(6)	1.86(2)
Sb(2A)-F(7)	1.90(2)	Sb(2A)-F(8)	1.81(3)
Sb(2A)-F(9)	1.92(3)	O(15)-C(34)	1.22(3)
C(34)-C(35)	1.50(3)	C(34)-C(36)	1.46(4)

TABLE 3.9: Interatomic angles (°) for

$[Ru_2(CO)_5(H_2O)\{\mu\text{-}(Pr^iO)_2PN(Et)P(OPr^i)_2\}_2](SbF_6)_2\cdot OC(CH_3)_2$ (7)

Ru(2)-Ru(1)-P(1)	87.9(1)	Ru(2)-Ru(1)-P(2)	84.6(1)
P(1)-Ru(1)-P(2)	172.5(1)	Ru(2)-Ru(1)-C(1)	83.1(4)
P(1)-Ru(1)-C(1)	87.7(4)	P(2)-Ru(1)-C(1)	92.5(4)
Ru(2)-Ru(1)-C(2)	176.9(4)	P(1)-Ru(1)-C(2)	89.3(4)
P(2)-Ru(1)-C(2)	98.1(4)	C(1)-Ru(1)-C(2)	95.4(6)
Ru(2)-Ru(1)-C(3)	87.8(4)	P(1)-Ru(1)-C(3)	91.1(4)
P(2)-Ru(1)-C(3)	87.4(4)	C(1)-Ru(1)-C(3)	170.8(5)
C(2)-Ru(1)-C(3)	93.7(6)	Ru(1)-Ru(2)-P(3)	89.4(1)
Ru(1)-Ru(2)-P(4)	88.0(1)	P(3)-Ru(2)-P(4)	176.3(1)
Ru(1)-Ru(2)-O(14)	89.4(2)	P(3)-Ru(2)-O(14)	89.2(2)
P(4)-Ru(2)-O(14)	93.4(2)	Ru(1)-Ru(2)-C(4)	86.5(4)
P(3)-Ru(2)-C(4)	90.3(4)	P(4)-Ru(2)-C(4)	86.9(4)
O(14)-Ru(2)-C(4)	175.9(5)	Ru(1)-Ru(2)-C(5)	177.0(4)
P(3)-Ru(2)-C(5)	90.1(4)	P(4)-Ru(2)-C(5)	92.7(4)
O(14)-Ru(2)-C(5)	87.6(5)	C(4)-Ru(2)-C(5)	96.5(6)
Ru(1)-P(1)-O(6)	117.5(4)	Ru(1)-P(1)-O(7)	111.2(4)
O(6)-P(1)-O(7)	101.6(5)	Ru(1)-P(1)-N(1)	116.7(4)
O(6)-P(1)-N(1)	103.8(5)	O(7)-P(1)-N(1)	104.3(5)
Ru(1)-P(2)-O(8)	113.8(4)	Ru(1)-P(2)-O(9)	120.9(4)
O(8)-P(2)-O(9)	102.1(5)	Ru(1)-P(2)-N(2)	114.1(4)
O(8)-P(2)-N(2)	103.0(5)	O(9)-P(2)-N(2)	100.6(5)
Ru(2)-P(3)-O(10)	105.3(5)	Ru(2)-P(3)-O(11)	119.3(4)
O(10)-P(3)-O(11)	109.9(7)	Ru(2)-P(3)-N(2)	116.3(4)
O(10)-P(3)-N(2)	107.5(6)	O(11)-P(3)-N(2)	98.0(5)
Ru(2)-P(4)-O(12)	118.6(4)	Ru(2)-P(4)-O(13)	116.8(4)
O(12)-P(4)-O(13)	99.9(5)	Ru(2)-P(4)-N(1)	115.9(4)
O(12)-P(4)-N(1)	100.7(5)	O(13)-P(4)-N(1)	102.1(5)
P(1)-O(6)-C(6)	129.5(11)	P(1)-O(7)-C(9)	134.8(12)
P(2)-O(8)-C(12)	126.5(11)	P(2)-O(9)-C(15)	131.4(10)
P(3)-O(10)-C(18)	137(2)	P(3)-O(11)-C(21)	125.6(11)
P(4)-O(12)-C(24)	123.6(8)	P(4)-O(13)-C(27)	128.5(8)
P(1)-N(1)-P(4)	119.9(6)	P(1)-N(1)-C(30)	117.3(10)
P(4)-N(1)-C(30)	119.9(10)	P(2)-N(2)-P(3)	116.4(6)
P(2)-N(2)-C(32)	124.4(9)	P(3)-N(2)-C(32)	118.9(9)
Ru(1)-C(1)-O(1)	177.5(11)	Ru(1)-C(2)-O(2)	178.0(12)

Ru(1)-C(3)-O(3)	179.3(11)	Ru(2)-C(4)-O(4)	175.3(11)
Ru(2)-C(5)-O(5)	177.0(12)	O(6)-C(6)-C(7)	104(2)
O(6)-C(6)-C(8)	104(2)	C(7)-C(6)-C(8)	121(2)
O(7)-C(9)-C(10)	107(2)	O(7)-C(9)-C(11)	116(2)
C(10)-C(9)-C(11)	111(2)	O(8)-C(12)-C(13)	107(2)
O(8)-C(12)-C(14)	108(2)	C(13)-C(12)-C(14)	110(2)
O(9)-C(15)-C(16)	105(2)	O(9)-C(15)-C(17)	107(2)
C(16)-C(15)-C(17)	115(2)	O(10)-C(18)-C(19)	102(2)
O(10)-C(18)-C(20)	116(2)	C(19)-C(18)-C(20)	121(2)
O(11)-C(21)-C(22)	105(2)	O(11)-C(21)-C(23)	103(2)
C(22)-C(21)-C(23)	120(2)	O(12)-C(24)-C(25)	108.8(13)
O(12)-C(24)-C(26)	108.8(13)	C(25)-C(24)-C(26)	104.5(14)
O(13)-C(27)-C(28)	107.6(14)	O(13)-C(27)-C(29)	106.0(13)
C(28)-C(27)-C(29)	109(2)	N(1)-C(30)-C(31)	111(2)
N(2)-C(32)-C(33)	106(2)	F(1)-Sb(1)-F(2)	175.5(7)
F(1)-Sb(1)-F(3)	84.5(8)	F(2)-Sb(1)-F(3)	92.9(8)
F(1)-Sb(1)-F(4)	87.6(9)	F(2)-Sb(1)-F(4)	94.8(9)
F(3)-Sb(1)-F(4)	171.2(10)	F(1)-Sb(1)-F(5)	90.1(7)
F(2)-Sb(1)-F(5)	86.1(7)	F(3)-Sb(1)-F(5)	86.6(8)
F(4)-Sb(1)-F(5)	89.6(9)	F(1)-Sb(1)-F(6)	92.7(7)
F(2)-Sb(1)-F(6)	90.9(7)	F(3)-Sb(1)-F(6)	88.9(8)
F(4)-Sb(1)-F(6)	95.3(9)	F(5)-Sb(1)-F(6)	174.5(7)
F(7)-Sb(2A)-F(8)	95.3(11)	F(7)-Sb(2A)-F(9)	87.0(10)
F(8)-Sb(2A)-F(9)	88.5(11)	O(15)-C(34)-C(35)	124(2)
O(15)-C(34)-C(36)	122(2)	C(35)-C(34)-C(36)	114(2)

TABLE 3.10: Fractional co-ordinates ($x10^4$) and equivalent isotropic temperature factors ($Å^2$, $x10^3$) for $[Ru_2(CO)_4\{\mu\text{-}OC(OEt)\}\{\mu\text{-}(MeO)_2PN(Et)P(OMe)_2\}_2]SbF_6$ (39)

	x/a	y/b	z/c	U_{eq}
Ru(1)	6776(1)	1024(1)	1718(1)	34(1)
Ru(2)	8536(1)	1995(1)	2501(1)	39(1)
P(1)	7948(3)	949(2)	970(1)	43(1)
P(2)	5540(2)	1181(2)	2428(1)	43(1)
P(3)	7286(3)	2317(2)	3168(2)	44(1)
P(4)	9901(3)	1611(3)	1907(2)	56(1)
O(1)	4680(9)	175(7)	794(5)	94(3)
O(2)	7755(9)	-627(6)	2330(5)	72(3)
O(3)	9484(9)	507(7)	3380(5)	80(3)
O(4)	10120(11)	3483(9)	3073(6)	111(4)
O(5)	6512(7)	2333(5)	1445(4)	48(2)
O(6)	7613(9)	3495(6)	1643(5)	75(3)
O(7)	7628(8)	1664(6)	420(4)	65(2)
O(8)	7816(10)	163(7)	512(5)	81(3)
O(9)	4169(7)	1373(6)	2114(4)	59(2)
O(10)	5270(8)	344(6)	2795(4)	59(2)
O(11)	7142(9)	3269(6)	3377(5)	69(3)
O(12)	7694(7)	1944(6)	3873(4)	63(2)
O(13)	10827(8)	2289(9)	1783(5)	89(3)
O(14)	10871(8)	909(7)	2229(4)	78(3)
N(1)	9394(8)	1144(6)	1210(4)	45(2)
N(2)	5888(8)	1943(6)	2991(5)	47(2)
C(1)	5428(12)	518(9)	1106(7)	58(3)*
C(2)	7376(10)	11(8)	2093(6)	45(3)*
C(3)	9164(10)	1074(8)	3059(6)	46(3)*
C(4)	9529(13)	2926(9)	2867(7)	63(4)*
C(5)	7430(11)	2697(8)	1776(6)	47(3)*
C(6)	6672(17)	3986(12)	1130(10)	96(5)*
C(7)	7202(25)	4021(18)	553(14)	149(9)*
C(8)	6467(15)	1651(11)	-9(9)	84(5)*
C(9)	7688(14)	-720(11)	688(8)	78(4)*
C(10)	3841(14)	2026(10)	1630(8)	71(4)*
C(11)	6125(15)	13(11)	3352(8)	79(4)*
C(12)	6785(14)	3942(10)	2914(8)	78(4)*

TABLE 3.10 (continued)

C(13)	8819(14)	2220(10)	4299(8)	77(4)*
C(14)	10339(19)	3086(13)	1420(11)	102(6)*
C(15)	11796(15)	1065(11)	2814(9)	84(5)*
C(16)	10199(12)	1045(9)	749(7)	61(3)*
C(17)	10961(15)	209(11)	882(8)	83(5)*
C(18)	5038(13)	2090(9)	3408(8)	69(4)*
C(19)	4325(17)	2892(12)	3270(9)	91(5)*
Sb(1)	2704(1)	1743(1)	4848(1)	68(1)
F(1)	3803(10)	2378(8)	-62(9)	163(5)
F(2)	1581(13)	4063(8)	-268(10)	180(6)
F(3)	3471(21)	3711(16)	587(9)	273(9)
F(4)	1884(13)	2758(9)	-914(5)	144(4)
F(5)	6449(15)	-1055(8)	5618(9)	174(6)
F(6)	1809(13)	2535(9)	239(7)	142(4)

* isotropic temperature factor.

$$\underline{U}_{eq} = \frac{1}{3} \Sigma_i \Sigma_j \underline{U}_{ij} \underline{a}^*_i \underline{a}^*_j (a_i \cdot a_j)$$

TABLE 3.11: Anistropic temperature factors ($Å^2$, $x10^3$) for

$[Ru_2(CO)_4\{\mu\text{-}OC(OEt)\}\{\mu\text{-}(MeO)_2PN(Et)P(OMe)_2\}_2]SbF_6$ (39)

	U(11)	U(22)	U(33)	U(23)	U(13)	U(12)
Ru(1)	30(1)	38(1)	31(1)	-3(1)	-1(1)	-4(1)
Ru(2)	29(1)	50(1)	36(1)	-14(1)	3(1)	-7(1)
P(1)	42(2)	53(2)	31(1)	-10(1)	4(1)	-7(1)
P(2)	31(1)	57(2)	39(2)	-4(1)	5(1)	-7(1)
P(3)	35(2)	56(2)	40(2)	-15(1)	6(1)	-3(1)
P(4)	35(2)	83(2)	51(2)	-25(2)	10(1)	-12(2)
O(1)	69(6)	104(8)	91(8)	-34(7)	-20(6)	-41(6)
O(2)	86(7)	59(6)	66(6)	4(5)	6(5)	18(5)
O(3)	67(6)	82(7)	82(7)	13(6)	2(5)	9(5)
O(4)	97(8)	126(10)	119(10)	-79(9)	41(8)	-71(8)
O(5)	39(4)	48(4)	50(5)	5(4)	-3(4)	3(4)
O(6)	93(7)	54(6)	70(6)	-3(5)	1(6)	-27(5)
O(7)	50(5)	87(7)	51(5)	14(5)	-2(4)	-8(5)
O(8)	95(8)	76(7)	76(7)	-21(6)	29(6)	-20(6)
O(9)	33(4)	84(6)	57(5)	0(5)	6(4)	-5(4)
O(10)	57(5)	68(6)	53(5)	10(5)	12(4)	-15(4)
O(11)	72(6)	69(6)	67(6)	-29(5)	15(5)	-3(5)
O(12)	44(5)	101(7)	42(5)	-10(5)	2(4)	2(5)
O(13)	50(5)	138(10)	86(7)	-38(8)	27(5)	-37(6)
O(14)	52(5)	120(9)	51(5)	-13(6)	-12(4)	32(6)
N(1)	46(5)	55(6)	31(5)	-7(4)	4(4)	-3(4)
N(2)	38(5)	62(6)	43(5)	-8(5)	14(4)	4(5)
Sb(1)	63(1)	68(1)	70(1)	-4(1)	6(1)	-1(1)
F(1)	93(8)	113(9)	266(18)	0(11)	8(10)	43(7)
F(2)	154(12)	99(9)	279(21)	19(11)	35(13)	50(8)
F(3)	303(24)	303(25)	168(16)	-180(18)	-41(16)	-56(20)
F(4)	198(14)	134(10)	78(7)	-4(7)	-15(8)	-23(10)
F(5)	198(15)	111(10)	254(19)	-13(11)	134(15)	23(9)
F(6)	161(11)	130(10)	157(11)	19(9)	80(10)	-34(9)

TABLE 3.12: Interatomic distances (Å) for

$[Ru_2(CO)_4\{\mu\text{-}OC(OEt)\}\{\mu\text{-}(MeO)_2PN(Et)P(OMe)_2\}_2]SbF_6$ (39)

Ru(1)-Ru(2)	2.777(1)	Ru(1)-P(1)	2.325(3)
Ru(1)-P(2)	2.324(3)	Ru(1)-O(5)	2.140(8)
Ru(1)-C(1)	1.961(14)	Ru(1)-C(2)	1.845(12)
Ru(2)-P(3)	2.306(3)	Ru(2)-P(4)	2.318(3)
Ru(2)-C(3)	1.914(12)	Ru(2)-C(4)	1.912(15)
Ru(2)-C(5)	2.091(12)	P(1)-O(7)	1.614(9)
P(1)-O(8)	1.565(10)	P(1)-N(1)	1.652(9)
P(2)-O(9)	1.596(8)	P(2)-O(10)	1.601(9)
P(2)-N(2)	1.686(10)	P(3)-O(11)	1.581(9)
P(3)-O(12)	1.597(9)	P(3)-N(2)	1.672(10)
P(4)-O(13)	1.570(11)	P(4)-O(14)	1.610(10)
P(4)-N(1)	1.653(9)	O(1)-C(1)	1.103(15)
O(2)-C(2)	1.163(14)	O(3)-C(3)	1.136(14)
O(4)-C(4)	1.13(2)	O(5)-C(5)	1.268(14)
O(6)-C(5)	1.312(15)	O(6)-C(6)	1.56(2)
O(7)-C(8)	1.44(2)	O(8)-C(9)	1.45(2)
O(9)-C(10)	1.45(2)	O(10)-C(11)	1.46(2)
O(11)-C(12)	1.45(2)	O(12)-C(13)	1.47(2)
O(13)-C(14)	1.51(2)	O(14)-C(15)	1.47(2)
N(1)-C(16)	1.51(2)	N(2)-C(18)	1.49(2)
C(6)-C(7)	1.50(3)	C(16)-C(17)	1.57(2)
C(18)-C(19)	1.50(2)		

TABLE 3.13: Interatomic angles (°) for

$[Ru_2(CO)_4\{\mu\text{-}OC(OEt)\}\{\mu\text{-}(MeO)_2PN(Et)P(OMe)_2\}_2]SbF_6$ (39)

Ru(2)-Ru(1)-P(1)	89.6(1)	Ru(2)-Ru(1)-P(2)	90.6(1)
P(1)-Ru(1)-P(2)	176.0(1)	Ru(2)-Ru(1)-O(5)	71.2(2)
P(1)-Ru(1)-O(5)	85.8(2)	P(2)-Ru(1)-O(5)	90.5(2)
Ru(2)-Ru(1)-C(1)	170.6(4)	P(1)-Ru(1)-C(1)	90.4(4)
P(2)-Ru(1)-C(1)	88.7(4)	O(5)-Ru(1)-C(1)	99.4(4)
Ru(2)-Ru(1)-C(2)	93.4(4)	P(1)-Ru(1)-C(2)	92.5(4)
P(2)-Ru(1)-C(2)	91.5(4)	O(5)-Ru(1)-C(2)	164.5(4)
C(1)-Ru(1)-C(2)	96.1(5)	Ru(1)-Ru(2)-P(3)	91.6(1)
Ru(1)-Ru(2)-P(4)	90.7(1)	P(3)-Ru(2)-P(4)	174.9(1)
Ru(1)-Ru(2)-C(3)	94.9(3)	P(3)-Ru(2)-C(3)	88.5(4)
P(4)-Ru(2)-C(3)	86.8(4)	Ru(1)-Ru(2)-C(4)	162.7(4)
P(3)-Ru(2)-C(4)	88.5(4)	P(4)-Ru(2)-C(4)	90.6(4)
C(3)-Ru(2)-C(4)	102.4(6)	Ru(1)-Ru(2)-C(5)	66.4(3)
P(3)-Ru(2)-C(5)	89.5(3)	P(4)-Ru(2)-C(5)	95.6(3)
C(3)-Ru(2)-C(5)	161.2(5)	C(4)-Ru(2)-C(5)	96.3(5)
Ru(1)-P(1)-O(7)	113.7(4)	Ru(1)-P(1)-O(8)	119.2(4)
O(7)-P(1)-O(8)	96.4(6)	Ru(1)-P(1)-N(1)	118.2(3)
O(7)-P(1)-N(1)	98.5(5)	O(8)-P(1)-N(1)	106.9(5)
Ru(1)-P(2)-O(9)	115.7(3)	Ru(1)-P(2)-O(10)	117.0(4)
O(9)-P(2)-O(10)	94.6(5)	Ru(1)-P(2)-N(2)	118.0(3)
O(9)-P(2)-N(2)	102.7(5)	O(10)-P(2)-N(2)	105.5(5)
Ru(2)-P(3)-O(11)	120.3(4)	Ru(2)-P(3)-O(12)	115.0(3)
O(11)-P(3)-O(12)	95.9(5)	Ru(2)-P(3)-N(2)	118.9(4)
O(11)-P(3)-N(2)	103.9(5)	O(12)-P(3)-N(2)	98.5(5)
Ru(2)-P(4)-O(13)	119.2(5)	Ru(2)-P(4)-O(14)	115.4(4)
O(13)-P(4)-O(14)	96.2(7)	Ru(2)-P(4)-N(1)	118.2(3)
O(13)-P(4)-N(1)	105.1(5)	O(14)-P(4)-N(1)	98.9(5)
Ru(1)-O(5)-C(5)	103.3(7)	C(5)-O(6)-C(6)	120.4(11)
P(1)-O(7)-C(8)	119.0(9)	P(1)-O(8)-C(9)	126.1(10)
P(2)-O(9)-C(10)	120.6(8)	P(2)-O(10)-C(11)	121.9(9)
P(3)-O(11)-C(12)	121.7(9)	P(3)-O(12)-C(13)	120.8(9)
P(4)-O(13)-C(14)	117.5(10)	P(4)-O(14)-C(15)	123.4(10)
P(1)-N(1)-P(4)	119.3(6)	P(1)-N(1)-C(16)	119.7(7)
P(4)-N(1)-C(16)	120.0(7)	P(2)-N(2)-P(3)	118.1(5)
P(2)-N(2)-C(18)	117.7(8)	P(3)-N(2)-C(18)	122.4(8)

TABLE 3.13 (continued)

Ru(1)-C(1)-O(1)	174.0(13)	Ru(1)-C(2)-O(2)	179.9(2)
Ru(2)-C(3)-O(3)	176.6(11)	Ru(2)-C(4)-O(4)	178.8(14)
Ru(2)-C(5)-O(5)	118.0(8)	Ru(2)-C(5)-O(6)	124.5(9)
O(5)-C(5)-O(6)	117.5(11)	O(6)-C(6)-C(7)	105(2)
N(1)-C(16)-C(17)	111.4(11)	N(2)-C(18)-C(19)	114.5(13)

TABLE 3.14: Fractional co-ordinates ($x10^4$) and equivalent isotropic temperature factors ($Å^2$, $x10^3$) for $[Ru_2(CO)_4\{\mu\text{-}OC(O)\}\{\mu\text{-}(Pr^iO)_2PN(Et)P(OPr^i)_2\}_2]$ (35)

	x/a	y/b	z/c	U_{eq}
Ru(1)	528(1)	7975(1)	3941(1)	50(1)
Ru(2)	-604(1)	8684(1)	3434(1)	52(1)
P(1)	-358(2)	7039(1)	4111(1)	55(1)
P(2)	1489(2)	8853(1)	3775(1)	55(1)
P(3)	275(2)	9650(2)	3306(1)	72(1)
P(4)	-1545(2)	7814(1)	3636(1)	56(1)
O(1)	1532(6)	7444(7)	4666(4)	144(4)
O(2)	1133(6)	6999(5)	3221(3)	103(3)
O(3)	-69(7)	7783(6)	2654(3)	126(3)
O(4)	-1882(6)	9626(5)	3069(3)	115(3)
O(5)	-71(5)	6216(4)	3988(2)	69(2)
O(6)	-544(4)	6899(4)	4601(2)	66(2)
O(7)	2258(4)	8541(4)	3533(2)	64(2)
O(8)	1945(4)	9258(4)	4150(2)	69(2)
O(9)	146(5)	387(4)	3576(4)	121(4)
O(10)	312(6)	10004(6)	2876(3)	137(4)
O(11)	-2166(5)	8062(4)	4002(3)	77(2)
O(12)	-2168(5)	7526(4)	3290(3)	83(2)
O(13)	-169(8)	8806(7)	4311(4)	148(4)
O(14)	-1010(16)	9441(13)	4245(7)	311(10)
N(1)	-1240(5)	7037(4)	3864(3)	65(2)
N(2)	1234(5)	9514(4)	3434(3)	64(2)
C(1)	1197(7)	7646(6)	4391(4)	79(3)
C(2)	911(8)	7364(6)	3487(4)	78(3)
C(3)	-251(8)	8124(7)	2951(4)	81(3)
C(4)	-1415(6)	9296(5)	3222(4)	68(3)
C(5)	509(7)	5796(8)	4244(4)	85(4)*
C(6)	1179(12)	5600(11)	3954(6)	131(6)*
C(7)	126(14)	5135(12)	4382(7)	162(7)*
C(8)	-611(7)	7430(8)	4929(4)	84(3)*
C(9)	-1471(11)	7481(10)	5033(6)	127(5)*
C(10)	-196(14)	7161(12)	5330(7)	159(8)*
C(11)	2916(8)	8173(8)	3755(4)	89(4)*
C(12)	2903(10)	7371(9)	3689(5)	112(5)*

TABLE 3.14 (continued)

C(13)	3619(12)	8509(11)	3527(6)	148(7)*
C(14)	1560(8)	9553(7)	4534(4)	90(4)*
C(15)	1472(10)	10364(9)	4508(5)	120(5)*
C(16)	2190(12)	9360(12)	4909(7)	156(7)*
C(17)	-486(10)	10911(11)	3536(6)	121(5)*
C(18)	-334(18)	11590(19)	3360(10)	228(13)*
C(19)	-799(17)	11121(18)	3963(10)	214(12)*
C(20)	-33(10)	9801(9)	2481(5)	114(5)*
C(21)	538(13)	9356(14)	2157(8)	175(9)*
C(22)	-424(12)	10522(13)	2321(8)	160(8)*
C(23)	-2731(8)	8665(7)	3975(4)	84(4)*
C(24)	-3624(13)	8375(12)	3854(7)	159(8)*
C(25)	-2762(11)	8999(10)	4439(6)	137(6)*
C(26)	-2095(9)	7576(8)	2831(5)	97(4)*
C(27)	-2916(12)	7813(11)	2690(7)	147(7)*
C(28)	-1784(13)	6835(13)	2670(7)	164(8)*
C(29)	-1832(9)	6450(8)	3991(5)	101(4)*
C(30)	-1843(11)	5792(12)	3676(7)	150(7)*
C(31)	1861(8)	10118(7)	3333(4)	89(4)*
C(32)	2316(10)	9971(8)	2944(5)	113(5)*
C(33)	-660(11)	9038(12)	4047(5)	150(7)

* isotropic temperature factor.

$$U_{eq} = \frac{1}{3} \Sigma_i \Sigma_j U_{ij} a_i^* a_j^* (a_i \cdot a_j)$$

TABLE 3.15: Anistropic temperature factors ($Å^2$, $\times 10^3$) for

$[Ru_2(CO)_4\{\mu\text{-}OC(O)\}\{\mu\text{-}(Pr^iO)_2PN(Et)P(OPr^i)_2\}_2]$ (35)

	U(11)	U(22)	U(33)	U(23)	U(13)	U(12)
Ru(1)	49(1)	47(1)	55(1)	4(1)	-5(1)	-2(1)
Ru(2)	45(1)	48(1)	62(1)	7(1)	-4(1)	-3(1)
P(1)	57(2)	45(1)	62(2)	5(1)	1(1)	-2(1)
P(2)	51(2)	49(1)	64(2)	1(1)	-7(1)	-5(1)
P(3)	52(2)	61(2)	102(2)	29(2)	-10(2)	-7(1)
P(4)	48(1)	51(1)	71(2)	3(1)	-5(1)	-8(1)
O(1)	111(8)	151(9)	170(12)	64(8)	-74(8)	-36(7)
O(2)	114(8)	92(6)	102(7)	-29(5)	17(6)	-4(5)
O(3)	148(10)	143(8)	88(7)	-25(6)	12(7)	11(7)
O(4)	93(7)	92(6)	160(10)	27(6)	-11(7)	3(5)
O(5)	76(5)	61(4)	69(5)	-7(3)	-1(4)	11(4)
O(6)	79(5)	55(4)	65(5)	1(3)	12(4)	-5(3)
O(7)	46(4)	68(4)	78(5)	6(4)	-2(3)	2(3)
O(8)	66(4)	67(4)	75(5)	-11(4)	-16(4)	-11(4)
O(9)	75(6)	61(5)	228(12)	-15(6)	29(7)	3(4)
O(10)	114(8)	174(10)	123(9)	84(8)	-67(7)	-70(7)
O(11)	69(5)	77(5)	86(6)	12(4)	10(4)	-8(4)
O(12)	92(6)	84(5)	73(5)	5(4)	-14(4)	-28(5)
O(13)	162(12)	139(10)	143(11)	20(8)	8(10)	-72(9)
O(14)	380(27)	291(22)	261(23)	-158(19)	216(22)	-178(21)
N(1)	56(5)	57(5)	83(6)	0(4)	-3(5)	-20(4)
N(2)	45(5)	55(5)	91(7)	18(4)	-19(4)	-13(4)
C(1)	75(8)	77(7)	84(8)	26(6)	-9(7)	-12(6)
C(2)	97(9)	55(6)	83(9)	-6(6)	4(7)	5(6)
C(3)	78(8)	82(8)	83(9)	-7(7)	16(7)	9(7)
C(4)	51(6)	45(5)	109(9)	15(6)	-20(6)	-1(5)
C(33)	178(18)	201(19)	69(11)	-46(11)	29(10)	-106(15)

TABLE 3.16: Interatomic distances (Å) for

$[Ru_2(CO)_4\{\mu\text{-}OC(O)\}\{\mu\text{-}(Pr^iO)_2PN(Et)P(OPr^i)_2\}_2]$ (35)

Ru(1)-Ru(2)	2.800(1)	Ru(1)-P(1)	2.315(3)
Ru(1)-P(2)	2.323(3)	Ru(1)-O(13)	2.233(13)
Ru(1)-C(1)	1.909(12)	Ru(1)-C(2)	1.920(12)
Ru(2)-P(3)	2.318(3)	Ru(2)-P(4)	2.319(3)
Ru(2)-C(3)	1.921(13)	Ru(2)-C(4)	1.879(10)
Ru(2)-C(33)	2.04(2)	P(1)-O(5)	1.606(7)
P(1)-O(6)	1.598(8)	P(1)-N(1)	1.679(9)
P(2)-O(7)	1.605(7)	P(2)-O(8)	1.589(8)
P(2)-N(2)	1.660(9)	P(3)-O(9)	1.592(10)
P(3)-O(10)	1.502(11)	P(3)-N(2)	1.686(9)
P(4)-O(11)	1.623(8)	P(4)-O(12)	1.602(8)
P(4)-N(1)	1.655(9)	O(1)-C(1)	1.10(2)
O(2)-C(2)	1.129(15)	O(3)-C(3)	1.16(2)
O(4)-C(4)	1.098(14)	O(5)-C(5)	1.477(15)
O(6)-C(8)	1.41(2)	O(7)-C(11)	1.470(15)
O(8)-C(14)	1.48(2)	O(9)-C(17)	1.43(2)
O(10)-C(20)	1.43(2)	O(11)-C(23)	1.446(15)
O(12)-C(26)	1.46(2)	O(13)-O(14)	1.83(3)
O(13)-C(33)	1.25(2)	O(14)-C(33)	1.13(3)
N(1)-C(29)	1.51(2)	N(2)-C(31)	1.55(2)
C(5)-C(6)	1.50(2)	C(5)-C(7)	1.42(3)
C(8)-C(9)	1.49(2)	C(8)-C(10)	1.53(3)
C(11)-C(12)	1.46(2)	C(11)-C(13)	1.51(3)
C(14)-C(15)	1.47(2)	C(14)-C(16)	1.63(3)
C(17)-C(18)	1.37(4)	C(17)-C(19)	1.50(4)
C(20)-C(21)	1.62(3)	C(20)-C(22)	1.54(3)
C(23)-C(24)	1.64(3)	C(23)-C(25)	1.59(2)
C(26)-C(27)	1.51(3)	C(26)-C(28)	1.52(3)
C(29)-C(30)	1.55(3)	C(31)-C(32)	1.47(2)

TABLE 3.17: Interatomic angles (°) for

$[Ru_2(CO)_4\{\mu\text{-}OC(O)\}\{\mu\text{-}(Pr^iO)_2PN(Et)P(OPr^i)_2\}_2]$ (35)

Ru(2)-Ru(1)-P(1)	91.4(1)	Ru(2)-Ru(1)-P(2)	92.1(1)
P(1)-Ru(1)-P(2)	175.9(1)	Ru(2)-Ru(1)-O(13)	68.7(4)
P(1)-Ru(1)-O(13)	91.5(4)	P(2)-Ru(1)-O(13)	91.7(4)
Ru(2)-Ru(1)-C(1)	166.0(4)	P(1)-Ru(1)-C(1)	89.0(4)
P(2)-Ru(1)-C(1)	88.1(4)	O(13)-Ru(1)-C(1)	97.4(5)
Ru(2)-Ru(1)-C(2)	93.6(4)	P(1)-Ru(1)-C(2)	88.5(4)
P(2)-Ru(1)-C(2)	89.2(4)	O(13)-Ru(1)-C(2)	162.2(5)
C(1)-Ru(1)-C(2)	100.4(5)	Ru(1)-Ru(2)-P(3)	90.3(1)
Ru(1)-Ru(2)-P(4)	90.1(1)	P(3)-Ru(2)-P(4)	172.3(1)
Ru(1)-Ru(2)-C(3)	90.3(4)	P(3)-Ru(2)-C(3)	93.3(4)
P(4)-Ru(2)-C(3)	94.4(4)	Ru(1)-Ru(2)-C(4)	165.2(4)
P(3)-Ru(2)-C(4)	87.9(3)	P(4)-Ru(2)-C(4)	89.7(3)
C(3)-Ru(2)-C(4)	104.5(5)	Ru(1)-Ru(2)-C(33)	68.3(6)
P(3)-Ru(2)-C(33)	87.8(6)	P(4)-Ru(2)-C(33)	85.2(6)
C(3)-Ru(2)-C(33)	158.6(7)	C(4)-Ru(2)-C(33)	97.0(7)
Ru(1)-P(1)-O(5)	114.8(3)	Ru(1)-P(1)-O(6)	117.8(3)
O(5)-P(1)-O(6)	98.5(4)	Ru(1)-P(1)-N(1)	117.7(3)
O(5)-P(1)-N(1)	98.7(4)	O(6)-P(1)-N(1)	106.1(4)
Ru(1)-P(2)-O(7)	115.6(3)	Ru(1)-P(2)-O(8)	118.7(3)
O(7)-P(2)-O(8)	97.2(4)	Ru(1)-P(2)-N(2)	116.9(3)
O(7)-P(2)-N(2)	98.7(4)	O(8)-P(2)-N(2)	106.3(4)
Ru(2)-P(3)-O(9)	116.4(4)	Ru(2)-P(3)-O(10)	120.1(4)
O(9)-P(3)-O(10)	97.9(6)	Ru(2)-P(3)-N(2)	117.5(3)
O(9)-P(3)-N(2)	97.0(5)	O(10)-P(3)-N(2)	103.8(5)
Ru(2)-P(4)-O(11)	116.9(3)	Ru(2)-P(4)-O(12)	118.6(3)
O(11)-P(4)-O(12)	98.8(4)	Ru(2)-P(4)-N(1)	118.5(3)
O(11)-P(4)-N(1)	97.0(4)	O(12)-P(4)-N(1)	103.1(4)
P(1)-O(5)-C(5)	122.6(7)	P(1)-O(6)-C(8)	128.2(7)
P(2)-O(7)-C(11)	122.7(7)	P(2)-O(8)-C(14)	124.5(7)
P(3)-O(9)-C(17)	127.1(11)	P(3)-O(10)-C(20)	131.8(10)
P(4)-O(11)-C(23)	126.0(7)	P(4)-O(12)-C(26)	127.1(8)
Ru(1)-O(13)-O(14)	140.0(10)	Ru(1)-O(13)-C(33)	102.8(12)
O(14)-O(13)-C(33)	37.2(12)	O(13)-O(14)-C(33)	42.0(13)
P(1)-N(1)-P(4)	118.4(5)	P(1)-N(1)-C(29)	117.6(8)
P(4)-N(1)-C(29)	120.1(8)	P(2)-N(2)-P(3)	120.6(5)

TABLE 3.17 (continued)

P(2)-N(2)-C(31)	117.4(7)	P(3)-N(2)-C(31)	120.2(7)
Ru(1)-C(1)-O(1)	174.8(11)	Ru(1)-C(2)-O(2)	179.4(11)
Ru(2)-C(3)-O(3)	177.3(12)	Ru(2)-C(4)-O(4)	174.5(11)
O(5)-C(5)-C(6)	106.5(11)	O(5)-C(5)-C(7)	107.2(13)
C(6)-C(5)-C(7)	110(2)	O(6)-C(8)-C(9)	106.3(11)
O(6)-C(8)-C(10)	111.0(12)	C(9)-C(8)-C(10)	106.3(14)
O(7)-C(11)-C(12)	111.4(11)	O(7)-C(11)-C(13)	100.7(11)
C(12)-C(11)-C(13)	109.8(13)	O(8)-C(14)-C(15)	110.8(11)
O(8)-C(14)-C(16)	103.6(11)	C(15)-C(14)-C(16)	108.5(13)
O(9)-C(17)-C(18)	119(2)	O(9)-C(17)-C(19)	110(2)
C(18)-C(17)-C(19)	102(2)	O(10)-C(20)-C(21)	116.0(14)
O(10)-C(20)-C(22)	104.2(14)	C(21)-C(20)-C(22)	118(2)
O(11)-C(23)-C(24)	112.4(11)	O(11)-C(23)-C(25)	104.5(11)
C(24)-C(23)-C(25)	107.7(13)	O(12)-C(26)-C(27)	103.5(12)
O(12)-C(26)-C(28)	108.0(13)	C(27)-C(26)-C(28)	118(2)
N(1)-C(29)-C(30)	111.9(12)	N(2)-C(31)-C(32)	113.7(11)
Ru(2)-C(33)-O(13)	120.0(14)	Ru(2)-C(33)-O(14)	139(2)
O(13)-C(33)-O(14)	101(2)		

TABLE 3.18: Fractional co-ordinates ($x10^4$) and equivalent isotropic temperature factors ($Å^2$, $x10^3$) for $[Ru_2(CO)_4(\mu\text{-}OOCCH_3)\{\mu\text{-}(Pr^iO)_2PN(Et)P(OPr^i)_2\}_2]PF_6$ (40)

	x/a	y/b	z/c	U_{eq}
Ru(1)	0	0	0	30(1)
Ru(2)	-198(1)	-2428(1)	-191(1)	33(1)
P(1)	1321(2)	779(2)	2129(2)	34(1)
P(2)	-1223(2)	-756(2)	-2121(2)	37(1)
P(3)	-1999(3)	-3241(2)	-2234(2)	40(1)
P(4)	1715(3)	-1616(2)	1807(2)	39(1)
O(1)	523(9)	2707(7)	268(8)	74(2)
O(2)	-2898(7)	-367(7)	26(6)	64(2)
O(3)	-2406(7)	-2491(6)	726(6)	67(2)
O(4)	-311(11)	-5078(7)	-560(8)	77(2)
O(5)	456(6)	1113(5)	2880(5)	43(1)
O(6)	2655(6)	2095(5)	2809(5)	44(1)
O(7)	-2383(7)	-179(6)	-2727(6)	49(1)
O(8)	-195(7)	-570(5)	-2742(5)	51(1)
O(9)	-3666(6)	-3796(5)	-2555(5)	53(1)
O(10)	-1912(7)	-4442(5)	-3167(6)	54(1)
O(11)	1678(8)	-2351(7)	2640(6)	61(2)
O(12)	3300(6)	-1516(6)	1899(5)	56(1)
O(13)	1989(5)	-22(4)	-84(5)	39(1)
O(14)	1429(6)	-2101(5)	-761(5)	45(1)
N(1)	2072(8)	-140(7)	2734(7)	36(1)
N(2)	-2150(10)	-2323(8)	-2943(8)	58(2)
C(1)	371(8)	1713(7)	171(7)	40(2)*
C(2)	-1764(8)	-237(7)	36(7)	40(2)*
C(3)	-1582(9)	-2477(7)	367(7)	45(2)*
C(4)	-216(9)	-4094(8)	-429(8)	51(2)*
C(5)	-224(11)	2073(9)	2892(9)	63(2)*
C(6)	918(14)	3349(12)	4031(11)	84(3)*
C(7)	-1613(16)	1587(13)	2977(13)	96(4)*
C(8)	3674(9)	2475(7)	2371(7)	47(2)*
C(9)	4153(13)	3884(11)	2853(11)	76(3)*
C(10)	4971(14)	2014(11)	2819(11)	80(3)*
C(11)	-3050(9)	663(8)	-2170(7)	50(2)*
C(12)	-3000(13)	1658(11)	-2620(11)	78(3)*

TABLE 3.18 (continued)

C(13)	-4607(14)	-138(11)	-2587(11)	80(3)*
C(14)	341(11)	667(9)	-2736(9)	67(2)*
C(15)	2037(17)	976(14)	-2287(14)	103(4)*
C(16)	-475(14)	527(11)	-4057(11)	83(3)*
C(17)	-4277(12)	-4777(9)	-2275(9)	67(2)*
C(18)	-4817(13)	-6076(11)	-3378(11)	79(3)*
C(19)	-5493(18)	-4447(14)	-2004(14)	104(4)*
C(20)	-538(11)	-4572(9)	-3140(9)	64(2)*
C(21)	-129(19)	-3969(16)	-3881(16)	119(5)*
C(22)	-815(15)	-5982(12)	-3595(12)	89(3)*
C(23)	435(11)	-3291(9)	2491(9)	63(2)*
C(24)	1039(15)	-4308(12)	2735(12)	93(3)*
C(25)	-154(17)	-2708(14)	3303(15)	108(4)*
C(26)	4015(14)	-2451(11)	2006(11)	80(3)*
C(27)	3693(22)	-3348(19)	796(19)	132(6)*
C(28)	5757(26)	-1444(21)	2837(20)	149(7)*
C(29)	3212(10)	426(8)	4047(8)	50(2)*
C(30)	2587(12)	513(10)	4915(10)	70(2)*
C(31)	-3074(12)	-2815(10)	-4325(9)	68(2)*
C(32)	-4691(19)	-2968(15)	-4739(15)	113(5)*
C(33)	2246(8)	-991(7)	-460(7)	41(2)*
C(34)	3586(13)	-862(10)	-629(10)	76(3)*
P(5)	-3695(4)	-6458(3)	494(3)	83(1)
F(1)	7186(21)	4755(13)	523(14)	239(5)
F(2)	7187(15)	4065(11)	1934(10)	161(4)
F(3)	5397(11)	2955(10)	-979(8)	132(3)
F(4)	5435(22)	2387(16)	469(14)	257(6)
F(5)	7287(20)	2766(18)	410(12)	224(6)
F(6)	5181(19)	4132(19)	610(14)	218(7)

* Isotropic temperature factor.

$$U_{eq} = \frac{1}{3} \Sigma_i \Sigma_j U_{ij} a_i^* a_j^* (a_i \cdot a_j)$$

TABLE 3.19: Anistropic temperature factors ($Å^2$, $x10^3$) for

$[Ru_2(CO)_4(\mu\text{-}OOCCH_3)\{\mu\text{-}(Pr^iO)_2PN(Et)P(OPr^i)_2\}_2]PF_6$ (40)

	U(11)	U(22)	U(33)	U(23)	U(13)	U(12)
Ru(1)	29(1)	32(1)	31(1)	12(1)	15(1)	11(1)
Ru(2)	34(1)	31(1)	35(1)	14(1)	17(1)	13(1)
P(1)	32(1)	37(1)	33(1)	12(1)	16(1)	13(1)
P(2)	38(1)	38(1)	34(1)	16(1)	15(1)	13(1)
P(3)	42(1)	31(1)	35(1)	9(1)	12(1)	10(1)
P(4)	37(1)	40(1)	40(1)	18(1)	16(1)	16(1)
O(1)	83(5)	43(3)	93(5)	34(4)	33(4)	25(4)
O(2)	46(3)	93(4)	83(4)	51(4)	45(3)	35(3)
O(3)	65(4)	85(4)	80(4)	44(4)	50(4)	33(3)
O(4)	111(6)	38(3)	80(5)	27(4)	40(5)	27(4)
O(5)	40(3)	59(3)	43(3)	23(2)	26(2)	26(2)
O(6)	34(3)	34(3)	43(3)	3(2)	13(2)	4(2)
O(7)	50(4)	51(3)	52(3)	29(3)	20(3)	24(3)
O(8)	67(4)	51(3)	43(3)	22(2)	33(3)	19(3)
O(9)	34(3)	50(3)	60(3)	19(3)	15(3)	3(2)
O(10)	63(4)	39(3)	56(3)	11(2)	32(3)	16(3)
O(11)	58(4)	64(4)	57(4)	39(3)	18(3)	11(3)
O(12)	41(3)	71(3)	62(3)	33(3)	22(3)	32(3)
O(13)	35(3)	40(3)	45(3)	14(2)	23(2)	14(2)
O(14)	46(3)	51(3)	46(3)	18(2)	28(3)	21(2)
N(1)	39(4)	34(3)	30(3)	11(3)	12(3)	18(3)
N(2)	61(5)	48(5)	40(4)	17(4)	3(4)	13(4)
P(5)	93(2)	69(2)	88(2)	28(1)	54(2)	13(2)
F(1)	249(17)	156(10)	182(12)	70(9)	52(12)	-88(11)
F(2)	194(12)	139(8)	109(7)	34(6)	65(8)	22(8)
F(3)	116(7)	167(9)	101(6)	50(6)	55(5)	26(6)
F(4)	233(18)	214(14)	151(11)	79(10)	12(11)	-108(13)
F(5)	241(16)	302(19)	139(10)	63(11)	75(11)	200(16)
F(6)	220(16)	299(21)	211(15)	109(15)	129(14)	191(16)

TABLE 3.20: Interatomic distances (Å) for

$[Ru_2(CO)_4(\mu\text{-}OOCCH_3)\{\mu\text{-}(Pr^iO)_2PN(Et)P(OPr^i)_2\}_2]PF_6$ (40)

Ru(1)-Ru(2)	2.806(1)	Ru(1)-P(1)	2.334(2)
Ru(1)-P(2)	2.324(2)	Ru(1)-O(13)	2.141(6)
Ru(1)-C(1)	1.942(8)	Ru(1)-C(2)	1.844(9)
Ru(2)-P(3)	2.336(2)	Ru(2)-P(4)	2.333(2)
Ru(2)-O(14)	2.132(7)	Ru(2)-C(3)	1.861(11)
Ru(2)-C(4)	1.919(10)	P(1)-O(5)	1.591(7)
P(1)-O(6)	1.609(5)	P(1)-N(1)	1.688(9)
P(2)-O(7)	1.583(8)	P(2)-O(8)	1.604(8)
P(2)-N(2)	1.700(8)	P(3)-O(9)	1.587(7)
P(3)-O(10)	1.616(7)	P(3)-N(2)	1.638(11)
P(4)-O(11)	1.606(10)	P(4)-O(12)	1.604(7)
P(4)-N(1)	1.675(8)	O(1)-C(1)	1.133(12)
O(2)-C(2)	1.169(12)	O(3)-C(3)	1.133(14)
O(4)-C(4)	1.118(13)	O(5)-C(5)	1.463(14)
O(6)-C(8)	1.462(13)	O(7)-C(11)	1.498(13)
O(8)-C(14)	1.481(14)	O(9)-C(17)	1.448(15)
O(10)-C(20)	1.470(15)	O(11)-C(23)	1.461(14)
O(12)-C(26)	1.48(2)	O(13)-C(33)	1.236(10)
O(14)-C(33)	1.285(9)	N(1)-C(29)	1.492(10)
N(2)-C(31)	1.523(13)	C(5)-C(6)	1.587(12)
C(5)-C(7)	1.53(2)	C(8)-C(9)	1.510(15)
C(8)-C(10)	1.54(2)	C(11)-C(12)	1.49(2)
C(11)-C(13)	1.52(2)	C(14)-C(15)	1.57(2)
C(14)-C(16)	1.54(2)	C(17)-C(18)	1.570(14)
C(17)-C(19)	1.54(3)	C(20)-C(21)	1.51(3)
C(20)-C(22)	1.54(2)	C(23)-C(24)	1.54(2)
C(23)-C(25)	1.48(2)	C(26)-C(27)	1.47(3)
C(26)-C(28)	1.68(2)	C(29)-C(30)	1.50(2)
C(31)-C(32)	1.53(2)	C(33)-C(34)	1.50(2)
P(5)-F(1)	1.55(2)	P(5)-F(2)	1.579(11)
P(5)-F(3)	1.611(9)	P(5)-F(4)	1.50(2)
P(5)-F(5)	1.53(2)	P(5)-F(6)	1.52(2)

TABLE 3.21: Interatomic angles (°) for

$[Ru_2(CO)_4(\mu\text{-}OOCCH_3)\{\mu\text{-}(Pr^iO)_2PN(Et)P(OPr^i)_2\}_2]PF_6$ (40)

Ru(2)-Ru(1)-P(1)	89.6(1)	Ru(2)-Ru(1)-P(2)	90.6(1)
P(1)-Ru(1)-P(2)	177.6(1)	Ru(2)-Ru(1)-O(13)	81.4(1)
P(1)-Ru(1)-O(13)	88.9(2)	P(2)-Ru(1)-O(13)	88.8(2)
Ru(2)-Ru(1)-C(1)	173.4(3)	P(1)-Ru(1)-C(1)	88.7(2)
P(2)-Ru(1)-C(1)	90.8(2)	O(13)-Ru(1)-C(1)	92.1(3)
Ru(2)-Ru(1)-C(2)	89.7(3)	P(1)-Ru(1)-C(2)	91.6(2)
P(2)-Ru(1)-C(2)	90.7(2)	O(13)-Ru(1)-C(2)	171.1(3)
C(1)-Ru(1)-C(2)	96.8(4)	Ru(1)-Ru(2)-P(3)	89.5(1)
Ru(1)-Ru(2)-P(4)	90.6(1)	P(3)-Ru(2)-P(4)	176.3(1)
Ru(1)-Ru(2)-O(14)	81.3(2)	P(3)-Ru(2)-O(14)	88.5(2)
P(4)-Ru(2)-O(14)	87.8(2)	Ru(1)-Ru(2)-C(3)	90.8(3)
P(3)-Ru(2)-C(3)	92.7(2)	P(4)-Ru(2)-C(3)	91.0(2)
O(14)-Ru(2)-C(3)	172.0(3)	Ru(1)-Ru(2)-C(4)	173.5(4)
P(3)-Ru(2)-C(4)	88.7(2)	P(4)-Ru(2)-C(4)	90.8(2)
O(14)-Ru(2)-C(4)	92.4(4)	C(3)-Ru(2)-C(4)	95.5(4)
Ru(1)-P(1)-O(5)	117.4(2)	Ru(1)-P(1)-O(6)	115.8(3)
O(5)-P(1)-O(6)	99.4(3)	Ru(1)-P(1)-N(1)	118.3(3)
O(5)-P(1)-N(1)	98.9(4)	O(6)-P(1)-N(1)	104.0(3)
Ru(1)-P(2)-O(7)	118.8(3)	Ru(1)-P(2)-O(8)	115.5(2)
O(7)-P(2)-O(8)	99.9(4)	Ru(1)-P(2)-N(2)	117.4(4)
O(7)-P(2)-N(2)	102.8(4)	O(8)-P(2)-N(2)	99.3(5)
Ru(2)-P(3)-O(9)	118.1(3)	Ru(2)-P(3)-O(10)	115.5(3)
O(9)-P(3)-O(10)	99.0(3)	Ru(2)-P(3)-N(2)	119.0(2)
O(9)-P(3)-N(2)	99.4(5)	O(10)-P(3)-N(2)	102.6(5)
Ru(2)-P(4)-O(11)	119.1(2)	Ru(2)-P(4)-O(12)	114.2(3)
O(11)-P(4)-O(12)	100.5(4)	Ru(2)-P(4)-N(1)	117.2(3)
O(11)-P(4)-N(1)	102.7(4)	O(12)-P(4)-N(1)	100.3(4)
P(1)-O(5)-C(5)	123.8(7)	P(1)-O(6)-C(8)	125.8(5)
P(2)-O(7)-C(11)	129.9(6)	P(2)-O(8)-C(14)	119.1(7)
P(3)-O(9)-C(17)	126.2(7)	P(3)-O(10)-C(20)	124.3(5)
P(4)-O(11)-C(23)	129.2(6)	P(4)-O(12)-C(26)	125.7(8)
Ru(1)-O(13)-C(33)	123.7(5)	Ru(2)-O(14)-C(33)	122.2(6)
P(1)-N(1)-P(4)	119.3(4)	P(1)-N(1)-C(29)	119.4(6)
P(4)-N(1)-C(29)	120.7(7)	P(2)-N(2)-P(3)	119.4(5)
P(2)-N(2)-C(31)	117.9(8)	P(3)-N(2)-C(31)	122.7(7)

TABLE 3.21 (continued)

Ru(1)-C(1)-O(1)	176.7(9)	Ru(1)-C(2)-O(2)	177.3(9)
Ru(2)-C(3)-O(3)	178.8(5)	Ru(2)-C(4)-O(4)	175.3(11)
O(5)-C(5)-C(6)	108.4(8)	O(5)-C(5)-C(7)	105.9(10)
C(6)-C(5)-C(7)	112.6(11)	O(6)-C(8)-C(9)	106.6(9)
O(6)-C(8)-C(10)	109.4(9)	C(9)-C(8)-C(10)	112.8(8)
O(7)-C(11)-C(12)	106.4(10)	O(7)-C(11)-C(13)	107.0(7)
C(12)-C(11)-C(13)	112.7(9)	O(8)-C(14)-C(15)	105.5(10)
O(8)-C(14)-C(16)	107.4(7)	C(15)-C(14)-C(16)	111.3(13)
O(9)-C(17)-C(18)	108.8(11)	O(9)-C(17)-C(19)	105.7(11)
C(18)-C(17)-C(19)	114.8(9)	O(10)-C(20)-C(21)	110.3(12)
O(10)-C(20)-C(22)	105.2(9)	C(21)-C(20)-C(22)	115.1(13)
O(11)-C(23)-C(24)	104.6(10)	O(11)-C(23)-C(25)	110.4(9)
C(24)-C(23)-C(25)	115.5(13)	O(12)-C(26)-C(27)	111.1(13)
O(12)-C(26)-C(28)	97.0(12)	C(27)-C(26)-C(28)	113(2)
N(1)-C(29)-C(30)	113.7(8)	N(2)-C(31)-C(32)	113.5(12)
O(13)-C(33)-O(14)	125.5(9)	O(13)-C(33)-C(34)	117.0(8)
O(14)-C(33)-C(34)	117.5(8)	F(1)-P(5)-F(2)	91.4(8)
F(1)-P(5)-F(3)	90.5(8)	F(2)-P(5)-F(3)	177.8(7)
F(1)-P(5)-F(4)	178.8(13)	F(2)-P(5)-F(4)	88.5(8)
F(3)-P(5)-F(4)	89.6(7)	F(1)-P(5)-F(5)	100.6(12)
F(2)-P(5)-F(5)	88.4(8)	F(3)-P(5)-F(5)	90.2(7)
F(4)-P(5)-F(5)	80.5(12)	F(1)-P(5)-F(6)	89.4(12)
F(2)-P(5)-F(6)	89.9(9)	F(3)-P(5)-F(6)	91.2(8)
F(4)-P(5)-F(6)	89.4(13)	F(5)-P(5)-F(6)	169.9(12)

TABLE 3.22: Fractional co-ordinates ($\times 10^4$) and equivalent isotropic temperature factors ($Å^2$, $\times 10^3$) for $[Ru_2(CO)_4(\mu\text{-}NC_5H_4O)\{\mu\text{-}(MeO)_2PN(Et)P(OMe)_2\}_2]PF_6$ (44)

	x/a	y/b	z/c	U_{eq}
Ru(1)	1220(1)	1033(1)	2500	33(1)
Ru(2)	1079(1)	3554(1)	3130(1)	37(1)
P(1)	535(1)	1072(2)	1688(3)	39(1)
P(2)	1909(1)	1199(2)	3300(3)	37(1)
P(3)	1627(1)	3406(3)	4525(2)	41(1)
P(4)	589(1)	3742(3)	1619(3)	50(1)
O(1)	1465(3)	-1657(7)	1865(9)	79(3)
O(2)	812(3)	142(10)	4744(8)	78(3)
O(3)	414(3)	2861(11)	4920(9)	93(3)
O(4)	957(4)	6341(8)	3728(11)	100(3)
O(5)	182(2)	706(7)	2629(8)	56(2)
O(6)	431(3)	178(6)	616(7)	55(2)
O(7)	2285(2)	1582(6)	2448(6)	44(2)
O(8)	2111(3)	-60(7)	3814(7)	56(2)
O(9)	1502(3)	3233(8)	5848(6)	56(2)
O(10)	1922(2)	4648(7)	4658(7)	56(2)
O(11)	767(3)	4412(7)	501(8)	75(2)
O(12)	178(3)	4624(8)	1868(11)	93(3)
O(13)	1574(3)	3810(6)	1912(6)	48(2)
N(1)	393(3)	2428(8)	1039(8)	51(2)
N(2)	1994(3)	2250(8)	4355(7)	45(2)
N(3)	1470(3)	1927(7)	965(7)	36(2)
C(1)	1382(4)	-652(10)	2041(10)	51(3)
C(2)	978(4)	489(11)	3922(10)	51(3)
C(3)	664(4)	3149(11)	4232(11)	54(3)
C(4)	1028(4)	5338(11)	3476(10)	56(3)
C(5)	-294(3)	676(14)	2363(16)	81(4)
C(6)	431(5)	-1202(11)	730(15)	80(4)
C(7)	2461(4)	729(13)	1585(11)	67(3)
C(8)	1888(4)	-843(12)	4683(13)	71(4)
C(9)	1258(5)	4199(16)	6484(13)	85(4)
C(10)	2126(5)	5222(13)	3687(12)	78(4)
C(11)	930(6)	5695(13)	498(16)	95(5)
C(12)	-149(4)	4391(18)	2658(26)	134(7)

C(13)	106(6)	2483(14)	-1(14)	92(4)
C(14)	326(9)	2435(20)	-1096(16)	133(7)
C(15)	2428(4)	2330(13)	4926(10)	60(3)
C(16)	2441(5)	1786(18)	6149(12)	91(5)
C(17)	1627(3)	3109(9)	985(9)	42(2)
C(18)	1852(4)	3640(11)	43(11)	60(3)
C(19)	1887(5)	2948(12)	-957(11)	70(3)
C(20)	1700(4)	1708(12)	-1018(10)	60(3)
C(21)	1507(4)	1286(10)	-57(9)	49(3)
P(5)	3543(1)	2876(3)	2801(3)	59(1)
F(1)	3341(3)	1608(7)	3243(10)	95(2)
F(2)	3750(3)	4123(9)	2368(16)	137(4)
F(3)	3458(7)	2451(12)	1517(11)	169(5)
F(4)	3606(7)	3234(12)	4047(11)	206(7)
F(5)	3979(3)	2160(11)	2849(20)	187(6)
F(6)	3106(3)	3550(10)	2773(17)	155(5)

$$U_{eq} = \frac{1}{3} \Sigma_i \Sigma_j U_{ij} a_i^* a_j^* (a_i \cdot a_j)$$

TABLE 3.23: Anistropic temperature factors ($Å^2$, $x10^3$) for

$[Ru_2(CO)_4(\mu\text{-}NC_5H_4O)\{\mu\text{-}(MeO)_2PN(Et)P(OMe)_2\}_2]PF_6$ (**44**)

	U(11)	U(22)	U(33)	U(23)	U(13)	U(12)
Ru(1)	34(1)	29(1)	36(1)	0(1)	2(1)	-4(1)
Ru(2)	37(1)	32(1)	42(1)	-6(1)	3(1)	-2(1)
P(1)	37(1)	33(1)	49(2)	0(1)	-6(1)	-5(1)
P(2)	34(1)	41(1)	37(1)	-2(1)	5(1)	1(1)
P(3)	44(2)	45(1)	35(1)	-8(1)	7(1)	-5(1)
P(4)	51(2)	31(1)	69(2)	0(1)	-15(2)	3(1)
O(1)	101(7)	33(4)	103(7)	-15(4)	-9(6)	15(4)
O(2)	76(6)	101(7)	56(5)	30(5)	17(5)	-2(5)
O(3)	76(7)	115(8)	90(7)	-14(7)	50(6)	-30(6)
O(4)	136(9)	47(5)	117(9)	-31(6)	-4(8)	18(5)
O(5)	30(3)	66(5)	71(5)	9(5)	-5(4)	-8(3)
O(6)	71(5)	36(4)	59(5)	-5(4)	-19(4)	-8(4)
O(7)	34(4)	56(4)	42(4)	-7(4)	10(3)	-2(3)
O(8)	62(5)	50(4)	56(5)	5(4)	-7(4)	11(4)
O(9)	62(5)	67(5)	38(4)	-6(4)	13(4)	11(4)
O(10)	57(5)	59(4)	52(4)	-20(4)	-2(4)	-21(4)
O(11)	107(7)	48(4)	71(6)	21(4)	-28(5)	-19(5)
O(12)	76(6)	49(5)	154(10)	-29(6)	-27(7)	21(4)
O(13)	65(5)	38(4)	40(4)	-4(3)	9(4)	-14(3)
N(1)	54(6)	39(5)	60(5)	1(4)	-25(5)	-3(4)
N(2)	41(5)	64(6)	30(4)	-5(4)	-2(4)	0(4)
N(3)	39(4)	35(4)	34(4)	-3(4)	4(4)	-12(3)
C(1)	56(7)	42(6)	54(6)	-3(5)	5(5)	-1(5)
C(2)	54(7)	48(6)	51(7)	5(6)	-7(6)	-4(5)
C(3)	39(7)	60(7)	63(7)	-10(6)	0(6)	1(5)
C(4)	65(8)	48(6)	54(7)	-5(5)	0(5)	-3(5)
C(5)	23(5)	102(10)	117(12)	0(11)	-3(7)	-2(6)
C(6)	110(12)	35(6)	95(11)	-11(7)	-12(10)	-19(6)
C(7)	63(8)	78(8)	59(7)	-20(7)	25(7)	3(7)
C(8)	52(8)	72(8)	90(10)	36(8)	-17(7)	2(6)
C(9)	95(11)	110(12)	51(7)	-26(8)	21(8)	27(9)
C(10)	98(10)	70(8)	66(8)	4(7)	5(8)	-45(8)
C(11)	128(14)	50(7)	107(13)	17(8)	-23(11)	-33(8)
C(12)	41(8)	150(16)	211(24)	-33(19)	32(13)	22(8)
C(13)	121(13)	70(8)	86(11)	9(8)	-73(10)	-13(9)

TABLE 3.23 (continued)

C(14)	226(25)	102(13)	72(12)	7(11)	-47(14)	-22(14)
C(15)	39(6)	94(9)	48(6)	-12(6)	-8(5)	-3(6)
C(16)	63(9)	159(16)	49(7)	1(9)	-9(7)	15(9)
C(17)	44(6)	43(5)	40(5)	2(5)	9(5)	-7(5)
C(18)	76(9)	51(6)	53(7)	5(6)	6(6)	-14(6)
C(19)	98(11)	67(8)	47(7)	-2(6)	22(7)	-10(7)
C(20)	69(8)	66(7)	45(7)	-4(6)	-5(6)	-14(6)
C(21)	60(7)	48(6)	39(6)	-13(5)	13(5)	1(5)
P(5)	49(2)	56(2)	72(2)	3(2)	3(1)	-1(1)
F(1)	72(5)	72(5)	140(8)	22(6)	20(6)	-12(4)
F(2)	74(5)	91(6)	248(17)	58(9)	20(8)	-22(5)
F(3)	277(19)	130(10)	102(8)	3(8)	-11(11)	19(11)
F(4)	401(27)	107(9)	111(10)	-20(8)	-105(15)	-11(13)
F(5)	61(5)	144(10)	356(24)	116(15)	22(10)	22(6)
F(6)	79(6)	114(7)	273(19)	47(11)	46(10)	35(5)

TABLE 3.24: Interatomic distances (Å) for

$[Ru_2(CO)_4(\mu\text{-}NC_5H_4O)\{\mu\text{-}(MeO)_2PN(Et)P(OMe)_2\}_2]PF_6$ (**44**)

Ru(1)-Ru(2)	2.797(1)	Ru(1)-P(1)	2.315(3)
Ru(1)-P(2)	2.326(3)	Ru(1)-N(3)	2.148(8)
Ru(1)-C(1)	1.924(11)	Ru(1)-C(2)	1.890(12)
Ru(2)-P(3)	2.339(3)	Ru(2)-P(4)	2.315(4)
Ru(2)-O(13)	2.094(8)	Ru(2)-C(3)	1.853(12)
Ru(2)-C(4)	1.934(12)	P(1)-O(5)	1.584(8)
P(1)-O(6)	1.587(8)	P(1)-N(1)	1.675(9)
P(2)-O(7)	1.574(7)	P(2)-O(8)	1.585(8)
P(2)-N(2)	1.667(9)	P(3)-O(9)	1.582(8)
P(3)-O(10)	1.608(8)	P(3)-N(2)	1.680(9)
P(4)-O(11)	1.569(10)	P(4)-O(12)	1.601(9)
P(4)-N(1)	1.655(9)	O(1)-C(1)	1.112(13)
O(2)-C(2)	1.136(15)	O(3)-C(3)	1.15(2)
O(4)-C(4)	1.121(15)	O(5)-C(5)	1.504(13)
O(6)-C(6)	1.466(13)	O(7)-C(7)	1.447(15)
O(8)-C(8)	1.47(2)	O(9)-C(9)	1.47(2)
O(10)-C(10)	1.42(2)	O(11)-C(11)	1.45(2)
O(12)-C(12)	1.38(3)	O(13)-C(17)	1.309(12)
N(1)-C(13)	1.49(2)	N(2)-C(15)	1.497(14)
N(3)-C(17)	1.341(12)	N(3)-C(21)	1.362(13)
C(13)-C(14)	1.43(3)	C(15)-C(16)	1.52(2)
C(17)-C(18)	1.40(2)	C(18)-C(19)	1.37(2)
C(19)-C(20)	1.44(2)	C(20)-C(21)	1.33(2)
P(5)-F(1)	1.563(9)	P(5)-F(2)	1.548(11)
P(5)-F(3)	1.567(14)	P(5)-F(4)	1.495(14)
P(5)-F(5)	1.548(10)	P(5)-F(6)	1.527(10)

TABLE 3.25: Interatomic angles (°) for

$[Ru_2(CO)_4(\mu\text{-}NC_5H_4O)\{\mu\text{-}(MeO)_2PN(Et)P(OMe)_2\}_2]PF_6$ (**44**)

Ru(2)-Ru(1)-P(1)	86.8(1)	Ru(2)-Ru(1)-P(2)	88.2(1)
P(1)-Ru(1)-P(2)	174.6(1)	Ru(2)-Ru(1)-N(3)	81.4(2)
P(1)-Ru(1)-N(3)	89.4(2)	P(2)-Ru(1)-N(3)	87.8(2)
Ru(2)-Ru(1)-C(1)	173.8(3)	P(1)-Ru(1)-C(1)	98.3(3)
P(2)-Ru(1)-C(1)	86.6(3)	N(3)-Ru(1)-C(1)	95.0(4)
Ru(2)-Ru(1)-C(2)	90.2(3)	P(1)-Ru(1)-C(2)	89.6(4)
P(2)-Ru(1)-C(2)	92.5(4)	N(3)-Ru(1)-C(2)	171.6(4)
C(1)-Ru(1)-C(2)	93.4(5)	Ru(1)-Ru(2)-P(3)	90.1(1)
Ru(1)-Ru(2)-P(4)	89.4(1)	P(3)-Ru(2)-P(4)	174.4(1)
Ru(1)-Ru(2)-O(13)	80.5(2)	P(3)-Ru(2)-O(13)	86.4(2)
P(4)-Ru(2)-O(13)	88.0(2)	Ru(1)-Ru(2)-C(3)	93.7(4)
P(3)-Ru(2)-C(3)	90.9(4)	P(4)-Ru(2)-C(3)	94.6(4)
O(13)-Ru(2)-C(3)	173.7(4)	Ru(1)-Ru(2)-C(4)	174.6(4)
P(3)-Ru(2)-C(4)	89.0(4)	P(4)-Ru(2)-C(4)	91.0(4)
O(13)-Ru(2)-C(4)	94.1(4)	C(3)-Ru(2)-C(4)	91.6(5)
Ru(1)-P(1)-O(5)	110.4(3)	Ru(1)-P(1)-O(6)	119.3(3)
O(5)-P(1)-O(6)	104.2(4)	Ru(1)-P(1)-N(1)	115.8(3)
O(5)-P(1)-N(1)	109.5(4)	O(6)-P(1)-N(1)	96.3(4)
Ru(1)-P(2)-O(7)	116.7(3)	Ru(1)-P(2)-O(8)	116.5(3)
O(7)-P(2)-O(8)	99.0(4)	Ru(1)-P(2)-N(2)	118.9(3)
O(7)-P(2)-N(2)	99.5(4)	O(8)-P(2)-N(2)	103.1(4)
Ru(2)-P(3)-O(9)	119.5(3)	Ru(2)-P(3)-O(10)	115.0(3)
O(9)-P(3)-O(10)	98.1(4)	Ru(2)-P(3)-N(2)	117.3(3)
O(9)-P(3)-N(2)	101.1(4)	O(10)-P(3)-N(2)	102.8(4)
Ru(2)-P(4)-O(11)	115.1(4)	Ru(2)-P(4)-O(12)	115.7(5)
O(11)-P(4)-O(12)	99.4(5)	Ru(2)-P(4)-N(1)	118.0(3)
O(11)-P(4)-N(1)	100.2(5)	O(12)-P(4)-N(1)	105.7(5)
P(1)-O(5)-C(5)	122.6(9)	P(1)-O(6)-C(6)	121.6(8)
P(2)-O(7)-C(7)	123.0(7)	P(2)-O(8)-C(8)	122.7(7)
P(3)-O(9)-C(9)	121.7(8)	P(3)-O(10)-C(10)	121.7(8)
P(4)-O(11)-C(11)	123.2(9)	P(4)-O(12)-C(12)	126.5(10)
Ru(2)-O(13)-C(17)	124.3(6)	P(1)-N(1)-P(4)	116.3(6)
P(1)-N(1)-C(13)	123.2(8)	P(4)-N(1)-C(13)	120.5(8)
P(2)-N(2)-P(3)	117.6(5)	P(2)-N(2)-C(15)	119.9(7)
P(3)-N(2)-C(15)	120.9(8)	Ru(1)-N(3)-C(17)	121.8(6)

TABLE 3.25 (continued)

Ru(1)-N(3)-C(21)	121.4(6)	C(17)-N(3)-C(21)	116.7(8)
Ru(1)-C(1)-O(1)	174.1(11)	Ru(1)-C(2)-O(2)	176.2(10)
Ru(2)-C(3)-O(3)	177.8(11)	Ru(2)-C(4)-O(4)	172.6(12)
N(1)-C(13)-C(14)	115(2)	N(2)-C(15)-C(16)	114.1(10)
O(13)-C(17)-N(3)	119.7(9)	O(13)-C(17)-C(18)	117.7(9)
N(3)-C(17)-C(18)	122.5(9)	C(17)-C(18)-C(19)	118.4(11)
C(18)-C(19)-C(20)	119.8(11)	C(19)-C(20)-C(21)	116.5(11)
N(3)-C(21)-C(20)	125.9(10)	F(1)-P(5)-F(2)	179.0(5)
F(1)-P(5)-F(3)	89.6(7)	F(2)-P(5)-F(3)	90.6(9)
F(1)-P(5)-F(4)	87.6(7)	F(2)-P(5)-F(4)	92.3(9)
F(3)-P(5)-F(4)	177.0(10)	F(1)-P(5)-F(5)	85.2(6)
F(2)-P(5)-F(5)	93.8(6)	F(3)-P(5)-F(5)	92.2(11)
F(4)-P(5)-F(5)	88.7(12)	F(1)-P(5)-F(6)	93.2(5)
F(2)-P(5)-F(6)	87.8(6)	F(3)-P(5)-F(6)	88.0(10)
F(4)-P(5)-F(6)	91.0(11)	F(5)-P(5)-F(6)	178.3(8)

CHAPTER 4

REACTION OF $[Ru_2(\mu\text{-}CO)(CO)_4\{\mu\text{-}(RO)_2PN(Et)P(OR)_2\}_2]$ (R = Me or Pr^i) WITH QUINONES AND WITH THE DIAZONIUM SALT $[PhN_2][PF_6]$

4.1 INTRODUCTION

Being electron-rich, the diruthenium diphosphazane-bridged derivatives $[Ru_2(\mu\text{-}CO)(CO)_4\{\mu\text{-}(RO)_2PN(Et)P(OR)_2\}_2]$ (R = Me or Pr^i) are expected to react with a wide range of electron-acceptor ligands such as TCNQ and TCNE. Indeed, the reactions of these compounds with TCNQ and TCNE have been the subject of a detailed investigation and have been found to afford radical anion salts of general formula $[Ru_2(CO)_5(TCNX)\{\mu\text{-}(RO)_2PN(Et)P(OR)_2\}_2]^{+}\cdot TCNX^{\cdot -}$ (R = Me or Pr^i; X = E or Q) which contain TCNX radical anions in both the inner and outer co-ordination spheres of the cation.

Quinones may similarly undergo reaction with electron-rich transition metal complexes to afford charge-transfer complexes. These electron-acceptor ligands play an integral role in many biological charge-transfer processes, particularly respiration and photosynthesis.[185-187] During these processes quinones are reversibly reduced to semiquinone radical anions, with the concomitant oxidation of the divalent metal centres.

Ortho-quinones tend to adopt the chelating co-ordination mode in bonding to transition metals although in some cases they have been shown to bridge two transition metals. For example, addition of tetrachloro-*o*-benzoquinone to the sulphur-bridged dirhodium species $[Rh_2(\mu\text{-}S)(CO)_2(\mu\text{-}dppm)_2]$ results in the formation of the catecholate derivative

$[Ru_2(\mu\text{-}S)(\mu\text{-}CO)(CO)(1,2\text{-}O_2C_6Cl_4)(\mu\text{-}dppm)_2]$ in which the quinone dianion chelates to a single rhodium atom,[188] whereas treatment of $[Ru(CO)_2(PPh_3)L]$ (L = η^4-2,3-dimethylbuta-1,3-diene) with tetrachloro-*o*-benzoquinone affords the catecholate-bridged dimer $[Ru(CO)_2(PPh_3)(\mu\text{-}o\text{-}O_2C_6Cl_4)]_2$.[189] In contrast, *p*-quinones may either co-ordinate to a transition metal through one of its carbonyl oxygen atoms in a unidentate fashion, or in a π manner.[190] The photochemical reactions of the dimolybdenum species $[MoCp(CO)_3]_2$ with a series of *p*-benzoquinones have been investigated by EPR spectroscopy. The paramagnetic products have been characterized as complexes of the form $[CpMo(CO)_3(p\text{-benzoquinone})]$ where $CpMo(CO)_3$, produced by photocleavage of the Mo-Mo bond in $[CpMo(CO)_3]_2$, is co-ordinated by the carbonyl oxygen in the *p*-benzoquinones.

In general, complexes containing quinone ligands can be readily reduced in two one-electron steps to afford semiquinone and catecholate products as illustrated below.

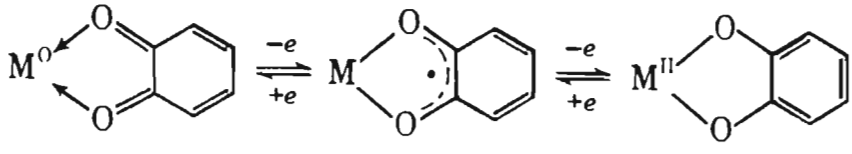

Scheme 4.1

The propensity to form complexes containing quinone ligands in which the quinone is co-ordinated as a quinone, semiquinone or catecholate ligand, will depend on the basicity of the metal as well as the oxidizing ability of the quinone.

A preliminary investigation of the reactivity of $[Ru_2(\mu\text{-}CO)(CO)_4\{\mu\text{-}(R\text{-}O)_2PN(Et)P(OR)_2\}_2]$ (R = Me or Pr^i) towards tetrachloro-*o*-benzoquinone has been undertaken previously in these laboratories. It was found that

addition of an equimolar amount of this quinone to the dinuclear ruthenium species leads to the formation of an unusual rearrangement product *viz.* $[Ru_2\{\mu\text{-}(RO)_2PN(Et)C(O)\}\{P(OR)_2OC_6Cl_4O\}(CO)_4\{\mu\text{-}(RO)_2PN(Et)P(OR)_2\}]$ (R = Me or Pr^i) (Figure 4.1), as described in Chapter 1. As

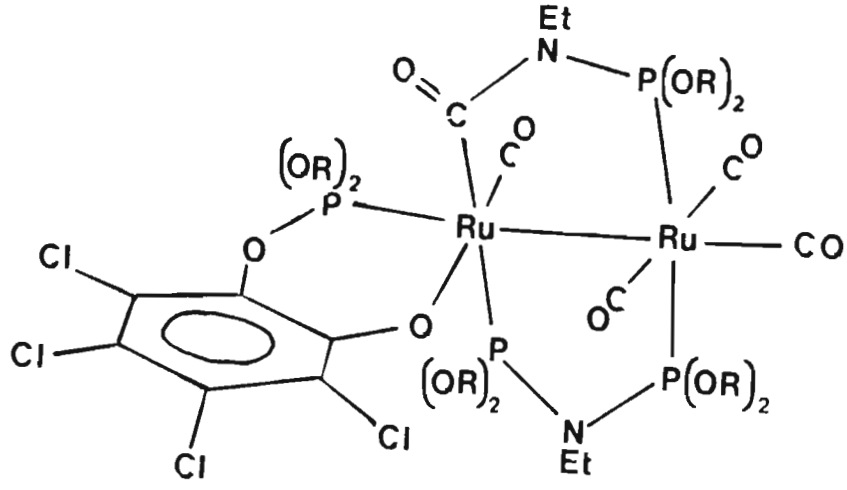

Figure 4.1

part of a programme aimed at the synthesis of metal-ligand charge-transfer salts, it has been our endeavour to investigate further reactions of the parent dinuclear complexes with related quinone ligands.

Aryldiazonium salts of the type $[ArN_2][PF_6]$ have been used extensively as one-electron oxidants and have, in many cases, produced routes to derivatives containing the aryldiazo ligand RN_2 on reaction with transition metal complexes.[191,192] Methods of introducing the RN_2 ligand include the displacement of another ligand[193] such as CO by RN_2^+, the oxidative addition of RN_2^+ to the complex and by the insertion of RN_2^+ into a metal-ligand bond.[194,195] The motivation for the study of complexes containing the aryldiazonium ions RN_2^+ is based upon the close relationship of co-ordinated RN_2^+ with co-ordinated N_2 or NO^+.

By analogy with the nitrosonium ion NO^+, aryldiazonium ions may co-ordinate to transition metals as a three-electron donor in a singly bent geometry (a) or as a one-electron donor in a doubly bent geometry (b), as depicted in Scheme 4.2.

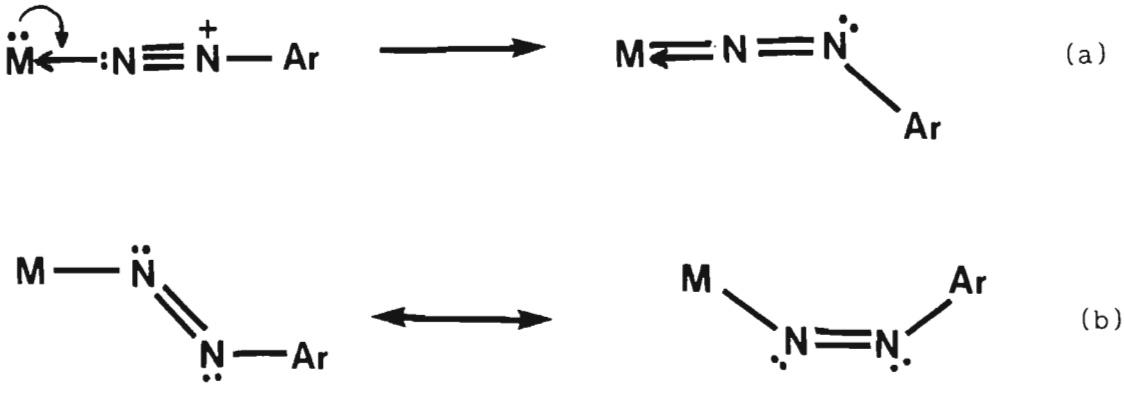

Scheme 4.2

The aryldiazenato-ligand may also bridge two metal atoms as a three-electron donor as shown below; bridging nitrosyls bound in a manner comparable to that shown in Figure 4.2 (a) are well known.

Figure 4.2

As expected, the aryldiazonium ion has been found to exhibit similar co-ordination behaviour to the nitrosonium ion NO^+. For example, reaction of the rhodium species [RhCl(PPP)] {PPP = $PhP[(CH_2)_3PPh_2]_2$} with NO^+ affords $[RhCl(NO)(PPP)]^+$ while reaction of this rhodium precursor with PhN_2^+ gives the phenyldiazenato species $[RhCl(N_2Ph)(PPP)]^+$. Significantly, it was found that warming the latter species in methanol

resulted in the formation of the hydrido species $[RhH(Cl)(PPP)]^+$ [197] and anisole, PhOMe. It is proposed that methanol is sufficiently acidic for H^+ to displace the aryldiazenate group as PhN_2^+ from the co-ordination sphere, probably via a phenyldiazene complex $[RhCl(NH{=}NPh)(PPP)]^{2+}$.

Transition metal complexes containing co-ordinated aryldiazenes (NH=NAr) such as phenyldiazenes, have been shown to be formed upon protonation of the corresponding aryldiazenato species. Of the two possible sites for protonation of the doubly bent aryldiazenato ligand, the available evidence is that protonation occurs at the nitrogen atom adjacent to the metal as illustrated in equation:

$$[RhCl_2(N_2Ar)(PPh_3)_2] \xrightarrow{HCl} [RhCl_3(NH{=}NAr)(PPh_3)_2]$$

No example is known of protonation at the second nitrogen atom or at both sites. Protonation of co-ordinated aryldiazonium ions therefore yields complexes containing co-ordinated aryldiazenes (NH=NAr) such as phenyldiazene, molecules that are quite unstable in the uncomplexed state. In contrast, protonation of the singly bent aryldiazenato ligand has been shown to occur at the second nitrogen atom. For example, protonation of $[ReCl_2(N_2Ph)(PMe_2Ph)_2(NH_3)]$ affords $[ReCl_2\{NN(H)Ph\}(PMe_2Ph)_2(NH_3)]^+$ where the observed dimensions of the X-ray crystal structure indicate the presence of a Re···N···N(H)Ph group.

Complexes containing aryldiazene ligands have also been shown to be formed through the insertion of ArN_2^+ into a metal-hydride bond. [198] For example, reaction of the platinum species $[PtHCl(PEt_3)_2]$ with aryldiazonium salts ArN_2^+ affords the aryldiazene species $[PtCl\{N(H){=}NAr\}(PEt_3)_2]^+$.

It has been established in these laboratories that reaction of the

diruthenium species $[Ru_2(\mu\text{-}CO)(CO)_4\{\mu\text{-}(RO)_2PN(Et)P(OR)_2\}_2]$ (R = Me or Pr^i) with NO^+ affords the nitrosyl-bridged derivatives $[Ru_2(\mu\text{-}NO)(CO)_4\text{-}\{\mu\text{-}(RO)_2PN(Et)P(OR)_2\}_2]^+$. The reactions of the parent diruthenium species with the phenyldiazonium salt $[PhN_2][PF_6]$ were investigated in order to draw comparisons between the reactivity of PhN_2^+ and NO^+ towards the diruthenium complexes.

4.2 REACTIONS OF $[Ru_2(\mu\text{-}CO)(CO)_4\{\mu\text{-}(RO)_2PN(Et)P(OR)_2\}_2]$ WITH QUINONES

As described above, as part of a programme aimed at extending the studies of the reactions of the electron-rich dinuclear compounds $[Ru_2(\mu\text{-}CO)(CO)_4\{\mu\text{-}(RO)_2PN(Et)P(OR)_2\}_2]$ (R = Me or Pr^i) with electron-acceptor ligands, their behaviour towards tetrachloro-*p*-benzoquinone has been investigated in detail. Treatment of a toluene solution of these complexes with a twice molar amount of this quinone was found to result in the immediate separation of a brown oil from solution. Washing this oil with toluene and ether and subsequent drying under reduced pressure led to it solidifying as a yellowish-brown microcrystalline material. The band pattern and the frequencies of the C-O stretching peaks in the infrared spectra of the products isolated were consistent with the compound being a monocationic pentacarbonyl species of the type $[Ru_2(CO)_5A\{\mu\text{-}(RO)_2PN(Et)P(OR)_2\}_2]^+$. The $^{31}P\{^1H\}$ nmr spectra of these products exhibited AA'BB' patterns of peaks of chemical shift identical to those of the AA'BB' patterns of peaks for the chloro species $[Ru_2(CO)_5Cl\{\mu\text{-}(RO)_2PN(Et)P(OR)_2\}_2]PF_6$ (R = Me or Pr^i). Furthermore, the UV-visible spectra of the products were found to contain two bands at 445 and 480 nm, readily assigned to the presence of free *p*-chloranil in its radical anion form,[199] while the infrared spectra contain a peak at 1520 cm^{-1} which is also attributed to the presence of a *p*-chloranil radical anion on the basis that the infrared spectrum of

K^+(*p*-chloranil)$^{\cdot-}$ contains a band at 1524 cm^{-1}. [200]

It is thus proposed that the brown product isolated is the chloro species $[Ru_2(CO)_5Cl\{\mu\text{-}(RO)_2PN(Et)P(OR)_2\}_2]^+$(*p*-chloranil)$^{\cdot-}$ {R = Pr^i; (**46**); R = Me (**47**)}, formed as a result of the direct chlorination of $[Ru_2(\mu\text{-}CO)(CO)_4\{\mu\text{-}(RO)_2PN(Et)P(OR)_2\}_2]$ by the quinone and with the cationic species thus produced separating from solution as the salt of the *p*-chloranil radical anion.

As established for the corresponding hexafluorophosphate salts, $[Ru_2(CO)_5Cl\{\mu\text{-}(Pr^iO)_2PN(Et)P(OPr^i)_2\}_2]^+$(*p*-chloranil)$^{\cdot-}$ and $[Ru_2(CO)_5Cl\text{-}\{\mu\text{-}(MeO)_2PN(Et)P(OMe)_2\}_2]^+$(*p*-chloranil)$^{\cdot-}$ were found to slowly decarbonylate in solution to afford products characterized as the tetracarbonyl derivatives $[Ru_2(\mu\text{-}Cl)(CO)_4\{\mu\text{-}(Pr^iO)_2PN(Et)P(OPr^i)_2\}_2]^+$(*p*-chloranil)$^{\cdot-}$ and $[Ru_2(\mu\text{-}Cl)(CO)_4\{\mu\text{-}(MeO)_2PN(Et)P(OMe)_2\}_2]^+$(*p*-chloranil)$^{\cdot-}$ respectively. The tetraisopropoxydiphosphazane-bridged species was best obtained by direct reaction of the co-ordinatively unsaturated species $[Ru_2(CO)_4\{\mu\text{-}(Pr^iO)_2PN(Et)P(OPr^i)_2\}_2]$ with *p*-chloranil in toluene with the product of this reaction which separated from solution being identified as $[Ru_2(\mu\text{-}Cl)(CO)_4\{\mu\text{-}(Pr^iO)_2PN(Et)P(OPr^i)_2\}_2]^+$(*p*-chloranil)$^{\cdot-}$.

The behaviour of *p*-chloranil towards $[Ru_2(\mu\text{-}CO)(CO)_4\{\mu\text{-}(RO)_2PN(Et)P\text{-}(OR)_2\}_2]$ is in contrast to that of *o*-chloranil which affords, as described earlier in the text, the unusual rearrangement product $[Ru_2\{\mu\text{-}(RO)_2PN(Et)C(O)\}\{P(OR)_2OC_6Cl_4O\}(CO)_4\{\mu\text{-}(RO)_2PN(Et)P(OR)_2\}]$ (R = Me or Pr^i) on reaction with the ruthenium dimer.

Interestingly, irradiation of $[Ru_2(CO)_5Cl\{\mu\text{-}(Pr^iO)_2PN(Et)P(OPr^i)_2\}_2]^+$(*p*-chloranil)$^{\cdot-}$ was found to result in the formation of a neutral compound characterized as the dichloro species $[Ru_2(\mu\text{-}Cl)Cl(CO)_3\{\mu\text{-}$

$(Pr^iO)_2PN(Et)P(OPr^i)_2\}_2]$ (**50**). The analogous tetramethoxydiphosphazane-bridged species $[Ru_2(\mu\text{-}Cl)Cl(CO)_3\{\mu\text{-}(MeO)_2PN(Et)P(OMe)_2\}_2]$ has been synthesized previously by the addition of chloride ions to $[Ru_2(\mu\text{-}Cl)(CO)_4\{\mu\text{-}(MeO)_2PN(Et)P(OMe)_2\}_2]PF_6$ in the presence of trimethylamine-N-oxide dihydrate.[131]

The infrared spectrum of $[Ru_2(\mu\text{-}Cl)Cl(CO)_3\{\mu\text{-}(Pr^iO)_2PN(Et)P(OPr^i)_2\}_2]$ (**50**) in the C-O stretching region is similar to that of the analogous tetramethoxydiphosphazane derivative while the $^{31}P\{^1H\}$ nmr spectrum measured in CD_2Cl_2 exhibits an AA'BB' pattern of peaks at 145.57 ppm.

4.3 REACTION OF $[Ru_2(\mu\text{-}CO)(CO)_4\{\mu\text{-}(RO)_2PN(Et)P(OR)_2\}_2]$ WITH $[PhN_2][PF_6]$

With the object of exploring further the redox and co-ordination chemistry of PhN_2^+ towards the diruthenium species $[Ru_2(\mu\text{-}CO)(CO)_4\{\mu\text{-}(RO)_2PN(Et)P(OR)_2\}_2]$, the tetraisopropoxydiphosphazane-bridged derivative was treated with a twice molar amount of $[PhN_2][PF_6]$ in methanol. Reaction was found to proceed rapidly at room temperature affording yellow crystals of a compound characterized as the phenyldiazene species $[Ru_2(CO)_5(NH{=}NPh)\{\mu\text{-}(Pr^iO)_2PN(Et)P(OPr^i)_2\}_2](PF_6)_2$ (**51**). The infrared spectrum of this compound, in the C-O stretching region, is similar to those of related dicationic pentacarbonyl species described in Chapter 2. The $^{31}P\{^1H\}$ nmr spectrum, measured in CD_2Cl_2, exhibits an AA'BB' pattern of peaks at 124.01 ppm, indicating the phosphorus atoms to be non-equivalent. The ^1H nmr spectrum exhibits resonances corresponding to the protons of the diphosphazane ligands as well as a broad singlet at 7.65 ppm, the integral of which corresponds to five protons and a broad singlet at 10.89 ppm, the integral of which corresponds to one proton. These two singlets are therefore assigned to the phenyl protons and diazene proton of the phenyldiazene ligand N(H)=NPh respectively.

These results are interpreted in terms of the addition of PhN_2^+ to $[Ru_2(\mu\text{-}CO)(CO)_4\{\mu\text{-}(Pr^iO)_2PN(Et)P(OPr^i)_2\}_2]$ in methanol resulting in the formation of a phenyldiazenato species $[Ru_2(CO)_5(N_2Ph)\{\mu\text{-}(Pr^iO)_2PN(Et)P(OPr^i)_2\}_2]^+$ followed by protonation of the diazenato ligand by methanol, affording the phenyldiazene species $[Ru_2(CO)_5\{N(H)=NPh\}\{\mu\text{-}(Pr^iO)_2PN(Et)P(OPr^i)_2\}_2]^{2+}$. This is consistent with the reaction pathway previously suggested for the reaction of $[RhCl(N_2Ph)(PPP)]^+$ with methanol; the product of this reaction *viz.* the hydrido complex $[RhCl(H)(PPP)]^+$ was proposed to be formed via the diazene species $[RhCl(NH=NPh)(PPP)]^{2+}$ as intermediate. Significantly, no reaction was observed to occur on addition of PhN_2^+ to the hydrido species $[Ru_2H(CO)_5\{\mu\text{-}(Pr^iO)_2PN(Et)P(OPr^i)_2\}_2]^+$ indicating that this complex is not an intermediate in the formation of the phenyldiazene species $[Ru_2(CO)_5(NH=NPh)\{\mu\text{-}(Pr^iO)_2PN(Et)P(OPr^i)_2\}_2]^{2+}$. The presence of a co-ordinated phenyldiazene ligand was established from a single crystal X-ray structure determination on $[Ru_2(CO)_5(NH=NPh)\{\mu\text{-}(Pr^iO)_2PN(Et)P(OPr^i)_2\}_2](PF_6)_2$; the stereochemistry of the dication is shown in Figure 4.3.

The two ruthenium atoms which are bridged by the tetraisopropoxydiphosphazane ligands, mutually *trans* with respect to each other, are separated by a distance of 2.908(1)Å, corresponding to a formal Ru-Ru bond. The stereochemistry about each ruthenium is essentially octahedral with one ruthenium atom containing three terminal carbonyl groups and the other two terminal carbonyl ligands and a phenyldiazene ligand; the latter occupies an equatorial position, similar to that for the benzonitrile in the related benzonitrile species $[Ru_2(CO)_5(NCPh)\{\mu\text{-}(Pr^iO)_2PN(Et)P(OPr^i)_2\}_2]^{2+}$ (see Chapter 2). The Ru(1)-N(3) distance of 2.103(7)Å is almost identical to that of the Ru-N distance for the benzonitrile species. The N(3)-N(4) separation of 1.222(11)Å is representative of a bond order of 2 and is comparable to the corresponding

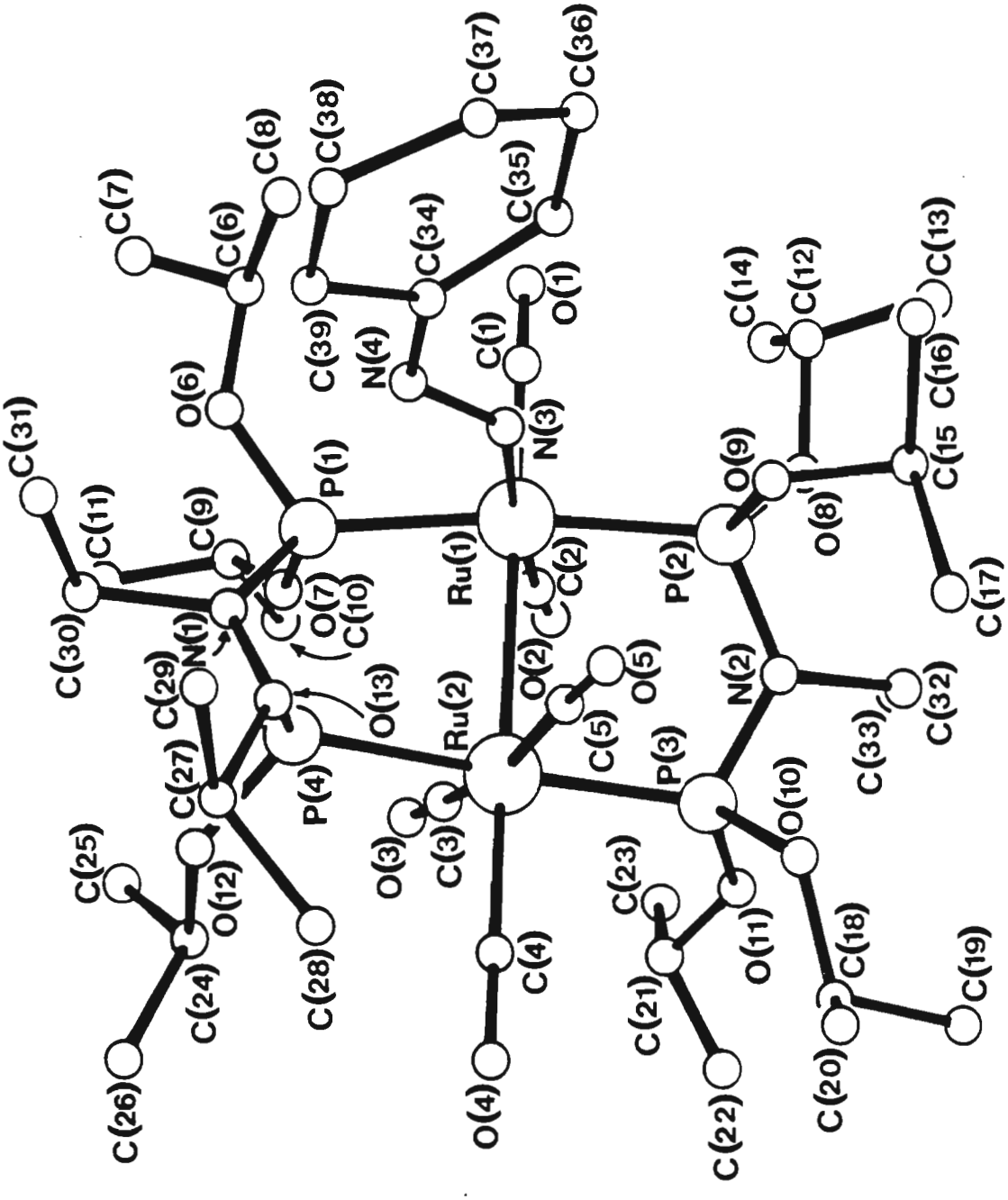

Figure 4.3: Structure of $[Ru_2(CO)_5\{N(H)=NPh\}\{\mu\text{-}(Pr^iO)_2PN(Et)P(OPr^i)_2\}_2]^{2+}$

separation for the platinum diazene species $[PtCl(NH{=}NC_6H_4F)(PEt_3)_2][ClO_4]$[201] {N-N 1.235(10)Å}. The Ru(1)-N(3)-N(4) angle of 130.9(6)° is slightly greater than the corresponding angle for the platinum diazene species (Pt-N-N 123.6°). The position of the proton of the diazene ligand was not located but its co-ordination to the nitrogen adjacent to the ruthenium atom may be inferred from the angles associated with the diazene group. This is in contrast to that observed for the rhenium species $[ReCl_2\{N{=}N(H)Ph\}(PMe_2Ph)_2(NH_3)]Br$ described above. A crystal structure determination of this compound established that protonation of the phenyldiazenato species $[ReCl_2(N_2Ph)(PMe_2Ph)(NH_3)]$ occurs at the second nitrogen atom, as reflected by a Re-N-N angle of 172(1)°.

Significantly, it was found that treatment of $[Ru_2(\mu\text{-}CO)(CO)_4\{\mu\text{-}(RO)_2PN(Et)P(OR)_2\}_2]$ with a twice molar amount of $[PhN_2][PF_6]$ in acetone was found not to afford the diazene species but the acetone solvento species $[Ru_2(CO)_5(acetone)\{\mu\text{-}(Pr^iO)_2PN(Et)P(OPr^i)_2\}_2](PF_6)_2$, identified spectroscopically (see Chapter 2); the phenyldiazonium salt is obviously functioning as a one-electron oxidant in this reaction. The aquo solvento species $[Ru_2(CO)_5(H_2O)\{\mu\text{-}(Pr^iO)_2PN(Et)P(OPr^i)_2\}_2](PF_6)_2$ was also formed in this reaction as a consequence of there being trace amounts of water present in the acetone solution.

4.4 EXPERIMENTAL

4.4.1 *Synthesis of* $[Ru_2Cl(CO)_5\{\mu\text{-}(RO)_2PN(Et)P(OR)_2\}_2]^+(p\text{-}chloranil)^{\cdot-}$ *(R = Me (**48**), Pr^i (**46**))*

A twice molar amount of 1,4-tetrachlorobenzoquinone (0.150 g, 0.610 mmol) was added to a solution of $[Ru_2(\mu\text{-}CO)(CO)_4\{\mu\text{-}(RO)_2PN(Et)P(OR)_2\}_2]$ (R = Me: 0.244 g, 0.305 mmol; R = Pr^i: 0.313 g, 0.305 mmol) in toluene

(5 ml) resulting in the immediate separation of a brown oil from the solution. The supernatant solution was decanted off and the oil which remained washed with toluene (3 x 3 ml) and ether (3 x 3 ml) and dried under reduced pressure to afford a brown microcrystalline material. This was spectroscopically identified as $[Ru_2Cl(CO)_5\{\mu\text{-}(RO)_2PN(Et)P(OR)_2\}_2]^+$(*p*-chloranil)$^{\bullet-}$. Yield; 55%. *M*(**48**) = 1083.1 g/mol; *M*(**46**) = 1306.6 g/mol.

4.4.2 *Synthesis of* $[Ru_2(\mu\text{-}Cl)(CO)_4\{\mu\text{-}(RO)_2PN(Et)P(OR)_2\}_2]^+$(*p*-chloranil)$^{\bullet-}$ (*R* = *Me* (**49**), Pr^i (**47**))

i) A twice molar amount of tetrachloro-*p*-benzoquinone (0.150 g, 0.610 mmol) was added to a solution of $[Ru_2(CO)_4\{\mu\text{-}(Pr^iO)_2PN(Et)P(OPr^i)_2\}_2]$ (0.310 g, 0.305 mmol) in toluene (5 ml) resulting in the immediate separation of a brown oil from the solution. The supernatant solution was decanted off and the oil which remained washed with toluene (3 x 3 ml) and ether (3 x 3 ml) and dried under reduced pressure to afford a brown microcrystalline material. This was spectroscopically identified as $[Ru_2(\mu\text{-}Cl)(CO)_4\{\mu\text{-}(Pr^iO)_2PN(Et)P(OPr^i)_2\}_2]^+$(*p*-chloranil)$^{\bullet-}$. Yield; 50%. *M*(**47**) = 1278.6 g/mol.

ii) Dissolution of $[Ru_2Cl(CO)_5\{\mu\text{-}(RO)_2PN(Et)P(OR)_2\}_2]^+$(*p*-chloranil)$^{\bullet-}$ in acetone was found to result in the formation of $[Ru_2(\mu\text{-}Cl)(CO)_4\{\mu\text{-}(RO)_2PN(Et)P(OR)_2\}_2]^+$(*p*-chloranil)$^{\bullet-}$, as established by monitoring this solution using $^{31}P\{^1H\}$ nmr and infrared spectroscopy.

4.4.3 *Synthesis of* $[Ru_2(\mu\text{-}Cl)Cl(CO)_3\{\mu\text{-}(Pr^iO)_2PN(Et)P(OPr^i)_2\}_2]$ (**50**)

A mixture of $[Ru_2Cl(CO)_5\{\mu\text{-}(Pr^iO)_2PN(Et)P(OPr^i)_2\}_2]^+$(*p*-chloranil)$^{\bullet}$ and $[Ru_2(\mu\text{-}Cl)(CO)_4\{\mu\text{-}(Pr^iO)_2PN(Et)P(OPr^i)_2\}_2]^+$(*p*-chloranil)$^{\bullet-}$ (0.200 g) in acetone was irradiated with ultraviolet light for 10 minutes. The sol-

vent was removed under reduced pressure and the title compound extracted into hexane (3 x 5 ml). Crystallization was effected by cooling this extract to -20°C. Yield: 35%. *M*(**50**) = 1040.00 g/mol.

4.4.4 *Synthesis of* $[Ru_2(CO)_5\{N(H)=NPh\}\{\mu\text{-}(Pr^iO)_2PN(Et)P(OPr^i)_2\}_2](PF_6)_2$ (**51**)

A twice molar amount of $[PhN_2][PF_6]$ (0.150 g, 0.600 mmol) was added to a solution of $[Ru_2(\mu\text{-}CO)(CO)_4\{\mu\text{-}(Pr^iO)_2PN(Et)P(OPr^i)_2\}_2]$ (0.300 g, 0.293 mmol) in methanol (10 ml) and the mixture stirred for 1h. Crystallization of the title compound was effected by cooling this solution to -20°C and allowing it to stand for 15h. Yield: 65%. *M*(**51**) = 1421.1 g/mol.

4.4.5 *Crystal Structure Determination of* $[Ru_2(CO)_5\{N(H)=NPh\}\{\mu\text{-}(Pr^iO)_2PN(Et)P(OPr^i)_2\}_2](PF_6)_2$ (**51**)

The method for the intensity data collection is described in Appendix A.3(a) while the general approach to the structure solution is given in Appendix A.3(b). The crystallographic data for (**51**) is summarized in Table 4.4, the fractional co-ordinates and isotropic thermal parameters are given in Table 4.5, the anisotropic thermal parameters in Table 4.6 and the interatomic distances in Table 4.7 and the interatomic angles in Table 4.8. The observed and calculated structure factors may be found on microfiche in an envelope fixed to the inside cover of this thesis.

TABLE 4.1

MICROANALYTICAL DATA

COMPLEX	ANALYSIS : Found (Calculated) % %C	%H	%N
50 $[Ru_2(\mu\text{-}Cl)Cl(CO)_3\{\mu\text{-}(Pr^iO)_2PN(Et)P(OPr^i)_2\}_2]$	36.82(35.79)	6.51(6.41)	2.74(2.69)
51 $[Ru_2(CO)_5\{N(H)=NPh\}\{\mu\text{-}(Pr^iO)_2PN(Et)P(OPr^i)_2\}_2](PF_6)_2$	32.96(34.48)	5.12(5.42)	3.94(4.13)

TABLE 4.2

INFRARED SPECTROSCOPIC DATA

COMPLEX	ν(C≡O), cm^{-1}	OTHER	MEDIUM	COLOUR
50	2001(s) 1985(s) 1933(vs) 1903(ms)		Hexane	Yellow
	1994(s) 1974(s) 1924(vs) 1898(ms)		Nujol	
51	2095(w) 2060(sh) 2038(s) 2018(s) 1990(m)		CH_2Cl_2	Yellow
	2095(w) 2060(s) 2041(sh) 2030(vs) 2023(s) 2005(s)		Nujol	

TABLE 4.3

^1H AND $^{31}P\{^1H\}$ NMR SPECTROSCOPIC DATA

COMPLEX	δ ^1H (ppm)	δ $^{31}P\{^1H\}$ (ppm)
50	1.10-1.55m (54H); 3.22-3.65m (4H); 4.59-4.88m (8H)	145.57 (AA'BB')[b]
51	1.18-1.58m (54H); 3.34-3.50m (4H); 4.68-4.84m (8H); 7.65s,br (5H); 10.89s,br, (1H)	124.01 (AA'BB')[a]

[a]Recorded in CD_2Cl_2. [b]Recorded in

TABLE 4.4

CRYSTAL DATA FOR

$[Ru_2(CO)_5\{N(H)NPh\}\{\mu\text{-}(Pr^iO)_2PN(Et)P(OPr^i)_2\}_2](PF_6)_2$ (**51**)

Formula	$C_{39}H_{72}F_{12}N_4O_{13}P_6Ru_2$
Molecular mass	1421.1
Crystal dimensions, mm	0.69 x 0.23 x 0.12
Crystal system	monoclinic
Space group	$P2_1/c$
a(Å)	13.679(3)
b(Å)	23.749(3)
c(Å)	19.496(3)
β(°)	98.48(2)
V(Å^3)	6264.2
Z	4
D_c (g cm^{-3})	1.51
F(000)	2912
λ(Mo-K_α) (Å)	0.71069
μ(Mo-K_α) (cm^{-1})	7.20
Reflections measured	9236
Unique reflections	7635
Observed reflections [$I > 3\sigma(I)$]	6078
Crystal stability	Decay = 24%
Absorption corrections	Applied
No. of parameters	686
R	0.065
R_w	0.073

TABLE 4.5: Fractional co-ordinates ($x10^4$) and equivalent isotropic temperature factors ($Å^2$, $x10^3$) for $[Ru_2(CO)_5\{N(H)=NPh\}\{\mu-(Pr^iO)_2PN(Et)P(OPr^i)_2\}_2](PF_6)_2$ (51)

	x/a	y/b	z/c	U_{eq}
Ru(1)	1722(1)	965(1)	1787(1)	38(1)
Ru(2)	3392(1)	753(1)	2863(1)	39(1)
P(1)	1321(2)	6(1)	1913(1)	43(1)
P(2)	2301(2)	1894(1)	1785(1)	42(1)
P(3)	4207(2)	1554(1)	2519(1)	45(1)
P(4)	2477(2)	26(1)	3289(1)	43(1)
O(1)	108(6)	1141(3)	572(4)	82(2)
O(2)	3043(6)	728(3)	705(4)	79(2)
O(3)	4147(5)	-73(3)	1837(4)	72(2)
O(4)	5126(5)	555(3)	4008(4)	75(2)
O(5)	2320(5)	1546(3)	3731(4)	67(2)
O(6)	224(5)	-221(3)	1749(4)	76(2)
O(7)	1941(5)	-378(3)	1466(4)	66(2)
O(8)	2162(4)	2259(3)	1098(3)	57(2)
O(9)	1777(4)	2225(2)	2336(3)	55(2)
O(10)	4468(4)	1980(3)	3133(4)	63(2)
O(11)	5220(4)	1512(3)	2231(4)	77(2)
O(12)	3053(4)	-485(3)	3647(3)	60(2)
O(13)	1919(5)	221(3)	3907(3)	61(2)
N(1)	1566(5)	-243(3)	2714(4)	48(2)
N(2)	3530(5)	1975(3)	1948(4)	47(2)
N(3)	812(5)	1211(3)	2514(4)	45(2)
N(4)	239(6)	940(4)	2809(4)	63(2)
C(1)	676(6)	1081(4)	1046(5)	48(2)
C(2)	2585(7)	801(4)	1136(5)	52(2)
C(3)	3874(7)	237(4)	2213(5)	55(2)
C(4)	4495(7)	627(4)	3586(5)	54(2)
C(5)	2689(7)	1257(4)	3398(5)	50(2)
C(6)	-618(7)	-57(5)	1223(7)	81(3)
C(7)	-1136(9)	-602(5)	1001(7)	91(4)
C(8)	-1246(8)	351(6)	1502(8)	106(4)
C(9)	1685(10)	-768(4)	940(7)	87(4)
C(10)	2537(14)	-780(7)	502(8)	131(6)
C(11)	1511(14)	-1371(6)	1235(8)	127(5)

TABLE 4.5 (continued)

C(12)	1209(7)	2409(4)	660(6)	66(3)
C(13)	1160(10)	3054(5)	663(7)	97(4)
C(14)	1307(11)	2165(6)	-42(6)	102(4)
C(15)	1863(7)	2833(3)	2528(5)	56(2)
C(16)	819(9)	3005(5)	2626(8)	95(4)
C(17)	2596(9)	2893(5)	3223(6)	74(3)
C(18)	5363(8)	2025(5)	3662(6)	81(3)
C(19)	6011(11)	2507(6)	3402(8)	118(5)
C(20)	5056(10)	2113(6)	4335(7)	100(4)
C(21)	5832(7)	1034(5)	2126(8)	79(3)
C(22)	6844(8)	1198(6)	2453(9)	105(4)
C(23)	5801(11)	934(8)	1354(9)	118(5)
C(24)	3932(7)	-782(4)	3459(6)	68(3)
C(25)	3605(11)	-1232(5)	2918(8)	100(4)
C(26)	4455(10)	-1027(6)	4124(8)	104(4)
C(27)	2202(9)	126(6)	4651(6)	84(3)
C(28)	3119(12)	409(11)	4938(8)	169(8)
C(29)	1318(12)	349(9)	4939(8)	142(7)
C(30)	1065(8)	-784(4)	2948(7)	72(3)
C(31)	191(10)	-619(6)	3336(7)	95(4)
C(32)	4008(7)	2499(4)	1715(5)	63(3)
C(33)	4416(9)	2404(5)	1009(7)	87(4)
C(34)	-346(7)	1233(5)	3249(6)	70(3)
C(35)	-626(10)	1789(5)	3097(9)	116(5)
C(36)	-1229(12)	2062(7)	3518(12)	121(6)
C(37)	-1385(17)	1812(13)	4093(12)	156(8)
C(38)	-1267(16)	1244(16)	4179(12)	226(12)
C(39)	-706(17)	936(10)	3745(11)	194(8)
P(5)	3169(2)	4383(1)	2150(2)	76(1)
P(6)	8143(3)	2410(2)	987(2)	100(1)
F(1)	3909(7)	3919(5)	2480(7)	166(4)
F(2)	2422(7)	4846(4)	1810(6)	155(4)
F(3)	3292(9)	4755(5)	2803(5)	168(4)
F(4)	2993(12)	4014(4)	1494(7)	202(5)
F(5)	2320(7)	4069(4)	2456(7)	158(4)
F(6)	4009(7)	4711(4)	1890(6)	158(4)
F(7)	8676(9)	2267(5)	335(5)	171(4)

TABLE 4.5 (continued)

F(8)	7827(11)	1808(5)	935(8)	215(5)
F(9)	7675(16)	2483(7)	1634(8)	287(8)
F(10)	8728(12)	2962(6)	1055(9)	249(7)
F(11)	7376(11)	2756(9)	587(8)	294(8)
F(12)	9107(11)	2084(6)	1436(6)	204(5)

$$\underline{U}_{eq} = \frac{1}{3} \Sigma_i \Sigma_j \underline{U}_{ij} \underline{a}_i^* \underline{a}_j^* (a_i \cdot a_j)$$

TABLE 4.6: Anistropic temperature factors ($Å^2$, $x10^3$) for

$[Ru_2(CO)_5\{N(H)=NPh\}\{\mu\text{-}(Pr^iO)_2PN(Et)P(OPr^i)_2\}_2](PF_6)_2$ (51)

	U(11)	U(22)	U(33)	U(23)	U(13)	U(12)
Ru(1)	32(1)	36(1)	44(1)	-1(1)	2(1)	1(1)
Ru(2)	29(1)	35(1)	50(1)	4(1)	1(1)	-2(1)
P(1)	34(1)	37(1)	58(1)	-6(1)	2(1)	-2(1)
P(2)	41(1)	36(1)	47(1)	3(1)	6(1)	1(1)
P(3)	33(1)	42(1)	62(2)	6(1)	7(1)	-5(1)
P(4)	37(1)	38(1)	54(1)	3(1)	4(1)	-5(1)
O(1)	75(5)	82(5)	80(6)	17(4)	-21(4)	-9(4)
O(2)	77(5)	96(6)	69(5)	-1(4)	27(4)	7(4)
O(3)	69(5)	73(5)	74(5)	-17(4)	14(4)	1(4)
O(4)	56(4)	86(5)	74(5)	4(4)	-19(4)	9(4)
O(5)	66(4)	62(4)	74(5)	-8(4)	15(4)	11(4)
O(6)	46(4)	60(4)	115(6)	-11(4)	-11(4)	-16(3)
O(7)	52(4)	66(4)	82(5)	-28(4)	10(4)	-9(3)
O(8)	55(4)	57(4)	58(4)	19(3)	2(3)	3(3)
O(9)	60(4)	37(3)	75(4)	-1(3)	30(3)	-3(3)
O(10)	45(4)	57(4)	80(5)	-5(3)	-11(3)	-12(3)
O(11)	43(4)	63(4)	127(7)	15(4)	25(4)	7(3)
O(12)	52(4)	51(4)	74(5)	8(3)	6(3)	3(3)
O(13)	60(4)	65(4)	59(4)	4(3)	14(3)	-9(3)
N(1)	44(4)	42(4)	58(5)	4(3)	7(3)	-9(3)
N(2)	38(4)	40(4)	61(5)	4(3)	5(3)	-3(3)
N(3)	35(4)	53(4)	50(4)	1(4)	16(3)	-3(3)
N(4)	47(5)	78(6)	70(6)	1(5)	24(4)	4(4)
C(1)	43(5)	44(5)	52(6)	3(4)	-9(4)	1(4)
C(2)	47(5)	54(6)	53(6)	-2(5)	3(5)	7(4)
C(3)	40(5)	70(7)	53(6)	4(5)	3(4)	-11(5)
C(4)	48(6)	45(5)	67(7)	-1(5)	2(5)	6(4)
C(5)	47(5)	44(5)	58(6)	7(5)	6(5)	-7(4)
C(6)	39(6)	71(7)	126(11)	-13(7)	-11(6)	-5(5)
C(7)	75(8)	72(8)	111(10)	-18(7)	-29(7)	-20(6)
C(8)	43(6)	125(11)	143(13)	-32(10)	-4(7)	21(7)
C(9)	97(9)	49(6)	113(10)	-36(7)	16(8)	-7(6)
C(10)	168(16)	141(14)	96(11)	-54(10)	61(11)	-13(12)
C(11)	201(17)	66(9)	122(13)	-27(8)	49(12)	-15(10)
C(12)	59(6)	48(6)	86(8)	20(5)	-11(5)	

TABLE 4.6 (continued)

C(13)	111(10)	76(8)	91(9)	20(7)	-29(8)	25(7)
C(14)	130(12)	128(12)	42(7)	8(7)	-7(7)	-24(9)
C(15)	69(6)	34(5)	61(6)	-4(4)	-5(5)	5(4)
C(16)	85(8)	55(7)	145(12)	-16(7)	21(8)	7(6)
C(17)	95(8)	65(7)	60(7)	0(5)	7(6)	4(6)
C(18)	69(7)	88(8)	76(8)	2(6)	-26(6)	-27(6)
C(19)	109(11)	101(10)	131(13)	-2(9)	-19(9)	-54(9)
C(20)	102(10)	128(12)	65(8)	-10(8)	-6(7)	-4(8)
C(21)	36(5)	83(8)	120(10)	-11(7)	15(6)	9(5)
C(22)	41(6)	96(10)	174(14)	-21(10)	7(7)	2(6)
C(23)	78(9)	165(16)	115(13)	-11(11)	24(9)	4(9)
C(24)	49(6)	57(6)	94(8)	13(6)	0(5)	18(5)
C(25)	108(10)	66(8)	123(11)	-17(8)	8(9)	10(7)
C(26)	103(10)	97(9)	105(11)	45(8)	-14(8)	40(8)
C(27)	66(7)	127(11)	59(7)	-7(7)	9(6)	1(7)
C(28)	84(11)	334(32)	81(11)	21(14)	-13(9)	-36(15)
C(29)	109(12)	229(22)	97(12)	-13(12)	45(10)	27(13)
C(30)	62(6)	40(5)	112(9)	9(6)	9(6)	-23(5)
C(31)	89(9)	102(10)	97(10)	-11(8)	26(7)	-56(8)
C(32)	64(6)	52(6)	71(7)	13(5)	4(5)	-22(5)
C(33)	91(9)	84(8)	89(9)	21(7)	28(7)	-12(7)
C(34)	31(5)	87(8)	93(8)	-5(7)	11(5)	6(5)
C(35)	98(10)	67(8)	203(17)	-41(10)	88(11)	-12(7)
C(36)	93(11)	104(12)	170(18)	-33(12)	38(12)	-6(9)
C(37)	133(18)	223(26)	105(15)	-69(17)	-1(14)	51(18)
C(38)	160(19)	400(44)	145(18)	120(25)	114(16)	106(26)
C(39)	215(21)	228(22)	176(18)	143(17)	152(18)	148(18)
P(5)	60(2)	63(2)	104(2)	2(2)	9(2)	-10(700)
P(6)	102(3)	98(3)	105(3)	9(2)	33(2)	-2(1)
F(1)	117(7)	152(9)	233(12)	50(8)	36(8)	42(6)
F(2)	114(7)	108(7)	234(12)	54(7)	-5(7)	14(5)
F(3)	209(12)	149(9)	146(9)	-36(7)	29(8)	-40(8)
F(4)	317(17)	110(8)	160(10)	-39(7)	-32(11)	4(9)
F(5)	108(7)	116(7)	259(13)	51(7)	61(8)	-20(5)
F(6)	113(7)	144(8)	234(12)	24(8)	86(8)	-20(6)
F(7)	215(12)	192(11)	114(8)	30(7)	57(8)	59(9)
F(8)	228(14)	157(11)	265(15)	-16(11)	58(13)	-79(10)

TABLE 4.6 (continued)

F(9)	440(26)	254(17)	217(15)	79(13)	213(18)	168(17)
F(10)	268(17)	155(11)	318(19)	-67(12)	26(15)	-100(11)
F(11)	171(12)	485(30)	214(15)	43(16)	-8(11)	198(16)
F(12)	238(14)	242(15)	137(9)	38(9)	47(9)	67(12)

TABLE 4.7: Interatomic distances (Å) for

$[Ru_2(CO)_5\{N(H)=NPh\}\{\mu\text{-}(Pr^iO)_2PN(Et)P(OPr^i)_2\}_2](PF_6)_2$ (51)

Ru(1)-Ru(2)	2.908(1)	Ru(1)-P(1)	2.363(2)
Ru(1)-P(2)	2.344(2)	Ru(1)-N(3)	2.103(7)
Ru(1)-C(1)	1.897(8)	Ru(1)-C(2)	1.898(10)
Ru(2)-P(3)	2.353(2)	Ru(2)-P(4)	2.355(2)
Ru(2)-C(3)	1.946(11)	Ru(2)-C(4)	1.930(9)
Ru(2)-C(5)	1.933(10)	P(1)-O(6)	1.582(7)
P(1)-O(7)	1.591(8)	P(1)-N(1)	1.657(8)
P(2)-O(8)	1.584(7)	P(2)-O(9)	1.585(7)
P(2)-N(2)	1.674(7)	P(3)-O(10)	1.567(7)
P(3)-O(11)	1.572(7)	P(3)-N(2)	1.670(7)
P(4)-O(12)	1.555(6)	P(4)-O(13)	1.587(7)
P(4)-N(1)	1.674(7)	P(5)-F(1)	1.569(11)
P(5)-F(2)	1.579(10)	P(5)-F(3)	1.538(11)
P(5)-F(4)	1.540(12)	P(5)-F(5)	1.569(11)
P(5)-F(6)	1.536(11)	P(6)-F(7)	1.591(12)
P(6)-F(8)	1.492(14)	P(6)-F(9)	1.51(2)
P(6)-F(10)	1.533(15)	P(6)-F(11)	1.46(2)
P(6)-F(12)	1.662(14)	O(1)-C(1)	1.125(11)
O(2)-C(2)	1.133(14)	O(3)-C(3)	1.141(13)
O(4)-C(4)	1.114(12)	O(5)-C(5)	1.116(12)
O(6)-C(6)	1.476(13)	O(7)-C(9)	1.389(14)
O(8)-C(12)	1.491(11)	O(9)-C(15)	1.492(10)
O(10)-C(18)	1.484(12)	O(11)-C(21)	1.442(13)
O(12)-C(24)	1.485(12)	O(13)-C(27)	1.464(13)
N(1)-C(30)	1.556(13)	N(2)-C(32)	1.507(12)
N(3)-N(4)	1.222(11)	N(4)-C(34)	1.437(15)
C(6)-C(7)	1.51(2)	C(6)-C(8)	1.45(2)
C(9)-C(10)	1.54(2)	C(9)-C(11)	1.58(2)
C(12)-C(13)	1.53(2)	C(12)-C(14)	1.51(2)
C(15)-C(16)	1.52(2)	C(15)-C(17)	1.568(14)
C(18)-C(19)	1.58(2)	C(18)-C(20)	1.45(2)
C(21)-C(22)	1.488(15)	C(21)-C(23)	1.52(2)
C(24)-C(25)	1.52(2)	C(24)-C(26)	1.50(2)
C(27)-C(28)	1.46(2)	C(27)-C(29)	1.50(2)
C(30)-C(31)	1.56(2)	C(32)-C(33)	1.58(2)

TABLE 4.7 (continued)

C(34)-C(35)	1.39(2)	C(34)-C(39)	1.35(3)
C(35)-C(36)	1.40(3)	C(36)-C(37)	1.31(4)
C(37)-C(38)	1.37(5)	C(38)-C(39)	1.43(4)

TABLE 4.8: Interatomic angles (°) for

$[Ru_2(CO)_5\{N(H)=NPh\}\{\mu\text{-}(Pr^iO)_2PN(Et)P(OPr^i)_2\}_2](PF_6)_2$ (51)

Ru(2)-Ru(1)-P(1)	85.9(1)	Ru(2)-Ru(1)-P(2)	86.2(1)
P(1)-Ru(1)-P(2)	172.1(1)	Ru(2)-Ru(1)-N(3)	92.4(2)
P(1)-Ru(1)-N(3)	91.6(2)	P(2)-Ru(1)-N(3)	88.5(2)
Ru(2)-Ru(1)-C(1)	176.5(3)	P(1)-Ru(1)-C(1)	93.4(3)
P(2)-Ru(1)-C(1)	94.5(3)	N(3)-Ru(1)-C(1)	91.1(3)
Ru(2)-Ru(1)-C(2)	87.0(3)	P(1)-Ru(1)-C(2)	92.8(3)
P(2)-Ru(1)-C(2)	87.0(3)	N(3)-Ru(1)-C(2)	175.5(3)
C(1)-Ru(1)-C(2)	89.6(4)	Ru(1)-Ru(2)-P(3)	90.5(1)
Ru(1)-Ru(2)-P(4)	88.8(1)	P(3)-Ru(2)-P(4)	173.1(1)
Ru(1)-Ru(2)-C(3)	86.8(3)	P(3)-Ru(2)-C(3)	95.9(3)
P(4)-Ru(2)-C(3)	90.9(3)	Ru(1)-Ru(2)-C(4)	178.9(3)
P(3)-Ru(2)-C(4)	88.9(3)	P(4)-Ru(2)-C(4)	91.6(3)
C(3)-Ru(2)-C(4)	94.2(4)	Ru(1)-Ru(2)-C(5)	83.2(3)
P(3)-Ru(2)-C(5)	87.0(3)	P(4)-Ru(2)-C(5)	86.1(3)
C(3)-Ru(2)-C(5)	169.7(4)	C(4)-Ru(2)-C(5)	95.7(4)
Ru(1)-P(1)-O(6)	122.4(3)	Ru(1)-P(1)-O(7)	110.2(3)
O(6)-P(1)-O(7)	105.1(4)	Ru(1)-P(1)-N(1)	115.1(3)
O(6)-P(1)-N(1)	97.1(4)	O(7)-P(1)-N(1)	105.2(4)
Ru(1)-P(2)-O(8)	121.2(2)	Ru(1)-P(2)-O(9)	106.2(2)
O(8)-P(2)-O(9)	106.9(3)	Ru(1)-P(2)-N(2)	116.0(3)
O(8)-P(2)-N(2)	95.2(4)	O(9)-P(2)-N(2)	110.9(3)
Ru(2)-P(3)-O(10)	111.6(3)	Ru(2)-P(3)-O(11)	122.0(3)
O(10)-P(3)-O(11)	101.6(4)	Ru(2)-P(3)-N(2)	115.7(2)
O(10)-P(3)-N(2)	99.4(3)	O(11)-P(3)-N(2)	103.5(4)
Ru(2)-P(4)-O(12)	118.0(3)	Ru(2)-P(4)-O(13)	113.2(3)
O(12)-P(4)-O(13)	99.0(4)	Ru(2)-P(4)-N(1)	115.2(3)
O(12)-P(4)-N(1)	106.4(3)	O(13)-P(4)-N(1)	103.0(4)
F(1)-P(5)-F(2)	179.3(7)	F(1)-P(5)-F(3)	94.6(6)
F(2)-P(5)-F(3)	86.2(6)	F(1)-P(5)-F(4)	87.3(7)
F(2)-P(5)-F(4)	92.0(6)	F(3)-P(5)-F(4)	177.3(8)
F(1)-P(5)-F(5)	88.8(6)	F(2)-P(5)-F(5)	91.3(5)
F(3)-P(5)-F(5)	87.5(7)	F(4)-P(5)-F(5)	90.6(7)
F(1)-P(5)-F(6)	91.3(6)	F(2)-P(5)-F(6)	88.6(5)
F(3)-P(5)-F(6)	89.2(6)	F(4)-P(5)-F(6)	92.7(7)
F(5)-P(5)-F(6)	176.7(7)	F(7)-P(6)-F(8)	84.5(8)

TABLE 4.8 (continued)

F(7)-P(6)-F(9)	173.8(8)	F(8)-P(6)-F(9)	90.8(9)
F(7)-P(6)-F(10)	87.6(9)	F(8)-P(6)-F(10)	165.5(9)
F(9)-P(6)-F(10)	96.2(10)	F(7)-P(6)-F(11)	94.1(8)
F(8)-P(6)-F(11)	109.0(10)	F(9)-P(6)-F(11)	91.1(10)
F(10)-P(6)-F(11)	83.6(10)	F(7)-P(6)-F(12)	84.2(6)
F(8)-P(6)-F(12)	77.9(8)	F(9)-P(6)-F(12)	90.9(9)
F(10)-P(6)-F(12)	89.3(8)	F(11)-P(6)-F(12)	172.8(10)
P(1)-O(6)-C(6)	132.1(7)	P(1)-O(7)-C(9)	133.8(7)
P(2)-O(8)-C(12)	126.9(6)	P(2)-O(9)-C(15)	128.5(6)
P(3)-O(10)-C(18)	130.4(6)	P(3)-O(11)-C(21)	131.4(7)
P(4)-O(12)-C(24)	129.4(7)	P(4)-O(13)-C(27)	128.4(7)
P(1)-N(1)-P(4)	121.5(4)	P(1)-N(1)-C(30)	122.3(6)
P(4)-N(1)-C(30)	115.8(6)	P(2)-N(2)-P(3)	120.0(4)
P(2)-N(2)-C(32)	120.4(6)	P(3)-N(2)-C(32)	118.1(5)
Ru(1)-N(3)-N(4)	130.9(6)	N(3)-N(4)-C(34)	118.5(9)
Ru(1)-C(1)-O(1)	174.6(9)	Ru(1)-C(2)-O(2)	173.9(8)
Ru(2)-C(3)-O(3)	178.7(9)	Ru(2)-C(4)-O(4)	179.3(10)
Ru(2)-C(5)-O(5)	176.7(8)	O(6)-C(6)-C(7)	105.0(9)
O(6)-C(6)-C(8)	111.1(10)	C(7)-C(6)-C(8)	113.7(10)
O(7)-C(9)-C(10)	107.1(10)	O(7)-C(9)-C(11)	111.8(11)
C(10)-C(9)-C(11)	110.7(12)	O(8)-C(12)-C(13)	105.8(8)
O(8)-C(12)-C(14)	103.9(9)	C(13)-C(12)-C(14)	113.4(10)
O(9)-C(15)-C(16)	104.4(8)	O(9)-C(15)-C(17)	108.7(7)
C(16)-C(15)-C(17)	110.9(9)	O(10)-C(18)-C(19)	105.9(9)
O(10)-C(18)-C(20)	108.7(9)	C(19)-C(18)-C(20)	115.9(11)
O(11)-C(21)-C(22)	104.8(10)	O(11)-C(21)-C(23)	109.4(10)
C(22)-C(21)-C(23)	110.7(12)	O(12)-C(24)-C(25)	109.9(8)
O(12)-C(24)-C(26)	105.7(10)	C(25)-C(24)-C(26)	112.3(10)
O(13)-C(27)-C(28)	113.2(11)	O(13)-C(27)-C(29)	101.9(10)
C(28)-C(27)-C(29)	112.8(14)	N(1)-C(30)-C(31)	109.7(8)
N(2)-C(32)-C(33)	111.9(8)	N(4)-C(34)-C(35)	119.5(12)
N(4)-C(34)-C(39)	117.9(13)	C(35)-C(34)-C(39)	122(2)
C(34)-C(35)-C(36)	119(2)	C(35)-C(36)-C(37)	118(2)
C(36)-C(37)-C(38)	121(2)	C(37)-C(38)-C(39)	120(2)
C(34)-C(39)-C(38)	116(2)		

CHAPTER 5

REACTIONS OF $[Ru_2(\mu\text{-}CO)(CO)_4\{\mu\text{-}(RO)_2PN(Et)P(OR)_2\}_2]$ WITH VARIOUS ALKYNES

5.1 INTRODUCTION

The co-ordination chemistry of alkynes and their reactivity patterns on metal sites has received, and continues to receive much attention.[202,203] An underlying objective of these investigations has been the development of homogeneous catalysts for reactions involving alkynes. The generation of dimetallacycles, in particular by the reaction of bimetallic transition metal carbonyls with alkynes, has been the subject of considerable study.[204-207] In these complexes the alkyne bridging the metal centres has been observed to adopt one of two bridging co-ordination modes; the $\mu\text{-}\sigma^2$ (" parallel") mode or the $\mu\text{-}\eta^2$ ("perpendicular") mode.

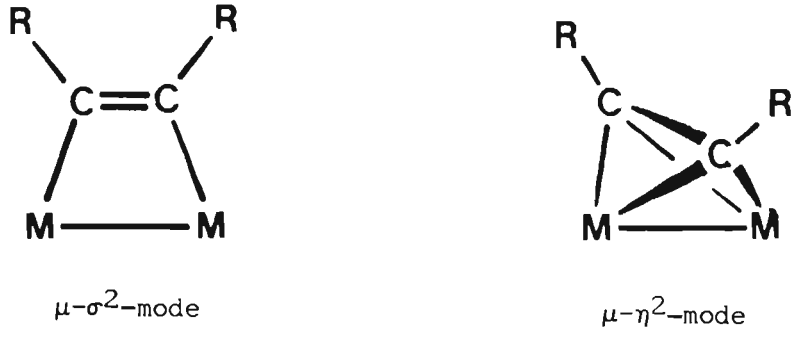

$\mu\text{-}\sigma^2$-mode $\mu\text{-}\eta^2$-mode

Figure 5.1

The more common architecture in binuclear alkyne complexes that are not constrained by additional binucleating ligands involves the $\mu\text{-}\eta^2$ alkyne bonding mode in which the alkyne is co-ordinated perpendicular to the metal-metal vector.[208,209] The $\mu\text{-}\sigma^2$-bound alkyne ligand in which the alkyne is co-ordinated parallel to the metal-metal vector has, however,

been frequently observed in binuclear rhodium and iridium complexes containing both bridging dppm and dmpm ligands,[206,210] although most of these rhodium and iridium compounds can only be prepared with very electron-deficient alkynes such as hexafluoro-2-butyne or dimethyl acetylenedicarboxylate. For example, reaction of the dirhodium species $[Rh_2Cl_2(\mu\text{-}CO)(\mu\text{-}Ph_2PNC_5H_4)_2]$ with electrophilic acetylenes affords the dimetallated alkyne derivatives $[Rh_2Cl_2(\mu\text{-}RC{=}CR')(\mu\text{-}Ph_2PNC_5H_4)_2]$ (R = R' = CO_2Me, CF_3; R = CO_2Me, R' = H).

The formal insertion of an alkyne into a metal-carbonyl bond to generate another type of dimetallacycle, *viz.* dimetallacyclopropenone species, has also been reported.[88,211] Knox *et al.* have shown that a variety of alkynes (HC_2H, MeC_2Me, PhC_2Ph, $MeO_2CC_2CO_2Me$, MeC_2H, PhC_2H and PhC_2Me) react with the di-iron cyclopentadienyl derivative $[Fe_2(CO)_4(\eta\text{-}C_5H_5)_2]$ under photochemical conditions to form dimetallacyclopropenone complexes of the type $[Fe_2(CO)(\mu\text{-}CO)\{\mu\text{-}\sigma\text{:}\eta^3\text{-}C(O)C_2R_2\}(\eta\text{-}C_5H_5)_2]$. Diphenylacetylene is the only acetylene that was found to react with the analogous ruthenium derivative $[Ru_2(CO)_4(\eta\text{-}C_5H_5)_2]$ under these conditions however, although the product of this reaction, $[Ru_2(CO)(\mu\text{-}CO)\{\mu\text{-}\sigma\text{:}\eta^3\text{-}C(O)C_2Ph_2\}(\eta\text{-}C_5H_5)_2]$ (Figure 5.2(a)), undergoes alkyne exchange on heating in toluene with HC_2H, MeC_2Me, MeC_2H, PhC_2H or PhC_2Me affording the respective dimetallacyclopropenone complexes; the

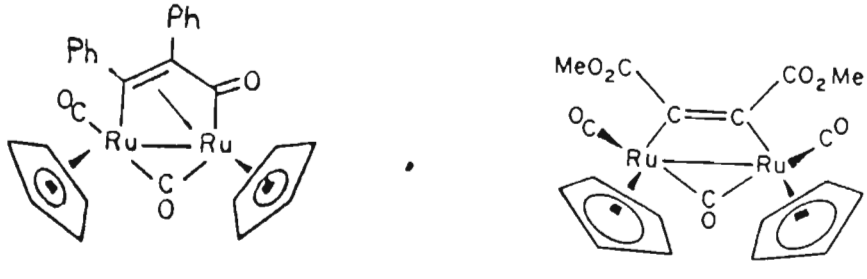

(a) (b)

Figure 5.2

dimetallacyclobutene complex $[Ru_2(CO)_2(\mu\text{-}CO)\{\mu\text{-}C_2(CO_2Me)_2\}(\eta\text{-}C_5H_5)_2]$ (Figure 5.2(b)) is generated when $[Ru_2(CO)(\mu\text{-}CO)\{\mu\text{-}\sigma\text{:}\eta^3\text{-}C(O)C_2Ph_2\}(\eta\text{-}C_5H_5)_2]$ is heated in the presence of the electron-deficient alkyne $MeO_2CC_2CO_2Me$.

Terminal alkynes (RC≡CH) have been shown to react with transition metal complexes by a number of different routes, the products of such reactions including π-complexes, as described above, as well as σ-bonded acetylide complexes, acetylide (hydrido) complexes and bridging and terminal vinylidene complexes. This variety arises from the bifunctionality offered by terminal alkynes, with metal-alkyne interactions occurring at either the C≡C bond or the acetylenic C-H bond. This bifunctionality[51] is illustrated by consideration of the reaction of the low-valent binuclear complex $[Rh_2(CO)_3(\mu\text{-}dppm)_2]$ with the terminal alkyne PhC≡CH. This reaction was found to afford an A-frame vinylidene complex, $[Rh_2(CO)_2(\mu\text{-}C{=}CHPh)(\mu\text{-}dppm)_2]$ (Figure 5.3 (a)), in addition to the non A-frame acetylene-bridged complex $[Rh_2(CO)_2(\mu\text{-}\eta^2\text{-}PhC{\equiv}CH)(\mu\text{-}dppm)_2]$ (Figure 5.3(b)), with the former being the thermodynamically preferred isomer.

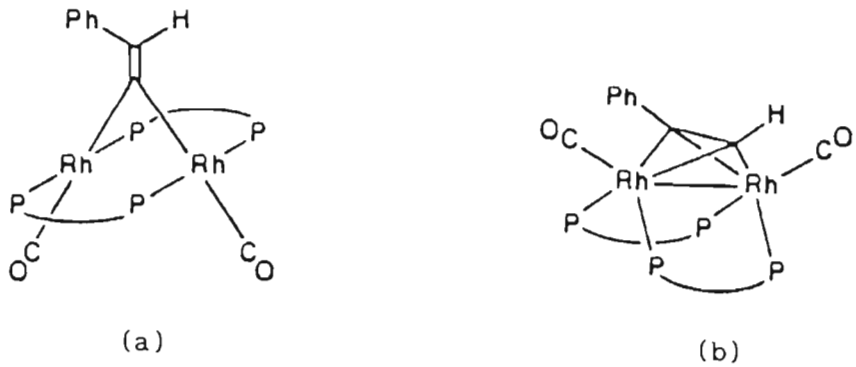

Figure 5.3

Vinylidene, the simplest unsaturated carbene, has never been observed experimentally as it undergoes an extremely fast 1,2-hydrogen shift to give acetylene. Substituted vinylidenes are similarly unstable. Unsub-

stituted and substituted vinylidenes can be stabilized by co-ordination to transition metals, however, with the first complex of this type, containing a diphenylvinylidene group, being reported in 1966.[212] This compound, $[Fe_2(\mu\text{-}C{=}CPh_2)(CO)_8]$, is obtained as a product of the reaction of $[Fe_2(CO)_9]$ with diphenylketene. Many other procedures for the synthesis of dinuclear vinylidene complexes have been developed. One method involves the reaction of terminal alkynes with suitable mononuclear or dinuclear precursors, an example being provided by the reaction of alk-1-ynes with two equivalents of $[Mn(CO)_2L(\eta\text{-}C_5H_5)]$ (L = CO or THF), from which the dimanganese vinylidene complexes $[Mn_2(CO)_4(\eta\text{-}C{=}CHR)(\eta\text{-}C_5H_5)_2]$ (R = H, Me, Ph, CO_2Me) are obtained.[213] A second method is based on the use of alkenes, as illustrated by the reaction of $Cl_2C{=}C(CN)_2$ with the highly nucleophilic anionic species $[Fe(CO)_2(\eta\text{-}C_5H_5)]^-$, which affords the *cis* and *trans* isomers of $[Fe_2(CO)_2(\mu\text{-}CO)\{\mu\text{-}C{=}C(CN)_2\}(\eta\text{-}C_5H_5)_2]$.[214] A third procedure involves the modification of bridging ligands. For example, nucleophilic attack by methyllithium on a bridging carbonyl ligand in $[Fe_2(CO)_2(\mu\text{-}CO)_2(\eta\text{-}C_5H_5)_2]$, followed by acidification, affords the μ-vinylidene complex $[Fe_2(CO)_2(\mu\text{-}CO)\{\mu\text{-}C{=}CH_2)(\eta\text{-}C_5H_5)_2]$.[215] Thermolysis of the metallacyclopropenone complex $[Ru_2(CO)(\mu\text{-}CO)\{\mu\text{-}\sigma{:}\eta^3\text{-}C(O)C_2H_2\}(\eta\text{-}C_5H_5)_2]$ has been found to produce the analogous *cis* and *trans* isomers of the μ-vinylidene complex $[Ru_2(CO)_2(\mu\text{-}CO)\{\mu\text{-}C{=}CH_2)(\eta\text{-}C_5H_5)_2]$[216]. This represents a fourth general method for the synthesis of vinylidene compounds.

Mononuclear vinylidene complexes have been extensively studied and their formation from terminal alkynes have been shown in many cases to occur via alkynyl(hydrido) intermediates,[217,218] according to the scheme illustrated below.

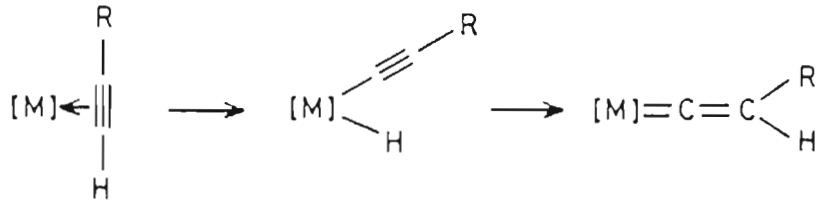

Scheme 5.1

Werner *et al.*[219] have established that the co-ordinatively unsaturated $14e^-$ species $[RhCl(PPr^i_3)_2]$ and $[IrCl(PPr^i_3)_2]$ are useful precursors for the synthesis of various square planar rhodium and iridium alkyne complexes, and that in the case of alk-1-ynes the derivatives *trans*-$[MCl(HC{\equiv}CR)(PPr^i_3)_2]$ rearrange in two consecutive steps to give firstly the alkynyl(hydrido) and subsequently the isomeric vinylidene metal derivatives. The reactions of the dihydride derivative $[IrH_2Cl(PPr^i_3)_2]$[220] with various alkynes have also been extensively investigated. With phenylacetylene this compound affords the alkynyl(hydrido) compound $[IrH(Cl)(C{\equiv}CPh)(PPr^i_3)_2]$, previously prepared by the intramolecular oxidation of the four-co-ordinate isomer *trans*-$[IrCl(PhC{\equiv}CH)(PPr^i_3)_2]$, whereas with acetylene, it affords almost instantaneously the vinylidene complex *trans*-$[IrCl(=C=CH_2)(PPr^i_3)_2]$, without the alkynyl(hydrido) species being observed as an intermediate.

A product, $[Re_2(\mu\text{-}H)(\mu\text{-}C{\equiv}CPh)(CO)_4(\mu\text{-dppm})_2]$,[42] containing both a bridging hydrido group and a bridging alkynyl ligand is produced on reaction of $[Re_2(CO)_6(\mu\text{-dppm})_2]$ with phenylacetylene at high temperature. This compound, in which the alkynyl ligand is involved in some fluxional process, was found not to rearrange to the vinylidene-bridged derivative, even at elevated temperatures.

The vinylidene-bridged complex $[Pd_2Cl_2(\mu\text{-}C{=}CH_2)(\mu\text{-dppm})_2]$[60] has been

prepared by heating a mixture of $[Pd(PPh_3)_4]$, dppm and $Cl_2C{=}CH_2$ in refluxing benzene. This compound is thermodynamically more stable than the isomeric σ^2-bonded alkyne species $[Pd_2Cl_2(\mu\text{-}\sigma^2\text{-}HC{=}CH)(\mu\text{-dppm})_2]$, synthesized by reaction of acetylene with $[Pd_2Cl_2(\mu\text{-dppm})_2]$, but significantly the latter could not be converted to the former.

Complexes containing a bridging vinylidene ligand have been shown to be susceptible to electrophilic attack, with the attack occurring at either the methylene carbon, or at the metal-metal bond. For example, protonation of the previously described dimanganese vinylidene species $[Mn_2(CO)_4(\mu\text{-}C{=}CH_2)(\eta\text{-}C_5H_5)_2]$ leads to the formation of the μ-carbyne complex $[Mn_2(CO)_4(\mu\text{-}CCH_3)(\eta\text{-}C_5H_5)_2]^+$,[221] whereas protonation of the dirhodium complex $[Rh_2(CO)_2(\mu\text{-}C{=}CH_2)(\eta\text{-indenyl})_2]$[222] affords the $\mu\text{-}\eta^1,\eta^2$-vinyl complex $[Rh_2(CO)_2(\mu\text{-}\eta^1,\eta^2\text{-}CH{=}CH_2)(\eta\text{-indenyl})_2]^+$, probably via initial attack on the Rh-Rh bond.

Transition metal acetylene and vinylidene complexes attract considerable interest because of their importance in catalysis. Acetylenes undergo a wide range of reactions catalyzed by metal complexes, both with themselves and with other compounds having multiple bonds to produce monomers, oligomers and polymers.[202] For example, a commercial process using $Ni(CO)_4$ as catalyst converts a mixture of acetylene, carbon monoxide and water into the useful monomer acrylic acid.

$$HC{\equiv}CH + CO + H_2O \xrightarrow[180^\circ\ 35\ atm]{Ni(CO)_4} \begin{array}{l} H \\ \diagdown \\ \quad C \\ \diagup \\ H \end{array} = \begin{array}{l} H \\ \diagup \\ C \\ \diagdown \\ CO_2H \end{array}$$

$[Ru_3(CO)_{12}]$ has been shown to catalyze the reaction of acetylene and carbon monoxide under a reducing atmosphere to afford *p*-catechol,[223] as shown in Scheme 5.3.

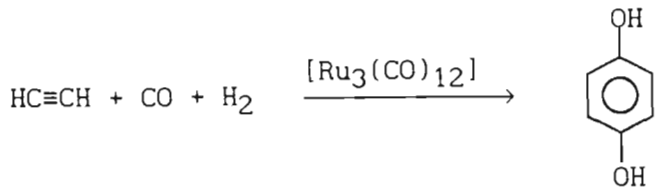

A previous study in these laboratories has shown that the diruthenium diphosphazane-bridged complexes $[Ru_2(\mu\text{-}CO)(CO)_4\{\mu\text{-}(RO)_2PN(Et)P(OR)_2\}_2]$ (R = Me or Pr^i) react with phenylacetylene in hexane under reflux to afford the vinylidene-bridged species $[Ru_2\{\mu\text{-}C{=}C(H)Ph\}(CO)_4\{\mu\text{-}(RO)_2PN(Et)P(OR)_2\}_2]$ (Figure 5.4(a)). This contrasts with the behaviour of the recently reported analogous ditertiary phosphine derivative $[Ru_2(\mu\text{-}CO)(CO)_4(\mu\text{-}Me_2PCH_2PMe_2)_2]$ which afforded σ^2-alkyne co-ordinated derivatives of the type $[Ru_2(\mu\text{-}\sigma^2\text{-}R'C{=}CR')(CO)_4(\mu\text{-}Me_2PCH_2PMe_2)_2]$ (R' = Ph or CO_2Me) (Figure 5.4(b)) on reaction with the internal alkynes diphenylacetylene and dimethyl acetylenedicarboxylate. A third type of product *viz.* the dimetallacyclopropenone complex $[Ru_2(\mu\text{-}C_2H_2CO)(CO)_5(\mu\text{-}dppm)]$ (Figure 5.4(c)) was found to be produced on reaction of the related hepta-carbonyl derivative $[Ru_2(\mu\text{-}CO)(CO)_6(\mu\text{-}dppm)]$[138] with acetylene in pentane at 0°C, although the σ^2-alkyne derivatives $[Ru_2(\mu\text{-}\sigma^2\text{-}R'C{=}CR')(CO)_6(\mu\text{-}dppm)]$ (R' = Ph or CO_2Me) (Figure 5.4(d)) were obtained on reaction with PhC≡CPh or with the less electron-rich alkyne $MeO_2CC{\equiv}CCO_2Me$.

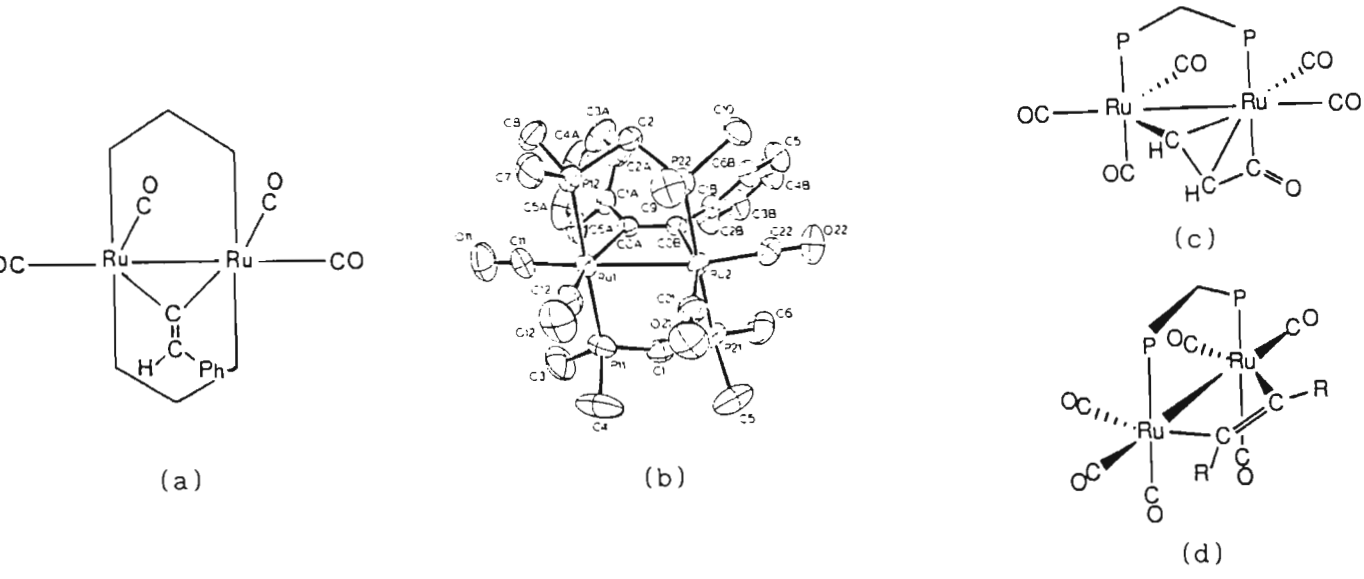

Figure 5.4

An objective of the research described in this chapter was to investigate the reactivity of the dinuclear diphosphazane-bridged derivatives $[Ru_2(\mu\text{-}CO)(CO)_4\{\mu\text{-}(RO)_2PN(Et)P(OR)_2\}_2]$ (R = Me, Pr^i) towards a range of alkynes, with the aim of establishing the reaction pathways for the formation of alkyne, vinylidene or metallacyclopropenone products.

5.2 REACTION OF $[Ru_2(\mu\text{-}CO)(CO)_4\{\mu\text{-}(RO)_2PN(Et)P(OR)_2\}_2]$ WITH ALKYNES

Passage of a stream of acetylene (HC≡CH) through a solution of the tetramethoxydiphosphazane-bridged derivative $[Ru_2(\mu\text{-}CO)(CO)_4\{\mu\text{-}(MeO)_2PN(Et)P(OMe)_2\}_2]$ in toluene at 80°C was found to result in a change in the colour of the solution from yellow to pale red and with time to pale yellow again. A yellow crystalline product was isolated in almost quantitative yield from this solution, the microanalysis of which was consistent with a compound of formulation $[Ru_2(CO)_4(HC{\equiv}CH)\{\mu\text{-}(MeO)_2PN(Et)P(OMe)_2\}_2]$. The infrared spectrum of this product in the C-O stretching region is very similar to that of the parent complex $[Ru_2(\mu\text{-}$

$CO)(CO)_4\{\mu\text{-}(MeO)_2PN(Et)P(OMe)_2\}_2]$, but with the peak corresponding to the stretching mode of the bridging carbonyl ligand in the latter, being absent. The $^{31}P\{^1H\}$ nmr spectrum of this species, measured in $CDCl_3$, exhibits two singlet resonances, at 155.79 and 153.00 ppm respectively, with the intensity of the latter upfield peak being more than ten-fold that of the former. The ^1H nmr spectrum in $CDCl_3$ is essentially the same as that of the parent complex, but containing an additional singlet at 7.11 ppm, the integral of which corresponds to two protons, as well as a much weaker quintet at 6.51 ppm; the integral of this quintet is approximately 3% of that of the singlet. The $^{13}C\{^1H\}$ nmr spectrum exhibits a quintet at 120.96 ppm with a DEPT analysis indicating that it corresponds to one or more equivalent carbon atoms each containing a single hydrogen atom. These results are interpreted in terms of two products having been formed in the reaction of $[Ru_2(\mu\text{-}CO)(CO)_4\{\mu\text{-}(MeO)_2\text{-}PN(Et)P(OMe)_2\}_2]$ with HC≡CH, and that the major product contains a symmetrically-bridging acetylene ligand. This species was later established to be the alkendiyl-bridged derivative $[Ru_2(CO)_4(\mu\text{-}\sigma^2\text{-}HC{=}CH)\{\mu\text{-}(MeO)_2PN(Et)P(OMe)_2\}_2]$ (**52**) (Figure 5.5) by means of X-ray

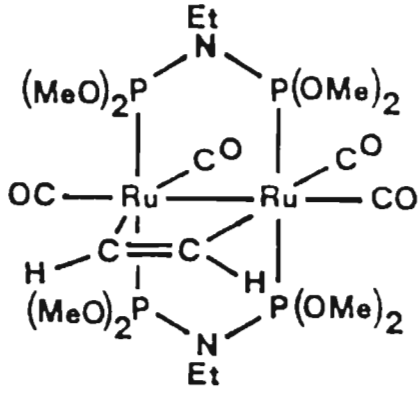

Figure 5.5: $[Ru_2(CO)_4(\mu\text{-}\sigma^2\text{-}HC{=}CH)\{\mu\text{-}(MeO)_2PN(Et)P(OMe)_2\}_2]$

crystallography. The minor product contributing to the weak "downfield" singlet at 155.79 ppm in the $^{31}P\{^1H\}$ nmr spectrum and to the weak

quintet at 6.51 ppm in the ^1H nmr spectrum was subsequently identified as the vinylidene-bridged isomer $[Ru_2(CO)_4(\mu\text{-}\eta^1\text{-}C{=}CH_2)\{\mu\text{-}(MeO)_2PN(Et)P(OMe)_2\}_2]$ (**53**) (*vide infra*).

The co-ordination of the acetylene in $[Ru_2(CO)_4(\mu\text{-}\sigma^2\text{-}HC{=}CH)\{\mu\text{-}(MeO)_2PN(Et)P(OMe)_2\}_2]$ as an alkendiyl group parallel to the ruthenium-ruthenium vector rather than as a η^2-alkyne perpendicular to this vector was confirmed, as indicated above, by means of an X-ray crystal structure determination. The stereochemistry of the compound is illustrated in Figure 5.6.

The structure is very similar to that of the parent compound $[Ru_2(\mu\text{-}CO)(CO)_4\{\mu\text{-}(MeO)_2PN(Et)P(OMe)_2\}_2]$[124] but with a σ^2-alkendiyl ligand bridging the two ruthenium atoms instead of a carbonyl group. The compound adopts an eclipsed configuration such that the four-membered dimetallacycle ring is planar. The two ruthenium atoms are separated by a distance of 2.867(1)Å which is slightly longer than that of the parent species $[Ru_2(\mu\text{-}CO)(CO)_4\{\mu\text{-}(MeO)_2PN(Et)P(OMe)_2\}_2]$ {2.801(2)Å}. The alkendiyl mode of co-ordination of the acetylene in $[Ru_2(CO)_4(\mu\text{-}\sigma^2\text{-}HC{=}CH)\{\mu\text{-}(MeO)_2PN(Et)P(OMe)_2\}_2]$ is the same as that established for the diphenylacetylene in $[Ru_2(CO)_4(\mu\text{-}\sigma^2\text{-}PhC{=}CPh)\{\mu\text{-}Me_2PCH_2PMe_2\}_2]$,[69] with the C-C distance of the acetylene in the former {1.31(2)Å} being almost identical to the analogous distance in the latter {1.329(6)Å}. The position of the hydrogen atoms of the alkendiyl group were not located.

The reaction of the tetraisopropoxydiphosphazane-bridged diruthenium complex $[Ru_2(\mu\text{-}CO)(CO)_4\{\mu\text{-}(Pr^iO)_2PN(Et)P(OPr^i)_2\}_2]$ with acetylene in toluene at 80°C was also observed to result in a change in the colour of the solution from pale yellow to pale red, to pale yellow. A yellow crystalline product was similarly isolated from this solution, the

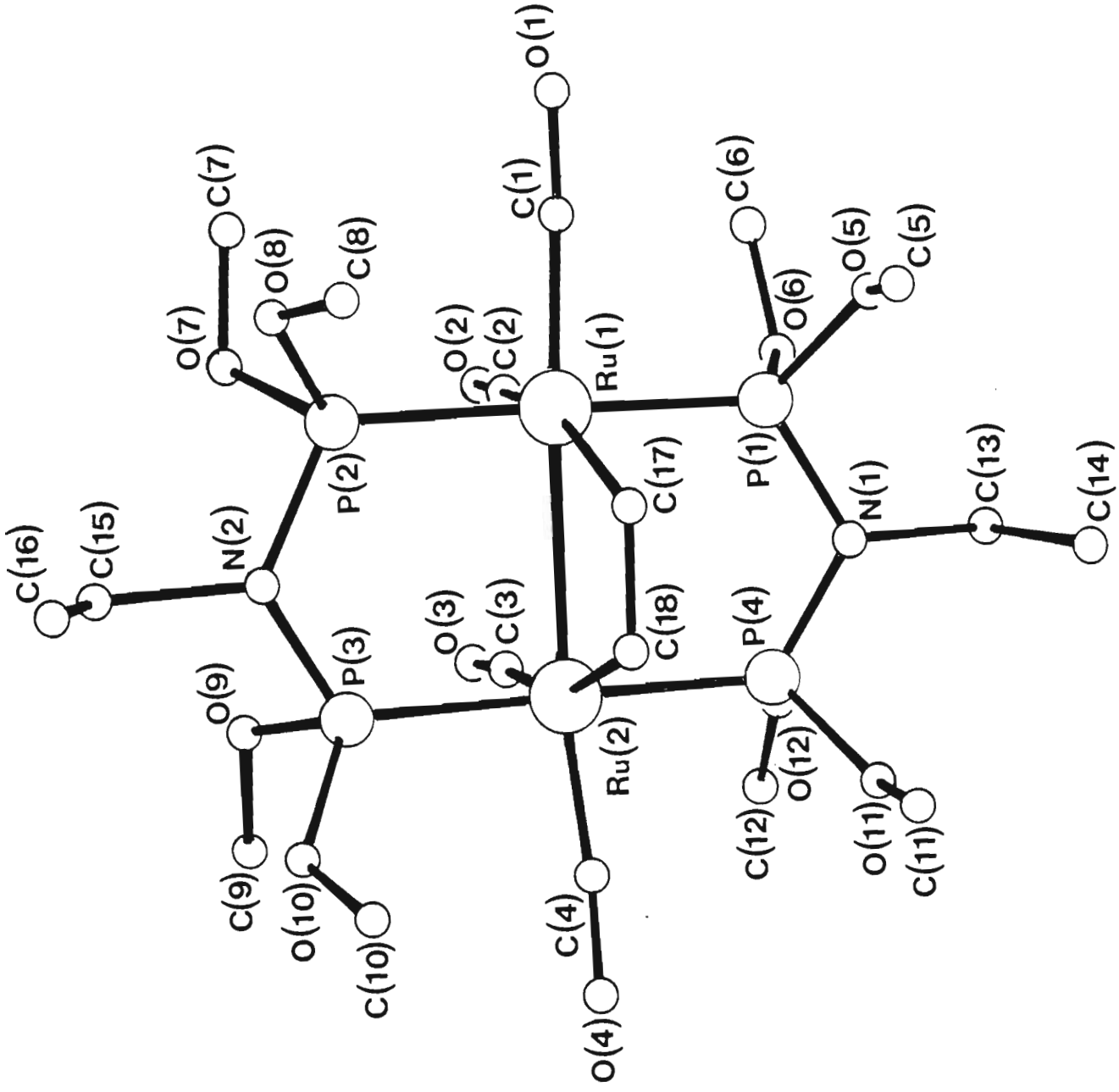

Figure 5.6: Structure of $[Ru_2(CO)_4(\mu\text{-}\sigma^2\text{-}HC{=}CH)\{\mu\text{-}(MeO)_2PN(Et)P(OMe)_2\}_2]$

microanalysis of which was consistent with the formulation $[Ru_2(CO)_4(HC{\equiv}CH)\{\mu\text{-}(Pr^iO)_2PN(Et)P(OPr^i)_2\}_2]$. The infrared spectrum of the product in the C-O stretching region is almost identical to that of the above alkendiyl species $[Ru_2(CO)_4(\mu\text{-}\sigma^2\text{-}HC{=}CH)\{\mu\text{-}(MeO)_2PN(Et)P(OMe)_2\}_2]$, while its $^{31}P\{^1H\}$ nmr spectrum, measured in $CDCl_3$, similar to that of the alkendiyl-bridged tetramethoxydiphosphazane product, exhibits two singlets. The intensity of the downfield singlet at 148.22 ppm is, however, more than ten times that of the singlet at 146.09 ppm. The ^1H nmr spectrum of this species in $CDCl_3$ contains a quintet at 6.41 ppm, the integral of which corresponds to two protons, as well as a much weaker singlet at 7.02 ppm, in addition to the resonances corresponding to the protons of the diphosphazane ligands. The integral of this singlet is approximately 8% of that of the above-mentioned quintet. The compound's $^{13}C\{^1H\}$ nmr spectrum exhibits a well-resolved quintet at 232.67 ppm and a less well-resolved quintet at 131.88 ppm. A DEPT analysis revealed that the former quintet corresponds to a quaternary carbon whereas the latter corresponds to a secondary carbon. The spectroscopic results are interpreted in terms of two products also being formed in the reaction of $[Ru_2(\mu\text{-}CO)(CO)_4\{\mu\text{-}(Pr^iO)_2PN(Et)P(OPr^i)_2\}_2]$ with HC≡CH but, in contrast to the corresponding reaction involving the tetramethoxydiphosphazane-bridged derivative, with the major product being a vinylidene-bridged derivative *viz.* $[Ru_2(CO)_4(\mu\text{-}\eta^1\text{-}C{=}CH_2)\{\mu\text{-}(Pr^iO)_2PN(Et)P(OPr^i)_2\}_2]$ (**55**) (Figure 5.7). Inherent crystal twinning prevented the structure of this compound being established by means of X-ray crystallography, but an X-ray crystal structure determination of the related methyl vinylidene species $[Ru_2(CO)_4(\mu\text{-}\eta^1\text{-}C{=}CHMe)\{\mu\text{-}(Pr^iO)_2PN(Et)P(OPr^i)_2\}_2]$ (*vide infra*) unequivocally established the formation of vinylidene-bridged products in the reactions of the diphosphazane-bridged derivatives $[Ru_2(\mu\text{-}CO)(CO)_4\{\mu\text{-}(RO)_2PN(Et)P(OR)_2\}_2]$ with terminal alkynes.

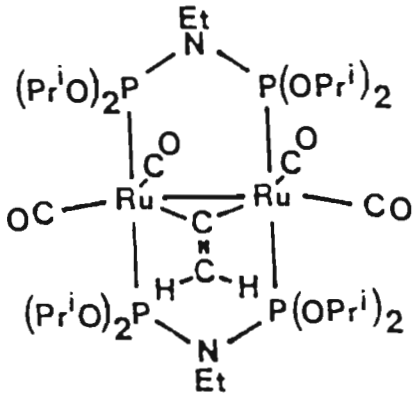

Figure 5.7: $[Ru_2(CO)_4(\mu\text{-}\eta^1\text{-}CCH_2)\{\mu\text{-}(Pr^iO)_2PN(Et)P(OPr^i)_2\}_2]$

The minor product contributing to the weaker singlet at 146.09 ppm in the $^{31}P\{^1H\}$ nmr spectrum and the singlet at 7.02 ppm in the ^1H nmr spectrum, is proposed to be the alkendiyl-bridged isomer $[Ru_2(CO)_4(\mu\text{-}\sigma^2\text{-}HC{=}CH)\{\mu\text{-}(Pr^iO)_2PN(Et)P(OPr^i)_2\}_2]$ (**54**) on the basis of the nmr spectroscopic data and by analogy with the spectroscopic data for the tetramethoxydiphosphazane derivative $[Ru_2(CO)_4(\mu\text{-}\sigma^2\text{-}HC{=}CH)\{\mu\text{-}(MeO)_2PN(Et)P(OMe)_2\}_2]$.

In summary, while the reaction of the less bulky tetramethoxydiphosphazane-bridged derivative $[Ru_2(\mu\text{-}CO)(CO)_4\{\mu\text{-}(MeO)_2PN(Et)P(OMe)_2\}_2]$ with acetylene affords the alkendiyl derivative $[Ru_2(CO)_4(\mu\text{-}\sigma^2\text{-}HC{=}CH)\{\mu\text{-}(MeO)_2PN(Et)P(OMe)_2\}_2]$ as the major isomer, the reaction of the more bulky tetraisopropoxydiphosphazane-bridged species $[Ru_2(\mu\text{-}CO)(CO)_4\{\mu\text{-}(Pr^iO)_2PN(Et)P(OPr^i)_2\}_2]$ with acetylene affords the vinylidene-bridged species $[Ru_2(CO)_4(\mu\text{-}\eta^1\text{-}C{=}CH_2)\{\mu\text{-}(Pr^iO)_2PN(Et)P(OPr^i)_2\}_2]$ as the major product. In an attempt to gain a fuller understanding of these reactions they were monitored at various temperatures by means of $^{31}P\{^1H\}$ nmr spectroscopy. Table 5.1 gives the percentage of the parent complex $[Ru_2(\mu\text{-}CO)(CO)_4\{\mu\text{-}(RO)_2PN(Et)P(OR)_2\}_2]$ (A), the alkendiyl-

bridged product $[Ru_2(CO)_4(\mu\text{-}\sigma^2\text{-}HC{=}CH)\{\mu\text{-}(RO)_2PN(Et)P(OR)_2\}_2]$ (B) and the vinylidene-bridged product $[Ru_2(CO)_4(\mu\text{-}\eta^1\text{-}C{=}CH_2)\{\mu\text{-}(RO)_2PN(Et)P(OR)_2\}_2]$ (C) in the reaction mixture at various time intervals for the reaction performed at 55°C .

R	10 min			30 min			60 min			90 min		
	A	B	C	A	B	C	A	B	C	A	B	C
Me	78	20	2	20	70	10	0	88	12	0	88	12
Pr^i	85	0	15	63	2	35	9	6	85	0	8	92

Table 5.1

Significantly, the reactions of the parent diruthenium species $[Ru_2(\mu\text{-}CO)(CO)_4\{\mu\text{-}(RO)_2PN(Et)P(OR)_2\}_2]$ (R = Me, Pr^i) with acetylene at 110°C were found to afford the alkendiyl- and vinylidene-bridged isomers in approximately the same ratios as those found for the reactions at 55°C, although shorter reaction times were required for the reaction to go to completion. A number of conclusions can be drawn from these results. Firstly, the ratios of the yields of the alkendiyl- and vinylidene-bridged isomers are independent of both the reaction temperature as well as the reaction time. Secondly, the tetraisopropoxydiphosphazane derivative $[Ru_2(\mu\text{-}CO)(CO)_4\{\mu\text{-}(Pr^iO)_2PN(Et)P(OPr^i)_2\}_2]$ reacts more rapidly with acetylene than its tetramethoxydiphosphazane-bridged analogue, while thirdly, it was evident that the two isomeric forms are not interconvertible, and appear to be formed via two different pathways.

The mixed-ligand species $[Ru_2(\mu\text{-}CO)(CO)_4\{\mu\text{-}(MeO)_2PN(Et)P(OMe)_2\}\{\mu\text{-}(Pr^iO)_2PN(Et)P(OPr^i)_2\}]$ which contains both the more bulky isopropoxy- and the less bulky methoxydiphosphazane ligands, was also reacted with acetylene and was found to afford a mixture of both the alkendiyl- and

vinylidene-bridged isomers $[Ru_2(CO)_4(\mu\text{-}\sigma^2\text{-}HC{=}CH)\{\mu\text{-}(MeO)_2PN(Et)P(OMe)_2\}\text{-}\{\mu\text{-}(Pr^iO)_2PN(Et)P(OPr^i)_2\}]$ (**56**) and $[Ru_2(CO)_4(\mu\text{-}\eta^1\text{-}C{=}CH_2)\{\mu\text{-}(MeO)_2PN\text{-}(Et)P(OMe)_2\}\{\mu\text{-}(Pr^iO)_2PN(Et)P(OPr^i)_2\}]$ (**57**). The $^{31}P\{^1H\}$ nmr spectrum of the "product" isolated from this reaction exhibited two sets of resonances of AA'BB' pattern of roughly equal intensity, centred at 151.04 and 153.78 ppm (measured in CD_2Cl_2) respectively. The ^1H nmr spectrum (Figure 5.8) measured in CD_2Cl_2 contained a singlet at 7.10 ppm and a quintet at 6.52 ppm of relative intensity 55:45, as well as resonances corresponding to the protons of the diphosphazane ligands. The $^{13}C\{^1H\}$ nmr spectrum (Figure 5.9) exhibits a well resolved quintet at 235.84 ppm and a less well resolved quintet at 132.67 ppm. A DEPT analysis showed the former to correspond to a quaternary carbon and the latter to a secondary carbon, and thus may be assigned as the α and β carbons of the vinylidene ligand in the complex $[Ru_2(CO)_4(\mu\text{-}\eta^1\text{-}C{=}CH_2)\{\mu\text{-}(MeO)_2PN(Et)P(OMe)_2\}\{\mu\text{-}(Pr^iO)_2PN(Et)P(OPr^i)_2\}]$. The $^{13}C\{^1H\}$ nmr spectrum also exhibits a quintet at 121.60 ppm, and the DEPT analysis indicates that this quintet corresponds to one or more equivalent carbon atoms, each containing a single hydrogen atom. The latter quintet is thus assigned to the acetylenic carbons in the alkendiyl-bridged species $[Ru_2(CO)_4(\mu\text{-}\sigma^2\text{-}HC{=}CH)\{\mu\text{-}(MeO)_2PN(Et)P(OMe)_2\}\{\mu\text{-}(Pr^iO)_2PN(Et)P(OPr^i)_2\}]$.

The tetraethoxydiphosphazane-bridged complex $[Ru_2(\mu\text{-}CO)(CO)_4\{\mu\text{-}(EtO)_2PN\text{-}(Et)P(OEt)_2\}_2]$ was likewise reacted with acetylene. The $CDCl_3$ $^{31}P\{^1H\}$ nmr spectrum of the product isolated from this reaction exhibits two singlet resonances at 150.54 and 147.56 ppm respectively, with the intensity of the latter being approximately three times that of the former. The ^1H nmr spectrum contains, in addition to the resonances of the protons of the diphosphazane ligand, a singlet at 7.01 ppm, and a quintet at 6.36 ppm, with the intensity of the former being three times that of the latter. Based on analogous spectroscopic results described

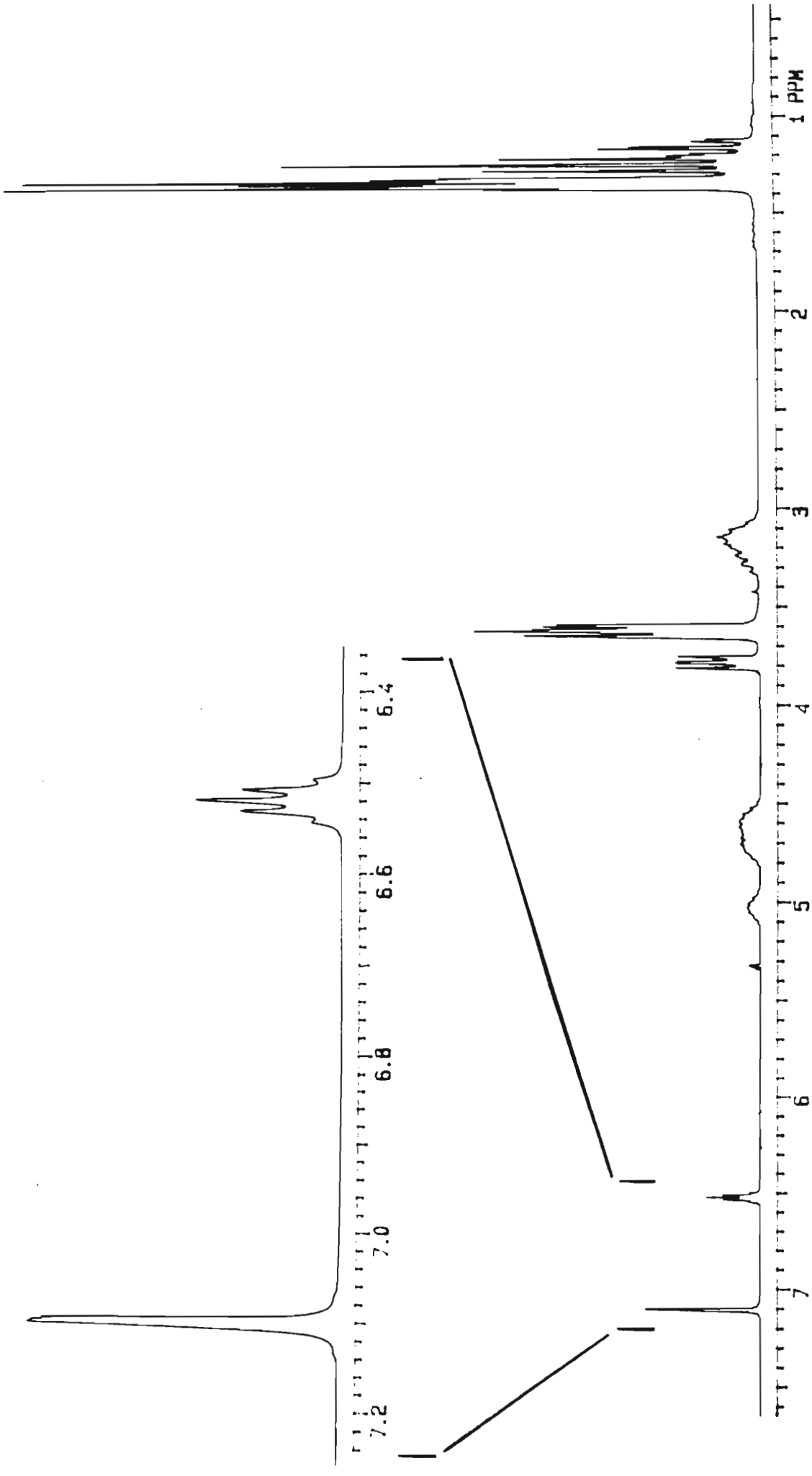

Figure 5.8: ^{1}H nmr spectrum of a mixture of **(56)** and **(57)** in CD_2Cl_2 (in ppm)

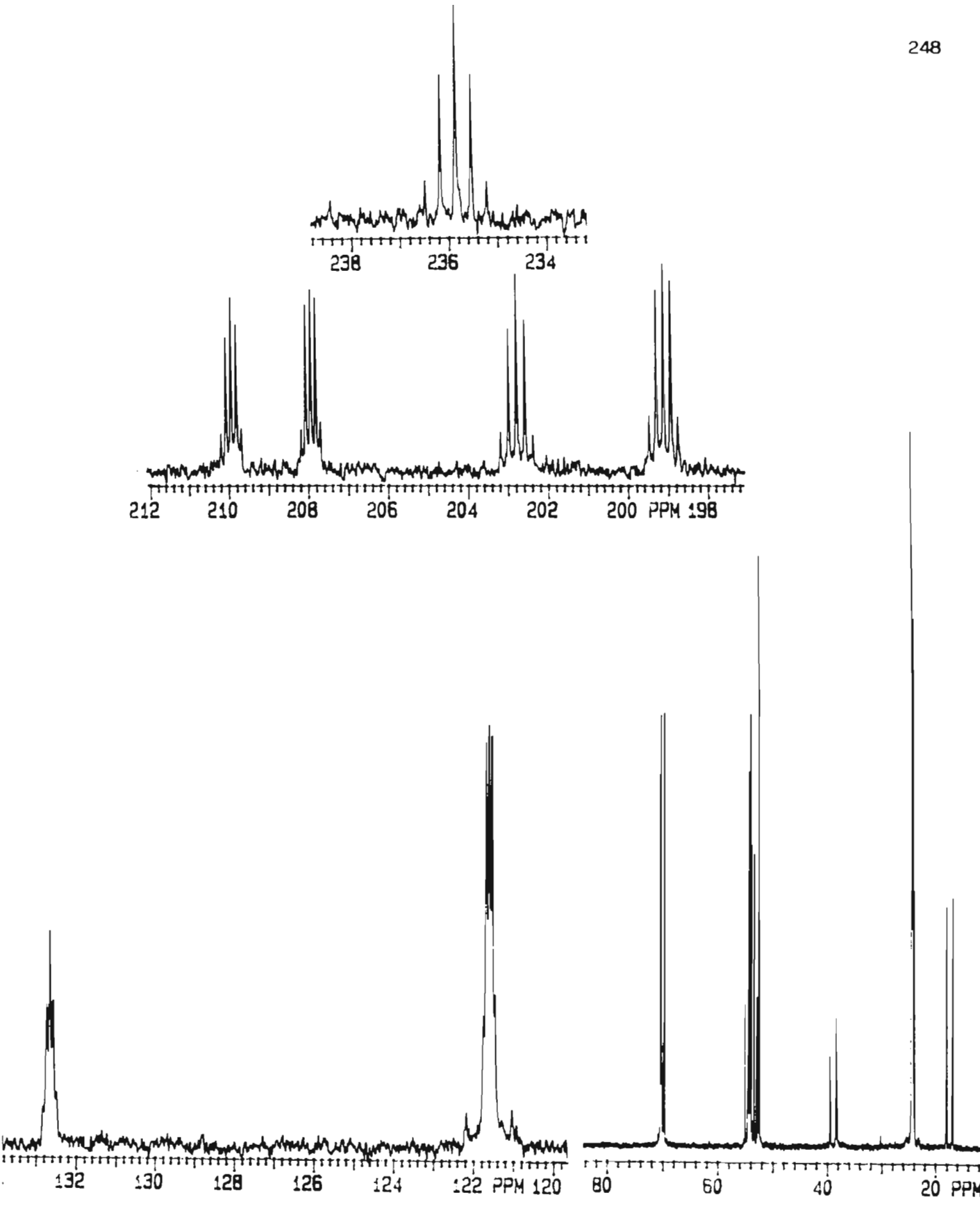

Figure 5.9: $^{13}C\{^1H\}$ nmr spectrum of a mixture of $[Ru_2(CO)_4(\mu\text{-}\sigma^2\text{-}HC{=}CH)\{\mu\text{-}(MeO)_2PN(Et)P(OMe)_2\}\{\mu\text{-}(Pr^iO)_2PN(Et)P(OPr^i)_2\}]$ (**56**) and $Ru_2(CO)_4(\mu\text{-}\eta^1\text{-}C{=}CH_2)\text{-}\{\mu\text{-}(MeO)_2PN(Et)P(OMe)_2\}\{\mu\text{-}(Pr^iO)_2PN(Et)P(OPr^i)_2\}]$ (**57**) in CD_2Cl_2 (in ppm)

above, it is concluded that the alkendiyl-bridged species $[Ru_2(CO)_4(\mu\text{-}\sigma^2\text{-}HC{=}CH)\{\mu\text{-}(EtO)_2PN(Et)P(OEt)_2\}_2]$ (**58**) is formed as the major product, and the vinylidene-bridged complex $[Ru_2(CO)_4(\mu\text{-}\eta^1\text{-}C{=}CH_2)\{\mu\text{-}(EtO)_2PN(Et)\text{-}P(OEt)_2\}_2]$ (**59**) as the minor isomer.

The contrasting co-ordination behaviour of acetylene towards the diruthenium complexes $[Ru_2(\mu\text{-}CO)(CO)_4\{\mu\text{-}(RO)_2PN(Et)P(OR)_2\}_2]$ (R = Me, Et and Pr^i) can be explained in terms of two different mechanistic pathways (*vide infra*) with the preferential adoption of either one being governed by the steric bulk of the bridging diphosphazane ligands. Stemming from this, it was concluded that reaction of the diruthenium complexes $[Ru_2(\mu\text{-}CO)(CO)_4\{\mu\text{-}(RO)_2PN(Et)P(OR)_2\}_2]$ (R = Me, Pr^i) with more bulky terminal acetylenes such as propyne, butyne or phenylacetylene should afford the vinylidene species $[Ru_2(CO)_4(\mu\text{-}\eta^1\text{-}C{=}CHR')\{\mu\text{-}(RO)_2PN(Et)\text{-}P(OR)_2\}_2]$ (R′ = Me, Et, Ph) in preference to the alkendiyl-bridged isomers $[Ru_2(CO)_4(\mu\text{-}\sigma^2\text{-}HC{=}CR')\{\mu\text{-}(RO)_2PN(Et)P(OR)_2\}_2]$. It was also concluded that as a consequence of the absence of an active hydrogen, reaction of the parent diruthenium complexes with internal acetylenes should afford solely alkendiyl-bridged derivatives. As described below, these conclusions were experimentally substantiated.

Reaction of the tetramethoxydiphosphazane-bridged species $[Ru_2(\mu\text{-}CO)\text{-}(CO)_4\{\mu\text{-}(MeO)_2PN(Et)P(OMe)_2\}_2]$ with propyne (HC≡CMe) in toluene at 80°C was found to afford both the alkendiyl- and vinylidene-bridged isomers, $[Ru_2(CO)_4(\mu\text{-}\sigma^2\text{-}HC{=}CMe)\{\mu\text{-}(MeO)_2PN(Et)P(OMe)_2\}_2]$ (**60**) and $[Ru_2(CO)_4(\mu\text{-}\eta^1\text{-}C{=}CHMe)\{\mu\text{-}(MeO)_2PN(Et)P(OMe)_2\}_2]$ (**61**) respectively, with the latter being the major isomer. The infrared spectrum in the C-O stretching region of the product isolated is similar to those of the alkendiyl- and vinylidene-bridged species $[Ru_2(CO)_4(\mu\text{-}\sigma^2\text{-}HC{=}CH)\{\mu\text{-}(MeO)_2PN(Et)P\text{-}(OMe)_2\}_2]$ and $[Ru_2(CO)_4(\mu\text{-}\eta^1\text{-}C{=}CH_2)\{\mu\text{-}(Pr^iO)_2PN(Et)P(OPr^i)_2\}_2]$ respec-

tively, as are the corresponding infrared spectra of the products isolated from the reactions described below. The $^{31}P\{^1H\}$ nmr spectrum, measured in $CDCl_3$, exhibits two singlets at 155.51 ppm and 152.91 ppm, with the intensity of the former being approximately five times that of the latter. The ^1H nmr spectrum exhibits a broad multiplet centred at 6.60 ppm, the integral of which corresponds to one proton, as well as a much weaker singlet at 7.18 ppm. A multiplet centred at 2.87 ppm (three protons) and a much weaker singlet at 1.60 ppm are also observed in addition to the resonances corresponding to the protons of the diphosphazane ligands. The $^{13}C\{^1H\}$ nmr spectrum exhibits quintets at 223.82 and 135.95 ppm and a singlet at 28.82 ppm assigned to the α, β and γ carbons respectively of the methylvinylidene ligand in $[Ru_2(CO)_4(\mu\text{-}\eta^1\text{-}C{=}CHMe)\{\mu\text{-}(MeO)_2PN(Et)P(OMe)_2\}_2]$. Significantly, weaker quintets at 132.60 and 120.56 ppm and a singlet at 29.72 ppm are assigned to the carbons of the alkendiyl ligand in $[Ru_2(CO)_4(\mu\text{-}\sigma^2\text{-}HC{=}CMe)\{\mu\text{-}(MeO)_2PN(Et)P(OMe)_2\}_2]$.

In contrast to that observed in the reaction described above, treatment of the tetraisopropoxydiphosphazane-bridged complex $[Ru_2(\mu\text{-}CO)(CO)_4\{\mu\text{-}(Pr^iO)_2PN(Et)P(OPr^i)_2\}_2]$ with HC≡CMe under the same conditions was found to lead to the formation of a vinylidene-bridged species, *viz.* $[Ru_2(CO)_4(\mu\text{-}\eta^1\text{-}C{=}CHMe)\{\mu\text{-}(Pr^iO)_2PN(Et)P(OPr^i)_2\}_2]$ (**62**), as the sole product. The $^{31}P\{^1H\}$ nmr spectrum of this compound, measured in $CDCl_3$, exhibits an AA'BB' pattern of resonances, centred at 148.43 ppm, while the $^{13}C\{^1H\}$ nmr spectrum exhibits a well resolved quintet at 221.84 ppm, a less well resolved quintet at 134.58 ppm and a singlet at 28.23 ppm. These resonances are readily assigned to the α, β and γ carbons respectively of the methyl vinylidene ligand. The ^1H nmr spectrum exhibits multiplets centred at 6.24 and 1.86 ppm, the integrals of which correspond to one and three protons and are therefore assigned to the

vinylidene and methyl protons of the methyl vinylidene ligand respectively.

A single crystal structure determination was carried out for $[Ru_2(CO)_4(\mu\text{-}\eta^1\text{-}C{=}CHMe)\{\mu\text{-}(Pr^iO)_2PN(Et)P(OPr^i)_2\}_2]$ which confirmed the presence of a bridging vinylidene ligand. Disorder of some of the isopropoxy groups of the diphosphazane ligands prevented refinement of the X-ray data to within acceptable limits however. A final R factor of 12% was obtained, and thus the interatomic distances and angles are not entirely reliable; the structure of this species is shown in Figure 5.10, with the carbon atoms of the diphosphazane ligands having been omitted.

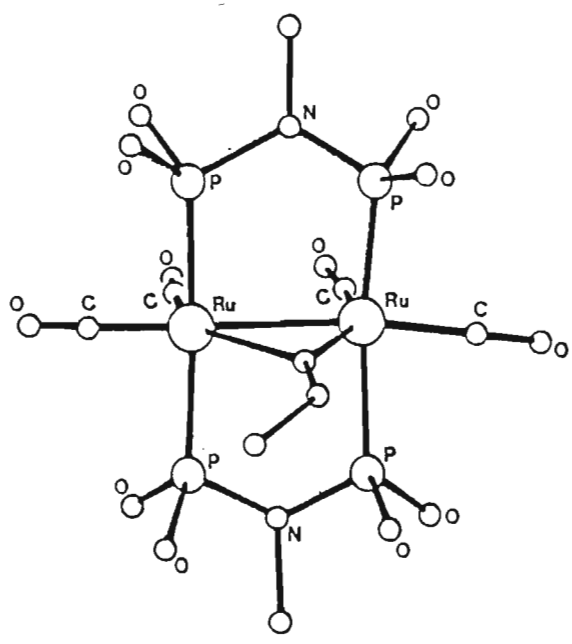

Figure 5.10: Structure of $[Ru_2(CO)_4(\mu\text{-}\eta^1\text{-}CCHMe)\{\mu\text{-}(Pr^iO)_2PN(Et)P(OPr^i)_2\}_2]$; the alkyl groups of the diphosphazane ligands have been omitted

It was found that reaction of the tetramethoxydiphosphazane-bridged derivative $[Ru_2(\mu\text{-}CO)(CO)_4\{\mu\text{-}(MeO)_2PN(Et)P(OMe)_2\}_2]$ with a slight excess of methyl propiolate ($HC{\equiv}CCO_2Me$) at 80°C in toluene afforded the

alkendiyl-bridged species $[Ru_2(CO)_4(\mu\text{-}\sigma^2\text{-}HC{=}CCO_2Me)\{\mu\text{-}(MeO)_2PN(Et)P(OMe)_2\}_2]$ (**63**) as the sole product. The $^{31}P\{^1H\}$ nmr spectrum of the compound in $CDCl_3$ exhibits a set of resonances of AA'BB' pattern, centred at 151.63 ppm. The presence of a methyl propiolate group was confirmed by the presence of a band at 1670 cm^{-1} in the infrared spectrum of the compound, assigned to its carbonyl stretching vibration and a singlet resonance at 9.08 ppm in its ^1H nmr spectrum, the integral of which corresponds to a single proton, assigned to the acetylenic proton of this group.

Consistent with the trends already established for the reactions of the diruthenium complexes with alkynes, reaction of the tetraisopropoxydiphosphazane-bridged complex $[Ru_2(\mu\text{-}CO)(CO)_4\{\mu\text{-}(Pr^iO)_2PN(Et)P(OPr^i)_2\}_2]$ with methyl propiolate in toluene at 80°C was found to afford a mixture of both the alkendiyl-bridged species, $[Ru_2(CO)_4(\mu\text{-}\sigma^2\text{-}HC{=}CCO_2Me)\{\mu\text{-}(Pr^iO)_2PN(Et)P(OPr^i)_2\}_2]$ (**64**) and the vinylidene-bridged species $[Ru_2(CO)_4(\mu\text{-}\eta^1\text{-}C{=}CHCO_2Me)\{\mu\text{-}(Pr^iO)_2PN(Et)P(OPr^i)_2\}_2]$ (**65**), with the former occurring as the major isomer. The $^{31}P\{^1H\}$ nmr spectrum of this mixture in $CDCl_3$ exhibits two AA'BB' sets of resonances, centred at 147.90 and 144.10 ppm; the ratio of the intensities of these AA'BB' patterns of peaks are approximately 1:3. The ^1H nmr spectrum of the mixture exhibits singlets at 9.12 and 3.54 ppm, assigned to the acetylenic proton and methyl protons respectively of the alkendiyl group of $[Ru_2(CO)_4(\mu\text{-}\sigma^2\text{-}HC{=}CCO_2Me)\{\mu\text{-}(Pr^iO)_2PN(Et)P(OPr^i)_2\}_2]$. A quintet centred at 7.35 ppm and a singlet at 3.59 ppm was assigned to the vinylidene proton and methyl protons of the methyl propiolate vinylidene ligand of $[Ru_2(CO)_4(\mu\text{-}\eta^1\text{-}C{=}CHCO_2Me)\{\mu\text{-}(Pr^iO)_2PN(Et)P(OPr^i)_2\}_2]$. The ratio of the integrals of the resonance for the acetylenic proton in $[Ru_2(CO)_4(\mu\text{-}\sigma^2\text{-}HC{=}CCO_2Me)\{\mu\text{-}(Pr^iO)_2PN(Et)P(OPr^i)_2\}_2]$ to those for the vinylidene proton in $[Ru_2(CO)_4(\mu\text{-}\eta^1\text{-}C{=}CHCO_2Me)\{\mu\text{-}(Pr^iO)_2PN(Et)P(OPr^i)_2\}_2]$ was found to be

approximately 3:1, as were the ratios of the resonances for the protons of the ester group of the two isomeric forms.

Significantly, it was possible to isolate the alkendiyl-bridged species $[Ru_2(CO)_4(\mu\text{-}\sigma^2\text{-}HC{=}CCO_2Me)\{\mu\text{-}(Pr^iO)_2PN(Et)P(OPr^i)_2\}_2]$ (**64**) in a pure state by fractional crystallization. Measurement of the $^{31}P\{^1H\}$ and ^1H nmr spectra of this compound confirmed the above assignment of the peaks in the spectra of the isomeric mixture. Most important, it was found that heating the pure alkendiyl-bridged species $[Ru_2(CO)_4(\mu\text{-}\sigma^2\text{-}HC{=}C\text{-}CO_2Me)\{\mu\text{-}(Pr^iO)_2PN(Et)P(OPr^i)_2\}_2]$ in refluxing toluene for several hours did not lead to the formation of the vinylidene-bridged isomer. This result again confirmed the observation that the alkendiyl- and vinylidene-bridged isomers are not interconvertible and that the formation of the vinylidene-bridged species does not occur via the alkendiyl-bridged isomer as intermediate.

Reaction of the diruthenium complexes $[Ru_2(\mu\text{-}CO)(CO)_4\{\mu\text{-}(RO)_2PN(Et)P\text{-}(OR)_2\}_2]$ (R = Me or Pr^i) with the more electrophilic internal alkyne dimethyl acetylenedicarboxylate ($MeO_2CC{\equiv}CCO_2Me$) at elevated temperatures in toluene was established to lead to the formation of the alkendiyl-bridged derivatives $[Ru_2(CO)_4(\mu\text{-}\sigma^2\text{-}MeO_2CC{=}CCO_2Me)\{\mu\text{-}(RO)_2PN(Et)P(OR)_2\}_2]$ (R = Me and Pr^i), in almost quantitative yield.

The infrared spectrum of the tetramethoxydiphosphazane-bridged derivative $[Ru_2(CO)_4(\mu\text{-}\sigma^2\text{-}MeO_2CC{=}CCO_2Me)\{\mu\text{-}(MeO)_2PN(Et)P(OMe)_2\}_2]$ (**66**) in the C-O stretching region exhibits a four-line pattern typical of tetracarbonyl complexes of this type, as well as a band at 1673 cm^{-1}, assigned to the stretching vibration of the carbonyls of the alkendiyl group. The $^{31}P\{^1H\}$ nmr spectrum of the compound, measured in $CDCl_3$, exhibits a singlet resonance at 148.45 ppm, while the presence of the

dimethyl acetylenedicarboxylate group was established by the presence of a singlet resonance at 3.50 ppm, the integral of which corresponds to six protons, in the ^{1}H nmr spectrum of the compound. The $^{13}C\{^{1}H\}$ nmr spectrum exhibits, in addition to resonances assigned to the carbon atoms of the diphosphazane ligands, two quintets at 206.39 and 196.28 ppm, assigned to the carbon atoms of the two axial and two equatorial carbonyl ligands respectively. In addition, a singlet at 173.95 and a quintet centred at 146.91 ppm was observed, the integrals of which correspond to two carbons each. These sets of peaks may readily be assigned to the carboxylate and acetylenic carbons of the alkendiyl ligand respectively. A peak at 50.99 ppm was assigned to the methyl carbon of the alkendiyl ligand.

The infrared spectrum of the tetraisopropoxydiphosphazane-bridged species $[Ru_2(CO)_4(\mu\text{-}\sigma^2\text{-}MeO_2CC{=}CCO_2Me)\{\mu\text{-}(Pr^iO)_2PN(Et)P(OPr^i)_2\}_2]$ (**67**) in the C-O stretching region is similar to that of the analogous tetramethoxydiphosphazane-bridged species. The $^{31}P\{^{1}H\}$ nmr spectrum of the compound, measured in $CDCl_3$, exhibits a singlet resonance at 140.91 ppm while the ^{1}H nmr spectrum contains, in addition to the resonances associated with the protons of the diphosphazane ligands, a singlet at 3.41 ppm, the integral of which corresponds to six protons, and is therefore assigned to the protons of the two methyl groups of the acetylenedicarboxylate ligand. The $^{13}C\{^{1}H\}$ nmr spectrum exhibits a singlet at 173.70 ppm, a quintet centred at 152.01 ppm and a singlet at 50.66 ppm, and by analogy to that described for the tetramethoxy-diphosphazane-bridged analogue, these peaks are assigned to the carboxylate, acetylenic and methyl carbons of the acetylenedicarboxylate ligand respectively.

Significantly, it was found that the less electron-deficient internal

acetylene diphenylacetylene (PhC≡CPh) does not react with the diruthenium complexes $[Ru_2(\mu\text{-}CO)(CO)_4\{\mu\text{-}(RO)_2PN(Et)P(OR)_2\}_2]$ (R = Me or Pr^i) under the above reaction conditions, in contrast to that established for the more electron-rich and less sterically constrained derivative $[Ru_2(\mu\text{-}CO)(CO)_4(\mu\text{-}Me_2PCH_2PMe_2)_2]$.[69] A change in the colour of the solution from pale yellow to an intense red was observed, however, on refluxing a mixture of $[Ru_2(\mu\text{-}CO)(CO)_4\{\mu\text{-}(RO)_2PN(Et)P(OR)_2\}_2]$ (R = Me, Pr^i) and PhC≡CPh in toluene. The increase in the electron density on the ruthenium atoms from $[Ru_2(\mu\text{-}CO)(CO)_4\{\mu\text{-}(RO)_2PN(Et)P(OR)_2\}_2]$ (R = Me, Pr^i) to $[Ru_2(\mu\text{-}CO)(CO)_4(\mu\text{-}Me_2PCH_2PMe_2)_2]$ is undoubtedly the major factor for the less electron-deficient alkyne, diphenylacetylene, reacting with the latter diruthenium species. The compound contributing to the red colour described was later established to be the co-ordinatively unsaturated diruthenium species $[Ru_2(CO)_4\{\mu\text{-}(RO)_2PN(Et)P(OR)_2\}_2]$, the synthesis and reactivity of which are discussed in Chapter 6.

5.3 MECHANISTIC STUDIES FOR THE FORMATION OF THE ALKENDIYL- AND VINYLIDENE-BRIDGED ISOMERS

It was found that the formation of the alkendiyl- and vinylidene-bridged complexes of the type $[Ru_2(CO)_4(\mu\text{-}\sigma^2\text{-}R'C{=}CR'')\{\mu\text{-}(RO)_2PN(Et)P(OR)_2\}_2]$ (R = Me, Pr^i; R′ = R″ = H, CO_2Me; R′ = H, R″ = Me, CO_2Me) and $[Ru_2(CO)_4(\mu\text{-}\eta^1\text{-}C{=}CHR')\{\mu\text{-}(RO)_2PN(Et)P(OR)_2\}_2]$ (R = Me, Pr^i; R′ = H, Me, Ph, CO_2Me) respectively, from $[Ru_2(\mu\text{-}CO)(CO)_4\{\mu\text{-}(RO)_2PN(Et)P(OR)_2\}_2]$ (R = Me, Pr^i) are irreversible, in that passage of carbon monoxide through solutions of these complexes at elevated temperatures does not lead to the formation of the parent diruthenium species $[Ru_2(\mu\text{-}CO)(CO)_4\{\mu\text{-}(RO)_2$-

$PN(Et)P(OR)_2\}_2]$.

It was also shown that the mechanism for the formation of both the above alkendiyl- and vinylidene-bridged isomers is a dissociative one, involving the loss of carbon monoxide. This is evidenced by the isolation of the tetracarbonyl co-ordinatively unsaturated species $[Ru_2(CO)_4\{\mu\text{-}(Pr^iO)_2PN(Et)P(OPr^i)_2\}_2]$ (*vide infra*), and its reactivity towards a range of alkynes. Significantly, reaction of $[Ru_2(CO)_4\text{-}\{\mu\text{-}(Pr^iO)_2PN(Et)P(OPr^i)_2\}_2]$ with HC≡CH, HC≡CMe, HC≡CPh and $HC{\equiv}CCO_2Me$ was found to proceed rapidly at room temperature. The ratios of the alkendiyl- and vinylidene-bridged isomers formed were essentially the same as those found for the reactions of the parent pentacarbonyl species $[Ru_2(\mu\text{-}CO)(CO)_4\{\mu\text{-}(Pr^iO)_2PN(Et)P(OPr^i)_2\}_2]$ with these alkynes. The tetracarbonyl co-ordinatively unsaturated species $[Ru_2(CO)_4\{\mu\text{-}(RO)_2\text{-}PN(Et)P(OR)_2\}_2]$ (R = Me, Pr^i) are thus shown to be intermediates in the formation of both the alkendiyl- and vinylidene-bridged isomers in the reactions of $[Ru_2(\mu\text{-}CO)(CO)_4\{\mu\text{-}(RO)_2PN(Et)P(OR)_2\}_2]$ with alkynes. This eliminates dimetallacyclopropenone compounds of the type $[Ru_2(CO)_4(\mu\text{-}C_2\text{-}R'R''CO)\{\mu\text{-}(RO)_2PN(Et)P(OR)_2\}_2]$ as possible intermediates in the formation of these species.

It has also been unequivocally established that formation of the vinylidene-bridged isomers of the type $[Ru_2(CO)_4(\mu\text{-}\eta^1\text{-}C{=}CHR')\{\mu\text{-}(RO)_2PN\text{-}(Et)P(OR)_2\}_2]$ (R = Me, Pr^i; R′ = H, Me, Ph, CO_2Me) are not formed via alkendiyl-bridged species of the type $[Ru_2(CO)_4(\mu\text{-}\sigma^2\text{-}HC{=}CR')\{\mu\text{-}(RO)_2P\text{-}N(Et)P(OR)_2\}_2]$ as intermediate. This is evidenced by, as discussed above, the ratios of alkendiyl- and vinylidene-bridged isomers being invariant to both reaction temperature and, more importantly, to reaction time. Also, the isolation of pure $[Ru_2(CO)_4(\mu\text{-}\sigma^2\text{-}HC{=}C\text{-}CO_2Me)\{\mu\text{-}(Pr^iO)_2PN(Et)P(OPr^i)_2\}_2]$ by fractional crystallization, and the

observation of its inability to isomerise to the vinylidene-bridged isomer at elevated temperatures, further confirms the absence of an interconversion process between the alkendiyl- and vinylidene-bridged isomers (*vide supra*).

The reactions of the unsaturated species $[Ru_2(CO)_4\{\mu\text{-}(Pr^iO)_2PN(Et)P(OPr^i)_2\}_2]$ with $HC{\equiv}CCO_2Me$, $PhC{\equiv}CH$ and $MeO_2CC{\equiv}CCO_2Me$ in C_6D_6 were monitored by means of $^{31}P\{^1H\}$ and ^1H nmr spectroscopy. The ^1H nmr spectrum of the monitored reaction of $[Ru_2(CO)_4\{\mu\text{-}(Pr^iO)_2PN(Et)P(OPr^i)_2\}_2]$ with $PhC{\equiv}CH$ exhibited triplets at -8.06 and -8.98 ppm while that of the reaction of $[Ru_2(CO)_4\{\mu\text{-}(Pr^iO)_2PN(Et)P(OPr^i)_2\}_2]$ with $HC{\equiv}C\text{-}CO_2Me$ exhibited triplets at -6.54 and -8.00 ppm. These results are interpreted in terms of the formation of the vinylidene-bridged isomers occurring via terminally-bonded hydrido intermediates. It is proposed that the first step [Scheme 5.4, PATHWAY (ii)] in this reaction involves either the co-ordination of the alkyne to a single ruthenium atom [Scheme 5.4, PATHWAY (iia)] followed by an intramolecular oxidative addition of the alkyne to give an intermediate containing a hydrido as well as a σ-bonded alkynyl ligand co-ordinated to the same ruthenium atom. Alternatively, the first step in this reaction may involve the co-ordination of the alkyne in the bridging mode perpendicular to the ruthenium-ruthenium vector [Scheme 5.4, PATHWAY (iib)] followed by its intramolecular oxidative addition to afford an intermediate in which the hydrido and alkynyl ligands are bonded to different ruthenium atoms.

The $^{31}P\{^1H\}$ and ^1H nmr spectra of the monitored reaction of $[Ru_2(CO)_4\{\mu\text{-}(Pr^iO)_2PN(Et)P(OPr^i)_2\}_2]$ with $MeO_2CC{\equiv}CCO_2Me$ did not provide evidence for the formation of any intermediates. This is interpreted in terms of the formation of the alkendiyl-bridged species occurring by addition of the alkyne across the ruthenium-ruthenium bond [Scheme 5.4, PATHWAY (i)].

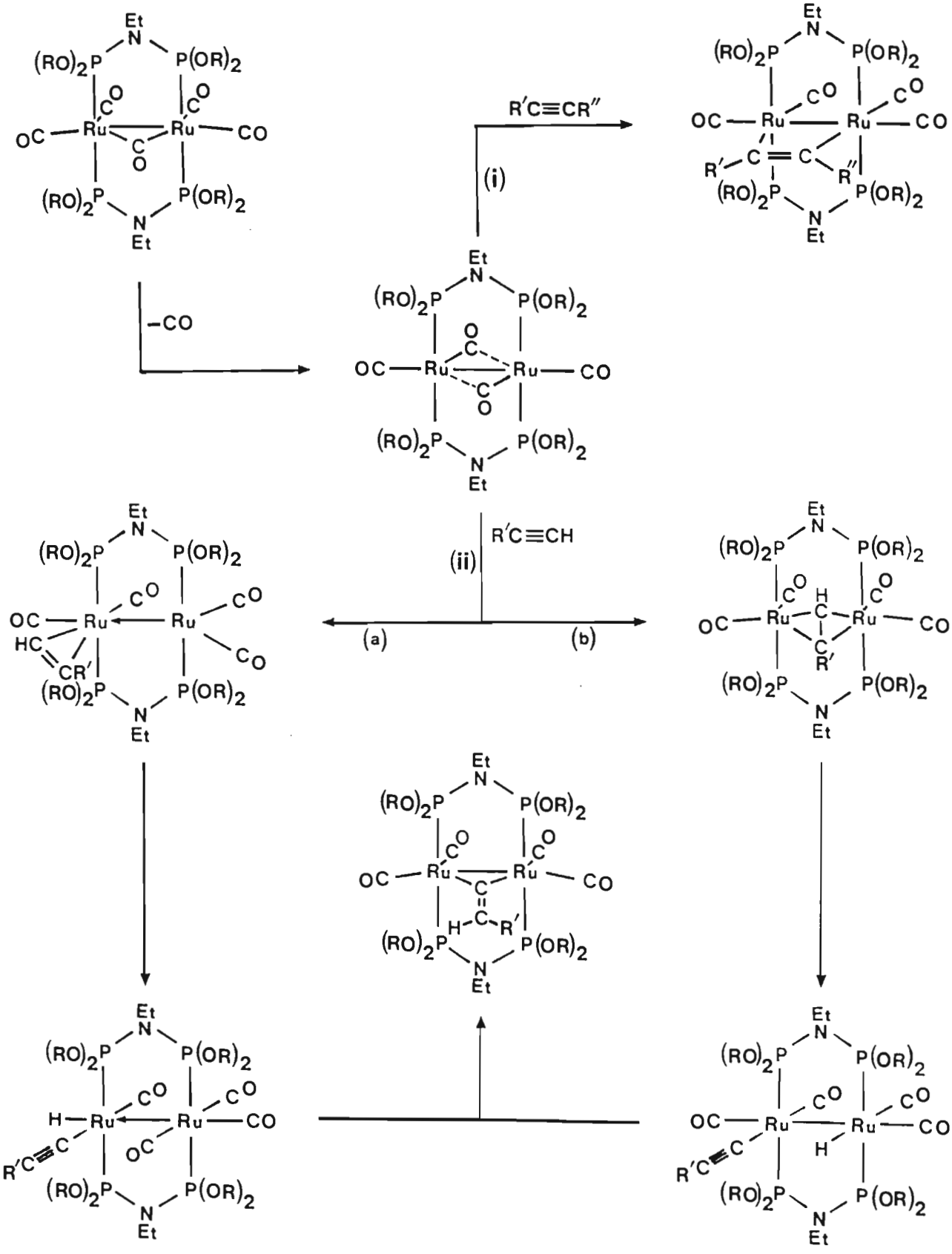

R = Me or Pr^{i}
R′ = H, Me, Ph or C(O)OMe
R″ = H or C(O)OMe

Scheme 5.4

5.4 PROTONATION STUDIES OF THE VINYLIDENE-BRIDGED SPECIES $[Ru_2(CO)_4(\mu\text{-}\eta^1\text{-}C{=}CHPh)\{\mu\text{-}(Pr^iO)_2PN(Et)P(OPr^iR)_2\}_2]$

In order to establish the preferred site of electrophilic attack on vinylidene-bridged complexes of the type $[Ru_2(CO)_4(\mu\text{-}\eta^1\text{-}C{=}CHR')\{\mu\text{-}(RO)_2PN(Et)P(OR)_2\}_2]$ (R = Me or Pr^i; R' = H, Me or Ph) by protons, the reaction of the phenyl vinylidene derivative $[Ru_2(CO)_4(\mu\text{-}\eta^1\text{-}C{=}CHPh)\{\mu\text{-}(Pr^iO)_2PN(Et)P(OPr^i)_2\}_2]$ with $HBF_4.OEt_2$ was investigated.

It was found that addition of excess $HBF_4.OEt_2$ to a solution of $[Ru_2(CO)_4(\mu\text{-}\eta^1\text{-}C{=}CHPh)\{\mu\text{-}(Pr^iO)_2PN(Et)P(OPr^i)_2\}_2]$ in ether results in the precipitation of a yellow solid from the solution. This solid was isolated and characterized as the μ-vinyl species $[Ru_2(CO)_4\{\mu\text{-}\eta^1,\eta^2\text{-}C(H){=}CHPh\}\{\mu\text{-}(Pr^iO)_2PN(Et)P(OPr^i)_2\}_2]BF_4$ (**68**). The infrared spectrum of this compound in the C-O stretching region exhibits a four-line pattern typical of a monocationic tetracarbonyl species. The $^{31}P\{^1H\}$ nmr spectrum, measured in CD_2Cl_2, exhibits an AA'BB' pattern of peaks centred at 135.54 ppm, reflecting the compound to have a asymmetric structure. The presence of a μ-vinyl group as opposed to a compound containing a μ-alkylidyne ligand was confirmed from the $^{13}C\{^1H\}$ nmr spectrum of the product. This spectrum exhibits two quintets at 94.71 and 144.01 ppm with a DEPT analysis showing a single proton to be bonded to each of the carbon atoms giving rise to these resonances. The ^1H nmr spectrum exhibits two broad multiplets at 5.50 and 8.30 ppm; the integrals of each of these corresponds to one proton, and are therefore assigned to the two protons of the vinyl group. The structure of $[Ru_2(CO)_4\{\mu\text{-}\eta^1,\eta^2\text{-}C(H){=}CHPh\}\{\mu\text{-}(Pr^iO)_2PN(Et)P(OPr^i)_2\}_2]BF_4$ was established unequivocally by means of single crystal X-ray structure determination; the stereochemistry of the cation is shown in Figure 5.11. The two ruthenium atoms, which are separated by a distance of 2.828(1)Å,

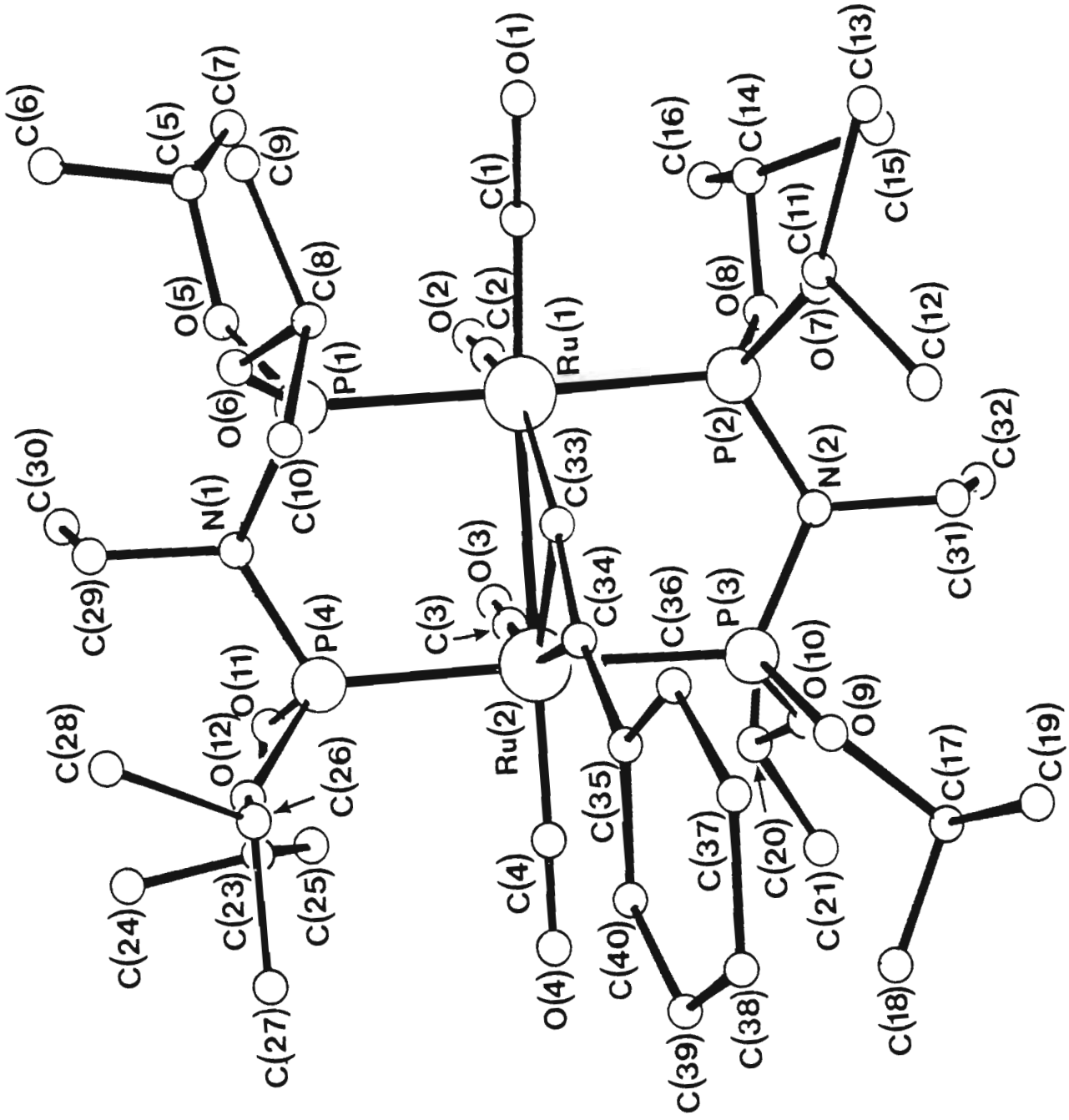

Figure 5.11:

Structure of $[Ru_2(CO)_4(\mu\text{-}\eta^1,\eta^2\text{-}C(H)=CHPh)\{\mu\text{-}(Pr^iO)_2PN(Et)P(OPr^i)_2\}_2]^+$

are bridged by a vinyl ligand as well as by two diphosphazane ligands *trans* disposed with respect to each other. In addition, two terminal carbonyl ligands are bonded to each ruthenium, one axially and the other equatorially. The cation adopts an eclipsed configuration, as reflected by P(1)-Ru(1)-Ru(2)-P(4) and P(2)-Ru(1)-Ru(2)-P(3) torsion angles of 6.8 and 4.9° respectively.

The bonding of vinyl fragments across metal-metal bonds has usually been described in terms of involving both σ- and π-donation[224,225] as shown in I below; description II has been used in cases where the metal-bridging carbon distances have been shown to be approximately equal, thus emphasizing the μ-carbenoid nature of this carbon.[226] The nmr

(I) (II)

Figure 5.12

spectroscopic properties of the bridging carbon and its attached hydrogen in complexes of this type (II) are considerably more downfield in frequency in relation to that of non-bridging carbon and its attached proton. The nmr spectroscopic properties of the bridging carbon in $[Ru_2(CO)_4\{\mu\text{-}\eta^1,\eta^2\text{-}C(H)=CHPh\}\{\mu\text{-}(Pr^iO)_2PN(Et)P(OPr^i)_2\}_2]^+$ ($^{13}C\{^1H\}$ δ 144.01 ppm) and its attached proton (^1H δ 8.30 ppm) and in particular the relatively upfield frequencies of the resonances under consideration are best interpreted in terms of description I. The carbon-metal bond lengths of the bridging carbon in μ-vinyl groups of this type are anticipated to be unequal. The μ-vinyl Ru-C distances in the cation $[Ru_2(CO)_4\{\mu\text{-}\eta^1,\eta^2\text{-}C(H)=CHPh\}\{\mu\text{-}(Pr^iO)_2PN(Et)\text{-}P(OPr^i)_2\}_2]^+$ follow these

trends with Ru(1)-C(33) 2.008(11)Å and Ru(2)-C(33) 2.261(10)Å. The non-bridging carbon-metal distance {Ru(2)-C(34) 2.382(11)Å} is, as expected, longer than those observed for the bridging carbon-metal distances. The C(33)-C(34) distance {1.24(2)Å} is that associated with a carbon-carbon double bond, providing further support for description I above. These observations contrast to those observed for the μ-vinyl species $[Fe_2(CO)_2(\mu\text{-}CO)(\mu\text{-}CHCH_2)(\eta\text{-}C_5H_5)_2]BF_4$ [227] in which the bridging carbon of the μ-vinyl ligand was established to bridge the two iron atoms symmetrically, as in description II above. Furthermore, the C-C distance {1.40(2)Å} of the vinyl ligand, in this compound is compatible with a C-C bond order of between one and two.

It is proposed that the formation of the μ-vinyl species $[Ru_2(CO)_4\{\mu\text{-}\eta^1,\eta^2\text{-}C(H)=CHPh\}\{\mu\text{-}(Pr^iO)_2PN(Et)P(OPr^i)_2\}_2]^+$ by protonation of the vinylidene species $[Ru_2(CO)_4\{\mu\text{-}\eta^1\text{-}C=CHPh\}\{\mu\text{-}(Pr^iO)_2PN(Et)P(OPr^i)_2\}_2]$ occurs via an alkenylidene hydrido species $[Ru_2(CO)_4(H)(C=CHPh\}\{\mu\text{-}(Pr^iO)_2PN(Et)P(OPr^i)_2\}_2]^+$ as intermediate, as illustrated in Scheme 5.5.

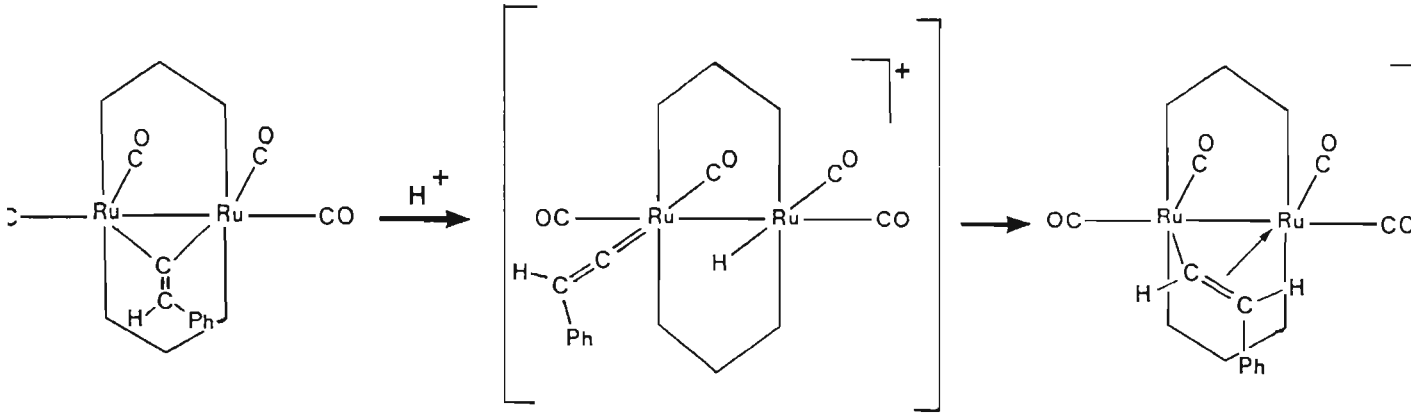

Scheme 5.5

The reaction of $HBF_4.OEt_2$ with $[Ru_2(CO)_4\{\mu\text{-}\eta^1\text{-}C=CHPh\}\{\mu\text{-}(Pr^iO)_2PN(Et)P(OPr^i)_2\}_2]$ has been monitored by means of $^{31}P\{^1H\}$ and ^1H nmr spectroscopy and was found to be extremely rapid, with no intermediates being

observed.

5.5 EXPERIMENTAL

5.5.1 *Synthesis of* $[Ru_2(CO)_4(\mu\text{-}\sigma^2\text{-}HC{=}CH)\{\mu\text{-}(R'O)_2PN(Et)P(OR')_2\}\{\mu\text{-}(R''O)_2PN(Et)P(OR'')_2\}]$ {$R' = R'' = Me$ (**52**); $R' = R'' = Et$ (**58**); $R' = R'' = Pr^i$ (**54**); $R' = Me$, $R'' = Pr^i$ (**56**)} *and* $[Ru_2(CO)_4(\mu\text{-}\eta^1\text{-}C{=}CH_2)\{\mu\text{-}(R'O)_2PN(Et)P(OR')_2\}\{\mu\text{-}(R''O)_2PN(Et)P(OR'')_2\}]$ {$R' = R''$ = Me (**53**); $R' = R'' = Et$ (**59**); $R' = R'' = Pr^i$ (**55**); $R' = Me$, $R'' = Pr^i$ (**57**)}

A stream of acetylene was passed slowly through a solution of $[Ru_2(\mu\text{-}CO)(CO)_4\{\mu\text{-}(R'O)_2PN(Et)P(OR')_2\}\{\mu\text{-}(R''O)_2PN(Et)P(OR'')_2\}]$ ($R' = R''$ = Me : 0.300 g, 0.375 mmol; $R' = R'' = Et$: 0.300 g, 0.329 mmol; $R' = R'' = Pr^i$: 0.300 g, 0.293 mmol; $R' = Me$, $R'' = Pr^i$: 0.300 g. 0.329 mmol) in toluene (15 ml) at 80°C for one hour. The pale yellow solution was filtered through a glass fibre fritte and the volume of the filtrate was concentrated under reduced pressure to *ca.* 3 ml. Crystallization of the title compounds as pale yellow crystals was achieved by addition of methanol (5 ml) to the solution which was then set aside at -10°C . Yield: 80-95%. *M* (**52**) = *M* (**53**) = 798.6 g/mol; *M* (**58**) = *M* (**59**) = 910.8 g/mol; *M* (**54**) = *M* (**55**) = 1023.0 g/mol; *M* (**56**) = *M* (**57**) = 910.8 g/mol.

5.5.2 *Synthesis of* $[Ru_2(CO)_4(\mu\text{-}\sigma^2\text{-}HC{=}CMe)\{\mu\text{-}(RO)_2PN(Et)P(OR)_2\}_2]$ {$R = Me$ (**60**)} *and* $[Ru_2(CO)_4(\mu\text{-}\eta^1\text{-}C{=}CHMe)\{\mu\text{-}(RO)_2PN(Et)P(OR)_2\}_2]$ {$R = Me$ (**61**); $R = Pr^i$ (**62**)}

A stream of propyne was passed slowly through a solution of $[Ru_2(\mu\text{-}CO)(CO)_4\{\mu\text{-}(RO)_2PN(Et)P(OR)_2\}_2]$ (R = Me : 0.200 g, 0.250 mmol; R = Pr^i : 0.200 g, 0.195 mmol) in toluene (15 ml) at 80°C for one hour.

The pale yellow solution was filtered through a glass fibre fritte and the volume of the filtrate was concentrated under reduced pressure to *ca.* 3 ml, to which methanol (5 ml) was added. The solution was cooled to -10°C to effect the separation of the title compounds in crystalline form. Yield: 80-90%. *M* (**60**) = *M* (**61**) = 812.6 g/mol; *M* (**62**) = 1037.1 g/mol.

5.5.3 *Synthesis of* $[Ru_2(CO)_4(\mu\text{-}\sigma^2\text{-}HC{=}CCO_2Me)\{\mu\text{-}(RO)_2PN(Et)P(OR)_2\}_2]$ *{R = Me (**63**); R = Pr^i (**64**)} and* $[Ru_2(CO)_4(\mu\text{-}\eta^1\text{-}C{=}CHCO_2Me)\{\mu\text{-}(RO)_2PN(Et)P(OR)_2\}_2]$ *{R = Pr^i (**65**)*

A solution of $[Ru_2(\mu\text{-}CO)(CO)_4\{\mu\text{-}(RO)_2PN(Et)P(OR)_2\}_2]$ (R = Me : 0.200 g, 0.250 mmol; R = Pr^i : 0.250 g, 0.244 mmol) and methyl propiolate (0.025 g, 0.298 mmol) in toluene (15 ml) was heated at 80°C for one hour. All volatiles were removed under reduced pressure and the yellow oil which remained was washed with cold methanol (3 x 3 ml, -10°C). The solid residue remaining was dissolved in toluene (3 ml) and methanol (5 ml) was added. The yellow microcrystalline product which separated, was washed with cold methanol (3 ml, -10°C) and dried under vacuum. Yield: 75-85%. *M* (**63**) = 856.60 g/mol; *M* (**64**) = *M* (**65**) = 1081.1 g/mol.

5.5.4 *Synthesis of* $[Ru_2(CO)_4(\mu\text{-}\sigma^2\text{-}MeO_2CC{\equiv}CCO_2Me)\{\mu\text{-}(RO)_2PN(Et)P(OR)_2\}_2]$ *{R = Me (**66**); R = Pr^i (**67**)}*

A solution of $[Ru_2(\mu\text{-}CO)(CO)_4\{\mu\text{-}(RO)_2PN(Et)P(OR)_2\}_2]$ (R = Me : 0.200 g, 0.250 mmol; R = Pr^i : 0.275 g, 0.269 mmol) and dimethyl acetylenedicarboxylate (0.040 g, 0.282 mmol) in toluene (15 ml) was heated at 80°C for one hour. All volatiles were removed under reduced pressure and the yellow solid which remained was washed with cold methanol (3 x 3 ml, -10°C). The solid residue remaining was dissolved in toluene (3 ml) and

crystallization of the title compounds as pale yellow crystals was achieved by addition of methanol to the solution which was then set aside at -10°C. Yield: 80-90%. *M* (**66**) = 914.6 g/mol; *M* (**67**) =1139.1 g/mol.

5.5.5 *Synthesis of* $[Ru_2(CO)_4\{\mu\text{-}\eta^1,\eta^2\text{-}C(H)=CHPh\}\{\mu\text{-}(Pr^iO)_2PN(Et)P\text{-}(OPr^i)_2\}_2]BF_4$ (**68**)

An excess of $HBF_4.OEt_2$ (0.100 g, 60% solution in Et_2O) was added to a solution of $[Ru_2(CO)_4(\mu\text{-}\eta^1\text{-}C=CHPh)\{\mu\text{-}(Pr^iO)_2PN(Et)P(OPr^i)_2\}_2]$ (0.200 g, 0.182 mmol) in diethyl ether (10 ml) and the mixture stirred for 20 minutes, during which time a pale yellow solid separated from solution. The volume of the solution was reduced *in vacuo* and pentane was added to effect further precipitation. The precipitate was filtered, washed with cold ether/pentane (1:1) and dried under vacuum. The title compound was obtained in crystalline form by crystallization from chloroform/pentane. Yield: 80%. *M* (**68**) = 1187.0 g/mol.

5.5.6 *Crystal Structure Determination of* $[Ru_2(CO)_4(\mu\text{-}\sigma^2\text{-}HC=CH)\{\mu\text{-}(MeO)_2PN(Et)P(OMe)_2\}_2]$ (**52**) *and* $[Ru_2(CO)_4\{\mu\text{-}\eta^1,\eta^2\text{-}C(H)=CHPh\}\{\mu\text{-}(Pr^iO)_2PN(Et)P(OPr^i)_2\}_2]BF_4$ (**68**)

The method for the intensity data collections is described in Appendix A.3(a) while the general approach to the structure solutions is given in Appendix A.3(b). For (**52**) the crystallographic data are given in Table 5.6, the fractional co-ordinates and isotropic thermal parameters in Table 5.7, the anisotropic thermal parameters in Table 5.8, the interatomic distances in Table 5.9, and the interatomic angles in Table 5.10. For each asymmetric unit one molecule lies in a general position and another lies across a centre of inversion, leading to disorder of

the latter. For (**68**) the crystallographic data are given in Table 5.6, the fractional co-ordinates and isotropic thermal parameters in Table 5.11, the anisotropic thermal parameters in Table 5.12, the interatomic distances in Table 5.13, and the interatomic angles in Table 5.14. The observed and calculated structure factors may be found on microfiche in an envelope fixed to the inside cover of the thesis.

TABLE 5.2

MICROANALYTICAL DATA

COMPLEX	ANALYSIS : Found (Calculated) % %C	%H	%N
52 $[Ru_2(CO)_4(\mu\text{-}\sigma^2\text{-}HC{=}CH)\{\mu\text{-}(MeO)_2PN(Et)P(OMe)_2\}_2]$	27.78(27.08)	4.49(4.55)	3.24(3.51)
and **53** $[Ru_2(CO)_4(\mu\text{-}\eta^1\text{-}C{=}CH_2)\{\mu\text{-}(MeO)_2PN(Et)P(OMe)_2\}_2]$			
54 $[Ru_2(CO)_4(\mu\text{-}\sigma^2\text{-}HC{=}CH)\{\mu\text{-}(Pr^iO)_2PN(Et)P(OPr^i)_2\}_2]$	39.86(39.91)	6.61(6.67)	2.47(2.74)
and **55** $[Ru_2(CO)_4(\mu\text{-}\eta^1\text{-}C{=}CH_2)\{\mu\text{-}(Pr^iO)_2PN(Et)P(OPr^i)_2\}_2]$			
56 $[Ru_2(CO)_4(\mu\text{-}\sigma^2\text{-}HC{=}CH)\{\mu\text{-}(MeO)_2PN(Et)P(OMe)_2\}\{\mu\text{-}(Pr^iO)_2PN(Et)P(OPr^i)_2\}]$	34.46(34.28)	5.86(5.77)	2.82(3.07)
and **57** $[Ru_2(CO)_4(\mu\text{-}\eta^1\text{-}C{=}CH_2)\{\mu\text{-}(MeO)_2PN(Et)P(OMe)_2\}$-$\{\mu\text{-}(Pr^iO)_2PN(Et)P(OPr^i)_2\}]$			
58 $[Ru_2(CO)_4(\mu\text{-}\sigma^2\text{-}HC{=}CH)\{\mu\text{-}(EtO)_2PN(Et)P(OEt)_2\}_2]$	34.46(34.28)	5.81(5.77)	2.82(3.07)
and **59** $[Ru_2(CO)_4(\mu\text{-}\eta^1\text{-}C{=}CH_2)\{\mu\text{-}(EtO)_2PN(Et)P(OEt)_2\}_2]$			
60 $[Ru_2(CO)_4(\mu\text{-}\sigma^2\text{-}HC{=}CMe)\{\mu\text{-}(MeO)_2PN(Et)P(OMe)_2\}_2]$	28.51(28.08)	4.87(4.72)	3.38(3.45)
and **61** $[Ru_2(CO)_4(\mu\text{-}\eta^1\text{-}C{=}CHMe)\{\mu\text{-}(MeO)_2PN(Et)P(OMe)_2\}_2]$			
62 $[Ru_2(CO)_4(\mu\text{-}\eta^1\text{-}C{=}CHMe)\{\mu\text{-}(Pr^iO)_2PN(Et)P(OPr^i)_2\}_2]$	41.50(40.53)	6.80(6.81)	2.68(2.70)
63 $[Ru_2(CO)_4(\mu\text{-}\sigma^2\text{-}HC{=}CCO_2Me)\{\mu\text{-}(MeO)_2PN(Et)P(OMe)_2\}_2]$	28.11(28.04)	4.50(4.48)	3.22(3.27)
64 $[Ru_2(CO)_4(\mu\text{-}\sigma^2\text{-}HC{=}CCO_2Me)\{\mu\text{-}(Pr^iO)_2PN(Et)P(OPr^i)_2\}_2]$	39.32(39.99)	6.45(6.54)	2.85(2.59)
and **65** $[Ru_2(CO)_4(\mu\text{-}\eta^1\text{-}C{=}CHCO_2Me)\{\mu\text{-}(Pr^iO)_2PN(Et)P(OPr^i)_2\}_2]$			
66 $[Ru_2(CO)_4(\mu\text{-}\sigma^2\text{-}MeO_2CC{=}CCO_2Me)\{\mu\text{-}(MeO)_2PN(Et)P(OMe)_2\}_2]$	28.84(28.88)	4.37(4.42)	3.09(3.06)
67 $[Ru_2(CO)_4(\mu\text{-}\sigma^2\text{-}MeO_2CC{=}CCO_2Me)\{\mu\text{-}(Pr^iO)_2PN(Et)P(OPr^i)_2\}_2]$	39.98(40.06)	6.28(6.38)	2.11(2.46)

Table 5.2 (continued)

COMPLEX	ANALYSIS : Found (Calculated) % %C	%H	%N
68 $[Ru_2(CO)_4\{\mu\text{-}\eta^1,\eta^2\text{-}C(H)=CHPh\}\{\mu\text{-}(Pr^iO)_2PN(Et)P(OPr^i)_2\}_2]BF_4$	40.61(40.47)	6.33(6.21)	2.29(2.36)

TABLE 5.3

INFRARED SPECTROSCOPIC DATA

COMPLEX	ν(C≡O), cm^{-1}				OTHER	MEDIUM	COLOUR
52 and	2001(s)	1964(vs)	1933(s)	1915(s)		Cyclohexane	Yellow
53	2000(s)	1963(vs)	1931(s)	1902(s)		Nujol	
54 and	1991(s)	1947(s)	1906(s)	1890(s)		Cyclohexane	Yellow
55	1989(s)	1942(s)	1904(s)	1882(s)		Nujol	
56 and	1998(s)	1957(s)	1923(ms)	1907(s)		Cyclohexane	Yellow
57	1990(s)	1951(s)	1921(sh)	1908(s)	1891(s)	Nujol	
58 and	1998(s)	1961(vs)	1928(ms)	1908(s)		Cyclohexane	Yellow
59	2000(s)	1959(s)	1919(ms)	1904(s)		Nujol	
60 and	1992(s)	1953(s)	1917(s)	1897(a)		Cyclohexane	Yellow
61	1987(s)	1952(s)	1917(s)	1898(s)		Nujol	
62	1986(s)	1943(s)	1905(s)	1888(s)		Cyclohexane	Yellow
	1976(s)	1939(s)	1901(s)	1881(s)		Nujol	
63	2007(s)	1973(vs)	1942(s)	1923(s)	1674(m), ν(C=O)	Cyclohexane	Yellow
	1999(s)	1958(vs)	1936(s)	1915(s)	1672(m), ν(C=O)	Nujol	
64 and	2000(s)	1963(vs)	1930(ms)	1908(s)	1665(m), ν(C=O)	Cyclohexane	Yellow
65	2000(s)	1968(s)	1928(ms)	1901(s)	1670(m), ν(C=O)	Nujol	
66	2000(s)	1978(vs)	1949(s)	1927(ms)	1675(ms), ν(C=O)	CCl_4	Yellow

TABLE 5.3 (continued)

COMPLEX	ν(C≡O), cm^{-1}				OTHER	MEDIUM	COLOUR
67	2001(s)	1967(vs)	1940(s)	1917(s)	1678(ms), ν(C=O)	Cyclohexane	Yellow
	2000(s)	1960(vs)	1938(s)	1910(s)	1670(ms), ν(C=O)	Nujol	
68	2033(s)	2001(vs)	1973(s)	1951(s)		CH_2Cl_2	Pale yellow
	2034(s)	2002(vs)	1970(ms)	1951(ms)			

vs = very strong, s = strong, ms = medium-strong, m = medium, sh = shoulder.

TABLE 5.4

^{1}H AND $^{31}P\{^{1}H\}$ NMR SPECTROSCOPIC DATA

COMPLEX	δ ^{1}H (ppm)	δ $^{31}P\{^{1}H\}$ (ppm)
52 and **53**	1.07t (6H); 3.02-3.21m (4H); 3.41-3.76m (24H); 7.11s (2H); 6.51q (w) (^{4}J(PC) 2.4Hz)	155.7(s,w), 153.00(s)[a]
54 and **55**	1.11-1.35m (54H); 3.02-3.16m (4H); 4.50-5.03m (8H); 6.34q (2H); (^{4}J(PH) 2.4Hz); 7.02s (w)	148.83(s), 146.10(s,w)[a]
56 and **57**	1.11-1.34m (30H); 3.04-3.30m (4H); 3.57-3.82m (12H); 4.50-5.13m (4H); 6.52q (^{4}J(PH) 2.4Hz) and 7.10s	153.78 (AA'BB')[c] 151.03 (AA'BB')[b,d]
58 and **59**	1.11t (6H); 1.15-1.28m (24H); 3.03-3.17m (4H); 3.62-4.35m (16H); 6.36q (w) (^{4}J(PH) 2.4Hz) and 7.01s	150.54(s)[c], 147.56(s)[a,d]
60 and **61**	1.07-1.20m (6H); 1.60s and 1.85-1.90m (3H); 2.96-3.25m (4H); 3.55-3.82m (24H); 6.43-6.61m and 7.25s (2H)	155.51 (AA'BB')[d], 152.91(s)[a,c]
62	1.16-1.33m (54H); 1.83-1.92m (3H); 3.00-3.20m (4H); 4.56-5.13m (8H); 6.20-6.34m (1H)	148.44 (AA'BB')[a]
63	1.06t (6H); 2.92-3.08m (4H); 3.50-3.64m (27H); 9.08s (1H)	151.63 (AA'BB')[a]
64 and **65**	1.10-1.45m (54H); 3.00-3.22m (4H); 3.54s and 3.59s (3H); 4.52-4.87m (8H); 7.35q (w) and 9.12s (1H)	144.09 (AA'BB')[c] 147.96 (AA'BB')[a,d]

TABLE 5.4 (Continued)

COMPLEX	δ ^{1}H (ppm)	δ $^{31}P\{^{1}H\}$ (ppm)
67	1.10-1.28m (54H); 2.90-3.10m (4H); 3.41s (6H); 4.40-5.05m (8H)	140.91(s)[a]
68	1.04-1.55m (54H); 3.15-3.51m (4H); 4.52-5.00m (8H); 5.45-5.60m (1H) 7.18-7.60m (5H); 8.20-8.44m (1H)	135.55 (AA'BB')[a]

t = triplet, m = multiplet, q = quintet, s = singlet, w = weak, AA'BB' = midpoint of AA'BB' pattern
[a]Recorded in $CDCl_3$, [b]Recorded in CD_2Cl_2, [c]Minor isomer, [d]Major isomer.

TABLE 5.5

$^{13}C\{^{1}H\}$ NMR SPECTROSCOPIC DATA

COMPLEX	δ $^{13}C\{^{1}H\}$ (ppm)[a]
52 and **53**	16.72s ($-NCH_2\mathit{C}H_3$); 38.08s ($-N\mathit{C}H_2CH_3$); 52.34s ($-O\mathit{C}H_3$); 53.98s ($-O\mathit{C}H_3$); 120.96q ($H\mathit{C}=\mathit{C}H$) (^2J(PC) 3.9Hz); 197.90q ($-\mathit{C}\equiv O$) (^2J(PC) 9.0 Hz); 206.14q ($-\mathit{C}\equiv O$) (^2J(PC) 6.3 Hz)
54 and **55**	17.82s ($-NCH_2\mathit{C}H_3$); 23.74-24.40m ($-OCH(\mathit{C}H_3)_2$); 37.79s ($-N\mathit{C}H_2CH_3$); 69.17-69.88m ($-O\mathit{C}H(CH_3)_2$); 131.88q ($C=\mathit{C}H_2$) (^3J(PC) 4.1 Hz); 203.83q ($-\mathit{C}\equiv O$) (^2J(PC) 10.3 Hz); 210.70q ($-\mathit{C}\equiv O$) (^2J(PC) 6.0 Hz); 232.67q ($\mathit{C}=CH_2$) (^2J(PC) 16.4 Hz)
56 and **57**	16.71s, 16.75s ($-NCH_2\mathit{C}H_3$); 23.84-24.26m ($-OCH(\mathit{C}H_3)_2$); 38.16s, 38.22s ($-N\mathit{C}H_2CH_3$); 52.36-54.89m ($O\mathit{C}H_3$); 69.60-70.34m ($-O\mathit{C}H(CH_3)_2$); 121,60q ($H\mathit{C}=\mathit{C}H$) (^2J(PC) 3.6 Hz); 132.67q ($C=\mathit{C}H_2$) (^3J(PC) 4.0 Hz); 199.09q ($-\mathit{C}\equiv O$) (^2J(PC) 9.0 Hz); 202.76q ($-\mathit{C}\equiv O$) (^2J(PC) 10.0 Hz); 207.91q ($-\mathit{C}\equiv O$) (^2J(PC) 6.1 Hz); 209.91q ($-\mathit{C}\equiv O$) (^2J(PC) 6.6 Hz); 235.84q ($\mathit{C}=CH_2$) (^2J(PC) 16.0 Hz)
60 and **61**	16.53s, 16.66s ($-NCH_2\mathit{C}H_3$); 28.82s ($C=C\mathit{H}CH_3$); 29.72s ($HC=C\mathit{C}H_3$); 36.47s, 36.74s ($-N\mathit{C}H_2CH_3$); 52.20-53.80m ($-O\mathit{C}H_3$, $-OCH(\mathit{C}H_3)_2$); 120.56q ($H\mathit{C}=CCH_3$) (^2J(PC) 3.8 Hz); 132.50q ($HC=\mathit{C}CH_3$); 135.95q ($C=\mathit{C}HCH_3$) (^2J(PC) 4.1 Hz); 200.05-209.00m ($-\mathit{C}\equiv O$); 223.82q ($\mathit{C}=CHCH_3$) (^2J(PC) 16 Hz)
62	17.57s ($-NCH_2\mathit{C}H_3$); 23.66-24.55m ($-OCH(\mathit{C}H_3)_2$); 28.23s ($C=C\mathit{H}CH_3$); 37.35s ($-N\mathit{C}H_2CH_3$); 68.77-69.69m ($-O\mathit{C}H(CH_3)_2$); 134.58q ($C=\mathit{C}HCH_3$) (^3J(PC) 4.6 Hz); 203.59m ($-\mathit{C}\equiv O$); 210.00m ($-\mathit{C}\equiv O$); 221.84q ($\mathit{C}=CHCH_3$) (^2J(PC) 16.2 Hz)
66	16.77s ($-NCH_2\mathit{C}H_3$); 39.23s ($-N\mathit{C}H_2CH_3$); 50.98s ($-CO_2\mathit{C}H_3$); 52.69s and 53.25s ($-O\mathit{C}H_3$); 146.91q ($CH_3O_2C\mathit{C}=\mathit{C}CO_2CH_3$) ($^2J$(PC) 4.1 Hz); 173.95s ($\mathit{C}O_2CH_3$); 196.28q ($-\mathit{C}\equiv O$) ($^2J$(PC) 9.0 Hz); 206.39q ($-\mathit{C}\equiv O$) ($^2J$(PC) 7.2 Hz)

TABLE 5.5 (continued)

COMPLEX	δ $^{13}C\{^{1}H\}$ (ppm)[a]
67	17.41s ($-NCH_2\mathit{C}H_3$); 24.08-24.60m ($-OCH(\mathit{C}H_3)_2$); 38.75s ($-N\mathit{C}H_2CH_3$); 38.75s ($-N\mathit{C}H_2CH_3$); 50.66s ($-CO_2\mathit{C}H_3$); 69.40s and 71.05s ($-O\mathit{C}H(CH_3)_2$); 152.01q ($CH_3O_2C\mathit{C}=\mathit{C}CO_2CH_3$) ($^{2}J$(PC) 3.6 Hz); 173.30s ($\mathit{C}OCH_3$); 197.15q ($-\mathit{C}\equiv O$) ($^{2}J$(PC) 9.0 Hz); 209.30q ($-\mathit{C}\equiv O$) ($^{2}J$(PC) 7.1 Hz)
68	17.17s ($-NCH_2\mathit{C}H_3$); 22.45-24.88m ($-OCH(\mathit{C}H_3)_2$); 39.26s ($-N\mathit{C}H_2CH_3$); 71.83-74.72m ($-O\mathit{C}H(CH_3)_2$); 94.71q ($CH=\mathit{C}HPh$); 126.17-128.49m (C_6H_5); 144.01q ($\mathit{C}H=CHPh$)

s = singlet, m = multiplet, q = quintet

[a]Recorded in $CDCl_3$

TABLE 5.6

CRYSTAL DATA FOR

$[Ru_2(CO)_4(\mu\text{-}\sigma^2HC{=}CH)\{\mu\text{-}(MeO)_2PN(Et)P(OMe)_2\}_2]$ (**52**)

AND $[Ru_2(CO)_4(\mu\text{-}\eta,\eta^1\text{-}CH{=}C(H)Ph)\{\mu\text{-}(Pr^iO)_2PN(Et)P(OPr^i)_2\}_2]BF_4$ (**68**)

	52	**68**
Formula	$C_{18}H_{36}N_2O_{12}P_4Ru_2$	$C_{40}H_{73}BF_4N_2O_{12}P_4Ru_2$
Molecular mass	798.6	1187.0
Crystal dimensions, mm	0.35 x 0.35 x 0.27	0.38 x 0.15 x 0.16
Crystal system	monoclinic	triclinic
Space group	$P2_1/c$	$P\bar{1}$
a(Å)	9.844(6)	12.362(2)
b(Å)	25.126(4)	20.725(4)
c(Å)	18.914(3)	22.550(3)
$\alpha(°)$	90	77.72(1)
$\beta(°)$	96.89(4)	84.40(1)
$\gamma(°)$	90	89.07(1)
V(Å^3)	4644.3	5617.9
Z	6	4
D_c (g cm^{-3})	1.71	1.40
F(000)	2412	2468
λ(Mo-K_α) (Å)	0.71069	0.71069
μ(Mo-K_α) (cm^{-1})	12.13	7.54
Reflections measured	6886	16053
Unique reflections	5889	13186
Observed reflections [$I > 3\sigma(I)$]	5073	9937
Crystal stability	Decay = 5%	No decay
Absorption corrections	Applied	Applied
No. of parameters	286	291
R	0.076	0.078
R_w	0.101	0.094

TABLE 5.7: Fractional co-ordinates ($x10^4$) and equivalent isotropic temperature factors ($Å^2$, $x10^3$) for $[Ru_2(CO)_4(\mu\text{-}\sigma^2\text{-}HC{=}CH)\{\mu\text{-}(MeO)_2PN(Et)P(OMe)_2\}_2]$ (52)

	x/a	y/b	z/c	U_{eq}
Ru(1A)	473(1)	1864(1)	4809(1)	47(1)
Ru(2A)	-2326(1)	1525(1)	4680(1)	49(1)
P(1A)	191(3)	2111(1)	3631(2)	60(1)
P(2A)	804(3)	1543(1)	5953(1)	54(1)
P(3A)	-2003(3)	1225(1)	5830(2)	62(1)
P(4A)	-2572(3)	1762(2)	3496(2)	65(1)
O(1A)	3507(11)	2025(4)	4874(6)	93(3)*
O(2A)	-223(11)	2990(5)	5232(5)	98(3)*
O(3A)	-3260(11)	2609(4)	5185(6)	98(3)*
O(4A)	-5020(11)	932(4)	4419(6)	97(3)*
O(5A)	1403(9)	1962(4)	3169(5)	80(2)*
O(6A)	146(10)	2743(4)	3466(5)	82(2)*
O(7A)	988(9)	1974(3)	6580(5)	72(2)*
O(8A)	2175(8)	1201(3)	6176(4)	69(2)*
O(9A)	-2641(10)	1575(4)	6415(6)	92(3)*
O(10A)	-2661(10)	679(4)	6008(5)	90(3)*
O(11A)	-3335(10)	1356(4)	2937(6)	94(3)*
O(12A)	-3481(11)	2303(4)	3271(6)	95(3)*
N(1A)	-1244(11)	1927(4)	3106(6)	72(3)*
N(2A)	-440(9)	1169(4)	6241(5)	58(2)*
C(1A)	2329(12)	1949(4)	4823(6)	58(3)*
C(2A)	16(11)	2554(5)	5088(6)	60(3)*
C(3A)	-2942(12)	2202(5)	4973(6)	66(3)*
C(4A)	-3976(12)	1160(5)	4511(7)	67(3)*
C(5A)	1906(18)	1429(8)	3130(10)	108(5)*
C(6A)	1356(17)	3050(6)	3655(9)	93(4)*
C(7A)	2157(16)	2328(6)	6651(8)	88(4)*
C(8A)	2632(14)	794(5)	5762(7)	76(3)*
C(9A)	-4126(20)	1641(8)	6422(11)	117(6)*
C(10A)	-2618(17)	202(7)	5575(10)	104(5)*
C(11A)	-2920(18)	836(7)	2888(10)	104(5)*
C(12A)	-4868(19)	2309(7)	3365(10)	108(5)*
C(13A)	-1394(18)	2072(8)	2313(9)	105(5)*
C(14A)	-1008(24)	1701(10)	1888(13)	140(7)*
C(15A)	-160(15)	930(6)	7003(8)	90(4)*

TABLE 5.7 (continued)

C(16A)	317(19)	375(8)	7024(10)	113(5)*
C(17A)	289(12)	1044(5)	4461(7)	68(3)*
C(18A)	-1002(11)	899(4)	4410(6)	60(3)*
RuB	4710(2)	544(1)	-168(1)	104(1)
P(1B)	3684(5)	625(2)	848(3)	94(1)
P(2B)	5867(7)	477(2)	-1138(2)	107(1)
O(1B)	4125(14)	1689(6)	-518(8)	132(4)*
O(2B)	7684(27)	926(10)	708(14)	119(7)*
O(2B')	8283(28)	-286(11)	1046(15)	128(8)*
O(3B)	4432(12)	1032(5)	1481(7)	112(4)*
O(4B)	2253(16)	934(7)	793(9)	146(5)*
O(5B)	5311(20)	759(8)	-1851(10)	183(7)*
O(6B)	7476(20)	784(8)	-1115(10)	183(7)*
Nb	3461(13)	89(5)	1341(7)	96(4)*
C(1B)	4323(15)	1237(7)	-378(8)	89(4)*
C(2B)	6645(29)	800(12)	427(15)	77(7)*
C(2B')	7217(33)	-373(14)	687(17)	91(8)*
C(3B)	4616(22)	1567(8)	1314(12)	126(7)*
C(4B)	1126(29)	724(11)	342(15)	169(10)*
C(5B)	3879(23)	760(9)	-2081(12)	132(7)*
C(6B)	7645(33)	1328(15)	-912(18)	198(12)*
C(7B)	2677(27)	149(11)	2022(15)	159(9)*
C(8B)	3567(31)	238(13)	2718(17)	191(11)*
C(9B)	6298(25)	442(11)	547(14)	67(6)*
C(10B)	6576(30)	-12(13)	706(16)	87(8)*

* isotropic temperature factor.

$$U_{eq} = \frac{1}{3} \Sigma_i \Sigma_j U_{ij} a_i^* a_j^* (a_i \cdot a_j)$$

TABLE 5.8: Anistropic temperature factors ($Å^2$, $x10^3$) for

$[Ru_2(CO)_4(\mu\text{-}\sigma^2\text{-}HC{=}CH)\{\mu\text{-}(MeO)_2PN(Et)P(OMe)_2\}_2]$ (52)

	U(11)	U(22)	U(33)	U(23)	U(13)	U(12)
Ru(1A)	42(1)	56(1)	42(1)	-1(1)	8(1)	-1(1)
Ru(2A)	43(1)	62(1)	43(1)	-1(1)	9(1)	-4(1)
P(1A)	56(2)	79(2)	48(2)	10(1)	11(1)	-8(1)
P(2A)	51(2)	73(2)	38(1)	-4(1)	6(1)	-1(1)
P(3A)	56(2)	86(2)	46(2)	4(1)	14(1)	-15(1)
P(4A)	52(2)	94(2)	47(2)	5(2)	2(1)	0(2)
RuB	201(2)	54(1)	52(1)	4(1)	-3(1)	18(1)
P(1B)	109(3)	78(2)	91(3)	-6(2)	-3(2)	13(2)
P(2B)	188(5)	72(3)	62(2)	8(2)	11(3)	-4(3)

TABLE 5.9: Interatomic distances (Å) for

$[Ru_2(CO)_4(\mu\text{-}\sigma^2\text{-}HC{=}CH)\{\mu\text{-}(MeO)_2PN(Et)P(OMe)_2\}_2]$ (52)

Ru(1A)-Ru(2A)	2.867(1)	Ru(1A)-P(1A)	2.298(3)
Ru(1A)-P(2A)	2.295(3)	Ru(1A)-C(1A)	1.836(11)
Ru(1A)-C(2A)	1.883(12)	Ru(1A)-C(17A)	2.165(13)
Ru(2A)-P(3A)	2.288(3)	Ru(2A)-P(4A)	2.301(3)
Ru(2A)-C(3A)	1.909(13)	Ru(2A)-C(4A)	1.859(12)
Ru(2A)-C(18A)	2.145(11)	P(1A)-O(5A)	1.604(10)
P(1A)-O(6A)	1.618(10)	P(1A)-N(1A)	1.690(11)
P(2A)-O(7A)	1.599(9)	P(2A)-O(8A)	1.614(8)
P(2A)-N(2A)	1.686(9)	P(3A)-O(9A)	1.600(11)
P(3A)-O(10A)	1.571(11)	P(3A)-N(2A)	1.644(9)
P(4A)-O(11A)	1.593(11)	P(4A)-O(12A)	1.656(11)
P(4A)-N(1A)	1.631(11)	O(1A)-C(1A)	1.168(14)
O(2A)-C(2A)	1.160(14)	O(3A)-C(3A)	1.155(15)
O(4A)-C(4A)	1.172(14)	O(5A)-C(5A)	1.43(2)
O(6A)-C(6A)	1.43(2)	O(7A)-C(7A)	1.45(2)
O(8A)-C(8A)	1.396(15)	O(9A)-C(9A)	1.47(2)
O(10A)-C(10A)	1.45(2)	O(11A)-C(11A)	1.37(2)
O(12A)-C(12A)	1.40(2)	N(1A)-C(13A)	1.53(2)
N(2A)-C(15A)	1.55(2)	C(13A)-C(14A)	1.32(3)
C(15A)-C(16A)	1.47(2)	C(17A)-C(18A)	1.31(2)
RuB-P(1B)	2.285(5)	RuB-P(2B)	2.279(5)
RuB-C(1B)	1.82(2)	RuB-C(2B)	2.19(3)
RuB-C(9B)	1.96(2)	RuB-RuB	2.847(2)
P(1B)-O(3B)	1.677(13)	P(1B)-O(4B)	1.60(2)
P(1B)-Nb	1.669(14)	P(2B)-O(5B)	1.56(2)
P(2B)-O(6B)	1.76(2)	O(1B)-C(1B)	1.18(2)
O(2B)-C(2B)	1.14(3)	O(2B)-C(9B)	1.83(4)
O(2B')-C(2B')	1.20(4)	O(2B')-C(10B)	1.86(4)
O(3B)-C(3B)	1.40(2)	O(4B)-C(4B)	1.42(3)
O(5B)-C(5B)	1.42(3)	O(6B)-C(6B)	1.42(4)
Nb-C(7B)	1.59(3)	C(2B)-C(9B)	1.00(3)
C(2B')-C(10B)	1.11(4)	C(7B)-C(8B)	1.51(4)
C(9B)-C(10B)	1.20(4)		

TABLE 5.10: Interatomic angles (°) for

$[Ru_2(CO)_4(\mu\text{-}\sigma^2\text{-}HC{=}CH)\{\mu\text{-}(MeO)_2PN(Et)P(OMe)_2\}_2]$ (52)

Ru(2A)-Ru(1A)-P(1A)	89.7(1)	Ru(2A)-Ru(1A)-P(2A)	90.1(1)
P(1A)-Ru(1A)-P(2A)	174.9(1)	Ru(2A)-Ru(1A)-C(1A)	168.6(4)
P(1A)-Ru(1A)-C(1A)	89.2(4)	P(2A)-Ru(1A)-C(1A)	89.9(4)
Ru(2A)-Ru(1A)-C(2A)	92.1(3)	P(1A)-Ru(1A)-C(2A)	91.1(4)
P(2A)-Ru(1A)-C(2A)	94.0(4)	C(1A)-Ru(1A)-C(2A)	99.2(5)
Ru(2A)-Ru(1A)-C(17A)	69.3(3)	P(1A)-Ru(1A)-C(17A)	88.0(3)
P(2A)-Ru(1A)-C(17A)	87.1(3)	C(1A)-Ru(1A)-C(17A)	99.3(5)
C(2A)-Ru(1A)-C(17A)	161.4(5)	Ru(1A)-Ru(2A)-P(3A)	89.7(1)
Ru(1A)-Ru(2A)-P(4A)	89.6(1)	P(3A)-Ru(2A)-P(4A)	175.2(1)
Ru(1A)-Ru(2A)-C(3A)	92.6(4)	P(3A)-Ru(2A)-C(3A)	91.7(4)
P(4A)-Ru(2A)-C(3A)	93.0(4)	Ru(1A)-Ru(2A)-C(4A)	166.4(4)
P(3A)-Ru(2A)-C(4A)	91.1(4)	P(4A)-Ru(2A)-C(4A)	88.4(4)
C(3A)-Ru(2A)-C(4A)	100.9(5)	Ru(1A)-Ru(2A)-C(18A)	68.4(3)
P(3A)-Ru(2A)-C(18A)	88.0(3)	P(4A)-Ru(2A)-C(18A)	87.3(3)
C(3A)-Ru(2A)-C(18A)	161.1(5)	C(4A)-Ru(2A)-C(18A)	98.0(5)
Ru(1A)-P(1A)-O(5A)	117.0(4)	Ru(1A)-P(1A)-O(6A)	116.7(4)
O(5A)-P(1A)-O(6A)	97.4(5)	Ru(1A)-P(1A)-N(1A)	119.4(4)
O(5A)-P(1A)-N(1A)	103.9(5)	O(6A)-P(1A)-N(1A)	98.8(5)
Ru(1A)-P(2A)-O(7A)	116.9(3)	Ru(1A)-P(2A)-O(8A)	116.9(3)
O(7A)-P(2A)-O(8A)	98.6(4)	Ru(1A)-P(2A)-N(2A)	118.3(3)
O(7A)-P(2A)-N(2A)	99.2(5)	O(8A)-P(2A)-N(2A)	103.6(4)
Ru(2A)-P(3A)-O(9A)	117.0(4)	Ru(2A)-P(3A)-O(10A)	118.5(4)
O(9A)-P(3A)-O(10A)	97.3(5)	Ru(2A)-P(3A)-N(2A)	119.6(3)
O(9A)-P(3A)-N(2A)	98.2(5)	O(10A)-P(3A)-N(2A)	102.2(5)
Ru(2A)-P(4A)-O(11A)	117.9(4)	Ru(2A)-P(4A)-O(12A)	117.0(4)
O(11A)-P(4A)-O(12A)	99.1(5)	Ru(2A)-P(4A)-N(1A)	120.7(4)
O(11A)-P(4A)-N(1A)	101.6(6)	O(12A)-P(4A)-N(1A)	96.4(5)
P(1A)-O(5A)-C(5A)	122.0(10)	P(1A)-O(6A)-C(6A)	118.7(9)
P(2A)-O(7A)-C(7A)	120.2(9)	P(2A)-O(8A)-C(8A)	124.1(8)
P(3A)-O(9A)-C(9A)	122.8(10)	P(3A)-O(10A)-C(10A)	124.0(10)
P(4A)-O(11A)-C(11A)	122.2(10)	P(4A)-O(12A)-C(12A)	118.8(10)
P(1A)-N(1A)-P(4A)	117.5(7)	P(1A)-N(1A)-C(13A)	119.1(9)
P(4A)-N(1A)-C(13A)	121.0(9)	P(2A)-N(2A)-P(3A)	118.3(6)
P(2A)-N(2A)-C(15A)	117.4(8)	P(3A)-N(2A)-C(15A)	121.6(8)
Ru(1A)-C(1A)-O(1A)	175.2(11)	Ru(1A)-C(2A)-O(2A)	176.2(11)

TABLE 5.10 (continued)

Ru(2A)-C(3A)-O(3A)	176.1(11)	Ru(2A)-C(4A)-O(4A)	178.6(11)
N(1A)-C(13A)-C(14A)	115(2)	N(2A)-C(15A)-C(16A)	114.3(13)
Ru(1A)-C(17A)-C(18A)	109.3(9)	Ru(2A)-C(18A)-C(17A)	112.9(9)
P(1B)-RuB-P(2B)	176.2(2)	P(1B)-RuB-C(1B)	89.7(5)
P(2B)-RuB-C(1B)	90.4(5)	P(1B)-RuB-C(2B)	89.2(7)
P(2B)-RuB-C(2B)	87.0(8)	C(1B)-RuB-C(2B)	88.7(9)
P(1B)-RuB-C(9B)	80.1(7)	P(2B)-RuB-C(9B)	96.4(8)
C(1B)-RuB-C(9B)	113.9(9)	C(2B)-RuB-C(9B)	27.1(9)
RuB-P(1B)-O(3B)	117.1(5)	RuB-P(1B)-O(4B)	117.6(6)
O(3B)-P(1B)-O(4B)	93.4(8)	RuB-P(1B)-Nb	119.9(5)
O(3B)-P(1B)-Nb	99.7(7)	O(4B)-P(1B)-Nb	104.7(8)
RuB-P(2B)-O(5B)	120.2(8)	RuB-P(2B)-O(6B)	118.9(7)
O(5B)-P(2B)-O(6B)	92.5(10)	C(2B)-O(2B)-C(9B)	29(2)
C(2B')-O(2B')-C(10B)	35(2)	P(1B)-O(3B)-C(3B)	118.8(12)
P(1B)-O(4B)-C(4B)	119(2)	P(2B)-O(5B)-C(5B)	120(2)
P(2B)-O(6B)-C(6B)	120(2)	P(1B)-Nb-C(7B)	119.1(13)
RuB-C(1B)-O(1B)	177(2)	RuB-C(2B)-O(2B)	177(3)
RuB-C(2B)-C(9B)	63(2)	O(2B)-C(2B)-C(9B)	117(3)
O(2B')-C(2B')-C(10B)	107(4)	Nb-C(7B)-C(8B)	116(2)
RuB-C(9B)-O(2B)	123(2)	RuB-C(9B)-C(2B)	90(2)
O(2B)-C(9B)-C(2B)	34(2)	RuB-C(9B)-C(10B)	116(2)
O(2B)-C(9B)-C(10B)	117(2)	C(2B)-C(9B)-C(10B)	147(3)
O(2B')-C(10B)-C(2B')	38(2)	O(2B')-C(10B)-C(9B)	127(3)
C(2B')-C(10B)-C(9B)	152(4)		

TABLE 5.11: Fractional co-ordinates ($\times 10^4$) and equivalent isotropic temperature factors ($Å^2$, $\times 10^3$) for $[Ru_2(CO)_4(\mu\text{-}\eta,\eta^1\text{-}CH{=}CHPh)\{\mu\text{-}(Pr^iO)_2PN(Et)P(OPr^i)_2\}_2]BF_4$ (68)

	x/a	y/b	z/c	U_{eq}
Ru(1A)	-2980(1)	-354(1)	2958(1)	48(1)
Ru(2A)	-3267(1)	-150(1)	1703(1)	46(1)
P(1A)	-3952(3)	601(1)	3025(1)	50(1)
P(2A)	-2093(3)	-1353(2)	2920(2)	60(1)
P(3A)	-2534(3)	-1188(2)	1642(2)	58(1)
P(4A)	-4059(3)	888(1)	1712(1)	50(1)
O(1A)	-3253(9)	-782(5)	4327(5)	97(3)*
O(2A)	-829(10)	363(6)	2880(6)	114(4)*
O(3A)	-1099(9)	553(6)	1477(5)	100(3)*
O(4A)	-3721(9)	44(5)	380(5)	92(3)*
O(5A)	-3400(7)	1105(4)	3341(4)	63(2)*
O(6A)	-5114(6)	531(4)	3397(4)	60(2)*
O(7A)	-2552(7)	-1974(4)	3434(4)	69(2)*
O(8A)	-857(8)	-1394(5)	3046(4)	80(3)*
O(9A)	-3443(7)	-1651(4)	1511(4)	72(2)*
O(10A)	-1685(9)	-1251(5)	1107(5)	90(3)*
O(11A)	-3370(7)	1495(4)	1304(4)	67(2)*
O(12A)	-5179(7)	1064(4)	1431(4)	64(2)*
N(1A)	-4129(7)	1131(4)	2360(4)	50(2)*
N(2A)	-1982(8)	-1618(5)	2261(4)	59(2)*
C(1A)	-3116(11)	-606(7)	3784(6)	70(3)*
C(2A)	-1640(12)	95(7)	2906(6)	73(4)*
C(3A)	-1943(12)	295(7)	1565(6)	74(4)*
C(4A)	-3576(10)	-54(6)	892(6)	59(3)*
C(5A)	-3395(10)	1064(6)	3981(6)	67(3)*
C(6A)	-4168(16)	1582(10)	4146(9)	114(6)*
C(7A)	-2216(15)	1097(9)	4143(9)	111(6)*
C(8A)	-5729(9)	-86(6)	3695(5)	55(3)*
C(9A)	-5973(14)	-39(8)	4345(8)	93(5)*
C(10A)	-6714(12)	-135(7)	3375(7)	78(4)*
C(11A)	-3713(11)	-2140(7)	3635(6)	74(4)*
C(12A)	-4097(13)	-2573(8)	3259(7)	91(5)*
C(13A)	-3700(16)	-2508(10)	4296(9)	118(6)*
C(14A)	-438(16)	-1426(10)	3645(9)	112(6)*

TABLE 5.11 (continued)

C(15A)	-220(22)	-2154(14)	3879(13)	169(9)*
C(16A)	605(23)	-1012(14)	3518(13)	171(10)*
C(17A)	-3383(14)	-2133(8)	1125(8)	95(5)*
C(18A)	-3806(17)	-1755(11)	523(10)	126(7)*
C(19A)	-4152(19)	-2727(12)	1465(11)	143(8)*
C(20A)	-856(16)	-772(9)	761(9)	108(5)*
C(21A)	-643(24)	-1043(14)	132(13)	180(11)*
C(22A)	124(21)	-811(13)	1053(12)	155(9)*
C(23A)	-3464(12)	1718(7)	621(7)	79(4)*
C(24A)	-4080(17)	2372(10)	522(9)	124(6)*
C(25A)	-2306(16)	1757(10)	329(9)	117(6)*
C(26A)	-6214(12)	711(7)	1627(7)	81(4)*
C(27A)	-6707(15)	669(9)	1066(9)	110(6)*
C(28A)	-6917(15)	1115(9)	2011(8)	104(5)*
C(29A)	-4552(11)	1829(7)	2392(6)	70(3)*
C(30A)	-3569(13)	2325(8)	2321(7)	88(4)*
C(31A)	-1600(12)	-2295(8)	2263(7)	84(4)*
C(32A)	-378(15)	-2349(9)	2124(9)	110(6)*
C(33A)	-4216(8)	-670(5)	2577(5)	46(2)*
C(34A)	-4825(9)	-771(6)	2202(5)	54(3)*
C(35A)	-5729(9)	-1085(5)	1994(5)	50(3)*
C(36A)	-6374(12)	-1502(7)	2425(7)	76(4)*
C(37A)	-7296(13)	-1812(8)	2247(8)	92(5)*
C(38A)	-7430(13)	-1718(8)	1637(7)	87(4)*
C(39A)	-6805(14)	-1304(9)	1231(8)	97(5)*
C(40A)	-5908(11)	-986(7)	1390(6)	69(3)*
B(1A)	6853(18)	2038(11)	5639(10)	96(6)*
F(1A)	6542(10)	2618(6)	5278(5)	136(4)*
F(2A)	7659(10)	1746(6)	5371(6)	146(4)*
F(3A)	7232(12)	2177(7)	6119(7)	164(5)*
F(4A)	5966(11)	1628(6)	5781(6)	150(4)*
Ru(1B)	2189(1)	3939(1)	3180(1)	46(1)
Ru(2B)	2375(1)	4200(1)	1896(1)	42(1)
P(1B)	3373(3)	4797(2)	3190(2)	60(1)
P(2B)	949(3)	3088(2)	3220(2)	69(1)
P(3B)	1009(3)	3441(2)	1893(1)	52(1)
P(4B)	3656(2)	5024(2)	1862(1)	52(1)

TABLE 5.11 (continued)

N(1B)	4011(8)	5165(5)	2516(5)	63(3)*
N(2B)	582(9)	2959(5)	2577(5)	69(3)*
O(1B)	1878(9)	3721(6)	4562(5)	102(3)*
O(2B)	4033(11)	3015(6)	3052(6)	116(4)*
O(3B)	4098(9)	3182(6)	1663(5)	100(3)*
O(4B)	2105(8)	4783(5)	573(5)	82(3)*
O(5B)	2751(8)	5354(5)	3471(5)	86(3)*
O(6B)	4392(10)	4648(6)	3585(6)	109(4)*
O(7B)	1456(12)	2342(7)	3466(7)	137(5)*
O(8B)	-93(15)	3000(9)	3662(8)	163(6)*
O(9B)	1374(7)	2869(4)	1522(4)	66(2)*
O(10B)	-37(8)	3701(4)	1588(4)	77(2)*
O(11B)	3395(7)	5718(4)	1468(4)	75(2)*
O(12B)	4821(7)	4926(4)	1559(4)	69(2)*
C(1B)	1998(10)	3833(6)	4022(6)	67(3)*
C(2B)	3310(13)	3377(8)	3086(7)	81(4)*
C(3B)	3435(11)	3578(7)	1744(6)	66(3)*
C(4B)	2176(9)	4556(6)	1069(5)	54(3)*
C(5B)	3131(19)	5847(12)	3776(11)	134(7)*
C(6B)	2628(23)	5616(14)	4451(13)	169(10)*
C(7B)	2381(37)	6398(22)	3534(20)	271(19)*
C(8B)	4695(31)	4093(23)	3920(17)	241(16)*
C(9B)	5106(46)	3818(25)	4533(19)	343(26)*
C(10B)	5454(48)	4508(25)	4184(30)	440(35)*
C(11B)	1678(25)	2071(15)	4064(13)	163(9)*
C(12B)	2676(39)	1829(22)	4176(19)	265(19)*
C(13B)	899(34)	1507(21)	4280(19)	251(17)*
C(14B)	-657(28)	3465(16)	3837(15)	189(12)*
C(15B)	-840(23)	3219(14)	4580(13)	172(10)*
C(16B)	-1889(31)	3435(18)	3713(16)	216(13)*
C(17B)	1345(13)	2972(8)	854(7)	84(4)*
C(18B)	2413(19)	2842(11)	587(10)	137(7)*
C(19B)	389(22)	2535(13)	795(12)	163(9)*
C(20B)	-496(11)	4373(7)	1467(6)	71(4)*
C(21B)	-1446(15)	4396(9)	1921(9)	108(5)*
C(22B)	-863(14)	4490(9)	811(8)	99(5)*
C(23B)	2282(11)	6023(7)	1415(6)	72(4)*

TABLE 5.11: (continued)

C(24B)	2346(16)	6447(10)	757(9)	114(6)*
C(25B)	2033(16)	6407(9)	1903(9)	111(6)*
C(26B)	5134(12)	5006(8)	889(7)	80(4)*
C(27B)	5612(17)	5695(10)	593(9)	120(6)*
C(28B)	5936(18)	4431(11)	844(10)	129(7)*
C(29B)	4804(14)	5733(9)	2481(8)	96(5)*
C(30B)	6003(21)	5460(12)	2541(11)	152(8)*
C(31B)	-423(18)	2501(12)	2571(10)	136(7)*
C(32B)	96(24)	1888(15)	2515(13)	176(10)*
C(33B)	1340(8)	4624(5)	2457(4)	41(2)*
C(34B)	848(8)	4742(5)	2917(5)	46(2)*
C(35B)	76(10)	5126(6)	3244(5)	58(3)*
C(36B)	-625(11)	5550(7)	2894(6)	72(4)*
C(37B)	-1423(13)	5918(8)	3204(8)	90(4)*
C(38B)	-1456(15)	5856(9)	3826(8)	101(5)*
C(39B)	-733(18)	5434(11)	4152(10)	123(6)*
C(40B)	41(12)	5082(7)	3856(7)	77(4)*
B(1B)	1162(45)	3519(29)	9022(26)	216(18)*
F(1B)	772(14)	2932(9)	9151(8)	189(6)*
F(2B)	1667(19)	3818(11)	9319(11)	242(9)*
F(3B)	303(12)	3975(7)	8718(7)	164(5)*
F(4B)	1776(20)	3618(12)	8452(12)	272(10)*

* isotropic temperature factor.

$$U_{eq} = \frac{1}{3} \Sigma_i \Sigma_j U_{ij} a_i^* a_j^* (a_i \cdot a_j)$$

TABLE 5.12: Anistropic temperature factors ($Å^2$, $x10^3$) for

$[Ru_2(CO)_4(\mu\text{-}\eta,\eta^1\text{-}CH{=}CHPh)\{\mu\text{-}(Pr^iO)_2PN(Et)P(OPr^i)_2\}_2]BF_4$ (68)

	U(11)	U(22)	U(33)	U(23)	U(13)	U(12)
Ru(1A)	52(1)	44(1)	46(1)	-3(1)	-9(1)	2(1)
Ru(2A)	54(1)	40(1)	41(1)	-4(1)	2(1)	2(1)
P(1A)	64(2)	44(2)	42(2)	-9(1)	-6(1)	1(1)
P(2A)	51(2)	50(2)	72(2)	2(2)	-6(2)	9(1)
P(3A)	63(2)	46(2)	61(2)	-12(1)	11(2)	8(1)
P(4A)	64(2)	42(2)	41(2)	-4(1)	-4(1)	7(1)
Ru(1B)	49(1)	47(1)	40(1)	-4(1)	-3(1)	10(1)
Ru(2B)	42(1)	42(1)	39(1)	-6(1)	-1(1)	4(1)
P(1B)	61(2)	68(2)	53(2)	-16(2)	-15(2)	1(2)
P(2B)	81(2)	67(2)	49(2)	5(2)	6(2)	-16(2)
P(3B)	56(2)	52(2)	48(2)	-11(1)	-4(1)	-2(1)
P(4B)	44(2)	56(2)	52(2)	-7(1)	1(1)	-3(1)

TABLE 5.13: Interatomic distances (Å) for

$[Ru_2(CO)_4(\mu\text{-}\eta,\eta^1\text{-}CH{=}CHPh)\{\mu\text{-}(Pr^iO)_2PN(Et)P(OPr^i)_2\}_2]BF_4$ (68)

Ru(1A)-Ru(2A)	2.828(1)	Ru(1A)-P(1A)	2.325(3)
Ru(1A)-P(2A)	2.341(3)	Ru(1A)-C(1A)	1.817(14)
Ru(1A)-C(2A)	1.894(15)	Ru(1A)-C(33A)	2.008(11)
Ru(2A)-P(3A)	2.346(3)	Ru(2A)-P(4A)	2.354(3)
Ru(2A)-C(3A)	1.858(15)	Ru(2A)-C(4A)	1.873(13)
Ru(2A)-C(33A)	2.261(10)	Ru(2A)-C(34A)	2.382(11)
P(1A)-O(5A)	1.580(10)	P(1A)-O(6A)	1.583(8)
P(1A)-N(1A)	1.691(9)	P(2A)-O(7A)	1.607(8)
P(2A)-O(8A)	1.580(10)	P(2A)-N(2A)	1.683(11)
P(3A)-O(9A)	1.577(10)	P(3A)-O(10A)	1.545(11)
P(3A)-N(2A)	1.688(10)	P(4A)-O(11A)	1.595(8)
P(4A)-O(12A)	1.583(9)	P(4A)-N(1A)	1.638(10)
O(1A)-C(1A)	1.20(2)	O(2A)-C(2A)	1.14(2)
O(3A)-C(3A)	1.16(2)	O(4A)-C(4A)	1.16(2)
O(5A)-C(5A)	1.43(2)	O(6A)-C(8A)	1.493(13)
O(7A)-C(11A)	1.49(2)	O(8A)-C(14A)	1.48(2)
O(9A)-C(17A)	1.46(2)	O(10A)-C(20A)	1.48(2)
O(11A)-C(23A)	1.52(2)	O(12A)-C(26A)	1.47(2)
N(1A)-C(29A)	1.54(2)	N(2A)-C(31A)	1.47(2)
C(5A)-C(6A)	1.51(2)	C(5A)-C(7A)	1.54(2)
C(8A)-C(9A)	1.49(2)	C(8A)-C(10A)	1.49(2)
C(11A)-C(12A)	1.47(2)	C(11A)-C(13A)	1.52(2)
C(14A)-C(15A)	1.52(3)	C(14A)-C(16A)	1.53(4)
C(17A)-C(18A)	1.55(3)	C(17A)-C(19A)	1.58(3)
C(20A)-C(21A)	1.63(4)	C(20A)-C(22A)	1.43(3)
C(23A)-C(24A)	1.53(3)	C(23A)-C(25A)	1.51(2)
C(26A)-C(27A)	1.47(3)	C(26A)-C(28A)	1.53(3)
C(29A)-C(30A)	1.58(2)	C(31A)-C(32A)	1.52(2)
C(33A)-C(34A)	1.24(2)	C(34A)-C(35A)	1.46(2)
C(35A)-C(36A)	1.36(2)	C(35A)-C(40A)	1.37(2)
C(36A)-C(37A)	1.45(2)	C(37A)-C(38A)	1.37(2)
C(38A)-C(39A)	1.31(2)	C(39A)-C(40A)	1.41(2)
B(1A)-F(1A)	1.37(2)	B(1A)-F(2A)	1.32(3)
B(1A)-F(3A)	1.31(3)	B(1A)-F(4A)	1.37(3)
Ru(1B)-Ru(2B)	2.818(1)	Ru(1B)-P(1B)	2.325(4)

TABLE 5.13 (continued)

Ru(1B)-P(2B)	2.338(4)	Ru(1B)-C(1B)	1.857(14)
Ru(1B)-C(2B)	1.82(2)	Ru(1B)-C(33B)	2.254(9)
Ru(1B)-C(34B)	2.356(10)	Ru(2B)-P(3B)	2.329(3)
Ru(2B)-P(4B)	2.332(3)	Ru(2B)-C(3B)	1.882(13)
Ru(2B)-C(4B)	1.893(12)	Ru(2B)-C(33B)	2.033(10)
P(1B)-N(1B)	1.676(10)	P(1B)-O(5B)	1.586(11)
P(1B)-O(6B)	1.602(13)	P(2B)-N(2B)	1.636(12)
P(2B)-O(7B)	1.662(15)	P(2B)-O(8B)	1.54(2)
P(3B)-N(2B)	1.690(10)	P(3B)-O(9B)	1.623(10)
P(3B)-O(10B)	1.558(10)	P(4B)-N(1B)	1.662(12)
P(4B)-O(11B)	1.568(9)	P(4B)-O(12B)	1.563(9)
N(1B)-C(29B)	1.53(2)	N(2B)-C(31B)	1.58(3)
O(1B)-C(1B)	1.18(2)	O(2B)-C(2B)	1.16(2)
O(3B)-C(3B)	1.18(2)	O(4B)-C(4B)	1.127(15)
O(5B)-C(5B)	1.45(3)	O(6B)-C(8B)	1.30(4)
O(7B)-C(11B)	1.40(3)	O(8B)-C(14B)	1.29(4)
O(9B)-C(17B)	1.48(2)	O(10B)-C(20B)	1.48(2)
O(11B)-C(23B)	1.51(2)	O(12B)-C(26B)	1.50(2)
C(5B)-C(6B)	1.57(4)	C(5B)-C(7B)	1.50(5)
C(8B)-C(9B)	1.51(6)	C(8B)-C(10B)	1.52(8)
C(9B)-C(10B)	1.53(7)	C(11B)-C(12B)	1.35(6)
C(11B)-C(13B)	1.50(5)	C(14B)-C(15B)	1.64(4)
C(14B)-C(16B)	1.58(5)	C(17B)-C(18B)	1.44(3)
C(17B)-C(19B)	1.53(3)	C(20B)-C(21B)	1.49(2)
C(20B)-C(22B)	1.56(2)	C(23B)-C(24B)	1.55(2)
C(23B)-C(25B)	1.50(3)	C(26B)-C(27B)	1.54(2)
C(26B)-C(28B)	1.55(3)	C(29B)-C(30B)	1.59(3)
C(31B)-C(32B)	1.44(4)	C(33B)-C(34B)	1.218(15)
C(34B)-C(35B)	1.48(2)	C(35B)-C(36B)	1.40(2)
C(35B)-C(40B)	1.36(2)	C(36B)-C(37B)	1.45(2)
C(37B)-C(38B)	1.38(3)	C(38B)-C(39B)	1.39(3)
C(39B)-C(40B)	1.40(3)	B(1B)-F(1B)	1.28(6)
B(1B)-F(2B)	1.22(7)	B(1B)-F(3B)	1.52(6)
B(1B)-F(4B)	1.40(6)		

TABLE 5.14: Interatomic angles (°) for

$[Ru_2(CO)_4(\mu\text{-}\eta,\eta^1\text{-}CH{=}CHPh)\{\mu\text{-}(Pr^iO)_2PN(Et)P(OPr^i)_2\}_2]BF_4$ (68)

Ru(2A)-Ru(1A)-P(1A)	90.3(1)	Ru(2A)-Ru(1A)-P(2A)	90.6(1)
P(1A)-Ru(1A)-P(2A)	176.5(1)	Ru(2A)-Ru(1A)-C(1A)	165.2(4)
P(1A)-Ru(1A)-C(1A)	89.9(4)	P(2A)-Ru(1A)-C(1A)	88.4(4)
Ru(2A)-Ru(1A)-C(2A)	99.5(4)	P(1A)-Ru(1A)-C(2A)	91.4(4)
P(2A)-Ru(1A)-C(2A)	91.7(4)	C(1A)-Ru(1A)-C(2A)	95.2(6)
Ru(2A)-Ru(1A)-C(33A)	52.5(3)	P(1A)-Ru(1A)-C(33A)	89.2(3)
P(2A)-Ru(1A)-C(33A)	88.7(3)	C(1A)-Ru(1A)-C(33A)	112.8(5)
C(2A)-Ru(1A)-C(33A)	152.0(5)	Ru(1A)-Ru(2A)-P(3A)	91.9(1)
Ru(1A)-Ru(2A)-P(4A)	91.3(1)	P(3A)-Ru(2A)-P(4A)	176.5(1)
Ru(1A)-Ru(2A)-C(3A)	86.4(4)	P(3A)-Ru(2A)-C(3A)	95.7(5)
P(4A)-Ru(2A)-C(3A)	85.9(5)	Ru(1A)-Ru(2A)-C(4A)	174.9(4)
P(3A)-Ru(2A)-C(4A)	87.8(4)	P(4A)-Ru(2A)-C(4A)	88.9(4)
C(3A)-Ru(2A)-C(4A)	98.7(6)	Ru(1A)-Ru(2A)-C(33A)	44.8(3)
P(3A)-Ru(2A)-C(33A)	86.4(3)	P(4A)-Ru(2A)-C(33A)	94.8(3)
C(3A)-Ru(2A)-C(33A)	131.1(5)	C(4A)-Ru(2A)-C(33A)	130.2(5)
Ru(1A)-Ru(2A)-C(34A)	75.6(3)	P(3A)-Ru(2A)-C(34A)	84.2(3)
P(4A)-Ru(2A)-C(34A)	95.2(3)	C(3A)-Ru(2A)-C(34A)	161.9(5)
C(4A)-Ru(2A)-C(34A)	99.4(5)	C(33A)-Ru(2A)-C(34A)	30.8(4)
Ru(1A)-P(1A)-O(5A)	116.1(3)	Ru(1A)-P(1A)-O(6A)	118.4(3)
O(5A)-P(1A)-O(6A)	100.2(5)	Ru(1A)-P(1A)-N(1A)	116.5(4)
O(5A)-P(1A)-N(1A)	97.4(5)	O(6A)-P(1A)-N(1A)	105.1(4)
Ru(1A)-P(2A)-O(7A)	114.9(4)	Ru(1A)-P(2A)-O(8A)	116.8(4)
O(7A)-P(2A)-O(8A)	99.1(5)	Ru(1A)-P(2A)-N(2A)	118.9(4)
O(7A)-P(2A)-N(2A)	105.5(5)	O(8A)-P(2A)-N(2A)	98.8(5)
Ru(2A)-P(3A)-O(9A)	109.9(4)	Ru(2A)-P(3A)-O(10A)	119.6(4)
O(9A)-P(3A)-O(10A)	98.5(6)	Ru(2A)-P(3A)-N(2A)	117.2(4)
O(9A)-P(3A)-N(2A)	105.7(5)	O(10A)-P(3A)-N(2A)	103.6(5)
Ru(2A)-P(4A)-O(11A)	114.2(3)	Ru(2A)-P(4A)-O(12A)	119.6(4)
O(11A)-P(4A)-O(12A)	97.5(4)	Ru(2A)-P(4A)-N(1A)	116.5(3)
O(11A)-P(4A)-N(1A)	97.9(5)	O(12A)-P(4A)-N(1A)	107.5(5)
P(1A)-O(5A)-C(5A)	126.6(7)	P(1A)-O(6A)-C(8A)	128.4(7)
P(2A)-O(7A)-C(11A)	126.5(8)	P(2A)-O(8A)-C(14A)	125.8(10)
P(3A)-O(9A)-C(17A)	130.2(9)	P(3A)-O(10A)-C(20A)	130.0(11)
P(4A)-O(11A)-C(23A)	121.8(8)	P(4A)-O(12A)-C(26A)	126.7(8)
P(1A)-N(1A)-P(4A)	121.9(6)	P(1A)-N(1A)-C(29A)	117.6(8)

P(4A)-N(1A)-C(29A)	119.7(7)	P(2A)-N(2A)-P(3A)	121.0(6)
P(2A)-N(2A)-C(31A)	118.8(8)	P(3A)-N(2A)-C(31A)	119.0(9)
Ru(1A)-C(1A)-O(1A)	177.0(12)	Ru(1A)-C(2A)-O(2A)	179.3(12)
Ru(2A)-C(3A)-O(3A)	177.7(13)	Ru(2A)-C(4A)-O(4A)	175.1(11)
O(5A)-C(5A)-C(6A)	107.0(11)	O(5A)-C(5A)-C(7A)	109.9(11)
C(6A)-C(5A)-C(7A)	117(2)	O(6A)-C(8A)-C(9A)	105.1(11)
O(6A)-C(8A)-C(10A)	109.8(9)	C(9A)-C(8A)-C(10A)	113.8(11)
O(7A)-C(11A)-C(12A)	108.7(12)	O(7A)-C(11A)-C(13A)	103.8(12)
C(12A)-C(11A)-C(13A)	110.8(13)	O(8A)-C(14A)-C(15A)	105(2)
O(8A)-C(14A)-C(16A)	106(2)	C(15A)-C(14A)-C(16A)	112(2)
O(9A)-C(17A)-C(18A)	104.0(14)	O(9A)-C(17A)-C(19A)	106.6(14)
C(18A)-C(17A)-C(19A)	113(2)	O(10A)-C(20A)-C(21A)	101(2)
O(10A)-C(20A)-C(22A)	112(2)	C(21A)-C(20A)-C(22A)	110(2)
O(11A)-C(23A)-C(24A)	107.5(13)	O(11A)-C(23A)-C(25A)	105.0(12)
C(24A)-C(23A)-C(25A)	115.1(14)	O(12A)-C(26A)-C(27A)	106.6(12)
O(12A)-C(26A)-C(28A)	107.4(13)	C(27A)-C(26A)-C(28A)	111.6(14)
N(1A)-C(29A)-C(30A)	110.3(10)	N(2A)-C(31A)-C(32A)	114.1(13)
Ru(1A)-C(33A)-Ru(2A)	82.8(4)	Ru(1A)-C(33A)-C(34A)	162.7(8)
Ru(2A)-C(33A)-C(34A)	80.0(7)	Ru(2A)-C(34A)-C(33A)	69.2(7)
Ru(2A)-C(34A)-C(35A)	134.5(8)	C(33A)-C(34A)-C(35A)	155.5(10)
C(34A)-C(35A)-C(36A)	117.1(11)	C(34A)-C(35A)-C(40A)	122.3(10)
C(36A)-C(35A)-C(40A)	120.5(12)	C(35A)-C(36A)-C(37A)	119.4(13)
C(36A)-C(37A)-C(38A)	118.4(13)	C(37A)-C(38A)-C(39A)	121(2)
C(38A)-C(39A)-C(40A)	122(2)	C(35A)-C(40A)-C(39A)	118.5(12)
F(1A)-B(1A)-F(2A)	113(2)	F(1A)-B(1A)-F(3A)	108(2)
F(2A)-B(1A)-F(3A)	105(2)	F(1A)-B(1A)-F(4A)	108(2)
F(2A)-B(1A)-F(4A)	110(2)	F(3A)-B(1A)-F(4A)	113(2)
Ru(2B)-Ru(1B)-P(1B)	92.2(1)	Ru(2B)-Ru(1B)-P(2B)	90.5(1)
P(1B)-Ru(1B)-P(2B)	176.9(1)	Ru(2B)-Ru(1B)-C(1B)	175.2(4)
P(1B)-Ru(1B)-C(1B)	86.3(4)	P(2B)-Ru(1B)-C(1B)	90.9(4)
Ru(2B)-Ru(1B)-C(2B)	83.2(5)	P(1B)-Ru(1B)-C(2B)	92.0(5)
P(2B)-Ru(1B)-C(2B)	90.0(5)	C(1B)-Ru(1B)-C(2B)	101.4(6)
Ru(2B)-Ru(1B)-C(33B)	45.6(3)	P(1B)-Ru(1B)-C(33B)	88.8(3)
P(2B)-Ru(1B)-C(33B)	91.9(3)	C(1B)-Ru(1B)-C(33B)	129.7(5)
C(2B)-Ru(1B)-C(33B)	128.8(5)	Ru(2B)-Ru(1B)-C(34B)	76.1(3)
P(1B)-Ru(1B)-C(34B)	87.9(3)	P(2B)-Ru(1B)-C(34B)	91.2(3)
C(1B)-Ru(1B)-C(34B)	99.2(5)	C(2B)-Ru(1B)-C(34B)	159.3(5)

TABLE 5.14 (continued)

C(33B)-Ru(1B)-C(34B)	30.5(4)	Ru(1B)-Ru(2B)-P(3B)	91.8(1)
Ru(1B)-Ru(2B)-P(4B)	90.2(1)	P(3B)-Ru(2B)-P(4B)	175.6(1)
Ru(1B)-Ru(2B)-C(3B)	100.6(4)	P(3B)-Ru(2B)-C(3B)	90.1(4)
P(4B)-Ru(2B)-C(3B)	93.5(4)	Ru(1B)-Ru(2B)-C(4B)	163.1(4)
P(3B)-Ru(2B)-C(4B)	87.6(4)	P(4B)-Ru(2B)-C(4B)	89.4(4)
C(3B)-Ru(2B)-C(4B)	96.3(5)	Ru(1B)-Ru(2B)-C(33B)	52.4(3)
P(3B)-Ru(2B)-C(33B)	88.2(3)	P(4B)-Ru(2B)-C(33B)	89.8(3)
C(3B)-Ru(2B)-C(33B)	152.9(5)	C(4B)-Ru(2B)-C(33B)	110.7(4)
Ru(1B)-P(1B)-N(1B)	116.4(4)	Ru(1B)-P(1B)-O(5B)	110.3(4)
N(1B)-P(1B)-O(5B)	107.3(5)	Ru(1B)-P(1B)-O(6B)	119.1(5)
N(1B)-P(1B)-O(6B)	99.8(6)	O(5B)-P(1B)-O(6B)	102.4(7)
Ru(1B)-P(2B)-N(2B)	118.2(4)	Ru(1B)-P(2B)-O(7B)	113.1(6)
N(2B)-P(2B)-O(7B)	97.1(7)	Ru(1B)-P(2B)-O(8B)	121.7(8)
N(2B)-P(2B)-O(8B)	105.4(8)	O(7B)-P(2B)-O(8B)	96.7(8)
Ru(2B)-P(3B)-N(2B)	116.0(4)	Ru(2B)-P(3B)-O(9B)	114.2(3)
N(2B)-P(3B)-O(9B)	99.3(5)	Ru(2B)-P(3B)-O(10B)	118.0(4)
N(2B)-P(3B)-O(10B)	106.2(5)	O(9B)-P(3B)-O(10B)	100.6(5)
Ru(2B)-P(4B)-N(1B)	118.6(4)	Ru(2B)-P(4B)-O(11B)	115.2(4)
N(1B)-P(4B)-O(11B)	105.9(5)	Ru(2B)-P(4B)-O(12B)	117.1(4)
N(1B)-P(4B)-O(12B)	97.9(5)	O(11B)-P(4B)-O(12B)	99.1(5)
P(1B)-N(1B)-P(4B)	121.8(6)	P(1B)-N(1B)-C(29B)	119.8(10)
P(4B)-N(1B)-C(29B)	117.5(9)	P(2B)-N(2B)-P(3B)	122.7(7)
P(2B)-N(2B)-C(31B)	120.6(10)	P(3B)-N(2B)-C(31B)	114.8(11)
P(1B)-O(5B)-C(5B)	131.8(12)	P(1B)-O(6B)-C(8B)	130(2)
P(2B)-O(7B)-C(11B)	126(2)	P(2B)-O(8B)-C(14B)	126(2)
P(3B)-O(9B)-C(17B)	121.9(8)	P(3B)-O(10B)-C(20B)	129.9(9)
P(4B)-O(11B)-C(23B)	126.0(7)	P(4B)-O(12B)-C(26B)	125.6(8)
Ru(1B)-C(1B)-O(1B)	175.6(12)	Ru(1B)-C(2B)-O(2B)	177.1(14)
Ru(2B)-C(3B)-O(3B)	178.5(11)	Ru(2B)-C(4B)-O(4B)	176.6(11)
O(5B)-C(5B)-C(6B)	104(2)	O(5B)-C(5B)-C(7B)	98(2)
C(6B)-C(5B)-C(7B)	102(2)	O(6B)-C(8B)-C(9B)	141(4)
O(6B)-C(8B)-C(10B)	87(3)	C(9B)-C(8B)-C(10B)	60(3)
C(8B)-C(9B)-C(10B)	60(4)	C(8B)-C(10B)-C(9B)	59(3)
O(7B)-C(11B)-C(12B)	120(3)	O(7B)-C(11B)-C(13B)	105(3)
C(12B)-C(11B)-C(13B)	107(3)	O(8B)-C(14B)-C(15B)	104(2)
O(8B)-C(14B)-C(16B)	112(3)	C(15B)-C(14B)-C(16B)	97(2)
O(9B)-C(17B)-C(18B)	108.3(14)	O(9B)-C(17B)-C(19B)	102.9(13)

TABLE 5.14: (continued)

C(18B)-C(17B)-C(19B)	119(2)	O(10B)-C(20B)-C(21B)	108.6(11)
O(10B)-C(20B)-C(22B)	105.9(12)	C(21B)-C(20B)-C(22B)	110.6(13)
O(11B)-C(23B)-C(24B)	104.3(11)	O(11B)-C(23B)-C(25B)	109.6(13)
C(24B)-C(23B)-C(25B)	114.3(13)	O(12B)-C(26B)-C(27B)	112.7(14)
O(12B)-C(26B)-C(28B)	104.0(12)	C(27B)-C(26B)-C(28B)	113.9(14)
N(1B)-C(29B)-C(30B)	110(2)	N(2B)-C(31B)-C(32B)	102(2)
Ru(1B)-C(33B)-Ru(2B)	82.0(3)	Ru(1B)-C(33B)-C(34B)	79.4(7)
Ru(2B)-C(33B)-C(34B)	161.3(8)	Ru(1B)-C(34B)-C(33B)	70.1(6)
Ru(1B)-C(34B)-C(35B)	136.4(8)	C(33B)-C(34B)-C(35B)	153.0(10)
C(34B)-C(35B)-C(36B)	116.9(11)	C(34B)-C(35B)-C(40B)	122.4(11)
C(36B)-C(35B)-C(40B)	120.7(12)	C(35B)-C(36B)-C(37B)	118.4(13)
C(36B)-C(37B)-C(38B)	120(2)	C(37B)-C(38B)-C(39B)	120(2)
C(38B)-C(39B)-C(40B)	121(2)	C(35B)-C(40B)-C(39B)	120.5(14)
F(1B)-B(1B)-F(2B)	131(5)	F(1B)-B(1B)-F(3B)	108(4)
F(2B)-B(1B)-F(3B)	109(4)	F(1B)-B(1B)-F(4B)	109(5)
F(2B)-B(1B)-F(4B)	104(4)	F(3B)-B(1B)-F(4B)	88(3)

CHAPTER 6

THE SYNTHESIS, REACTIVITY AND ELECTROCHEMISTRY OF THE CO-ORDINATIVELY UNSATURATED SPECIES $[Ru_2(CO)_4\{\mu\text{-}(RO)_2PN(Et)P(OR)_2\}_2]$

2.1 INTRODUCTION

Considerable attention has been focused on the mechanism of activation of small molecules by dinuclear and polynuclear transition metal complexes with the object of developing and understanding cluster catalysis and of modelling the chemisorption of small molecules on metal surfaces.[5] The prime objective in the design of complexes which will function as homogeneous catalysts for various organic reactions is the development of systems which readily give rise to formally co-ordinatively unsaturated species or which themselves are co-ordinatively unsaturated. Such complexes will provide ready access of the substrate molecules to a metal atom. These types of complexes are also an attractive target in synthetic chemistry since they may be employed as precursors in the synthesis under mild conditions of products which are not generally accessible by other routes.[228,229] For example, the development of the triosmium solvento species $[Os_3(CO)_{10}L_2]$ (L = cyclooctene, acetonitrile) greatly expanded the chemistry of triosmium dodecacarbonyl by making the osmium centres more accessible to substrates compared to those in the parent cluster $[Os_3(CO)_{12}]$. The related unsaturated dihydride $[Os_3(\mu\text{-}H)_2(CO)_{10}]$, has also been extremely important in developing the chemistry of osmium clusters.

Binuclear unsaturated transition metal complexes in particular have attracted considerable attention because of their potential role in catalysis. For example, the co-ordinatively unsaturated binuclear

rhodium species $[Rh_2(\mu\text{-}H)_2\{Pr^i{}_2P(CH_2)_nPPr^i{}_2\}_2]$ (n = 2, 3 or 4) have been shown to catalyze the hydrogenation of alkenes.[230] The dinuclear complex $[Rh_2(CO)_2(\mu\text{-dppm})_2]$ is an effective catalyst for the hydrogenation of acetylene to ethylene[231] while $[Pd_2Cl_2(\mu\text{-dppm})_2]$ readily catalyzes the cyclotrimerisation of alkynes;[48] the catalytic properties of both complexes is associated with their ability to readily add alkynes in the bridging position.

Some typical unsaturated dinuclear carbonyl and diphosphorus ligand-bridged carbonyl derivatives which have been reported include $[M_2(\mu\text{-}H)_2(CO)_8]^{2-}$ (M = Cr, Mo or W),[232] $[Re_2(\mu\text{-}H)_2(CO)_8]$,[233] $[Mn_2(\mu\text{-}H)_2(CO)_6\{\mu\text{-}(EtO)_2POP(OEt)_2\}]$,[234,235] $[Mn_2(\mu\text{-}H)_2(CO)_6(\mu\text{-dppm})]$[235,236] and $[Mn_2(\mu\text{-}H)_2(CO)_4(\mu\text{-dppm})_2]$.[37] Complexes of this type have been found to be valuable synthetic precursors because they react under mild conditions with other transition metal compounds as well as with a range of small organic molecules. These reactions involve both the formal insertion of the substrate into a metal-hydrogen bond as well as the displacement of dihydrogen via reductive elimination. For example, reaction of $[Mn_2(\mu\text{-}H)_2(CO)_4(\mu\text{-dppm})_2]$ with methyl isonitrile affords $[Mn_2(\mu\text{-}H)(\mu\text{-MeN=CH})(CO)_4(\mu\text{-dppm})_2]$ whereas $[Mn_2(CO)_6(\mu\text{-dppm})_2]$ is produced on reaction with carbon monoxide (Scheme 6.1).

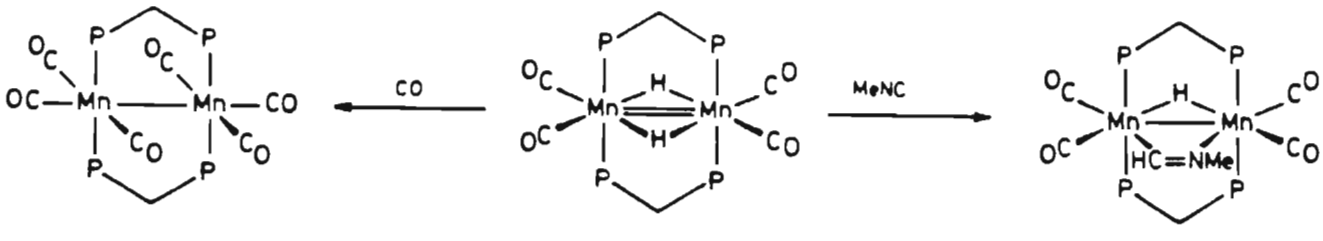

Scheme 6.1

Significantly, the manganese-manganese distance for $[Mn_2(\mu\text{-}H)_2(CO)_6(\mu\text{-dppm})]$ {2.699(2)Å} is considerably shorter than that for

$[Mn_2(CO)_{10}]$[237] and corresponds to that expected for a metal-metal double bond, which is in agreement with the formal unsaturation predicted for the molecule on the basis of electron counting.

The carbonyl-bridged dimanganese compound $[Mn_2(\mu\text{-}\eta^2\text{-}CO)(CO)_4(\mu\text{-}dppm)_2]$ represents, on the other hand, an example of a related dinuclear compound which can be formally converted to an unsaturated species, in this case through the bridging carbonyl reverting from a four-electron to a two-electron ligand. This compound is formed on thermolysis of the parent hexacarbonyl species $[Mn_2(CO)_6(\mu\text{-}dppm)_2]$.

Dinuclear co-ordinatively unsaturated species have also been shown to be formed under photochemical as opposed to thermal conditions, and in many cases involve the loss of carbon monoxide. For instance, the photochemistry of the diruthenium·cyclopentadienyl species $[Ru_2(\mu\text{-}CO)_2(CO)_2(\eta\text{-}C_5H_5)_2]$ has been studied,[238-240] and has been shown to decarbonylate under ultraviolet radiation with the concurrent formation of the 17 electron radical species $[Ru(\eta\text{-}C_5H_5)(CO)_2]\cdot$ (Figure 6.1(a)) as well as small amounts of the triply carbonyl-bridged species $[Ru_2(\mu\text{-}CO)_3(\eta\text{-}C_5H_5)_2]$ (Figure 6.1(b)). These products react with CO under thermal or

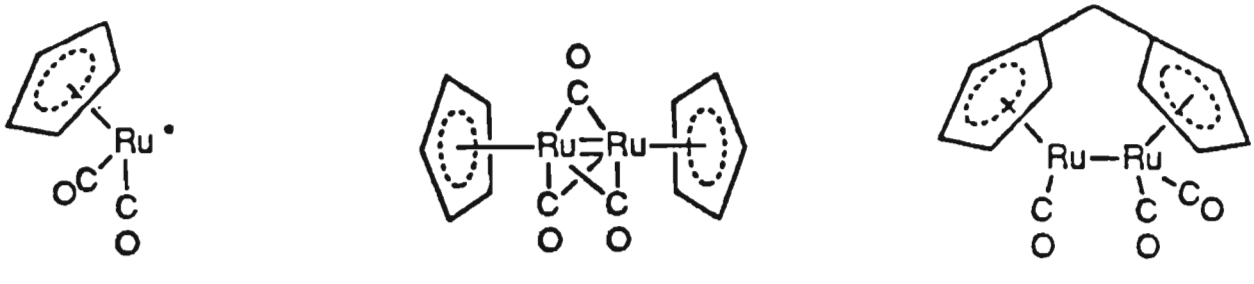

(a) (b) (c)

Figure 6.1

photochemical conditions to produce the parent complex $[Ru_2(CO)_4(\eta\text{-}C_5H_5)_2]$. On the other hand, photolysis of the related species

$[Ru_2(CO)_4\{(\eta^5\text{-}C_5H_4)_2CH_2\}]$, in which the cyclopentadienyl ligands are linked via a methylene group, leads to the generation of the co-ordinatively unsaturated tricarbonyl species $[Ru_2(CO)_3\{(\eta^5\text{-}C_5H_4)_2CH_2\}]$ (Figure 6.1(c)) in which all three carbonyl groups co-ordinate terminally. This species was also observed to add carbon monoxide under photochemical conditions as well as to react with dinitrogen to produce a co-ordinatively saturated dinitrogen species $[Ru_2N_2(CO)_3\{(\eta^5\text{-}C_5H_4)_2CH_2\}]$.

The biradical species $\cdot(CO)_4Re(\mu\text{-}\bar{L}\bar{L})Re(CO)_4\cdot$ ($\bar{L}\bar{L}$ = dppm, dmpm) have been observed as transient species following laser flash photolysis of $[Re_2(CO)_8(\mu\text{-}\bar{L}\bar{L})]$. These biradicals readily undergo recombination, electron transfer and halogen atom transfer reactions.

6.2 SYNTHESIS OF THE CO-ORDINATIVELY UNSATURATED SPECIES $[Ru_2(CO)_4\{\mu\text{-}(RO)_2PN(Et)P(OR)_2\}_2]$

It was found that the heating of a solution of the parent dimer $[Ru_2(\mu\text{-}CO)(CO)_4\{\mu\text{-}(Pr^iO)_2PN(Et)P(OPr^i)_2\}_2]$ in toluene under an atmosphere of dinitrogen or argon results in a change in the colour of the solution from yellow to pale red; no change in the colour was observed upon cooling this red solution back to room temperature. A $^{31}P\{^1H\}$ nmr spectrum of this solution exhibited a single resonance, readily assigned to the phosphorus atoms of the parent complex $[Ru_2(\mu\text{-}CO)(CO)_4\{\mu\text{-}(Pr^iO)_2PN(Et)P(OPr^i)_2\}_2]$ while an infrared spectrum of this solution confirmed the parent dinuclear complex to be the sole species present in solution. It was therefore concluded that the compound contributing to the red colour in solution was present in only trace amounts and is probably formed as a result of the loss of carbon monoxide from the parent complex. With the objective of displacing carbon monoxide from $[Ru_2(\mu\text{-}$

$CO)(CO)_4\{\mu\text{-}(Pr^iO)_2PN(Et)P(OPr^i)_2\}_2]$ a stream of argon was passed through a solution of this compound in toluene at elevated temperatures. This resulted in a change in the colour of the solution from pale red to an intense purple from which a purple-black crystalline compound, characterized as the co-ordinatively unsaturated species $[Ru_2(CO)_4\{\mu\text{-}(Pr^iO)_2PN(Et)P(OPr^i)_2\}_2]$ (**69**), could be isolated.

The solid-state infrared spectrum of $[Ru_2(CO)_4\{\mu\text{-}(Pr^iO)_2PN(Et)P(OPr^i)_2\}_2]$ in the CO stretching region contains two bands at 1864 and 1820 cm^{-1}. The $^{31}P\{^1H\}$ nmr spectrum of the compound in C_6D_6 exhibits a singlet at 158.85 ppm, while the ^1H nmr spectrum contains only resonances corresponding to the protons of the bridging diphosphazane ligands. The $^{13}C\{^1H\}$ nmr spectrum exhibits resonances assigned to the carbon atoms of the diphosphazane ligands as well as downfield quintets at 203.50 and 220.21 ppm respectively, assigned to the carbon atoms of the carbonyl ligands. This is interpreted in terms of the unsaturated compound containing two sets on non-equivalent carbonyl ligands. In contrast, the $^{13}C\{^1H\}$ nmr spectrum of the parent complex $[Ru_2(\mu\text{-}CO)(CO)_4\{\mu\text{-}(Pr^iO)_2PN(Et)P(OPr^i)_2\}_2]$ exhibits a broad set of resonances in the region 220.95 - 222.20 ppm, indicative of the carbonyl ligands in this compound being involved in a rapid fluxional process.

The structure of $[Ru_2(CO)_4\{\mu\text{-}(Pr^iO)_2PN(Et)P(OPr^i)_2\}_2]$ was established X-ray crystallographically and revealed the presence of two typically semi-bridging carbonyl ligands as well as two terminally bonded carbonyl groups collinear with the ruthenium-ruthenium vector. The Ru-C(2)-O(2) bond angle of the semi-bridging carbonyl ligand of 153.5(9)° can only be interpreted in terms of these equatorial carbonyl ligands not functioning as four-electron donors and on this basis, with no unusual short contact distances being apparent, the compound must be considered

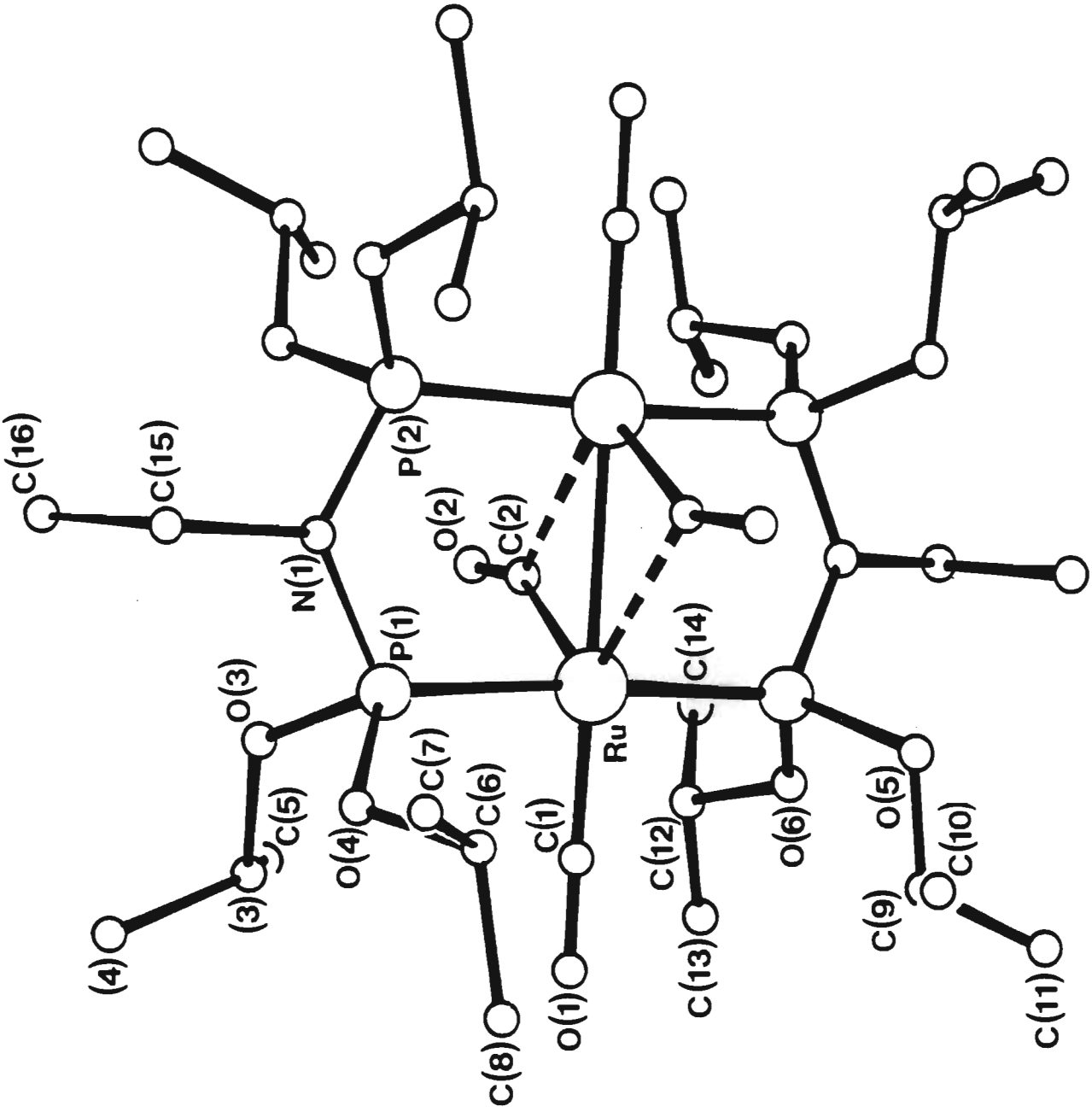

Figure 6.2: Structure of $[Ru_2(\mu_{SB}\text{-}CO)_2(CO)_2\{\mu\text{-}(Pr^iO)_2PN(Et)P(OPr^i)_2\}_2]$

as being co-ordinatively unsaturated. The ruthenium-ruthenium distance of 2.763(1)Å is marginally shorter than that for $[Ru_2(\mu\text{-}CO)(CO)_4\{\mu\text{-}(MeO)_2PN(Et)P(OMe)_2\}_2]$ {2.801(2)Å} and longer than that expected for a typical ruthenium-ruthenium double bond. The structure shows the compound adopts an essentially eclipsed configuration with a P(1)-Ru-Ru'-P(2') torsion angle of 4.75(8)°. Each atom in the molecule is related to another through a centre of inversion located midway between the two ruthenium atoms. The stereochemistry of $[Ru_2(\mu_{SB}\text{-}CO)_2(CO)_2\{\mu\text{-}(Pr^iO)_2PN(Et)P(OPr^i)_2\}_2]$ is illustrated in Figure 6.2 and the interatomic distances and angles of the metal-carbonyl fragment are depicted in Figure 6.3.

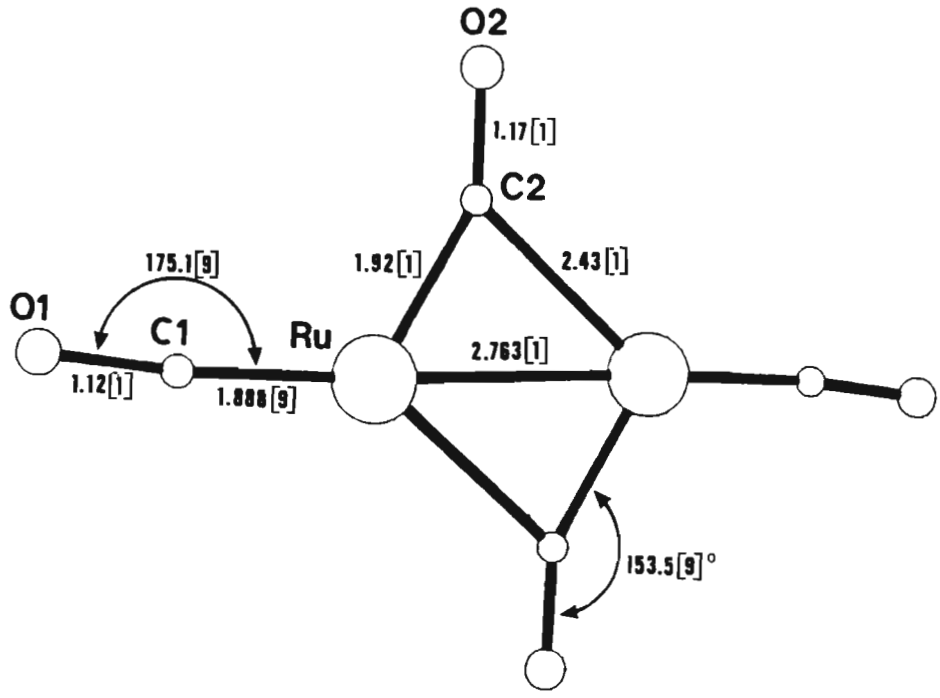

Figure 6.3

Semi-bridging carbonyl ligands such as those described in $[Ru_2(\mu_{SB}\text{-}CO)_2(CO)_2\{\mu\text{-}(Pr^iO)_2PN(Et)P(OPr^i)_2\}_2]$ have been shown to occur in a wide range of compounds. They may result, in the first instance, through steric crowding, examples of which are provided by the dimolybdenum com-

plexes of formula $[(\eta\text{-}C_5H_5)_2Mo_2(CO)_4(RC{\equiv}CR)]$[241] for which a symmetrical structure would have been predicted (Figure 6.4(a)). On the basis of an

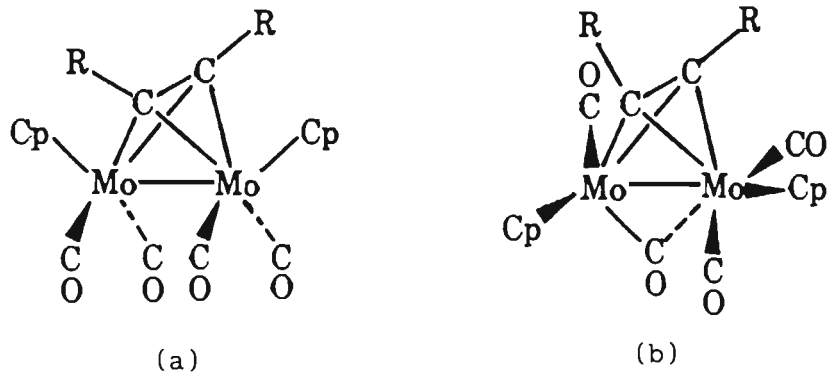

Figure 6.4

X-ray crystal structure determination it was established that one carbonyl ligand is forced into the vicinity of the Mo-Mo bond, opposite to the η^2-bound alkyne, to allow the cyclopentadienyl rings to move away from the R groups (Figure 6.4(b)). The frequency of the C-O stretching vibration associated with this carbonyl ligand is, as a consequence, considerably lowered (to *ca.* 1840 cm^{-1}).

Semi-bridging carbonyl ligands have also been observed to occur in inherently unsymmetrical environments such as that in $[Fe_2(\mu\text{-}CO)(\mu_{SB}\text{-}CO)(CO)_5(bipy)]$ (Figure 6.5(a)).[242] This prototypical example exhibits

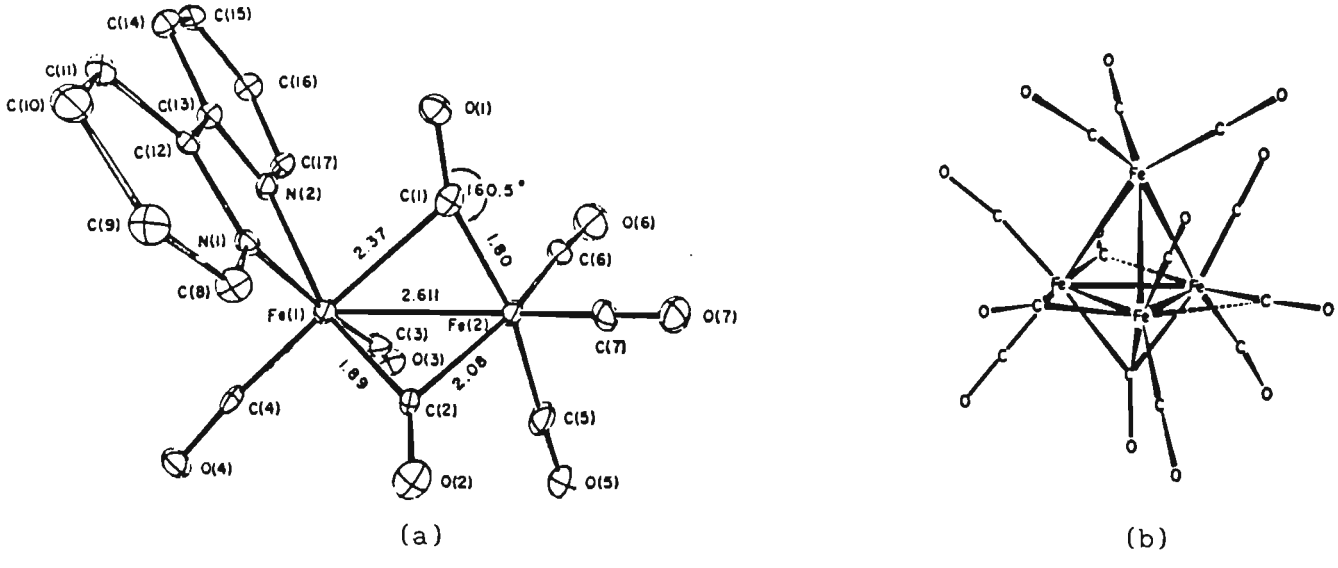

Figure 6.5: Structures of $[Fe_2(\mu\text{-}CO)(\mu_{SB}\text{-}CO)(CO)_5(bipy)]$ (a) and $[Fe_4(CO)_{13}]^{2-}$ (b)

a peak at 1850 cm^{-1} in its infrared spectrum, attributed to the presence of a semi-bridging carbonyl ligand. It has also been shown that cyclic sets of semi-bridging carbonyls may occur, as found in the carbonylate anion $[Fe_4(CO)_{13}]^{2-}$, shown in Figure 6.5(b). The structure of this compound revealed mean Fe-C distances of 1.82 and 2.28Å and a mean Fe-C-O angle of 155°, with respect to the three semi-bridging carbonyl ligands.

On the basis of the structure established for $[Ru_2(\mu_{SB}\text{-}CO)_2(CO)_2\{\mu\text{-}(Pr^iO)_2PN(Et)P(OPr^i)_2\}_2]$ it is not unreasonable to propose that this compound occurs as a diradical and, consistent with this, it reacts immediately with carbon tetrachloride affording the previously synthesized dichloro species $[Ru_2Cl_2(CO)_4\{\mu\text{-}(Pr^iO)_2PN(Et)P(OPr^i)_2\}_2]$. This is analogous to the reaction of the photolysis product of $[Re_2(CO)_8(\mu\text{-dppm})]$[243,244] with CCl_4, described above. The lack of a signal in the ESR spectrum of $[Ru_2(\mu_{SB}\text{-}CO)_2(CO)_2\{\mu\text{-}(Pr^iO)_2PN(Et)P(OPr^i)_2\}_2]$ may be attributed to anti-ferromagnetic coupling. On the other hand, on the basis of the chemistry established for this compound, it would appear that the molecule contains a metal-metal double bond on the basis that it undergoes typical addition reactions such as with dihydrogen and alkynes (see Section 6.3). The relatively small difference in the ruthenium-ruthenium distances for $[Ru_2(\mu_{SB}\text{-}CO)_2(CO)_2\{\mu\text{-}(Pr^iO)_2PN(Et)P(OPr^i)_2\}_2]$ and $[Ru_2(\mu\text{-}CO)(CO)_4\{\mu\text{-}(MeO)_2PN(Et)P(OMe)_2\}_2]$ may be explained in terms of the bridging diphosphazane ligands effecting stuctural constraints.

The UV-visible spectrum of $[Ru_2(\mu_{SB}\text{-}CO)_2(CO)_2\{\mu\text{-}(Pr^iO)_2PN(Et)P(OPr^i)_2\}_2]$ in THF exhibits an absorption band at 553 nm, as compared to the UV-visible spectrum of the parent species $[Ru_2(\mu\text{-}CO)(CO)_4\{\mu\text{-}(Pr^iO)_2PN(Et)P\text{-}(OPr^i)_2\}_2]$ in which a band at 353 nm is observed. This charge-transfer band is within the region expected for a compound containing a metal-

metal double bond such as that observed for the dirhodium species $[Rh_2(\eta\text{-}C_5Me_5)_2(CO)_2]$ (λ_{max} 582 nm)[245] or for a diradical species such as $\cdot(OC)_4RePCy_2(CH_2)_2Cy_2PRe(CO)_4\cdot$ (λ_{max} 550 nm).

The synthesis of the co-ordinatively unsaturated species $[Ru_2(CO)_4\{\mu\text{-}(Pr^iO)_2PN(Et)P(OPr^i)_2\}_2]$ has also been achieved by adopting a number of other procedures, for example by pyrolysis of solid $[Ru_2(\mu\text{-}CO)(CO)_4\{\mu\text{-}(Pr^iO)_2PN(Et)P(OPr^i)_2\}_2]$ or $[Ru_2H_2(CO)_4\{\mu\text{-}(Pr^iO)_2PN(Et)P(OPr^i)_2\}_2]$ *(vide infra)* at 80°C under high vacuum, or by passage of a stream of argon through a toluene solution of the dihydrido species $[Ru_2H_2(CO)_4\{\mu\text{-}(Pr^iO)_2PN(Et)P(OPr^i)_2\}_2]$ at 80°C . The latter procedure was found to be the most efficient in terms of achieving a rapid high-yield synthesis of the unsaturated species. The synthesis of this compound may also be effected by an entirely different route *viz.* that involving the oxidation of the parent dimer $[Ru_2(\mu\text{-}CO)(CO)_4\{\mu\text{-}(Pr^iO)_2PN(Et)P(OPr^i)_2\}_2]$ by silver(I) salts in THF in the presence of trace amounts of water. As described in Chapter 3, the product of this reaction, *viz.* the dicationic aquo solvento species $[Ru_2(CO)_5(H_2O)\{\mu\text{-}(Pr^iO)_2PN(Et)P(OPr^i)_2\}_2]^{2+}$, may be readily deprotonated to give the neutral carbon dioxide adduct $[Ru_2(CO)_4\{\mu\text{-}OC(O)\}\{\mu\text{-}(Pr^iO)_2PN(Et)P(OPr^i)_2\}_2]$. This compound is readily decarboxylated on heating, to afford the co-ordinatively unsaturated species $[Ru_2(CO)_4\{\mu\text{-}(Pr^iO)_2PN(Et)P(OPr^i)_2\}_2]$. Significantly, this compound reacts quantitatively with carbon monoxide to produce the parent complex $[Ru_2(\mu\text{-}CO)(CO)_4\{\mu\text{-}(Pr^iO)_2PN(Et)P(OPr^i)_2\}_2]$, thereby completing the redox cycle.

The synthesis of the analogous tetramethoxydiphosphazane-bridged derivative $[Ru_2(CO)_4\{\mu\text{-}(MeO)_2PN(Et)P(OMe)_2\}_2]$ has similarly been achieved but, significantly, the parent complex $[Ru_2(\mu\text{-}CO)(CO)_4\{\mu\text{-}(MeO)_2PN(Et)P(OMe)_2\}_2]$ could not be converted entirely to $[Ru_2(CO)_4\{\mu\text{-}(Me-$

$O)_2PN(Et)P(OMe)_2\}_2]$ using any of the procedures described above for the synthesis of the analogous tetraisopropoxydiphosphazane-bridged derivative.

6.3 REACTIVITY OF $[Ru_2(CO)_4\{\mu\text{-}(Pr^iO)_2PN(Et)P(OPr^i)_2\}_2]$ TOWARDS VARIOUS SMALL MOLECULE COMPOUNDS

Not surprisingly, $[Ru_2(CO)_4\{\mu\text{-}(Pr^iO)_2PN(Et)P(OPr^i)_2\}_2]$ is highly reactive and reacts spontaneously with appropriate electrophiles, nucleophiles and radical sources. Thus, addition of carbon monoxide to a solution of the unsaturated species $[Ru_2(CO)_4\{\mu\text{-}(Pr^iO)_2PN(Et)P(O\text{-}Pr^i)_2\}_2]$ at room temperature resulted in the quantitative formation of the parent pentacarbonyl derivative $[Ru_2(\mu\text{-}CO)(CO)_4\{\mu\text{-}(Pr^iO)_2PN(Et)P(O\text{-}Pr^i)_2\}_2]$. Passage of a stream of ^{13}C-enriched carbon monoxide through a solution of the unsaturated species is therefore an effective means of producing a ^{13}C-enriched sample of $[Ru_2(\mu\text{-}CO)(CO)_4\{\mu\text{-}(Pr^iO)_2PN(Et)P\text{-}(OPr^i)_2\}_2]$ which may prove useful in monitoring reactions involving these complexes using $^{13}C\{^1H\}$ nmr spectroscopy.

Addition of an excess of the alkynes, HC≡CH, HC≡CMe, HC≡CPh, $HC{\equiv}CCO_2Me$ and $MeO_2CC{\equiv}CCO_2Me$ led to the formation of vinylidene-bridged products of the type $[Ru_2(CO)_4(\mu\text{-}\eta^1\text{-}C{=}CHR)\{\mu\text{-}(Pr^iO)_2PN(Et)P(OPr^i)_2\}_2]$ and/or alkendiyl-bridged derivatives of formula $[Ru_2(CO)_4(\mu\text{-}\sigma^2\text{-}RC{=}CR')\{\mu\text{-}(Pr^iO)_2PN(Et)P(OPr^i)_2\}_2]$. The identities of these products were confirmed by comparison of their $^{31}P\{^1H\}$ nmr spectra with those of the products obtained from the reactions of the pentacarbonyl species $[Ru_2(\mu\text{-}CO)(CO)_4\{\mu\text{-}(Pr^iO)_2PN(Et)P(OPr^i)_2\}_2]$ with various alkynes (see Chapter 5). Significantly, the relative yields of the vinylidene- and alkendiyl-bridged isomers from the reactions of the unsaturated species with various alkynes were found to be the same as those from the

reactions of the parent pentacarbonyl species with these alkynes.

The room temperature reaction of $[Ru_2(CO)_4\{\mu\text{-}(Pr^iO)_2PN(Et)P(OPr^i)_2\}_2]$ with dihydrogen in toluene was found to result in an immediate change in the colour of the solution from purple to yellow-orange. Orange crystals of the product of this hydrogenation could be isolated from this solution and were characterized as the dihydrido species $[Ru_2H_2(CO)_4\{\mu\text{-}(Pr^iO)_2PN(Et)P(OPr^i)_2\}_2]$ (**70**). The synthesis of this compound is best achieved however by passage of a stream of dihydrogen gas through a solution of the parent pentacarbonyl species $[Ru_2(\mu\text{-}CO)(CO)_4\{\mu\text{-}(Pr^iO)_2PN(Et)P(OPr^i)_2\}_2]$ in toluene at 80°C. The $^{31}P\{^1H\}$ nmr spectrum of $[Ru_2H_2(CO)_4\{\mu\text{-}(Pr^iO)_2PN(Et)P(OPr^i)_2\}_2]$, measured in C_6D_6, exhibits a singlet at 159.25 ppm, while its ^1H nmr spectrum contains resonances corresponding to the protons of the diphosphazane ligands as well as a well-resolved quintet at -8.36 ppm, the integral of which corresponds to two protons. The chemical shift of this quintet is indicative of the compound containing terminally-bonded hydride ligands. The solid state infrared spectrum of the compound in the C-O stretching region exhibits strong peaks at 1994 and 1933 cm^{-1} and a weaker band at 1878 cm^{-1} with the latter being tentatively assigned to a ruthenium-hydrogen stretching vibration. This assignment is based upon the infrared spectrum of the related structurally characterized disolvento species $[Ru_2(CO)_4(NCPh)_2\{\mu\text{-}(Pr^iO)_2PN(Et)P(OPr^i)_2\}_2](SbF_6)_2$ which contains two strong bands in the carbonyl region of its infrared spectrum *(vide infra)*. The $^{13}C\{^1H\}$ nmr spectrum exhibits a broad set of resonances in the range 203.4 - 203.7 ppm assigned to the carbon atoms of the carbonyl ligands, indicating the carbonyl and hydride ligands are involved in a rapid fluxional process in solution. The molecular structure of this compound was established X-ray crystallographically, and is illustrated in Figure 6.6. A salient feature of the structure is

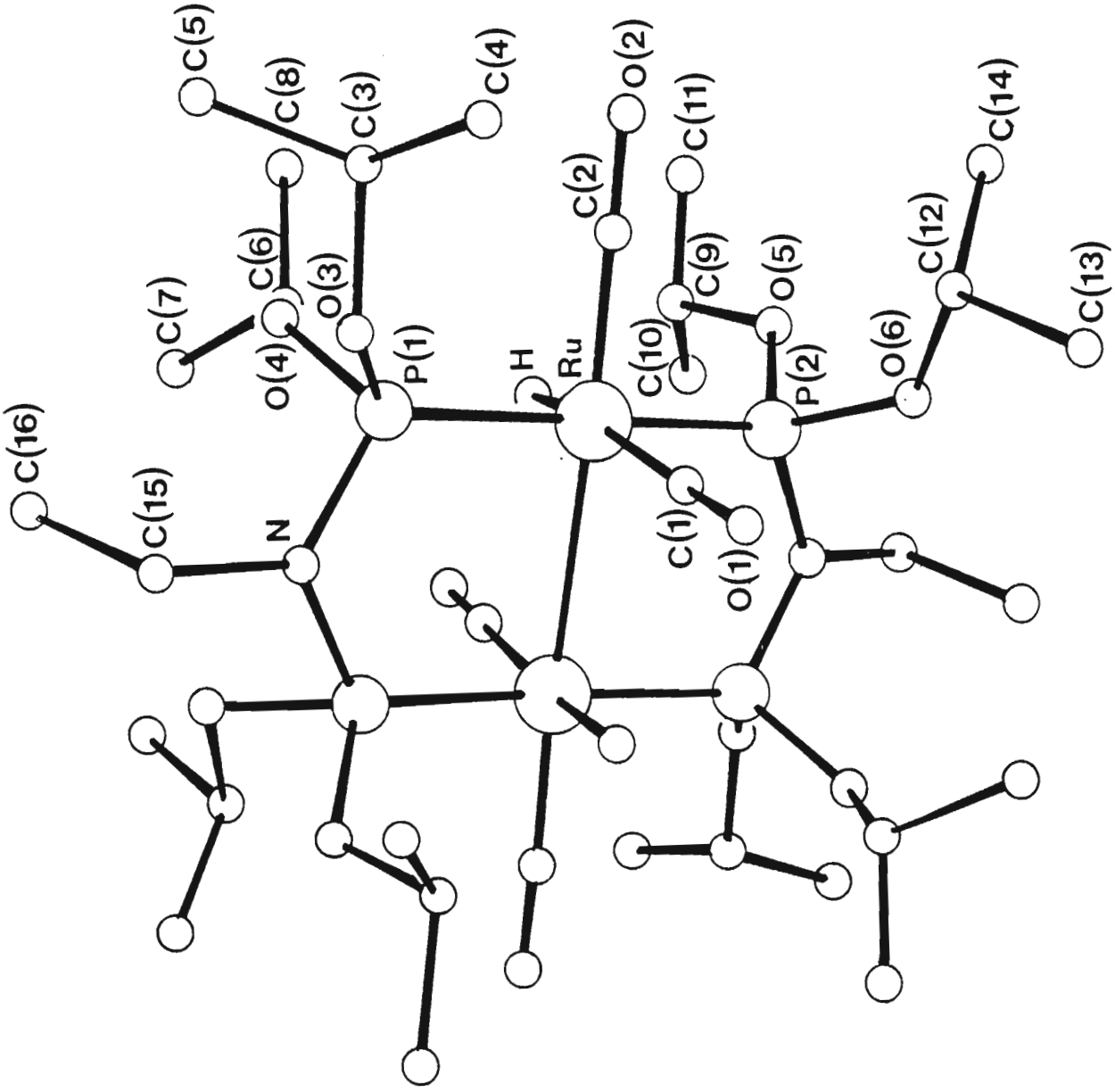

Figure 6.6: Structure of $[Ru_2H_2(CO)_4\{\mu\text{-}(Pr^iO)_2PN(Et)P(OPr^i)_2\}_2]$

that the hydrogen atoms are bonded terminally and occupy an equatorial site on each ruthenium atom. This is in contrast to the chloro groups in $[Ru_2Cl_2(CO)_4\{\mu\text{-}(MeO)_2PN(Et)P(OMe)_2\}_2]$ which, as established X-ray crystallographically, are bonded in axial positions. The molecule contains a centre of inversion located midway between the two ruthenium atoms, and adopts a near eclipsed configuration {P(1)-Ru-Ru'-P(2)' = 8.6(1)°}; the geometry at each ruthenium atom is essentially octahedral. The ruthenium atoms are separated by a distance of 2.911(1)Å which is slightly longer than that for the tetramethoxydiphosphazane-bridged parent species $[Ru_2(\mu\text{-}CO)(CO)_4\{\mu\text{-}(MeO)_2PN(Et)P(OMe)_2\}_2]$ *(vide supra)*. The positions of the hydride ligands were located and found to be at a distance of 1.72(6)Å from the ruthenium atoms. This distance is slightly longer than that for a typical terminal Ru-H bond as found in $[RuH(H_2)I(PCy_3)_2]$[246-248] for which a Ru-H distance of 1.51(5)Å has been determined.

An interesting feature of the crystals of $[Ru_2H_2(CO)_4\{\mu\text{-}(Pr^iO)_2PN(Et)P(OPr^i)_2\}_2]$, isolated as orange rectangular blocks, is their dichroic behaviour; when viewed down one crystal plane they appeared pale yellow whereas when viewed through another plane at approximately 90°C to the former, their colour was blood red.

The dihydrido species was found to readily reductively eliminate dihydrogen to afford the co-ordinatively unsaturated species $[Ru_2(CO)_4\{\mu\text{-}(Pr^iO)_2PN(Et)P(OPr^i)_2\}_2]$. In fact, merely applying a vacuum to a solution of $[Ru_2H_2(CO)_4\{\mu\text{-}(Pr^iO)_2PN(Et)P(OPr^i)_2\}_2]$ at room temperature results in the formation of the unsaturated species, although heat is required for this reaction to go to completion. The dihydrido species is thus also highly reactive, affording the parent pentacarbonyl species $[Ru_2(\mu\text{-}CO)(CO)_4\{\mu\text{-}(Pr^iO)_2PN(Et)P(OPr^i)_2\}_2]$ on reaction with carbon mon-

oxide, the vinylidene-bridged and/or alkendiyl-bridged species, $[Ru_2(CO)_4(\mu\text{-}\eta^1\text{-}C{=}CHR)\{\mu\text{-}(Pr^iO)_2PN(Et)P(OPr^i)_2\}_2]$ and $[Ru_2(CO)_4(\mu\text{-}\sigma^2\text{-}RC{=}CR')\{\mu\text{-}(Pr^iO)_2PN(Et)P(OPr^i)_2\}_2]$ respectively, on reaction with alkynes, and the diiodo species $[Ru_2I_2(CO)_4\{\mu\text{-}(Pr^iO)_2PN(Et)P(OPr^i)_2\}_2]$ on reaction with iodine. The reaction of $[Ru_2H_2(CO)_4\{\mu\text{-}(Pr^iO)_2PN(Et)P\text{-}(OPr^i)_2\}_2]$ with alkynes is in contrast to that observed for the reaction of the related dimanganese dihydrido species $[Mn_2(\mu\text{-}H)_2(CO)_6(\mu\text{-dppm})]$ with acetylene, which results in the insertion of the alkyne into a M-H bond producing $[Mn_2(\mu\text{-}H)(\mu\text{-}\eta^1,\eta^2\text{-}CH{=}CH_2)(CO)_6(\mu\text{-dppm})]$.

The chemistry of metal-hydrides is particularly relevant in homogeneous catalysis,[249-252] and the hydride ligand ranks only second to phosphorus donor ligands in playing a crucial role therein. For example, the highly active compound $[HRuCl(PPh_3)_3]$[253] is used extensively as a hydrogenation catalyst.

The first well-defined, although unstable hydrides $[H_2Fe(CO)_4]$ and $[H_2Co(CO)_4]$ were discovered by Hieber and Leutert in 1931,[254] and a vast number of transition metal compounds containing hydride ligands have since been reported. Some hydrides can be prepared directly by reaction of an appropriate precursor with dihydrogen. The initial step in the hydrogen addition is arguably the formation of a molecular dihydrogen complex, several of which have more recently been identified and fully characterized.[255,256] The attack of the hydrogen molecule at an electron-rich centre is accompanied by a transfer of electron density from the metal to the antibonding σ^*-orbital of the dihydrogen molecule, leading to bond weakening and the formation of two *cis*-M-H bonds via a three-centre addition mechanism as depicted below:

Scheme 6.2

The oxidative addition of dihydrogen is a special case compared to other substances that can be added oxidatively in that despite the high H-H bond energy (450 kJ mol^{-1}), oxidative addition often occurs with great facility. The reactions are commonly reversible at 25°C at atmospheric pressure. For example the square planar iridium complex $[IrCl(CO)(PPh_3)_2]$ reversibly adds dihydrogen to form the dihydrido species $[H_2IrCl(CO)(PPh_3)_2]$. The formation of dihydrido species by oxidative addition of dihydrogen to co-ordinatively unsaturated species usually occurs with even greater ease, illustrated by the reaction of the violet coloured compound $[RhCl(Pr^i_3)_2]$ with dihydrogen to produce $[RhClH_2(Pr^i_3)_2]$.

The oxidative addition or reductive elimination of dihydrogen to or from binuclear complexes has been well documented.[257-259] In each case hydrogen addition is thought to occur at a single metal site, rather than co-operatively at two metals. A mechanism involving oxidative addition across or reductive elimination of dihydrogen from two metal centres has not been favoured in the past because this involves a four-centre transition state which is orbitally forbidden (Scheme 6.3); there is evidence for a binuclear mechanism in some cases, however.[97,260,261]

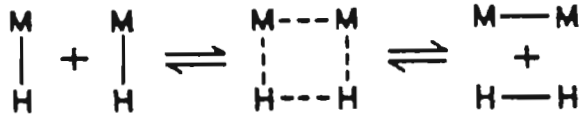

Scheme 6.3

Reactions in which dihydrogen reversibly displaces co-ordinated carbon monoxide in transition metal complexes are relatively rare. Two examples[257,262] in which this has been shown to occur are provided by

the reactions represented by the equations below.

$$[Ir(CO)_3(PPh_3)_2] + H_2 \rightleftharpoons [IrH_2(CO)_2(PPh_3)_2] + CO$$

$$[Os_3(CO)_{12}] + H_2 \rightleftharpoons [Os_3H_2(CO)_{10}] + 2CO$$

The first reported binuclear complex having this property is the complex ion $[Pt_2H_2(\mu\text{-}H)(\mu\text{-}dppm)_2]^+$ [263] which reacts reversibly with carbon monoxide to give dihydrogen and a hydridoplatinum(I) complex cation $[Pt_2H(CO)(\mu\text{-}dppm)_2]^+$. The dihydrido species $[Pt_2H_2(\mu\text{-}H)(\mu\text{-}dppm)_2]^+$ was found to be thermally stable and the reductive elimination of hydrogen from this derivative has been shown to be induced only by addition of soft donor ligands or under photochemical conditions.[261] A more recently reported heterobimetallic complex $[(CO)_2Ru(\mu\text{-}CO)(\mu\text{-}dppm)_2Mo(CO)_3]$[264] has been shown to lose carbon monoxide upon heating in vacuo to afford a red compound identified as the metal-metal double-bonded species $[(CO)Ru(\mu\text{-}CO)_2(\mu\text{-}dppm)_2Mo(CO)_2]$. This compound reacts reversibly with dihydrogen at room temperature in toluene to produce a dihydride species $[(CO)_2Ru(\mu\text{-}H)_2(\mu\text{-}dppm)_2Mo(CO)_3]$ (Scheme 6.4) in which the hydride ligands bridge

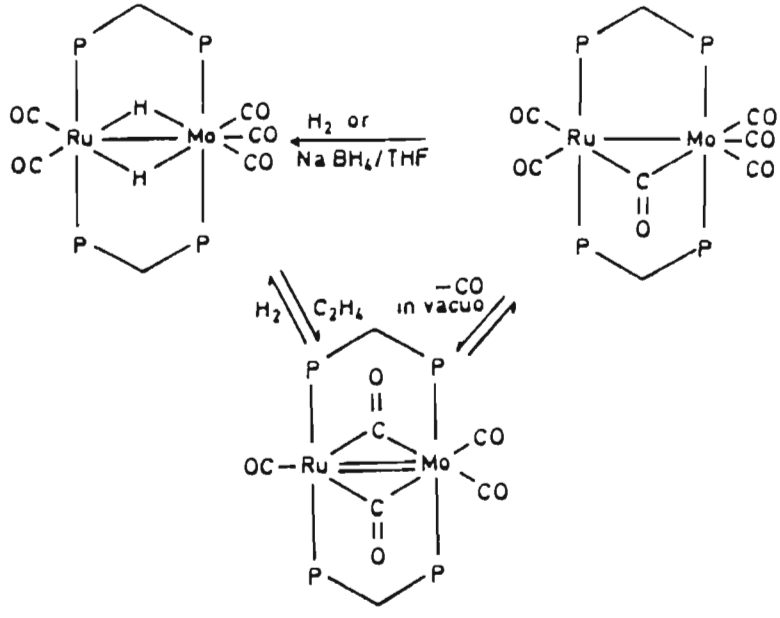

Scheme 6.4

the two metal atoms, in contrast to that observed for the diruthenium species $[Ru_2H_2(CO)_4\{\mu\text{-}(Pr^iO)_2PN(Et)P(OPr^i)_2\}_2]$.

Ditertiaryphosphine-bridged derivatives of dirhodium have also shown interesting redox properties. For example, the sodium borohydride reduction of the dirhodium derivative $[Rh_2Cl_2(CO)_2(\mu\text{-dppm})_2]$ results in the formation of the dihydrido species $[Rh_2(\mu\text{-}H)_2(CO)_2(\mu\text{-dppm})_2]$ from which dihydrogen is readily eliminated to form the metal-metal bonded species $[Rh_2(CO)_2(\mu\text{-dppm})_2]$, which in turn reacts irreversibly with carbon monoxide to form $[Rh_2(CO)_3(\mu\text{-dppm})_2]$.[45]

The co-ordinatively unsaturated species $[Ru_2(CO)_4\{\mu\text{-}(Pr^iO)_2PN(Et)P(OPr^i)_2\}_2]$ and to a lesser extent the dihydrido species $[Ru_2H_2(CO)_4\{\mu\text{-}(Pr^iO)_2PN(Et)P(OPr^i)_2\}_2]$ are highly reactive towards dioxygen, particularly in solution. Thus, exposing a solution of the unsaturated species in toluene to dioxygen or air was found to result in a change in the colour of the solution from purple to pale yellow. A white crystalline compound was isolated from this solution and identified as the dioxygen species $[Ru_2(\mu\text{-}O_2)(CO)_4\{\mu\text{-}(Pr^iO)_2PN(Et)P(OPr^i)_2\}_2]$ (**71**). The compound was established to be neutral by virtue of its solubility in hexane, as well as from the low frequencies observed for the C-O stretching bands in its infrared spectrum. The band pattern of these peaks is typical of that of a tetracarbonyl species of the type $[Ru_2(\mu\text{-}X)(CO)_4\{\mu\text{-}(Pr^iO)_2PN(Et)P(OPr^i)_2\}_2]$. The $^{31}P\{^1H\}$ nmr spectrum of this species, measured in C_6D_6, exhibits a singlet at 135.35 ppm, consistent with a compound having a symmetrical structure. A ^1H nmr spectrum exhibits only resonances corresponding to the protons of the diphosphazane ligands.

This dioxygen species is stable in air and inert to attack by both

carbon monoxide and dihydrogen.

Molecular oxygen has been shown to react reversibly with a range of transition metal complexes with such reactions being crucial to life processes, for example in oxygenation of hemogloblin and myoglobin. The first synthetic oxygen carrier was Vaska's compound $[IrCl(CO)(PPh_3)_2]$ which reversibly adds dioxygen to afford $[O_2IrCl(CO)(PPh_3)_2]$.[265] While this compound is diamagnetic, a paramagnetic species $[RhCl(O_2)(PPr^i_3)_2]$ was found to be reversibly formed on reaction of $[RhCl(PPr^i_3)_2]$ with dioxygen, and in which the dioxygen is co-ordinated as a superoxo ligand. A ruthenium dioxygen species *viz.* $[RuO_2(Cl)(NO)(PPh_3)_2]$, obtained from the reaction of $[RuCl(CO)(NO)(PPh_3)_2]$ with oxygen, has also been reported[266] but in this case the addition appeared to be irreversible. This dioxygen species exhibits a strong absorption in its infrared spectrum at 875 cm^{-1}, assigned to the O-O stretching vibration of a η^2-peroxo group.

$[Ru_2(CO)_4\{\mu\text{-}(Pr^iO)_2PN(Et)P(OPr^i)_2\}_2]$ was found to react almost instantaneously with nitric oxide, sulphur dioxide and stannous chloride affording $[Ru_2(\mu\text{-}NO)(CO)_4\{\mu\text{-}(Pr^iO)_2PN(Et)P(OPr^i)_2\}_2]^+$, $[Ru_2(\mu\text{-}SO_2)(CO)_4\{\mu\text{-}(Pr^iO)_2PN(Et)P(OPr^i)_2\}_2]$ and $[Ru_2(\mu\text{-}SnCl_2)(CO)_4\{\mu\text{-}(Pr^iO)_2PN(Et)P(OPr^i)_2\}_2]$ respectively, all of which have previously been synthesized by reaction of the parent pentacarbonyl species $[Ru_2(\mu\text{-}CO)(CO)_4\{\mu\text{-}(Pr^iO)_2PN(Et)P(OPr^i)_2\}_2]$ with the appropriate substrate.

Interestingly, $[Ru_2(CO)_4\{\mu\text{-}(Pr^iO)_2PN(Et)P(OPr^i)_2\}_2]$ also reacts spontaneously with sulphur powder at room temperature in toluene affording, in almost quantitative yield, the sulphide-bridged species $[Ru_2(\mu\text{-}S)(CO)_4\{\mu\text{-}(Pr^iO)_2PN(Et)P(OPr^i)_2\}_2]$ (**74**). The synthesis of this compound using this procedure is advantageous to that previously discussed (see

Chapter 2), in that high yields are obtained in a one-step reaction.

As discussed previously, the unsaturated species $[Ru_2(CO)_4\{\mu\text{-}(Pr^iO)_2PN(Et)P(OPr^i)_2\}_2]$ is formed via the loss of carbon dioxide from $[Ru_2(CO)_4\{\mu\text{-}OC(O)\}\{\mu\text{-}(Pr^iO)_2PN(Et)P(OPr^i)_2\}_2]$ and it was therefore envisaged that carbon dioxide might react with the unsaturated species to afford the carbon dioxide adduct. This adduct has been shown to be readily protonated to the aquo solvento species $[Ru_2(CO)_5(H_2O)\{\mu\text{-}(Pr^iO)_2PN(Et)P(OPr^i)_2\}_2]^{2+}$. This compound may be readily reduced under appropriate conditions to give water and the parent pentacarbonyl species $[Ru_2(\mu\text{-}CO)(CO)_4\{\mu\text{-}(Pr^iO)_2PN(Et)P(OPr^i)_2\}_2]$, which in turn may be decarbonylated under thermal conditions to afford the unsaturated species. This pathway is summarized in the scheme below; all intermediates in the cycle

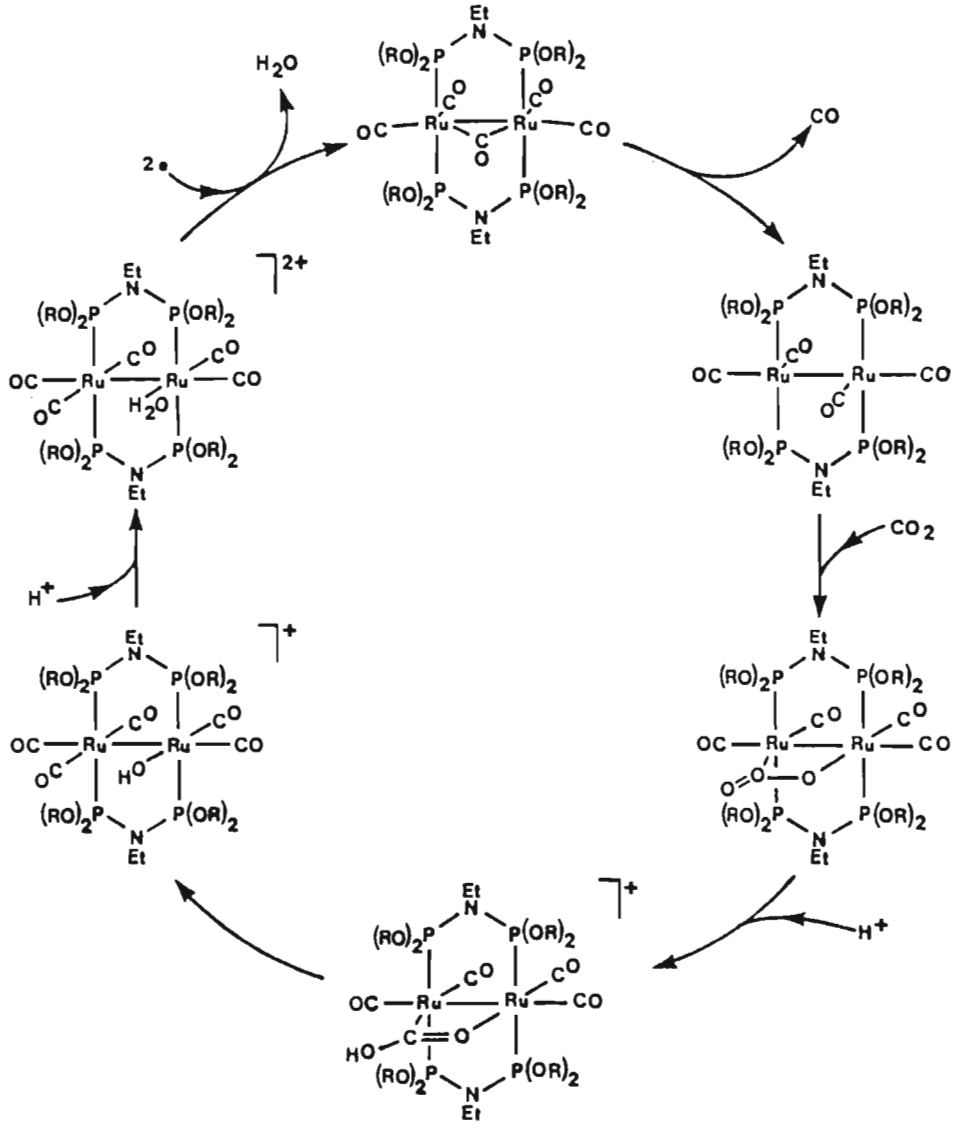

have been isolated and characterized and each step but one has been confirmed. The only step required for this cycle to be complete is that involving the reaction of $[Ru_2(CO)_4\{\mu\text{-}(Pr^iO)_2PN(Et)P(OPr^i)_2\}_2]$ with carbon dioxide, but this has as yet not been achieved. More suprisingly is that $[Ru_2(CO)_4\{\mu\text{-}(Pr^iO)_2PN(Et)P(OPr^i)_2\}_2]$ also appears to be inert towards carbon disulphide.

The co-ordinatively unsaturated species appears to be inert towards dinitrogen at room temperature and atmospheric pressure. This assumption is based upon the spectroscopic properties of $[Ru_2(CO)_4\{\mu\text{-}(Pr^iO)_2PN(Et)P(OPr^i)_2\}_2]$ being identical under both an atmosphere of dinitrogen and argon.

$[Ru_2(CO)_4\{\mu\text{-}(Pr^iO)_2PN(Et)P(OPr^i)_2\}_2]$ was found to be unstable in carbon tetrachloride affording the dichloro species $[Ru_2Cl_2(CO)_4\{\mu\text{-}(Pr^iO)_2PN(Et)P(OPr^i)_2\}_2]$, as mentioned above, but appears to be relatively stable in chloroform and dichloromethane. It is also stable in organonitrile solvents such as benzonitrile and acetonitrile, although solubility in the latter is poor.

6.4 ELECTROCHEMISTRY OF $[Ru_2(CO)_4\{\mu\text{-}(Pr^iO)_2PN(Et)P(OPr^i)_2\}_2]$

The electrochemistry of the parent pentacarbonyl complexes $[Ru_2(\mu\text{-}CO)(CO)_4\{\mu\text{-}(RO)_2PN(Et)P(OR)_2\}_2]$ (R = Me, Pr^i) has been discussed in Chapter 2. Because of the presence of four strongly electron-donating phosphorus atoms and only five carbonyl groups, these dinuclear complexes are electron-rich and, as such, are readily oxidized. On this basis, the co-ordinatively unsaturated species $[Ru_2(CO)_4\{\mu\text{-}(Pr^iO)_2PN(Et)P(OPr^i)_2\}_2]$ may be considered as being even more electron-rich and should be similarly readily oxidized. The electrochemistry of $[Ru_2(CO)_4\{\mu\text{-}$

$(Pr^iO)_2PN(Et)P(OPr^i)_2\}_2]$ has therefore been studied and the preliminary results of this investigation are discussed below.

Figure 6.7 shows the CV of $[Ru_2(CO)_4\{\mu\text{-}(Pr^iO)_2PN(Et)P(OPr^i)_2\}_2]$ measured

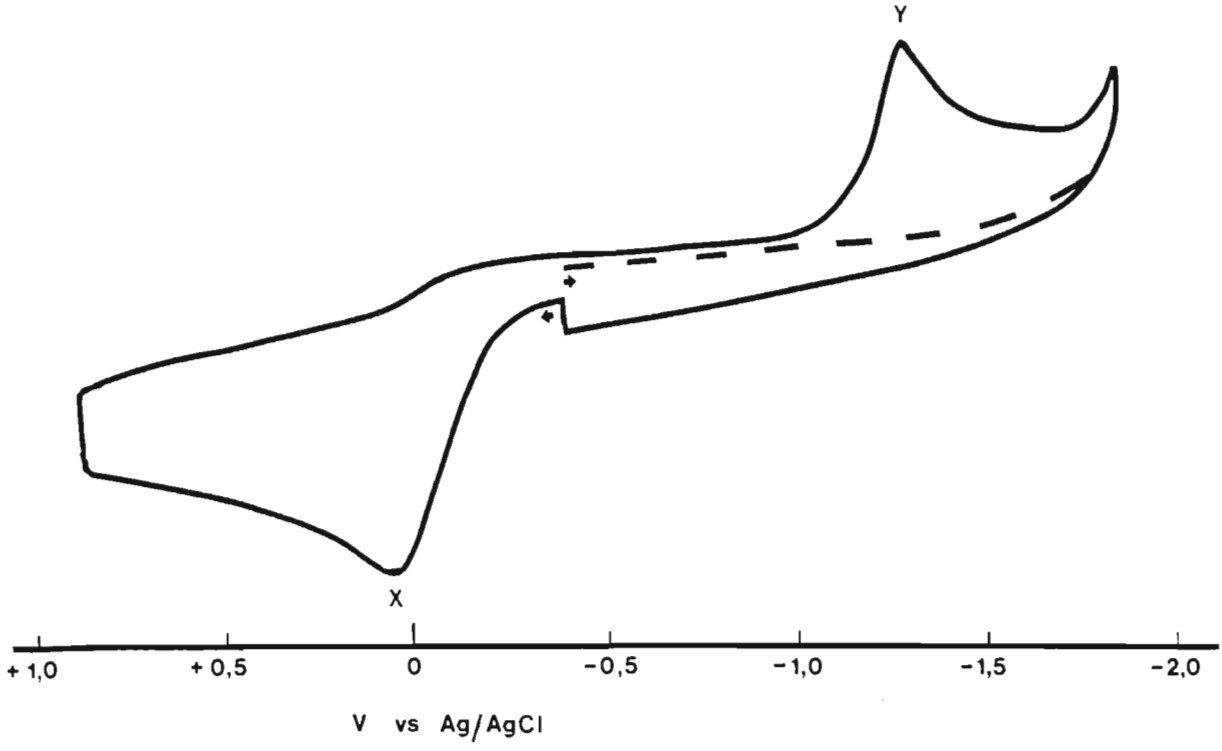

Figure 6.7: CV of 1.0m*M* $[Ru_2(\mu_{SB}\text{-}CO)_2(CO)_2\{\mu\text{-}(Pr^iO)_2PN(Et)P(OPr^i)_2\}_2]$ in benzonitrile (0.1*M* TBAP) at Pt (298 K, 200 mV s^{-1})

in benzonitrile; co-workers have since established that similar CV's are obtained in acetone and dichloromethane. In contrast to the CV of $[Ru_2(\mu\text{-}CO)(CO)_4\{\mu\text{-}(Pr^iO)_2PN(Et)P(OPr^i)_2\}_2]$ which reveals two oxidation waves, only one broad and irreversible wave is observed in the CV of this species on scanning anodically. Moreover, the height of this peak (i_{pa} μA at 200 mV s^{-1}) is approximately double that observed for the primary oxidation wave in the CV of the pentacarbonyl species $[Ru_2(\mu\text{-}CO)(CO)_4\{\mu\text{-}(Pr^iO)_2PN(Et)P(OPr^i)_2\}_2]$ (i_{pa} μA at 200 mV s^{-1}). This oxidation is therefore proposed to be associated with an overall two electron-transfer reaction. Interestingly, the potential of this oxidation is more anodic than that of the primary oxidation of

$[Ru_2(\mu\text{-}CO)(CO)_4\{\mu\text{-}(Pr^iO)_2PN(Et)P(OPr^i)_2\}_2]$. This may be explained in terms of a partial redistribution of electron density occurring onto the semi-bridging carbonyls of $[Ru_2(\mu\text{-}CO)(CO)_4\{\mu\text{-}(Pr^iO)_2PN(Et)P(OPr^i)_2\}_2]$, thereby resulting in the oxidation potential of this compound being more positive. The potential of the 2-electron oxidation is considerably more cathodic than the potential of the second oxidation wave for $[Ru_2(\mu\text{-}CO)(CO)_4\{\mu\text{-}(Pr^iO)_2PN(Et)P(OPr^i)_2\}_2]$ however. The appearance of a broad cathodic wave (X, Figure 6.7) in the reverse scan is also significant. It has been possible to confirm at least for benzonitrile as solvent that the species formed following the removal of two electrons from $[Ru_2(CO)_4\{\mu\text{-}(Pr^iO)_2PN(Et)P(OPr^i)_2\}_2]$, and which is subsequently reduced at X in the reverse scan (Figure 6.7), is the dicationic disolvento species $[Ru_2(CO)_4(NCPh)_2\{\mu\text{-}(Pr^iO)_2PN(Et)P\text{-}(OPr^i)_2\}_2]^{2+}$. This was confirmed by synthesis of its hexafluoroantimonate salt *(vide infra)* and measurement of its CV in benzonitrile. The primary reduction peak in the CV (Figure 6.8) coincides with peak X in

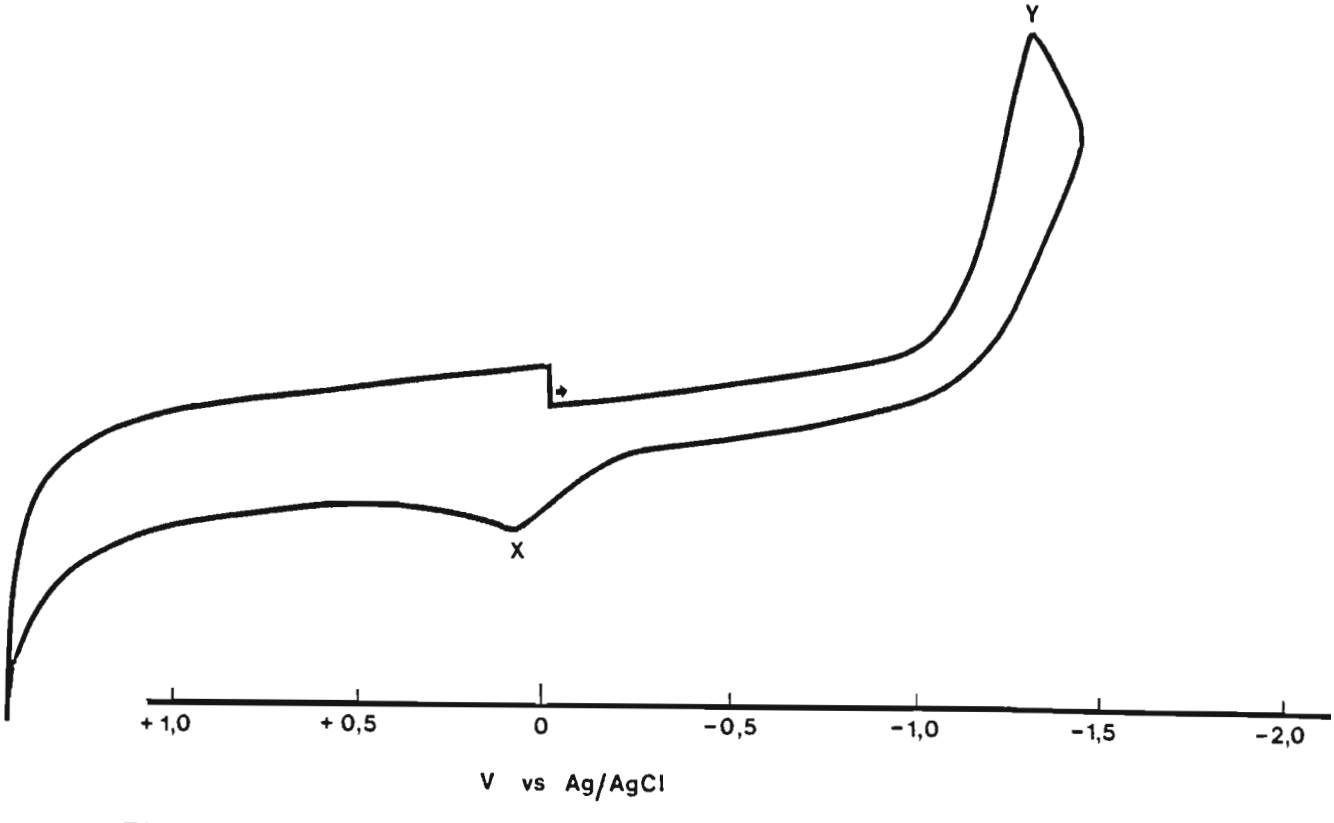

Figure 6.8: CV of 1.0m*M* $[Ru_2(CO)_4(NCPh)_2\{\mu\text{-}(Pr^iO)_2PN(Et)P(OPr^i)_2\}_2]\text{-}(SbF_6)_2$ in benzonitrile (0.1*M* TBAP) at Pt (298 K, 200 mV s^{-1})

the CV of the parent compound $[Ru_2(CO)_4\{\mu\text{-}(Pr^iO)_2PN(Et)P(OPr^i)_2\}_2]$ and, furthermore, an anodic wave is obtained in the reverse scan which corresponds to the oxidation wave of the parent unsaturated complex $[Ru_2(CO)_4\{\mu\text{-}(Pr^iO)_2PN(Et)P(OPr^i)_2\}_2]$.

6.5 REACTIONS OF $[Ru_2(CO)_4\{\mu\text{-}(Pr^iO)_2PN(Et)P(OPr^i)_2\}_2]$ WITH SILVER(I) SALTS IN BENZONITRILE

The electrochemical investigation of $[Ru_2(CO)_4\{\mu\text{-}(Pr^iO)_2PN(Et)P(OPr^i)_2\}_2]$, described above, revealed that this unsaturated species is readily oxidized electrochemically to afford a dicationic disolvento species of the type $[Ru_2(CO)_4(solvent)_2\{\mu\text{-}(Pr^iO)_2PN(Et)P(OPr^i)_2\}_2]^{2+}$. The synthesis of these disolvento compounds may also be achieved by the use of one-electron oxidants such as silver(I) salts. Thus, treatment of a suspension of $[Ru_2(CO)_4\{\mu\text{-}(Pr^iO)_2PN(Et)P(OPr^i)_2\}_2]$ in benzonitrile with a twice molar amount of $AgSbF_6$ was found to result in the immediate separation of metallic silver from a pale yellow solution. A white crystalline compound was isolated from this solution, the microanalysis of which was consistent with the formulation $[Ru_2(CO)_4(NCPh)_2\{\mu\text{-}(Pr^iO)_2PN(Et)P(OPr^i)_2\}_2](SbF_6)_2$. The infrared spectrum of this compound in the C-O stretching region exhibits two bands at 2023 and 1985 cm^{-1}; the frequencies of these peaks are considerably higher then those for the two C-O stretching bands observed in the infrared spectrum of $[Ru_2(CO)_4\{\mu\text{-}(Pr^iO)_2PN(Et)P(OPr^i)_2\}_2]$. A peak at 2260 cm^{-1} is also observed in the infrared spectrum of the dibenzonitrile species, readily assigned to the C-N stretching vibration of the co-ordinated benzonitrile ligands. The ^1H nmr spectrum of this compound exhibits resonances corresponding to the protons of the bridging diphosphazane ligands as well as a multiplet in the range 7.74 - 8.02 ppm, the integral of which corresponds to ten protons and which confirms the presence of two co-ordinated

benzonitrile ligands. The $^{31}P\{^{1}H\}$ nmr spectrum exhibits a singlet at 131.76 ppm reflecting a compound having a symmetrical structure. On the basis of the infrared spectrum of this compound it is proposed that the benzonitrile ligands are both co-ordinated in an equatorial position; the infrared spectrum of $[Ru_2(CO)_4(NCPh)_2\{\mu\text{-}(Pr^iO)_2PN(Et)P(OPr^i)_2\}_2]^{2+}$ in the C-O stretching region more closely resembles that of the dihydride species $[Ru_2H_2(CO)_4\{\mu\text{-}(Pr^iO)_2PN(Et)P(OPr^i)_2\}_2]$ than that of the dichloro species $[Ru_2Cl_2(CO)_4\{\mu\text{-}(Pr^iO)_2PN(Et)P(OPr^i)_2\}_2]$ which were structurally found to have hydrido and chloro ligands co-ordinated in equatorial,equatorial and axial,axial positions respectively.

The structure of $[Ru_2(CO)_4(NCPh)_2\{\mu\text{-}(Pr^iO)_2PN(Et)P(OPr^i)_2\}_2](SbF_6)_2$ was determined X-ray crystallographically; the stereochemistry of the dication is illustrated in Figure 6.9. The most important feature of the structure is the presence of two benzonitrile ligands co-ordinated in equatorial positions to each ruthenium atom. The ruthenium-ruthenium distance {2.849(4)Å} is marginally shorter than that of the penta-carbonyl benzonitrile solvento species {2.890(3)Å}, discussed in Chapter 2. The cation adopts a staggered conformation as reflected by P(1)-Ru(1)-Ru(2)-P(2) and P(3)-Ru(2)-Ru(1)-P(4) torsion angles of 30.7 and 29.3° respectively.

The electrochemistry of $[Ru_2(CO)_4(NCPh)_2\{\mu\text{-}(Pr^iO)_2PN(Et)P(OPr^i)_2\}_2](SbF_6)_2$ has been investigated and is discussed in Section 6.3.

Disolvento species of the type $[Ru_2(CO)_4(solvent)_2\{\mu\text{-}(Pr^iO)_2PN(Et)P(OPr^i)_2\}_2](SbF_6)_2$ (solvent = RCN, acetone, THF, water) are expected to be excellent precursors in the synthesis of a wide range of new compounds. This assumption is based upon $[Ru_2(CO)_4(solvent)_2\{\mu\text{-}(Pr^iO)_2PN(Et)P(OPr^i)_2\}_2]^{2+}$ having two labile ligands which may readily be displaced by a

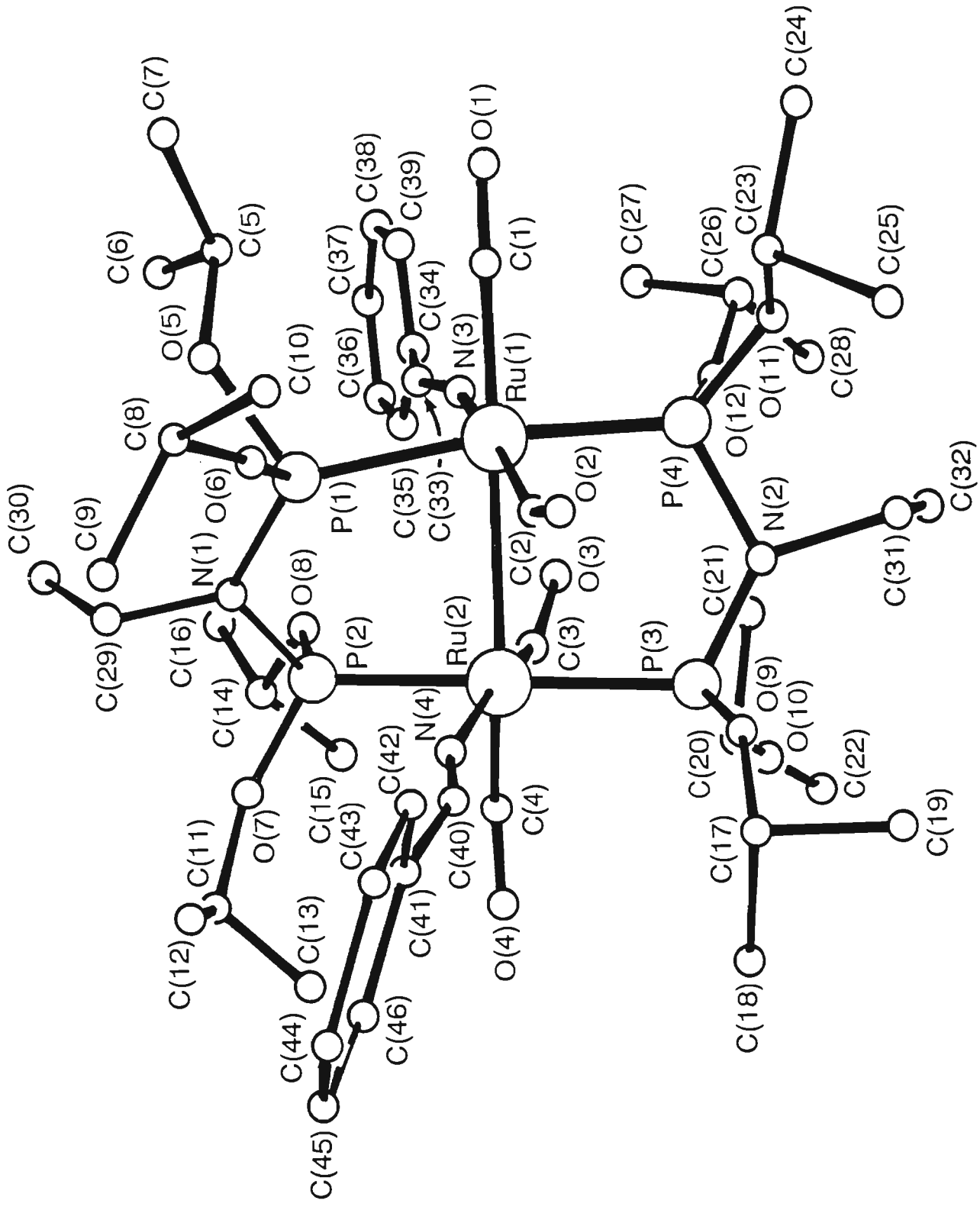

Figure 6.9: Structure of $[Ru_2(CO)_4(NCPh)_2\{\mu\text{-}(Pr^iO)_2PN(Et)P(OPr^i)_2\}_2]^{2+}$

variety of neutral and anionic ligands.

6.6 EXPERIMENTAL

6.6.1 *Synthesis of* $[Ru_2(\mu_{SB}\text{-}CO)_2(CO)_2\{\mu\text{-}(Pr^iO)_2PN(Et)P(OPr^i)_2\}_2]$ (**69**)

i) A stream of argon was passed slowly through a solution of $[Ru_2(\mu\text{-}CO)(CO)_4\{\mu\text{-}(Pr^iO)_2PN(Et)P(OPr^i)_2\}_2]$, (0.250 g, 0.244 mmol), $[Ru_2H_2(CO)_4\{\mu\text{-}(Pr^iO)_2PN(Et)P(OPr^i)_2\}_2]$ (0.250 g, 0.250 mmol) or $[Ru_2(CO)_4\{\mu\text{-}OC(O)\}\{\mu\text{-}(Pr^iO)_2PN(Et)P(OPr^i)_2\}_2]$ (0.250 g, 0.240 mmol) in toluene (15 ml) at 80°C for 45 minutes. The volume of the purple solution was concentrated under reduced pressure to *ca.* 3 ml. Crystallisation of the title compound as purple/black crystals was achieved by cooling this solution to -20°C for 15 hours. Yield: 80-90%. *M* (**69**) = 997.0 g/mol.

ii) Solid $[Ru_2H_2(CO)_4\{\mu\text{-}(Pr^iO)_2PN(Et)P(OPr^i)_2\}_2]$ (0.250 g, 0.250 mmol) was heated *in vacuo* at 80°C for 6 hours. The purple solid was recrystallized from toluene at -20°C. Yield: 60-70%.

6.6.2 *Synthesis of* $[Ru_2H_2(CO)_4\{\mu\text{-}(Pr^iO)_2PN(Et)P(OPr^i)_2\}_2]$ (**70**)

A stream of dihydrogen was passed slowly through a solution of $[Ru_2(\mu\text{-}CO)(CO)_4\{\mu\text{-}(Pr^iO)_2PN(Et)P(OPr^i)_2\}_2]$, (0.250 g, 0.244 mmol), in toluene at 80°C for 45 minutes. The yellow solution was cooled to room temperature under a flow of dihydrogen and was concentrated under reduced pressure to *ca.* 3 ml. Crystallisation of the title compound as yellow/orange crystals was achieved by cooling this solution to -20°C for 15 hours. Yield: 80-90%. *M* (**70**) = 999.0 g/mol.

6.6.3 *Synthesis of* $[Ru_2(O_2)(CO)_4\{\mu\text{-}(Pr^iO)_2PN(Et)P(OPr^i)_2\}_2]$ (**71**)

A solution of $[Ru_2(\mu_{SB}\text{-}CO)_2(CO)_2\{\mu\text{-}(Pr^iO)_2PN(Et)P(OPr^i)_2\}_2]$, (0.300 g, 0.301 mmol), at room temperature, was exposed to a stream of dioxygen for 2 minutes or to air for 10 hours. The resultant yellow solution was evaporated under reduced pressure affording an orange-yellow solid which was washed with cold methanol (3 x 3 ml, -20°C) and dried under vacuum. Yield: 50-60%. *M* (**71**) = 1029.0 g/mol.

6.6.4 *Synthesis of* $[Ru_2Cl_2(CO)_4\{\mu\text{-}(Pr^iO)_2PN(Et)P(OPr^i)_2\}_2]$ (**72**)

Solid $[Ru_2(\mu_{SB}\text{-}CO)_2(CO)_2\{\mu\text{-}(Pr^iO)_2PN(Et)P(OPr^i)_2\}_2]$, (0.200 g, 0.201 mmol), was added to freshly distilled carbon tetrachloride (10 ml) and the solution stirred for 5 minutes. The solvent was removed under reduced pressure and the title compound crystallized from n-hexane. Yield: 80-90%.

6.6.5 *Synthesis of* $[Ru_2(\mu\text{-}SO_2)(CO)_4\{\mu\text{-}(Pr^iO)_2PN(Et)P(OPr^i)_2\}_2]$ (**73**)

A stream of sulphur dioxide was passed slowly through a solution of $[Ru_2(\mu_{SB}\text{-}CO)_2(CO)_2\{\mu\text{-}(Pr^iO)_2PN(Et)P(OPr^i)_2\}_2]$, (0.200 g, 0.201 mmol), in toluene (5 ml) at room temperature for 1 minute, resulting in a change in colour of the solution from purple to pale yellow. The volume of the solution was reduced to *ca.* 1 ml and n-hexane was added, resulting in the precipitation of the title compound in crystalline form. Yield: 90%.

6.6.6 *Synthesis of* $[Ru_2(\mu\text{-}S)(CO)_4\{\mu\text{-}(Pr^iO)_2PN(Et)P(OPr^i)_2\}_2]$ (**74**)

Solid sulphur powder (0.100 g) was added to a solution of $[Ru_2(\mu_{SB}\text{-}$

$CO)_2(CO)_2\{\mu\text{-}(Pr^iO)_2PN(Et)P(OPr^i)_2\}_2]$, (0.200 g, 0.201 mmol), in toluene (5 ml) at room temperature resulting in an immediate change in colour of the solution from purple to orange. The solvent was removed under reduced pressure and the residue was extracted with n-hexane (3 x 5 ml). The combined extracts were evaporated to dryness and the resultant orange solid was crystallized from methanol. Yield: 80%.

6.6.7 *Synthesis of* $[Ru_2(CO)_4(NCPh)_2\{\mu\text{-}(Pr^iO)_2PN(Et)P(OPr^i)_2\}_2](SbF_6)_2$ (**75**)

A twice molar amount of a solution of $AgSbF_6$ (0.207 g, 0.602 mmol), in benzonitrile (2 ml) was added to a solution of $[Ru_2(\mu_{SB}\text{-}CO)_2\text{-}(CO)_2\{\mu\text{-}(Pr^iO)_2PN(Et)P(OPr^i)_2\}_2]$, (0.300 g, 0.301 mmol) in benzonitrile (10 ml) and the mixture stirred for five hours, during which time a precipitate of silver metal formed. The pale yellow solution was filtered through a glass fibre fritte and the volume of the filtrate was concentrated under reduced pressure to *ca.* 2 ml. Toluene (2 ml) was added to the solution resulting in the separation of the title compound in crystalline form. Recrystallization was achieved from a dichloromethane/ether mixture. Yield: 70%. *M* (**74**) = 1674.7 g/mol.

6.6.8 Electrochemical Procedures

The electrochemical techniques employed were direct current rotating disc electrode and cyclic voltammetry. All experiments were performed under a pure, dry argon atmosphere. The benzonitrile solvent used in the work was purified by repeated distillations under argon using established procedures. TBAP was used in 0.1 *M* concentration as the supporting electrolyte; the sample concentration was 10^{-3} *M*. The TBAP was recrystallized from a 9:1 ethanol/water mixture and dried *in vacuo*

at 100°C. The purity of the solvent system was checked by running a blank voltammogram before each measurement.

All experiments employed a conventional three-electrode cell, with a platinum spiral wire auxillary electrode and a reference electrode comprising a AgCl-coated spiral silver wire dipped into a 0.1 *M* solution of TBAP in benzonitrile and separated from the electrolyte solution by a fine fritte. All potentials are quoted relative to the Ag/AgCl reference electrode, against which the [ferrocene]$^{+/o}$ couple had an $E_{\frac{1}{2}}$ value of 0.44 V in benzonitrile (ΔE_p = 75 mV at 100 mV s^{-1}). Ferrocene was added to the solution under investigation at the end of each experiment as an internal standard to check on the stability of the reference electrode.

The working electrode was a platinum disc electrode of local construction (University of Natal, Faculty of Science, Mechanical Instrument Workshop) which was rotated at 500 rpm for the RDE voltammogams. Its surface was freshly polished using 2-6 μm diamond paste until no scratches were observed at tenfold magnification. Before being inserted into the solution, the electrode was rinsed with acetone and distilled water and dried in a warm air stream.

6.6.9 *Crystal Structure Determination on* $[Ru_2(\mu_{SB}\text{-}CO)_2(CO)_2\{\mu\text{-}(Pr^iO)_2P\text{-}N(Et)P(OPr^i)_2\}_2]$ (69), $[Ru_2H_2(CO)_4\{\mu\text{-}(Pr^iO)_2PN(Et)P(OPr^i)_2\}_2]$ (70) *and* $[Ru_2(CO)_4(NCPh)_2\{\mu\text{-}(Pr^iO)_2PN(Et)P(OPr^i)_2\}_2](SbF_6)_2$ (75)

The method for the intensity data collection is described in Appendix A3(a), while the general approach to structure solutions is given in Appendix A.3(b). The crystallographic data for **69**, **70** and **75** are summarized in Table 6.5, the fractional co-ordinates and isotropic

thermal parameters in Tables 6.6, 6.10 and 6.14 respectively, the aniostropic thermal parameters in Tables 6.7, 6.11 and 6.15 respectively, the interatomic distances in Tables 6.8, 6.12 and 6.16 respectively and the interatomic angles in Tables 6.9, 6.13 and 6.17 respectively. The observed and calculated structure factors may be found on microfiche in an envelope fixed to the inside back cover of this thesis.

TABLE 6.1

MICROANALYTICAL DATA

	COMPLEX	ANALYSIS : Found (Calculated) % %C	%H	%N
69	$[Ru_2(\mu\text{-}CO)_2(CO)_2\{\mu\text{-}(Pr^iO)_2PN(Et)P(OPr^i)_2\}_2]$	38.94(38.55)	6.84(6.69)	2.85(2.81)
70	$[Ru_2H_2(CO)_4\{\mu\text{-}(Pr^iO)_2PN(Et)P(OPr^i)_2\}_2]$	39.03(38.47)	6.78(6.88)	2.61(2.80)
71	$[Ru_2(\mu\text{-}O_2)(CO)_4\{\mu\text{-}(Pr^iO)_2PN(Et)P(OPr^i)_2\}_2]$	nm		
75	$[Ru_2(CO)_4(NCPh)_2\{\mu\text{-}(Pr^iO)_2PN(Et)P(OPr^i)_2\}_2](SbF_6)_2$	32.18(32.99)	4.59(4.58)	2.91(3.34)

TABLE 6.2

INFRARED SPECTROSCOPIC DATA

COMPLEX	$\nu(C\equiv O)$, cm^{-1}			OTHER	MEDIUM	COLOUR
69	1880(s)	1782(m)			Cyclohexane	Purple
	1864(s)	1821(m)	1781(sh)		Nujol	
	1864(s)	1820(m)	1781(ms)		KBr disk	
70	1997(m)	1935(s)		1886(w), ν(Ru-H)	n-hexane	Yellow
	1994(ms)	1993(s)		1878(m), ν(Ru-H)	Nujol	
71	2010(m)	1986(s)	1957(ms) 1929(m)		n-hexane	White
75	2045(sh)	2027(s)	1987(s)	2165(w), $\nu(C\equiv N)$	CH_2Cl_2	White
	2023(s)	1985(s)		2160(w), $\nu(C\equiv N)$	Nujol	

TABLE 6.3

^{1}H AND $^{31}P\{^{1}H\}$ NMR SPECTROSCOPIC DATA

COMPLEX	δ ^{1}H (ppm)	δ $^{31}P\{^{1}H\}$ (ppm)
69	1.24-1.52m (54H); 3.62-3.66m (4H); 4.90-5.10m (8H)	158.85(s)[a]
70	1.20-1.64m (54H); 3.42-3.80m (4H); 4.95-5.05m (8H); -8.39q (2H) ($^{2}J_{P-H}$11.1 Hz	159.25(s)[a]
71	1.20-1.55m (54H); 3.55-3.71m (4H); 4.91-5.16m (8H)	135.35(s)[a]
75	1.37-1.54m (54H); 3.55-3.72m (4H); 4.88-5.21m (8H); 7.74-8.02m (10H)	131.76(s)[b]

[a]Recorded in C_6D_6, [b]Recorded in acetone-d_6, m = multiplet, q = quintet, s = singlet.

TABLE 6.4

$^{13}C\{^{1}H\}$ NMR SPECTROSCOPIC DATA

COMPLEX	δ $^{13}C\{^{1}H\}$ (ppm)[a]
69	17.80s ($-NCH_2\underline{C}H_3$); 23.48-25.13m ($-OCH(\underline{C}H_3)_2$); 38.07s ($-N\underline{C}H_2CH_3$); 69.84-71.31m ($O\underline{C}H(CH_3)_2$); 203.50q ($-\underline{C}\equiv O$); 220.21q ($-\underline{C}\equiv O$)
70	17.93s ($-NCH_2\underline{C}H_3$); 23.46-24.90m ($-OCH(\underline{C}H_3)_2$); 40.36s ($-N\underline{C}H_2CH_3$); 69.59-70.78m ($-O\underline{C}H(CH_3)_2$); 203.42-203.67m ($-\underline{C}\equiv O$)

- singlet, m = multiplet, q = quintet

Table 6.5 (continued)

CRYSTAL DATA FOR

$[Ru_2(CO)_4(NCPh)_2\{\mu\text{-}(Pr^iO)_2PN(Et)P(OPr^i)_2\}_2](SbF_6)_2$ (75)

	75
Formula	$C_{46}H_{76}N_4O_{12}F_{12}P_4Ru_2Sb_2$
Molecular mass	1674.7
Crystal dimensions, mm	0.19 x 0.15 x 0.08
Crystal system	monoclinic
Space group	$P2_1/a$
a(Å)	19.126(3)
b(Å)	16.152(2)
c(Å)	23.481(6)
α(°)	90
β(°)	111.96(1)
γ(°)	90
V(Å^3)	6727.4
Z	4
D_c (g cm^{-3})	1.65
F(000)	3336
λ(Mo-K_α) (Å)	0.71069
μ(Mo-K_α) (cm^{-1})	14.21
Reflections measured	9646
Unique reflections	6350
Observed reflections [$I > 3\sigma(I)$]	2580
Crystal stability	Decay = 6.2%
Absorption corrections	Applied
No. of parameters	239
R	0.108
R_w	0.127

TABLE 6.6: Fractional co-ordinates ($\times 10^4$) and equivalent isotropic temperature factors ($Å^2$, $\times 10^3$) for $[Ru_2(\mu\text{-}CO)_2(CO)_2\{\mu\text{-}(Pr^iO)_2PN(Et)P(OPr^i)_2\}_2]$ (69)

	x/a	y/b	z/c	U_{eq}
Ru	4591(1)	94(1)	837(1)	39(1)
P(1)	5591(1)	-793(2)	1896(1)	38(1)
P(2)	3510(1)	812(2)	-162(1)	40(1)
O(1)	3695(4)	615(10)	2623(6)	91(2)
O(2)	5473(4)	2643(7)	561(5)	77(2)
O(3)	5994(3)	189(5)	2767(4)	49(1)
O(4)	5407(3)	-2044(5)	2610(4)	50(1)
O(5)	2828(3)	-219(5)	-378(4)	49(1)
O(6)	3039(3)	2024(5)	257(4)	48(1)
N(1)	6371(4)	-1260(7)	1364(4)	44(1)
C(1)	4041(5)	368(10)	1975(7)	56(2)
C(2)	5203(5)	1571(11)	452(8)	66(3)
C(3)	5598(5)	637(9)	3622(7)	55(2)*
C(4)	6050(9)	83(13)	4567(13)	105(5)*
C(5)	5555(8)	2124(15)	3542(11)	109(4)*
C(6)	4834(5)	-3069(10)	2293(7)	56(2)*
C(7)	5244(7)	-4451(14)	2320(10)	97(4)*
C(8)	4280(8)	-3038(16)	3038(11)	115(5)*
C(9)	2422(5)	-845(9)	427(7)	55(2)*
C(10)	2622(8)	-2312(13)	492(11)	98(4)*
C(11)	1579(8)	-625(15)	133(11)	104(4)*
C(12)	3391(5)	3168(9)	861(6)	53(2)*
C(13)	2826(6)	3561(12)	1586(8)	80(3)*
C(14)	3568(7)	4284(13)	131(10)	91(3)*
C(15)	7026(5)	-2010(10)	2009(7)	69(3)*
C(16)	7631(6)	-1006(12)	2503(9)	79(3)*

* isotropic temperature factor.

$$U_{eq} = \frac{1}{3} \Sigma_i \Sigma_j U_{ij} a_i^* a_j^* (a_i . a_j)$$

TABLE 6.7: Anistropic temperature factors ($Å^2$, $\times 10^3$) for

$[Ru_2(\mu\text{-}CO)_2(CO)_2\{\mu\text{-}(Pr^iO)_2PN(Et)P(OPr^i)_2\}_2]$ (69)

	U(11)	U(22)	U(33)	U(23)	U(13)	U(12)
Ru	45(1)	38(1)	35(1)	4(1)	1(1)	6(1)
P(1)	49(1)	31(1)	34(1)	3(1)	-1(1)	-1(1)
P(2)	47(1)	33(1)	37(1)	-1(1)	0(1)	5(1)
O(1)	77(5)	140(7)	59(4)	8(5)	22(4)	15(5)
O(2)	93(5)	54(4)	86(5)	1(4)	11(4)	-11(4)
O(3)	54(3)	51(3)	41(3)	-7(2)	-3(3)	-7(3)
O(4)	68(4)	35(3)	45(3)	10(2)	-7(3)	-10(3)
O(5)	57(4)	49(3)	41(3)	2(2)	-2(3)	-5(3)
O(6)	52(3)	42(3)	48(3)	-7(2)	-4(3)	11(2)
N(1)	51(4)	42(4)	37(3)	3(3)	-9(3)	6(3)
C(1)	50(5)	76(6)	41(5)	8(5)	-1(4)	16(5)
C(2)	44(5)	62(6)	92(7)	30(6)	5(5)	6(5)

TABLE 6.8: Interatomic distances (Å) for

$[Ru_2(\mu\text{-}CO)_2(CO)_2\{\mu\text{-}(Pr^iO)_2PN(Et)P(OPr^i)_2\}_2]$ (69)

Ru-P(1)	2.312(2)	Ru-P(2)	2.317(2)
Ru-C(1)	1.888(9)	Ru-C(2)	1.915(10)
Ru-Ru	2.763(1)	P(1)-O(3)	1.621(6)
P(1)-O(4)	1.614(5)	P(1)-N(1)	1.665(7)
P(2)-O(5)	1.580(6)	P(2)-O(6)	1.589(5)
O(1)-C(1)	1.124(11)	O(2)-C(2)	1.168(12)
O(3)-C(3)	1.455(10)	O(4)-C(6)	1.462(11)
O(5)-C(9)	1.474(10)	O(6)-C(12)	1.489(10)
N(1)-C(15)	1.554(11)	C(3)-C(4)	1.52(2)
C(3)-C(5)	1.48(2)	C(6)-C(7)	1.55(2)
C(6)-C(8)	1.45(2)	C(9)-C(10)	1.498(15)
C(9)-C(11)	1.51(2)	C(12)-C(13)	1.497(13)
C(12)-C(14)	1.522(15)	C(15)-C(16)	1.553(15)

TABLE 6.9 Interatomic angles (°) for

$[Ru_2(\mu\text{-}CO)_2(CO)_2\{\mu\text{-}(Pr^iO)_2PN(Et)P(OPr^i)_2\}_2]$ (69)

P(1)-Ru-P(2)	174.1(1)	P(1)-Ru-C(1)	89.2(3)
P(2)-Ru-C(1)	87.7(3)	P(1)-Ru-C(2)	92.3(3)
P(2)-Ru-C(2)	93.5(3)	C(1)-Ru-C(2)	116.5(5)
Ru-P(1)-O(3)	117.2(2)	Ru-P(1)-O(4)	117.8(2)
O(3)-P(1)-O(4)	98.2(3)	Ru-P(1)-N(1)	117.1(2)
O(3)-P(1)-N(1)	98.6(3)	O(4)-P(1)-N(1)	104.7(3)
Ru-P(2)-O(5)	117.9(2)	Ru-P(2)-O(6)	117.2(2)
O(5)-P(2)-O(6)	98.2(3)	P(1)-O(3)-C(3)	122.1(5)
P(1)-O(4)-C(6)	122.5(5)	P(2)-O(5)-C(9)	123.5(5)
P(2)-O(6)-C(12)	124.3(5)	P(1)-N(1)-C(15)	119.6(5)
Ru-C(1)-O(1)	175.1(9)	Ru-C(2)-O(2)	153.5(9)
O(3)-C(3)-C(4)	106.3(8)	O(3)-C(3)-C(5)	105.9(9)
C(4)-C(3)-C(5)	116.0(11)	O(4)-C(6)-C(7)	107.8(8)
O(4)-C(6)-C(8)	106.0(9)	C(7)-C(6)-C(8)	110.1(10)
O(5)-C(9)-C(10)	109.0(8)	O(5)-C(9)-C(11)	106.4(8)
C(10)-C(9)-C(11)	111.9(9)	O(6)-C(12)-C(13)	106.2(7)
O(6)-C(12)-C(14)	108.1(7)	C(13)-C(12)-C(14)	114.0(8)
N(1)-C(15)-C(16)	111.3(8)		

TABLE 6.10: Fractional co-ordinates ($\times 10^4$) and equivalent isotropic temperature factors ($Å^2$, $\times 10^3$) for $[Ru_2H_2(CO)_4\{\mu\text{-}(Pr^iO)_2PN(Et)P(OPr^i)_2\}_2]$ (70)

	x/a	y/b	z/c	U_{eq}
Ru	-394(1)	-1224(1)	5252(1)	28(1)
P(1)	1611(1)	141(1)	7202(1)	29(1)
P(2)	-2115(1)	-2584(1)	3200(1)	29(1)
N	2367(3)	1865(3)	7793(3)	34(1)
O(1)	-2633(4)	-747(4)	6284(4)	86(1)
O(2)	-830(4)	-3857(3)	5495(3)	71(1)
O(3)	1243(3)	-52(3)	8387(2)	40(1)
O(4)	3050(3)	-69(3)	7459(2)	46(1)
O(5)	-1905(3)	-3805(2)	2428(2)	41(1)
O(6)	-3913(3)	-3542(3)	2914(2)	44(1)
C(1)	-1805(5)	-907(4)	5903(4)	46(1)
C(2)	-645(5)	-2833(4)	5433(3)	43(1)
C(3)	1035(6)	-1254(4)	8622(4)	60(1)
C(4)	-517(7)	-1920(6)	8689(6)	92(2)
C(5)	2360(8)	-748(7)	9843(5)	93(2)
C(6)	3656(5)	-453(5)	6549(4)	63(1)
C(7)	5263(8)	792(7)	6917(6)	89(2)
C(8)	3711(9)	-1690(7)	6549(10)	134(3)
C(9)	-449(6)	-3620(5)	2419(4)	61(1)
C(10)	-264(10)	-3353(9)	1277(8)	116(3)
C(11)	-545(11)	-4961(9)	2332(9)	129(3)
C(12)	-4511(5)	-4334(4)	3586(4)	48(1)
C(13)	-5970(6)	-4304(6)	3551(5)	77(1)
C(14)	-4802(7)	-5789(5)	2977(5)	78(1)
C(15)	3404(5)	2785(4)	9161(3)	48(1)
C(16)	5045(6)	3031(5)	9546(5)	75(1)
H	823(56)	-1366(48)	4553(43)	74(14)*

* isotropic temperature factor.

$$U_{eq} = \frac{1}{3} \Sigma_i \Sigma_j U_{ij} a_i^* a_j^* (a_i . a_j)$$

TABLE 6.11: Anistropic temperature factors ($Å^2$, $x10^3$) for

$[Ru_2H_2(CO)_4\{\mu\text{-}(Pr^iO)_2PN(Et)P(OPr^i)_2\}_2]$ (70)

	U(11)	U(22)	U(33)	U(23)	U(13)	U(12)
Ru	27(1)	25(1)	26(1)	11(1)	7(1)	12(1)
P(1)	30(1)	30(1)	28(1)	13(1)	9(1)	16(1)
P(2)	28(1)	26(1)	28(1)	11(1)	8(1)	11(1)
N	35(2)	27(1)	26(1)	7(1)	6(1)	10(1)
O(1)	75(2)	104(3)	106(3)	45(2)	62(2)	55(2)
O(2)	84(2)	44(2)	72(2)	29(2)	11(2)	31(2)
O(3)	52(2)	39(1)	31(1)	19(1)	17(1)	22(1)
O(4)	44(2)	60(2)	39(1)	18(1)	9(1)	36(1)
O(5)	43(1)	34(1)	41(1)	12(1)	14(1)	20(1)
O(6)	31(1)	45(1)	46(1)	24(1)	12(1)	10(1)
C(1)	40(2)	49(2)	50(2)	25(2)	22(2)	21(2)
C(2)	47(2)	37(2)	38(2)	18(2)	7(2)	19(2)
C(3)	73(3)	50(2)	57(3)	40(2)	20(2)	24(2)
C(4)	76(4)	80(4)	98(4)	52(4)	33(3)	17(3)
C(5)	103(4)	98(4)	65(3)	49(3)	7(3)	49(4)
C(6)	47(3)	90(3)	55(3)	15(2)	18(2)	49(3)
C(7)	84(4)	102(5)	106(5)	53(4)	57(4)	55(4)
C(8)	121(6)	85(4)	227(10)	46(5)	105(7)	73(4)
C(9)	61(3)	65(3)	59(3)	13(2)	24(2)	42(2)
C(10)	138(6)	158(7)	145(6)	103(6)	109(6)	101(6)
C(11)	171(8)	139(7)	195(9)	98(6)	112(7)	138(7)
C(12)	45(2)	46(2)	46(2)	27(2)	22(2)	12(2)
C(13)	56(3)	94(4)	90(4)	45(3)	42(3)	36(3)
C(14)	91(4)	43(3)	93(4)	34(3)	45(3)	22(3)
C(15)	50(2)	43(2)	24(2)	7(2)	0(2)	16(2)
C(16)	52(3)	69(3)	52(3)	2(2)	-14(2)	21(2)

TABLE 6.12 : Interatomic distances (Å) for

$[Ru_2H_2(CO)_4\{\mu\text{-}(Pr^iO)_2PN(Et)P(OPr^i)_2\}_2]$ (70)

Ru-P(1)	2.297(1)	Ru-P(2)	2.288(1)
Ru-C(1)	1.942(5)	Ru-C(2)	1.873(5)
Ru-H	1.72(6)	Ru-Ru	2.911(1)
P(1)-N	1.679(3)	P(1)-O(3)	1.614(3)
P(1)-O(4)	1.595(4)	P(2)-O(5)	1.615(3)
P(2)-O(6)	1.611(3)	N-C(15)	1.505(4)
O(1)-C(1)	1.128(7)	O(2)-C(2)	1.159(6)
O(3)-C(3)	1.449(7)	O(4)-C(6)	1.454(7)
O(5)-C(9)	1.444(7)	O(6)-C(12)	1.437(6)
C(3)-C(4)	1.504(9)	C(3)-C(5)	1.518(8)
C(6)-C(7)	1.535(8)	C(6)-C(8)	1.476(12)
C(9)-C(10)	1.531(12)	C(9)-C(11)	1.505(13)
C(12)-C(13)	1.528(9)	C(12)-C(14)	1.523(8)
C(15)-C(16)	1.537(8)		

TABLE 6.13: Interatomic angles (°) for

$[Ru_2H_2(CO)_4\{\mu\text{-}(Pr^iO)_2PN(Et)P(OPr^i)_2\}_2]$ (70)

P(1)-Ru-P(2)	171.4(0)	P(1)-Ru-C(1)	91.4(1)
P(2)-Ru-C(1)	97.1(1)	P(1)-Ru-C(2)	90.7(1)
P(2)-Ru-C(2)	88.8(1)	C(1)-Ru-C(2)	102.4(2)
P(1)-Ru-H	91.9(13)	P(2)-Ru-H	79.5(13)
C(1)-Ru-H	172(2)	C(2)-Ru-H	85(2)
Ru-P(1)-N	118.6(1)	Ru-P(1)-O(3)	117.2(1)
N-P(1)-O(3)	95.9(2)	Ru-P(1)-O(4)	117.8(1)
N-P(1)-O(4)	105.8(2)	O(3)-P(1)-O(4)	97.5(2)
Ru-P(2)-O(5)	116.1(1)	Ru-P(2)-O(6)	118.2(1)
O(5)-P(2)-O(6)	97.2(1)	P(1)-N-C(15)	121.5(3)
P(1)-O(3)-C(3)	121.4(3)	P(1)-O(4)-C(6)	126.6(3)
P(2)-O(5)-C(9)	124.5(2)	P(2)-O(6)-C(12)	126.1(3)
Ru-C(1)-O(1)	178.6(5)	Ru-C(2)-O(2)	177.4(3)
O(3)-C(3)-C(4)	107.0(5)	O(3)-C(3)-C(5)	107.6(4)
C(4)-C(3)-C(5)	112.6(5)	O(4)-C(6)-C(7)	108.3(4)
O(4)-C(6)-C(8)	108.3(6)	C(7)-C(6)-C(8)	112.3(6)
O(5)-C(9)-C(10)	109.4(6)	O(5)-C(9)-C(11)	105.2(6)
C(10)-C(9)-C(11)	111.2(7)	O(6)-C(12)-C(13)	104.7(5)
O(6)-C(12)-C(14)	110.0(4)	C(13)-C(12)-C(14)	114.0(4)
N-C(15)-C(16)	114.6(4)		

TABLE 6.14: Fractional co-ordinates ($x10^4$) and equivalent isotropic temperature factors ($Å^2$, $x10^3$) for $[Ru_2(CO)_4(NCPh)_2\{\mu\text{-}(Pr^iO)_2PN(Et)P(OPr^i)_2\}_2](SbF_6)_2$ (75)

	x/a	y/b	z/c	U_{eq}
Ru(1)	1830(3)	519(5)	4710(4)	63(2)
Ru(2)	3137(3)	457(4)	5285(2)	39(1)
P(1)	1944(13)	-893(17)	5029(14)	74(6)
P(2)	3146(10)	-942(12)	5020(10)	34(4)
P(3)	3110(13)	1886(18)	5592(14)	89(7)
P(4)	1845(7)	1919(10)	4517(8)	37(3)
O(1)	485(33)	542(40)	4166(32)	125(20)*
O(2)	1917(24)	897(34)	6262(25)	83(17)*
O(3)	2943(19)	973(27)	3697(20)	59(12)*
O(4)	4536(22)	405(29)	5624(24)	83(13)*
N(1)	2555(21)	-1437(18)	5168(20)	47(9)*
N(2)	2508(25)	2392(16)	5120(23)	45(8)*
N(3)	1751(25)	272(33)	3660(27)	67(16)*
N(4)	3171(18)	113(23)	6384(21)	36(10)*
C(1)	965(18)	526(24)	4371(19)	22(8)*
C(2)	2033(20)	750(25)	5761(24)	35(10)*
C(3)	3186(32)	744(42)	4443(35)	84(21)*
C(4)	3939(46)	386(60)	5394(48)	130(33)*
O(5)	1348(13)	-1496(18)	4523(14)	35(8)*
C(5)	878(13)	-1414(18)	3777(14)	131(6)*
C(6)	1032(13)	-1965(18)	3230(14)	131(6)*
C(7)	262(13)	-1673(18)	3794(14)	131(6)*
H(1)	853(13)	-780(18)	3595(14)	191(170)*
O(6)	1740(14)	-1105(30)	5538(21)	154(21)*
C(8)	1506(14)	-1488(30)	6061(21)	131(6)*
C(9)	2025(14)	-1926(30)	6677(21)	131(6)*
C(10)	1237(14)	-831(30)	6413(21)	131(6)*
H(2)	1156(14)	-1930(30)	5766(21)	191(170)*
O(7)	3720(14)	-1475(30)	5478(21)	161(29)*
C(11)	4221(14)	-1703(30)	6166(21)	131(6)*
C(12)	3993(14)	-1749(30)	6809(21)	131(6)*
C(13)	4726(14)	-1059(30)	6349(21)	131(6)*
H(3)	4400(14)	-2297(30)	6094(21)	191(170)*
O(8)	3080(10)	-1094(13)	4132(13)	21(5)*
C(14)	3559(10)	-1521(13)	3973(13)	131(6)*

TABLE 6.14 (continued)

C(15)	4049(10)	-907(13)	3976(13)	131(6)*
C(16)	3290(10)	-1929(13)	3205(13)	131(6)*
H(4)	3762(10)	-1986(13)	4397(13)	191(170)*
O(9)	3124(12)	2086(18)	6393(14)	46(8)*
C(17)	3401(12)	2060(18)	7225(14)	131(6)*
C(18)	4105(12)	2024(18)	7424(14)	131(6)*
C(19)	3287(12)	2933(18)	7489(14)	131(6)*
H(5)	3175(12)	1517(18)	7378(14)	191(170)*
O(10)	3648(18)	2442(32)	5453(21)	88(16)*
C(20)	3762(18)	2320(32)	4751(21)	131(6)*
C(21)	3138(18)	2496(32)	4101(21)	131(6)*
C(22)	4181(18)	3053(32)	4721(21)	131(6)*
H(6)	3954(18)	1679(32)	4806(21)	191(170)*
O(11)	1318(27)	2532(57)	4412(35)	158(36)*
C(23)	931(27)	2407(57)	4859(35)	131(6)*
C(24)	273(27)	2665(57)	4329(35)	131(6)*
C(25)	1132(27)	3089(57)	5476(35)	131(6)*
H(7)	1012(27)	1746(57)	5042(35)	191(170)*
O(12)	1737(28)	2218(35)	3737(24)	150(23)*
C(26)	1380(28)	2517(35)	2968(24)	131(6)*
C(27)	1339(28)	1768(35)	2442(24)	131(6)*
C(28)	1805(28)	3145(35)	2785(24)	131(6)*
H(8)	944(28)	2754(35)	3004(24)	191(170)*
C(29)	2626(27)	-2314(38)	5352(30)	81(17)*
C(30)	2537(67)	-2893(77)	4659(65)	239(52)*
C(31)	2388(138)	3472(89)	4714(123)	51(75)*
C(32)	2420(75)	3788(100)	4412(82)	214(65)*
C(33)	1774(28)	-61(39)	3048(28)	56(17)*
C(34)	1685(15)	-121(22)	2318(14)	36(11)*
C(35)	2206(15)	-270(22)	2151(14)	52(12)*
C(36)	2144(15)	-491(22)	1421(14)	79(14)*
C(37)	1560(15)	-564(22)	858(14)	66(15)*
C(38)	1040(15)	-415(22)	1024(14)	98(22)*
C(39)	1102(15)	-193(22)	1755(14)	85(19)*
C(40)	3254(30)	132(39)	6943(32)	46(18)*
C(41)	3290(28)	-163(38)	7814(23)	91(25)*
C(42)	2806(28)	-63(38)	8061(23)	113(27)*

TABLE 6.14 (continued)

C(43)	2890(28)	-246(38)	8806(23)	194(60)*
C(44)	3458(28)	-529(38)	9304(23)	195(47)*
C(45)	3943(28)	-629(38)	9056(23)	131(32)*
C(46)	3859(28)	-446(38)	8311(23)	91(21)*
Sb(1)	720(4)	5381(4)	3266(3)	82(2)
F(1)	529(4)	6189(4)	2569(3)	121(13)*
F(2)	911(4)	4572(4)	3964(3)	396(64)*
F(3)	325(4)	5933(4)	3768(3)	154(21)*
F(4)	1114(4)	4828(4)	2764(3)	130(14)*
F(5)	1421(4)	5912(4)	3806(3)	212(25)*
F(6)	19(4)	4849(4)	2727(3)	190(23)*
Sb(2)	4266(4)	-222(5)	1716(5)	115(2)
F(7)	5005(4)	-264(5)	2477(5)	327(46)*
F(8)	3527(4)	-180(5)	954(5)	197(22)*
F(9)	4017(4)	-1106(5)	2101(5)	297(41)*
F(10)	4514(4)	661(5)	1330(5)	203(23)*
F(11)	4543(4)	-903(5)	1166(5)	265(43)*
F(12)	3990(4)	458(5)	2265(5)	273(40)*

* isotropic temperature factor.

$$U_{eq} = \frac{1}{3} \Sigma_i \Sigma_j U_{ij} a_i^* a_j^* (a_i \cdot a_j)$$

TABLE 6.15: Anistropic temperature factors ($Å^2$, $x10^3$) for

$[Ru_2(CO)_4(NCPh)_2\{\mu\text{-}(Pr^iO)_2PN(Et)P(OPr^i)_2\}_2](SbF_6)_2$ (75)

	U(11)	U(22)	U(33)	U(23)	U(13)	U(12)
Ru(1)	39(5)	44(4)	106(5)	-22(3)	26(4)	10(3)
Ru(2)	35(4)	43(4)	34(3)	-19(2)	5(2)	10(3)
P(1)	53(14)	62(15)	87(13)	12(11)	3(10)	-5(11)
P(2)	33(11)	31(8)	52(8)	9(7)	33(8)	14(7)
P(3)	95(19)	77(16)	136(19)	-39(13)	92(16)	-27(12)
P(4)	19(8)	26(7)	51(7)	-4(6)	-5(6)	9(6)
Sb(1)	101(5)	71(4)	84(3)	-2(3)	48(4)	-16(3)
Sb(2)	98(6)	78(4)	154(5)	24(4)	31(4)	8(4)

TABLE 6.16: Interatomic distances (Å) for

$[Ru_2(CO)_4(NCPh)_2\{\mu\text{-}(Pr^iO)_2PN(Et)P(OPr^i)_2\}_2](SbF_6)_2$ (75)

Ru(1)-Ru(2)	2.849(4)	Ru(1)-P(1)	2.35(3)
Ru(1)-P(4)	2.29(2)	Ru(1)-N(3)	1.99(5)
Ru(1)-C(1)	1.89(4)	Ru(1)-C(2)	1.92(4)
Ru(2)-P(2)	2.32(2)	Ru(2)-P(3)	2.39(3)
Ru(2)-N(4)	2.15(4)	Ru(2)-C(3)	1.72(6)
Ru(2)-C(4)	1.82(10)	P(1)-N(1)	1.62(5)
P(1)-O(5)	1.68(4)	P(1)-O(6)	1.28(4)
P(2)-N(1)	1.72(5)	P(2)-O(7)	1.56(4)
P(2)-O(8)	1.66(3)	P(3)-N(2)	1.59(5)
P(3)-O(9)	1.55(4)	P(3)-O(10)	1.65(4)
P(4)-N(2)	1.73(5)	P(4)-O(11)	1.54(7)
P(4)-O(12)	1.50(5)	O(1)-C(1)	1.05(7)
O(2)-C(2)	1.12(5)	O(3)-C(3)	1.37(7)
O(4)-C(4)	1.30(10)	N(1)-C(29)	1.45(6)
N(3)-C(33)	1.31(7)	N(4)-C(40)	1.01(5)
C(3)-C(4)	2.09(11)	O(5)-C(5)	1.446(0)
O(5)-O(6)	1.92(5)	C(5)-C(6)	1.516(0)
C(5)-C(7)	1.516(0)	C(5)-H(1)	1.076(0)
O(6)-C(8)	1.446(0)	C(8)-C(9)	1.516(0)
C(8)-C(10)	1.516(0)	C(8)-H(2)	1.076(0)
O(7)-C(11)	1.446(0)	C(11)-C(12)	1.516(0)
C(11)-C(13)	1.516(0)	C(11)-H(3)	1.076(0)
O(8)-C(14)	1.446(0)	C(14)-C(15)	1.516(0)
C(14)-C(16)	1.516(0)	C(14)-H(4)	1.076(0)
O(9)-C(17)	1.477(0)	C(17)-C(18)	1.554(0)
C(17)-C(19)	1.553(0)	C(17)-H(5)	1.118(0)
O(10)-C(20)	1.477(0)	C(20)-C(21)	1.553(0)
C(20)-C(22)	1.554(0)	C(20)-H(6)	1.118(0)
O(11)-C(23)	1.477(0)	C(23)-C(24)	1.554(0)
C(23)-C(25)	1.554(0)	C(23)-H(7)	1.118(0)
O(12)-C(26)	1.477(0)	C(26)-C(27)	1.554(0)
C(26)-C(28)	1.553(0)	C(26)-H(8)	1.118(0)
C(29)-C(30)	1.57(11)	C(31)-C(32)	.8(2)
C(33)-C(34)	1.34(5)	C(34)-C(35)	1.395(0)
C(34)-C(39)	1.395(0)	C(35)-C(36)	1.395(0)

TABLE 6.16 (continued)

C(36)-C(37)	1.395(0)	C(37)-C(38)	1.395(0)
C(38)-C(39)	1.395(0)	C(40)-C(41)	1.70(7)
C(41)-C(42)	1.395(0)	C(41)-C(46)	1.395(0)
C(42)-C(43)	1.395(0)	C(43)-C(44)	1.395(0)
C(44)-C(45)	1.395(0)	C(45)-C(46)	1.395(0)
Sb(1)-F(1)	1.800(0)	Sb(1)-F(2)	1.800(0)
Sb(1)-F(3)	1.800(0)	Sb(1)-F(4)	1.800(0)
Sb(1)-F(5)	1.800(0)	Sb(1)-F(6)	1.800(0)
Sb(2)-F(7)	1.801(0)	Sb(2)-F(8)	1.801(0)
Sb(2)-F(9)	1.801(0)	Sb(2)-F(10)	1.801(0)
Sb(2)-F(11)	1.802(0)	Sb(2)-F(12)	1.800(0)

TABLE 6.17: Interatomic angles (°) for

$[Ru_2(CO)_4(NCPh)_2\{\mu\text{-}(Pr^iO)_2PN(Et)P(OPr^i)_2\}_2](SbF_6)_2$ (75)

Ru(2)-Ru(1)-P(1)	82.2(8)	Ru(2)-Ru(1)-P(4)	91.0(5)
P(1)-Ru(1)-P(4)	172.5(9)	Ru(2)-Ru(1)-N(3)	94(2)
P(1)-Ru(1)-N(3)	92(2)	P(4)-Ru(1)-N(3)	92(2)
Ru(2)-Ru(1)-C(1)	177.1(11)	P(1)-Ru(1)-C(1)	95.7(14)
P(4)-Ru(1)-C(1)	91.1(13)	N(3)-Ru(1)-C(1)	88(2)
Ru(2)-Ru(1)-C(2)	78.0(13)	P(1)-Ru(1)-C(2)	87.6(14)
P(4)-Ru(1)-C(2)	87.9(13)	N(3)-Ru(1)-C(2)	172(2)
C(1)-Ru(1)-C(2)	100(2)	Ru(1)-Ru(2)-P(2)	92.6(6)
Ru(1)-Ru(2)-P(3)	86.4(8)	P(2)-Ru(2)-P(3)	177.8(6)
Ru(1)-Ru(2)-N(4)	91.5(11)	P(2)-Ru(2)-N(4)	87.8(11)
P(3)-Ru(2)-N(4)	90.3(12)	Ru(1)-Ru(2)-C(3)	94(2)
P(2)-Ru(2)-C(3)	93(2)	P(3)-Ru(2)-C(3)	89(2)
N(4)-Ru(2)-C(3)	175(3)	Ru(1)-Ru(2)-C(4)	165(3)
P(2)-Ru(2)-C(4)	83(3)	P(3)-Ru(2)-C(4)	99(3)
N(4)-Ru(2)-C(4)	102(3)	C(3)-Ru(2)-C(4)	72(3)
Ru(1)-P(1)-N(1)	125(2)	Ru(1)-P(1)-O(5)	115(2)
N(1)-P(1)-O(5)	106(2)	Ru(1)-P(1)-O(6)	115(3)
N(1)-P(1)-O(6)	107(3)	O(5)-P(1)-O(6)	79(2)
Ru(2)-P(2)-N(1)	110.1(13)	Ru(2)-P(2)-O(7)	119(2)
N(1)-P(2)-O(7)	103(2)	Ru(2)-P(2)-O(8)	111.2(11)
N(1)-P(2)-O(8)	109(2)	O(7)-P(2)-O(8)	103(2)
Ru(2)-P(3)-N(2)	117(2)	Ru(2)-P(3)-O(9)	117(2)
N(2)-P(3)-O(9)	98(2)	Ru(2)-P(3)-O(10)	113(2)
N(2)-P(3)-O(10)	102(3)	O(9)-P(3)-O(10)	108(2)
Ru(1)-P(4)-N(2)	113.1(13)	Ru(1)-P(4)-O(11)	127(3)
N(2)-P(4)-O(11)	106(3)	Ru(1)-P(4)-O(12)	118(2)
N(2)-P(4)-O(12)	107(3)	O(11)-P(4)-O(12)	80(3)
P(1)-N(1)-P(2)	116(2)	P(1)-N(1)-C(29)	126(4)
P(2)-N(1)-C(29)	118(4)	P(3)-N(2)-P(4)	123(2)
P(3)-N(2)-C(31)	132(9)	P(4)-N(2)-C(31)	100(9)
Ru(1)-N(3)-C(33)	166(5)	Ru(2)-N(4)-C(40)	161(5)
Ru(1)-C(1)-O(1)	178(5)	Ru(1)-C(2)-O(2)	154(5)
Ru(2)-C(3)-O(3)	154(5)	Ru(2)-C(3)-C(4)	56(3)
O(3)-C(3)-C(4)	150(5)	Ru(2)-C(4)-O(4)	167(7)
Ru(2)-C(4)-C(3)	52(3)	O(4)-C(4)-C(3)	138(7)

TABLE 6.17 (continued)

P(1)-O(5)-C(5)	132.7(13)	P(1)-O(5)-O(6)	41.1(14)
C(5)-O(5)-O(6)	150(2)	O(5)-C(5)-C(6)	109.6(0)
O(5)-C(5)-C(7)	109.6(0)	C(6)-C(5)-C(7)	109.2(0)
O(5)-C(5)-H(1)	109.5(0)	C(6)-C(5)-H(1)	109.4(0)
C(7)-C(5)-H(1)	109.4(0)	P(1)-O(6)-O(5)	60(2)
P(1)-O(6)-C(8)	170(3)	O(5)-O(6)-C(8)	113.4(14)
O(6)-C(8)-C(9)	109.6(0)	O(6)-C(8)-C(10)	109.6(0)
C(9)-C(8)-C(10)	109.2(0)	O(6)-C(8)-H(2)	109.6(0)
C(9)-C(8)-H(2)	109.4(0)	C(10)-C(8)-H(2)	109.4(0)
P(2)-O(7)-C(11)	153(2)	O(7)-C(11)-C(12)	109.6(0)
O(7)-C(11)-C(13)	109.6(0)	C(12)-C(11)-C(13)	109.2(0)
O(7)-C(11)-H(3)	109.5(0)	C(12)-C(11)-H(3)	109.4(0)
C(13)-C(11)-H(3)	109.4(0)	P(2)-O(8)-C(14)	120.2(10)
O(8)-C(14)-C(15)	109.6(0)	O(8)-C(14)-C(16)	109.6(0)
C(15)-C(14)-C(16)	109.2(0)	O(8)-C(14)-H(4)	109.6(0)
C(15)-C(14)-H(4)	109.4(0)	C(16)-C(14)-H(4)	109.4(0)
P(3)-O(9)-C(17)	154(2)	O(9)-C(17)-C(18)	105.3(0)
O(9)-C(17)-C(19)	105.3(0)	C(18)-C(17)-C(19)	104.6(0)
O(9)-C(17)-H(5)	104.0(0)	C(18)-C(17)-H(5)	118.1(0)
C(19)-C(17)-H(5)	118.1(0)	P(3)-O(10)-C(20)	119(2)
O(10)-C(20)-C(21)	105.3(0)	O(10)-C(20)-C(22)	105.3(0)
C(21)-C(20)-C(22)	104.6(0)	O(10)-C(20)-H(6)	104.0(0)
C(21)-C(20)-H(6)	118.1(0)	C(22)-C(20)-H(6)	118.1(0)
P(4)-O(11)-C(23)	118(3)	O(11)-C(23)-C(24)	105.3(0)
O(11)-C(23)-C(25)	105.3(0)	C(24)-C(23)-C(25)	104.6(0)
O(11)-C(23)-H(7)	104.0(0)	C(24)-C(23)-H(7)	118.1(0)
C(25)-C(23)-H(7)	118.1(0)	P(4)-O(12)-C(26)	157(2)
O(12)-C(26)-C(27)	105.3(0)	O(12)-C(26)-C(28)	105.3(0)
C(27)-C(26)-C(28)	104.6(0)	O(12)-C(26)-H(8)	104.0(0)
C(27)-C(26)-H(8)	118.1(0)	C(28)-C(26)-H(8)	118.1(0)
N(1)-C(29)-C(30)	114(5)	N(2)-C(31)-C(32)	149(29)
N(3)-C(33)-C(34)	157(6)	C(33)-C(34)-C(35)	116(3)
C(33)-C(34)-C(39)	123(3)	C(35)-C(34)-C(39)	120.0(0)
C(34)-C(35)-C(36)	120.0(0)	C(35)-C(36)-C(37)	120.0(0)
C(36)-C(37)-C(38)	120.0(0)	C(37)-C(38)-C(39)	120.0(0)
C(34)-C(39)-C(38)	120.0(0)	N(4)-C(40)-C(41)	161(6)
C(40)-C(41)-C(42)	123(3)	C(40)-C(41)-C(46)	116(3)

TABLE 6.17 (continued)

C(42)-C(41)-C(46)	120.0(0)	C(41)-C(42)-C(43)	120.0(0)
C(42)-C(43)-C(44)	120.0(0)	C(43)-C(44)-C(45)	120.0(0)
C(44)-C(45)-C(46)	120.0(0)	C(41)-C(46)-C(45)	120.0(0)
F(1)-Sb(1)-F(2)	180.0(0)	F(1)-Sb(1)-F(3)	90.0(0)
F(2)-Sb(1)-F(3)	90.0(0)	F(1)-Sb(1)-F(4)	90.0(0)
F(2)-Sb(1)-F(4)	90.0(0)	F(3)-Sb(1)-F(4)	180.0(0)
F(1)-Sb(1)-F(5)	90.0(0)	F(2)-Sb(1)-F(5)	90.0(0)
F(3)-Sb(1)-F(5)	90.0(0)	F(4)-Sb(1)-F(5)	90.0(0)
F(1)-Sb(1)-F(6)	90.0(0)	F(2)-Sb(1)-F(6)	90.0(0)
F(3)-Sb(1)-F(6)	90.0(0)	F(4)-Sb(1)-F(6)	90.0(0)
F(5)-Sb(1)-F(6)	180.0(0)	F(7)-Sb(2)-F(8)	180.0(0)
F(7)-Sb(2)-F(9)	90.0(0)	F(8)-Sb(2)-F(9)	90.0(0)
F(7)-Sb(2)-F(10)	90.0(0)	F(8)-Sb(2)-F(10)	90.0(0)
F(9)-Sb(2)-F(10)	180.0(0)	F(7)-Sb(2)-F(11)	90.0(0)
F(8)-Sb(2)-F(11)	90.0(0)	F(9)-Sb(2)-F(11)	89.9(0)
F(10)-Sb(2)-F(11)	90.1(0)	F(7)-Sb(2)-F(12)	89.9(0)
F(8)-Sb(2)-F(12)	90.1(0)	F(9)-Sb(2)-F(12)	90.1(0)
F(10)-Sb(2)-F(12)	89.9(0)	F(11)-Sb(2)-F(12)	179.9(0)

APPENDIX A: GENERAL EXPERIMENTAL DETAILS

A.1 INSTRUMENTATION

Carbon, hydrogen and nitrogen analyses were performed by the Microanalytical Laboratory, University of Natal, Pietermaritzburg. Phosphorus, iodine and chlorine analyses were performed by Analytische Laboratorien, Gummersbach, Germany.

All infrared spectra were recorded for nujol mulls and solutions using a Perkin-Elmer 457 infrared spectrometer.

$^{31}P\{^{1}H\}$ nmr spectra were recorded on a Varian FT-80A spectrometer. ^{1}H and $^{13}C\{^{1}H\}$ nmr spectra were recorded on a Varian FT-80A or a Gemini 200 spectrometer. Deuterated solvents were employed in all cases.

Electrochemical measurements were performed using a PAR 175 universal programmer, a PAR 173 potentiostat, fitted with a PAR 176 current follower and connected to a HP 7045A X-Y recorder, and a locally made coulometer (University of Natal, Electronics Workshop).

A.2. EXPERIMENTAL TECHNIQUES

All reactions, except where otherwise indicated, were carried out under an atmosphere of dinitrogen. Standard Schlenk type apparatus was used.

a) Chemical reagents. The chemicals used during the course of this investigation were either obtained from commercial suppliers or synthesized by previously published methods as indicated in Appendix B. The chemicals obtained commercially were used without further

purification.

b) Photochemical reactor. The ultraviolet reactor comprised of a water-cooled, nitrogen-cooled 125 watt Philips HPW 125W U-V lamp placed in a double-armed jacket, one arm comprising a condensor attachment, the other attached to a nitrogen bubbler.

c) Solvents. The solvents were freshly distilled and dried before use using standard procedures[267] except for cylcohexane and pentane which were used in Analar Grade purity without further purification. Solvents used for electrochemical purposes and for the synthesis of solvento species were purified according to the procedures described by C.K. Mann.[268]

A.3. CRYSTAL STRUCTURE DETERMINATIONS

a) Data Collection. The intensities of the reflections were measured at 22°C with an Enraf-Nonius CAD-4 diffractometer using graphite monochromated Mo-K_α radiation.

Cell constants were obtained by fitting the setting angles of 25 high-order reflections. During data collection, the orientation matrix was redetermined if any of the setting angles of three reflections, measured every 200 reflections, deviated by more than 0.1° from the theoretical value. Three standard reflections were measured every hour to check on any possible decomposition of the crystal. An ω-2θ scan with a variable speed up to a maximum of 5.49° min^{-1} was used. The ω-angle changed as $a_\omega + b_\omega \tan\theta$ (°), the horizontal aperture as $a_h + b_h \tan\theta$ (mm), but was limited to the range 1, 3-5, 9 mm. The vertical slit was fixed at 4 mm. Optical values of a_ω, b_ω, a_h and b_h were determined for each

crystal by a critical evaluation of peak shape for several reflections with different values of θ using the program OTPLOT (Omega-Theta plot; Enraf-Nonius diffractometer control program, 1988D). Where applicable, a linear decay correction was applied using the mean value of linear curves fitted through three intensity control reflections, measured at regular time intervals. Data were corrected for Lorentz and polarisation effects, and where possible for absorption by the psi-scan (empirical) method.[269]

b) Structural solution and refinement. Direct methods or the Patterson function were used to solve the phase problem. Once a suitable phasing model was found successive applications of Fourier and difference Fourier techniques allowed the location of the remaining non-hydrogen atoms. In general, hydrogen atoms were not located but, where the location of a hydrogen atom was particularly important, a difference Fourier, calculated with the low angle reflections weighted relative to the high angle reflections, was employed. Weighted full-matrix least-squares methods were always used to refine the structure; the weighting scheme was chosen so as to find the smallest variation of the mean value of $\omega(F_o-F_c)^2$ as a function of the magnitude of F_o. R, R_w and the weighting scheme are defined as follows:

$$R = \frac{\Sigma|F_o-F_c|}{\Sigma|F_o|}, \quad R_w = \frac{\Sigma\omega^{\frac{1}{2}}|F_o-F_c|}{\Sigma\omega^{\frac{1}{2}}|F_o|}$$

and $\omega = 2.84/(\sigma(F)^2 + 0.0002F^2)$.

Scattering factor data were taken from reference 270. For all these calculations, the programs SHELX-76[271] and SHELX-86[272] were employed. Occasionally the program MULTAN-82[273] was used to solve the phase

problem. Plotting of the structures was performed using the program PLUTO-78[274] while the tabulation of fractional co-ordinates, thermal parameters, interatomic distances and angles was achieved using the program TABLES.[275]

APPENDIX B: SOURCES OF CHEMICALS

1. Commercially available chemicals (used without further purification)

i) Chemicals obtained from Aldrich Chemical Company Inc.:
$HBF_4.OEt_2$, methyl propiolate, silver trifluoroacetate, trifluoroacetic acid.

ii) Chemicals obtained from British Drug Houses Ltd.:
pyridine, NH_4PF_6, tetrabutyl ammonium iodide, silver acetate, 1,4-tetrachlorobenzoquinone, phenol, dimethyl sulphide, thiophene, acetic acid, iodine.

iii) Chemicals obtained from Ega Chemie:
diphenyl acetylene.

iv) Chemicals obtained from Fluka AG:
thiophenol, TBAP.

v) Chemicals obtained from Holpro Analytics Pty Ltd.:
formic acid, KOH.

vi) Chemicals obtained from Jansen Chimica:
$HPF_6.H_2O$.

vii) Chemicals obtained from Matheson Company Inc.:
hydrogen sulphide, methyl acetylene, sulphur dioxide.

viii) Chemicals obtained from E. Merck:
benzonitrile, acetonitrile, CD_3OD, acetone-d_6. CD_2Cl_2, C_6D_6, $CDCl_3$, CCl_4, phenyl acetylene, dimethylacetylenedicarboxylate, triethylamine, NaH, 4,4'-bipyridine, silver benzoate, carbon disulphide, PhNCS, diethyl ketone, nitromethane, tetrahydrothiophene, benzoic acid, pyrazol, 2-oxypyridinate.

ix) Chemicals obtained from Monsanto Research Corporation:
^{13}CO

x) Chemicals obtained from Saarchem Pty Ltd:

sodium acetate, sulphur powder.

xi) Chemicals obtained from Sigma Chemical Company:

$Me_3NO.2H_2O$.

xii) Chemicals obtained from Strem Chemicals:

$Ru_3(CO)_{12}$.

2. Chemicals synthesized by published methods

The diphosphazane ligands $(RO)_2PN(Et)P(OR)_2$ (R = Me,Et or Pr^i) were synthesized in two steps. The first step involved synthesis of the chloro-precursor $Cl_2PN(Et)PCl_2$ by the method of J.F. Nixon,[276] while the second involved reactions of the chloro-precursor with the appropriate alcohol to produce the required ligand.[277]

Sodium pyrazolate and sodium-2-oxypyridinate were prepared by reacting equivalent amounts of pyrazol- or 2-oxypyridinate with sodium hydride in THF. Reduction of the solvent volume and addition of ether precipitated the white salt.

Sodium methoxide and sodium mercaptide were prepared by reacting methanol or thiophenol with sodium metal. Addition of ether precipitated the white salt.

The phenyl diazonium salt $PhN_2^+PF_6^-$ was prepared by treatment of aniline with sodium nitrite and conc. hydrochloric acid, followed by addition of HPF_6.[278]

APPENDIX C: PUBLICATION LIST

The following is a list of publications which have emerged from work performed during the course of this investigation:

1. K.J. Edwards, J.S. Field, R.J. Haines, B. Homan, J. Sundermeyer and S.F. Woollam; Synthesis of three-, four-, and five-membered dimetalloheterocyclic compounds by reaction of the hydride $[Ru_2H(CO)_5\{\mu\text{-}(RO)_2PN(Et)P(OR)_2\}_2][PF_6]$ (R = Me or Pr^i) with unsaturated systems of the type X≡Y and X′=Y′=Z′. Crystal structures of representative examples of the three types of products; *J. Organomet. Chem., 386* (1990) C1-C6.

2. J.S. Field, R.J. Haines, U. Honrath, J. Sundermeyer and S.F. Woollam; Synthesis of the solvento species $[Ru_2(CO)_5(solvent)\{\mu\text{-}(RO)_2PN(Et)P(OR)_2\}_2]^{2+}$ and its potential as a source of a wide range of dinuclear derivatives of ruthenium; *J. Organomet. Chem., 395* (1990) C9-C15.

3. J.S. Field, R.J. Haines, J. Sundermeyer and S.F. Woollam; Ready deprotonation of the protic solvento species $[Ru_2(CO)_5(R'OH)\{\mu\text{-}(RO)_2PN(Et)P(OR)_2\}_2]^{2+}$ (R = Me or Pr^i; R′ = H, Me, Et, etc.) and the formation of $[Ru_2(CO)_4\{\mu\text{-}OC(O)\}\{\mu\text{-}(RO)_2PN(Et)P(OR)_2\}_2]$ containing carbon dioxide in a bridging co-ordination mode; *J. Chem. Soc., Chem. Commun.,* (1990) 985-988.

4. J.S. Field, A.M.A. Francis, R.J. Haines, and S.F. Woollam; Electrochemical behaviour of ditertiary phosphine and diphosphazane-bridged derivatives of diruthenium nonacarbonyl; *J. Organomet. Chem., 412,* (1991) 383-396.

5. J.S. Field, R.J. Haines, E. Minshall, C.N. Sampson, J. Sundermeyer, S.F. Woollam, C.C. Allen and J.C.A. Boeyens; Electrophilic attack on diphosphazane-bridged derivatives of diruthenium nonacarbonyl by halogens, *J. Chem. Soc., Dalton Trans.,* (1991) 2761

6. J.S. Field, R.J. Haines, J. Sundermeyer and S.F. Woollam; Synthesis and reactivity of the formally unsaturated diruthenium diphosphazane-bridged species $[Ru_2(CO)_4\{\mu\text{-}(RO)_2PN(Et)P(OR)_2\}_2]$ (R = Me or Pr^i); *J.*

Chem. Soc., Chem. Commun., (1991) 1382.

7. J.S. Field, R.J. Haines, J. Sundermeyer and S.F. Woollam; Contrasting co-ordination behaviour of acetylene and other alkynes towards the di-ruthenium complexes $[Ru_2(\mu\text{-}CO)(CO)_4\{\mu\text{-}(RO)_2PN(Et)P(OR)_2\}_2]$ and $[Ru_2(CO)_4\{\mu\text{-}(RO)_2PN(Et)P(OR)_2\}_2]$ (R = Me or Pr^i); (1991) in press.

8. J.S. Field, R.J. Haines, E. Minshall, C.N. Sampson, J. Sundermeyer and S.F. Woollam; Protonation of the diphosphazane ligand-bridged derivatives of nonacarbonyl by protic acids with co-ordinating and non co-ordinating conjugate bases; (1991) in press.

9. D.W. Engel, J.S. Field, R.J. Haines, J. Sundermeyer and S.F. Woollam; Contrasting co-ordination behaviour of the electron-acceptor ligands 1,2- and 1,4-tetrachlorobenzoquinone towards the diruthenium diphosphazane-bridged derivatives $[Ru_2(\mu\text{-}CO)(CO)_4\{\mu\text{-}(RO)_2PN(Et)P(OR)_2\}_2]$ (R = Me or Pr^i); (1991) submitted for publication.

10. J.S. Field, R.J. Haines, J. Sundermeyer and S.F. Woollam; Oxidation of diphosphazane-bridged derivatives of diruthenium nonacarbonyl by silver(I) salts in the protic solvents R'OH (R = H, Me or Et) : Formation and rearrangement of products of the type $[Ru_2(CO)_5(HA)\{\mu\text{-}(RO)_2PN(Et)P(OR)_2\}_2]^{2+}$ (R = Me or Pr^i) in which the co-ordinated acid HA is of a conjugate base with potential ligating properties; (1992) submitted for publication.

11. D.W. Engel, J.S. Field, R.J. Haines, E.C. Horsfield, U. Honrath, J. Sundermeyer and S.F. Woollam; Reactions of diphosphazane-bridged derivatives of diruthenium nonacarbonyl with metal-containing electrophiles : Formation of the solvento species $[Ru_2(CO)_5(solvent)\{\mu\text{-}(RO)_2PN(Et)P(OR)_2\}_2]^{2+}$ (R = Me or Pr^i) and its reactivity towards various nucleophiles; (1992) in preparation.

12. J.S. Field, R.J. Haines, M.W. Stewart, J. Sundermeyer and S.F. Woollam, Synthesis and reactivity of the formally unsaturated diphosphazane-bridged species $[Ru_2(CO)_4\{\mu\text{-}(RO)_2PN(Et)P(OR)_2\}_2]$ (R = Me or Pr^i); (1992) in preparation.

REFERENCES

1. F.A. Cotton and G. Wilkinson, *Advanced Inorganic Chemistry,* Fifth Edition, John Wiley and Sons, USA (1988).
2. W. Keim, *J. Organomet. Chem., 372* (1989), 15.
3. M.E. Dry, *J. Organomet. Chem., 372* (1989), 117.
4. C.P. Kubiak and R. Eisenberg, *J. Am. Chem. Soc, 99* (1977), 6129.
5. R. Poilblanc, *Inorg. Chim. Acta., 62* (1982), 75.
6. B.R. Sutherland and M. Cowie, *Organometallics, 4* (1985), 1637.
7. B.R. Sutherland and M. Cowie, *Organometallics, 4* (1985), 1801.
8. T.G. Shenck, J.M. Downes, C.R.C. Milne, P.B. Mackenzie, H. Boucher, J. Whelan and B. Bosnich, *Inorg. Chem., 24* (1985), 2334.
9. L.C. Mond and C. Longer, *J. Chem. Soc.,* (1891), 1090.
10. R.V.G. Ewens and M.W. Lister, *Tran. Faraday Soc., 35* (1939), G81.
11. W. Manchot and W.J. Manchot, *Z. Anorg. Allgem. Chem., 226* (1936), 385.
12. W. Hieber and H. Stallman, *Z. Elektrochem., 49* (1943), 288.
13. K. Noack, *Helv. Chim. Acta, 45* (1962), 1847.
14. J. Dewar and H.O. Jones, *Proc. Roy. Soc., A, 76* (1905), 573.
15. H.M. Powell and R.V.G. Ewens, *J. Chem. Soc.,* (1939), 286.
16. F.A. Cotton and J.M. Troup, *J. Am. Chem. Soc., 96* (1974), 3438.
17. P.S. Brateman and W.J. Wallace, *J. Organomet. Chem., 30* (1971), C17.
18. J.R. Moss and W.A.G. Graham, *J. Chem. Soc., Chem. Commun.,* (1970), 835.
19. J.R. Moss and W.A.G. Graham, *J. Chem. Soc., Dalton Trans.,* (1977), 95.
20. C.H Wei and L.F. Dahl, *J. Am. Chem. Soc., 91* (1969), 1351.
21. E.R. Corey and L.F. Dahl, *Inorg. Chem., 1* (1962), 521.

22. M.R. Churchill, F.J. Hollander and J.P. Hutchinson, *Inorg. Chem.*, *16* (1977), 2655.

23. R. Poilblanc, *J. Organomet. Chem.*, *94* (1975), 241.

24. M. Cowie and S.K. Dwight, *Inorg. Chem.*, *19*, (1980), 2500.

25. F.A. Cotton, R.J. Haines, B.E. Hanson and J.C. Sekutowski, *Inorg. Chem.*, *17* (1978), 2010.

26. M.M. de V Steyn, Ph.D. Thesis, University of South Africa, (1989).

27. C.A. Tolman, *Chem. Rev.*, *77* (1977), 313.

28. M.G. Newton, R.B. King, M. Chang, N.S. Pantaleo and J. Gimeno, *J. Chem. Soc., Chem. Commun.*, (1977), 531.

29. R.B. King, J. Gimeno and T.J. Lotz, *Inorg. Chem.*, *17* (1978), 2401.

30. G. de Leeuw, M.Sc. Thesis, University of Natal, (1984).

31. M.I. Bruce, M.L. Williams and B.K. Nicholson, *J. Organomet. Chem.*, *258* (1983), 63.

32. D.S. Payne, J.A.A. Mokuolo and J.C. Speakman, *J. Chem. Soc.*, (1973), 1443.

33. G.M. Brown, J.E. Finhott, R.B. King and K.W. Bibber, *Inorg. Chem.*, *17* (1978), 2010.

34. B. Chaudret, B. Delavaux and R. Poilblanc, *Coord. Chem. Reviews*, *86* (1988), 191.

35. R.J. Puddephatt, *Chem. Soc., Rev.*, *12* (1983), 99.

36. M.G. Newton, R.B. King, T.W. Lee, L. Norskov-Lauritzen and V. Kumar, *J. Chem. Soc., Chem. Commun.*, (1982), 201.

37. H.C. Aspinall and A.J. Deeming, *J. Chem. Soc., Chem. Commun.*, (1983), 838.

38. R. Carreno, V. Riera, M.A. Ruiz, Y. Jeannin and M. Philoche-Levisalles, *J. Chem. Soc., Chem. Commun.*, (1990), 15.

39. R. Colton and C.J. Commons, *Aust. J. Chem.*, *28* (1975), 1673.

40. C.J. Commons and B.F. Hoskins, *Aust. J. Chem.*, *28* (1975), 1663.

41. T.W. Turney, *Inorg. Chim. Acta.*, *64* (1982), L141.

42. K. Lee and T.L. Brown, *Organometallics, 4* (1985), 1025.

43. K. Lee and T.L. Brown, *Organometallics, 4* (1985), 1030.

44. L.J. Tortorelli, C. Woods and A.T. McPhail, *Inorg. Chem., 29* (1990), 2726.

45. C. Woodcock and R. Eisenberg, *Inorg. Chem., 23,* (1984), 4207.

46. J.J. Jenkins, J.P. Ennett and M. Cowie, *Organometallics, 7* (1988), 1845.

47. C. Woods, L.J. Tortorelli, D.P. Rillema, J.L.E. Burn and J.G. DePriest, *Inorg. Chem., 28* (1989) 1673.

48. C.P. Kubiak and R. Eisenberg, *J. Am. Chem. Soc., 102* (1980), 3637.

49. C. Woodcock and R. Eisenberg, *Inorg. Chem., 24* (1985), 1285.

50. S.I. Hommeltoft, D.H. Berry and R. Eisenberg, *J. Am. Chem. Soc., 108* (1986), 5345.

51. D.H. Berry and R. Eisenberg, *Organometallics, 6* (1987), 1796.

52. A.L. Balch, *J. Am. Chem. Soc., 98* (1976), 8049.

53. J.T. Mague and S.H. DeVries, *Inorg. Chem., 19* (1980), 3743.

54. A.L. Balch and B. Tulyathan, *Inorg. Chem., 18* (1979), 1224.

55. J.T. Mague and A.R. Sanger, *Inorg. Chem., 18,* (1979), 2060.

56. C.L. Lee, C.T. Hunt and A.L. Balch, *Organometallics, 1* (1982), 824.

57. C.P. Kubiak, C. Woodcock and R. Eisenberg, *Inorg. Chem., 19* (1980) 2733.

58. B.A. Vaartstra, K.N. O'Brien, R. Eisenberg and M. Cowie, *Inorg. Chem., 27* (1988), 3668.

59. A.L. Balch, K.M. Waggoner and M.M. Olmstead, *Inorg. Chem., 27* (1988), 4511.

60. S.J. Higgins and B.L. Shaw, *J. Chem. Soc., Chem. Commun.,* (1986), 1629.

61. S. Muralidharan, J.H. Espenson and S.A. Ross, *Inorg. Chem., 25,* (1986), 2557.

62. T.S. Cameron, P.A. Gardner and K.R. Grundy, *J. Organomet. Chem.*, *212* (1981), C19.

63. C.L. Lee, C.T. Hunt and A.L. Balch, *Inorg. Chem.*, *20*, (1981), 2098.

64. C.P. Kubiak, C. Woodcock and R. Eisenberg, *Inorg. Chem.*, *21* (1982) 2119.

65. A.A. Frew, R.H. Hill, L. Manojlovic-Muir, K.W. Muir and R.J. Puddephatt, *J. Chem. Soc., Chem. Commun.*,, (1982), 198.

66. M. Lehmann and G. Wilkinson, *J. Chem. Soc., Dalton Trans.*, (1981), 191.

67. G. de Leeuw, J.S. Field, R.J. Haines, B. McCulloch, E. Meintjies, F. Monberg, G.M. Olivier, P. Ramdial, C.N. Sampson, B. Sigwarth, N.D. Steen and K.G. Moodley, *J. Organomet. Chem.*, *275* (1984), 95.

68. A.R. Chakravarty, F.A. Cotton, M.P. Diebold, D.B. Lewis and W.J. Roth, *J. Am. Chem. Soc.*, *108* (1986), 971.

69. K.A. Johnson and W.L. Gladfelter, *Organometallics*, *8* (1989), 2866.

70. D.L. Davies, B.P. Gracey, V. Guerchais, S.A.R. Knox and A.G. Orpen, *J. Chem. Soc., Chem. Commun.*, (1984), 841.

71. N.G. Connolly, N.J. Farrow, B.R. Gracey, S.A.R. Knox and G.A. Orpen, *J. Chem. Soc., Chem. Commun.*, (1985), 14.

72. J.A. Clucas, M.H. Harding, B.S. Nicholls and A.K. Smith, *J. Chem. Soc., Dalton Trans.*, (1985), 1835.

73. M.I. Bruce and M.L. Williams, *J. Organomet. Chem.*, *306* (1986), 115.

74. T.D. Tilley, R.H. Grubbs and J.E. Bercaw, *Organometallics*, *3* (1984), 274.

75. V. Koelle and J. Kossakowski, *J. Chem. Soc., Chem. Commun.*, (1988), 549.

76. H. Suzuki, H. Omori and Y. Moro-Oka, *Organometallics*, *7* (1988), 2579.

77. T. Arthur and J.A Stephenson, *J. Organomet. Chem.*, *208* (1981), 369.

78. T. Arthur, D.R. Robertson, D.A. Tocker and T.A Stephenson, *J. Organomet. Chem., 208* (1981), 389.

79. T.A. Stephenson and G. Wilkinson, *J. Inorg, Nucl. Chem., 28* (1966), 2285.

80. R. Friary and G.W. Kirby, *J. Chem. Soc., Chem. Commun.,* (1984), 1383.

81. H. Taube, *Ann. N.Y. Acad. Sci., 313* (1978), 496.

82. C. Creutz and H. Taube, *J. Am. Chem. Soc., 95* (1973), 1086.

83. M.J. Powers and T.J. Meyer, *Inorg. Chem., 17* (1978), 2955.

84. E.O Fischer *et al. Z. Naturforsch., B, 17* (1962), 420.

85. M.A. Bennet, M.I. Bruce and T.W. Matheson, *Comprehensive Organometallic Chemistry, Vol. IV,* Pergamon, Oxford (1982), 691.

86. M.O. Albers, D.J. Robinson and E. Singleton, *Coord, Chem. Rev., 79* (1987), 1

87. A.F. Dyke, S.A.R. Knox, P.J. Naish and G.E. Taylor, *J. Chem. Soc., Chem. Commun.,* (1980), 409.

88. A.F. Dyke, S.A.R. Knox, P.J. Naish and G.E. Taylor, *J. Chem. Soc., Dalton Trans.,* (1982), 1297.

89. J. Evans and G.S. McNulty, *J. Chem. Soc., Dalton Trans.,* (1983), 639.

90. R.E. Colborn, D.L. Davies, A.F. Dyke, A. Endesfelder, S.A.R. Knox, A.G. Orpen and D. Plaas, *J. Chem. Soc., Dalton Trans.,* (1983), 2661.

91. D.L. Davies, S.A.R. Knox, K.A. Mead, M.J. Morris and P. Woodward, *J. Chem. Soc., Dalton Trans.,* (1984), 2293.

92. A.F. Dyke, S.A.R. Knox, P.J. Naish and G.E. Taylor, *J. Chem. Soc., Chem. Commun.,* (1980), 803.

93. P.Q. Adams, D.L. Davies, A.F. Dyke, S.A.R. Knox, K.A. Mead and P. Woodward, *J. Chem. Soc., Chem. Commun.,* (1983), 222.

94. A. Stasunik and N. Malisch, *J. Organomet. Chem., 270,* (1984), C56.

95. N.C. Doherty, M.J. Fildes, N.J. Forrow, S.A.R. Knox, K.A. MacPherson and A.G. Orpen, *J. Chem. Soc., Chem. Commun.*, (1986), 1355.

96. N.J. Forrow and S.A.R. Knox, *J. Chem. Soc., Chem. Commun.*, (1984), 679.

97. K.P.C. Vollhardt and T.W. Weideman, *J. Am. Chem. Soc., 105* (1983), 1676.

98. E.A. Seddon and K.R. Seddon, in R.J.H. Clarke (Ed.), *The Chemistry of Ruthenium,* Monograph 19, Elsevier Science Publishers, B.V. Amsterdam (1984).

99. G.R. Crookes, B.F.G. Johnson, J. Lewis, I.G. Williams and G. Gamlen, *J. Chem. Soc., (A),* (1969), 2761.

100. F. Neumann and G. Süss-Fink, *J. Organomet. Chem., 367* (1989), 175.

101. M. Spohn, T. Vogt and J. Strähle, *Naturforsch, B, 41B* (1986), 1373.

102. M. Rotem, Y. Shuo, I. Goldberg and U. Shmeuli, *Organometallics, 3* (1984), 1758.

103. M. Rotem, Y. Shuo, I. Goldberg and U. Shmeuli, *J. Organomet. Chem., 314* (1986), 185.

104. J.G. Bullitt and F.A. Cotton, *Inorg. Chim. Acta, 5* (1971), 406.

105. J. Jenck, P. Kalck, E. Pinelli, M. Siani and A. Thorez, *J. Chem. Soc., Chem. Commun.*, (1988), 1428.

106. M. Rotem and Y. Shuo, *Organometallics, 2* (1983), 1689.

107. U. Matteoli, G. Menchi, M. Bianchi and F. Piacenti, *J. Organomet. Chem., 299* (1986), 233.

108. M. Bianchi, U. Matteoli, G. Menchi, P. Frediani and F. Piacenti, *J Organomet. Chem., 240* (1982), 65.

109. R.W. Hills, S.J. Sherlock, M. Cowie, E. Singleton and M.M. de V Steyn, *Inorg. Chem., 29* (1990), 3161.

110. M. Cowie, S.J. Sherlock, E. Singleton and M.M. de V Steyn, *J. Organomet. Chem., 361* (1989), 353.

111. M. Cowie, S.J. Sherlock, E. Singleton and M.M. de V Steyn, *Organometallics, 7* (1988), 1663.

112. S.A.R. Knox and F.G.A. Stone, *J. Chem. Soc., (A),* (1969), 2559.

113. S.A.R. Knox and F.G.A. Stone, *J. Chem. Soc., (A),* (1971), 2874.

114. J.A.K. Howard, S.L. Killett and P. Woodward, *J. Chem. Soc., Dalton Trans.,* (1975), 2333.

115. C.E. Kampe and H.D. Kaesz, *Inorg. Chem., 23* (1984), 4646.

116. J.A. Cabeza, C. Landazuri, L.A. Oro, A. Tiripicchio and M. Tiripicchio-Camellini, *J. Organomet. Chem., 322* (1987), C16.

117. S.J. Sherlock, M. Cowie, E. Singleton and M.M. de V Steyn, *J. Organomet. Chem., 361* (1989), 353.

118. H. Schumann and J. Opitz, *J. Organomet. Chem., 186* (1980), 91.

119. A. Colombie, G. Lavigne and J.J. Bonnet, *J. Chem. Soc., Dalton Trans.,* (1986), 899.

120. M. Cooke, M. Green and D. Kirkpatrick, *J. Chem. Soc., (A),* (1968), 1507.

121. R.E. Dessy, A.L. Rheingold and G.D. Howard, *J. Chem. Soc., 94* (1972), 746.

122. N.K. Bhattacharryya, T.J. Coffy, W. Quintana, T.A. Salupo, J.C. Bricker, T.B. Shay, M. Payne and S.G. Shore, *Organometallics, 9* (1990), 2368.

123. L. Hsu, N. Bhattacharryya and S.G. Shore, *Organometallics, 4* (1985), 1483.

124. G. de Leeuw, J.S. Field, R.J. Haines, B. McCulloch, E. Meintjies, F. Monberg, G.M. Olivier, P. Ramdial, C.N. Sampson, B. Sigwarth, N.D. Steen and K.G. Moodley, *J. Organomet. Chem., 275* (1984), 99.

125. A.L. du Preez, I.L. Marais, R.J. Haines, A. Pidcock and M. Safari, *J. Chem. Soc., Dalton Trans.,* (1981), 1918.

126. D.W. Engel, K.G. Moodley, L. Subramony and R.J. Haines, *J. Organomet. Chem., 349* (1988), 393.

127. J.S. Field, R.J. Haines, E. Minshall, C.N. Sampson and J. Sundermeyer, *J. Organomet. Chem., 309* (1986), C21.

128. J.S. Field, R.J. Haines, C.N. Sampson, J. Sundermeyer and K.G. Moodley, *J. Organomet. Chem., 322* (1987), C7.

129. K.J. Edwards, J.S. Field, R.J. Haines, B. Homann, J. Sundermeyer and S.F. Woollam, *J. Organomet. Chem., 386* (1990), C1.

130. J.S. Field, R.J. Haines, E. Minshall, C.N. Sampson and J. Sundermeyer, *J. Organomet. Chem., 327* (1987), C18.

131. J.S. Field, R.J. Haines, E. Minshall, C.N. Sampson, J. Sundermeyer and S.F. Woollam, submitted for publication.

132. D.W. Engel, R.J. Haines, E.C. Horsfield and J. Sundermeyer, *J. Chem. Soc., Chem. Commun.*, (1989), 1457.

133. S. Guy, M.Sc. Thesis, University of Natal, (1991).

134. J.S. Field, R.J. Haines, C.N. Sampson and J. Sundermeyer, *J. Organomet. Chem., 310* (1986), C42.

135. D.W. Engel, J.S. Field, R.J. Haines, J. Sundermeyer and S.F. Woollam, submitted for publication.

136. S.E. Bell, J.S. Field, R.J. Haines and J. Sundermeyer, submitted for publication.

137. J. Sundermeyer, unpublished results.

138. G. Kiel and J. Takats, *Organometallics, 8* (1989), 839.

139. K.A. Johnson and W.L. Gladfelter, *Organometallics, 9* (1990), 2101.

140. J.S. Field, A.M.A. Francis and R.J. Haines, *J. Organomet. Chem., 356* (1988), C23.

141. J.S. Field, A.M.A. Francis, R.J. Haines and S.F. Woollam, *J. Organomet. Chem., 412* (1991), 383.

142. R.J. Haines and A.L. du Preez, *Inorg. Chem., 11* (1972), 330.

143. G. Bruno, S.L. Schlaro, P. Piraino and F. Faraone, *Organometallics, 4* (1985), 1098.

144. J.A. Ladd, H. Hope and A.L. Balch, *Organometallics, 3* (1984), 1838.

145. W.A. Hermann and W. Kalcher, *Chem. Ber., 118* (1985), 3861.

146. H. Werner and R. Werner, *Chem. Ber., 115* (1982), 3766.

147. W.D. Rohrbach and V. Boekeheide, *J. Organomet. Chem., 48* (1983), 3673.

148. A.J. Lindsey, G. Wilkinson, M. Motevalli and M.B. Hursthouse, *J. Chem. Soc., Dalton Trans.,* (1985), 2321; *ibid* (1987), 2723.

149. B. Callan, A.R. Manning and F.S. Stephens, *J. Organomet. Chem., 331* (1987), 357.

150. B. Callan and A.R. Manning, *J. Organomet. Chem., 252* (1983), C81.

151. N.G. Connelly, N.J. Forrow, S.A.R. Knox, K.A. Macpherson and A.G. Orpen, *J. Chem. Soc., Chem. Commun.,* (1985), 16.

152. N.M. Doherty, J.A.K. Howard, S.A.R. Knox, N.J. Terrill and M.I. Yates, *J. Chem. Soc., Chem. Commun.,* (1989), 638.

153. B.N. Storhoff and H.C. Lewis, *Coord. Chem. Rev., 23* (1977), 1.

154. B. Storhoff and A.J Infante, *Inorg. Chem., 13* (1974), 3044.

155. G.A. Foulds, B.F.G. Johnson and J. Lewis, *J. Organomet. Chem., 296* (1985), 147.

156. A.J. Lindsey, G. Wilkinson, M. Motevalli and M.B. Hursthouse, *J. Chem. Soc., Dalton Trans.,* (1985), 2321.

157. K. Krogh-Jespersen, X. Zhang, J.D. Westbrook, R. Fikar, K. Nayak, W. Kwik, J.A. Potenza and H. Schugar, *J. Am. Chem. Soc., 111* (1989), 4082.

158. R.G. Pearson, *J. Am. Chem. Soc., 85* (1963), 3533.

159. S.P. Deraniyagala and K.R. Grundy, *Inorg. Chem., 24* (1985), 50.

160. M.J. Chen, H.M. Feder and J.W. Rathke, *J. Am. Chem. Soc., 101* (1979), 1589.

161. R. Pruette, *Adv. Organomet. Chem., 17* (1979), 1.

162. P.C. Ford, R.G. Rinker, R.M. Laine, C. Ungermann, V. Landis and S.A. Moya, *J. Am. Chem. Soc., 100* (1978), 4595.

163. K.M. Doxsee and R.H. Grubbs, *J. Am. Chem. Soc., 103* (1981), 7696.

164. C.H. Cheng, L. Kuritzkes and R. Eisenberg, *J. Organomet. Chem., 190* (1980), C21.

165. T. Cole, R. Ramage, K. Cann and R. Pettit, *J. Am. Chem. Soc., 102* (1980), 6182.

166. R.J. Trautman, D.C. Gross and P.C. Ford, *J. Am. Chem. Soc., 107* (1985), 2355.

167. D.C. Gross and P.C. Ford, *J. Am. Chem. Soc., 107* (1985), 585.

168. J.C. Bricker, C.C. Nagel, A.A.Bhattacharyya and S.G. Shore, *J. Am. Chem. Soc., 107* (1985), 377.

169. G. Süss-Fink, *Angew. Chem., Int. Ed. Engl., 21* (1982), 73.

170. M.Aresta and C.F. Nobile, *J. Chem. Soc., Chem. Commun.,* (1975), 636.

171. D.J. Darensbourg, R.A. Kudaroski, *Adv. Organomet. Chem., 22* (1983), 129.

172. G. Wilkinson and F.G.A. Stone, *Comprehensive Organometallic Chemisty,* E.W. Abel, Eds., Pergamon: New York, 1982, Vol 8, Chapter 50.

173. M.G. Mason, J.A. Ibers, *J. Am. Chem. Soc., 104* (1982), 5153.

174. J.R. Sweet, W.A.G. Graham, *Organometallics, 1* (1982), 982.

175. J.H. Merrifield and J.A. Gladysz, *Organometallics, 2* (1983), 782.

176. D.J. Darensbourg, *Israel J. Chem., 15* (1976), 247.

177. N. Grice, S.C. Kao and R. Pettit, *J. Am. Chem. Soc., 101* (1979), 1627.

178. S. Gamburotta, F. Arena, C.J. Floriani and P.F. Zanazzi, *J. Am. Chem. Soc., 104* (1982), 5082.

179. E.G. Lundquist, J.C. Huffman, K. Folting, B.E. Mann and K.G. Caulton, *Inorg. Chem., 29* (1990), 128.

180. M.E. Volpin and I.S. Kolomnikov, *Pure Appl. Chem., 33* (1973), 567.

181. M.E. Volpin and I.S. Kolomnikov, *Organomet. React., 3* (1975), 313.

182. C.M. Jensen, Y.J. Chen and H.D. Kaesz, *J. Am. Chem. Soc., 106* (1984), 4046.

183. C.J. Cardin, S.B. Colbran, B.F.G. Johnson, J. Lewis and P.R. Raithby, *J. Chem. Soc., Chem. Commun.*, (1986), 1288.

184. D.J. Darensbourg and A. Rokicki, *Organometallics, 1* (1982), 1685.

185. R.Bentley and I.M. Campbell, *The chemistry of Quinonoid Compounds;* S. Patai, Ed., Wiley: New York, 1974, Part 2, Chapter 13.

186. A.A. Konstantinov and E.K. Ruage, *Biorg. Khim., 3* (1977), 787.

187. C.A. Wraight, *FEBS Lett., 93* (1978), 283.

188. J.A. Ladd, M.M. Olmstead and A.L. Balch, *Inorg. Chem., 23* (1984), 2318.

189. N.G. Connelly, I. Manners, J.R.C. Protheroe and M.W. Whitely, *J. Chem. Soc., Dalton Trans.*, (1984), 2713.

190. G.M. Bodner and T.R. Engelmann, *J. Organomet. Chem., 88* (1975), 391.

191. D. Sutton, *Chem. Soc. Rev.*, (1975), 443.

192. C.F. Barrientos-Penna, A.B. Gilchrist, A.H. Klahn-Oliva, A.J. Lee Hanlan and D. Sutton, *Organometallics, 4* (1985), 478.

193. R.B. King and M.B. Bisnette, *J. Am. Chem. Soc., 86* (1964), 5694.

194. G.W. Parshall, *J. Am. Chem. Soc., 89* (1967), 1822.

195. K.R. Laing, S.D. Robinson and M.F. Uttley, JCSCC (1973), 1673.

196. N.G. Connelly, *Inorg. Chim. Acta. Rev., 6* (1972), 47.

197. T.E. Nappier and D.W. Meek, *J. Am. Chem. Soc., 75* (1973), 4194.

198. E.M. Kosower, *Acc. Chem. Res., 4* (1971), 193.

199. S. Matsuzaki, T. Mitsuishi and K. Toyoda, *Bull. Chem. Soc., Japan, 55* (1982), 3377.

200. Y. Iida, *Bull. Chem. Soc., Japan, 43* (1970), 345.

201. S.D. Ittel and J.A. Ibers, *J. Am. Chem. Soc., 96* (1974), 4804.

202. S. Otsuka and A. Nakamura, *Adv. in Organomet. Chem., 14* (1976), 245.

203. K.P.C. Volhardt, *Acc. Chem. Res., 10* (1977), 1.

204. N.D. Feasey, S.A.R. Knox, A.G. Orpen, M.J. Winter, *New J. Chem., 12* (1988), 1581.

205. F.A. Cotton, J.D. Jamerson and B.R. Stults, *J. Am. Chem. Soc., 98* (1976), 1774.

206. M. Cowie and T.J. Southern, *Inorg. Chem., 21* (1982), 246.

207. Y. Koie, S. Shinoda, Y. Saito, B.J. Fitzgerald and C.G. Pierpont, *Inorg. Chem., 19* (1980), 770.

208. E.L. Meutterties, W.R. Pretzer, M.G. Thomas, B.F. Beier, D.L. Thorn, V.W. Day and A.B. Anderson, *J. Am. Chem. Soc., 100* (1978), 2090.

209. N.M. Boag, M. Green, J.A.K. Howard, J.L. Spencer, R.F.D. Stansfied, F.G.A. Stone, M.D.O. Thomas, J. Vicente and P. Woodward, *J. Chem. Soc., Chem. Commun.,* (1977), 930.

210. A.L. Balch, C. Lee, C.H. Lindsey, M.M. Olmstead, *J. Organomet. Chem., 177* (1979), C22.

211. W.A. Hermann, *Angew. Chem., Int. Ed. Engl., 21* (1982), 117.

212. O.S. Mills and A.D. Redhouse, *J. Chem. Soc., Chem. Commun.,* (1966), 444.

213. A.N. Nesmeyanov, G.G. Aleksandrov, A.B. Antonova, K.N. Anisimov, N.E. Kolobova and Y.T. Struchkov, *J. Organomet. Chem.,* 110 (1976), C36.

214. R.B. King and M.S. Saran, *J. Am. Chem. Soc., 94* (1972), 1784.

215. M. Cooke, D.L. Davies, J.E. Guerchais, S.A.R. Knox, K.A. Mead, J. Roué, and P. Woodward, *J. Chem. Soc., Chem. Commun.,* (1981), 862.

216. D.L. Davies, A.F. Dyke, A. Endersfelder, S.A.R. Knox, P.J. Naish, A.G. Orpen and D. Plaas, *J. Organomet. Chem., 198* (1980), C43.

217. K.R. Birdwhistell, T.L. Tonker and J.L. Templeton, *J. Am. Chem. Soc., 107* (1985), 4474.

218. F.J. Garcia Alfonso, A. Höhn, J. Wolf, H. Otto and H. Werner, *Angew. Chem., Int. Ed. Engl., 24* (1985), 406.

219. A. Höhn, H. Otto, M. Dziallas and H. Werner, *J. Chem. Soc., Chem. Commun.*, (1987), 852.

220. H. Werner, A Höhn and M Schultz, *J. Chem. Soc., Dalton Trans.*, (1991), 777.

221. L.N. Lewis, J.C. Huffman and K.G. Caulton, *J. Am. Chem. Soc., 102* (1980), 403.

222. Y.N. Al-Obaidi, M. Green, N.D. White and G.E. Taylor, *J. Chem. Soc., Dalton Trans.*, (1982), 319.

223. E. Weiss, W. Hübel and R. Merenyi, *Chem. Ber., 95* (1962), 1155.

224. A.G. Orpen, D. Pippard, G.M. Sheldrick and D.J. Field, *Acta Crystallogr., Sect. B, 34* (1975), 2466.

225. B.F.G. Johnson, J. Lewis, A.G. Orpen, P.R. Raithby and K.D. Rouse, *J. Chem. Soc., Dalton Trans.*, (1981), 788.

226. Y.N. Al-Obaidi, P.K. Baker, M. Green, N.D. White and G.E. Taylor, *J. Chem. Soc., Dalton Trans.*, (1981), 2321.

227. A.G. Orpen, *J. Chem. Soc., Dalton Trans.*, (1983), 1427.

228. E.L. Meutterties, *Chem. Eng. News, 60* (1982), 28.

229. E.L. Meutterties, *Science, 196* (1977), 839.

230. M.D. Fryzuk, W.E. Piers, F.W.B. Einstein and T. Jones, *Can. J. Chem., 67* (1989), 883.

231. C.L. Lee, C.T. Hunt and A.L. Balch, *Inorg. Chem., 20* (1981), 2498.

232. J.T. Lin, G.P. Hagen and J.E. Ellis, *J. Am. Chem. Soc., 105* (1983), 2296.

233. M.J. Bennet, W.A.G. Graham, J.K. Hayano and W.L. Hutcheon, *J. Am. Chem. Soc., 94* (1972), 6232.

234. V. Riera, M.A. Ruiz, A. Tiripicchio and M. Tiripicchio-Camellini, *J. Chem. Soc., Chem. Commun.*, (1985), 1505.

235. F.J. Garcia-Alfonso, M. Garcia-Sanz, V. Riera, M.A. Ruiz, A. Tiripicchio and M. Tiripicchio-Camellini, *Angew. Chem., Int. Ed. Engl., 27* (1988), 1167.

236. M.J. Mays, D.W. Prest and P.R. Raithby, *J. Chem. Soc., Chem. Commun.*, (1980), 171; idem, *J. Chem. Soc., Dalton Trans.*, (1982), 2021.

237. A. Almenningen, G.G. Jacobsen and H.M. Seip, *Acta. Chem. Scand., 23* (1969), 685.

238. P.E. Bloyce, A.K. Campen, R.H. Hooker, A.J. Rest, N.R. Thomas, T.E. Bitterwolf and J.E. Shade, *J. Chem. Soc., Dalton Trans.*, (1990), 2833.

239. R.H. Hooker, K.A. Mohamoud and A.J. Rest, *J. Chem. Soc., Chem. Commun.*, (1983), 1022.

240. R.H. Hooker and A.J. Rest, *J. Chem. Soc., Dalton Trans.*, (1990), 1221.

241. W.I. Bailey, M.H. Chisholm, F.A. Cotton and L.A. Rankel, *J. Am. Chem. Soc., 100* (1978), 5764.

242. F.A. Cotton and J.M. Troup, *J. Am. Chem. Soc., 96* (1974), 1233.

243. K-W. Lee, W.T. Pennington, A.W. Cordes and T.L. Brown, *J. Am. Chem. Soc.,, 107* (1985), 631.

244. K-W. Lee, J.M. Hanckel and T.L. Brown, *J. Am. Chem. Soc., 108* (1986), 2266.

245. A. Nutton and P.M. Maitlis, *J. Organomet. Chem., 166* (1979), C21.

246. D.G. Hamilton and R.H. Crabtree, *J. Am. Chem. Soc., 110* (1988), 4126.

247. T. Arliguie, B. Chaudret, R.H. Morris and A. Sella, *Inorg. Chem., 27* (1988), 599.

248. C. Hampton, W.R. Cullen, B.R. James, J. Charland, *J. Am. Chem. Soc., 110* (1988), 6198.

249. M.L.H. Green and D.J. Jones, *Adv. Inorg. Chem. Radiochem.*, *7* (1965), 115.

250. H.D. Kaesz and R.B. Saillant, *Chem. Rev.*, *72* (1972), 231.

251. D.M. Roundhill, *Adv. Organomet. Chem.*, *13* (1975), 273.

252. D.S. Moore and S.D. Robinson, *Chem. Soc. Rev.*, *12* (1983), 415.

253. P.S. Hallman, B.R. McGarvey and G. Wilkinson, *J. Chem. Soc., (A)*, (1968), 3134.

254. W. Hieber and F. Leutert *Naturwissenschaften, 19* (1931), 360.

255. G.J. Kubas, R.R. Ryan, B.I. Swanson, P.J. Vergamini and H.J. Wasserman, *J. Am. Chem. Soc.*, 106 (1984), 450.

256. R.H. Crabtree and M. Lavin, *J. Chem. Soc., Chem. Commun.*, (1985), 794 and 1661.

257. S.A.R. Knox, J.W. Koepke, M.A. Andrews and H.D. Kaesz, *J. Am. Chem. Soc., 97* (1975), 3942.

258. J.J. Bonnet, A. Thorez, A. Maisonnat, J. Galy and R. Poilblanc, *J. Am. Chem. Soc., 101* (1979), 5940.

259. M.P. Brown, J.R. Fisher, R.H. Hill, R.J. Puddephatt and K.R. Seddon, *Inorg. Chem., 20* (1981), 3516.

260. S.G. Davies, J. Hibberd, S.J. Simpson and O. Watts, *J. Organomet. Chem., 238* (1982), C7.

261. R.H. Hill and R.J. Puddephatt, *J. Am. Chem. Soc., 105* (1983), 5797.

262. M.J. Church, M.J. Mays, R.N.F. Simpson and F.P. Stefanini, *J. Chem. Soc., (A)*, (1970), 2909.

263. J.R. Fisher, A.J. Mills, S. Sumner, M.P. Brown, M.A. Thomson, R.J. Puddephatt, A.A. Frew, L. Manojlovic-Muir and K.W. Muir, *Organometallics, 1* (1982), 1421.

264. B. Chaudret, F. Dahan and S. Sabo, *Organometallics, 4* (1985), 1490.

265. L. Vaska, *Science, 140* (1963), 810.

266. K.R. Laing and W.R. Roper, *J. Chem. Soc., Chem. Commun.*, (1968), 1556.

267. D.D. Perrin, W.L.F. Armarego and D.R. Perrin, "Purification of Laboratory Chemicals", Pergamon, Oxford, 1966.

268. C.K. Mann, *Electroanal. Chem., 3* (1969), 57.

269. A.C.T. North, D.C. Philips and F.S. Mathews, *Acta. Crystallogr., Sect. A, 24* (1968), 351.

270. "International Tables for X-ray Crystallography", Kynoch Press, Birmingham, Vol 4 (1974), pp 99, 149.

271. G.M. Sheldrick, SHELX-76, Program for Crystal Structure Determination, University of Cambridge, 1976.

272. G.M. Sheldrick, SHELX-86, Program for Crystal Structure Determination, University of Göttingen, 1986.

273. P. Main, MULTAN-82, A System of Computer Programs for the Automatic Solution of Crystal Structures from X-ray Diffraction Data, University of York, 1982.

274. S. Motherwell and W. Clegg, PLUTO-78, Program for Plotting Molecular and Crystal Structures, University of Göttingen, 1978.

275. D.C. Liles, TABLES, Program for Tabulation of Crystallographic Data, Council for Scientific and Industrial Research (Pretoria), 1988.

276. J.F. Nixon, *J. Chem. Soc., (A)*, (1968), 2689.

277. E. Meintjies, Ph.D. Thesis, University of Natal, (1981).

278. K.G. Rutherford, W. Redmond and J. Rigamonti. *J. Organomet. Chem., 26* (1961), 5149.